

Carbonyl Catalysis: Hydrolysis of Organophosphorus Compounds and Application in Prebiotic Chemistry

**By
Binjie Li**

A thesis submitted in partial fulfillment of the requirements for the
Ph. D. degree in chemistry

Ottawa-Carleton Chemistry Institute
University of Ottawa

Candidate

Supervisor

Binjie Li

Prof. André M. Beauchemin

Abstract

Since late 1990s, organocatalysis has been widely explored in many aspects and achieved various difficult transformations. In this field, carbonyl catalysis, which could be traced back to 1860 has been developed with impressive progress including asymmetric variants. Over the years, major activation modes were developed for carbonyl catalysis including exploiting temporary intramolecularity to form catalytic tethers and transient intramolecular nucleophiles, dioxirane formation and imine formation. On the other hand, electrophilic activation is also an important area of organocatalysis where impressive progress has been achieved. However, limited examples were reported to achieve the electrophilic activation via carbonyl catalysis. Organophosphorus compounds are crucially important in many aspects in organic chemistry. Many approaches were developed for asymmetric organophosphorus compounds. In this work, different types of organophosphorus compounds were used as the substances for aldehyde-catalyzed hydrolysis reactions.

The first part of this thesis illustrated the strategy to combine carbonyl catalysis and electrophilic activation. The hydrolysis of organophosphorus compounds containing P(=O)-N bond were investigated based on Jencks and Gilchrist's preliminary results with formaldehyde as the catalyst to promote the hydrolysis of one inorganic substance, phosphoramidate. This Chapter describes a systematic research to identify a superior catalyst, *o*-phthalaldehyde, and develop catalytic hydrolyses of various organophosphorus compounds containing P(=O)-NHR subunits. Gratifyingly, the reaction proved efficient with phosphinic amides and phosphoramidates. Moreover, chemoselectivity was also studied and selective hydrolysis of the P(=O)-N bonds in the presence of P(=O)-OR bonds could be accomplished.

The second part of this thesis demonstrated the further development of one of the major modes of carbonyl catalysis. Formaldehyde was identified as the efficient catalyst to react with α -amino phosphonates to form the transient intramolecular nucleophile, which facilitated the subsequent hydrolysis reactions. In this Chapter, different primary and secondary α -amino phosphonates with phenol as the leaving group, were tested in the reaction conditions. As a result, a vast of mono esters of α -amino phosphoric acids could be formed as the products.

Finally, the last portion of this thesis applied the methodologies developed in Chapter 2 to prebiotic chemistry. A prebiotic-related aldehyde, glycolaldehyde was studied as the catalyst for the hydrolysis of organophosphorus compounds containing P(=O)-N bond, including phosphinic amides and phosphoramidates. Additionally, other prebiotic important substances, diamidophosphate (DAP) and monoamidophosphate (MAP) were also investigated for potential glycolaldehyde-catalyzed phosphorylation reaction under aqueous conditions. In the presence of catalytic amount of glycolaldehyde, 1) when water was used as the nucleophile, the hydrolysis of DAP and MAP were significantly improved; 2) when other phosphate nucleophiles were added to compete with water, DAP could act as a phosphorylating reagent to phosphorylate other phosphate nucleophiles.

Overall, the results presented in this thesis investigated two different activation modes, electrophilic activation and transient intramolecular nucleophiles, for carbonyl catalysis to hydrolyze different organophosphorus compounds, phosphinic amides, phosphoramidates and α -amino phosphonates. The application of carbonyl catalysis to prebiotic chemistry was also achieved especially with the phosphorylation reaction with DAP.

Acknowledgement

Pursuing a PhD is a tough process, and studying abroad makes this even more difficult. This is an amazing experience, however, I do not think that I could reach this stage without the support and love from my family and friends.

First, I must thank André for giving me this great opportunity to join the group. André has provided a lot of guidance and support during these five years for research. André is also an amazing supervisor who has great respect on other different cultures and exceptional patience with a Chinese girl who barely spoke English.

I also want to thank the Beauchemin group. Special thanks to Sampada Chitale, Amanda Bongers and Pouyan Zahedi. Thank you for helping me a lot when I first came to Ottawa. Without your help, the first year would have been very tough especially with the winter. A huge thanks to the colleagues that I have collaborate with, Ryan Simard, Claudia EI-Nachef and Philippe Lemire. Without your help, the developments made in the lab would not have been possible. I must thank the colleagues that help me a lot with the English when I wrote the thesis, Ryan Ivanovich, Josh Derasp, Jasper Quartus, David Brzezinski and William Gagné Monfette. More broadly, I want to thank all the members in Beauchemin lab for making this group a great place to do research and that it has been my pleasure to work with all of you. I also want to thank all the Chinese friends in the department for your support and company. It is my great honor to make friends with all of you.

Finally, I want to thank my lovely big family and my parents for their unconditional love and support. I am very very lucky to be your daughter. Without your guidance and amazing model of what it means to be a couple and a family, I wouldn't be who I am today. Special thanks to my partner in life, none of this would be possible without your

endless love and support. I am looking forward to moving back to explore the new chapter of our life together.

You have to believe in yourself. That is the secret of success.

— *Charles Chaplin*

Table of Contents

Abstract	II
Acknowledgement	IV
Table of Contents	VII
List of Abbreviations	X
List of Figures	XIV
List of Schemes	XV
List of Tables	XX
Chapter 1	1
Introduction	1
1.1 Development of organocatalysis	1
1.2. Carbonyl Catalysis	5
1.2.1 Inducing temporary intramolecularity	8
Intramolecular nucleophiles: <i>in situ</i> formation of transient intramolecular nucleophiles	9
Tethering reagents: formation of mixed aminal tethers	14
1.2.2. Asymmetric epoxidation via dioxirane formation	20
1.2.3 Iminium/imine formation.....	22
Increased acidity/reactivity	23
Providing catalytic directing group.....	28
1.3. Electrophilic activation	29
1.3.1 Nucleophilic catalysis	31
1.3.2 Brønsted acid catalysis.....	36
1.4 Conclusion	39
Chapter 2	41
Electrophilic activation via carbonyl catalysis: <i>o</i>-Phthalaldehyde catalyzed hydrolysis of organophosphinic amides and related compounds	41
2.1 Introduction.....	41
2.1.1 Electrophilic activation via carbonyl catalysis	41
2.1.2 Importance of catalytic reactions of organophosphorus compounds....	44
2.1.3 Importance of hydrolysis reaction	52
2.1.4 Hydrolysis of P(=O)-N bond	53
Acidic and basic conditions for hydrolysis of P(=O)-N motif.....	53
Lewis acid catalyzed hydrolysis of P(=O)-N motif.....	54
Metal catalyzed hydrolysis of P(=O)-N motif	55
Fluoride ion mediated hydrolysis.....	57
2.2 Results and discussion	58
2.2.1 Optimization with primary phosphinic amide	58
2.2.2 Optimization with secondary phosphinic amide.....	61
2.2.3 Reaction time monitoring	64
2.2.4 Substrate scope for the hydrolysis reaction	67
2.2.5 Comparison of catalytic efficiency between formaldehyde and <i>o</i> -	

phthalaldehyde	72
2.3 Kinetic resolution.....	74
2.3.1 General introduction for kinetic resolution.....	74
2.3.3 Results and discussion	77
2.4 Summary and outlook.....	79
Chapter 3	81
Carbonyl catalysis via transient intramolecular nucleophiles: Formaldehyde catalyzed mono-hydrolysis of α-amino phosphonates	81
3.1 Introduction.....	81
3.2 Importance of α -amino phosphonates and derivatives	81
3.3. Hydrolysis of α -amino phosphonates	86
Hydrolysis under acidic conditions.....	86
Hydrolysis under basic conditions	87
Selected examples for other conditions	89
3.4 Results and discussion	90
3.4.1 Optimization of the reaction conditions.....	91
3.4.2 Efforts toward isolation of the product	98
Study for extraction.....	98
Replacement of a water-soluble base.....	99
<i>In situ</i> derivation of the product.....	100
Recrystallization with free amino substrates.....	101
Resin exchange	102
3.4.3 Substrate scope.....	103
3.4.4. Preliminary study for weaker leaving group.....	107
3.4.5. Preliminary trials toward kinetic resolution of chiral α -amino phosphonates.....	109
3.5 Conclusion	114
Chapter 4	115
Application of Carbonyl Catalysis in Prebiotic Chemistry.....	115
4.1 General introduction on prebiotic chemistry	115
4.2 Glycolaldehyde in Prebiotic chemistry.....	118
4.2.1 Formation of ribonucleotides.....	119
4.2.2 Formation of imidazoles and oxazoles	121
4.2.3 Formation of sugars: Formose synthesis.....	123
4.3 Glycolaldehyde catalyzed hydrolysis of Strecker adduct	125
4.3.1 Strecker reaction	125
4.3.2 Hydration of α -aminonitriles (Strecker adduct).....	126
4.3.3 Glycolaldehyde catalyzed hydration reaction of α -aminonitriles	128
4.4 Results and Discussion: Comparison of catalytic efficiency of glycolaldehyde vs formaldehyde.....	130
4.5 Phosphorylation process	133
4.5.1 Prebiotic phosphorylation	134
Orthophosphates as phosphorylating reagents.....	135
Poly-phosphates as phosphorylating reagents	136

DAP as a common phosphorylating source	136
4.5.2 Results and Discussion: Glycolaldehyde-catalyzed phosphorylation with DAP	141
4.6 Conclusion and future work	165
Chapter 5	166
Conclusion	166
Claims to Original Research	168
Publication from This Work	168
Presentations from This Work	169
Oral presentation	169
Poster presentation	169
Chapter 6	170
Experiment Section	170
6.1. General Information	170
6.2. Experimental section for Chapter 2	171
General procedure for the synthesis of diphenylphosphinic amides and diphenylphosphoramidates.	171
General procedure to generate products	171
Phosphinic Amides	173
Phosphoramidates	185
Chiral aldehydes	194
6.3. Experimental section for Chapter 3	196
General procedure for the synthesis of α -amino phosphonates	196
General procedure for the synthesis of secondary α -amino phosphonates ..	197
General procedure for the synthesis of mono ester of α -amino phosphonates	197
α -Amino phosphonates	199
Mono ester of α -Amino phosphonates	210
6.4. Experiment section for Chapter 4	220
General procedure to generate products with glycolaldehyde or formaldehyde	220
General procedure when DAP or MAP were used	221
Appendix I	226
NMR and HPLC spectra data	226
<i>Spectra for starting materials in Chapter 2</i>	226
<i>Spectra for chiral aldehydes in Chapter 2</i>	274
<i>HPLC data for racemic in Chapter 2</i>	276
<i>Spectra for starting materials in Chapter 3</i>	278
<i>Spectra for products in Chapter 3</i>	301
<i>HPLC data for racemic in Chapter 3</i>	323

List of Abbreviations

Ac	acetyl
A, U, G, C	adenine, uracil, guanine, cystine
AcOH	acetic acid
AcOAc	acetic anhydride
ADP	adenosinediphosphate
Ar	aromatic group
ATP	adenosinetriphosphate
ATPase	adenosinetriphosphatase
aq	aqueous
BINOL	1,1'-Bi-2-naphthol
Bn	benzyl
Boc	<i>tert</i> -butoxycarbonyl
Bu	butyl
<i>t</i> BuOH	<i>tert</i> -butanol
Bz	benzoyl
<i>n</i> Bu	butyl
<i>s</i> BuLi	<i>sec</i> -butyllithium
°C	degree Celsius
C ₆ H ₆	benzene
C ₆ F ₆	hexafluorobenzene
Cat.	catalyst
Cp ^x	chiral cyclopentadienyl complex
Cy	cyclohexyl
δ	chemical shift in parts per million
D	deuterium (Solvent); doublet
DABCO	1,4-diazabicyclo[2.2.2]octane
DBU	1,8-diazabicyclo(5.4.0)undec-7-ene

DCM	dichloromethane
de	diastereomeric excess
DMF	dimethylformamide
DMAP	4-dimethylaminopyridine
DMSO	dimethyl sulfoxide
DNA	deoxyribonucleic acid
DNBA	3,5-dinitrobenzoic acid
dr	Diastereomeric ratio
ee	Enantiomeric excess
eq./equiv.	equivalent
Et	ethyl
er	enantiomeric ratio
EWG	electron-withdrawing group
g	gram
h	hours
HRMS	high-resolution mass spectroscopy
Hz	Hertz
<i>i</i>	iso
IR	Infrared
<i>J</i>	coupling constant
K	equilibrium constant
LA	Lewis acid
LUMO	Lowest unoccupied molecular orbital
<i>m</i>	meta
M	molar; metal
Me	methyl
MeCN/CH ₃ CN	acetonitrile
MeOH	methanol
mg	milligram

min	minute
mL	millilitre
mol	Mole
mmol	millimole
Ms	mesylate
NEt ₃	triethylamine
Nu	nucleophile
NMR	nuclear magnetic resonance
<i>o</i>	ortho
<i>p</i>	para
Ph	phenyl
PhCH ₃ /PhMe	toluene
pr	propyl
<i>i</i> Pr	isopropyl
R (R [#])	carbon-based substituent
RNA	ribonucleic acid
rt/r.t.	room temperature
s	second
<i>s</i>	selectivity factor
<i>t</i>	tertiary
TBAF	tetra- <i>n</i> -butylammonium fluoride
TBD	triazabicyclodecene
THF	tetrahydrofuran
Tf	triflate
TFA	trifluoroacetic acid
TLC	thin layer chromatography
TMS	trimethylsilyl
Ts	tosyl
UV	ultra-violet

ΔG	change in Gibbs-free energy
ΔH	change in enthalpy
ΔS	change in entropy

List of Figures

Figure 3.1. ^{31}P NMR for preliminary results of weak leaving group (OEt).....	107
Figure 4.1. Background reaction (without glycolaldehyde and NH_4OTs)	143
Figure 4.2. Glycolaldehyde catalyzed activation of DAP under full reaction conditions.....	144
Figure 4.3. Enhanced spectrum for $t = 3.5$ h.....	145
Figure 4.4. Control experiment in the presence of glycolaldehyde	147
Figure 4.5. Control reaction (in the presence of NH_4OTs , without glycolaldehyde)	148
Figure 4.6. Stacked spectra for different reaction conditions at 3.5 h	149
Figure 4.7. Potential effect of anion by changing NH_4OTs to NH_4Cl	150
Figure 4.8. Potential effect of additives by changing NH_4OTs to NaCl	151
Figure 4.9. Stacked spectra for different additives at 3.5 h	152
Figure 4.10. Formaldehyde catalyzed activation of DAP under full reaction conditions.....	153
Figure 4.11. Formaldehyde activated DAP (only in the presence of formaldehyde)	154
Figure 4.12. Comparison of catalytic efficiency between glycolaldehyde and formaldehyde	155
Figure 4.13. Glycolaldehyde-catalyzed activation of DAP in the presence of NH_4Cl and Na_3PO_4	156
Figure 4.14. Glycolaldehyde catalyzed activation of DAP in the presence of $(\text{NH}_4)_2\text{HPO}_4$	157
Figure 4.15. Glycolaldehyde catalyzed activation of DAP in the presence of $\text{NH}_4\text{H}_2\text{PO}_4$	158
Figure 4.16. Comparison for activation of DAP under different conditions after 45 min (in presence of glycolaldehyde).....	159
Figure 4.17. Glycolaldehyde catalyzed activation of DAP at 50°C	161
Figure 4.18. Glycolaldehyde catalyzed activation of MAP	162
Figure 4.19. Investigation of ribose as a potential catalyst.....	164

List of Schemes

Scheme 1.1. Enamine catalysis in general	3
Scheme 1.2. Comparison of iminium catalysis and Lewis acid catalysis	4
Scheme 1.3. First example of carbonyl catalysis from Liebig	6
Scheme 1.4. Hydration and hydrolysis via transient intramolecular nucleophiles	6
Scheme 1.5. Major activation modes of carbonyl catalysis	7
Scheme 1.6. Carbonyl catalysis via a transient intramolecular nucleophile	9
Scheme 1.7. Carbonyl promoted hydration and hydrolysis reaction	10
Scheme 1.8. CO ₂ -catalyzed ester hydrolysis by Wieland	10
Scheme 1.9. Aldehyde-catalyzed hydrolysis of α -amino ester.....	11
Scheme 1.10. Carbonyl catalysis for methanolysis of α -hydroxy esters.....	11
Scheme 1.11. Carbonyl catalysis for the hydrolysis of amides	12
Scheme 1.12. Hydration of α -amino nitriles	13
Scheme 1.13. Selected examples of carbonyl compounds catalyzed hydration reaction for α -amino nitriles	13
Scheme 1.14. Aldehyde-catalyzed hydration reaction of α -amino nitriles from Beauchemin group	14
Scheme 1.15. Step-wise process for tethering strategy and selected examples	15
Scheme 1.16. <i>In situ</i> tether formation and metal catalysis combination strategy from Waser.....	16
Scheme 1.17. Catalytic tethering strategy	17
Scheme 1.18. Unusual formation of vicinal diamines via a hydroamination pathway from Knight.....	17
Scheme 1.19. Hydroamination via catalytic tether formation from Beauchemin	18
Scheme 1.20. Proposed catalytic cycle for Cope-type hydroamination via aldehyde catalysis.....	19
Scheme 1.21. Aldehydes catalyzed highly enantioselective intermolecular hydroamination	19
Scheme 1.22. Formaldehyde catalyzed diastereoselective intermolecular hydroamination	20
Scheme 1.23. Carbonyl compounds catalyzed asymmetric epoxidation	22
Scheme 1.24. Transamination pathways in Nature	23

Scheme 1.25. Comparison of the roles of carbonyl compounds in different reactions	24
Scheme 1.26. α -Alkylation of free amines from Guo	25
Scheme 1.27. Catalytic asymmetric activation of glycine esters from Guo	26
Scheme 1.28. Chiral aldehyde catalyzed asymmetric Mannich-type reaction	27
Scheme 1.29. Triple catalytic system (chiral aldehyde catalysis/Lewis acid catalysis/transition metal catalysis)	28
Scheme 1.30. Imine formation as a directing group	29
Scheme 1.31. Electrophilic activation in general	30
Scheme 1.32. Early studies regarding DMAP as a catalyst	32
Scheme 1.33. Kinetic resolution in the presence of chiral DMAP	33
Scheme 1.34. Fuji's DMAP catalyst	33
Scheme 1.35. Fu's DMAP-based catalyst	34
Scheme 1.36. Addition of alcohols to ketenes	34
Scheme 1.37. Rearrangement of <i>O</i> -acylated enolates	35
Scheme 1.38. Acylation of alcohols by anhydrides	35
Scheme 1.39. Other catalysts to realize electrophilic activation	36
Scheme 1.40. Activation of different substrates through Brønsted acid catalysis	37
Scheme 1.41. Early examples of application of chiral phosphoric acids as organocatalysts	38
Scheme 1.42. Bi-functional activation via chiral phosphoric acid	38
Scheme 1.43. Selected other chiral Brønsted acids	39
Scheme 1.44. Selected activation modes for electrophilic activation	39
Scheme 2.1. Comparison between nucleophilic catalysis and electrophilic catalysis	42
Scheme 2.2. Formaldehyde-catalyzed hydrolysis of phosphoramidate	43
Scheme 2.3. Aldehyde catalyzed formation of nitriles from amides	44
Scheme 2.4. Diastereoselective nucleophilic substitution for P-stereogenic compounds	46
Scheme 2.5. Enantioselective deprotonation for P-stereogenic compounds	46
Scheme 2.6. Catalytic asymmetric arylation	46
Scheme 2.7. A selected example for C-H activation to prepare P-chiral compounds	47
Scheme 2.8. Ir-catalyzed reaction to build P-stereogenic compounds	48
Scheme 2.9. Selected examples for useful phosphorothioates	48

Scheme 2.10. P(III)-based traditional methods towards phosphorothioates	49
Scheme 2.11. P(V)-based chiral reagents from Baran.....	50
Scheme 2.12. Selected example for the synthesis of chiral phosphorothioate oligonucleotides.....	50
Scheme 2.13. Cross-coupling to afford S-aryl phosphorothioates	51
Scheme 2.14. Stereoselective synthesis of prodrugs	52
Scheme 2.15. Hydrolysis of ATP to ADP with the release of energy.....	53
Scheme 2.16. Hydrolysis under acidic conditions	54
Scheme 2.17. Hydrolysis under basic conditions.....	54
Scheme 2.18. Deprotection of diphenylphosphinyl group to afford free amines.....	55
Scheme 2.19. Hydrolysis of imidazolide-activated nucleotides.....	55
Scheme 2.20. Mg-catalyzed hydrolysis of imidazolide-activated nucleotides	56
Scheme 2.21. Zn-catalyzed hydrolysis.....	57
Scheme 2.22. Fluoride ion mediated hydrolysis	57
Scheme 2.23. Study on the amount of NH ₄ OTs	61
Scheme 2.24. Control experiment with tertiary phosphinic amides.....	74
Scheme 2.25. A representative example for kinetic resolution	74
Scheme 2.26. A representative example of chiral-catalyst-permitted kinetic resolution	75
Scheme 2.27. General outline for kinetic resolution	76
Scheme 3.1. General structures for α -amino phosphonates and derivatives.....	82
Scheme 3.2. α -amino phosphonates and derivatives.....	83
Scheme 3.3. Structure of dehydrophos and dehydroalanine and other useful compounds	84
Scheme 3.4. α -Amino phosphonic acid as a potential inhibitor of aminopeptidase N/CD13	84
Scheme 3.5. General scheme for diaryl α -amino phosphonates as the inhibitor for serine protease.....	85
Scheme 3.6. Mono hydrolysis of diphenyl free α -amino phosphonates under acidic conditions.....	86
Scheme 3.7. Mono hydrolysis of diethyl α -amino phosphonate under acidic conditions.....	87
Scheme 3.8. Mono hydrolysis under basic conditions	87

Scheme 3.9. Mono hydrolysis with different reagents under basic conditions	88
Scheme 3.10. Mono hydrolysis of dialkyl phosphonate under basic conditions	89
Scheme 3.11. Two-step procedure to generate monoester of α -amino phosphonic acids	89
Scheme 3.12. Selected examples for mono hydrolysis of α -amino phosphonates.....	90
Scheme 3.13. Proposed carbonyl catalysis to achieve the mono hydrolysis reaction .	91
Scheme 3.14. Reaction to study the extraction order	98
Scheme 3.15. Reactions for water-soluble base	99
Scheme 3.16. Reaction for in situ derivation of the product	100
Scheme 3.17. Reactions for the study of recrystallization	101
Scheme 3.18. Amino acid vs monoester of α -amino phosphonate.....	102
Scheme 3.19. Reaction for resin exchange.....	103
Scheme 3.20. Hydrolysis under acidic conditions	109
Scheme 3.21. Attempts to prepare proposed substrate	113
Scheme 4.1. Plausible prebiotic synthesis of key prebiotic biomolecules	116
Scheme 4.2. Oró's prebiotic synthesis of adenine.....	118
Scheme 4.3. Preparation of glycolaldehyde in prebiotic manner.....	119
Scheme 4.4. Prebiotic synthesis of activated ribonucleotides from Sutherland.....	120
Scheme 4.5. Prebiotic synthesis of ribonucleotides from Benner.....	121
Scheme 4.6. Structure of histidine.....	122
Scheme 4.7. Glycolaldehyde as the precursor for imidazoles and oxazoles.....	123
Scheme 4.8. Most accepted mechanism for Formose reaction	124
Scheme 4.9. Strecker Reaction to produce α -aminonitriles	126
Scheme 4.10. Carbonyl compounds promoted the formation of amino acids from α -aminonitriles	126
Scheme 4.11. Proposed catalytic cycle for formaldehyde-catalyzed hydration of α -aminonitriles	127
Scheme 4.12. Glycolaldehyde catalyzed hydration of α -aminonitriles.....	129
Scheme 4.13. Observed intermediate of glycolaldehyde-catalyzed hydration reaction of α -aminonitriles.....	129
Scheme 4.14. Comparison of 10 and 20 mol% amount of formaldehyde and glycolaldehyde	132
Scheme 4.15. An outline for the process of glycolysis	134

Scheme 4.16. Selected examples for phosphorylated biomolecules	134
Scheme 4.17. An outline for phosphorylation process	135
Scheme 4.18. Structures of trimetaphosphate and cyclic triphosphate	136
Scheme 4.19. Generation of DAP from cyclo-trimetaphosphate	137
Scheme 4.20. Phosphorylation of aldoses with DAP	137
Scheme 4.21. Intramolecular phosphorylation of α -hydroxy aldehyde with DAP ...	138
Scheme 4.22. DAP as phosphorylating reagent to prepare phosphoenol pyruvate...	139
Scheme 4.23. Imidazole activated phosphorylation process of DAP.....	139
Scheme 4.24. DAP as the phosphorylating reagent for different building blocks	140
Scheme 4.25. Activation of DAP through glycolaldehyde catalysis	141
Scheme 4.26. Self-condensation of DAP in water at pH 6 from Krishnamurthy group	142

List of Tables

Table 2.1. Screening of catalysts for the hydrolysis of diphenylphosphinic amide 1n	59
Table 2.2. Survey of additives of the hydrolysis of diphenylphosphinic amide 1n	60
Table 2.3. Screening of possible catalysts for the hydrolysis of diphenylphosphinic amide	62
Table 2.4. Survey of additives for the hydrolysis of diphenylphosphinic amide 1a	63
Table 2.5. Solvent effects screening for the hydrolysis of diphenylphosphinic amide 1a	64
Table 2.6. Monitor the reaction time.	65
Table 2.7. Substrate scope for the catalytic hydrolysis of P(=O)-NHR reagents, including control experiments for selected substrates in the absence of <i>o</i> -phthalaldehyde	68
Table 2.8. Substrate scope for the chemoselective hydrolysis of P(=O)-NHR reagents and results of control experiments of selected examples in the absence of <i>o</i> -phthalaldehyde	70
Table 2.9. Comparison of catalytic efficiency between <i>o</i> -phthalaldehyde and formaldehyde	72
Table 2.10. Preliminary results for kinetic resolution	78
Table 3.1. Aldehyde scan for the mono hydrolysis reaction	92
Table 3.2. Mono hydrolysis with different amount of glycolaldehyde	93
Table 3.3. Base screening for the hydrolysis reaction	94
Table 3.4. Solvent effects for the mono hydrolysis reaction	95
Table 3.5. Ratio examination between solvent and water	96
Table 3.6. Re-investigate the aldehydes with optimal conditions	97
Table 3.7. Substrate scope for primary α -amino phosphonates	104
Table 3.8. Substrate scope for secondary α -amino phosphonates	106
Table 3.9. Preliminary study for kinetic resolution to prepare chiral α -amino phosphonates with chiral glyceraldehyde	110
Table 3.10. Preliminary study for kinetic resolution to prepare chiral α -amino phosphonates	111

Table 4.1. Review on aldehyde screening for model primary and secondary substrates	131
Table 4.2. Comparison of the catalytic efficiency between glycolaldehyde and formaldehyde	133

Chapter 1

Introduction

This thesis includes work in the area of organocatalysis using carbonyl compounds, which has been used to enable different chemical transformations via four major well-established activation modes. These achievements will be discussed in detail (Chapter 1). However, very limited examples were reported for electrophilic activation via carbonyl catalysis. Thus, carbonyl catalysis was further investigated to achieve electrophilic activation (Chapter 2). Additionally, little effort was made to apply carbonyl catalysis for organophosphorus compounds. Thus, one of the major activation modes was further studied to solve the challenging mono hydrolysis of α -amino phosphonates (Chapter 3). Finally, the activation mode, electrophilic activation via carbonyl catalysis was applied into the field of prebiotic chemistry. The use of DAP as a potential phosphorylation reagent via this activation mode was systematically investigated in the presence of glycolaldehyde as a catalyst (Chapter 4).

1.1 Development of organocatalysis

Organocatalysis, the application of organic molecules as catalysts, has been documented for more than a century; however this research field arguably only blossomed in the late 1990s. Nowadays, it is widely recognized that organocatalysis is an important branch of catalysis and often enantioselective synthesis alongside

enzymatic catalysis and organometallic catalysis.¹

Between 1968 and 1997, only relatively few examples of using small organic molecules as catalysts were reported to achieve highly enantioselective asymmetric reactions. Among these, the focus was largely on the individual transformation that had been studied. Unfortunately, there were no clear statements about the potential benefits of using organocatalysts, or demonstration of the new concepts to be broadly applicable.² In the late 1990s, pioneering work from Shi³, Yang⁴ and Denmark⁵ and their co-workers indicated that chiral ketones could be used as catalysts for asymmetric epoxidation of simple alkenes. Later on, Jacobsen⁶ and Corey⁷ reported the first examples of hydrogen-bonding catalysis for asymmetric Strecker reactions. The concept of short peptides was introduced by Miller and his co-workers for the asymmetric kinetic resolution of alcohols.⁸ The collection of these works demonstrated for the first time, organic molecules could be successfully utilized to solve long-standing challenging transformations, even though there was no clear definition of organocatalysis to be a research field. By 2000, the field of organocatalysis was cemented by two key papers: 1) enamine catalysis from List, Lerner and Barbas⁹ which indicated that small organic molecules such as proline^{2c,10} could potentially mimic enzymatic systems via similar general mechanisms (**Scheme 1.1**); and 2) iminium catalysis from Macmillan and co-workers which really conceptualized

¹ D. W. C. MacMillan, *Nature* **2008**, 455, 304.

² Early examples: (a) Z. G. Hajos, D. R. Parrish, *Asymmetric synthesis of optically active polycyclic organic compounds*. German patent DE 2102623 (1971). (b) U. Eder, G. R. Sauer, R. Wiechert, *Optically active 1,5-indanone and 1,6-naphthalenedione derivatives*. German patent DE 2014757 (1971). (c) Z. G. Hajos, D. R. Parrish, *J. Org. Chem.* **1974**, 39, 1615.

³ Y. Tu, Z.-X. Wang, Y. Shi, *J. Am. Chem. Soc.* **1996**, 118, 9806.

⁴ D. Yang, Y.-C. Yip, M.-W. Tang, M.-K. Wong, J.-H. Zheng, K.-K. Cheung, *J. Am. Chem. Soc.* **1996**, 118, 491.

⁵ S. E. Denmark, Z. Wu, C. M. Crudden, H. Matsuhashi, *J. Org. Chem.* **1997**, 62, 8288.

⁶ M. Sigman, E. N. Jacobsen, *J. Am. Chem. Soc.* **1998**, 120, 4901.

⁷ E. J. Corey, M. J. Grogan, *Org. Lett.* **1999**, 1, 157.

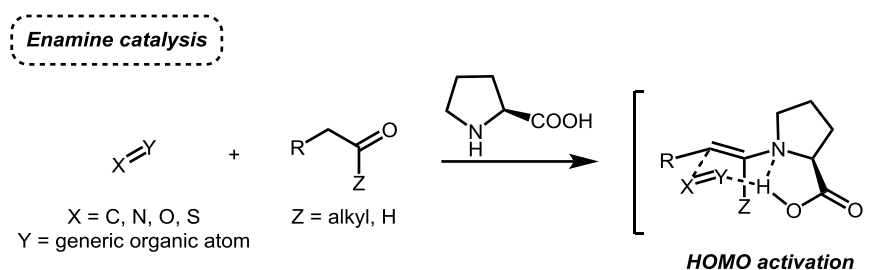
⁸ S. J. Miller, G. T. Copeland, N. Papaioannou, T. E. Horstmann, E. M. Ruel, *J. Am. Chem. Soc.* **1998**, 120, 1629.

⁹ B. List, R. A. Lerner, C. F. Barbas, *J. Am. Chem. Soc.* **2000**, 122, 2395.

¹⁰ Early example: U. Eder, G. Sauer, R. Wiechert, *Angew. Chem. Int. Ed.* **1971**, 10, 496.

organocatalysis¹¹ (**Scheme 1.2**).

The important work from List and co-workers⁹ demonstrated the first example of the use of a non-metallic small molecule, proline which is also inexpensive, readily accessible, water soluble and nontoxic, to realize the intermolecular Aldol reaction with moderate to good yields and enantioselectivities. The enantioselectivities were achieved relying on the Zimmerman-Traxler model favoring *Re* face attack with L-Proline (**Scheme 1.1**). This enamine catalysis was claimed to be bi-functional catalysis, where on one hand, the nitrogen of the proline could react with one substrate to form the enamine intermediate; while on the other hand the carboxylic acid could interact with the electrophile *via* hydrogen bonding or other electrostatic interactions.¹ After this inspiring work, enamine catalysis has been widely developed for enantioselective α -carbonyl functionalization and many different transformations have been achieved such as intramolecular α -alkylation, Mannich reaction, Michael addition, α -amination/oxygenation/halogenation/sulphenylation, *etc.*¹²



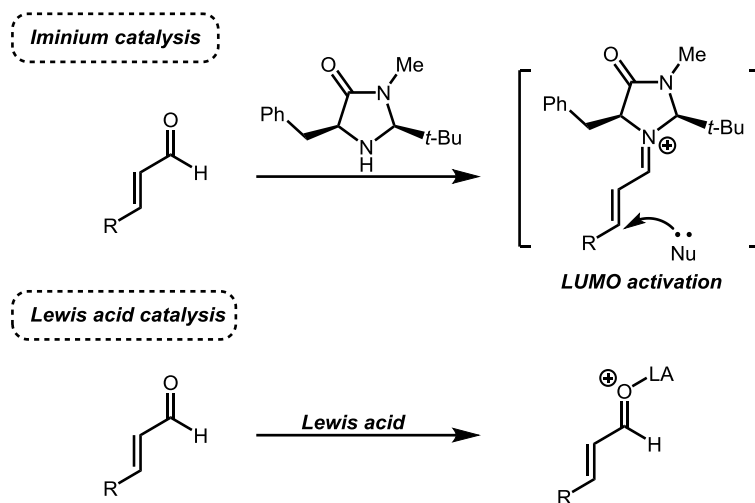
Scheme 1.1. Enamine catalysis in general

In 2000, MacMillan and co-workers reported a new strategy to apply a chiral amine as an organocatalyst for enantioselective Diels-Alder reactions.¹¹ This iminium catalysis was first designed and introduced for asymmetric organic transformations, which were previously promoted by Lewis acids. The chiral amine as the catalyst reacted reversibly

¹¹ K. A. Ahrendt, C. J. Borths, D. W. C. MacMillan, *J. Am. Chem. Soc.* **2000**, *122*, 4243.

¹² For a review on enamine catalysis, please see: S. Mukherjee, J. W. Yang, S. Hoffmann, B. List, *Chem. Rev.* **2007**, *107*, 5471.

with the α,β -unsaturated aldehydes to form the iminium. This activation mode of LUMO lowering has led to various chemical transformations, for instance conjugate Friedel-Crafts reaction, ketone Diels-Alder reaction, Mukaiyama-Michael reaction and conjugate hydride reduction/amination/oxygenation/sulphenylation, *etc.*¹³



Scheme 1.2. Comparison of iminium catalysis and Lewis acid catalysis

After these two groundbreaking examples from List and MacMillan, the field of organocatalysis exploded and various chemical transformations including enantioselective examples were achieved.

Organometallic catalysis dominated asymmetric catalysis for a long time, and of course greatly contributed to the development of this field. However, nowadays, organocatalysis is emerging as a strategy with the potential of being less toxic, less polluting and more economically feasible than organometallic catalysis in some cases. Organocatalysis has been used as a versatile synthetic method to accelerate different types of difficult reactions. These achievements usually rely on the reversible formation of covalent bonds or non-covalent interactions to realize efficient activation and stereocontrol.¹⁴ This included different types of organocatalysis, for example, the use

¹³ G. Lelais, D. W. C. MacMillan, *Aldrichim. Acta* **2006**, 39, 79.

¹⁴ B.-J. Li, R. D. Simard, A. M. Beauchemin, *Chem. Commun.* **2017**, 53, 8667.

of amines, iminiums and nitrogen-heterocyclic-carbenes, chiral phosphoric acids as catalysts, supramolecular organocatalysts, immobilized organocatalysts, photo-organocatalysts, *etc.*¹⁵ In particular, in this context, carbonyl compounds could be used not only as reagents to form activated nucleophiles or electrophiles, via enamine catalysis and LUMO lowering through unsaturated iminium ions as discussed above (**Scheme 1.1** and **Scheme 1.2**), but as highly efficient organocatalysts, to achieve different types of reactions based on a variety of activation modes.^{16,17} Asymmetric variants of other activation modes also rapidly emerged (e.g. acyl anion formation using chiral carbene organocatalysts).¹⁸ The following section will focus on recent developments of (asymmetric) carbonyl catalysis according to different activation modes.

1.2. Carbonyl Catalysis

Carbonyl catalysis is an essential branch of organocatalysis, which can be traced back to 1860 when Liebig showed that cyanogen could only be hydrated in the presence of acetaldehyde as a catalyst¹⁹ (**Scheme 1.3**).

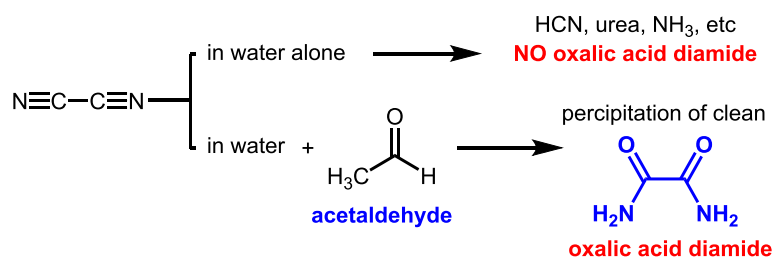
¹⁵ (a) V. D. G. Oliveira, M. F. D. C. Cardoso, L. D. S. M. Forezi, *Catalysts* **2018**, *8*, 605. For selected books: (b) A. Berkessel, H. Gröger, *Asymmetric Organocatalysis: From Biomimetic Concepts to Applications in Asymmetric Synthesis*, Wiley-VCH, Weinheim, **2005**. (c) B. List, *Asymmetric Organocatalysis*, Springer-Verlag, Berlin, Heidelberg, **2009**. (d) R. R. Torres, *Stereoselective Organocatalysis: Bond Formation Methodologies and Activation Modes*, John Wiley & Sons, Inc., Hoboken, New Jersey, **2013**. (e) Peter I. Dalko, *Comprehensive Enantioselective Organocatalysis: Catalysts, Reactions, and Applications*, Wiley-VCH, Weinheim, **2013**; For selected recent reviews: (f) C. M. Volla, I. Atodiresei, M. Rueping, *Chem. Rev.* **2014**, *114*, 2390. (g) B. S. Donslund, T. K. Johansen, P. H. Poulsen, K. S. Halskov, K. A. Jørgensen, *Angew. Chem. Int. Ed.* **2015**, *54*, 13860. (h) T. James, M. van Gemmeren, B. List, *Chem. Rev.* **2015**, *115*, 9388. (i) Y. Qin, L. Zhu, S. Luo, *Chem. Rev.* **2017**, *117*, 9433. (j) F. Vetica, P. Chauhan, S. Dochain, D. Enders, *Chem. Soc. Rev.* **2017**, *46*, 1661. (k) G. Zhan, W. Du, Y. C. Chen, *Chem. Soc. Rev.* **2017**, *46*, 1675. (l) M. Silvi, P. Melchiorre, *Nature* **2018**, *554*, 41.

¹⁶ For carbonyl catalysis review: (a) R. Pascal, *Eur. J. Org. Chem.* **2003**, 1813. (b) K. L. Tan, *ACS Catal.* **2011**, *1*, 877. (c) M. J. O'Donnell, *Acc. Chem. Res.* **2004**, *37*, 506. (d) H. Vogt, S. Brase, *Org. Biomol. Chem.* **2007**, *5*, 406.

¹⁷ B.-J. Li, C. El-Nachef, A. M. Beauchemin, *Chem. Commun.* **2017**, *53*, 13192.

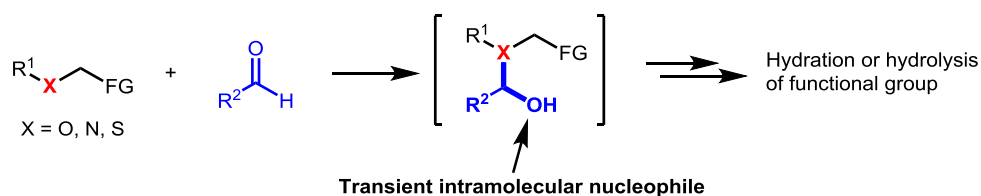
¹⁸ See a book about carbene chemistry: *N-Heterocyclic Carbenes in Synthesis*, S. P. Nolan, (Ed.), Wiley-VCH, Weinheim, **2006**.

¹⁹ J. von Liebig, *Justus Liebigs Ann. Chem.* **1860**, *113*, 246.



Scheme 1.3. First example of carbonyl catalysis from Liebig

It took *ca.* 100 years to realize that aldehydes could be applied to facilitate hydration and hydrolysis reactions.²⁰ These early examples utilized the ability of carbonyl compounds to reversibly form hemiacetals and hemiaminals to introduce a transient intramolecular nucleophile (**Scheme 1.4**). This could accelerate the reactions significantly to realize difficult hydration and hydrolysis reactions under mild conditions. This will be discussed in detail in Section 1.2.1.



Scheme 1.4. Hydration and hydrolysis via transient intramolecular nucleophiles

Even through the beginning of carbonyl catalysis could be dated back to 1860, steady growth only occurred over the past two decades. For example, aldehydes were found to be the catalysts in different types of reactions, such as early contributions to use biomimetic pyridoxal cyclophanes for asymmetric aldol reactions,²¹ Baylis-Hillman reaction when aryl aldehydes were used,²² photo-organocatalysis of atom-transfer

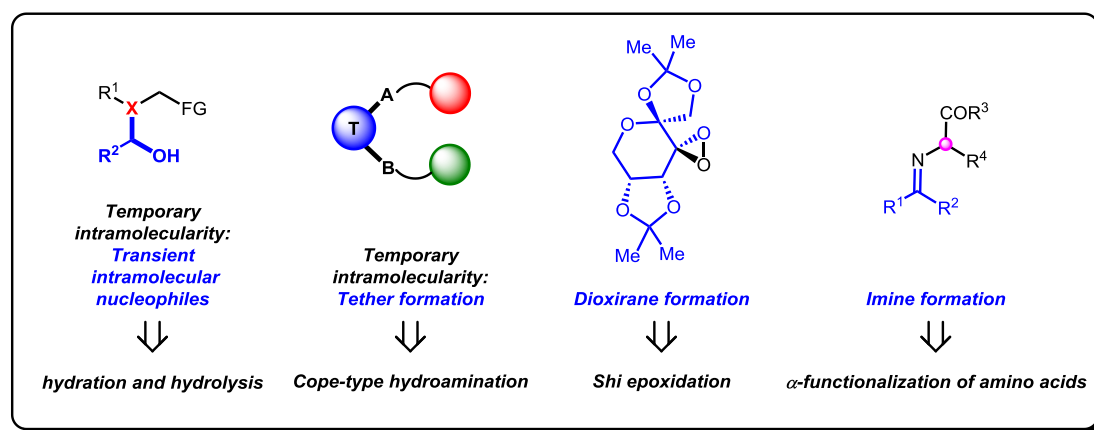
²⁰ For early examples: (a) V. T. Wieland, F. Jaenicke, *Justus Liebigs Ann. Chem.* **1956**, 599, 125. (b) V. T. Wieland, R. Lambert, H. U. Lang, G. Schramm, *Justus Liebigs Ann. Chem.* **1956**, 597, 181. (c) W. P. Jencks and M. Gilchrist, *J. Am. Chem. Soc.* **1964**, 86, 1410. (d) B. Capon, R. Capon, *Chem. Commun.* **1965**, 502. (e) R. W. Hay, L. Main, *Aust. J. Chem.* **1968**, 21, 155. For aldehyde catalysis of the formose reaction, see: (f) R. Breslow, *Tetrahedron Lett.* **1959**, 1, 22.

²¹ (a) H. Kuzuhara, N. Watanabe, M. Ando, *J. Chem. Soc. Chem. Commun.* **1987**, 95. (b) J. T. Koh, L. Delaude, R. Breslow *J. Am. Chem. Soc.* **1994**, 116, 11234.

²² K. E. Price, S. J. Broadwater, B. J. Walker, D. T. McQuade, *J. Org. Chem.* **2005**, 70, 3980.

radical addition to alkenes via energy-transfer pathway,²³ and dehydrative *N*-alkylation of amines and amides with alcohols,²⁴ etc.

More specifically, carbonyl compounds were extensively utilized 1) to facilitate hydration and hydrolysis reactions; 2) to act as a tethering reagent especially in the context of induced temporary intramolecularity; 3) as chiral catalysts for Shi asymmetric alkene epoxidation; and 4) for α -functionalization of amino acids and derivatives. In this context, reliable methodologies to prepare chiral molecules in a highly enantioselective manner were also discovered. This rapid development could be attributed to the discovery of different general and reliable activation modes of carbonyl catalysis. Activation modes in carbonyl catalysis including the formation of transient intramolecular nucleophiles, tether formation to induce temporary intramolecularity, dioxirane formation, and iminium/imine formation, will be discussed accordingly (**Scheme 1.5**). The application of carbonyl catalysis in the field of prebiotic chemistry will be discussed in detail separately in Chapter 4.



Scheme 1.5. Major activation modes of carbonyl catalysis

²³ E. Arceo, E. Montroni, P. Melchiorre, *Angew. Chem. Int. Ed.* **2014**, 53, 12064.

²⁴ Q. Xu, Q. Li, X. Zhu, J. Chen, *Adv. Synth. Catal.* **2013**, 355, 73.

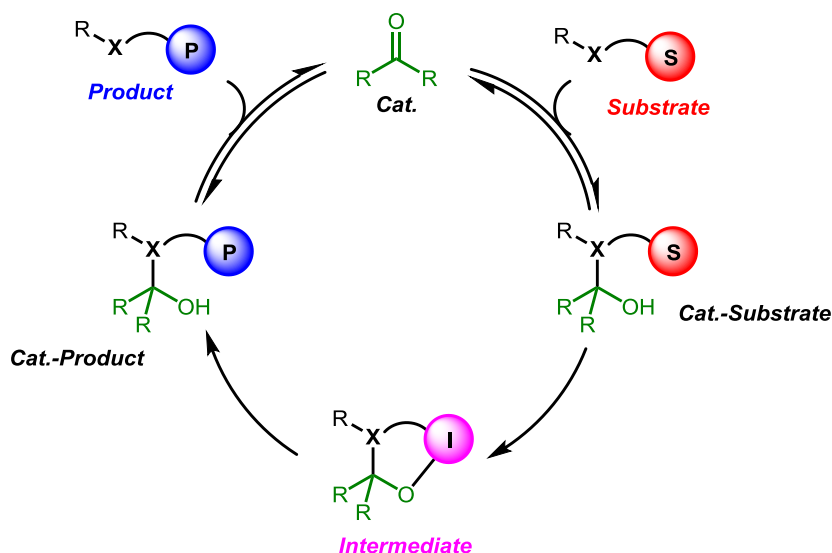
1.2.1 Inducing temporary intramolecularity

In general, most organic chemistry reactions could be classified as intermolecular reactions; one of the key aspects to achieve this type of reactions is to overcome the overall negative entropy change in Gibbs free energy ($\Delta G = \Delta H - T\Delta S$). In Nature, enzymes are found to perform a favorable binding process to pre-arrange substrates in a reactive orientation, which for normal intermolecular reactions costs a large entropic penalty; however, enzymes minimize this entropic penalty (e.g. by associative interactions with one or both reagents) to facilitate the subsequent step, which results in the overall rate acceleration of the reaction.^{16b} This strategy, induced temporary intramolecularity, by converting a bimolecular step into an uni-molecular step was known to accelerate the reaction on the order of 10^4 to 10^8 at 1 M^{16b,17}.

Inspired by enzymatic systems, the application of reversible covalent bonding to induce temporary intramolecularity was extended into organocatalysis. This activation mode pays the entropic penalty to bind two molecules together, therefore in theory this could be used to activate any bi-molecular step^{16b}. Because of the ability of carbonyl compounds to form hemiacetals and hemiaminals reversibly, carbonyl compounds were therefore developed as catalysts to enable challenging reactions under mild conditions. In this context, carbonyl catalysis was exploited to induce temporary intramolecularity from two major pathways: 1) *in situ* formation of transient intramolecular nucleophiles; and 2) serving as covalent tethering reagents to combine different components together, therefore converting bi-molecular reactions into uni-molecular steps to increase the reactivity and selectivity.

Intramolecular nucleophiles: *in situ* formation of transient intramolecular nucleophiles

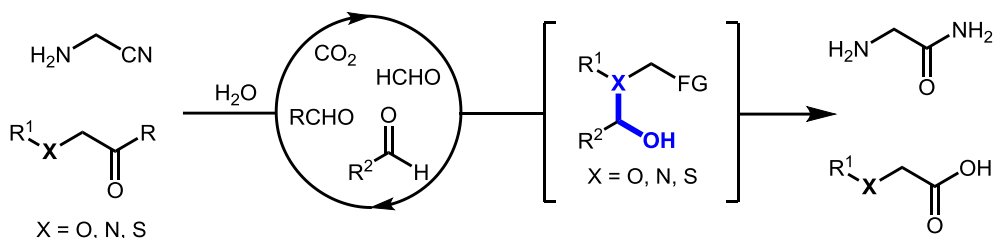
One aspect of inducing temporary intramolecularity where carbonyl catalysis was proficient was the hydrolysis and hydration reactions through the formation of hemiacetals and hemiaminals. This methodology often required properly functionalized reagents that could incorporate a transient oxygen atom as an intramolecular nucleophile. As demonstrated in **Scheme 1.6**, the carbonyl catalyst and the substrate were bound together to form the 'cat.-substrate' adduct reversibly. Therefore, in the adduct, the newly-formed intramolecular nucleophile can be perfectly positioned to activate the substrate to undergo an intramolecular reaction, followed by the subsequent reaction to release the desired products. As a result, a significant rate acceleration can be achieved.



Scheme 1.6. Carbonyl catalysis via a transient intramolecular nucleophile

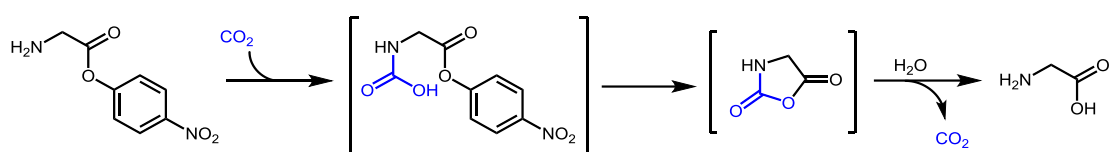
This activation mode incorporated by carbonyl catalysis could allow faster hydrations and hydrolysis with different substrates types (**Scheme 1.7**). The nucleophilic **X** component on the substrates is normally an amine or thiol which have a higher tendency

to react with the carbonyl catalysts to form the corresponding hemiaminals and hemithioacetals. In some cases, alcohols were also incorporated to form hemiacetals for hydrolysis reactions²⁵.



Scheme 1.7. Carbonyl promoted hydration and hydrolysis reaction

In 1956, Wieland and co-workers demonstrated the hydrolysis of a glycine ester with the help of bicarbonate^{20a,b}. In their proposed mechanism, a carbamic acid was produced from the free amine and carbon dioxide, then this intermediate went through the cyclization to form Leuchs anhydride, then hydrolysis of the anhydride would form the acid product and release one molecule of carbon dioxide, thereby completing the catalytic cycle. As shown in the **Scheme 1.8**, a temporary intramolecular nucleophile was formed to assist the difficult hydrolysis of an ester group, and carbon dioxide was used and reproduced in this reaction by serving as a catalyst.

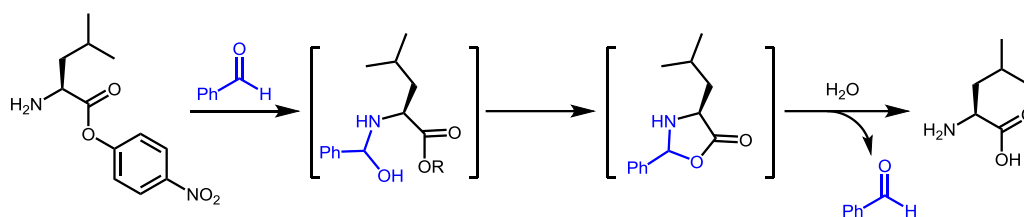


Scheme 1.8. CO₂-catalyzed ester hydrolysis from Wieland

Following this seminal report, there were several examples using aromatic aldehydes to accelerate the hydrolysis of *p*-nitrophenyl esters of amino acids via similar mechanism^{20d,e} (**Scheme 1.9**). First, the amino group would attack the aromatic aldehyde to form the intramolecular nucleophile, which would cyclize to form the

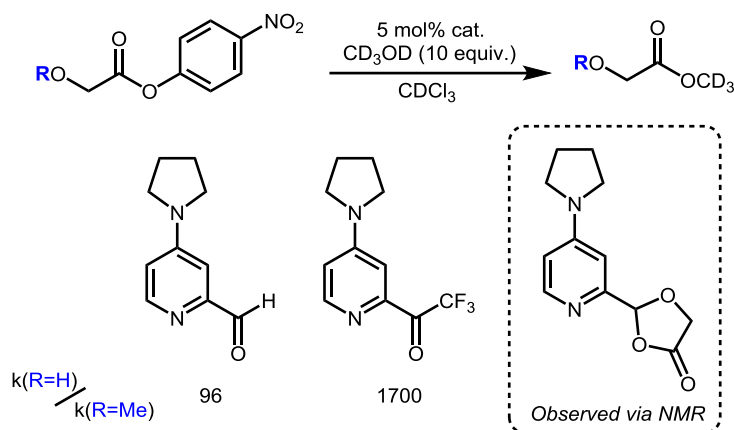
²⁵ (a) W. P. Jencks, *Prog. Phys. Org. Chem.* **1964**, 2, 63. (b) P. C. R. Le Henaff, *Seances Acad. Sci. C.* **1966**, 262, 1667.

oxazolidinone. Upon hydrolysis, an amino acid would be formed as the product.



Scheme 1.9. Aldehyde-catalyzed hydrolysis of α -amino ester

Decades later, the use of temporary intramolecularity via carbonyl catalysis has also been extended to the methanolysis of α -hydroxy esters.²⁶ It was discovered by Sammakia and co-workers that, compared to α -methoxy esters, α -hydroxy esters would undergo methanolysis significantly faster in the presence of aldehydes and ketones and in support of this proposal (as highlighted in **Scheme 1.10**) a key intermediate was observed during the reaction.

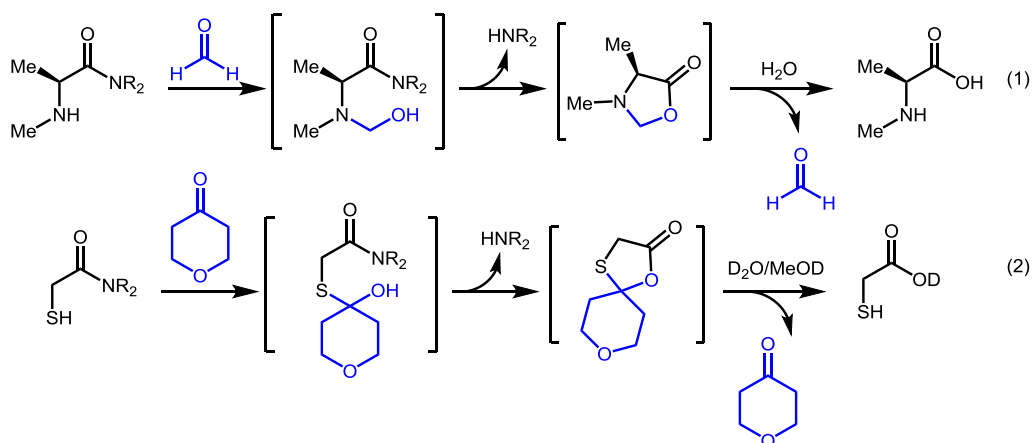


Scheme 1.10. Carbonyl catalysis for methanolysis of α -hydroxy esters

The hydrolysis of amide bonds under mild conditions, which was a long-standing problem in organic chemistry has attracted continuous attention. In Nature, proteases that enable the sequence-specific hydrolysis of peptides have evolved to induce a significant rate acceleration. From the aspect of synthetic chemistry, to hydrolyze the

²⁶ (a) T. Sammakia, T. B. Hurley, *J. Am. Chem. Soc.* **1996**, *118*, 8967. (b) T. Sammakia, T. B. Hurley, *J. Org. Chem.* **1999**, *64*, 4652. (c) T. Sammakia, T. B. Hurley, *J. Org. Chem.* **2000**, *65*, 974.

amides, strong acidic or basic conditions upon heating were normally required.²⁷ However, employing temporary intramolecularity from carbonyl catalysis to provide an intramolecular nucleophile was proposed to solve the problem. Commeyras and co-workers reported that in the presence of formaldehyde, α -amino amides could form hemiaminals by reacting with formaldehyde, then the intramolecular nucleophiles underwent cyclization to form an oxazolidinone intermediate. Eventually, the hydrolysis of this intermediate would produce the α -amino acids as the products^{28a} (**Scheme 1.11**, equation 1). Later on, this strategy was further applied by Seto and co-workers to perform the hydrolysis of α -thioamides. They figured out that in the presence of ketones, the rate of hydrolysis of α -thioamides was ~ 1500 times faster^{28b} (**Scheme 1.11**, equation 2).



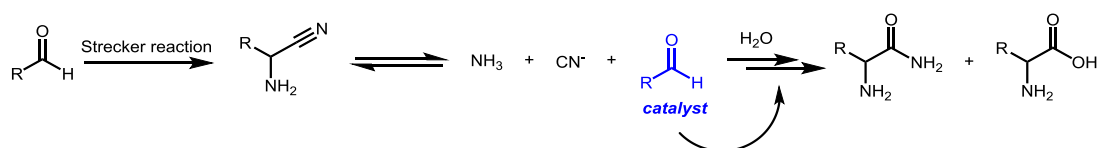
Scheme 1.11. Carbonyl catalysis for the hydrolysis of amides

Additionally, the hydration of α -amino nitriles, which are readily accessible from the Strecker reaction afford natural and unnatural amino amide and acid derivatives.^{16b} This hydration reaction has important synthetic applications. However, this transformation needs highly acidic or basic conditions with increased temperature, and as a result, it

²⁷ C. O'Connor, *Q. Rev. Chem. Soc.* **1970**, *24*, 553.

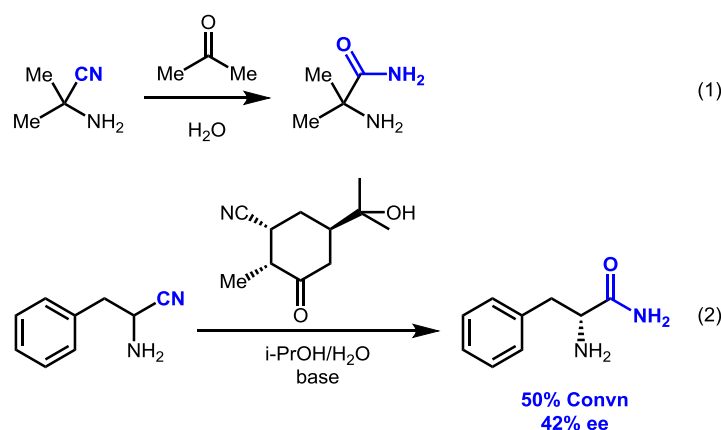
²⁸ (a) R. Pascal, M. Lasperas, J. Taillades, A. Commeyras, *New J. Chem.* **1987**, *11*, 235. For α -thioamide hydrolysis, see: (b) M. Ghosh, J. L. Conroy, C. T. Seto, *Angew. Chem. Int. Ed.* **1999**, *38*, 514.

was possible to over-hydrolyze the substance directly to carboxylic acids and cause the formation of polymeric side products.²⁹ In 1970's, Commeyras and co-workers discovered a pathway to afford amino amides and acids. They observed compared to unfunctionalized nitriles, α -amino nitriles were found to react faster towards hydration in the presence of aldehydes and ketones which were generated from the decomposition of α -amino nitriles³⁰ (**Scheme 1.12**).



Scheme 1.12. Hydration of α -amino nitriles

Therefore, adding ketones as catalysts could improve the efficiency of the hydrolysis process. This was validated by the addition of acetone to the reaction that demonstrated the dramatically increased yields and reduced reaction time, however acetone and base were used in large excess³¹ (**Scheme 1.13**, equation 1). Moreover, an enantiopure ketone was used for kinetic resolution of α -amino nitriles, but as a result only modest enantioselectivity was produced (**Scheme 1.13**, equation 2).



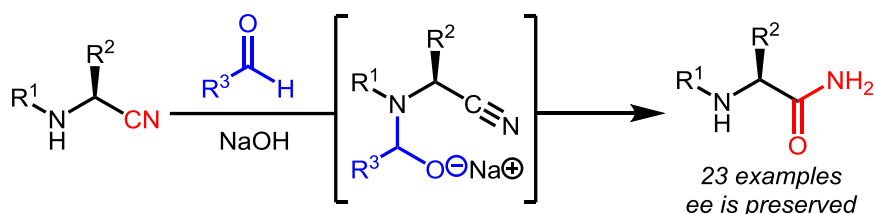
Scheme 1.13. Selected examples of carbonyl compounds catalyzed hydration reaction for α -amino nitriles

²⁹ J. N. Moorthy, N. Singhal, *J. Org. Chem.* **2005**, *70*, 1926.

³⁰ R. Pascal, J. Taillades, A. Commeyras, *Bull. Soc. Chim. Fr. II* **1978**, 3-4, 177.

³¹ (a) R. Pascal, J. Taillades, A. Commeyras, *Tetrahedron* **1978**, *34*, 2275. (b) R. Pascal, J. Taillades, A. Commeyras, *Tetrahedron* **1980**, *36*, 2999. (c) R. Sola, J. Taillades, J. Brigidou, A. Commeyras, *New J. Chem.* **1989**, *13*, 881.

In 2016, the Beauchemin group continued with carbonyl catalysis and developed a directed hydration of α -amino nitriles with various primary and secondary substrates³² (Scheme 1.14). It was proposed to operate through temporary intramolecularity, and built on the seminal contributions of Commeyras group in this field.^{28a,30,31} The high catalytic activity observed with formaldehyde and broad scopes were useful for the syntheses of unnatural amino acids.¹⁷ Importantly, they also observed no erosion in enantiopurity under the reaction conditions. This work demonstrated a truly catalytic protocol for hydration of α -amino nitriles via temporary intramolecularity under mild conditions and also explored catalytic activity of simple carbohydrates.



Scheme 1.14. Aldehyde-catalyzed hydration reaction of α -amino nitriles from Beauchemin group

Tethering reagents: formation of mixed aminal tethers

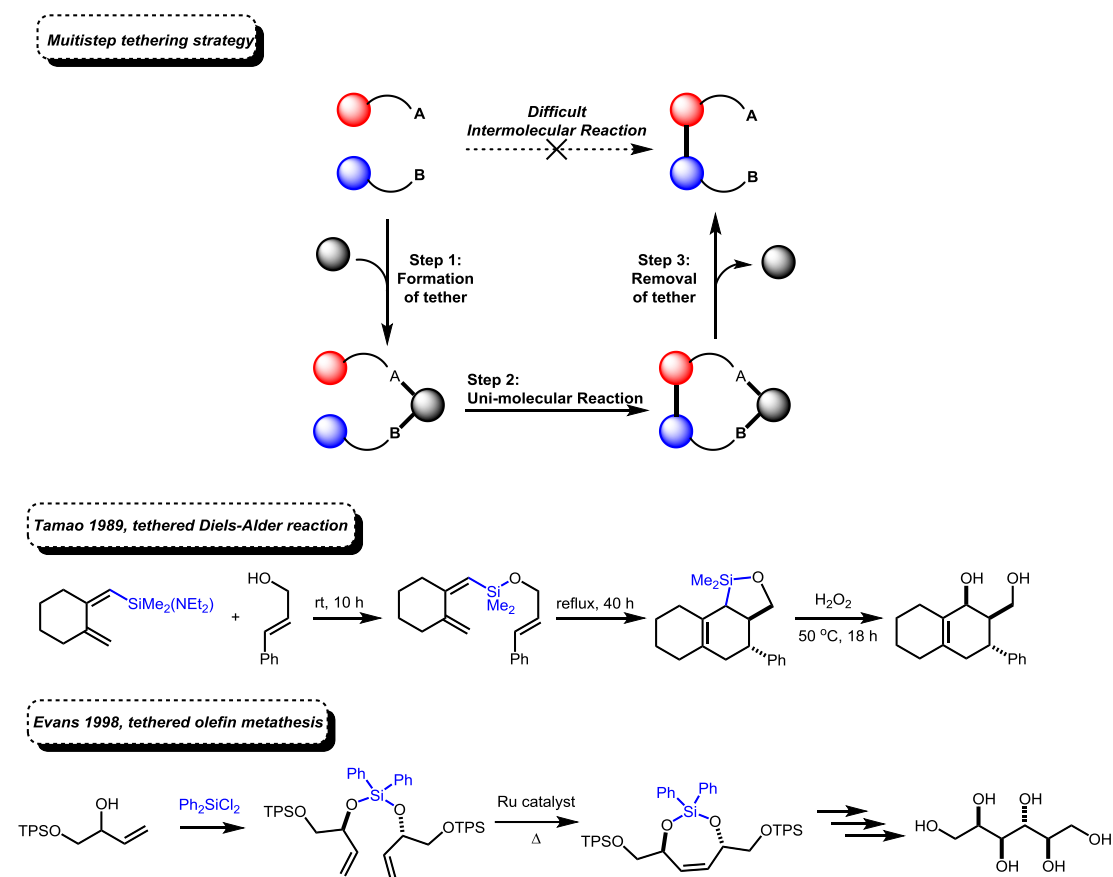
Carbonyl catalysis has also demonstrated great catalytic efficiency as a tethering reagent to induce temporary intramolecularity, therefore converting bi-molecular steps into uni-molecular steps for enhanced reactivity. This strategy was successfully applied for difficult Cope-type hydroamination reactions.

Generally, employing covalent tethering reagents has been used for a long time, for different reactions for example, intermolecular Diels-Alder reactions,³³ olefin and

³² S. Chitale, J. S. Derasp, B. Hussain, K. Tanveer, A. M. Beauchemin, *Chem Commun.* **2016**, 52, 13147.

³³ Selected examples: (a) K. Tamao, K. Kobayashi, Y. Ito, *J. Am. Chem. Soc.* **1989**, *111*, 6478. (b) S. M. Sieburth, L. Fensterbank, *J. Org. Chem.* **1992**, *57*, 5279. (c) G. Stork, T. Y. Chan, G. A. Breault, *J. Am. Chem. Soc.* **1992**, *114*, 7578. (d) R. A. Batey, A. N. Thadani, A. J. Lough, *J. Am. Chem. Soc.* **1999**, *121*, 450. (e) G. Stork, T. Y. Chan, *J. Am. Chem. Soc.* **1995**, *117*, 6595. (f) M. S. Abaee, D. E. Ward, *Org. Lett.* **2000**, *2*, 3937.

enyne metathesis,³⁴ metal-catalyzed reactions,³⁵ and radical reactions³⁶, *etc.* It also achieved impressive progress for enhancing regio-, chemo- and stereoselectivity in various transformations. However, previous methods suffered from additional steps to first install the tethering reagent and then remove the tether, which limited the efficiency of this strategy.³⁷ Selected examples are shown in **Scheme 1.15**.



Scheme 1.15. Stepwise process for tethering strategy and selected examples

In situ tether formation and metal catalysis combination has also been developed trying

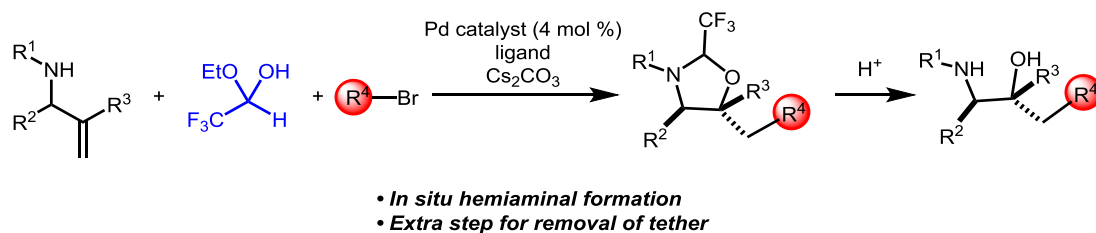
³⁴ Selected examples: (a) D. J. O'Leary, S. J. Miller, R. H. Grubbs, *Tetrahedron Lett.* **1998**, *39*, 1689. (b) V. S. Murthy, P. A. Evans, *J. Org. Chem.* **1998**, *63*, 6768. (c) P. A. Evans, J. Cui, G. P. Buffone, *Angew. Chem. Int. Ed.* **2003**, *42*, 1734. (d) K. T. Sprott, M. D. McReynolds, P. R. Hanson, *Org. Lett.* **2001**, *3*, 3939.

³⁵ One of the first examples with a stoichiometric tether in a total synthesis: A. Mayasundari, D. G. J. Young, *Tetrahedron Lett.* **2001**, *42*, 203.

³⁶ Selected examples: (a) H. Nishiyama, T. Kitajima, M. Matsumoto, K. Itoh, *J. Org. Chem.* **1984**, *49*, 2298. (b) G. Stork, M. Kahn, *J. Am. Chem. Soc.* **1985**, *107*, 500. (c) A. Kurek-Tyrlik, J. Wicha, G. Snatzke, *Tetrahedron Lett.* **1988**, *29*, 4001. (d) A. Kurek-Tyrlik, J. Wicha, A. Zarecki, G. Snatzke, *J. Org. Chem.* **1990**, *31*, 4445. (e) R. A. Batey, D. V. Smil, *Angew. Chem. Int. Ed.* **1999**, *38*, 1798.

³⁷ (a) R. Amoroso, G. Cardillo, C. Tomasini, *Heterocycles* **1992**, *34*, 349. For early reviews, see: (b) F. Diederich, P. J. Stang, *Templated Organic Synthesis*, Wiley-VCH, Chichester, UK, **2000**. (c) M. Bols, T. Skrydstrup, *Chem. Rev.* **1995**, *95*, 1253; (d) L. Fensterbank, M. Malacria, S. M. Sieburth, *Synthesis* **1997**, 813. (e) D. R. Gauthier Jr., K. S. Zandi, K. J. Shea, *Tetrahedron* **1998**, *54*, 2289.

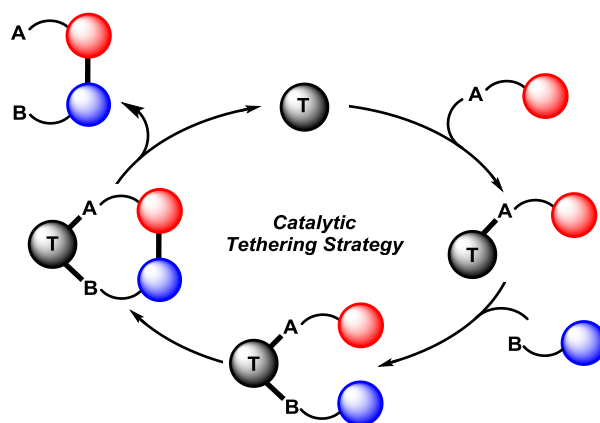
to solve the problem. In 2015, Waser and co-workers published the combination of palladium-catalysis and a tethering strategy to prepare vicinal amino alcohols via carboc-etherification. This work showed that it was extremely important to use the hemiacetal of trifluoroacetaldehyde, which is highly electron deficient for *in situ* formation of the hemiaminal in order to achieve high yields, and regio- and diastereoselectivity. This is a successful example of the use of tethering strategy beyond the world of organocatalysis. The reaction could be performed with broad scope and various functional groups were well-tolerated³⁸ (**Scheme 1.16**). However, a stoichiometric amount of trifluoroacetaldehyde was used in this reaction, which also required a subsequent removal step for the tether to reach the final products.



Scheme 1.16. *In situ* tether formation and metal catalysis combination strategy from Waser

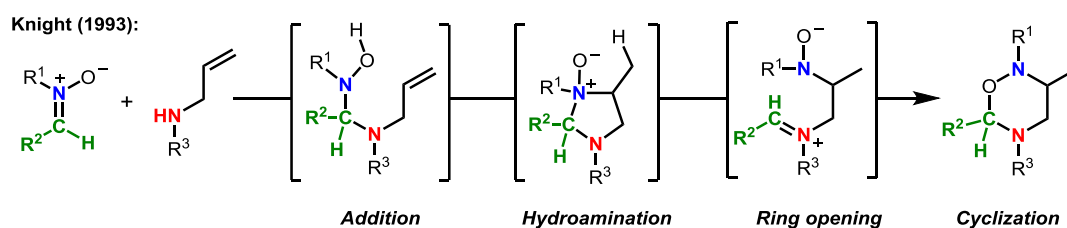
It is surprising that catalytic variants of tethering reaction are rare (**Scheme 1.17**), especially considering the large body of literature on temporary tethers. The Beauchemin group noticed that carbonyl compounds were able to form aminals and acetals reversibly even under mild conditions, which suggested carbonyl catalysis could be able to form transient tethers capable of transferring bimolecular reactions to unimolecular reactions.

³⁸ (a) U. Orcel, J. Waser, *Angew. Chem. Int. Ed.* **2015**, *54*, 5250. For following development and review, please see: (b) U. Orcel, J. Waser, *Angew. Chem. Int. Ed.* **2016**, *55*, 12881. (c) U. Orcel, J. Waser, *Chem. Sci.* **2017**, *8*, 32.



Scheme 1.17. Catalytic tethering strategy

During the exploration for possible tethering systems, the pioneering work of Knight was found to be an attractive starting point.³⁹ The Knight group observed the unusual formation of vicinal diamines via a hydroamination pathway (**Scheme 1.18**). This reaction started from nitrones, going through subsequent addition of amines, hydroamination, ring-opening and cyclization to give vicinal diamines as the products. In this reaction, aldehydes were used stoichiometrically to provide nitrones as the substrates and eventually ended up in the products. However, the formation of mixed amins as the intermediates, by facilitating ring opening, made it highly possible to achieve catalytic reactivity under a similar reaction manifold.

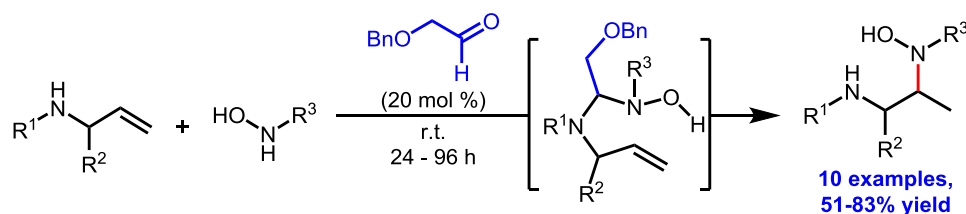


Scheme 1.18. Unusual formation of vicinal diamines via a hydroamination pathway from Knight

In 2011, the Beauchemin group reported an aldehyde-catalyzed Cope-type

³⁹ (a) M. B. Gravestock, D. W. Knight, S. R. Thornton, *J. Chem. Soc. Chem. Commun.* **1993**, 169. (b) K. E. Bell, M. P. Coogan, M. B. Gravestock, D. W. Knight, S. R. Thornton, *Tetrahedron Lett.* **1997**, 38, 8545. (c) M. B. Gravestock, D. W. Knight, K. M. Abdul Malik, S. R. Thornton, *J. Chem. Soc. Perkin Trans. 1*, **2000**, 3292.

hydroamination of allylic amines via *in situ* temporary intramolecularity⁴⁰ (**Scheme 1.19**). Aldehydes would first pre-associate the reagents, and the formation of the aminal temporary tethers depending on the nature of the nitron precursors. This temporary intramolecularity was induced by destabilized aldehydes and allowed the reactions to occur under remarkably mild conditions. As a result, the challenging intermolecular Cope-type hydroamination was reported under catalytic metal-free conditions. However, it was also noticed that this catalytic reaction could only take place with terminal allylic amines. Additionally, steric hindrance of the reagents also limited the synthetic application of this aldehyde-catalyzed hydroamination reaction.

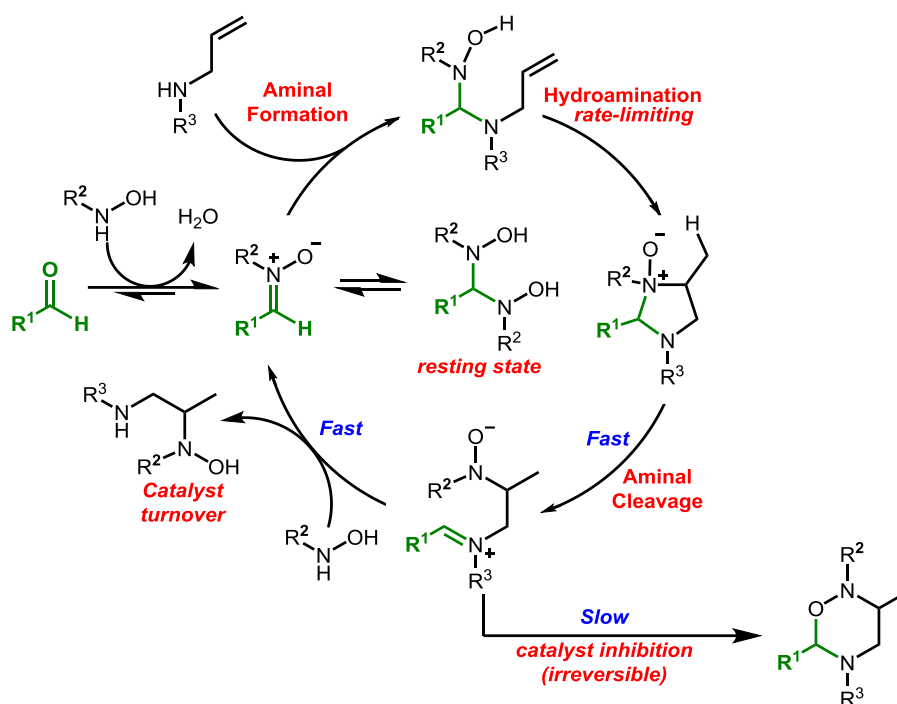


Scheme 1.19. Hydroamination via catalytic tether formation from Beauchemin

Therefore, mechanistic studies were also carefully performed and a more accurate catalytic cycle for aldehyde-catalyzed Cope-type hydroamination was proposed⁴¹ (**Scheme 1.20**). The hydroamination step was found to be the rate-limiting step and a catalyst-inhibition pathway was also identified. The mechanistic study also indicated that the simpler catalysts, for example formaldehyde, are more efficient because of the increased ability to form the transient mixed aminal tethers and also to favor the subsequent steps.

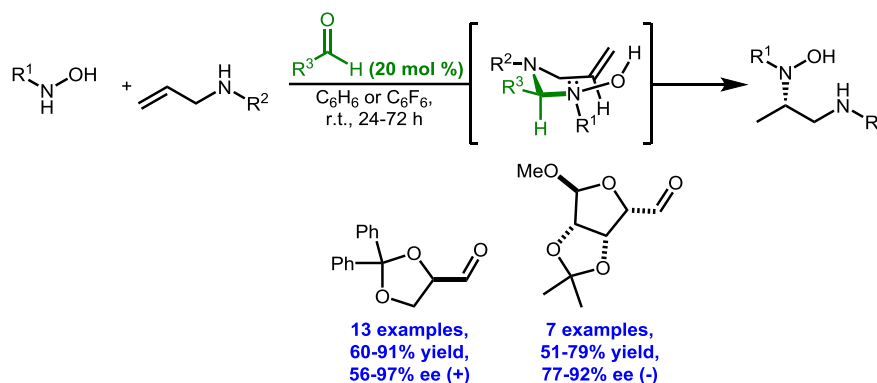
⁴⁰ M. J. MacDonald, D. J. Schipper, P. J. Ng, J. Moran, A. M. Beauchemin, *J. Am. Chem. Soc.* **2011**, *133*, 20100.

⁴¹ N. Guimond, M. J. MacDonald, V. Lemieux, A. M. Beauchemin, *J. Am. Chem. Soc.* **2012**, *134*, 16571.



Scheme 1.20. Proposed catalytic cycle for Cope-type hydroamination via aldehyde catalysis

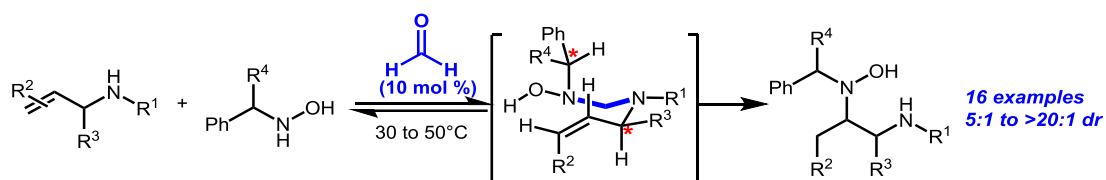
Gratifyingly, this strategy was also successfully extended to achieve high enantioselectivity with the identification of two pseudo-enantiomeric catalysts⁴² (**Scheme 1.21**). These two chiral aldehydes are readily prepared from commercially available precursors. These catalysts led to the highest enantioselectivity for a Cope-type hydroamination at that time. This showed that inducing asymmetry only through temporary intramolecularity can be realized by chiral aldehydes as the catalysts.



Scheme 1.21. Aldehydes catalyzed highly enantioselective intermolecular hydroamination

⁴² M. J. MacDonald, C. R. Hesp, D. J. Schipper, M. Pesant, A. M. Beauchemin, *Chem. Eur. J.* **2013**, *19*, 2597.

Moreover, continuous efforts finally led to the development of efficient diastereoselective intermolecular hydroamination reactions in which formaldehyde could act as an efficient tethering catalyst, and the diastereoselectivity was controlled by the use of chiral allylic amines or chiral hydroxylamines (**Scheme 1.22**). With the use of formaldehyde as the catalyst to form the temporary tether, the formation of the nitron and temporary tether proved more favorable compared to other aldehydes. This discovery significantly improved the substrate scope and even internal alkenes could be utilized in this reaction system, which led to largely improved synthetic efficiency of this reaction.



Scheme 1.22. Formaldehyde catalyzed diastereoselective intermolecular hydroamination

Overall, these results, especially with the excellent control of enantio- and diastereoselectivity for Cope-type hydroamination reactions, highlighted opportunities for high synthetic efficiency in the field of catalytic carbonyl catalysis based on temporary intramolecularity.

1.2.2. Asymmetric epoxidation via dioxirane formation

As discussed above, carbonyl catalysis achieved impressive progress for hydration/hydrolysis and hydroamination reactions via temporary intramolecularity. Additionally, carbonyl catalysis also had great achievements in the field of asymmetric epoxidation.

Optically active epoxides are valuable intermediates and synthons for further chemical

transformations. Numerous approaches have been developed for the synthesis of enantioenriched epoxides, such as chiral titanium catalysts,⁴³ epoxidation of allylic alcohols with the use of vanadium-catalysts⁴⁴ and nucleophilic epoxidation,⁴⁵ etc. Among these, asymmetric epoxidation for unfunctionalized olefins catalyzed by chiral ketones via dioxirane formation has also made a significant contribution.⁴⁶ It was known that *in situ* formation of dioxiranes occurs from ketones and Oxone (2KHSO₅·KHSO₄·K₂SO₄). Therefore, the use of a catalytic amount of ketone could be realized in theory. However, the practical development of an efficient chiral ketone was found to be challenging. The early exploration provided the products with only 9-20% enantioselectivity.⁴⁷ With continuous efforts from different chemists, Yang and co-workers provided a C₂ symmetric cyclic chiral ketone to realize this asymmetric epoxidation.⁴⁸ However, the enantioselectivity for most of the substrates was under 50% ee. Finally a carbohydrate-based ketone was reported by Shi and co-workers in 1996³ (**Scheme 1.23**). This system used a fructose-derived ketone as the catalyst and Oxone as the oxidant and proved to be highly effective for asymmetric epoxidation of trans-trisubstituted olefins bearing no allylic alcohol group under remarkably mild conditions. The products could be generated with up to 84% yields, up to >95% ee. This chiral ketone-catalyzed epoxidation could be considered as a representative example in the field of carbonyl catalysis to achieve asymmetric transformation. Further development

⁴³ For reviews, see: (a) T. Katsuki, V. S. Martin, *Org. React.* **1996**, *48*, 1. (b) R. A. Johnson, K. B. Sharpless, *In Catalytic Asymmetric Synthesis*; Ojima, I. Ed.; VCH: New York, **2000**, Chapter 6A.

⁴⁴ (a) N. Murase, Y. Hoshino, M. Oishi, H. Yamamoto, *J. Org. Chem.* **1999**, *64*, 338. (b) Y. Hoshino, H. Yamamoto, *J. Am. Chem. Soc.* **2000**, *122*, 10452. (c) W. Zhang, A. Basak, Y. Kosugi, Y. Hoshino, H. Yamamoto, *Angew. Chem. Int. Ed.* **2005**, *44*, 4389. (d) Z. Bourhani, A. V. Malkov, *Chem. Commun.* **2005**, 4592. (e) A. V. Malkov, Z. Bourhani, P. Kočovský, *Org. Biomol. Chem.* **2005**, *3*, 3194.

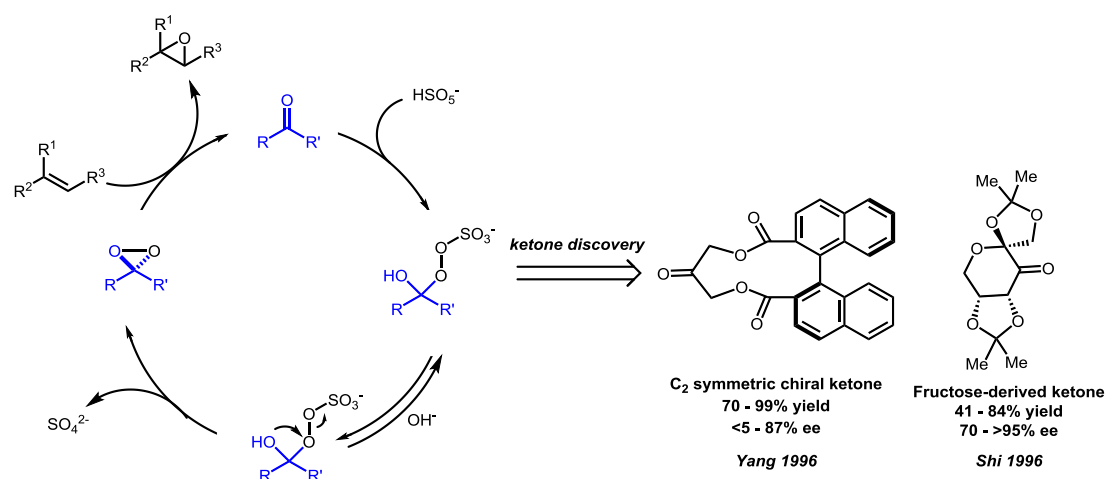
⁴⁵ For reviews, see: (a) M. J. Porter, J. Skidmore, *Chem. Commun.* **2000**, 1215. (b) C. Lauret, S. M. Roberts, *Aldrichimica Acta.* **2002**, *35*, 47. (c) T. Nemoto, T. Ohshima, M. J. Shibasaki, *Synth. Org. Chem. Jpn.* **2002**, *60*, 94. (d) D. R. Kelly, S. M. Roberts, *Biopolymers* **2006**, *84*, 74. (e) M. Shibasaki, M. Kanai, S. Matsunaga, *Aldrichimica Acta.* **2006**, *39*, 31.

⁴⁶ O. A. Wong, Y. Shi, *Chem. Rev.* **2008**, *108*, 3958.

⁴⁷ (a) R. Curci, M. Fiorentino, M. R. Serio, *Chem. Commun.* **1984**, 155. (b) R. Curci, L. D'Accolti, M. Fiorentino, and A. Rosa, *Tetrahedron Lett.* **1995**, *36*, 5831. (c) D. S. Brown, B. A. Marples, P. Smith and L. Walton, *Tetrahedron* **1995**, *51*, 3587.

⁴⁸ D. Yang, Y. C. Yip, M. W. Tang, M. K. Wong, J. H. Zheng, K. K. Cheung, *J. Am. Chem. Soc.* **1996**, *118*, 491.

also yielded different chemical transformations.⁴⁶



Scheme 1.23. Carbonyl compounds catalyzed asymmetric epoxidation

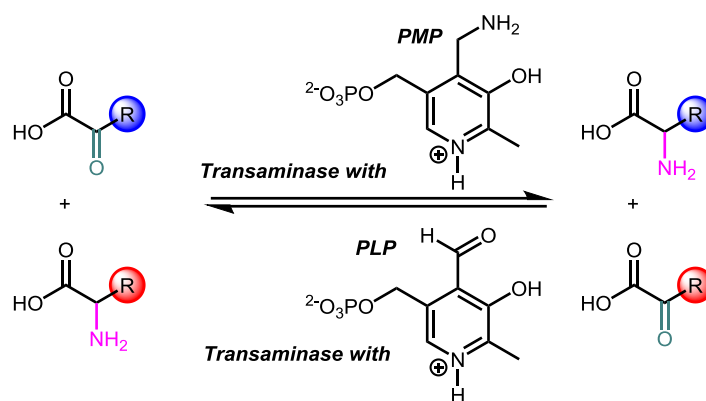
1.2.3 Iminium/imine formation

More recently, carbonyl catalysis via *in situ* formation of iminium/imine using carbonyl compounds as catalysts or co-catalysts has significantly progressed.

In Nature, iminium intermediates have been involved significantly in biological transamination pathways, which are among the most important biological processes. This transformation was catalyzed by transaminase with pyridoxal 5'-phosphate (PLP) and pyridoxamine 5'-phosphate (PMP)⁴⁹ (**Scheme 1.24**). Inspired by enzymatic system, continuous efforts have been made to develop efficient catalytic reaction to mimic this important enzymatic reactivity.⁵⁰

⁴⁹ For selected reviews on enzymatic transamination, see: (a) D. Zhu, L. Hua, *J. Biotechnol.* **2009**, *4*, 1420. (b) J. Ward, R. Wohlgemuth, *Curr. Org. Chem.* **2010**, *14*, 1914. (c) D. Koszelewski, K. Tauber, K. Faber, W. Kroutil, *Trends Biotechnol.* **2010**, *28*, 324.

⁵⁰ Selected representative example: L. Shi, C. Tao, Q. Yang, Y. E. Liu, J. Chen, J. Chen, J. Tian, F. Liu, B. Li, Y. Du, B. Zhao, *Org. Lett.* **2015**, *17*, 5784.



Scheme 1.24. Transamination pathways in Nature

In this context different transformations using iminium/imine formation via carbonyl catalysis could be achieved in two ways: 1) *in situ* formation of iminium/imine between carbonyl compounds and α -amino acid derivatives could increase the acidity and reactivity at the α -C-center of α -amino acid derivatives. This ‘simple’ but elegant strategy was used to promote the α -alkylation and racemization⁵¹ of α -amino acids and derivatives, and 2) carbonyl compounds were also successfully used to act as (catalytic) directing groups to increase control in metal-catalyzed reactions.¹⁷

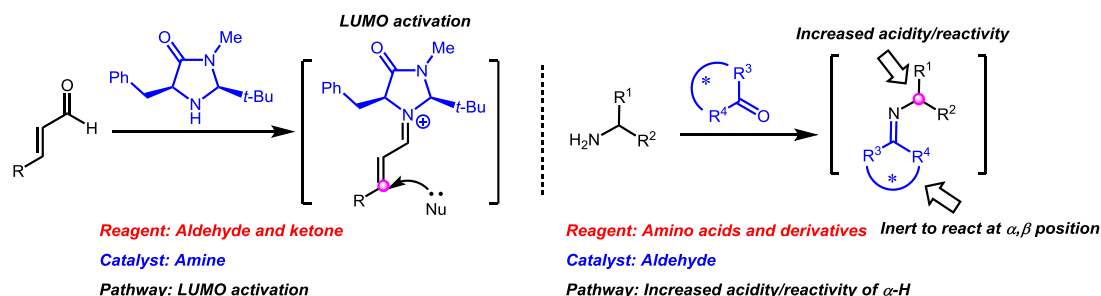
Increased acidity/reactivity

In organocatalysis, as mentioned in Section 1.1, iminium intermediates have been extensively investigated. Previously, this catalytic activation mode was realized via the LUMO activation of α,β -unsaturated carbonyl compounds (**Scheme 1.25**, left). Therefore, the role of carbonyl compounds and amines in this activation strategy is a substrate and catalyst respectively.

In carbonyl catalysis, aldehydes, which normally had the limited reactivity at α,β -positions, were applied as catalysts to react with the substrates bearing an amino group

⁵¹ S. Yamada, C. Hongo, R. Yoshioka, I. Chibata, *J. Org. Chem.* **1983**, *48*, 843.

to form the iminium/imine intermediates. As a result, the α -C of amines was activated with increased acidity/reactivity to undergo subsequent reactions to achieve difficult chemical transformations (Scheme 1.25, right).



Scheme 1.25. Comparison of the roles of carbonyl compounds in different reactions

In order to realize the α -functionalization of amines, many strategies were developed with *N*-protected amines or secondary/tertiary amines.⁵² In particular, chiral phase-transfer catalysis and transition metal catalysis obtained significant achievements.⁵³ However, it was an indirect method and required the installation of protecting groups on the amine with stoichiometric aldehydes or ketones, and then to release the free amino compounds, after the removal of the protection group.⁵⁴ However, carbonyl compounds could provide the solutions to activate the α -C of amino group.⁵⁵ By taking advantage of iminium/imine *in situ* formation to increase the acidity and reactivity, an

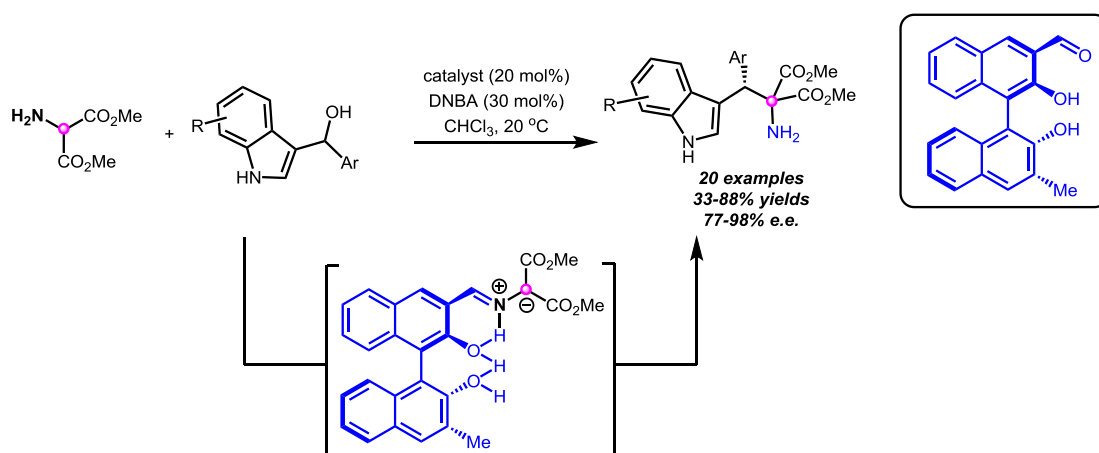
⁵² Selected reviews about α -functionalization of amine: (a) C. S. Yeung, V. M. Dong, *Chem. Rev.* **2011**, *111*, 1215. (b) C. Liu, H. Zhang, W. Shi, A. Lei, *Chem. Rev.* **2011**, *111*, 1780. (c) C.-J. Li, *Acc. Chem. Res.* **2009**, *42*, 335. (d) C.-L. Sun, B.-J. Li, Z.-J. Shi, *Chem. Rev.* **2011**, *111*, 1293. (e) S.-I. Murahashi, D. Zhang, *Chem. Soc. Rev.* **2008**, *37*, 1490. (f) C. K. Prier, D. A. Rankic, D. W. C. MacMillan, *Chem. Rev.* **2013**, *113*, 5322.

⁵³ For selected reviews: (a) A. E. Taggi, A. M. Hafez, T. Lectka, *Acc. Chem. Res.* **2003**, *36*, 10. (b) M. J. O'Donnell, *Acc. Chem. Res.* **2004**, *37*, 506. (c) B. Lygo, B. I. Andrews, *Acc. Chem. Res.* **2004**, *37*, 518. (d) T. Hashimoto, K. Maruoka, *Chem. Rev.* **2007**, *107*, 5656. (e) K. Maruoka, T. Ooi, T. Kano, *Chem. Commun.* **2007**, 1487. (f) U. Kazmaier, *Org. Chem. Front.* **2016**, *3*, 1541. For recent examples: (g) L. Wei, S. M. Xu, Q. Zhu, C. Che, C. J. Wang, *Angew. Chem.* **2017**, *129*, 12480; *Angew. Chem. Int. Ed.* **2017**, *56*, 12312. (h) X. Huo, R. He, J. Fu, J. Zhang, G. Yang, W. Zhang, *J. Am. Chem. Soc.* **2017**, *139*, 9819. (i) L. Wei, Q. Zhu, S. M. Xu, X. Chang, C. J. Wang, *J. Am. Chem. Soc.* **2018**, *140*, 1508. (j) X. Huo, J. Zhang, J. Fu, R. He, W. Zhang, *J. Am. Chem. Soc.* **2018**, *140*, 2080.

⁵⁴ Q. Wang, Q. Gu, S.-L. You, *Angew. Chem. Int. Ed.* **2019**, *58*, 2.

⁵⁵ (a) X.-H. Chen, W.-Q. Zhang, L.-Z. Gong, *J. Am. Chem. Soc.* **2008**, *130*, 5652. (b) J. Yu, L. He, X.-H. Chen, J. Song, W.-J. Chen, L.-Z. Gong, *Org. Lett.* **2009**, *11*, 4946. (c) N. Li, J. Song, X.-F. Tu, B. Liu, X.-H. Chen, L.-Z. Gong, *Org. Biomol. Chem.* **2010**, *8*, 2016. (d) Y.-K. Liu, H. Liu, W. Du, L. Yue, Y.-C. Chen, *Chem. Eur. J.* **2008**, *14*, 9873. (e) H. Park, K. M. Kim, A. Lee, S. Ham, W. Nam, J. Chin, *J. Am. Chem. Soc.* **2007**, *129*, 1518. (f) K. M. Kim, H. Park, H.-J. Kim, J. Chin, W. Nam, *Org. Lett.* **2005**, *7*, 3525. (g) J. Chin, D. C. Kim, H.-J. Kim, F. B. Panosyan, K. M. Kim, *Org. Lett.* **2004**, *6*, 2591. (h) S. M. So, K. Moozesh, A. J. Lough, J. Chin, *Angew. Chem. Int. Ed.* **2014**, *53*, 829.

ice-breaking example of BINOL-derived chiral aldehyde catalyzed enantioselective α -alkylation of 2-aminomalonates was documented by Guo and co-workers⁵⁶ (**Scheme 1.26**). In this work, the α -C-H bond of amines was activated through the formation of imines, therefore leading to the increased acidity/reactivity at the α -C center. As a result, an efficient approach for enantioselective direct α -alkylation of *N*-unprotected amino esters was achieved with moderate to good yields and good to excellent enantioselectivities.



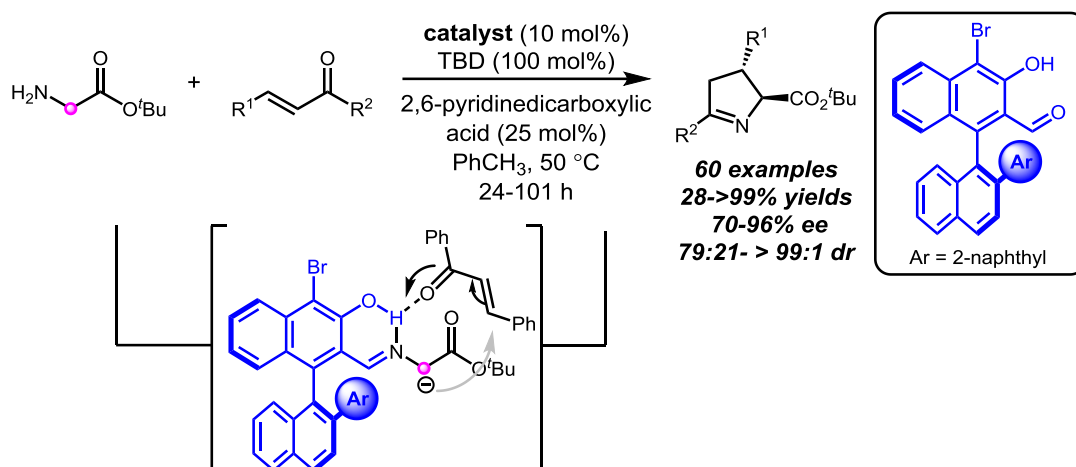
Scheme 1.26. α -Alkylation of free amines from Guo

Later on, the same group discovered a novel BINOL-based bifunctional chiral aldehyde catalyst, and applied this for the catalytic asymmetric activation of glycine esters which underwent a nucleophilic conjugation addition reaction⁵⁷ (**Scheme 1.27**). *In situ* formation of imine intermediates generated an active α -nucleophilic carbon center by increasing the α -C-H bond acidity, and the steric properties on the chiral catalysts influenced the stereocontrol in the reaction. With this efficient protocol, a broad substrate scope was developed with high yields and enantioselectivity. In the absence of the hydroxyl group or using its *O*-methylated analogue on the aldehyde catalyst, the

⁵⁶ B. Xu, L.-L. Shi, Y.-Z. Zhang, Z.-J. Wu, L.-N. Fu, C.-Q. Luo, L.-X. Zhang, Y.-G. Peng, Q.-X. Guo, *Chem. Sci.* **2014**, *5*, 1988.

⁵⁷ W. Wen, L. Chen, M.-J. Luo, Y. Zhang, Y.-C. Chen, Q. Ouyang, Q.-X. Guo, *J. Am. Chem. Soc.* **2018**, *140*, 9774.

reaction did not occur. Their DFT results suggested that this newly-designed chiral aldehyde catalyst served as an elegant bifunctional catalyst in which the hydroxyl group was extremely important for not only the condensation between aldehyde catalyst and glycine ester, but the subsequent nucleophilic addition step. Other amino acid derivatives such as amides as the substrates were reported.

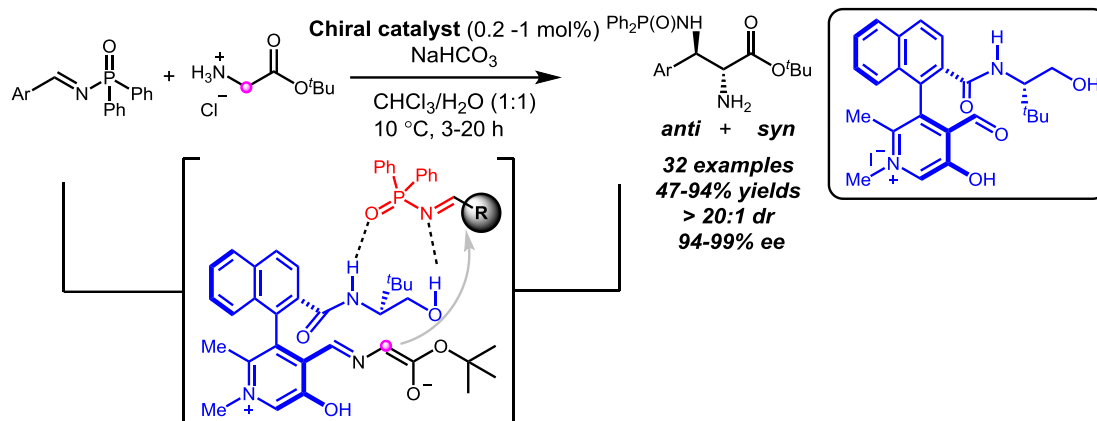


Scheme 1.27. Catalytic asymmetric activation of glycine esters from Guo

Very recently, Zhao, Yuan and co-workers developed a novel *N*-quaternized biaryl axially chiral pyridoxal catalyst and successfully applied this catalyst to a Mannich-type reaction⁵⁸ (**Scheme 1.28**). As a result, under remarkably mild conditions, various α,β -diamino acid esters could be synthesized, with excellent diastereo- and enantioselectivities, modest to excellent yields, and with surprisingly low catalyst loading (0.2-1 mol%). In their proposed mechanism, the reaction was initiated by the condensation between the chiral aldehyde catalyst and glycinate to form the imine intermediate, thereby increasing the acidity and reactivity of the α -H in glycinate. Moreover, the reaction could not take place without the *N*-methylation of the chiral catalyst; the reactivity and stereoselectivity were largely inhibited by the methylation

⁵⁸ (a) J. Chen, X. Gong, J. Li, Y. Li, J. Ma, C. Hou, G. Zhao, W. Yuan, B. Zhao, *Science* **2018**, *360*, 1438. For another example of aldehyde catalysis via imine/iminium intermediates, please see: (b) reference 48.

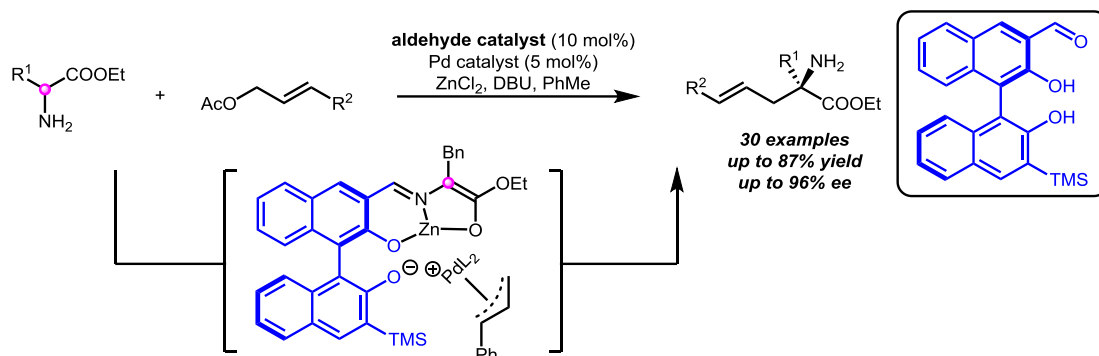
of the N-H or hydroxyl group of the side chain in the chiral catalyst. In summary, this newly-designed bifunctional carbonyl catalyst could not only activate both substrates via hydrogen-bonding and imine formation, but pre-organize reagents through proximity and orientation effects.



Scheme 1.28. Chiral aldehyde catalyzed asymmetric Mannich-type reaction

In 2019, Guo and co-workers⁵⁹ combined chiral aldehyde catalysis with Lewis acid catalysis and transition metal catalysis together to build a triple catalytic system. Eventually, the enantioselective α -allylic alkylation of amino acid esters was achieved. This efficient triple catalytic system was first introduced by Guo and co-workers to prepare optically active α,α -disubstituted α -amino esters with high yields and enantioselectivities (**Scheme 1.29**). Their preliminary mechanistic study demonstrated that the chiral aldehyde catalyst could not only react with α -amino esters to afford the iminium/imine, thereby the acidity and reactivity of α -H was significantly increased to promote the subsequent nucleophilic attack, but also support that the hydroxyl group could coordinate with the π -allyl Pd(II) species to improve the reactivity.

⁵⁹ (a) L. Chen, M.-J. Luo, F. Zhu, W. Wen, Q.-X. Guo, *J. Am. Chem. Soc.* **2019**, *141*, 5159.



Scheme 1.29. Triple catalytic system (chiral aldehyde catalysis/Lewis acid catalysis/transition metal catalysis)

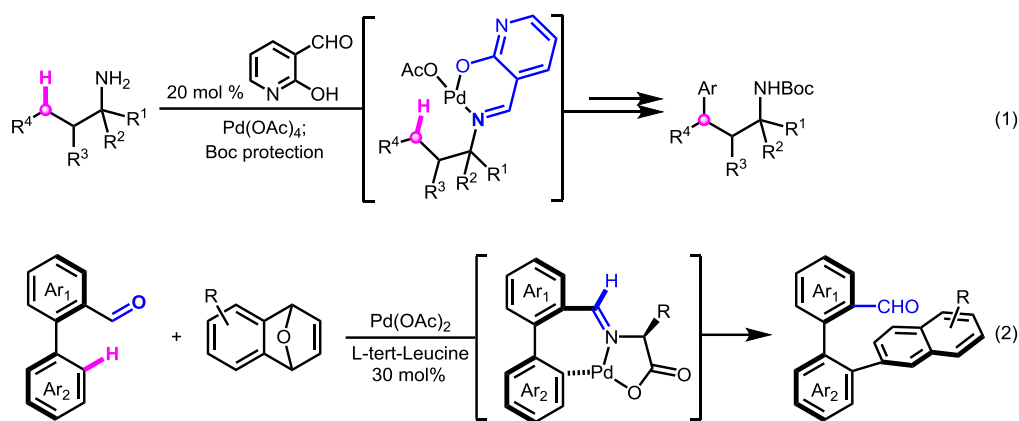
Providing catalytic directing group

Using aldehydes as catalytic transient directing groups is a recently developed strategy in the field of C-H activation. Traditionally, the directing groups were a part of the reagents or were installed covalently in prior steps, and in some cases, the reluctant removal of directing groups also limited the synthetic applicability of this approach. However, the development of catalytic directing groups, which first bond to the substrates transiently and then detach reversibly, do not require additional steps for the pre-functionalization of the substrates and subsequent removal. A representative example was reported by the Yu group, in which an efficient Pd-catalyzed C-H activation of free amines was achieved by forming a catalytic transient directing group⁶⁰ (**Scheme 1.30**, equation 1). The directed reactivity at the Pd metal center was permitted by the *in situ* formation of imine intermediates. Impressive achievements using intramolecular directing aldehyde were also reported by Shi and co-workers⁶¹ (**Scheme 1.30**, equation 2). This strategy has been studied extensively in order to achieve excellent control on reactivity and selectivity in metal-catalyzed reactions.⁶²

⁶⁰ Y. Wu, Y.-Q. Chen, T. Liu, M. D. Eastgate, J.-Q. Yu, *J. Am. Chem. Soc.* **2016**, *138*, 14554.

⁶¹ G. Liao, H.-M. Chen, Y.-N. Xia, B. Li, Q.-J. Yao, B.-F. Shi, *Angew. Chem. Int. Ed.* **2019**, *58*, 11464.

⁶² (a) Y. Liu, H. Ge, *Nat. Chem.* **2017**, *9*, 26. (b) A. Yada, W. Liao, Y. Sato, M. Murakami, *Angew. Chem. Int. Ed.* **2017**, *56*, 1073. (c) A. R. Ickes, S. C. Ensign, A. K. Gupta, K. L. Hull, *J. Am. Chem. Soc.* **2014**, *136*, 11256. (d) C.-H. Jun, H. Lee, J.-B. Hong, *J. Org. Chem.* **1997**, *62*, 1200. (e) F.-L. Zhang, K. Hong, T.-J. Li, H. Park, J.-Q. Yu,



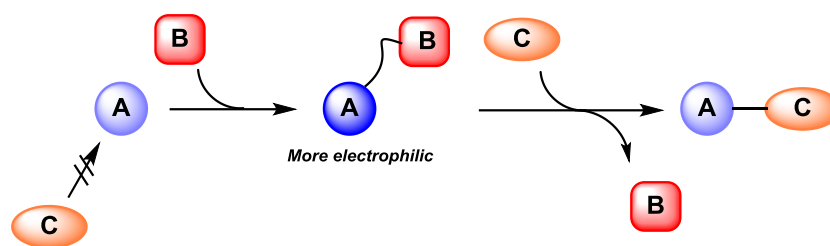
Scheme 1.30. Imine formation as a directing group

In this section, the major approaches to realize carbonyl catalysis have been discussed, including inducing temporary intramolecularity via the formation of tethers or transient intramolecular nucleophiles, asymmetric epoxidation via dioxirane formation and iminium/imine formation to perform α -functionalization of amines and directed C-H activation. Reactions that were discovered based on different activation modes will be introduced in Chapter 2, 3 and 4 in detail. Due to the types of activation presented in this thesis, other types of organocatalytic activation will be discussed for the following sections of the introduction.

1.3. Electrophilic activation

Besides carbonyl catalysis, another important branch of activation modes in organocatalysis is electrophilic activation (**Scheme 1.31**). Unlike carbonyl catalysis, a typical electrophilic activation process could be viewed as the enhancement of the electrophilic character of a given chemical species due to the covalent or non-covalent interaction with an electrophile.

Science **2016**, *351*, 252. Selected reviews on directed metal-catalyzed reactions, see: (f) G. Rousseau, B. Breit, *Angew. Chem. Int. Ed.* **2011**, *50*, 2450; (g) D.-S. Kim, W.-J. Park, C.-H. Jun, *Chem. Rev.* **2017**, *117*, 8977. (h) C.-H. Jun, H. Lee, J.-B. Hong, *J. Org. Chem.* **1997**, *62*, 1200. (i) F.-L. Zhang, K. Hong, T.-J. Li, H. Park, J.-Q. Yu, *Science* **2016**, *351*, 252.



Scheme 1.31. Electrophilic activation in general

In many cases, this interaction donates a pair of electrons into a reactive vacant orbital, or a LUMO, on the electrophile. Electrophilic activation could be realized using Lewis acid catalysts,⁶³ Brønsted acid catalysts^{63a}, hydrogen bonding catalysts^{6,64}, iminium ion formation^{1,11,65}, late- or post-transition-metal catalysts⁶⁶, or others⁶⁷. Efficient electrophilic activation has been exploited for different chemical transformations. However, only two of the catalytic activation modes will be discussed in detail here. One of the activation modes is the DMAP-promoted electrophilic activation. The other is the Brønsted acid-facilitated electrophilic activation, in which chiral phosphoric acid, one type of the organophosphorus compounds played an essential role. This specific choice is loosely related to the contents of this document, in that the reactions investigated in this thesis were related to organophosphorus compounds, and that chiral phosphoric acids are widely accepted as being a versatile class of organocatalysts.

⁶³ (a) A. Fürstner, P. W. Davies, *Angew. Chem. Int. Ed.* **2007**, *46*, 3410. (b) T. Caneque, F. M. Truscott, R. Rodriguez, G. Maestri, M. Malacria, *Chem. Soc. Rev.* **2014**, *43*, 2916. (c) M. C. Lipke, A. L. Liberman-Martin, T. D. Tilley, *Angew. Chem. Int. Ed.* **2017**, *56*, 2260.

⁶⁴ (a) M. S. Taylor, E. N. Jacobsen, *Angew. Chem. Int. Ed.* **2006**, *45*, 1520. (b) A. G. Doyle, E. N. Jacobsen, *Chem. Rev.* **2007**, *107*, 5713. (c) H. Miyabe, Y. Takemoto, *Carbonyl and Imine Activation. In Comprehensive Organic Synthesis*, 2nd ed.; P. Knochel, G. A. Molander, Eds.; Elsevier: Amsterdam, **2014**; p 751. For seminal papers, see: (d) M. S. Sigman, P. Vachal, E. N. Jacobsen, *Angew. Chem. Int. Ed.* **2000**, *39*, 1279.

⁶⁵ (a) W. S. Jen, J. J. M. Wiener, D. W. C. MacMillan *J. Am. Chem. Soc.* **2000**, *122*, 9874. (b) A. Erkkilä, I. Majander P. M. Pihko, *Chem. Rev.* **2007**, *107*, *12*, 5416.

⁶⁶ (a) J. A. Labinger, J. E. Bercaw, *Nature* **2002**, *417*, 507. (b) D. L. Davies, S. M. Donald, O. Al-Duajj, S. A. Macgregor, M. Pölleth, *J. Am. Chem. Soc.* **2006**, *128*, 4210. For a book, please see: (c) J. A. Labinger, in *Alkane C–H Activation by Single-Site Metal Catalysis*. P. J. Pérez, (Ed.), Springer, **2012**, p17-72.

⁶⁷ (a) D. Kaiser, N. Maulide, *J. Org. Chem.* **2016**, *81*, 4421. (b) D. Mahajan, V. Kumar, A. Rana, C. Lal Meena, N. Sharma, Y. Kumar, *Synthesis* **2018**, *50*, 3902.

1.3.1 Nucleophilic catalysis

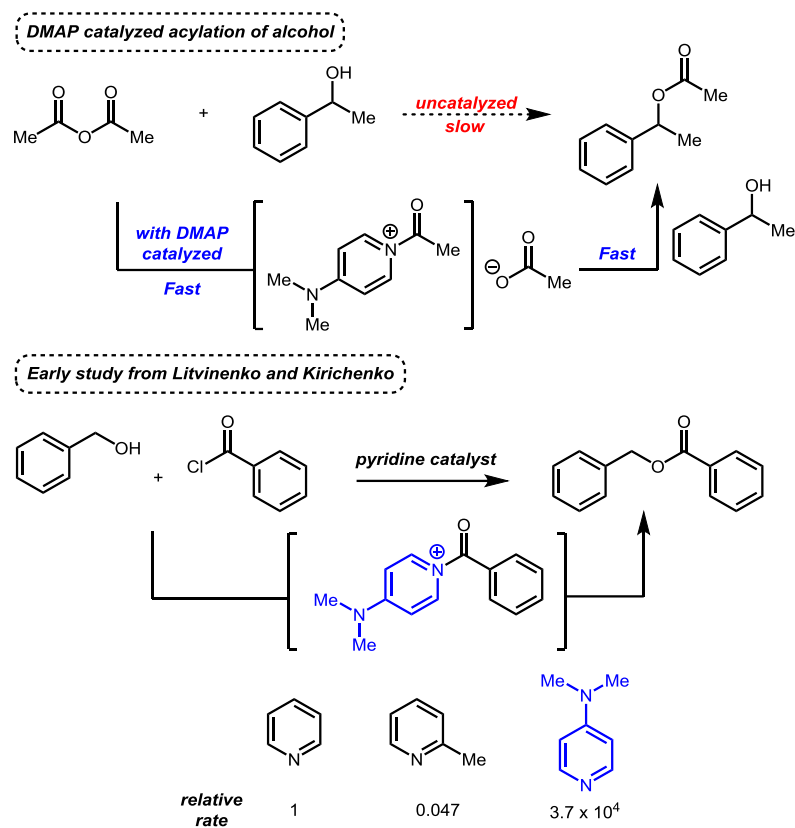
Electrophilic activation through nucleophilic catalysis seems like a contradiction. However, this is a well-developed area via a different mechanism from what has been discussed above. In the field of nucleophilic catalysis, 4-(dimethylamino)pyridine (DMAP) has proved to be a particularly useful nucleophilic catalysts.⁶⁸ For instance, the acylation of alcohols with the use of anhydrides in which DMAP served as a catalyst is one of the most encountered examples.⁶⁹ The first use of DMAP in organic synthesis could be dated back to 1960s. In 1967, Litvinenko and Kirichenko found that in the benzylation of 3-chloroaniline, DMAP could provide a 10^4 -fold faster rate compared to pyridine.⁷⁰ This enhancement of reaction rate was achieved by nucleophilic addition of DMAP to generate a more reactive intermediate, therefore by this activation, the carbonyl is more electrophilic and has a better leaving group. However, as also indicated by Litvinenko and Kirichenko, simply adding a methyl group at the 2-position of the pyridine would dramatically decrease the reactivity⁷¹ (**Scheme 1.32**).

⁶⁸ For a review: R. P. Wurz, *Chem. Rev.* **2007**, *107*, 5570.

⁶⁹ G. C. Fu, *Acc. Chem. Res.* **2000**, *33*, 412.

⁷⁰ (a) L. M. Litvinenko, A. I. Kirichenko, *Dokl. Akad. Nauk. SSSR* **1967**, *176*, 97.

⁷¹ L. I. Bondarenko, A. I. Kirichenko, L. M. Litvinenko, I. N. Dmitvenko, V. D. Kobets, *Zh. Org. Khim.* **1981**, *17*, 2588.



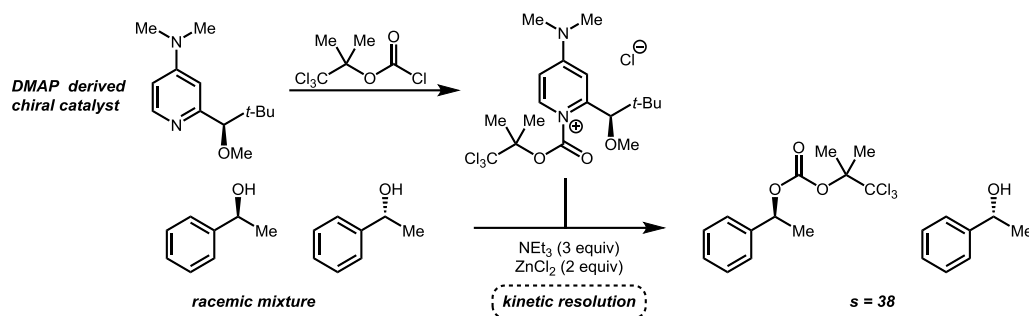
Scheme 1.32. Early studies regarding DMAP as a catalyst

Soon after, Steglich and Höfle showed that DMAP was used as a catalyst for the acetylation of 1-methylcyclohexanol, which is a sterically congested alcohol.⁷² After these independent initial studies, the application of DMAP as a catalyst to achieve different chemical transformation was studied broadly.

Vedejs and Chen documented the first successful application of a chiral DMAP catalyst in 1996.⁷³ In their original report, a kinetic resolution of racemic secondary alcohols was achieved using a 2-substituted chiral DMAP as a chiral acylating agent (**Scheme 1.33**).

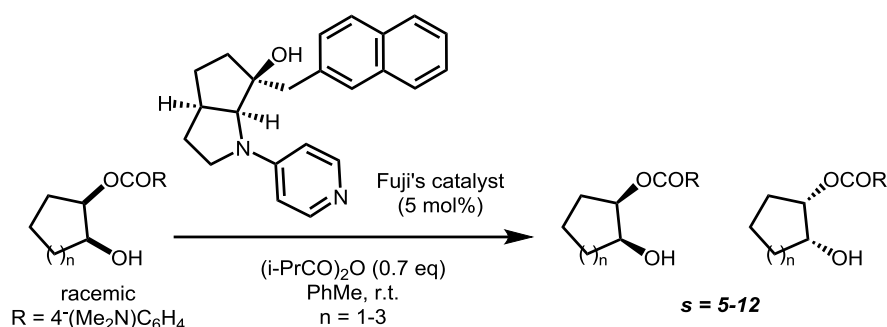
⁷² (a) W. Steglich, G. Höfle, *Angew. Chem. Int. Ed.* **1969**, 8, 981. (b) G. Höfle, W. Steglich, *Synthesis* **1972**, 619.

⁷³ E. Vedejs, X. Chen, *J. Am. Chem. Soc.* **1996**, 118, 1809.



Scheme 1.33. Kinetic resolution in the presence of chiral DMAP

Other 2-substituted chiral DMAP reagents were also discovered by Vedejs and Chen for different kinetic resolution,⁷⁴ however, unfortunately, Vedejs was not able to apply this type of chiral DMAP reagents to be a chiral catalysts, as stoichiometric amounts were always used. It was probably due to the steric demand at the 2-position on the pyridine nitrogen preventing efficient catalytic turnover. Later on, Fuji and co-workers developed a chiral 4-pyrrolidinopyridine derivative as a chiral catalyst with the stereogenic centers located at the para position to the pyridine nitrogen⁷⁵ (**Scheme 1.34**). In order to achieve catalytic activity, their catalyst was designed to have a remote stereocenter however this also led to reduced selectivity.



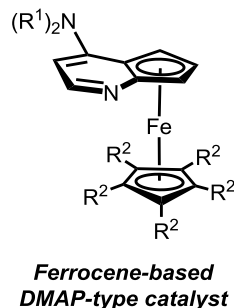
Scheme 1.34. Fuji's DMAP catalyst

In 1996, a planar-chiral ferrocene-fused DMAP derivative was reported by Fu and co-

⁷⁴ (a) E. Vedejs, M. Jure, *Angew. Chem. Int. Ed.* **2005**, *44*, 3974. (b) E. Vedejs, X. Chen, *J. Am. Chem. Soc.* **1997**, *119*, 2584. (c) E. Vedejs, X. Chen, U.S. Patent 5, 646, 287, **1997**.

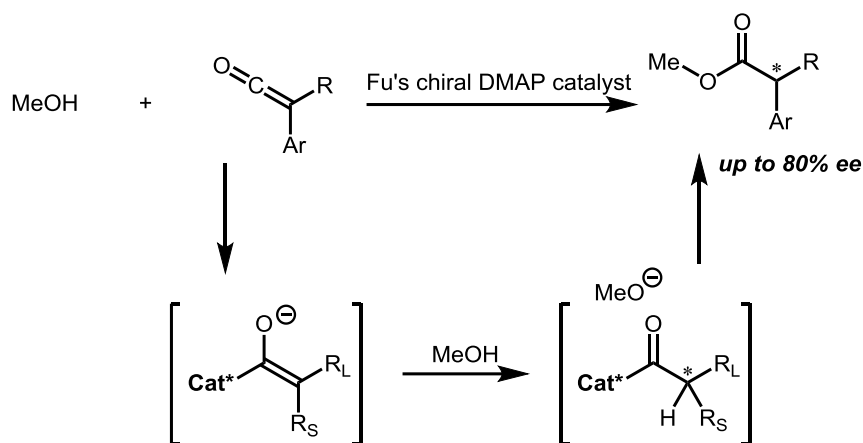
⁷⁵ (a) T. Kawabata, M. Nagato, K. Takasu, K. Fuji, *J. Am. Chem. Soc.* **1997**, *119*, 3169. (b) T. Kawabata, K. Yamamoto, Y. Momose, H. Yoshida, Y. Nagaoka, K. Fuji, *Chem. Commun.* **2001**, 2700.

workers⁷⁶ (**Scheme 1.35**) and they also extended this to the analogous ruthenocyl-fused derivatives.⁷⁷ They successfully utilized these DMAP derivatives as chiral catalysts in a variety of different asymmetric transformation.^{69,78}



Scheme 1.35. Fu's DMAP-based catalyst

In the presence of ferrocene-based DMAP-type catalysts, the addition of alcohols to ketenes could be realized with up to 80% ee⁷⁹ (**Scheme 1.36**).



Scheme 1.36. Addition of alcohols to ketenes

In addition, this type of chiral catalyst could also be used for the rearrangement of various 4-substituted *O*-acylated azlactones, providing up to 92% ee and up to 94% yield (**Scheme 1.37**). The products from the rearrangement could be transferred to α -

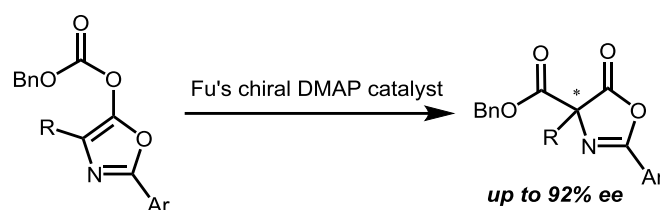
⁷⁶ J. C. Ruble, G. C. Fu, *J. Org. Chem.* **1996**, *61*, 7230.

⁷⁷ C. E. Garrett, G. C. Fu, *J. Am. Chem. Soc.* **1998**, *120*, 7479.

⁷⁸ (a) G. C. Fu, *Acc. Chem. Res.* **2004**, *37*, 542.

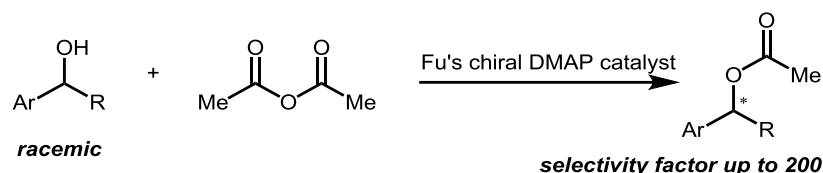
⁷⁹ For other ketene additions: (a) B. L. Hodous, J. C. Ruble, G. C. Fu, *J. Am. Chem. Soc.* **1999**, *121*, 2637. (b) B. L. Hodous, G. C. Fu, *J. Am. Chem. Soc.* **2002**, *124*, 10006. (c) C. Schaefer, G. C. Fu, *Angew. Chem. Int. Ed.* **2005**, *44*, 4606. (d) E. C. Lee, K. M. McCauley, G. C. Fu, *Angew. Chem. Int. Ed.* **2007**, *46*, 977. (e) X. Dai, T. Nakai, J. A. C. Romero, G. C. Fu, *Angew. Chem. Int. Ed.* **2007**, *46*, 4367.

substituted α -amino acids going through the ring-opening of azlactones.⁸⁰



Scheme 1.37. Rearrangement of *O*-acylated enolates

This catalyst has also been applied for the acylation of alcohols with anhydrides. The kinetic resolution of secondary alcohols was also widely studied by other groups as mentioned above. With Fu's ferrocene-based DMAP-type catalysts, the selectivity factor could be up to 200⁸¹ (**Scheme 1.38**).



Scheme 1.38. Acylation of alcohols by anhydrides

Several asymmetric chemical transformations were discovered with Fu's chiral DMAP catalysts, including kinetic resolution of different substances,⁸² coupling reaction with imines to form β -lactams,⁸³ and other ketene [2+2] cycloadditions.⁸⁴ Because of their various applications, Fu's ferrocene-fused DMAP derived catalysts have been accepted, in the field of asymmetric nucleophilic catalysis, as a reference standard.⁸⁵ Other chiral nucleophilic catalyst were developed, for example, Suga's BINOL-derived catalyst⁸⁶

⁸⁰ J. C. Ruble, G. C. Fu, *J. Am. Chem. Soc.* **1998**, *120*, 11532.

⁸¹ (a) J. C. Ruble, H. A. Latham, G. C. Fu, *J. Am. Chem. Soc.* **1997**, *119*, 1492. (b) J. C. Ruble, J. Tweddell, G. C. Fu, *J. Org. Chem.* **1998**, *63*, 2794. (c) B. Tao, J. C. Ruble, D. A. Hoic, G. C. Fu, *J. Am. Chem. Soc.* **1999**, *121*, 5091.

⁸² For acylation of racemic benzylic amines, see: (a) Y. Ie, G. C. Fu, *Chem. Commun.* **2000**, *119*. (b) S. Arai, S. Bellemin-Lapponnaz, G. C. Fu, *Angew. Chem. Int. Ed.* **2001**, *40*, 234. For 2-substituted indolines, see: (c) F. O. Arp, G. C. Fu, *J. Am. Chem. Soc.* **2006**, *128*, 14264.

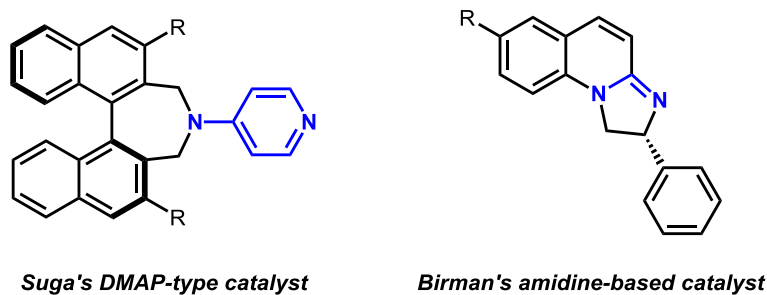
⁸³ B. L. Hodous, G. C. Fu, *J. Am. Chem. Soc.* **2002**, *124*, 1578.

⁸⁴ (a) J. E. Wilson, G. C. Fu, *Angew. Chem. Int. Ed.* **2004**, *43*, 6358. (b) E. C. Lee, B. L. Hodous, E. Bergin, C. Shih, G. C. Fu, *J. Am. Chem. Soc.* **2005**, *127*, 11586. (c) J. M. Berlin, G. C. Fu, *Angew. Chem. Int. Ed.* **2008**, *47*, 7048. (d) M. Dochnahl, G. C. Fu, *Angew. Chem. Int. Ed.* **2009**, *48*, 2391.

⁸⁵ T. Cruchter, M. G. Medvedev, X. Shen, T. Mietke, K. Harms, M. Marsch, E. Meggers, *ACS Catal.* **2017**, *7*, 5151.

⁸⁶ H. Mandai, K. Fujii, H. Yasuhara, K. Abe, K. Mitsudo, T. Korenaga, S. Suga, *Nat. Commun.* **2016**, *7*, 11297.

and Birman's amidine-based catalyst⁸⁷ (Scheme 1.39).



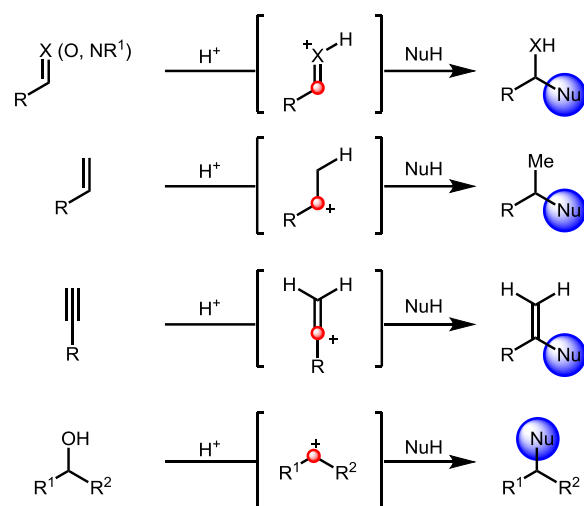
Scheme 1.39. Other catalysts to realize electrophilic activation

1.3.2 Brønsted acid catalysis

In the field of electrophilic activation, Brønsted acid catalysis has been thoroughly explored. Simply, a proton donor could be defined as a Brønsted acid. Brønsted acids can activate different substrates such as carbonyls, imines, alkenes, alkynes and hydroxyl groups to convert them into a better electrophile for subsequent nucleophilic addition⁸⁸ (Scheme 1.40). Compared to Lewis acids, Brønsted acids are more user-friendly and more stable, leading to a longer shelf-life. This makes Brønsted acid catalysis fit well within the practical consideration of organocatalysis, of which a selling feature is that it remain environmentally benign and suitable for the development of large-scale synthesis.

⁸⁷ (a) V. B. Birman, H. Jiang, *Org. Lett.* **2005**, *7*, 3445. (b) V. B. Birman, X. Li, H. Jiang, E. W. Uffman, *Tetrahedron* **2006**, *62*, 285. (c) X. Li, H. Jiang, E. W. Uffman, L. Guo, Y. Zhang, X. Yang, V. B. Birman, *J. Org. Chem.* **2012**, *77*, 1722. Recent review: (d) V. B. Birman, *Aldrichimica Acta.* **2016**, *49*, 23.

⁸⁸ T. Akiyama, K. Mori, *Chem. Rev.* **2015**, *115*, 9277.

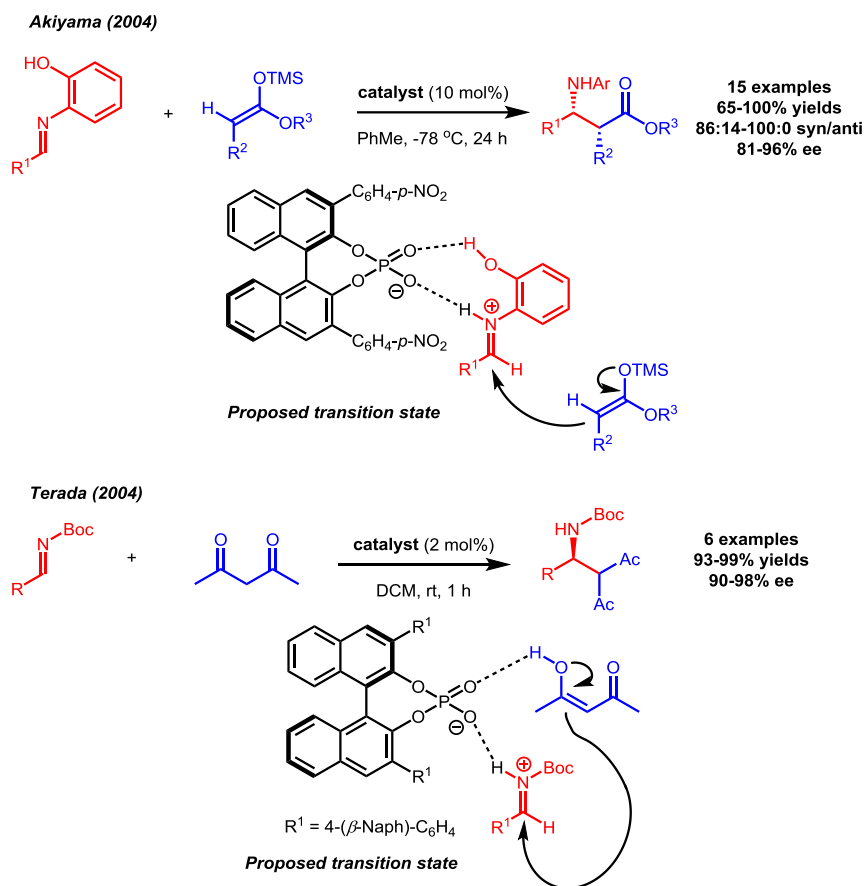


Scheme 1.40. Activation of different substrates through Brønsted acid catalysis

Brønsted acid catalysis is a well-developed area and many impressive transformations have been achieved, in which BINOL-derived chiral phosphoric Brønsted acids made a considerable impact. In the field of organic synthesis, the use of BINOL-derived phosphoric acid has been studied for more than 40 years, however their use as catalysts only sparked interest around 15 years ago.⁸⁹ Ground-breaking examples were reported in 2004 when the asymmetric Mannich reaction catalyzed by chiral phosphoric Brønsted acids was independently reported by the research groups of Akiyama and Terada. With BINOL-derived chiral phosphoric acids, the chiral amines were afforded in excellent enantioselectivity⁹⁰ (**Scheme 1.41**).

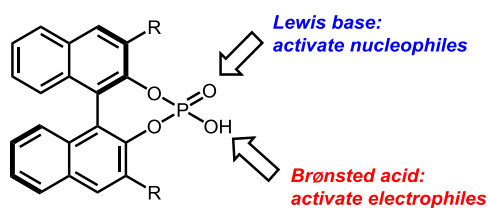
⁸⁹ D. Parmar, E. Sugiono, S. Raja, M. Rueping, *Chem. Rev.* **2014**, *114*, 9047.

⁹⁰ (a) T. Akiyama, J. Itoh, K. Yokota, K. Fuchibe, *Angew. Chem. Int. Ed.* **2004**, *43*, 1566. (b) D. Uraguchi, M. Terada, *J. Am. Chem. Soc.* **2004**, *126*, 5356. For a review on chiral phosphoric acid as asymmetric catalysts, see: (c) S. J. Connon, *Angew. Chem. Int. Ed.* **2006**, *45*, 3909.



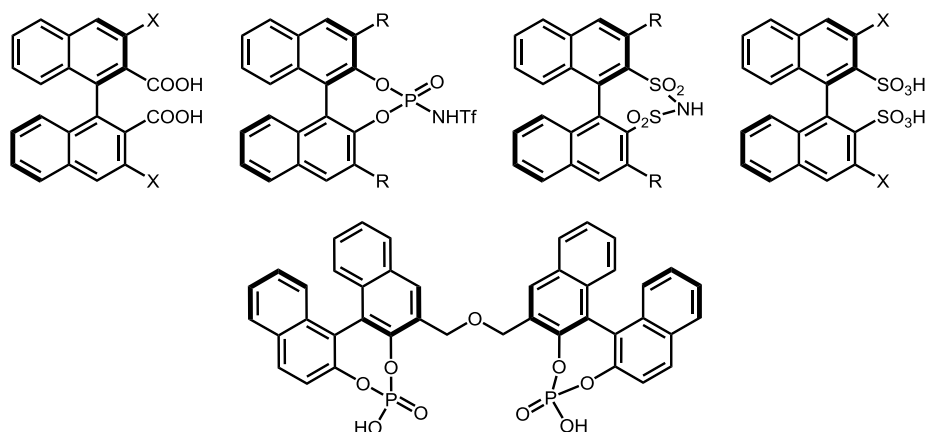
Scheme 1.41. Early examples of application of chiral phosphoric acids as organocatalysts

The success of these types hinges on the following properties^{90c}: 1) The structures of BINOL-derived chiral phosphoric acids are conformationally rigid and stereochemical information can be transferred from the axially chiral substituents onto the substrates; 2) The catalytic efficiency was based on a single acidic proton; and 3) The phosphoryl moiety could serve as a Lewis base, which results in more pre-organization via bi-functional activation of the nucleophilic and electrophilic elements (**Scheme 1.42**).



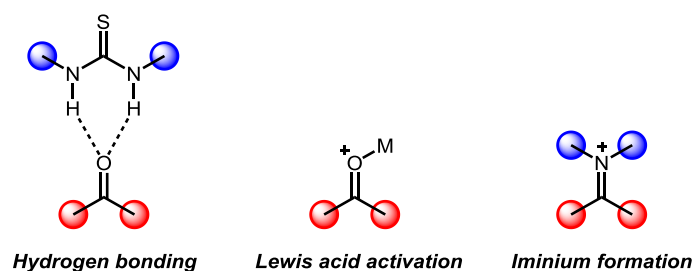
Scheme 1.42. Bi-functional activation via chiral phosphoric acid

These elegant reports formed the foundation for a new type of Brønsted acid catalyst. After their reports, a large number of chiral phosphoric-acid-catalyzed reactions were developed based on this electrophilic activation mode. Moreover, a range of BINOL-derived Brønsted-acid catalysts, such as dicarboxylic acids, disulfonic acids, and disulfonimides, were also developed^{88,89} (Scheme 1.43).



Scheme 1.43. Selected other chiral Brønsted acids

Other catalytic modes for electrophilic activation also had impressive achievements, such as hydrogen bonding, Lewis acid activation and iminium formation, *etc* (Scheme 1.44). However, these examples are not directly related to the current thesis, and will therefore not be discussed in this Chapter.



Scheme 1.44. Selected activation modes for electrophilic activation

1.4 Conclusion

As exemplified above, both carbonyl catalysis and electrophilic activation have made

contributions to the development of organocatalysis. Surprisingly, there are limited examples for the combination of these two activation modes. As will be discussed in the next chapters, the use of hydrolysis of organophosphorus compounds will be a suitable example to demonstrate the pathway to achieve 1) electrophilic activation via carbonyl catalysis; 2) carbonyl catalysis via the formation of transient intramolecular nucleophiles to accelerate the hydrolysis of organophosphorus compounds. Additionally, the further application of these methodologies will be applied to the field of prebiotic chemistry.

The reaction discussed in this thesis is the hydrolysis of two types of organophosphorus compounds. The acceleration for the hydrolysis reaction of P-N bond via carbonyl catalysis will be discussed in Chapter 2.

Chapter 2

Electrophilic activation via carbonyl catalysis: *o*-Phthalaldehyde catalyzed hydrolysis of organophosphinic amides and related compounds

2.1 Introduction

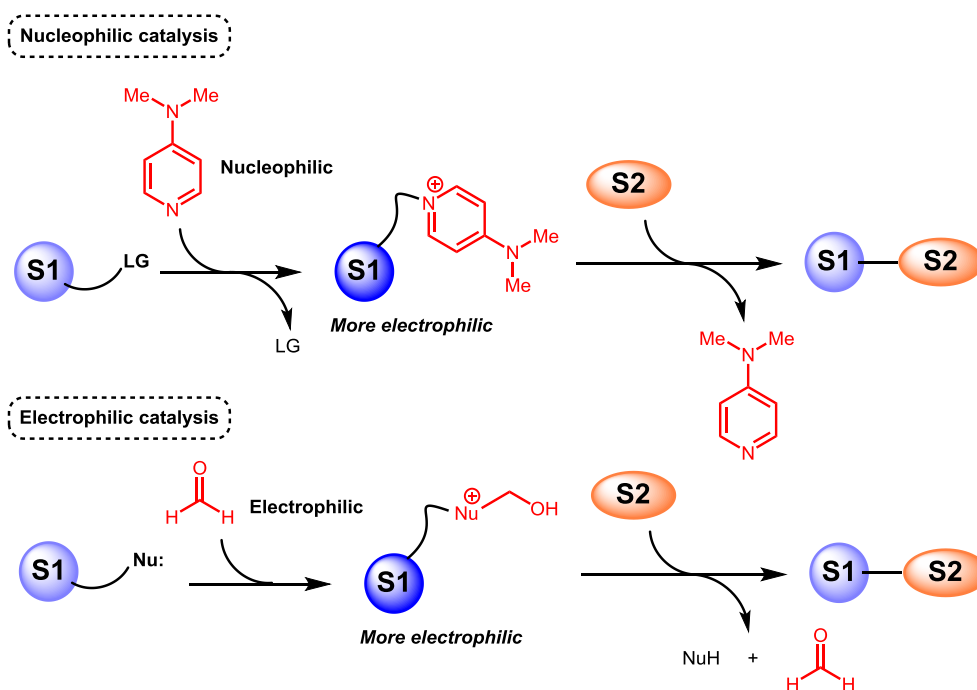
This chapter will focus on the combination of carbonyl catalysis and electrophilic activation to discover the *o*-phthalaldehyde as an efficient catalyst to promote the hydrolysis reaction of organophosphinic amides and other related compounds that contain the P(=O)-N motif. A comparison of reactivity and catalytic efficiency between *o*-phthalaldehyde and formaldehyde will also be presented. Notably, the chemoselective hydrolysis of the P(=O)-N bonds could be accomplished in the presence of P(=O)-O bonds. Eventually, preliminary efforts towards a kinetic resolution providing access to enantiopure materials were also made.

2.1.1 Electrophilic activation via carbonyl catalysis

As discussed in Chapter 1, separately, both carbonyl catalysis and electrophilic activation have allowed much progress in the field of organocatalysis. However, limited examples were described combining both of these strategies. Over 50 years ago, the pioneering work of Jencks and Gilchrist demonstrated that the hydrolysis of phosphoramidate could be catalyzed by formaldehyde.⁹¹ They proposed that this reaction was achieved via *electrophilic catalysis*. As discussed in Chapter 1,

⁹¹ W. P. Jencks, M. Gilchrist. *J. Am. Chem. Soc.* **1964**, 867, 1410.

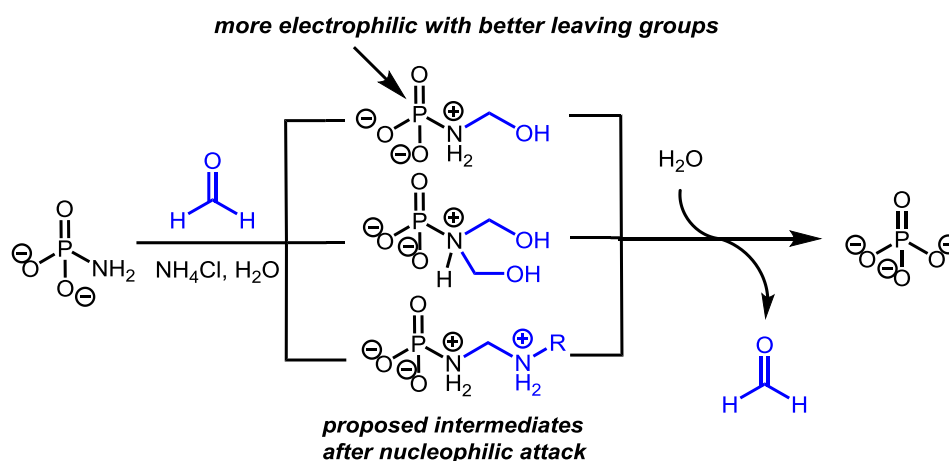
nucleophilic catalysis was well-known in the field of organocatalysis, especially with DMAP chemistry. In this context, catalysts, such as DMAP would attack the substrates to form unstable intermediates to achieve the overall electrophilic activation of the substrates (**Scheme 2.1**). However, *electrophilic catalysis* was less well known at that time. In general, substrates with a nucleophilic component would attack the catalysts, such as aldehydes to form more reactive intermediates. As a result, these intermediates were more electrophilic with a better leaving group towards the subsequent reactions (**Scheme 2.1**).



Scheme 2.1. Comparison between nucleophilic catalysis and electrophilic catalysis

Jencks and Gilchrist observed that in the presence of formaldehyde the hydrolysis of a phosphoramidate was accelerated. And this reaction was a true catalytic process with sub-stoichiometric amount of formaldehyde. They proposed that in the reaction system, the amino group on the substrate would attack the formaldehyde to form different protonated species, in which the phosphorus center was more electrophilic to undergo hydrolysis with a better leaving group as shown in **Scheme 2.2**. Therefore, the

electrophilic activation was achieved through formaldehyde catalysis. However, in their study only one inorganic substrate was studied in this reaction, therefore the universality of this catalytic system waited for further investigation, especially for organophosphorus compounds.

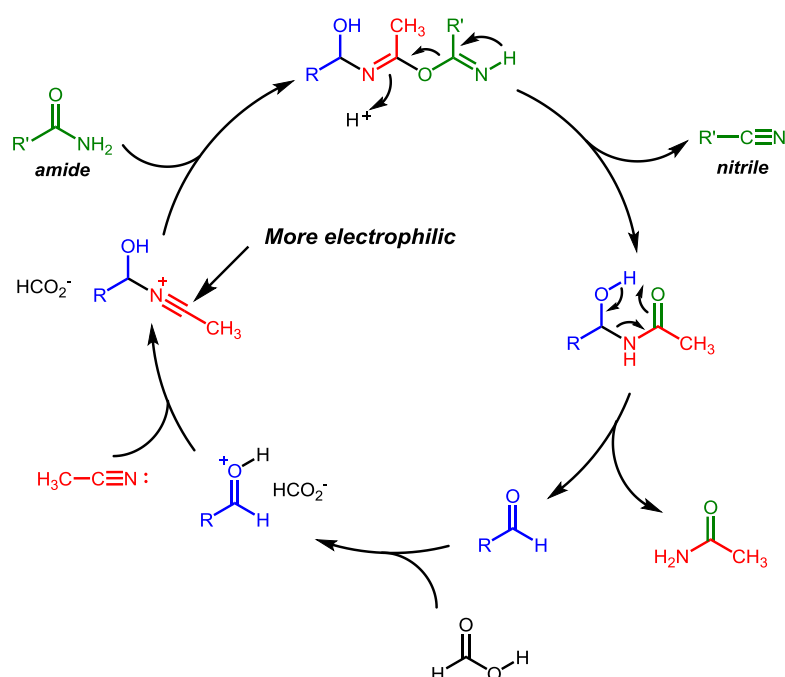


Scheme 2.2. Formaldehyde-catalyzed hydrolysis of phosphoramidate

Another example of electrophilic activation of acetonitrile via carbonyl catalysis was reported by Mioskowski and co-workers. They described the aldehyde-catalyzed conversion of primary amides to nitriles as shown in **Scheme 2.3**.⁹² They suggested a reaction mechanism in which the aldehyde acted as a relay for transferring water from the amide to acetonitrile which is the solvent in the reaction. First, the protonated aldehyde underwent nucleophilic attack by a molecule of acetonitrile forming the reactive nitrilium intermediate. This highly electrophilic species could then undergo a nucleophilic attack by primary amides. The following steps would generate the desired products. Notably, in this proposed mechanism, the initial steps were also the electrophilic activation of acetonitrile via aldehyde catalysis. However, it was necessary to mention that no clear evidence was observed for the formation of highly reactive nitrilium or other intermediates. Besides, the addition of formic acid could not be

⁹² M.-P. Heck, A. Wagner, C. Mioskowski, *J. Org. Chem.* **1996**, *61*, 6486.

replaced by other acids such as acetic and trifluoroacetic acid.



Scheme 2.3. Aldehyde catalyzed formation of nitriles from amides

As we can see, the electrophilic activation via carbonyl catalysis holds promise for the development of organocatalytic transformations, yet has received very little attention from the synthetic community. As a result of our continued interest in aldehyde-catalyzed reaction and the preliminary results from Jencks and Gilchrist, we decided to undertake a systematic study of the aldehyde-catalyzed transformation of organophosphorus compounds.

2.1.2 Importance of catalytic reactions of organophosphorus compounds

Phosphorus is the 11th most common element in Earth Crust, playing a fundamental but important role in biological systems. For example, for humans it is important for bone formation, cell membranes, the creation of DNA and others. Besides, in agriculture phosphorus is one the three nutrients (nitrogen, potassium and phosphorus) in

commercial fertilizer and its essential role for food production cannot be ignored. In academia, organophosphorus compounds made significant contributions to the development of organic chemistry, coordination chemistry, and organocatalysis, including the chiral phosphoric acids that were introduced in Chapter 1. Additionally, they are also valuable commodities for various industrial applications in the field of medicine, materials science, and drug discovery.⁹³ In Nature, phosphorus is largely distributed as calcium phosphate $\text{Ca}_5\text{X}(\text{PO}_4)_3$ ($\text{X} = \text{F}, \text{Cl}, \text{or OH}$), which drastically limited the organophosphorus compounds that exist naturally.⁹⁴ However, this gap did not prevent chemists from synthesizing organophosphorus compounds and utilizing them in various applications. The first example of an organophosphorus compound, β -aminoethyl phosphonic acid, was isolated in 1959 from rumen protozoa.⁹⁵ Since then, more and more approaches have been developed for the preparation of organophosphorus compounds, including recently the catalytic synthesis for the P-stereogenic containing compounds.

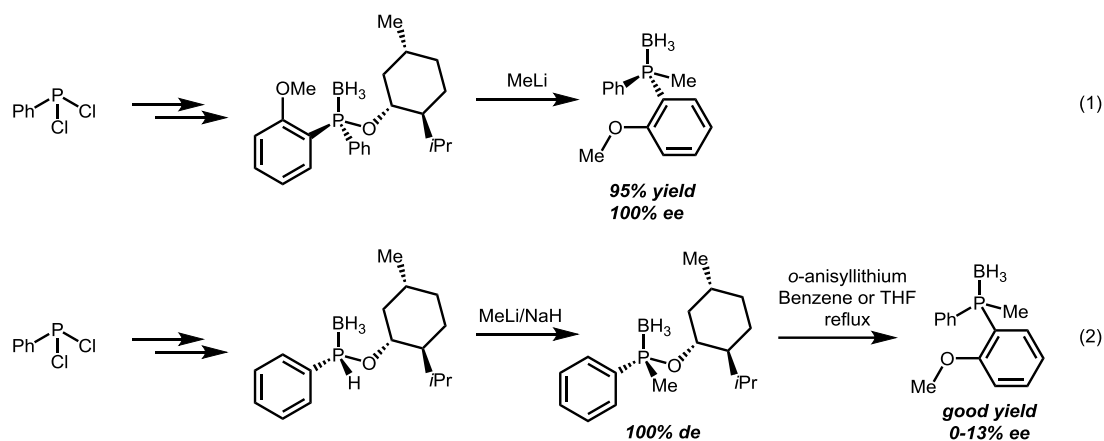
Previously, stoichiometric amounts of chiral auxiliaries were used for preparing P-stereogenic compounds. For example, optically active alcohols and amines were often applied to directly install the P-stereogenic center through nucleophilic substitution in excellent yields and stereocontrol⁹⁶ (**Scheme 2.4**, equation 1). However, depending on the reaction conditions, this reaction could suffer the erosion of the enantiomeric excess in some cases (**Scheme 2.4**, equation 2).

⁹³ Y.-M. Cui, Y. Lin, L.-W. Xu, *Coord. Chem. Rev.* **2017**, *330*, 37.

⁹⁴ M. Dutartre, J. Bayardon, S. Juge, *Chem. Soc. Rev.* **2016**, *45*, 5771.

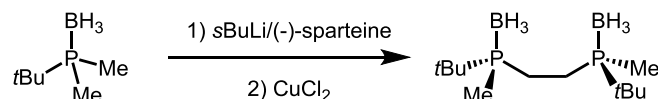
⁹⁵ M. Horiguchi, M. Kandatsu, *Nature* **1959**, *184*, 901.

⁹⁶ T. Imamoto, T. Oshiki, T. Onozawa, T. Kusumoto, K. Sato, *J. Am. Chem. Soc.* **1990**, *112*, 5244.



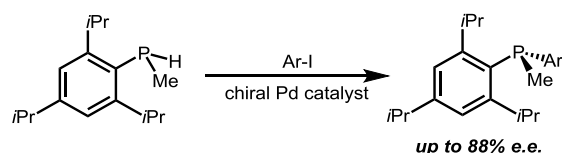
Scheme 2.4. Diastereoselective nucleophilic substitution for P-stereogenic compounds

Another conventional method to introduce the P-stereogenic center is via an enantioselective deprotonation. For example, starting from prochiral dimethylarylyphosphine boranes, then enantioselectively deprotonating of one of the methyl groups with a chiral sparteine-alkyllithium, eventually can lead to P-stereogenic compounds⁹⁷ (**Scheme 2.5**).



Scheme 2.5. Enantioselective deprotonation for P-stereogenic compounds

Moreover, desymmetrization or dynamic kinetic resolution by metallo-, organo- and biocatalytic asymmetric synthesis to make this type of P-stereogenic center is also an applicable strategy⁹⁸ (**Scheme 2.6**).

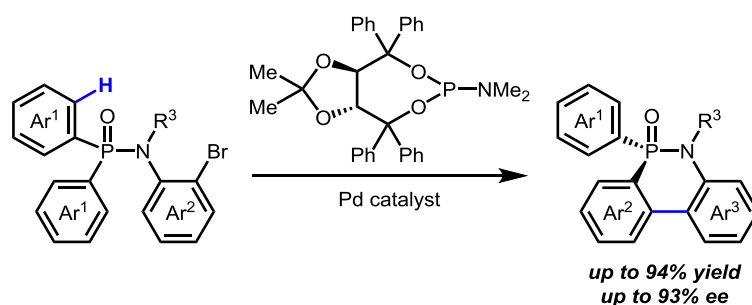


Scheme 2.6. Catalytic asymmetric arylation

⁹⁷ T. Imamoto, J. Watanabe, Y. Wada, H. Masuda, H. Yamada, H. Tsuruta, S. Matsukawa, K. Yamaguchi, *J. Am. Chem. Soc.* **1998**, *120*, 1635.

⁹⁸ N. F. Blank, J. R. Moncarz, T. J. Bruncker, C. Scriban, B. J. Anderson, O. Amir, D. S. Glueck, L. N. Zakharov, J. A. Golen, C. D. Incarvito, A. L. Rheingold, *J. Am. Chem. Soc.* **2007**, *129*, 6847.

Furthermore, C-H functionalization, which is more atom- and step-economic has started to gain traction in efforts to build different chiral organophosphorus compounds such as P-stereogenic compounds and axially chiral organophosphorus compounds. For example, in 2015, Duan and co-workers reported the asymmetric synthesis of P-stereogenic heterocycles in excellent yields and stereoselectivities via palladium-catalyzed enantioselective intramolecular C-H arylation. P-N cleavage could be accomplished using organolithium as nucleophiles without erosion of the enantiomeric ratio to prepare biaryl monophosphine oxides⁹⁹ (Scheme 2.7).



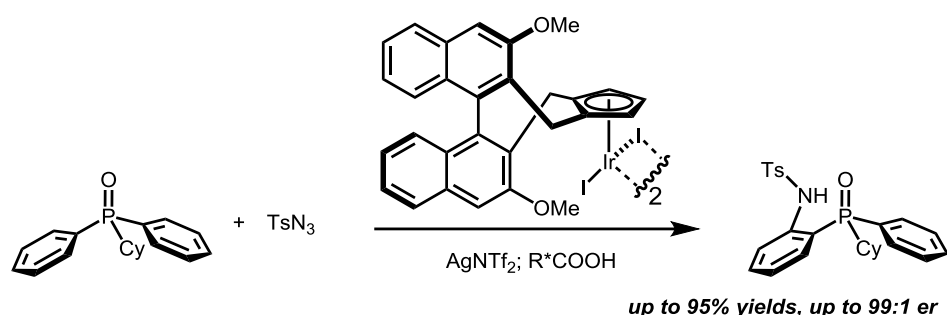
Scheme 2.7. A selected example for C-H activation to prepare P-chiral compounds

Another impressive contribution in C-H functionalization to build chiral phosphorus compounds was reported by Cramer and co-workers in 2017.¹⁰⁰ They utilized an efficient iridium (III) catalyst that bear an atropchiral cyclopentadienyl ligand to directly amidate phosphine oxides. The enantioselective transformation was enabled by the strong cooperative effect between the Cp^x ligand and a chiral carboxylic acid, phthaloyl *t*-leucine. As a result, chiral phosphorus compounds bearing a P-stereogenic center were formed with up to 95% yields and up to 99:1 er. Moreover, the subsequent enantiospecific reductive reaction provided the valuable P(III)-stereogenic compounds in good yields and excellent enantiomeric ratio. This type of the chiral phosphorus

⁹⁹ (a) Z.-Q. Lin, W.-Z. Wang, S.-B. Yan, W.-L. Duan, *Angew. Chem. Int. Ed.* **2015**, *54*, 6265. For a recent review for C-H functionalization to make chiral phosphorus compounds, see: (b) Y.-M. Cui, Y. Lin, L.-W. Xu, *Coord. Chem. Rev.* **2017**, *330*, 37.

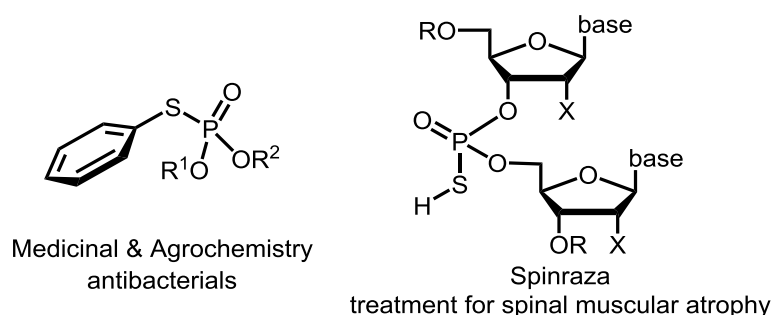
¹⁰⁰ Y.-S. Jang, M. Dieckmann, N. Cramer, *Angew. Chem. Int. Ed.* **2017**, *56*, 15088.

compounds could be applied as useful ligands and catalysts (**Scheme 2.8**).



Scheme 2.8. Ir-catalyzed reaction to build P-stereogenic compounds

Additionally, efforts have also been made to prepare another important class of P-stereogenic compounds, phosphorothioates, which are widely used as chiral catalysts. Meanwhile they are found in many important agrochemicals and top-selling pharmaceuticals such as Spinraza (\$ 125,000/dose) (**Scheme 2.9**).

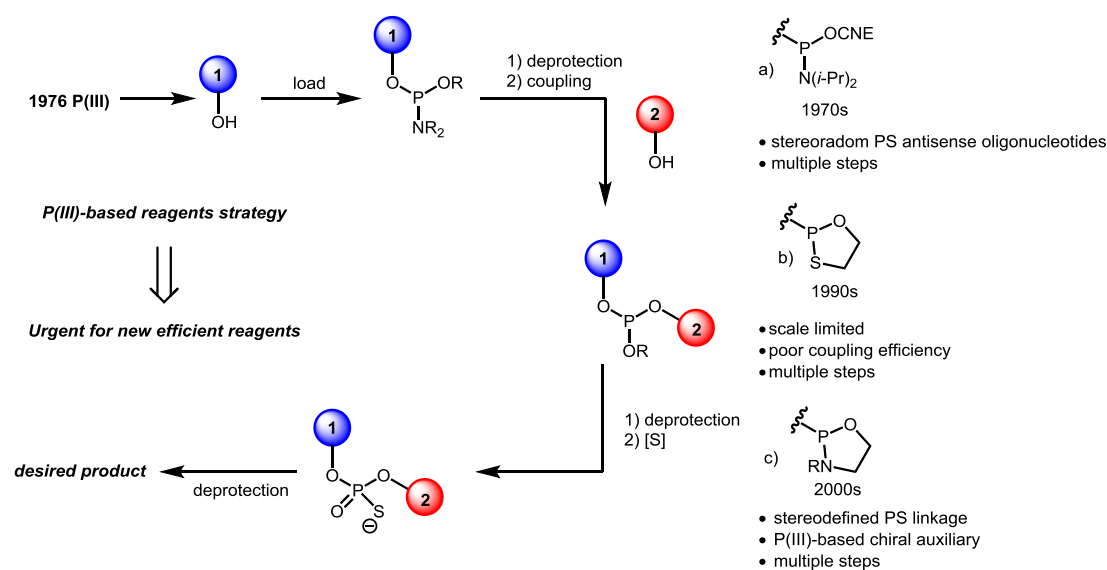


Scheme 2.9. Selected examples for useful phosphorothioates

However, the enantioselective synthesis of these species has been a long-standing problem in organic chemistry.¹⁰¹ For a long time, indirect multistep strategies were

¹⁰¹ (a) N. Iwamoto, D. C. D. Butler, N. Svrzikapa, S. Mohapatra, I. Zlatev, D. W. Y. Sah, Meena, S. M. Standley, G. Lu, L. H. Apponi, M. Frank-Kamenetsky, J. J. Zhang, C. Vargeese, G. L. Verdine, *Nat. Biotechnol.* **2017**, *35*, 845. (b) S. L. Beaucage, M. H. Caruthers, *Tetrahedron Lett.* **1981**, *22*, 1859. (c) M. H. Caruthers, in *Synthesis and Applications of DNA and RNA*, S. A. Narang, Ed. Academic Press, **1987**, pp. 47–94. (d) N. Oka, M. Yamamoto, T. Sato, T. Wada, *J. Am. Chem. Soc.* **2008**, *130*, 16031. (e) Y. Nukaga, K. Yamada, T. Ogata, N. Oka, T. Wada, *J. Org. Chem.* **2012**, *77*, 7913. (f) N. Oka, T. Kondo, S. Fujiwara, Y. Maizuru, T. Wada, *Org. Lett.* **2009**, *11*, 967. (g) W. J. Stec, A. Grajkowski, M. Koziolkiewicz, B. Uznanski, *Nucleic Acids Res.* **1991**, *19*, 5883. (h) W. J. Stec, A. Grajkowski, A. Kobylanska, B. Karwowski, M. Koziolkiewicz, K. Misiura, A. Okruszek, A. Wilk, P. Guga, M. Boczkowska, *J. Am. Chem. Soc.* **1995**, *117*, 12019. (i) W. J. Stec, B. Karwowski, M. Boczkowska, P. Guga, M. Koziolkiewicz, M. Sochacki, M. W. Wieczorek, J. Błaszczyk, *J. Am. Chem. Soc.* **1998**, *120*, 7156. (j) P. Guga, W. J. Stec, *Curr. Protoc. Nucleic Acid Chem.* **2003**, *14*, 4.17.1. (k) N. Iwamoto, N. Oka, T. Sato, T. Wada, *Angew. Chem. Int. Ed.* **2009**, *48*, 496. (l) R. P. Iyer, D. Yu, N.-H. Ho, W. Tan, S. Agrawal, *Tetrahedron Asymmetry* **1995**, *6*, 1051. (m) M. Guo, D. Yu, R. P. Iyer, S. Agrawal, *Bioorg. Med. Chem. Lett.* **1998**, *8*, 2539. (n) A. Wilk, A. Grajkowski, L. R. Phillips, S. L. Beaucage, *J. Am. Chem. Soc.* **2000**, *122*, 2149. (o) M. Li, H. L. Lightfoot, F. Halloy, A. L. Malinowska, C. Berk, A. Behera, D. Schümperli, J. Hall, *Chem. Commun.* **2017**, *53*, 541.

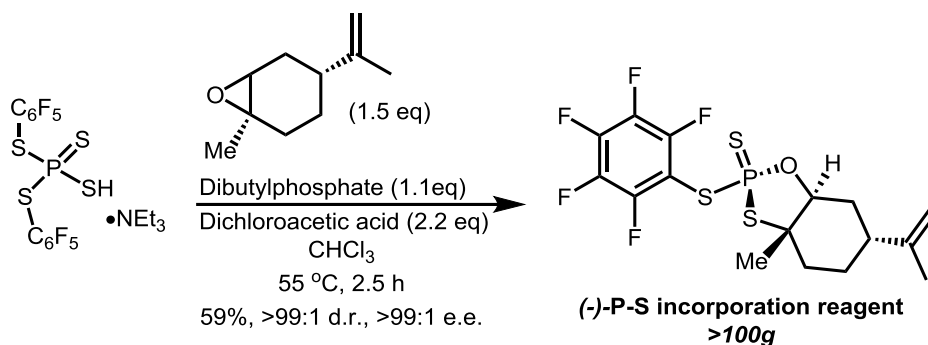
developed to obtain these compounds in enantiopure fashion. Such developments significantly relied on P(III)-based reagents (**Scheme 2.10**). Among these, easily scalable methods to prepare phosphorothioates faced the problem to achieve stereochemistry at phosphorus. On the other hand, when successful pathways to build P-stereogenic centers were developed, it was difficult to manufacture the designed products in large-scale manner (**Scheme 2.10**, reagents a, b and c).



Scheme 2.10. P(III)-based traditional methods towards phosphorothioates

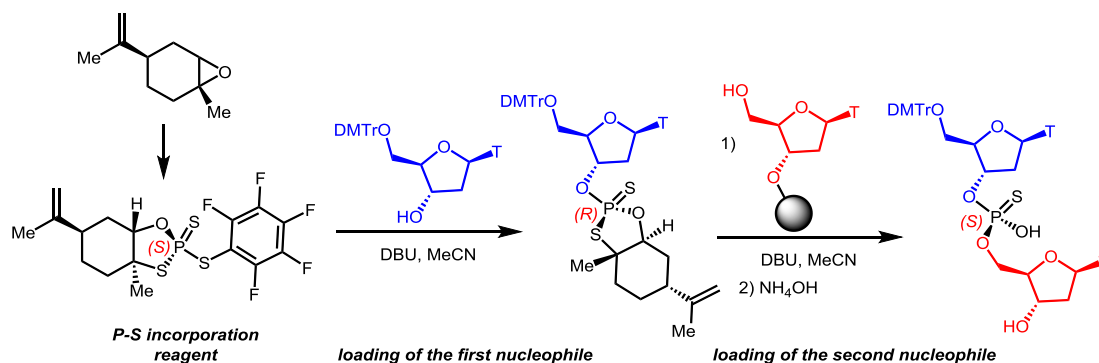
In 2018, a fundamentally different but groundbreaking method was described by Baran and co-workers to build chiral phosphorothioates.¹⁰² They developed a powerful limonene-derived P(V) phosphorus-sulfur incorporation reagent to directly afford chiral phosphorothioate oligonucleotides via auxiliary control (**Scheme 2.11**). This efficient P(V)-based chiral reagent is readily available from a 3-step sequence in large scale.

¹⁰² K. W. Knouse, J. N. deGruyter, M. A. Schmidt, B. Zheng, J. C. Vantourout, C. Kingston, S. E. Mercer, I. M. McDonald, R. E. Olsen, Y. Zhu, C. Hang, J. Zhu, C. Yuan, Q. Wang, P. Park, M. D. Eastgate, P. S. Baran, *Science* **2018**, *361*, 1234.



Scheme 2.11. P(V)-based chiral reagents from Baran

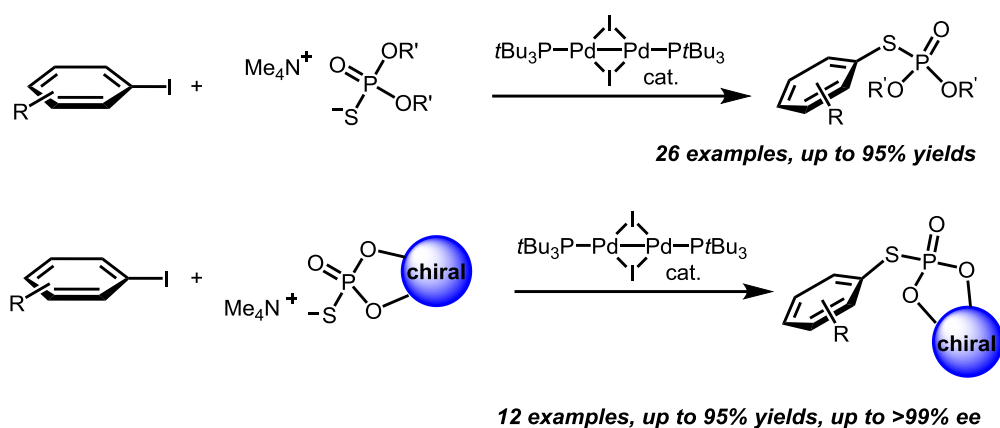
With this newly-discovered reagent, a variety of chiral phosphorothioate oligonucleotides were afforded in a stereocontrolled fashion through an inexpensive but efficient and operation-friendly process (**Scheme 2.12**).



Scheme 2.12. Selected example for the synthesis of chiral phosphorothioate oligonucleotides

More recently, Schoenebeck and co-workers successfully developed a catalytic system as a direct coupling strategy to prepare phosphorothioates.¹⁰³ This approach directly coupled the aryl iodides with phosphorothioate salts in the presence of dinuclear Pd(I) catalyst. Eventually, a variety of *S*-aryl phosphorothioates could be prepared with up to 95% yields. Meanwhile, they also employed chiral phosphorothioate salts under the reaction conditions. Gratifyingly, the chirality of the chiral phosphorothioate salts could be retained in the products with high functional group tolerance (**Scheme 2.13**).

¹⁰³ X.-Y. Chen, M. Pu, H.-G. Cheng, T. Sperger, F. Schoenebeck, *Angew. Chem. Int. Ed.* **2019**, *58*, 11395.



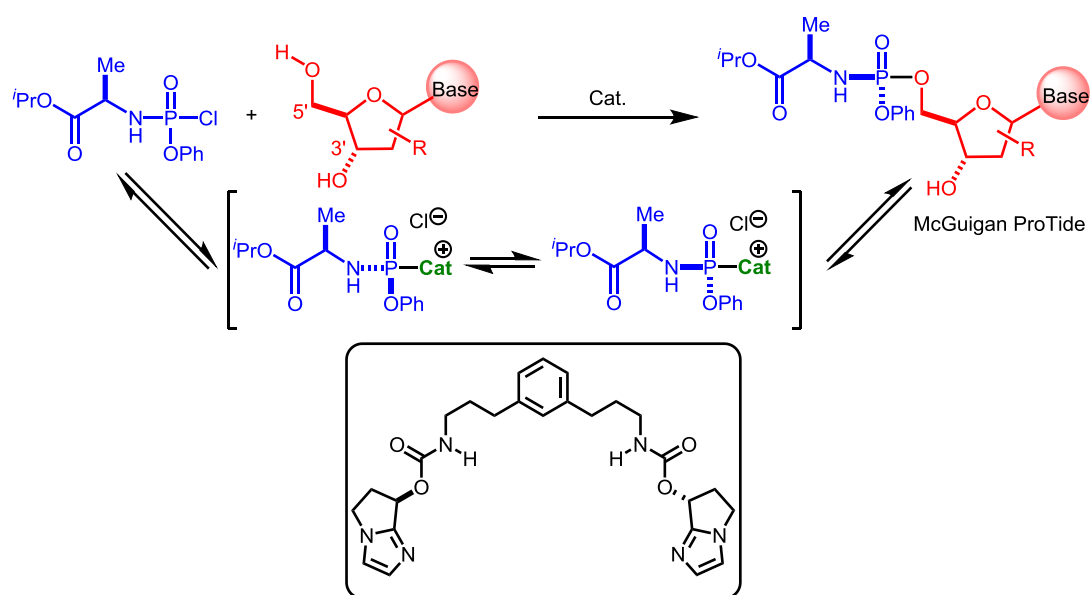
Scheme 2.13. Cross-coupling to afford *S*-aryl phosphorothioates

With all of these introduced approaches to achieve P-stereogenic compounds, there was a gap of a truly catalytic stereoselective protocol to afford this class of chiral compounds that could not be ignored. Notably, on the market, many antiviral and anticancer drugs are nucleosides.¹⁰⁴ Phosphorylation of the nucleoside is one of the important biological processes. In order to prepare these P-stereogenic prodrugs, traditional approaches were limited to the application of chiral phosphorylating reagents or chiral auxiliaries.¹⁰⁵ Finally, an example of a direct catalytic stereoselective process to install P-stereogenic phosphoramidates to nucleosides was reported in 2017^{105a} (**Scheme 2.14**). DiRocco and co-workers from Merck designed a practical small-molecule catalyst which could achieve high stereoselectivity at phosphorus to form P-O bonds. This process, which was in the absence of chiral auxiliaries, started from a racemic substance, then followed by nucleophilic attack with the catalyst to form a more electrophilic intermediate,

¹⁰⁴ L. P. Jordheim, D. Durantel, F. Zoulim, C. Dumontet, *Nat. Rev. Drug Discov.* **2013**, *12*, 447.

¹⁰⁵ (a) D. A. DiRocco, Y. Ji, E. C. Sherer, A. Klapars, M. Reibarkh, J. Dropinski, R. Mathew, P. Malignes, A. M. Hyde, J. Limanto, A. Brunskill, R. T. Ruck, L.-C. Campeau, I. W. Davies, *Science* **2017**, *356*, 426. For other catalytic reactions to prepare organophosphorus compounds, see: (b) J. S. Harvey, V. Gouverneur, *Chem. Commun.* **2010**, *46*, 7477. (c) M. Dutartre, J. Bayardon, S. Juge, *Chem. Soc. Rev.* **2016**, *45*, 5771. (d) Y. N. Ma, S. X. Li, S. D. Yang, *Acc. Chem. Res.* **2017**, *50*, 1480. (e) Y. Toda, M. Pink, J. N. Johnston, *J. Am. Chem. Soc.* **2014**, *136*, 14734. (f) Z. J. Du, J. Guan, G. J. Wu, P. Xu, L. X. Gao, F. S. Han, *J. Am. Chem. Soc.* **2015**, *137*, 632. (g) L. Liu, A. A. Zhang, Y. Wang, F. Zhang, Z. Zuo, W. X. Zhao, C. L. Feng, W. Ma, *Org. Lett.* **2015**, *17*, 2046. (h) R. Beaud, R. J. Phipps, M. J. Gaunt, *J. Am. Chem. Soc.* **2016**, *138*, 13183. (i) Z. Huang, X. Huang, B. Li, C. Mou, S. Yang, B. A. Song, Y. R. Chi, *J. Am. Chem. Soc.* **2016**, *138*, 7524. (j) K. M. Lim, T. Hayashi, *J. Am. Chem. Soc.* **2017**, *139*, 8122. (k) Y. N. Ma, M. X. Cheng, S. D. Yang, *Org. Lett.* **2017**, *19*, 600. (l) Y. Sun, N. Cramer, *Angew. Chem. Int. Ed.* **2017**, *56*, 364. (m) Z. Lian, B. N. Bhawal, P. Yu, B. Morandi, *Science* **2017**, *356*, 1059.

eventually would provide a chiral biologically active pronucleotide with excellent yields and enantioselectivities. The whole process to obtain enantiopurity completely relied on the catalyst under remarkably mild conditions. This small-molecular catalyst worked as a multifunctional catalyst, that in the transition state electrostatic stabilization, nucleophile activation and leaving group activation were all apparent. This example closely mimics how the enzymatic systems operate.



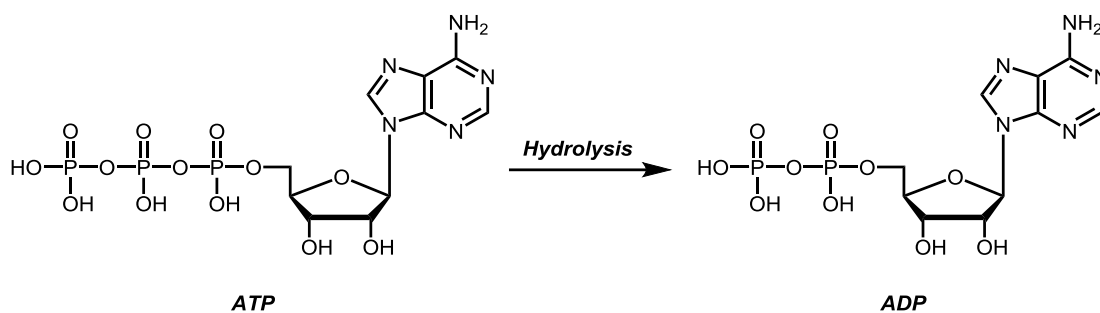
Scheme 2.14. Stereoselective synthesis of prodrugs

2.1.3 Importance of hydrolysis reaction

In chemistry and biochemistry, hydrolysis and hydration reactions are fundamentally important. In Nature, many different enzymes have evolved to catalyze these reactions, often with stereocontrol, under remarkably mild conditions.¹⁷ For example, Phospholipase A₂, the first recognized phospholipase, is a calcium-dependent enzyme to catalyze the cleavage of phospholipids to generate fatty acids and lysophospholipids.¹⁰⁶ ATPase, the sodium/potassium adenosine triphosphatase is an

¹⁰⁶ H. Wu, L. Yu, Y. Tong, A. Ge, S. Yau, M. Osawa, S. Ye, *Biochim. Biophys. Acta*, **2013**, 1828, 642

essential enzyme to catalyze the transformation from ATP to ADP (**Scheme 2.15**). This process is one of the well-known processes of dephosphorylation reaction to release energy.¹⁰⁷ Other reactive enzymes are also discovered for the hydrolysis of glycosides,¹⁰⁸ peptides¹⁰⁹ and DNA¹¹⁰.



Scheme 2.15. Hydrolysis of ATP to ADP with the release of energy

2.1.4 Hydrolysis of P(=O)-N bond

Hydrolysis of P(=O)-N bond has attracted intense attention because of their application as protecting groups for amines, amino acids and peptides.¹¹¹ At the same time, it was investigated as a remediation method to detoxify agrochemicals bearing this P(=O)-N motifs.¹¹² Previous studies have developed conventional conditions to accomplish this chemical transformation.

Acidic and basic conditions for hydrolysis of P(=O)-N motif

For instance, this hydrolysis could be achieved under strongly acidic conditions. The

¹⁰⁷ S. P. Gupta, *Chem. Rev.* **2012**, *112*, 3171

¹⁰⁸ (a) J. R. K. Cairns, A. Esen, *Cell. Mol. Life Sci.*, **2010**, *67*, 3389. (b) R. G. Spiro, *Cell. Mol. Life Sci.*, **2004**, *61*, 1025; (c) A. Ardevol, C. Rovira, *J. Am. Chem. Soc.* **2015**, *137*, 7528.

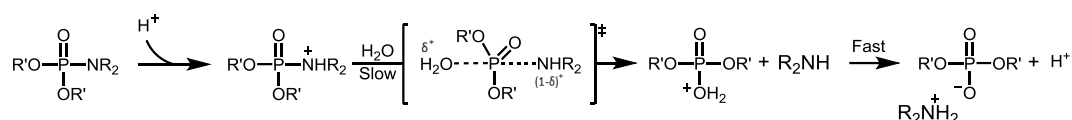
¹⁰⁹ (a) T. Nuijens, P. J. L. M. Quaedflieg, H.-D. Jakubke, in *Enzyme Catalysis in Organic Synthesis*, Drauz, Gröger and May, Eds, Wiley-VCH Verlag GmbH and Co. KGaA, Weinheim, **2012**, pp. 675–748. (b) M. S. Wolfe, *Chem. Rev.* **2009**, *109*, 1599. (c) J. Z. Long, B. F. Cravatt, *Chem. Rev.* **2011**, *111*, 6022.

¹¹⁰ (a) S. S. David, S. D. Williams, *Chem. Rev.* **1998**, *98*, 1221. (b) A. C. Drohat, C. T. Coey, *Chem. Rev.* **2016**, *116*, 12711.

¹¹¹ (a) P. G. M. Wuts, *Greene's Protective Groups in Organic Synthesis*, John Wiley & Sons, Inc., 5th edn, **2014**, p. 1083. (b) H. M. I. Osborn, J. B. Sweeney, B. Howson, *Synlett.* **1994**, 145.

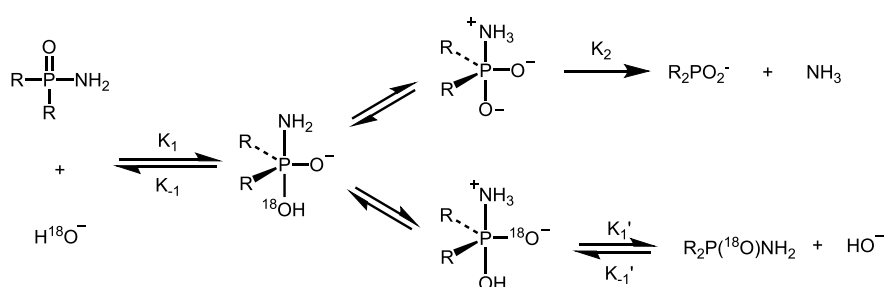
¹¹² A. W. Garrison, C. E. Boozer, *J. Am. Chem. Soc.* **1968**, *90*, 3486.

substrates were protonated in the acidic conditions to form more reactive intermediates with a better leaving group. A mechanism was suggested as below (**Scheme 2.16**). A bi-molecular transition state was proposed for this substitution process.¹¹³ It was shown experimentally that increased steric hindrance on nitrogen atom slowed down the reaction rate.



Scheme 2.16. Hydrolysis under acidic conditions

An important study for hydrolysis of P(=O)-N bonds under basic conditions was performed by Haake and Koizumi.¹¹⁴ Their investigation suggested that when a strong nucleophile such as hydroxide was used, hydrolysis of phosphinamides was no more reactive than carboxylic amides in basic conditions even at 90 °C. In other words, unactivated P(=O)-N bond was not labile towards nucleophilic attack. A penta-coordinate intermediate was suggested in the proposed mechanism (**Scheme 2.17**).



Scheme 2.17. Hydrolysis under basic conditions

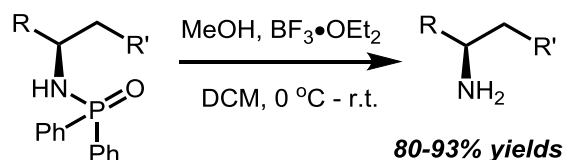
Lewis acid catalyzed hydrolysis of P(=O)-N motif

Lewis acids have also been used to perform the deprotection of *N*-diphenylphosphinyl

¹¹³ (a) M. J. P. Harger, *J. Chem. Soc., Perkin Trans.* **1977**, *1*, 605. (b) J. D. Chanley, E. Feageson, *J. Am. Chem. Soc.* **1958**, *80*, 2686. (c) J. D. Chanley, E. Feageson, *J. Am. Chem. Soc.* **1963**, *85*, 1181. (d) also see ref 111.

¹¹⁴ T. Koizumi, P. Haake, *J. Am. Chem. Soc.* **1973**, *95*, 8073.

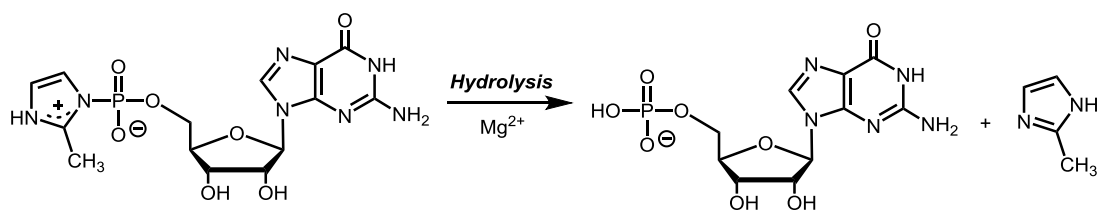
amines. Sweeney and Osborn^{11b} found that in the presence of methanolic boron trifluoride etherate, the deprotection of N-diphenylphosphinyl aziridines to break the P(=O)-N bond was achieved smoothly and provided functionalized amines in good yields (**Scheme 2.18**).



Scheme 2.18. Deprotection of diphenylphosphinyl group to afford free amines

Metal catalyzed hydrolysis of P(=O)-N motif

Metal-catalyzed hydrolysis of P(=O)-N motif of phosphoramidates have also attracted attention. Although it was not suitable for the development of green chemistry or metal-free catalytic approaches, metal catalyzed hydrolysis of P(=O)-N motif has found some useful applications. In 1989, Alberas and co-workers reported an example in which magnesium ion was able to catalyze the hydrolysis reaction of P(=O)-N bond in imidazolid-activated nucleotides¹¹⁵ (**Scheme 2.19**).

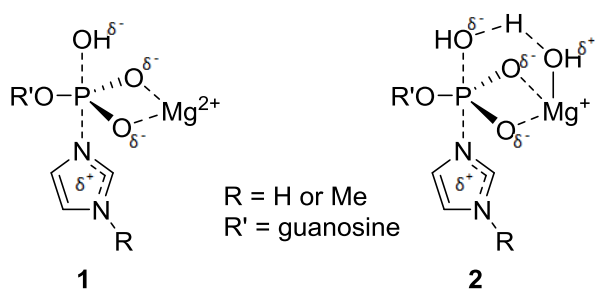


Scheme 2.19. Hydrolysis of imidazolid-activated nucleotides

In their study, two possible transition states were proposed, based on various experimental studies for this divalent magnesium catalyzed hydrolytic cleavage of P(=O)-N bond (**Scheme 2.20**). The stabilization of the first transition state was achieved

¹¹⁵ A. Kanavarioti, C. F. Bernasconi, D. L. Doodokyan, D. J. Alberas, *J. Am. Chem. Soc.* **1989**, *111*, 7247.

via the complexation of Mg^{2+} and the two phosphate oxygens. A repulsive interaction existed between the Mg^{2+} and a partial positive charge. The partial positive charge was in the imidazole moiety which was delocalized, and also served as an effective leaving group (**Scheme 2.20**, transition state **1**). It was also possible to realize the catalysis via the transition state **2**, implicating the reaction between substrate with $MgOH^+$. In contrast, besides the interaction of the Mg^{2+} with the phosphate oxygens as described for transition state **1**, transition state **2** also involved the induced intramolecularity, which was also previously reported by Herschlag and Jencks in the $MgOH^+$ -catalyzed hydrolysis of phosphorylated pyridines¹¹⁶ (**Scheme 2.20**, transition state **2**).

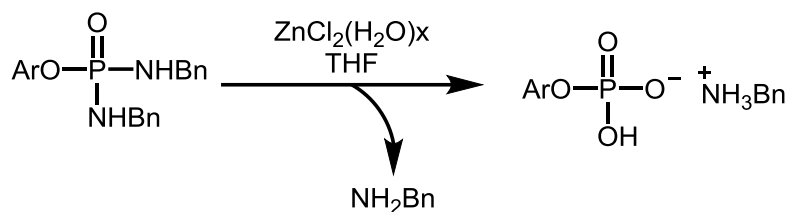


Scheme 2.20. Mg-catalyzed hydrolysis of imidazolide-activated nucleotides

More advances have been achieved for applying metals to catalyze hydrolysis of phosphoramidates.¹¹⁷ More recently, Rankumar and co-workers reported a $ZnCl_2$ -promoted hydrolysis of $P(=O)$ -N bonds of phosphoramidates in the presence of water, in which $ZnCl_2$ was suggested to serve as a mild Lewis acid (**Scheme 2.21**). However, the mono-hydrolysis of these compounds cannot be achieved under the reaction conditions.

¹¹⁶ D. Herschlag, W. P. Jencks, *Biochemistry* **1990**, *29*, 5172.

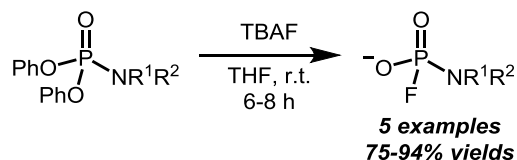
¹¹⁷ S. Kingsley, A. Vij, V. Chandrasekhar, *Inorg. Chem.* **2001**, *40*, 6057.



Scheme 2.21. Zn-catalyzed hydrolysis

Fluoride ion mediated hydrolysis

An interesting example of fluoride-ion-mediated hydrolysis of phosphoramidates was reported in 2008. Murai and co-workers found that when phosphoramidates were treated with TBAF, fluoride-ion-mediated hydrolysis would generate phosphoramidate fluoridic acid monoester salts as the product (**Scheme 2.22**). This means in the presence of fluoride source, the P(=O)-O ester bond was more labile than the P(=O)-N bond. However, the presence of fluoride in the final product limited the synthetic application of this approach to some extent. In addition, the cleavage of P(=O)-N bond cannot be targeted via this approach.¹¹⁸



Scheme 2.22. Fluoride ion mediated hydrolysis

These examples suggested that the hydrolysis of P(=O)-N amide bonds is challenging since conventional methods involved harsh conditions with strong acids or bases, or involved metal-based processes. Especially, forcing conditions made it difficult to determine the functional group compatibility of existing methods. Metal-catalyzed reactions were generally considered not to be environmentally-friendly. Given the

¹¹⁸ (a) T. Murai, T. Takenaka, S. Inaji, Y. Tonomura, *Chem. Lett.* **2008**, 37, 1198. For metallic promoted hydrolysis reaction, please see: (b) ref 116. (c) P. Malik, D. Chakraborty, V. Ramkumar, *Polyhedron* **2010**, 29, 2142.

importance of catalytic reactions to realize hydrolysis reactions especially for organophosphorus compounds, we decided to re-investigate the preliminary but promising work from Jencks and Gilchrist.⁹¹ With a comprehensive study on this aldehyde-catalyzed hydrolysis of phosphinic amides, we tried to broaden this reaction to hydrolyze organophosphorus compounds under mild conditions.

This development would have broader implications in aldehyde catalysis, should allow broad functional group compatibility and could potentially allow the hydrolysis of P(=O)-N amide bonds in the presence of P(=O)-O ester bonds. Moreover, such a strategy sets the foundation for the development of kinetic resolution making use of chiral aldehyde catalysis providing access to valuable P-chiral centers.

2.2 Results and discussion

The investigation started with two different model substrates that one was a primary phosphinic amide and the other was a secondary phosphinic amide. A series of surveys were performed to optimize the reaction conditions.

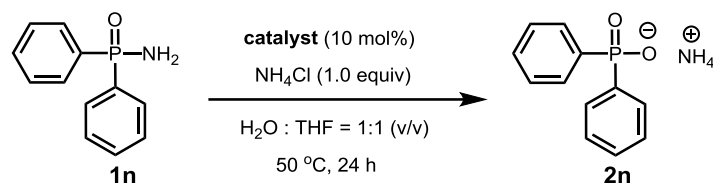
2.2.1 Optimization with primary phosphinic amide

The hydrolysis reaction was first tested with diphenylphosphinic amide **1n**, a simple primary phosphinic amide, as our model substrate. Gratifyingly, under conditions that are similar to those found in Jencks' report,⁹¹ the hydrolysis reaction of substrate **1n** occurred (**Table 2.1**), and the corresponding product was produced in 85% NMR yield in the presence of formaldehyde (10 mol%) and NH₄Cl (1.0 eq) in THF/H₂O at 50 °C. Delightfully, besides formaldehyde, other aldehydes such as glycolaldehyde (**3b**), glyoxylic acid (**3c**), and *o*-phthalaldehyde¹¹⁹ (**3f**) also showed good catalytic efficiency.

¹¹⁹ P. Schmidt, L. Zhou, K. Tishinov, K. Zimmermann, D. Gillingham, *Angew. Chem. Int. Ed.* **2014**, *53*, 10928.

In fact, the good reactivity demonstrated by *o*-phthalaldehyde attracted our attention especially when compared to the other two aromatic di-aldehyde **3g** (*meta*) and **3h** (*para*) that did not work for the hydrolysis reaction. These results indicated the ortho position relation was essential for the promoted catalytic activity.

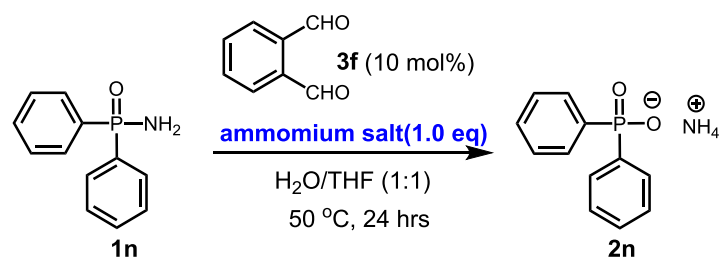
Table 2.1. Screening of catalysts for the hydrolysis of diphenylphosphinic amide **1n**^a



 3a 85%	 3b 77%	 3c 71%	 3d 45%	 3e 32%
 3f 83%	 3g NR	 3h NR	 3i 30%	 3j 23%
 3k 0.1 eq 15% 0.2 eq 57%	 3l 7%	 3m 6%	 3n 4%	 3o 3%

^a Reaction conditions: **1n** (0.2 mmol), NH_4Cl (0.2 mmol) and **catalyst** (0.02 mmol) in 0.2 mL of THF and 0.2 mL of H_2O at 50 °C for 24 h in a sealed tube. The yield was determined by ^1H NMR analysis using 1,3,5-trimethoxybenzene as an internal standard.

Considering the surprisingly good performance of *o*-phthalaldehyde, the further optimization of reaction conditions was carried on with *o*-phthalaldehyde as the catalyst. First, the optimization of the effect of the additive was investigated. As illustrated in **Table 2.2**, different ammonium salts were tested in the reaction. Both NH_4OTf and NH_4Cl proved efficient for the hydrolysis reaction, but NH_4OTf gave a slightly better result.

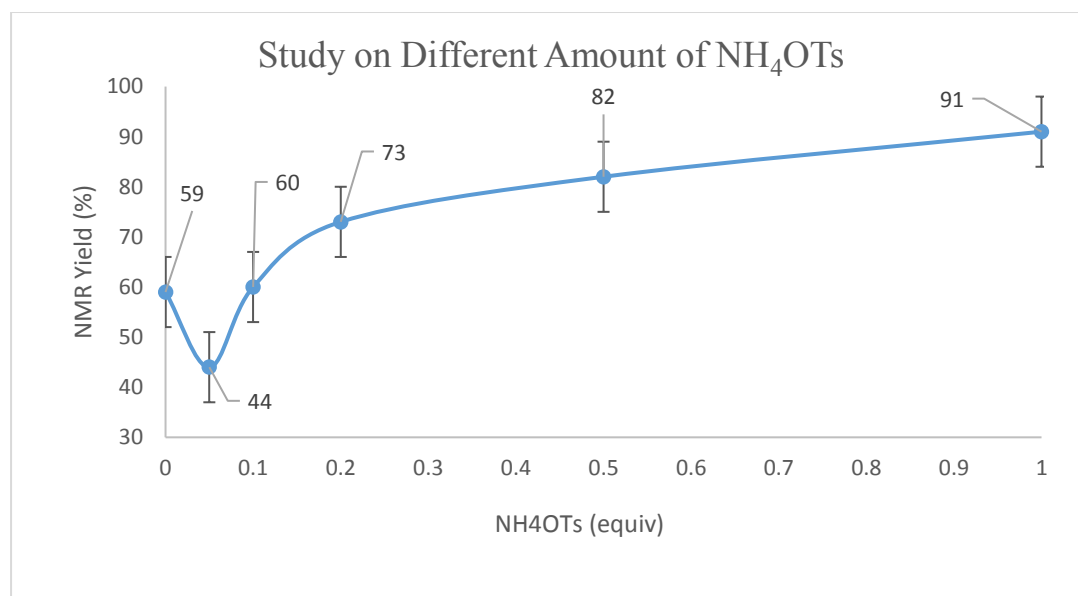
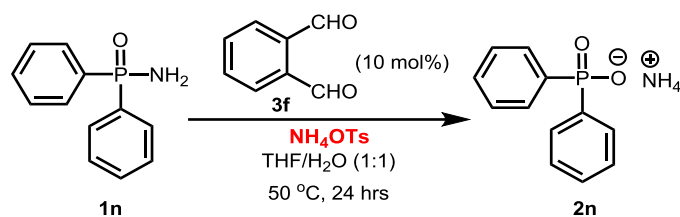
Table 2.2. Survey of additives of the hydrolysis of diphenylphosphinic amide **1n**^a

Entry ^a	Ammonium salt	Yield (%) ^b
1	NH₄OTs	91
2	NH ₄ Cl	83
3	NH ₄ I	74
4	NH ₄ OMs	70
5	NH ₄ OCOH	23
6	NH ₄ OAc	N.R.
7	NH ₄ OH	N.R.

^a Reaction conditions: **1n** (0.2 mmol), **ammonium salt** (0.2 mmol) and **3f** (0.02 mmol) in 0.2 mL of solvent and 0.2 mL of H₂O at 50 °C for 24 h in a sealed tube. ^b Determined by ¹H NMR analysis using 1,3,5-trimethoxybenzene as an internal standard.

Next, the study on the amount of NH₄OTs was then performed. Effort was made to realize the reaction with a catalytic amount of the additive. As we can see from **Scheme 2.23**, the reaction occurred even without the help of NH₄OTs. However, catalytic amounts of the NH₄OTs resulted in a decrease reaction rate. This study demonstrated the necessity to perform the reaction with stoichiometric amount of the NH₄OTs.

Scheme 2.23. Study on the amount of NH₄OTs

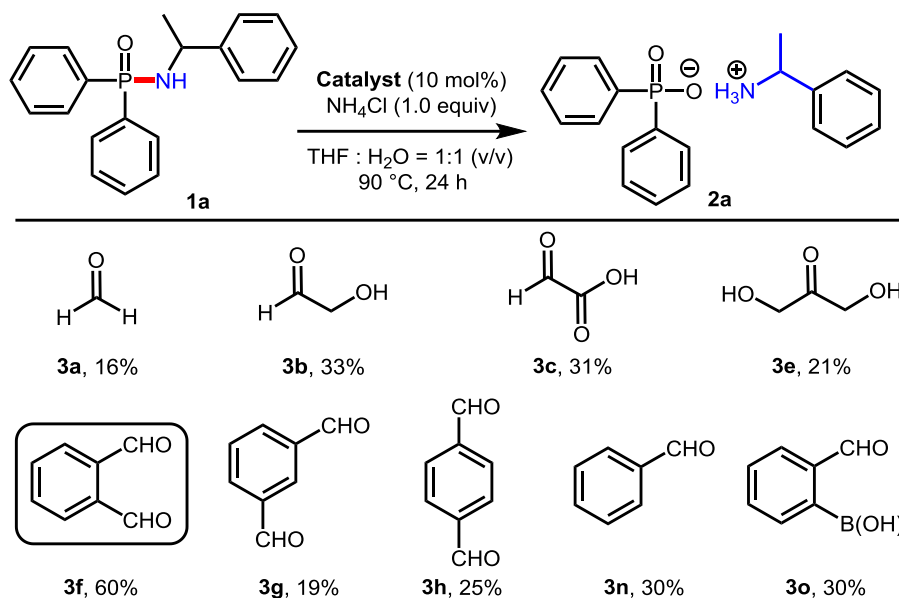


^aReaction conditions: **1n** (0.2 mmol), NH₄OTs and **3f** (0.02 mmol) in 0.2 mL of THF and 0.2 mL of H₂O at 50 °C for 24 h in a sealed tube. The yield was determined by ¹H NMR analysis using 1,3,5-trimethoxybenzene as an internal standard.

2.2.2 Optimization with secondary phosphinic amide

The results from primary phosphinic amide **1n** served as a guideline to continue further investigation for secondary phosphinic amides. Therefore, efforts were made to continue investigation of the optimal reaction conditions for secondary phosphinic amides (Table 2.3).

Table 2.3. Screening of possible catalysts for the hydrolysis of diphenylphosphinic amide^a



^a Reaction conditions: **1a** (0.2 mmol), NH₄Cl (0.2 mmol) and **3** (0.02 mmol) in 0.2 mL of THF and 0.2 mL of H₂O at 90 °C for 24 h in a sealed tube. The yield was determined by ¹H NMR analysis using 1,3,5-trimethoxybenzene as an internal standard.

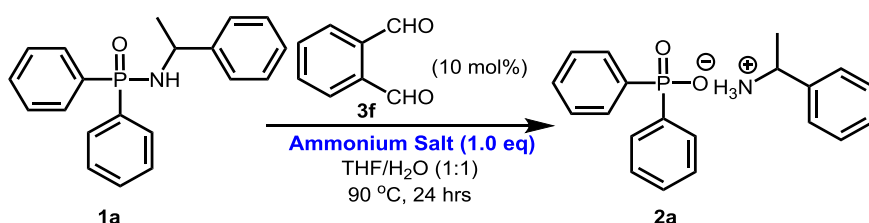
The studies started with a hindered substrate *P,P*-diphenyl-*N*-(1-phenylethyl)phosphinic amide **1a** as a model substrate to further investigate the catalytic activity of potential aldehyde catalysts (**Table 2.3**). However, the formaldehyde-catalyzed hydrolysis reaction with secondary phosphinic amides did not perform as expected. As shown in **Table 2.3**, the hydrolysis reaction of **1a** did occur however, the NMR yield for the corresponding product was 16% even at an increased temperature, 90 °C. Considering the steric hindrance around nitrogen atom, formaldehyde (**3a**) was not the only catalyst that suffered from the low catalytic activity. Glycolaldehyde (**3b**) and glyoxylic acid (**3c**) had a slight improvement, but unacceptable efficiency. Dihydroxyacetone **3e**, benzaldehyde **3n**, and 2-formylbenzeneboronic acid **3o**¹²⁰ also worked to a similar extent. However, surprisingly, *o*-phthalaldehyde (**3f**), standing out from other aldehydes, improved this

¹²⁰ P. Schmidt, C. Stress, D. Gillingham, *Chem. Sci.* **2015**, *6*, 3329.

reaction significantly with this hindered secondary phosphinic amide. The other two aromatic aldehydes **3g** and **3h** did not perform the reaction as efficiently as **3f**.

Considering these results for both primary and secondary phosphinic amides together, *o*-phthalaldehyde was identified as a more reactive catalyst for this hydrolysis reaction to cleave P(=O)-N amide bonds. Therefore, optimization was continued using *o*-phthalaldehyde as the optimal catalyst for this hydrolysis reaction. Further optimization of this reaction system was then performed. First, optimization of different additives was screened (**Table 2.4**).

Table 2.4. Survey of additives for the hydrolysis of diphenylphosphinic amide **1a**^a



Entry ^a	Ammonium salt	Solvent	Yield (%) ^b
1	NH ₄ Cl	THF	60
2	MeNH ₂ •HCl	THF	40
3	Pyrrolidine•HCl	THF	42
4	(<i>n</i> -Bu) ₃ N•HCl	THF	52
5	NH₄OTs	THF	75
6	NH ₄ OAc	THF	10
7	NH ₄ OCOH	THF	N.R.
8	-	THF	36

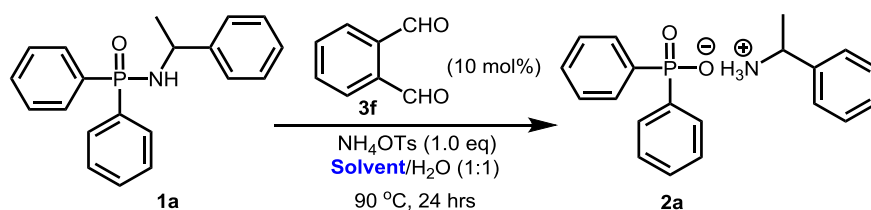
^aReaction conditions: **1a** (0.2 mmol), **ammonium salt** (0.2 mmol) and **3f** (0.02 mmol) in 0.2 mL of solvent and 0.2 mL of H₂O at 90 °C for 24 h in a sealed tube. ^bDetermined by ¹H NMR analysis using 1,3,5-trimethoxybenzene as an internal standard.

It was clearly demonstrated that the hydrolysis reaction benefited from the addition of NH₄Cl (**Table 2.4**, entries **1** and **8**). Other modification of the additive from ammonium salts to amine-derived salts such as primary, secondary and tertiary amines did not significantly improve the reaction (**Table 2.4**, entries **2**, **3** and **4**). Other ammonium salts were also tested for the hydrolysis reaction. It was interesting to find that the reaction

was slightly dependent on the nature of the counteranion. The higher acidity of the conjugate acid, the better activity (**Table 2.4**, entries **1**, **5-7**). In the survey for both primary and secondary phosphinic amides, NH₄OTs worked more efficiently than other additives to improve the reactions.

Screening for solvent effects revealed acetonitrile as the best solvent for this catalytic reaction (**Table 2.5**, entries **1-5**). The process was further improved by increasing the amount of *o*-phthalaldehyde to 20 mol% and the corresponding phosphinic acid could be isolated in 91% yield (**Table 2.5**, entry **6**). Importantly, it is worth mentioning that in the absence of *o*-phthalaldehyde, only trace amount of the product was detected (**Table 2.5**, entry **7**). This highlights the crucial role of the *o*-phthalaldehyde, allowing the reaction to proceed.

Table 2.5. Solvent effects screening for the hydrolysis of diphenylphosphinic amide **1a**^a



Entry ^a	Ammonium salt	Solvent	Yield (%) ^b
1	NH ₄ OTs	THF	75
2	NH ₄ OTs	DMF	38
3	NH ₄ OTs	DMSO	59
4	NH ₄ OTs	1,4-Dioxane	69
5	NH ₄ OTs	MeCN	82
6^c	NH₄OTs	MeCN	99 (91)^d
7 ^e	NH ₄ OTs	MeCN	4

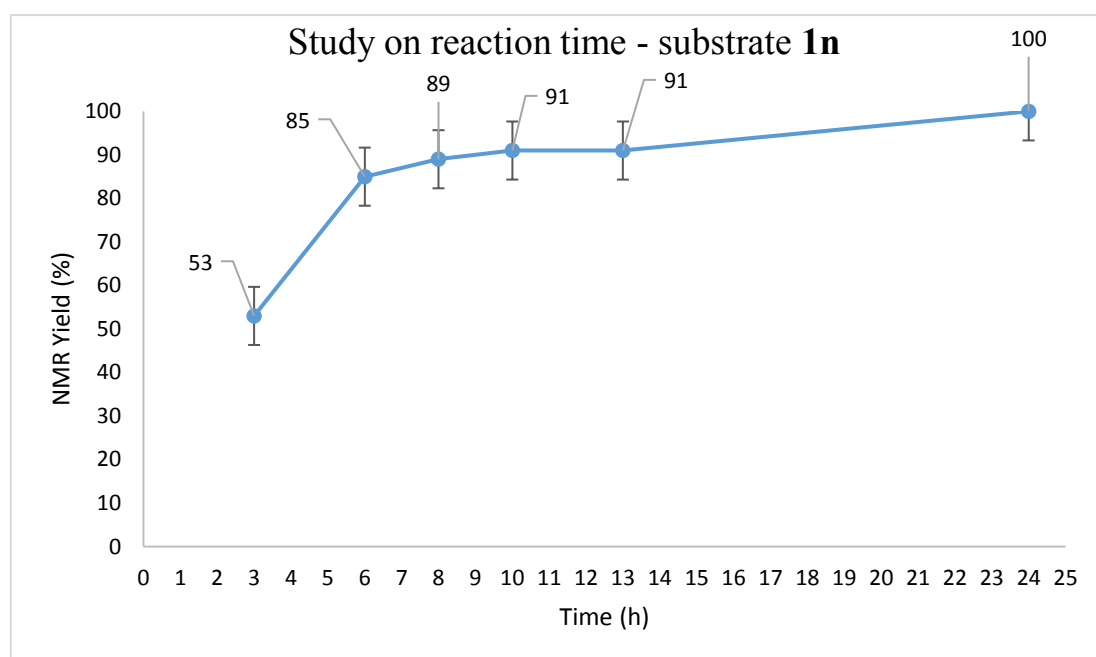
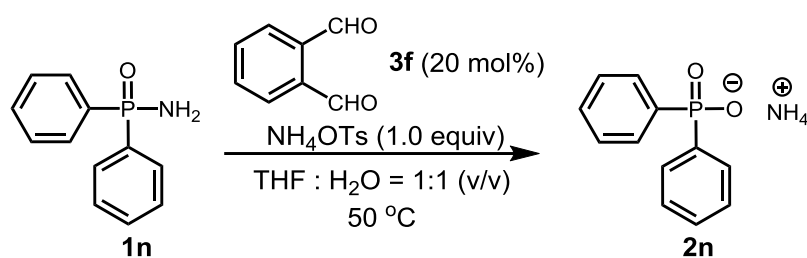
^a Reaction conditions: **1a** (0.2 mmol), NH₄OTs (0.2 mmol) and **3f** (0.02 mmol) in 0.2 mL of solvent and 0.2 mL of H₂O at 90 °C for 24 h in a sealed tube. ^b Determined by ¹H NMR analysis using 1,3,5-trimethoxybenzene as an internal standard. ^c **3f** (0.04 mmol) was used. ^d Isolated yield based on diphenylphosphinic acid. ^e Without *o*-phthalaldehyde.

2.2.3 Reaction time monitoring

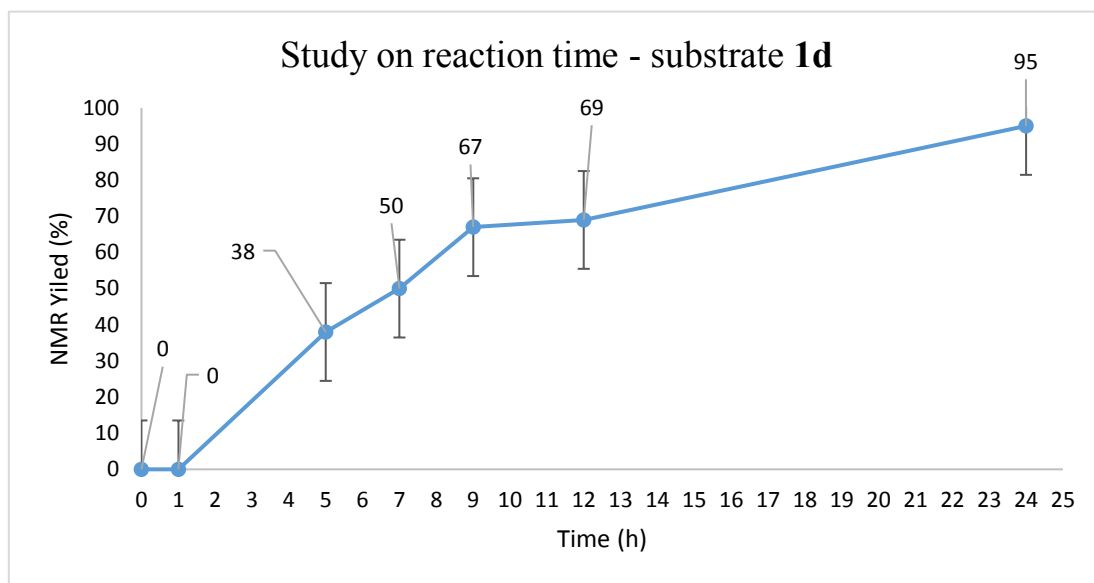
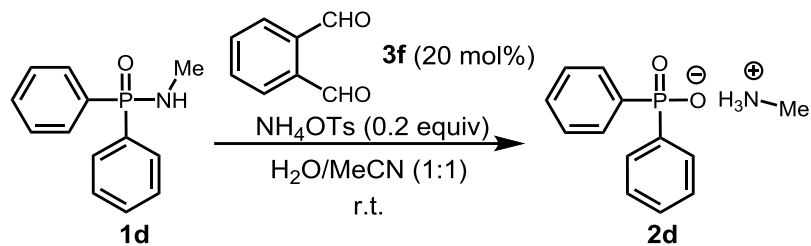
In order to have a better understanding about the reaction time, this reaction was

monitored for the period of 24 hours (**Table 2.6**). First the reaction was monitored for the primary substrate with the standard conditions. As we can see from the NMR study, the reaction was reasonably efficient and could achieve excellent yields in only several hours. However, for the other two secondary substrates, the reaction needed 24 hours to achieve excellent reactivity.

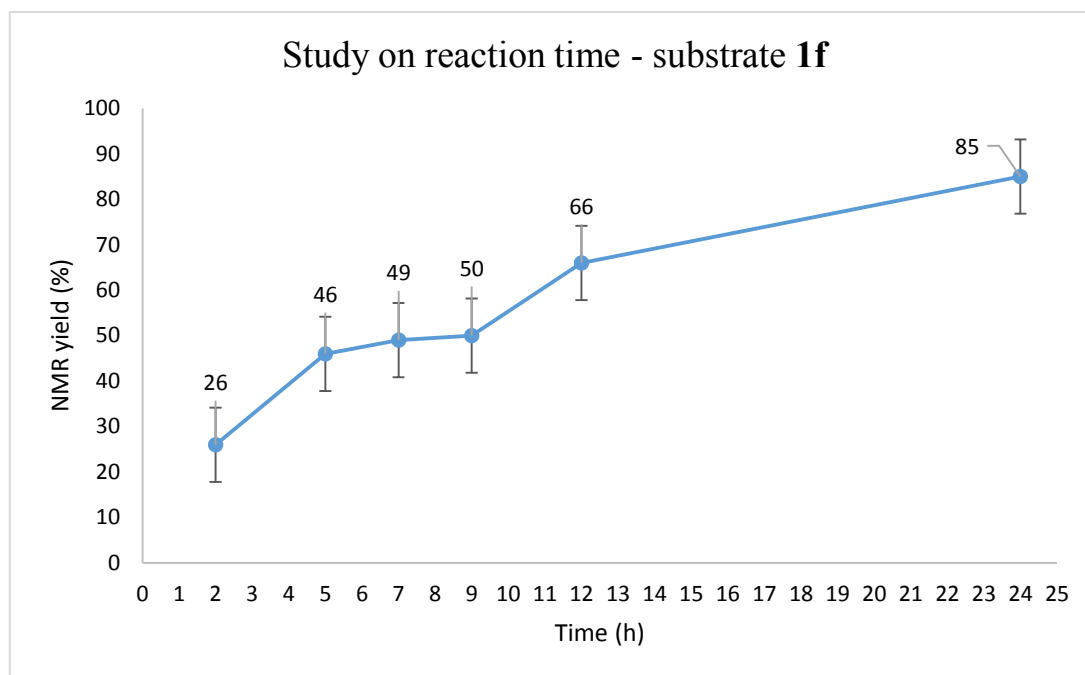
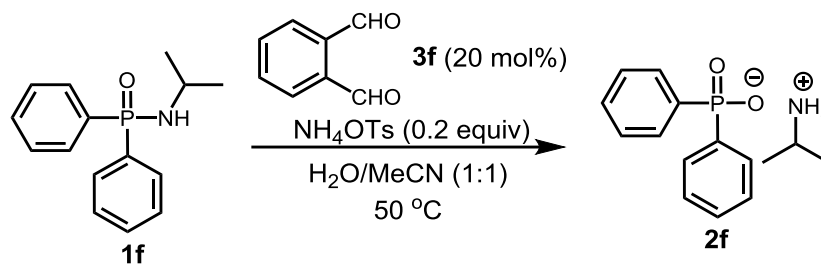
Table 2.6. Monitor the reaction time.



Reaction conditions: **1n** (0.2 mmol), NH_4OTs (0.2 mmol) and **3f** (0.04 mmol) in 0.2 mL of THF and 0.2 mL of H_2O at 50 °C for 24 h in a sealed tube. The reaction was monitored by ^1H NMR analysis using 1,3,5-trimethoxybenzene as an internal standard.



Reaction conditions: **1d** (0.2 mmol), NH_4OTs (0.04 mmol) and **3f** (0.04 mmol) in 0.2 mL of MeCN and 0.2 mL of H_2O at r.t. for 24 h in a sealed tube. The reaction was monitored by ^1H NMR analysis using 1,3,5-trimethoxybenzene as an internal standard.



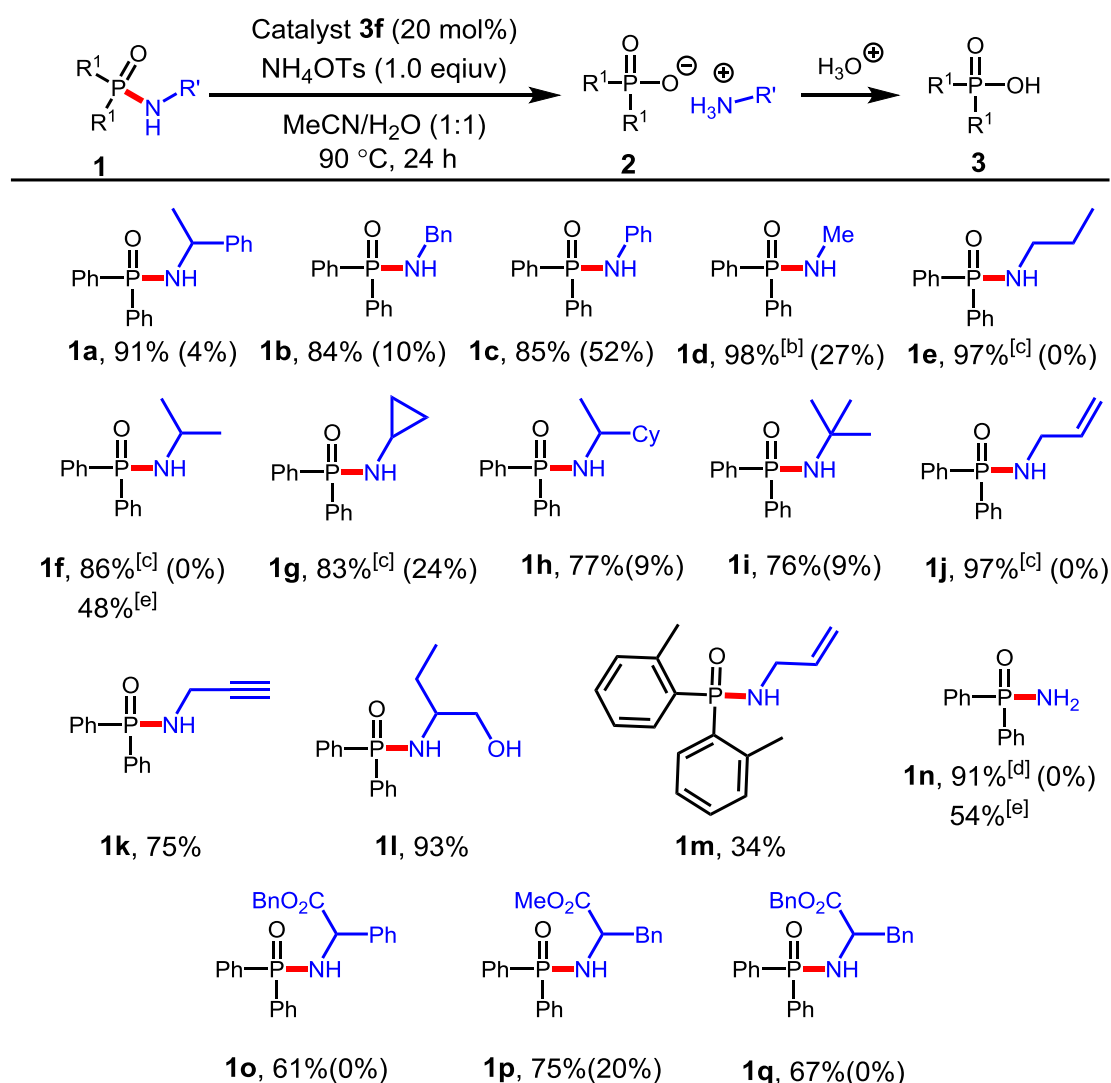
Reaction conditions: **1f** (0.2 mmol), NH_4OTs (0.04 mmol) and **3f** (0.04 mmol) in 0.2 mL of MeCN and 0.2 mL of H_2O at $50\text{ }^\circ\text{C}$ for 24 h in a sealed tube. The reaction was monitored by ^1H NMR analysis using 1,3,5-trimethoxybenzene as an internal standard.

2.2.4 Substrate scope for the hydrolysis reaction

With the identified optimal conditions in hand, we continued to investigate the universality of the hydrolysis reaction by testing different organophosphorus compounds containing P(=O)-N motif. These results are summarized in **Table 2.7**, which clearly showed the yields for the hydrolysis reactions. In parallel, the results for the corresponding control experiments in the absence of *o*-phthalaldehyde were shown in the parentheses in **Table 2.7**. Some of the substrates, such as **1h**, **1o**, **1p**, **1q**, **1s**, **1w**, **1v**, **1x** and **1y** were prepared with the help of a very talented undergraduate student, Mr. Ryan Simard who was under my supervision for an honor's project. Control

experiments with substrates **1a**, **1h** and **1q** were performed by Ryan Simard. The isolation process for the purification of the product was also carefully discovered by Ryan Simard. As shown in **Table 2.7**, a variety of diphenyl phosphinic amides were hydrolyzed efficiently in the catalytic system, provided isolated products in good yields.

Table 2.7. Substrate scope for the catalytic hydrolysis of P(=O)-NHR reagents, including control experiments for selected substrates in the absence of *o*-phthalaldehyde^a



^a Reaction conditions: **1** (0.2 mmol), NH₄OTs (0.2 mmol) and **3f** (0.04 mmol) in 0.2 mL of solvent and 0.2 mL of H₂O at 90 °C for 24 h in a sealed tube. NMR yields between parentheses are related to similar reactions performed without adding **3f**. Amine component of hydrolysis reaction of **1a** was isolated in 87% yield. ^b NH₄OTs (0.04 mmol) was used at r.t. ^c NH₄OTs (0.04 mmol) and **3f** (0.04 mmol) were used at 50 °C. ^d Performed in THF (0.2 mL) and H₂O (0.2 mL) at 50 °C. ^e Performed at room temperature with 0.2 mL of MeCN and 0.2 mL of H₂O.

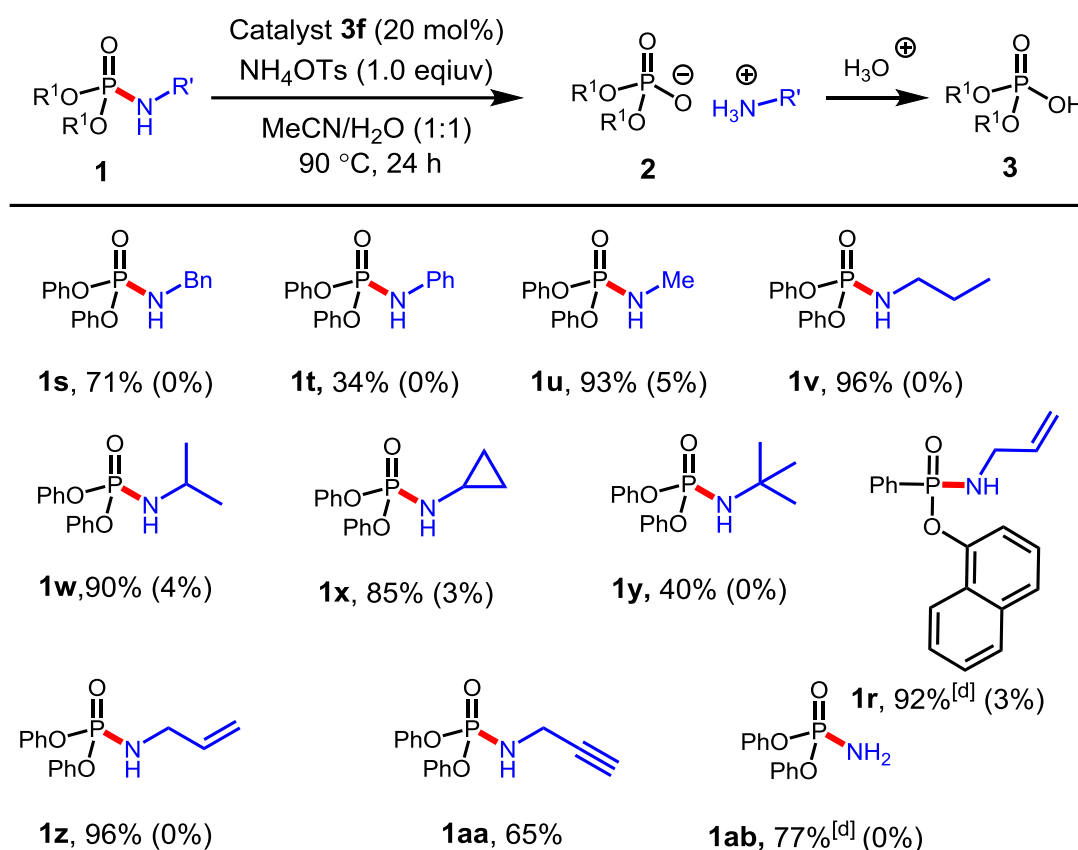
As shown in **Table 2.7**, substrates that contained aromatic groups on the nitrogen

substituent, such as *N*-phenylethyl- (**1a**), *N*-benzyl- (**1b**) and *N*-phenyl- (**1c**) diphenyl phosphinic amides, could be efficiently hydrolyzed in high yields (84-91%). The big difference between the reactions and the control experiments demonstrated necessity of using *o*-phthalaldehyde as catalyst (4-52% in the absence of *o*-phthalaldehyde *Vs* 84-91% with *o*-phthalaldehyde for substrates **1a**, **1b** and **1c**). Other substrates having alkyl groups on the nitrogen atom were also amenable to the transformation. For instance, *N*-methyl diphenyl phosphinic amide (**1d**) could undergo the hydrolysis reaction at room temperature with catalytic amount of both *o*-phthalaldehyde and NH₄OTs, providing the diphenyl phosphinic acid in 98% yield, which demonstrated much better reactivity than the control experiment. Diphenyl phosphinic amides with *N*-propyl- (**1e**), *N*-isopropyl- (**1f**), and *N*-cyclopropyl- (**1g**) substituents could be hydrolyzed even with catalytic amount of NH₄OTs under relatively mild conditions (50 °C). Other substrates containing hindered groups on nitrogen atom **1h** and **1i** also proceeded well under the standard reaction conditions. Additionally, substrates bearing different functional groups such as alkene (**1j**), alkyne (**1k**) and alcohol (**1l**) were also compatible in the reaction conditions with yields between 75 and 97%. However, when the steric hindrance around phosphorus center was increased, the substrate **1m** underwent a more difficult hydrolysis process resulting in an isolated yield of 34% of the corresponding acid. As mentioned above, the primary diphenyl phosphinic amide **1n** could be hydrolyzed under mild conditions. The product could be formed at 50 °C with 91% isolated yield, and 54% isolated yield at room temperature. Moreover, phosphinic amides derived from amino esters were also tested. As expected, substrates **1o**, **1p** and **1q** reacted well under the reaction conditions with modest yields.

This observation of excellent hydrolysis reactions of the diphenyl phosphinic amides proved encouraging, leading to study the hydrolysis reaction of another class of

organophosphorus compounds, the phosphoramidates. Inherently, this implied selective hydrolysis of the P(=O)-N bond in the presence of P(=O)-O bond. Gratifyingly, under the standard reaction conditions, a range of phosphoramidates were chemoselectively hydrolyzed (**Table 2.8**).

Table 2.8. Substrate scope for the chemoselective hydrolysis of P(=O)-NHR reagents and results of control experiments of selected examples in the absence of *o*-phthalaldehyde^a



^a Reaction conditions: **1** (0.2 mmol), NH_4OTs (0.2 mmol) and **3f** (0.04 mmol) in 0.2 mL of solvent and 0.2 mL of H_2O at $90\text{ }^\circ\text{C}$ for 24 h in a sealed tube. Results between parentheses related to similar reactions performed without adding **3f**. ^d Performed in THF (0.2 mL) and H_2O (0.2 mL) at $50\text{ }^\circ\text{C}$.

The control experiments with substrates **1s**, **1u**, **1w**, and **1x** were carried out with Ryan Simard. As we can see from the results, *N*-benzyl diphenyl phosphoramidate (**1s**) can be transferred to the desired acid product in 71% yield. However, the analogue, *N*-phenyl diphenyl phosphoramidate (**1t**) was more reluctant to be hydrolyzed in the reaction conditions, affording the product only in a 34% yield. This difference was expected since the nucleophilicity of the *N*-phenyl substrate was largely reduced

because of delocalization, supporting that this nucleophilicity is important to form the covalent adduct between the substrate and the aldehyde catalyst and realize efficient electrophilic activation. In contrast, other *N*-alkyl substrates such as *N*-methyl (**1u**), *N*-propyl (**1v**), *N*-isopropyl (**1w**) and *N*-cyclopropyl (**1x**) diphenyl phosphoramidates could be hydrolyzed efficiently in the reaction conditions, generating the products in high yields (85-96%). The control experiments demonstrated it was indeed necessary for the presence of the aldehyde catalyst (0-5% for control experiments Vs 85-96% for reactions for substrates **1u**, **1v**, **1w** and **1x**). The substrate containing a hindered *t*-butyl substituent (**1y**) could also be hydrolyzed chemoselectively, but with reduced efficiency generating the product in 40% yield. Other substrates bearing functional groups such as an alkene group (**1z**) and an alkyne group (**1aa**) were well tolerated in the reaction conditions. It was interesting to realize the catalytic hydrolysis for a hybridized substrate *o*-naphthyl phenylphosphoramidate (**1r**), which could generate the product in 92% yield. Moreover, the simple primary diphenyl phosphoramidate worked well under relatively mild conditions: the reaction temperature could be reduced from 90 °C to 50 °C.

Overall, comparing the results for phosphinic amides and phosphoramidates, phosphoramidates proved less labile towards the catalytic hydrolysis reaction. This may be due to the different electronic effect around the phosphorus center towards the nucleophilic attack by water molecule. This is in agreement with the general trend that the substitution reactions with diphenyl phosphoryl chloride (OPh)¹²¹ is generally more difficult than diphenyl (Ph) phosphinic chloride.¹²²

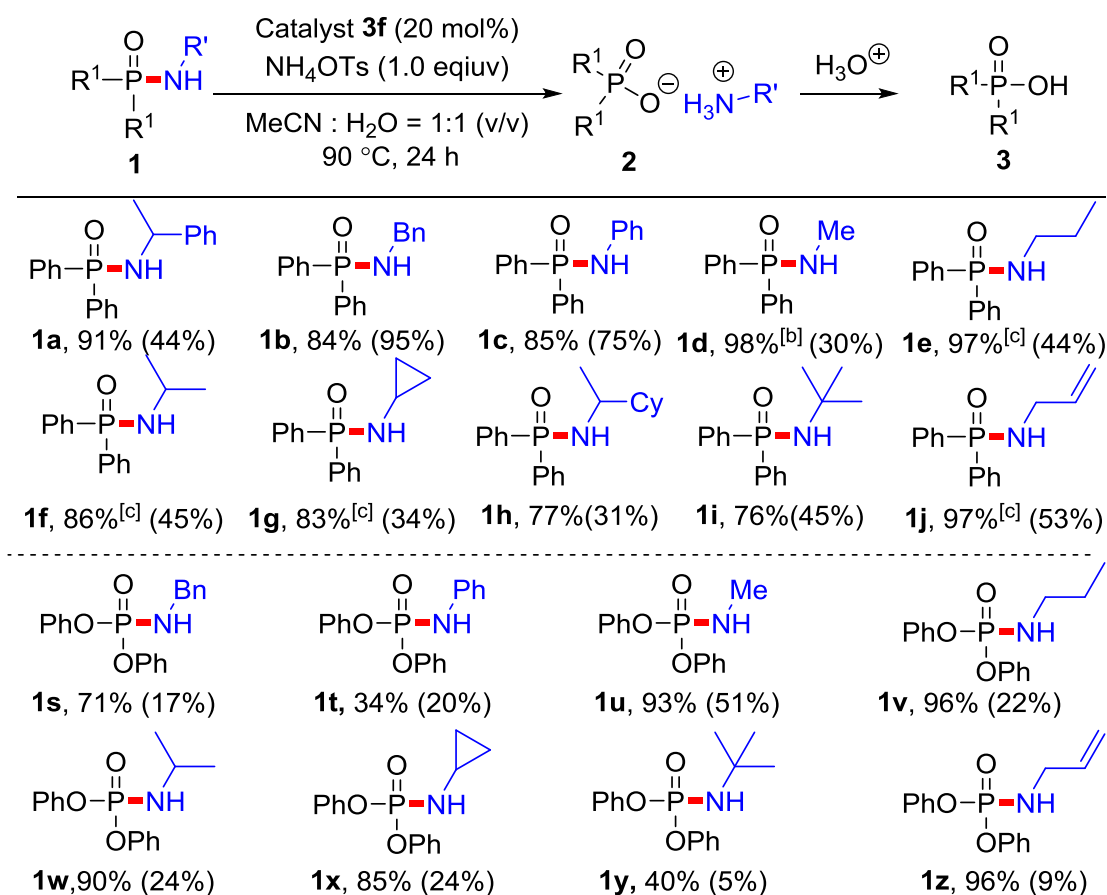
¹²¹ C.-Y. Liu, V. D. Pawar, J.-Q. Kao, C.-T. Chen, *Adv. Syn. Catal.* **2010**, 352, 188.

¹²² L. Horner, R. Gehring, *Phosphorus Sulfur Relat. Elem.* **1981**, 11, 157.

2.2.5 Comparison of catalytic efficiency between formaldehyde and *o*-phthalaldehyde

During our investigation for this hydrolysis reaction, we also noticed the good catalytic efficiency that formaldehyde demonstrated especially with the primary amide **1n**. As mentioned above, in Jencks' report,⁹¹ they found the important role of formaldehyde to catalyze the hydrolysis of the phosphoramidate. In order to have a better understanding about the catalytic efficiency between formaldehyde and *o*-phthalaldehyde, we proceeded to study a thorough comparison on a range of substrates (**Table 2.9**).

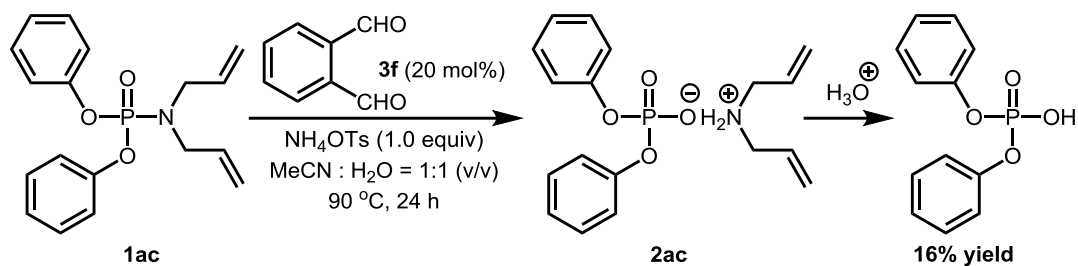
Table 2.9. Comparison of catalytic efficiency between *o*-phthalaldehyde and formaldehyde^a



^a Reaction conditions: **1** (0.2 mmol), NH₄OTs (0.2 mmol) and **3f** (0.04 mmol) in 0.2 mL of solvent and 0.2 mL of H₂O at 90 °C for 24 h in a sealed tube. NMR yields between parentheses are related to similar reactions performed using 20 mol% of formaldehyde. ^b NH₄OTs (0.04 mmol) was used at r.t. ^c NH₄OTs (0.04 mmol) and **3f** (0.04 mmol) were used at 50 °C.

As shown above, this comparison demonstrated a significantly improved reactivity of *o*-phthalaldehyde. Indeed, *o*-phthalaldehyde showed better catalytic efficiency for 17 of 18 substrates than formaldehyde. In particular, for 7 of 10 substrates of diphenyl phosphinic amides, the yields of formaldehyde were even less than 50%, however, *o*-phthalaldehyde could generate the product in good to excellent yields. For the other 8 substrates of diphenyl phosphoramidates that were tested, *o*-phthalaldehyde reacted better for the catalytic hydrolysis reactions, while the reactivity demonstrated by formaldehyde was still low: indeed, the yields for 7 of 8 substrates were less than 50%. Overall, this comparison clearly demonstrated the difference of catalytic reactivity between formaldehyde and *o*-phthalaldehyde to hydrolyze the P(=O)-N motif in organophosphorus compounds. The electrophilic activation through *o*-phthalaldehyde could be realized for this hydrolytic transformation.

To explain this increased reactivity, our current hypothesis is the superior ability of *o*-phthalaldehyde to form the covalent adduct between the *o*-phthalaldehyde and substrates, similar to the intermediate that Jencks and Gilchrist proposed (**Scheme 2.2**), which lead to a better electrophilic activation directly at the phosphorus center. Additionally, the need for the addition of ammonium salt suggested that this additive may facilitate formation of the adduct. However, unfortunately, experiments to further investigate the possible intermediates by ¹H NMR and ³¹P NMR were not successful. Efforts were also made to gain more insights regarding the kinetics, however it was not successful due to the solubility issue. Instead, a tertiary substrate was tested as a control experiment, in which the product was isolated in 16% yield (**Scheme 2.24**). This again supports that in this reaction, the formation of a covalent adduct between the substrates and *o*-phthalaldehyde is required to realize electrophilic activation.



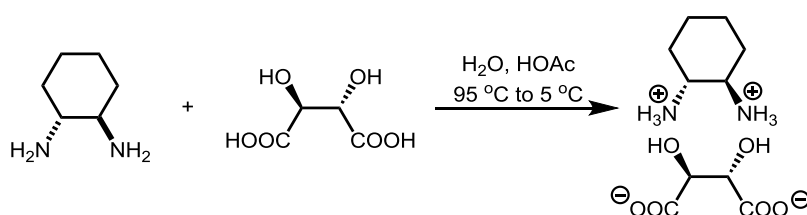
Scheme 2.24. Control experiment with tertiary phosphinic amides

2.3 Kinetic resolution

As introduced in Section 2.1.2, given the importance of catalytic reaction to prepare P-stereogenic compounds, kinetic resolution was selected for further investigation. Kinetic resolution is an efficient method to separate enantiomers from a racemic mixture. In general, different approaches were attempted to separate enantiomers.

2.3.1 General introduction for kinetic resolution

1) The classic resolution is to utilize a chiral resolving reagent, a stoichiometric amount, to generate a pair of diastereomers then separate them. This process is a physical separation¹²³ (**Scheme 2.25**).



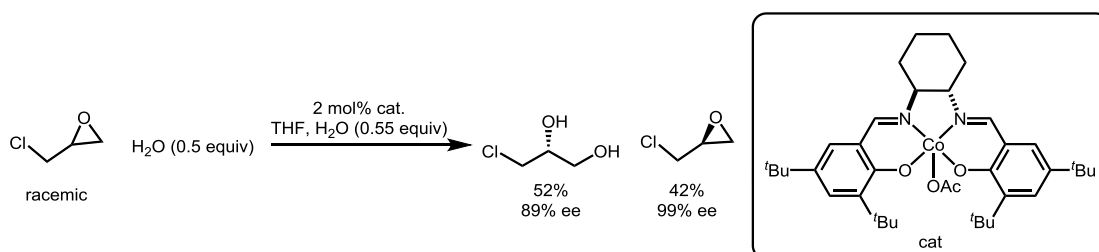
Scheme 2.25. A representative example for kinetic resolution

2) Using chiral chromatography is also developed to realize the separation, which is also a physical separation to employ a chiral stationary phase to differentiate enantiomers.

3) Kinetic resolution is to use a chiral catalyst or reagent to realize the resolution process.

¹²³ J. F. Larrow, E. N. Jacobsen, Y. Gao, Y. Hong, X. Nie, C. M. Zepp, *J. Org. Chem.* **1994**, *59*, 1939.

Unlike the physical separation, kinetic resolution is based on the different reactivity of enantiomeric substrates. Indeed, in the presence of a chiral catalyst or reagent, one enantiomer of the racemic mixture can react faster. The first kinetic resolution was discovered by Louis Pasteur in 1858, which was an example for enzymatic kinetic resolution.¹²⁴ Racemic ammonium tartrate was treated with *Penicillium glaucum*, in which it was noticed that one enantiomer was consumed faster than the other one. Different enzymatic kinetic resolution were discovered, which generally were highly selective however, the substrate scopes were limited. Meanwhile, increasing amounts of examples of non-enzymatic kinetic resolutions have been developed in the field of organic chemistry. An impressive example for non-enzymatic kinetic resolution was reported by Jacobsen and co-workers in 1997¹²⁵ (**Scheme 2.26**). In this hydrolytic kinetic resolution, important and valuable terminal epoxides (starting materials) and 1,2-diols (products) were afforded in high yields with high enantiomeric enrichment.¹²⁶



Scheme 2.26. A representative example of chiral-catalyst-permitted kinetic resolution

As discussed above in Section 1.2.1, the Beauchemin group demonstrated that two chiral aldehydes that could be obtained rapidly from commercial precursors (D-mannitol and D-mannose), can access to either enantiomer of the diamine products in excellent enantioselectivities in Cope-type hydroamination reactions⁴² (**Scheme 1.21**).

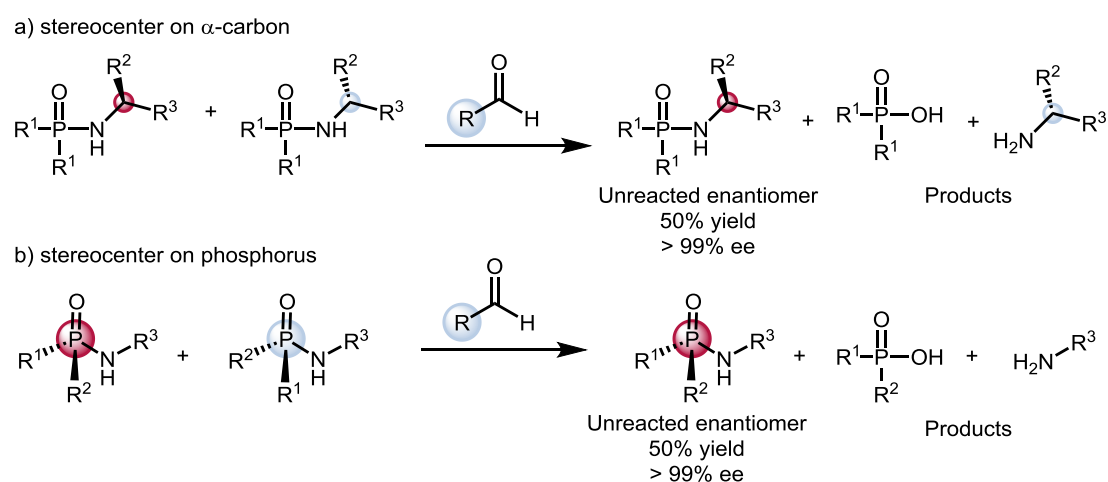
¹²⁴ L. Pasteur *C. R. Hebd. Seances Acad. Sci.* **1858**, 46, 615.

¹²⁵ M. Tokunaga, J. F. Larrow, F. Kakiuchi, E. N. Jacobsen, *Science* **1997**, 277, 936.

¹²⁶ Selected examples of reviews on kinetic resolution: (a) E. Vedejs, M. Jure, *Angew. Chem. Int. Ed.* **2005**, 44, 3974. (b) H. B. Kagan, J. C. Fiaud, in *Topics in Stereochemistry* E. Eliel, S. H. Wilen, (Eds), John Wiley & Sons: New York, **1988**, Vol. 18, 249.

This clearly indicated that aldehyde catalysis was an efficient method to transfer the stereochemical information on the chiral aldehydes to the products. This previous achievement clearly indicated that the stereoinformation could be transferred from the chiral aldehydes in right system. Therefore, after the investigation of the substrate scopes of the phosphinic amides and phosphoramidate, and the comparison of the catalytic efficiency between *o*-phthalaldehyde and formaldehyde, inspired by our previous work on enantioselective Cope-type hydroamination, and as a natural step to achieve more challenging goals, we moved on to attempt some enantiomeric enrichment through the kinetic resolution to achieve chiral phosphorus compounds.

In our reaction system, the substrates can contain one chiral center either on the α -carbon center or directly on the phosphorus center (**Scheme 2. 27**). When the stereocenter is on the α -carbon, we expected to target the recovered unreacted substrates since no chiral phosphorus compound would be afforded in the products after the hydrolytic cleavage of P(=O)-N bond. In the cases that the stereocenter is directly located on the phosphorus center, the detection of enantiomeric excess would also rely on the recovered unreacted substrates for easier separation and measurement.



Scheme 2. 27. General outline for kinetic resolution

2.3.3 Results and discussion

Our investigation could be summarized in **Table 2.10**. As it was shown, four different chiral aldehydes were utilized in this hydrolysis reaction. In particular, the bicyclic aldehyde **3p** proved to be significantly efficient for enantioselective hydroamination.⁴² And four different starting materials were tested. After 21 hours, the substances were recovered to examine the enantiomeric excess. The yields for the recovered starting materials were highlighted in blue. The smaller the yields were, the better the reactivity was.

Table 2.10. Preliminary results for kinetic resolution^a

Entry	3p	3q	3r	3s
	36% 0% ee	-	53% 0% ee	59% 0% ee
1a	37% ^b 0% ee ^b	0% ee	0% ee	0% ee
	72% 0% ee	-	91% 0% ee	80% 0% ee
1x	<1% conv. ^b 0% ee ^b	0% ee ^b	0% ee	0% ee
	24% 0% ee	21% 0% ee	21% 0% ee	-
1l				
	>99% conv.	>99% conv.	>99% conv.	68% 0% ee
1r	65% ^c 0% ee ^c	93% ^c 0% ee ^c	78% ^c 0% ee ^c	-
	96% ^d 0% ee ^d	62% ^d 0% ee ^d	-	-

^a Reaction conditions: **1** (0.2 mmol), NH₄OTf (0.2 mmol) and **chiral aldehydes** (0.04 mmol) in 0.2 mL of MeCN and 0.2 mL of H₂O at 90 °C for 24 h in a sealed tube. Then the starting materials were recovered and measured for ee and the yields were highlighted in **blue** for recovered starting material. ^b Reactions were performed in THF/H₂O instead of MeCN. ^c Reactions were carried out at 70 °C. ^d The temperature for the reactions were 50 °C.

First, diphenyl phosphinic amide **1a** was tested with different chiral aldehydes. Among the different chiral aldehydes, aldehyde **3p** showed good catalytic efficiency, and only 36% of the diphenyl phosphinic amide was recovered. However, no enantiomeric excess was achieved with all of these four chiral aldehydes. Changing the solvent to THF did not favor the reaction efficiency and enantiomeric excess.

Furthermore, diphenyl phosphoramidate **1x** was also tested in the reaction conditions. The reactivity was much slower with the four chiral aldehydes than the one with diphenyl phosphinic amides **1a**. Unfortunately, the enantiomeric excess was not improved by changing the starting material. Changing the solvent to THF was not helpful for both the reactivity and enantiomeric excess.

Moreover, another type of substrate **1l** with an intramolecular nucleophile was applied in the reaction. This substance was rapidly transformed to diphenyl phosphinic acid. Only 21-24% of the starting material was recovered after 21 hours with three chiral aldehydes. Unfortunately, the enantiomeric excess was still not improved. The starting material was recovered as racemic mixtures.

Eventually, substance **1r** was used which demonstrated the excellent reactivity with three different chiral aldehydes at 90 °C. Therefore, the reaction temperature was reduced to 70 °C and 50 °C. The reactivity was decreased that the starting material could be recovered, however, the enantiomeric excess was still the same. From then on, no more optimization was then performed since the preliminary results were not encouraging.

2.4 Summary and outlook

In summary, over 50 years ago, Jencks and Gilchrist documented an example of

aldehyde-catalyzed hydrolysis reaction of a phosphoramidate. They proposed that the reaction involved electrophilic activation. Herein, this reactivity was improved and these substrate scope was established: the methodology proved applicable to a range of organophosphorus compounds including phosphinic amides and phosphoramidates bearing the P(=O)-N subunit. Moreover, *o*-phthalaldehyde served as a general catalyst in this hydrolysis reaction, demonstrating superior activity to formaldehyde, which allowed the reaction to occur under relatively mild conditions. This chemoselective catalytic system allows the deprotection of *N*-protected derivatives, and could also potentially serve as a remediation method to hydrolyze agrochemicals bearing this P(=O)-N motif. This rare example of hydrolysis reaction that realized by organocatalysis via electrophilic activation could be further investigated for other chemical transformations.

In the future, further development for this methodology could be extended to other phosphorylation reactions. For example, other nucleophiles such as amines, alcohols, thiols and phosphoramidates could be utilized in the reaction system. Even if preliminary explorations did not prove encouraging, the kinetic resolution could be further studied, either to provide chiral phosphorus compounds or to achieve resolution of stereocenter on the α -carbon substituents. The next chapter will describe another example of activation mode for aldehyde catalysis with organophosphorus compounds.

Chapter 3

Carbonyl catalysis via transient intramolecular nucleophiles: Formaldehyde catalyzed mono-hydrolysis of α -amino phosphonates

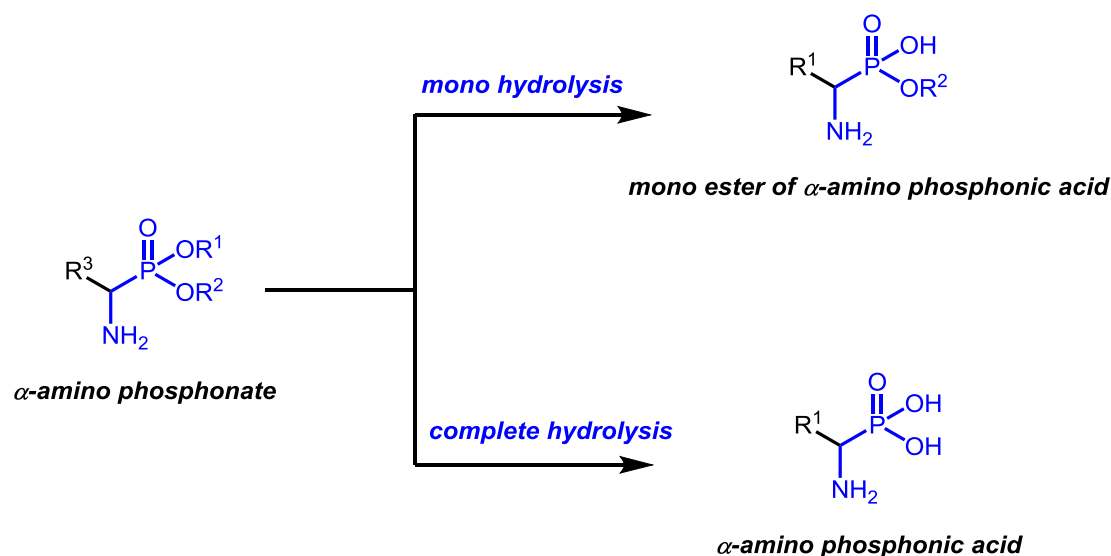
3.1 Introduction

In order to discover further application of carbonyl catalysis, this Chapter will continue to explore the hydrolysis reaction of another type of organophosphorus compounds, α -amino phosphonates. The importance of α -amino phosphonates and derivatives will be introduced. Traditional methods for the hydrolysis (mono hydrolysis and complete hydrolysis) of this type of compounds will be discussed. Carbonyl catalysis was proposed to achieve the challenging mono-hydrolysis as the amino group of α -amino phosphonates is perfectly positioned to incorporate the transient intramolecular nucleophile. Moreover, preliminary results for kinetic resolution will be presented.

3.2 Importance of α -amino phosphonates and derivatives

α -Amino phosphonic acids are structural analogues of natural amino acids. It is known that in biological systems, amino acids are fundamental building blocks for peptides. Therefore, α -amino phosphonates, α -amino phosphonic acids and monoesters of α -amino phosphonic acids (**Scheme 3.1**) are important classes of compounds and the studies related to their chemistry and biology have been developed into a prosperous field of phosphorus chemistry.¹²⁷

¹²⁷ A. Mucha, P. Kafarski, L. Berlicki, *J. Med. Chem.* **2011**, *54*, 5955.



Scheme 3.1. General structures for α -amino phosphonates and derivatives

Thus, continuous efforts have been made for their synthesis and applications in different aspects (**Scheme 3.2**). For example, α -amino phosphonates and derivatives have remarkable potential in medicinal chemistry¹²⁷ and also have found widespread applications in enzyme inhibitors,¹²⁸ antibacterial agents,¹²⁹ herbicides,¹³⁰ antibiotics,¹³¹ and pharmacological agents.¹³²

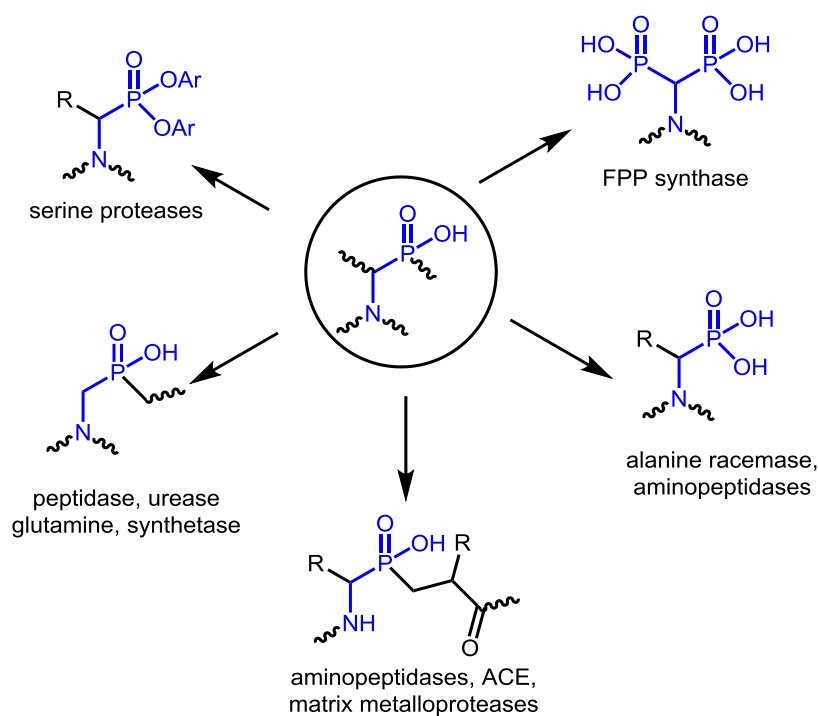
¹²⁸ (a) M. C. Allen, W. Fuhrer, B. Tuck, R. Wade, J. M. Wood, *J. Med. Chem.* **1989**, *32*, 1652. (b) E. W. Logusch, D. M. Walker, J. F. McDonald, G. C. Leo, J. E. Franz, *J. Org. Chem.* **1988**, *53*, 4069. (c) J.-L. Montchamp (Ed.) *Phosphorus Chemistry I Asymmetric Synthesis and Bioactive Compounds*, Springer, Switzerland **2015**.

¹²⁹ J. G. Allen, F. R. Atherton, M. J. Hall, C. H. Hassall, S. W. Holmes, R. W. Lambert, L. J. Nisbet, P. S. Ringrose, *Nature* **1978**, *272*, 56.

¹³⁰ M. K. Mao, J. E. Franz, *Synthesis* **1991**, 1991, 920.

¹³¹ (a) R. Hirschmann, A. B. Smith 3rd, C. M. Taylor, P. A. Benkovic, S. D. Taylor, K. M. Yager, P. A. Springler, S. J. Venkovic, *Science* **1994**, *265*, 234; (b) A. B. Smith, C. M. Taylor, S. J. Venkovic, R. Hirschmann, *Tetrahedron Lett.* **1994**, *35*, 6853.

¹³² (a) F. R. Atherton, C. H. Hassall, R. W. Lambert, *J. Med. Chem.* **1986**, *29*, 29. (b) J. G. L. Allen, F. R. Atherton, C. H. Hassall, R. W. Lambert, L. J. Nisbet, P. S. Ringrose, *Nature* **1978**, *272*, 56. (c) J. G. Allen, F. R. Atherton, M. J. Hall, C. H. Hassall, R. W. Lambert, L. J. Nisbet, P. S. Ringrose, *Antimicrob. Agents Chemother.* **1979**, *15*, 684.



Scheme 3.2. α -amino phosphonates and derivatives

In particular, the mono hydrolysis products, mono ester of α -amino phosphonic acids, also have essential applications. For instance, dehydrophos (**Scheme 3.3**) was discovered in 1984 and was produced by *Streptomyces luridus*. It shows broad antibacterial activity against both Gram-positive and Gram-negative bacteria.¹³³ Later on, further modifications of dehydrophos by Kuemin and van der Donk,¹³⁴ Aínsa, Sayago, Cativiela and their co-workers¹³⁵ to try to improve the antibacterial ability have been proved to be unsuccessful so far. Moreover, compounds **A** and **B** exhibited inhibition on the serine β -lactamases¹³⁶ and dipeptide analogue **C** was also found to inhibit to metalloenzyme leucine aminopeptidase.¹³⁷ The macro cyclic compound **D**

¹³³ R. D. Johnson, R. S. Gordee, R. M. Kastner, S. H. Larsen, E. E. Ose, *Antibiotic A53868 and Process for Production Thereof*. U.K. Patent 2,127,413, **1984**; Eli Lilly.

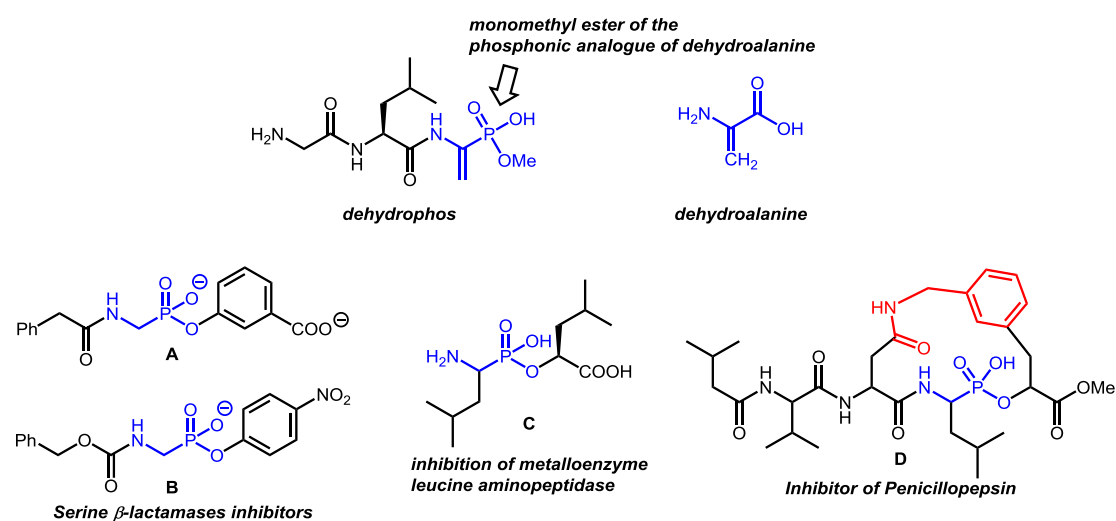
¹³⁴ M. Kuemin, W. A. van der Donk, *Chem. Commun.* **2010**, 46, 7694.

¹³⁵ M. M. Jiménez-Andreu, A. Lucía Quintana, J. A. Aínsa, F. J. Sayago, C. Cativiela, *Org. Biomol. Chem.* **2019**, 17, 1097.

¹³⁶ (a) R. F. Pratt, *Science* **1989**, 246, 917. (b) N. Li, J. Rahil, M. E. Wright, R. F. Pratt. *Bioorg. Med. Chem.* **1997**, 5, 1783.

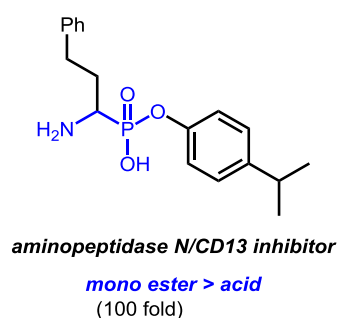
¹³⁷ P. P. Giannousis, P. A. Bartlett, *J. Med. Chem.* **1987**, 30, 1603.

was also found to be an efficient inhibitor of Penicillopepsin.¹³⁸



Scheme 3.3. Structure of dehydrophos and dehydroalanine and other useful compounds

Recently, Oleksyszyn and co-workers found that monoesters of α -amino phosphonic acids (**Scheme 3.4**) are potential inhibitors of aminopeptidase N/CD13. This enzyme is important in tumour angiogenesis. Notably, they noticed that some monoester derivatives of α -amino phosphonic acids demonstrated higher inhibition potency than corresponding α -amino phosphonic acids toward aminopeptidase N/CD13.¹³⁹

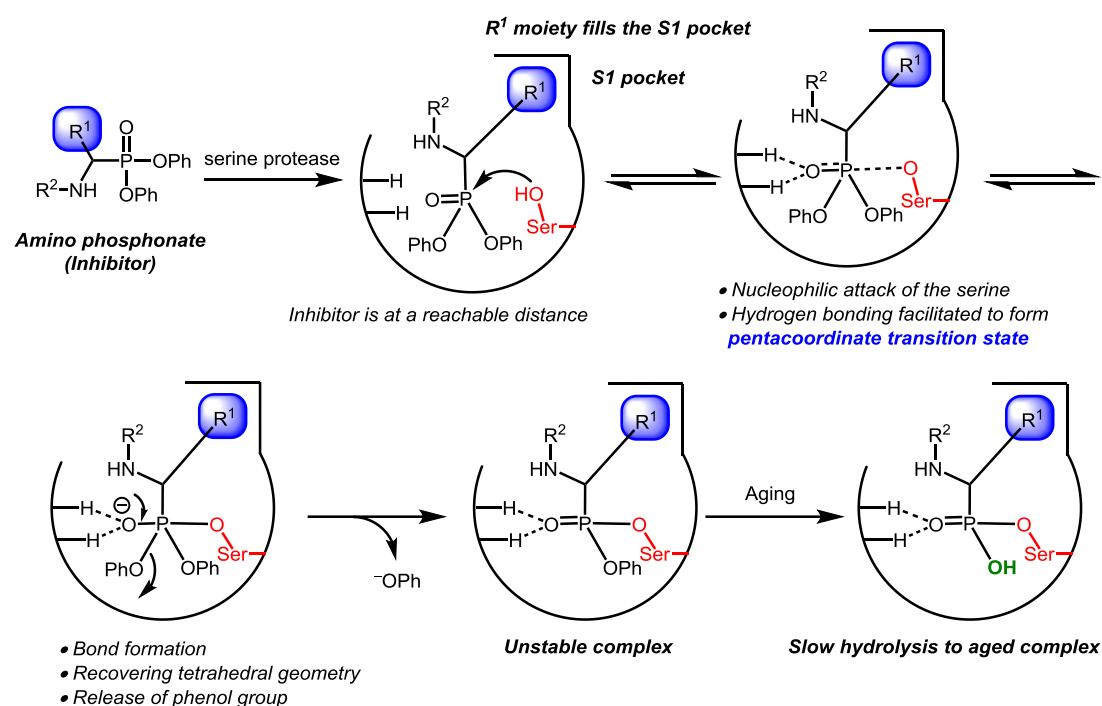


Scheme 3.4. α -Amino phosphonic acid as a potential inhibitor of aminopeptidase N/CD13

¹³⁸ (a) W. W. Smith, P. A. Bartlett, *J. Am. Chem. Soc.* **1998**, *120*, 4622. (b) M. E. Fraser, N. C. J. Strynadka, P. A. Bartlett, J. E. Hanson, M. N. G. James, *Biochem.* **1992**, *31*, 5201. (c) D. Suárez, N. Díaz, *J. Chem. Inf. Model.* **2017**, *57*, 2045.

¹³⁹ R. Grzywa, A. M. Sokol, M. Sieńczyk, M. Radziszewicz, B. Kościółek, M. P. Carty, J. Oleksyszyn, *Bioorg. Med. Chem.* **2010**, *18*, 2930.

Additionally, some diaryl α -amino phosphonates were found to be potential serine protease inhibitors.¹⁴⁰ The general mechanism for this type of inhibition was presented below (**Scheme 3.5**). First, the diaryl α -amino phosphonates approach the serine protease such that R^1 would enter the S1 pocket, meanwhile, phosphonates would also enter the reactive site. Nucleophilic attack of the hydroxyl group on serine would form the pentacoordinate transition state. This process is facilitated by hydrogen bonding in the reaction site. Then the bond forms between the serine and phosphorus center and the phenol group is released to re-build the tetrahedral geometry. Finally, this complex would be slowly hydrolyzed to its mono ester form (aged complex), which is more stable.



Scheme 3.5. General scheme for diaryl α -amino phosphonates as the inhibitor for serine protease¹⁴⁰

With these examples, the importance of monoester of α -amino phosphonic acids were clearly demonstrated. Therefore, the approaches to obtain these compounds were

¹⁴⁰ C. Moreno-Cinos, E. Sasseti, I. G. Salado, G. Witt, S. Benramdane, L. Reinhardt, C. D. Cruz, J. Joossens, P. Van der Veken, H. Brötz-Oesterhelt, P. Tammela, M. Winterhalter, P. Gribbon, B. Windshügel, K. Augustyns, *J. Med. Chem.* **2019**, *62*, 774.

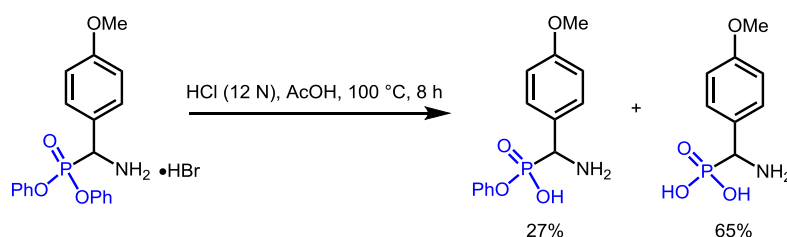
developed and the hydrolysis of α -amino phosphonates was one of these methods to achieve these compounds.

3.3. Hydrolysis of α -amino phosphonates

The hydrolysis of α -amino phosphonates to produce monoester of α -amino phosphonic acids can be realized under different mild conditions. However, one of the major difficulties for the hydrolysis of α -amino phosphonate is that, with slightly harsher conditions, the complete hydrolysis would occur to generate α -amino phosphonic acids.¹⁴¹ Moreover, the mono hydrolysis of dialkyl α -aminophosphonates required harsh conditions compared to the hydrolysis reaction of diphenyl α -aminophosphonates. In this section, hydrolysis reactions under acidic and basic conditions will be discussed.

Hydrolysis under acidic conditions

The hydrolysis of α -amino phosphonates under acidic conditions was inefficient, as both mono hydrolysis and complete hydrolysis were observed in most cases. For example, acidic conditions were reported to be unselective for the unprotected diphenyl α -amino phosphonates¹⁴² (Scheme 3.6).



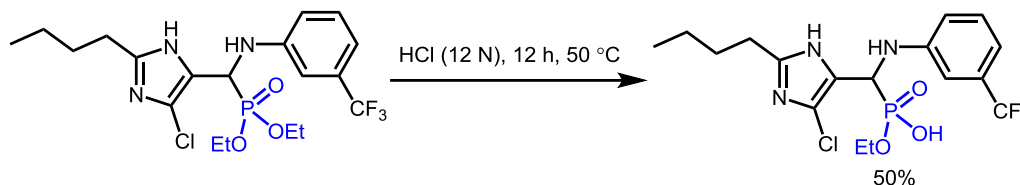
Scheme 3.6. Mono hydrolysis of diphenyl free α -amino phosphonates under acidic conditions

On the other hand, the mono hydrolysis of dialkyl α -amino phosphonates could be

¹⁴¹ C. S. Demmer, N. Krogsgaard-Larsen, L. Bunch, *Chem. Rev.* **2011**, *111*, 7981

¹⁴² S. Miroslaw, G. Waldemar, *Process for preparation of monoaryl (1-aminoalkyl)phosphonates by partial acid hydrolysis of diaryl [1-(alkoxycarbonylamino)alkyl]phosphonates with hydrochloric acid in acetic acid*, Pol. Patent 202822, 31 July, **2009**.

achieved in acidic conditions. For instance, when a diethyl phosphonate was heated at 50 °C, in the presence of concentrated hydrochloric acid, the mono ethyl ester of α -amino phosphonate was formed in only 50% yield¹⁴³ (**Scheme 3.7**).

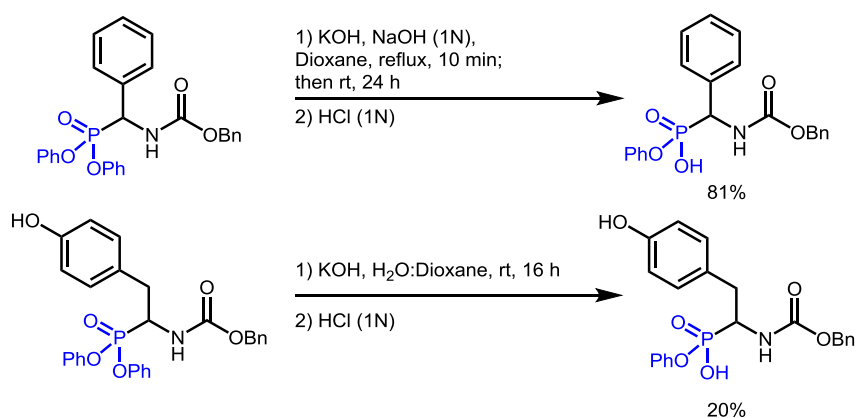


Scheme 3.7. Mono hydrolysis of diethyl α -amino phosphonate under acidic conditions

Hydrolysis under basic conditions

As demonstrated above, the hydrolysis of α -amino phosphonate was not as efficient as expected, since it was difficult to avoid the formation of completely hydrolyzed products. Thus, reactions were also developed for the hydrolysis under basic conditions.

The mono hydrolysis of diaryl phosphonates could be achieved under basic conditions in high yields.¹⁴⁴ However, in the presence of sensitive functional groups such as a hydroxyl group, the mono hydrolysis reaction could only afford the products in very low yields¹⁴⁰ (**Scheme 3.8**).

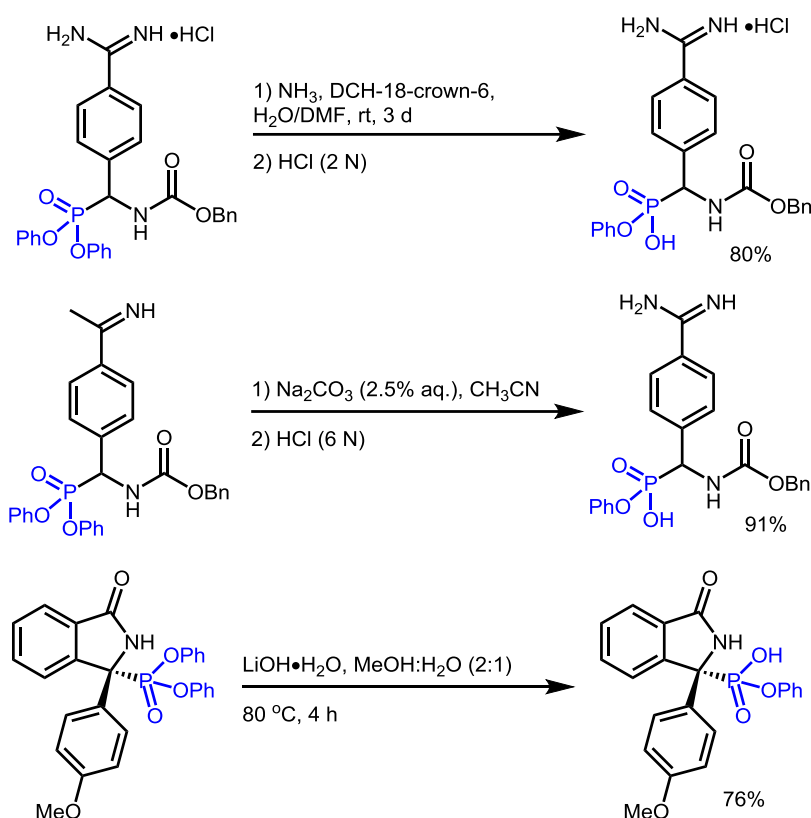


Scheme 3.8. Mono hydrolysis under basic conditions

¹⁴³ W.-W. Gao, S. Rasheed, V. Tangadanchu, Y. Sun, X.-M. Peng, Y. Cheng, F.-X. Zhang, J.-M. Lin, C.-H. Zhou, *Sci. China Chem.* **2017**, *60*, 769.

¹⁴⁴ M. G. v. Górnica, A. Czernicka, P. Młynarz, W. Balcerzak, P. Kafarski, *Beilstein J. Org. Chem.* **2014**, *10*, 741.

Other basic conditions were also reported for the mono hydrolysis reactions. For example, hydrophobic ammonium ions could catalyze the hydrolysis of diphenyl phosphonates, however, the isolated yields were not provided for this method.¹⁴⁵ Ammonia solution,¹⁴⁶ Na_2CO_3 ¹⁴⁷ and $\text{LiOH}\cdot\text{H}_2\text{O}$ ¹⁴⁸ could also promote the mono hydrolysis of diphenyl phosphonates (**Scheme 3.9**).



Scheme 3.9. Mono hydrolysis with different reagents under basic conditions

For the mono hydrolysis of dialkyl α -amino phosphonates, a common method is to reflux in the presence of NaOH .¹⁴⁹ However, this method could only afford moderate yields in some cases¹⁵⁰ (**Scheme 3.10**). Other bases were also used for the hydrolysis

¹⁴⁵ P. Kafarski, B. Lejczak, P. Plucinski, *Tetrahedron* **1987**, *43*, 799.

¹⁴⁶ J. C. Powers, D. S. Jackson, L. Ni, US Patent 5952307, **1999**.

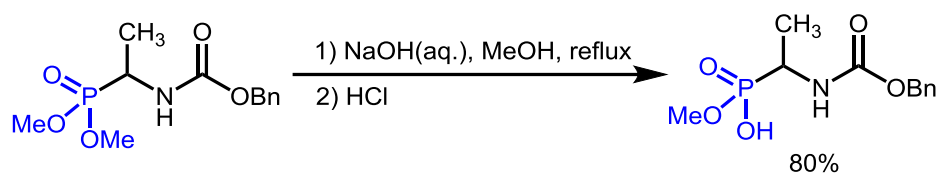
¹⁴⁷ Y. Nishiyama, H. Taguchi, J.-Q. Luo, Y.-X. Zhou, G. Burr, S. Karle, S. Paul, *Archives of Biochemistry and Biophysics* **2002**, *402*, 281.

¹⁴⁸ A. Suneja, R. A. Unhale, V. K. Singh, *Org. Lett.* **2017**, *19*, 476.

¹⁴⁹ C. Jia, K.-W. Yang, C.-C. Liu, L. Feng, J.-M. Xiao, L.-S. Zhou, Y.-L. Zhang, *Bioorg. Med. Chem. Lett.* **2012**, *22*, 482.

¹⁵⁰ C. Zou, W. Zou, Y. Hua, Q. Dang, *Substituted pyrimidines*, WO Patent 2013040790A1, 28 March, **2013**.

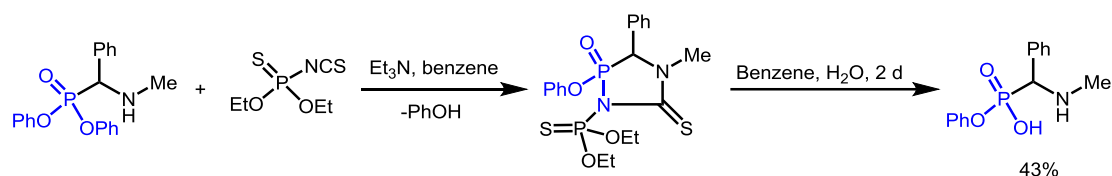
reactions, for example, NaOEt/ethylamine¹⁵¹ and DABCO.¹⁵²



Scheme 3.10. Mono hydrolysis of dialkyl phosphonate under basic conditions

Selected examples for other conditions

Formation of monoesters of α -amino phosphonic acids could also be achieved through a two-step procedure¹⁵³ (**Scheme 3.11**). First, diphenyl (α -methylamino)benzylphosphonate is reacted with diethyl isothiocyantophosphate to generate the 1,3,4-triazaphospholidine-2-thiones. Then, the product could be hydrolyzed in a mixture of benzene/H₂O to afford the monoester of α -amino phosphonic acids. However, the long reaction time was not that ideal.



Scheme 3.11. Two-step procedure to generate monoester of α -amino phosphonic acids

Other reagents were could also be used to achieve mono hydrolysis of dialkyl α -amino phosphonates. For example, reactions using KOTMS,¹⁵⁴ NaI,¹⁵⁵ LiBr,¹⁵⁶ and

¹⁵¹ T. E. Ali, S. A. Abdel-Aziz, S. M. El-Edfawy, E.-H. A. Mohamed, S. M. Abdel-Kariem, *Synth. Commun.* **2014**, *44*, 3610.

¹⁵² M. Hoffmann, *Phosphorus, Sulfur Silicon Relat. Elem.* **1998**, *134*, 109.

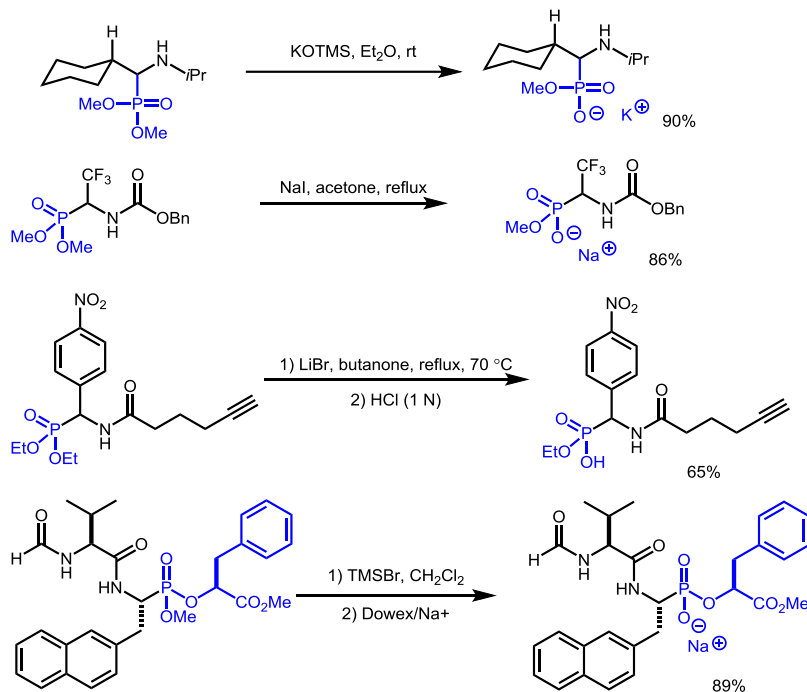
¹⁵³ N. A. Khailova, A. A. Shaimardanova, G. M. Saakyan, T. A. Zyablikova, N. M. Azancheev, D. B. Krivolapov, A. T. Gubaidullin, I. A. Litvinov, R. Z. Musin, G. A. Chmutova, M. A. Pudovik, A. N. Pudovik, *Russian Journal of General Chemistry (Zh. Obshch. Khim.)* **2003**, *73*, 1213.

¹⁵⁴ K. Moonen, *Synthesis of 4-phosphono- β -lactams and related azaheterocyclic phosphonates*. Ghent University, Ph.D. thesis, **2006**.

¹⁵⁵ P. de Medina, L. S. Ingrassia, M. E. Mulliez, *J. Org. Chem.* **2003**, *68*, 8424.

¹⁵⁶ S. Serim, P. Baer, S. H. L. Verhelst, *Org. Biomol. Chem.* **2015**, *13*, 2293.

TMSBr¹⁵⁷ were developed. As shown below, these reaction conditions can afford the mono esters in moderate to high yields. Unfortunately, reactions with a free amino groups were not reported.

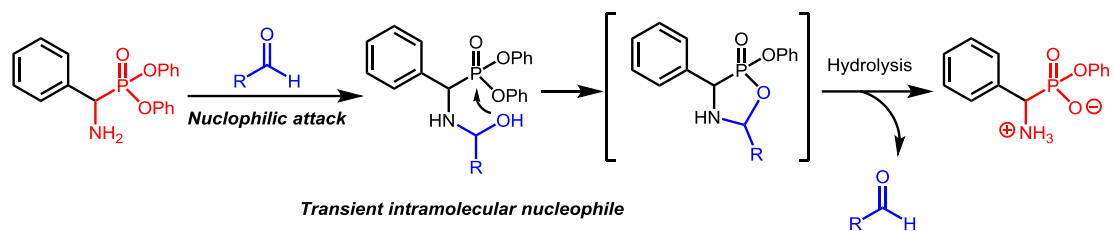


Scheme 3.12. Selected examples for mono hydrolysis of α -amino phosphonates

3.4 Results and discussion

For the development of a more efficient mono hydrolysis reaction of α -amino phosphonates, carbonyl catalysis was proposed that the amino group of α -amino phosphonates was perfectly set to incorporate the transient intramolecular nucleophile (**Scheme 3.13**). Since the product exists in the salt form, only monohydrolysis was expected. Indeed, the nucleophilic NH_2 -group would be protonated, thus preventing for further aldehyde-catalyzed hydrolysis, and the negative charge on the phosphorus atom would also help disfavor subsequent hydrolyses.

¹⁵⁷ J. H. Meyer, P. A. Bartlett, *J. Am. Chem. Soc.* **1998**, *120*, 4600.

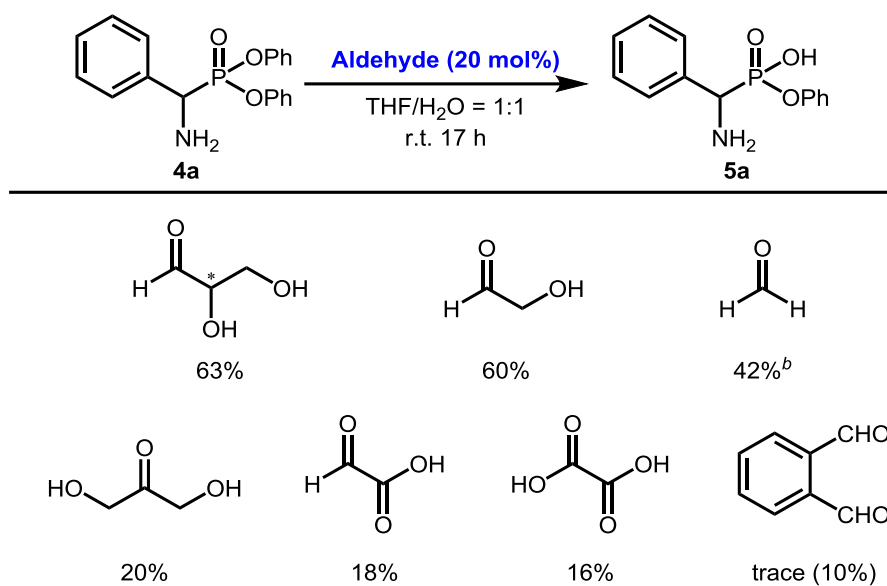


Scheme 3.13. Proposed carbonyl catalysis to achieve the mono hydrolysis reaction

3.4.1 Optimization of the reaction conditions

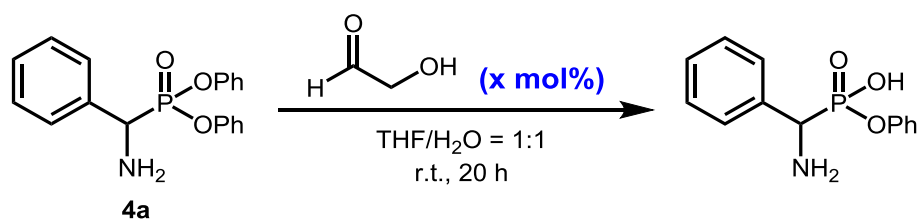
The investigation started with the use of **4a** as the model substrate to test the possibility for this reactivity. First, several aldehydes that were previously shown to work efficiently for the hydrolysis of P(=O)-N motif (Chapter 2) were tested. Delightfully, as shown in **Table 3.1**, the intended reactivity did occur, and several aldehydes showed reasonable reactivity and that the mono-hydrolyzed product was formed. For example, glyceraldehyde, glycolaldehyde, and formaldehyde all showed modest yields. Interestingly, *o*-phthalaldehyde only gave trace of the product. It is worth mentioning that the product precipitated when formaldehyde was used. This allowed facile isolation of the pure product to confirm the structure. In the absence of any aldehydes, a dimer was observed under the reaction conditions.

Table 3.1. Aldehyde scan for the mono hydrolysis reaction^a



^a Reaction conditions: **4a** (0.1 mmol) and **catalyst** (20 mol%) in 0.5 mL of THF and 0.5 mL of H₂O at room temperature for 17 h in a sealed tube. The yield was determined by ¹H NMR analysis using 1,3,5-trimethoxybenzene as an internal standard. ^b Full conversion, however also generated the dimerization byproduct.

Considering the price of glycerinaldehyde and the similar results between glycerinaldehyde and glycolaldehyde, the investigation was continued with the use of glycolaldehyde as the optimal aldehyde. Then the effect of changing the amount of glycolaldehyde was tested (**Table 3.2**).

Table 3.2. Mono hydrolysis with different amount of glycolaldehyde^a

Entry ^a	Amount of aldehyde	Yield (%)
1	5 mol%	37%
2	10 mol%	49%
3	20 mol%	60%^b / 67%^c
4	30 mol%	64%

^aReaction conditions: **4a** (0.1 mmol) and **catalyst** (x mol%) in 0.5 mL of THF and 0.5 mL of H₂O at room temperature for 20 h in a sealed tube. The yield was determined by ¹H NMR analysis using 1,3,5-trimethoxybenzene as an internal standard. ^b The reaction was 17 h. ^c The reaction time was lengthened to 24 h.

It was found that in the presence of **5 mol%**, **10 mol%**, **20 mol%**, and **30 mol%** of glycolaldehyde, the product was formed in **37%**, **49%**, **60%**, and **64%** yields respectively. However, with **30 mol%** of the glycolaldehyde, the yield (**64%**) did not increase significantly when compared to the **60%** yield with **20 mol%** of glycolaldehyde. Finally, by increasing the reaction time to 24 hours, the yield could be increased to 67% with 20 mol% of the glycolaldehyde. Then we tried to improve the reactivity with the addition of different bases (**Table 3.3**).

Table 3.3. Base screening for the hydrolysis reaction^a

4a

Entry	Base	Amount	Time	Yield (%)
1	-	-	24 h	67
2	<i>N</i> -methylmorpholine	1.0 eq	20 h	88
3	<i>i</i> Pr ₂ NEt	1.0 eq	20 h	87
4	DBU	1.0 eq	20 h	82
5	DABCO	1.0 eq	20 h	74
6	DMAP	1.0 eq	20 h	73
7	<i>N</i> -methylmorpholine	0.2 eq	24 h	81
8	<i>i</i>-Pr₂NEt	0.2 eq	24 h	84(20^b)
9	DBU	0.2 eq	24 h	81
10	NH ₄ OTs	0.2 eq	24 h	75
11		0.2 eq	24 h	66

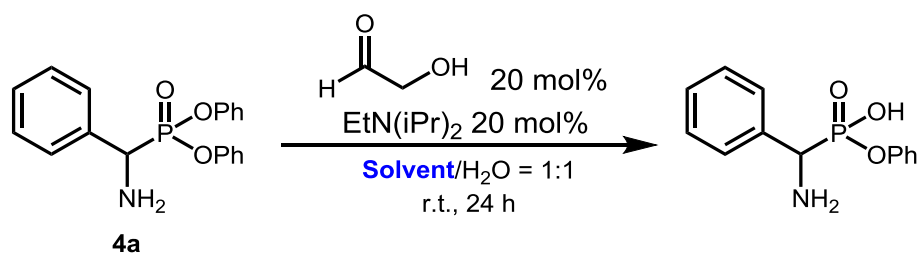
^a Reaction conditions: **4a** (0.1 mmol) and **catalyst** (20 mol%) in 0.5 mL of Solvent and 0.5 mL of H₂O at room temperature in a sealed tube. The yield was determined by ¹H NMR analysis using 1,3,5-trimethoxybenzene as an internal standard. ^b The reaction was performed in the absence of glycolaldehyde.

First, stoichiometric amounts of the selected bases were tested (**Table 3.3**, entries **2-6**).

These bases all provided increased yields when comparing to the reaction in the absence of any base (entry **1**). Both *N*-methylmorpholine (entry **2**, 88%) and diisopropylethylamine (entry **3**, 87%) gave similar yields. DBU, DABCO, and DMAP could also afford the product with slightly decreased yields (entries **4-6**). Then we examined how a catalytic amount of base with a longer reaction time could impact the reaction (entries **7-11**). *N*-methylmorpholine (81%), diisopropylethylamine (84%), and DBU (81%) could produce the product with good yields (entries **7-9**).

Diisopropylethylamine was the most efficient base since the product was obtained with slightly increased yields when compared to the other selected bases. With this in hand, we then continued to investigate the solvent effect (**Table 3.4**). Different solvents were examined for the reaction conditions.

Table 3.4. Solvent effects for the mono hydrolysis reaction^a



Entry	Solvent	Yield (%)
1	1,4-dioxane	90
2	THF	84
3	Ethanol	81
4	MeCN	76
5	Acetone	65
6	<i>t</i> -BuOH	54 ^b

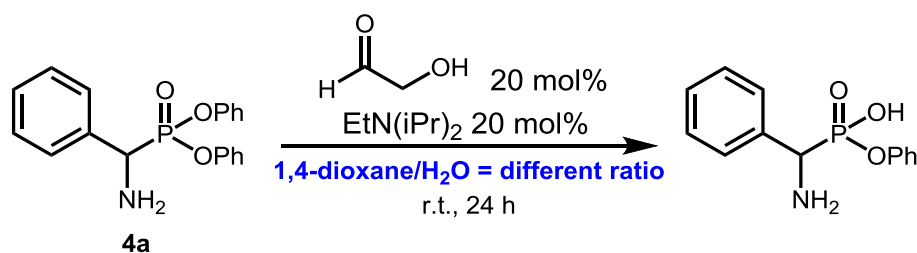
^aReaction conditions: **4a** (0.1 mmol), glycolaldehyde (20 mol%) and EtN(*i*Pr)₂ (20 mol%) in 0.5 mL of THF and 0.5 mL of H₂O at room temperature for 24 h in a sealed tube. The yield was determined by ¹H NMR analysis using 1,3,5-trimethoxybenzene as an internal standard. ^b The reaction was 18 h.

Among these different solvents, 1,4-dioxane could provide the monoester of α -amino phosphoric acid with excellent yield (**Table 3.4**, entry **1**). THF and ethanol as the solvent could also generate the desired product with good yields (entries **2** and **3**). Other solvents for example, acetonitrile, acetone, and *t*BuOH could also be used as the solvent to perform the reaction, however with decreased yields (entries **4-6**). Therefore, 1,4-dioxane was used as the solvent of choice for further optimization.

Furthermore, the ratio between 1,4-dioxane and water was also inspected (**Table 3.5**). When the ratio was 1:1, the reaction could generate the product in 90%

yield (**Table 3.5**, entry **1**). Changing the ratio between solvent and water, either more solvent (entries **2-4**) or more water (entries **5-7**) the reaction was not as efficient as that in entry **1**. Entries **2-7** in **Table 3.5** were performed with the help of a graduate student, Mr. Philippe Lemire.

Table 3.5. Ratio examination between solvent and water^a

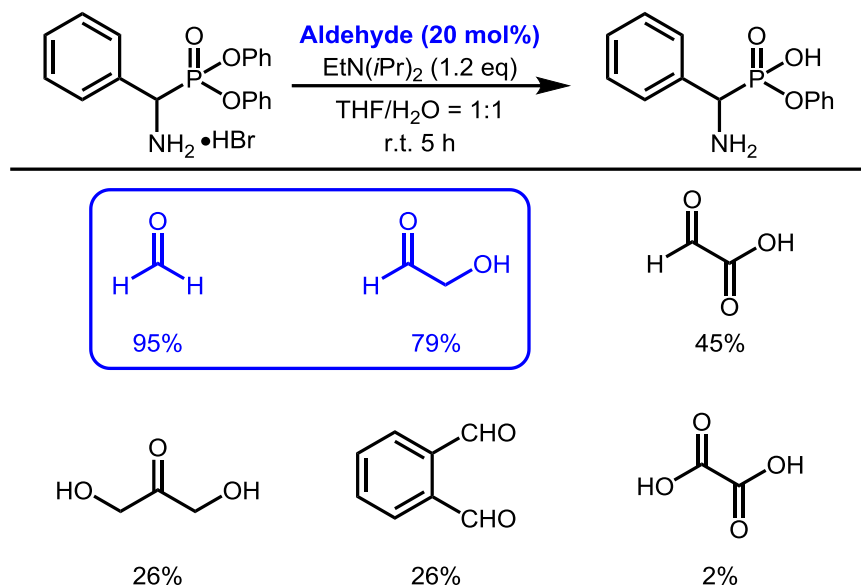


Entry	1,4-dioxane/H ₂ O ratio	Yield (%)
1	1:1	90
2	2:1	81
3	3:1	79
4	4:1	72
5	1:2	81
6	1:3	79
7	1:4	72

^aReaction conditions: **4a** (0.1 mmol) and glycolaldehyde (20 mol%) in 0.5 mL of THF and 0.5 mL of H₂O at room temperature for 20 h in a sealed tube. The yield was determined by ¹H NMR analysis using 1,3,5-trimethoxybenzene as an internal standard.

Moreover, we were wondering how different aldehydes would react with these optimal conditions especially in the presence of a catalytic amount of base. Meanwhile, we also figured out that the HBr salt of the α -amino phosphonate could also be utilized as the starting material, providing that an additional equivalent of the base was utilized. Therefore, we tested the reaction with different aldehydes under the optimized conditions (**Table 3.6**).

Table 3.6. Re-investigate the aldehydes with optimal conditions^a



^a Reaction conditions: α -amino phosphonate HBr (0.1 mmol), **catalyst** (0.02 mmol) and $\text{EtN}(i\text{Pr})_2$ (0.14 mmol) in 0.5 mL of THF and 0.5 mL of H_2O at room temperature for 17 h in a sealed tube. The yield was determined by ^1H NMR analysis using 1,3,5-trimethoxybenzene as an internal standard.

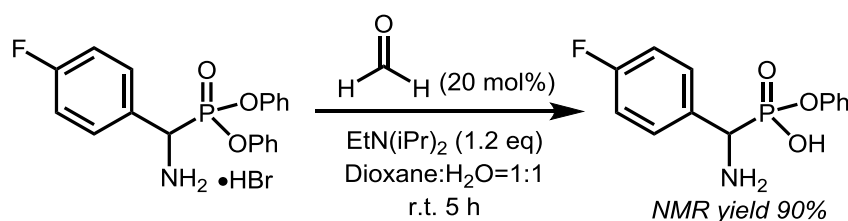
Surprisingly, formaldehyde demonstrated better catalytic efficiency among different aldehydes, generating the product in a 95% yield. And the reaction time was reduced to 5 hours with the use of formaldehyde, meanwhile, the reaction was more selective without the formation of byproducts. Within the same reaction time, the glycolaldehyde could also catalyze the hydrolysis reaction, albeit in a somewhat lower yield. Other aldehydes also promoted this reaction but with decreased efficiency. With this re-investigation of the catalysts under optimal conditions, formaldehyde proved to be the most efficient for this aldehyde-catalyzed hydrolysis reaction. It was also found out that the order of addition mattered: it was very important to add the base last in order to achieve excellent reactivity.

3.4.2 Efforts toward isolation of the product

After the optimal conditions had been found, we continued to work on the procedure to isolate the product. In the infancy of this project, the product could be isolated via recrystallization with methanol/ether when the reaction conditions was only with catalytic amount of aldehyde, THF and water. However, with the optimal conditions, especially the addition of the base, isolation became an issue. In order to develop a general procedure, instead of relying on the nature of the product to precipitate from the reaction mixture, efforts were made towards the isolation of the mono-hydrolyzed product.

Study for extraction

First, the reaction as shown below (**Scheme 3.14**) was performed to investigate the procedure for isolation. After 5 hours, the starting material was undetectable by TLC and reaction solution did not have any precipitate. Then, two different extraction orders were tested to isolate the product for the reaction as shown below (**Scheme 3.14**).



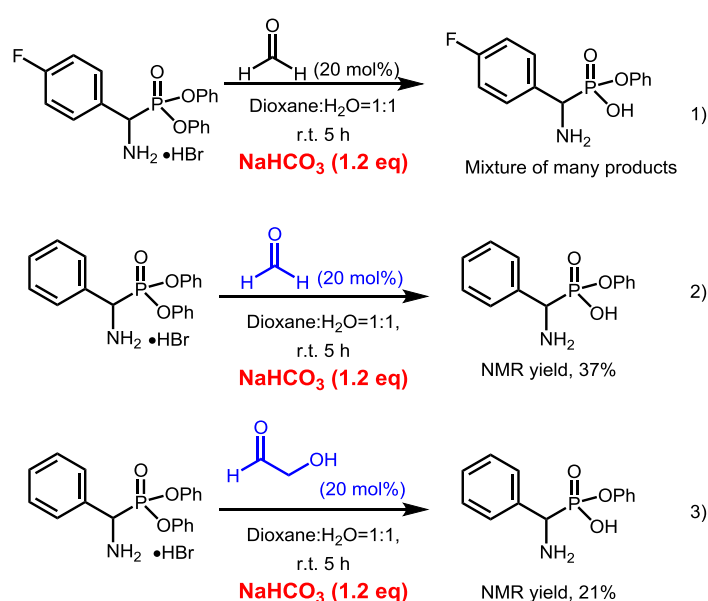
1) First, after the completion, the reaction mixture was transferred into a round bottom flask. 5 mL of ethanol was added twice to assist the evaporation of water. After the evaporation, 10 mL of a 1:1 mixture of H₂O : brine was added into the flask. Subsequently, a mixture of 10:1 DCM : MeOH (11 mL) was added twice

to perform the extraction in a separation funnel. The organic layer was dried with Na_2SO_4 and then concentrated. After, ^1H NMR was then taken. Unfortunately, using this procedure the product was only found in the aqueous phase.

2) The second procedure was as follows: after the completion, the reaction mixture was transferred into a round bottom flask. A saturated brine solution (5 mL) was added. At the moment of the addition, the solution became turbid with solid precipitate. Then 10:1 DCM: MeOH (11 mL) was added twice to perform the extraction in a separation funnel. The organic layer was concentrated and dried, and ^1H NMR was then taken. Unfortunately, ^1H NMR did not show the products. Thus, efforts to perform extractions were not successful.

Replacement of a water-soluble base

Since the isolation problem was due to the new addition of the organic base, it was hypothesized that a water-soluble base may help to solve the problem. Then a water-soluble base, sodium bicarbonate was tested as below (Scheme 3.15).

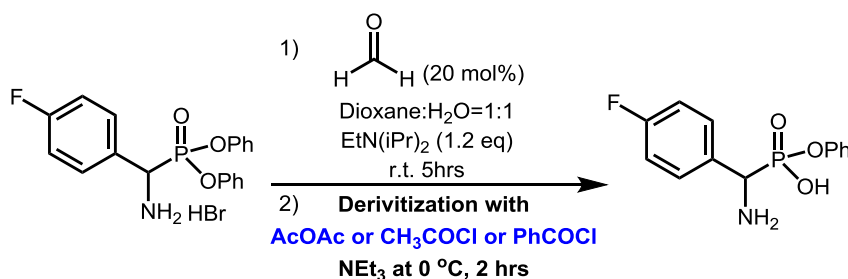


Scheme 3.15. Reactions for water-soluble base

However, after 5 hours the ^1H NMR for this reaction showed a mixture of different compounds (Scheme 3.15, equation 1). Then the model substrate was tested for this reaction with formaldehyde and glycolaldehyde respectively. Unfortunately, before a new isolation procedure could be developed, the ^1H NMR yield for these two reactions were disappointing (Formaldehyde 37% NMR yield; Glycolaldehyde 21% NMR yield). Therefore, further investigation with other water-soluble bases was not performed.

***In situ* derivation of the product**

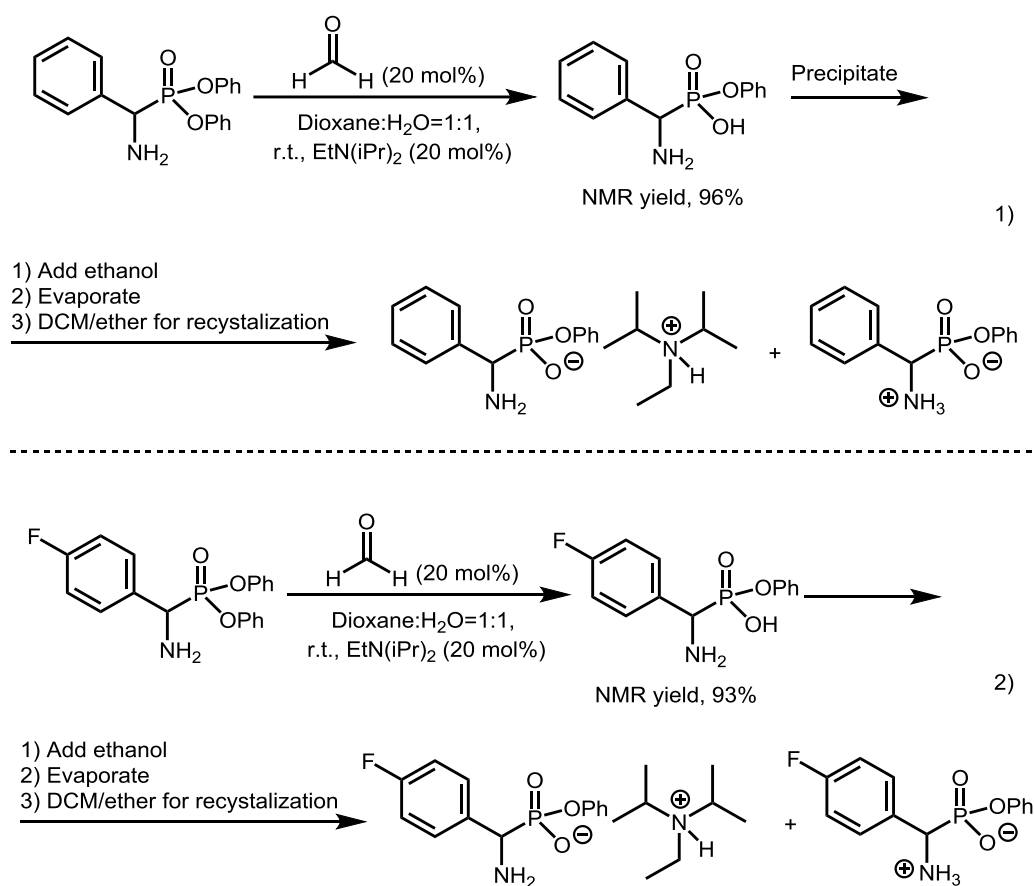
In order to come up with a generic isolation procedure, *in situ* protection of the product was further examined as a potential solution for the problem. The reaction was shown as below (Scheme 3.16). After 5 hours, TLC was taken for the reaction indicating excellent conversion of the starting material. Then the acylation was carried out with AcOAc/ NEt_3 at $0\text{ }^\circ\text{C}$ for 2 hours. The result of this derivation from TLC and ^1H NMR showed a mixture of many products. The method was not further investigated. Later on, other acylation reagents, CH_3COCl and PhCOCl were also tested for the *in situ* derivation. Unfortunately, results from TLC and ^1H NMR analysis did not show any promise, hence this was not pursued further.



Scheme 3.16. Reaction for *in situ* derivation of the product

Recrystallization with free amino substrates

With all these efforts, the discovery of an isolation procedure was more difficult than originally anticipate. Then we started to think that this un-smooth process for the discovery might be due to the HBr salt of substrates. Then the following investigation was based on the free amino substrates. The reactions showed below were achieved in excellent NMR yields (**Scheme 3.17**).



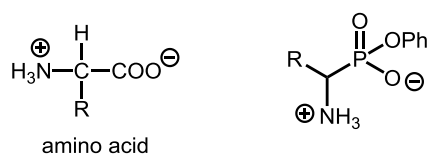
Scheme 3.17. Reactions for the study of recrystallization

The model substrate was used in the first reaction, precipitation of the product from the reaction mixture occurred during the reaction. Then ethanol was added to assist the evaporation. Afterwards, a DCM/ether mixture was utilized for the recrystallization. Delightfully, the formation of solid was observed. Then the product from recrystallization was examined with ^1H NMR. The ^1H NMR

demonstrated that the products existed as a combination of two salts as shown in **Scheme 3.17**. It was also the same when the *para*-fluoro substrate was applied for this procedure. Furthermore, reducing the amount of the base to 5 mol% decreased the catalytic efficiency with significantly lower yield of the product, even at a higher temperature (50 °C). However, this provided a possible pathway that ion exchange could be a potential solution.

Resin exchange

Given the fact that the desired product is a zwitterion, similar to amino acids (**Scheme 3.18**), the possibility to use ion-exchange resins used to isolate amino acids attracted the attention.¹⁵⁸

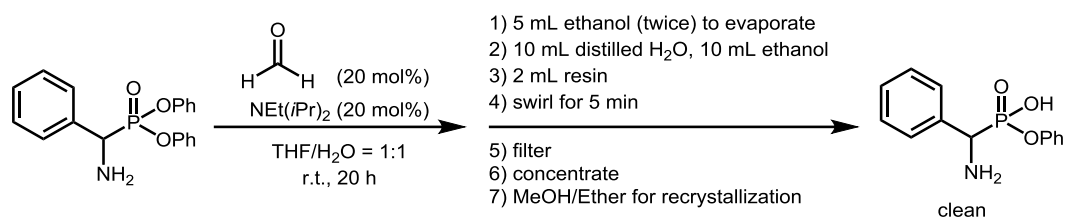


Scheme 3.18. Amino acid vs monoester of α -amino phosphonate

Therefore, an isolation procedure involving ion-exchange resin was proposed (**Scheme 3.19**). After the completion, the reaction mixture was transferred into a round bottom flask. 5 mL of ethanol was added twice to assist the evaporation of water. After the evaporation, 10 mL of distilled water and 10 mL of ethanol was added, followed by the addition of 2 mL of resin and after 5 minutes, the resin was filtered and the resultant mixture was concentrated. Then recrystallization was performed with a MeOH/ether mixture. The product of recrystallization was collected and examined by ¹H NMR. Surprisingly, this process could provide the clean product with 63% yield. Therefore, the procedure to isolate the clean

¹⁵⁸ P. E. Hare, P. A. St. John, M. H. Engel, *Ion-Exchange Separation of Amino Acids* In: G. C. Barrett (eds) *Chemistry and Biochemistry of the Amino Acids*. 1985, Springer, Dordrecht.

product was discovered.

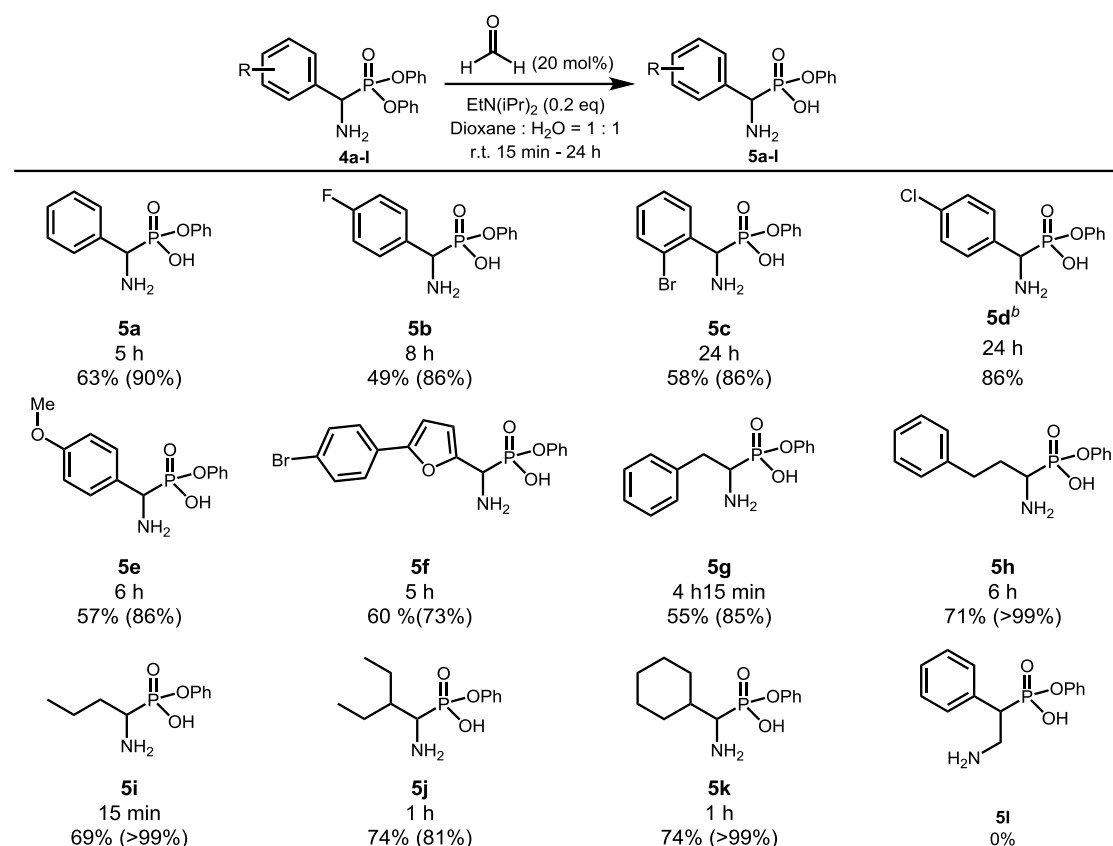


Scheme 3.19. Reaction for resin exchange

3.4.3 Substrate scope

With the optimal conditions and a reliable isolation procedure discovered, the substrate scopes were next examined. **Table 3.7** and **Table 3.8** summarize the results for the mono hydrolysis reaction. A variety of primary α -amino phosphonates were first examined in the reaction conditions, and evaluation of secondary α -amino phosphonates followed. Gratifyingly, the reaction conditions enabled the synthesis of a vast array of products, and the isolation procedure proved to be reliable.

As shown in **Table 3.7**, diverse primary α -amino phosphonates were tested in the reaction conditions, including α -aromatic and α -alkyl substrates. The ¹H NMR yields were also obtained for most of the substrates and are shown in parentheses.

Table 3.7. Substrate scope for primary α -amino phosphonates^a

^a Reaction conditions: α -amino phosphonates (0.1 mmol), catalyst (20 mol%) and NEt(*i*Pr)₂ (20 mol%) in 0.5 mL of 1,4-dioxane and 0.5 mL of H₂O at room temperature in a sealed tube. The yields in parentheses were determined by ¹H NMR analysis using 1,3,5-trimethoxybenzene as an internal standard. ^b The reaction was performed with 1g of starting material.

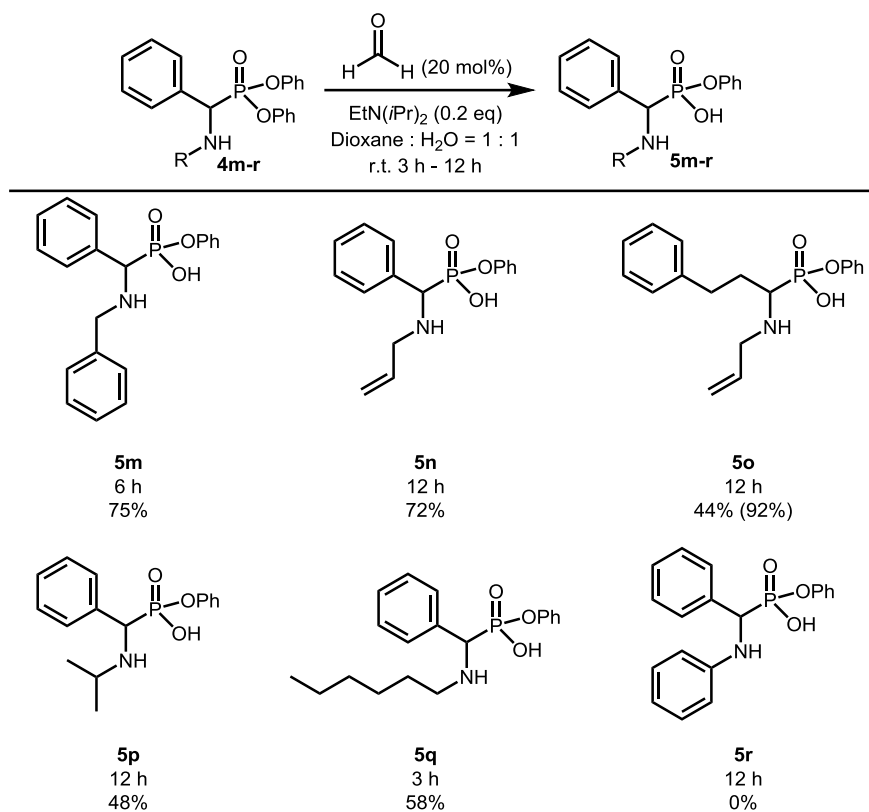
The model substrate **4a** could generate the desired product in 63% yield after the isolation procedure. Substrates bearing a range of aromatic substituents were also tested under the reaction conditions. For example, the substrate **4b** bearing a para-fluoro group was able to generate the corresponding product in 49% yield. Substrate **4c** containing ortho-bromo group proceeded through the hydrolysis reaction to provide the mono ester of the phosphonic acid in 58% yield within 24 hours. A gram-scale reaction was performed with the substrate **4d**, possessing a para-chloro substituent. Gratifyingly, this reaction could afford the product in 86% yield after recrystallization. The electron-rich substrate **4e** containing para-methoxy group was also examined in the reaction

conditions. The mono hydrolysis reaction was completed in 6 hours, providing the product in 57% after isolation. A substrate bearing a heterocyclic motif at the α -position could also convert smoothly, forming the product in 60% yield. The reaction conditions were next extended to α -alkyl substrates. Two α -amino phosphonates containing embedded aromatic groups were utilized as substrates for this hydrolysis reaction. Substrate **4g** with an α -benzyl group could give the product in 55% yield. The other substrate **4h** containing an α -phenylethyl group could produce the product in 71% yield. The reactions with substrates **4i**, **4j**, and **4k** were carried out by Mr. Philippe Lemire. Gratifyingly, these substrates reacted more efficiently and could be obtained within one hour and the isolation procedure using the resin was also reliable for α -alkyl substrates. For example, the substrate **4i** with α -propyl group could be hydrolyzed to the corresponding acid in 15 min and the product could be isolated in 69% yield. The other two substrates, **4j** and **4k**, could also be hydrolyzed within one hour and provided the corresponding products in 74% yields.

Overall, these results show that a noticeable loss of products occurs, a likely result of isolation procedure, considering that a recrystallization operation is required for this reaction. It is worth mentioning that the β -amino phosphonate (**4l**) was also tested under the reaction conditions. As predicted, this substrate was reluctant to undergo hydrolysis. Given our previous finding that catalytic activity proceeds more favorably with 5-membered compared to 6-membered transition states, this failed attempt also provides indirect support of the proposed mechanism for this aldehyde-catalyzed reaction (**Scheme 3.13**).

Several secondary α -amino phosphonates were also inspected under the reaction conditions (**Table 3.8**). Gratefully, the isolation procedure again worked for these substrates.

Table 3.8. Substrate scope for secondary α -amino phosphonates^a



^a Reaction conditions: α -amino phosphonates (1 mmol), catalyst (20 mol%) and $\text{NEt}(i\text{Pr})_2$ (20 mol%) in 5 mL of 1,4-dioxane and 5 mL of H_2O at room temperature in a sealed tube. The yields in parentheses were determined by ^1H NMR analysis using 1,3,5-trimethoxybenzene as an internal standard.

N-Benzyl (**4m**) and *N*-allyl (**4n**) phosphonates could be hydrolyzed to mono phosphonic acid in 75% yield and 72% yields, respectively. The substrate with an α -phenylethyl group (**4o**) was applied to the reaction conditions, providing the product in 42% yield in 12 hours. The ^1H NMR yields were obtained for **4o** and is shown in parentheses, highlighting again that the isolation process is only moderately effective. *N*-Alkyl substrates such as **4p** and **4q** were also inspected in this hydrolysis reaction, and the corresponding products could be generated in good yields. A control experiment was carried on the substrate **4r** containing a *N*-phenyl group. As expected, this substrate was stubborn towards the hydrolytic conditions due to the lower nucleophilicity of the aniline nitrogen. This failed result also suggested an important role for this nucleophilic

nitrogen atom in the mechanism.

3.4.4. Preliminary study for weaker leaving group

Our initial study regarding other leaving groups (e.g. ethoxy group) was not promising and very little reactivity was observed. Prof. Gagosz suggested the addition of phenol when this project was presented in Seminar II. In theory, phenol could replace the ethoxy group to facilitate the subsequent hydrolysis reaction. The summary of preliminary results are show below based on ^{31}P NMR.

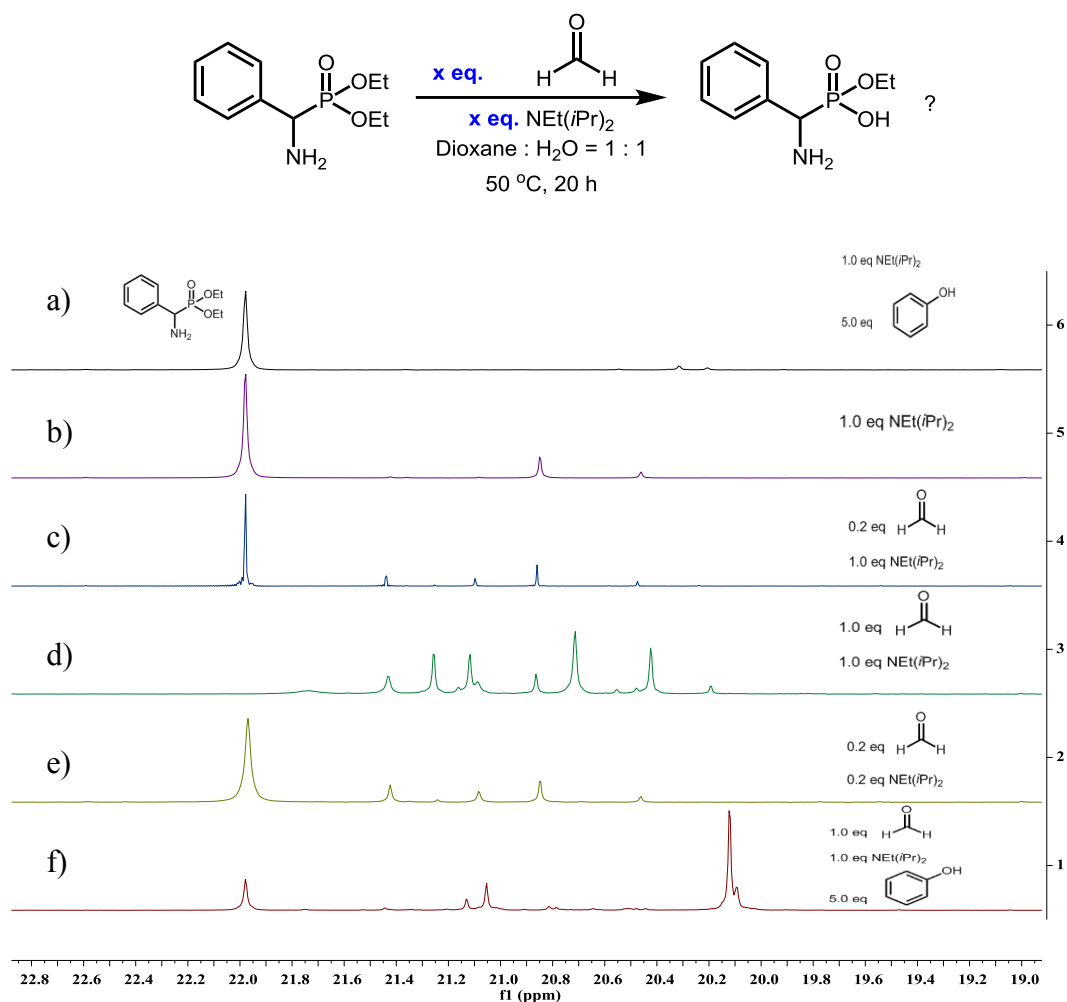
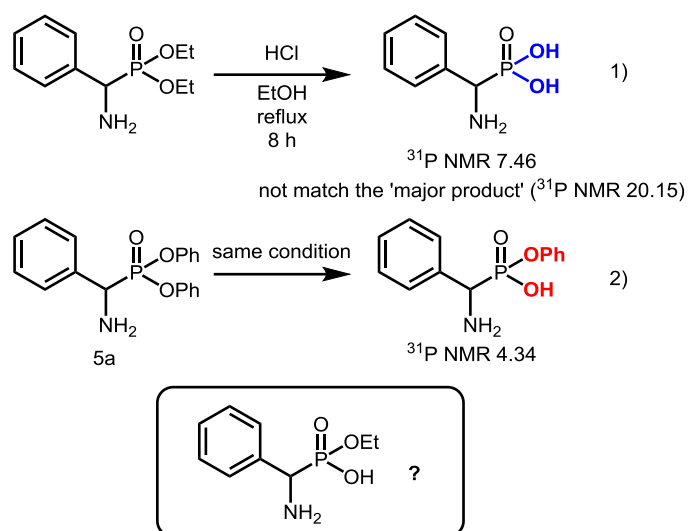


Figure 3.1. ^{31}P NMR for preliminary results of weak leaving group (OEt)

The reaction was first carried out merely in the presence of stoichiometric amount of the base (**Figure 3.1, b**). This control experiment indicated the limited reactivity of the

substrate. The addition of 20 mol% of formaldehyde did not improve the situation, however the ^{31}P NMR showed more phosphorus-containing substances were formed (**Figure 3.1**, c). The use of a stoichiometric amount of formaldehyde completely changed the reactivity so that >99% conversion was observed with the newly-formed, complicated phosphorus species (**Figure 3.1**, d). Reducing the amount of both formaldehyde and base dropped the reactivity dramatically (**Figure 3.1**, e). Surprisingly with the suggestion to add phenol into the reaction, reactivity increased and one major product was formed according the ^{31}P NMR (**Figure 3.1**, f). A control experiment in the absence of formaldehyde showed limited reactivity (**Figure 3.1**, a), which clearly demonstrated that the addition of stoichiometric amount of formaldehyde facilitates the reactivity. Continuous efforts were made to isolate the major product. Unfortunately, the isolation procedure developed above was not working and for this reaction, the structural confirmation was not successful.

Instead, we tried to prepare potential products (mono hydrolysis and complete hydrolysis) under acidic conditions (**Scheme 3.20**). The first hydrolysis reaction was performed with the substrate containing OEt group. The reaction yielded the complete hydrolysis product (**Scheme 3.20**, equation 1). The model substrate **4a** was also tested in the acidic conditions, surprisingly that mono hydrolysis product was generated in the same conditions (**Scheme 3.20**, equation 2). The ^{31}P NMR of complete hydrolysis product did not match the major product in **Figure 3.1**, f. Unfortunately, other investigation was not further performed due to the limited time available before writing this thesis.

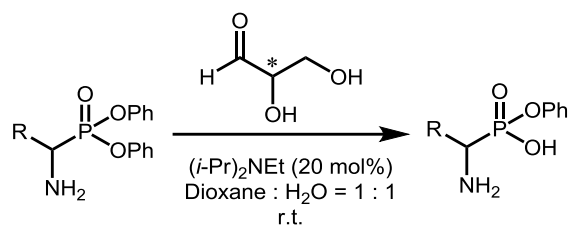


Scheme 3.20. Hydrolysis under acidic conditions

3.4.5. Preliminary trials toward kinetic resolution of chiral α -amino phosphonates

As mentioned in Chapter 2, Section 2.3, preparing chiral phosphorus compounds via kinetic resolution has always been one of the goals. Thus, in parallel, the chiral aldehyde **3p**, which proved to be efficient for asymmetric hydroamination,⁴² was utilized to examine the possibility to achieve chiral α -amino phosphonates. The preliminary results are summarized in **Table 3.9** and **Table 3.10**.

Table 3.9. Preliminary study for kinetic resolution to prepare chiral α -amino phosphonates with chiral glyceraldehyde^a

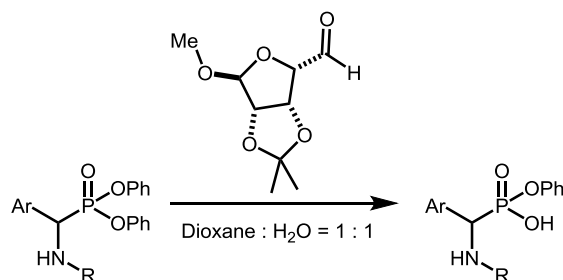


Entry	Substrates	Amount of aldehyde	Base (0.2 eq)	Time	e.e. (%)
1	 4m	0.2 eq	0.2 eq	4 h	0
2		0.2 eq	-	4 h	0
3	 4g	0.2 eq	-	4 h	6

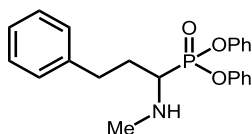
^a Reaction conditions: α -amino phosphonates (0.3 mmol), glyceraldehyde (20 mol%) and $\text{NEt}(\text{iPr})_2$ (20 mol%) in 1.5 mL of 1,4-dioxane and 1.5 mL of H_2O at room temperature in a sealed tube. After 4 hours, the starting material were isolated to determine the ee by chiral HPLC analysis. The conversion of the starting material was not determined for the first trials.

The model substrate **4m** was first tested for kinetic resolution. After 4 hours, unreacted starting material was isolated to determine ee. However, no enantioselectivity was observed with/without base (**Table 3.9**, entries 1 and 2). With the model substrate, the α -position might be easy to racemize due to the acidic proton. Then the reaction was carried out with substrate **4g**, in which the aromatic group was located at β -position. In this reaction, delightfully, 6% ee was detected from the unreacted starting material (**Table 3.9**, entry 3). Even the enantioselectivity was not significant, this was still a good sign that the kinetic resolution could be realized under optimal conditions. The chiral aldehyde **3p**, which was proved to be efficient for highly enantioselective hydroamination was further applied in this reaction. The results are summarized in **Table 3.10**.

Table 3.10. Preliminary study for kinetic resolution to prepare chiral α -amino phosphonates^a



Entry	Substrates	Amount of aldehyde	Base (0.2 eq)	Temp (°C)	Solvent	Time	e.e. (%)	Conversion (%) ^b
1	 4g	1.0 eq	-	r.t.	Dioxane	5.5 h	11	N/A
2	 4h	1.0 eq	-	r.t.	Dioxane	4.5 h	19	N/A
3		0.5 eq	NMM	r.t.	Dioxane	1.5 h	11	N/A
4		0.5 eq	Quinine	r.t.	Dioxane	1.5 h	20	N/A
5		1.0 eq	Quinine	r.t.	Dioxane	10 min	N/A	>99
6	 4m	-	-	70	Dioxane	40 min	-	47
7		1.0 eq	-	70	Dioxane	40 min	25	>99
8		0.5 eq	-	70	Dioxane	40 min	20	61
9		0.5 eq	-	70	Acetone	40 min	22	61
10		0.5 eq	-	70	MeCN	40 min	11	72
11		0.5 eq	-	70	THF	40 min	4	42
12		0.5 eq	-	70	<i>t</i> -BuOH	40 min	-5	61



Proposed substrate

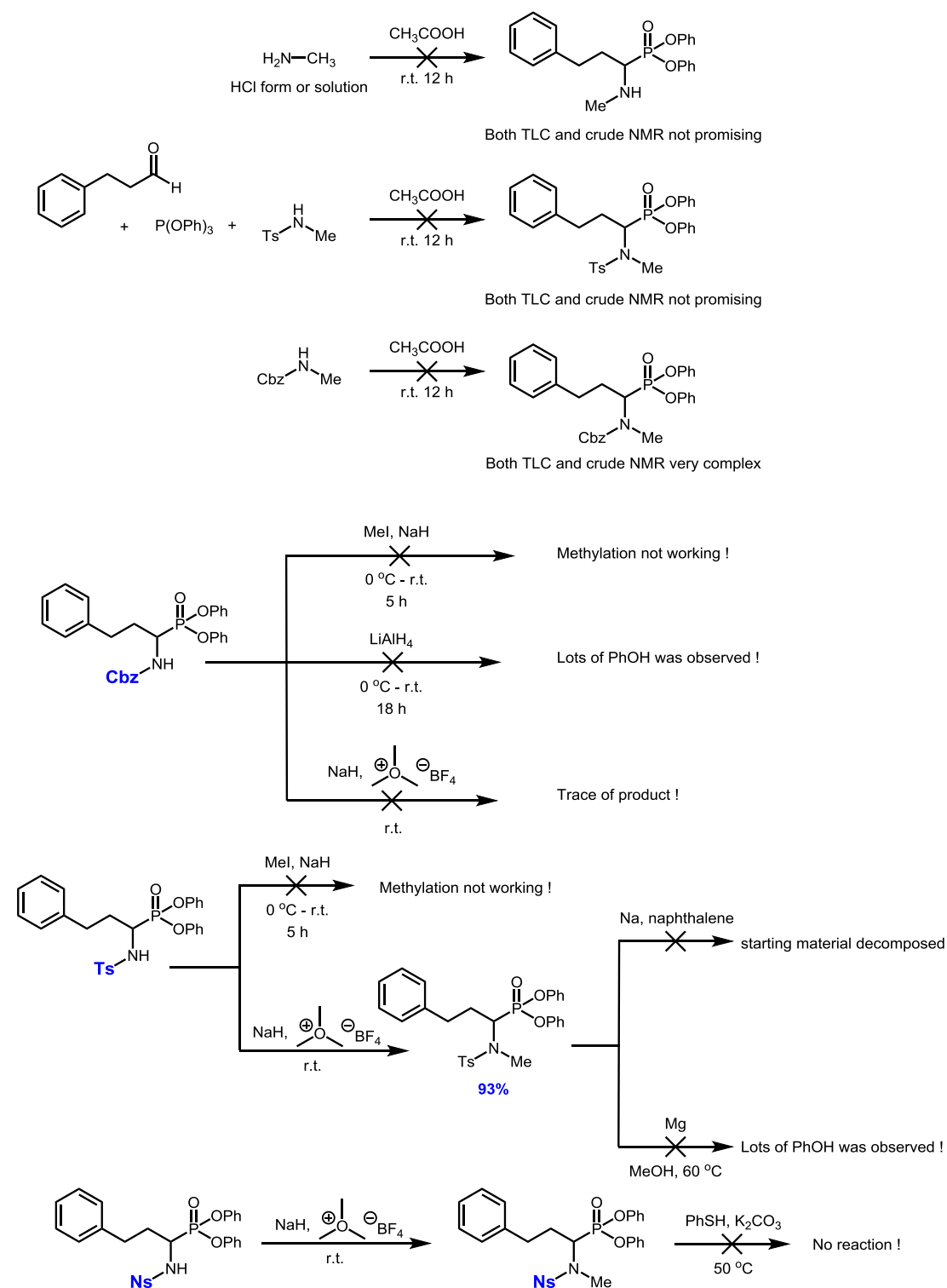
^a Reaction conditions: α -amino phosphonates (0.2 mmol), glyceraldehyde (x mol%) and base (x mol%) in 1.0 mL of 1,4-dioxane and 1.0 mL of H₂O at different temperature in a sealed tube. The unreacted starting material was isolated to determine the ee by chiral HPLC analysis. ^b Conversions are based on ³¹P NMR.

With a stoichiometric amount of chiral aldehyde **3p**, a slightly increased ee was observed with the unreacted substance **4g** (Table 3.10, entry 1, 11% ee). Then another substance **4h** with aromatic group at γ -position was further tested. With this substrate, the enantioselectivity was slightly increased to 19% ee (entry 2). Addition of a racemic base (*N*-methylmorphonine) or a chiral base (quinine) was also ineffective (entries 3-5).

A secondary substrate **4m** containing an *N*-benzyl group was further applied under the reaction conditions. This catalyst has a limited reactivity with substrate **4m** at room temperature, therefore the reactions were carried out at 70 °C. In the absence of the chiral aldehyde, the starting material gave 47% conversion (entry 6). With the addition of stoichiometric amount of the chiral catalyst (entry 7), the efficiency of the reaction was improved significantly and the leftover trace of starting material was enriched in one enantiomer (25% ee). With the quantity of chiral aldehyde reduced to 50 mol%, (entry 8) 61% of starting material was converted and the un-reacted starting material was determined to have 20% ee. Different solvents, including acetone, acetonitrile, THF, and *t*-BuOH were inspected for the kinetic resolution conditions (entries 8-12). Unfortunately, the enantiomeric purity was not improved (-5 – 22% ee).

Combining all these results, a possible substrate (Table 3.10, entry 13), which has a less acidic α -proton and a minimal steric hindrance around a secondary nitrogen atom

was proposed for this kinetic resolution reaction. However, lots of efforts was made to synthesize this substrate, unfortunately, no success was achieved (**Scheme 3.21**).



Scheme 3.21. Attempts to prepare proposed substrate

Even though current results do not establish efficient kinetic resolution conditions,

these studies demonstrate that with the suitable conditions such as chiral aldehydes, solvents and chiral bases, there is possibility to achieve this goal. My time with the Beauchemin group has almost come to the end, but I hope, these preliminary studies provide a foundation for other colleagues to investigate further.

3.5 Conclusion

To sum up, by exploring carbonyl catalysis to install transient intramolecular nucleophiles, formaldehyde successfully catalyzed mono hydrolysis of α -amino phosphonates under mild conditions. As a result, various monoester of α -amino phosphonic acids were obtained as the products. This approach proved applicable to a array of primary and secondary α -amino phosphonates. Furthermore, a reliable method to isolate the desired product was also discovered. Moreover, even if preliminary explorations only achieved limited enantioselectivity, the kinetic resolution could be further studied to come up with optimal conditions. The next chapter will describe the carbonyl catalysis in prebiotic chemistry, and a prebiotic-relevant aldehyde will be introduced for the applications in prebiotic chemistry and further explored as a catalyst for different reactions.

Chapter 4

Application of Carbonyl Catalysis in Prebiotic Chemistry

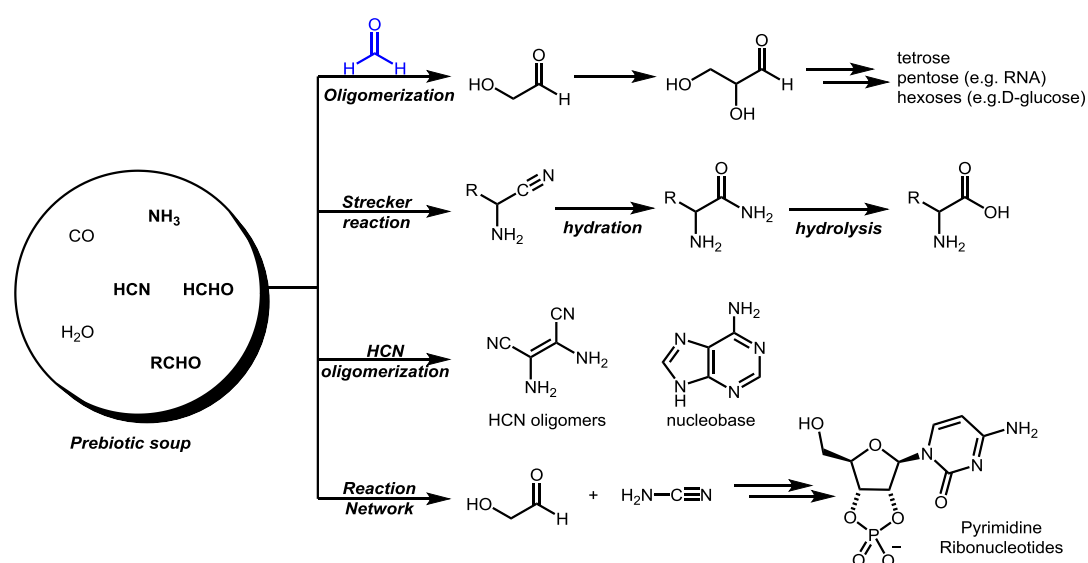
It has been demonstrated that simple aldehydes such as *o*-phthalaldehyde (Chapter 2) and formaldehyde (Chapter 3) can act as efficient catalysts for hydrolysis reactions through electrophilic activation and exploiting temporary intramolecularity to facilitate difficult intermolecular reactions. Given our interests in ‘origin of life’ chemistry¹⁵⁹ and as a natural development for the methodology described in Chapter 2, we wondered if carbonyl catalysis could potentially be applied in the field of prebiotic chemistry. We continued to exploit the role of prebiotic relevant aldehydes in the synthesis of amino acids and hydrolysis of organophosphorus compounds to address the catalytic efficiency of these aldehydes as mimics of hydratase and hydrolase enzymes. Furthermore, efforts were made to establish that phosphoryl transfer reactions were possible under aldehyde-catalyzed conditions.

4.1 General introduction on prebiotic chemistry

Arguably, one of the most fundamental questions, not only for scientists but also for everyone who takes time to wonder is “How did life originate?” The age of Earth is approximately 4.5 billion years; the emergence of life could not predate the existence of Earth unless an extraterrestrial environment served as a resource for the origin of life. So far, however, Earth is still the only known planet to harbour life. The earliest

¹⁵⁹ M. P. Jamshidi, M. J. MacDonald, A. M. Beauchemin, *Origins Life Evol. Biosphere* **2017**, *47*, 405.

evidence of micro-organisms could be dated to 3.77 to 4.28 billion years ago and was found in rocks in Quebec.¹⁶⁰ Currently it is extremely difficult to study or deduce the mechanism of the origin of life and impossible to know the exact progress for it. Prebiotic chemistry, in the literal sense, means the chemistry before biotic development. One of the major aspects of prebiotic chemistry is that scientists find ways to collect evidence and propose possible theories for the formation of important complex biomolecules such as amino acids, nucleotides and lipids from simpler and smaller precursors, including formaldehyde, formamide, ammonia, urea, hydrogen cyanide, etc¹⁶¹ (**Scheme 4.1**). These complex molecules cannot be identified as life itself, however they are essential for evolution into complex systems and the eventual establishment of life.



Scheme 4.1. Plausible prebiotic synthesis of key prebiotic biomolecules

In 1924, Alexandr Ivanovich Oparin, a biochemist from The Soviet Union, elucidated his theory about the ‘primordial soup’, a chemical mixture in which life on ancient

¹⁶⁰ M. S. Dodd, D. Papineau, T. Grenne, J. F. Slack, M. Rittner, F. Pirajno, J. O’Neil and C. T. S. Little, *Nature* **2017**, 543, 60.

¹⁶¹ (a) S. L. Miller, L. E. Orgel, *The Origins of Life on Earth* Prentice-Hall, Englewood Cliffs, N.J., **1974**. (b) A. Lazcano, *Journal of Molecular Evolution* **2016**, 83, 214.

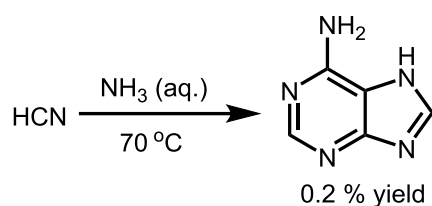
Earth developed gradually through a lengthy period of chemical evolution.¹⁶² Unfortunately, Oparin did not test his theory experimentally. However, in 1953, Stanley L. Miller who was a graduate student of Harold Urey utilized electric discharges in a reducing atmosphere (CH₄, NH₃, H₂O and H₂) to simulate the primitive Earth conditions and capture any compounds formed.¹⁶³ As a result, Miller reported in this prebiotic soup the detection of the formation of glycine after two days; and the other amino acids after two weeks. The analytic techniques at that time were more limited and the samples were further investigated to show the formation of over 20 amino acids after several decades.¹⁶⁴ This suggested chemical evolution could have been a possible pathway which led to achieve those building blocks on the early Earth. This influential experiment is known as Miller-Urey experiment, which has been one of the most discussed experiments in the field of prebiotic chemistry. The formation of other complex molecules from simple precursors has also attracted increasing attention. One experiment that is worth mentioning is Oró's synthesis of adenine¹⁶⁵ (**Scheme 4.2**). Adenine is one of the four nitrogenous bases that make up nucleic acid and is highly important for the generation of self-replicating biological systems. Oró's experiment demonstrated that, in a solution of ammonia, at 70 °C, HCN oligomerized and eventually generated adenine in low yield. Moreover, starting with more advanced HCN oligomer intermediates, including 4-aminoimidazole-5-carboxamide, adenine was produced in higher yields.^{165a}

¹⁶² A. Lazcano, *ACS Nano* **2018**, *12*, 9643.

¹⁶³ S. L. Miller, *Science* **1953**, *117*, 528.

¹⁶⁴ (a) J. L. Bada, *Earth and Planetary Science Letters* **2004**, *226*, 1. (b) E. T. Parker, M. Zhou, A. S. Burton, D. P. Glavin, J. P. Dworkin, R. Krishnamurthy, F. M. Fernández, J. L. Bada, *Angew. Chem. Int. Ed.* **2014**, *53*, 8132.

¹⁶⁵ (a) J. Oró, *Nature* **1961**, *4794*, 1193. (b) J. Oró, A. P. Kimball, *Arch. Biochem. Biophys.* **1961**, *94*, 217. (c) J. Oró, A. P. Kimball, *Arch. Biochem. Biophys.* **1961**, *96*, 293.



Scheme 4.2. Oró's prebiotic synthesis of adenine

To sum up, prebiotic chemistry mainly focused on chemical establishment of complex building blocks for life before biotic process. Gratifyingly, this has achieved some impressive progress and the listed results suggest it was possible to produce the complex molecules of life from simpler precursors.¹⁶⁶ The importance and application of carbonyl compounds in prebiotic chemistry will be further discussed.

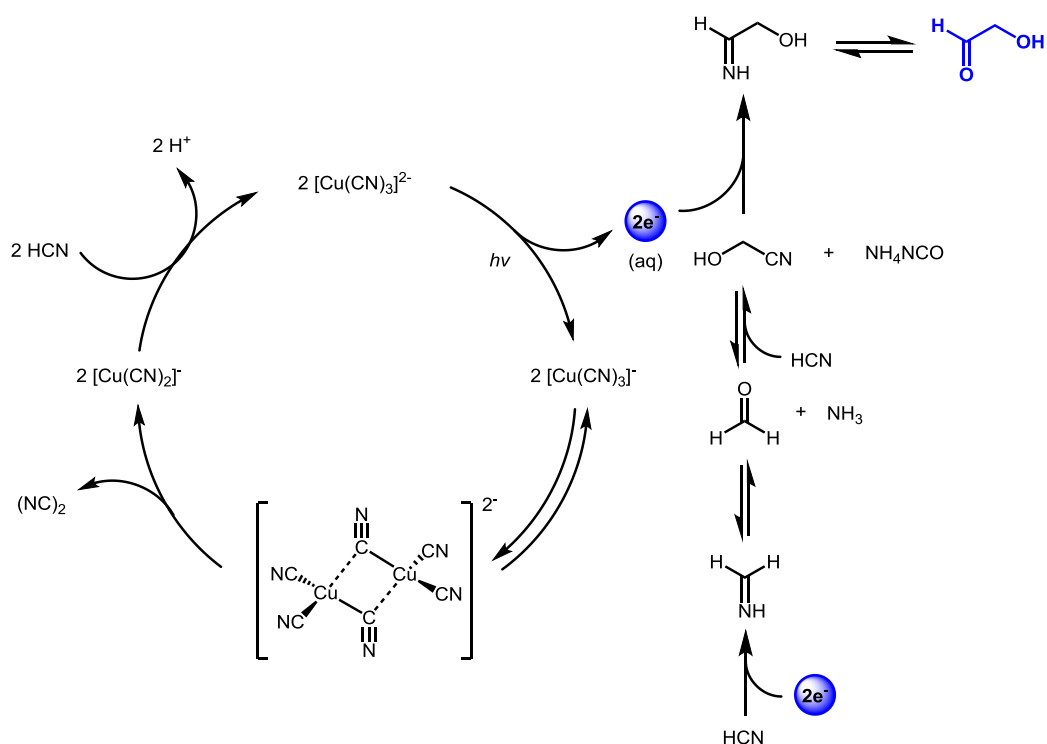
4.2 Glycolaldehyde in Prebiotic chemistry

In the context of prebiotic chemistry, small molecules such as simple carbonyl compounds have attracted significant attention in many aspects. Glycolaldehyde, which is the simplest monosaccharide unit, is one of the key prebiotic precursors for many subunit systems. Glycolaldehyde is also the only monosaccharide sugar to date that has been detected in interstellar clouds.¹⁶⁷ Additionally, it is plausible to prepare glycolaldehyde from photochemical homologation of formaldehyde in a prebiotic manner¹⁶⁸ (**Scheme 4.3**). In 2012, Sutherland and co-workers demonstrated that in the presence of cyanometallates, glycolaldehyde could be prepared from HCN with the help of ultraviolet irradiation.

¹⁶⁶ A. W. Schwartz, M. Goverde, *Journal of Molecular Evolution* **1982**, 18, 351.

¹⁶⁷ (a) J. M. Hollis, F. J. Lovas, P. R. Jewell, *Astrophys. Journal Lett.* **2000**, 540, L107. (b) P. Wang, Y. Hu, H. Zhan, J. Chen, *RSC Adv.* **2017**, 7, 6242.

¹⁶⁸ (a) D. Ritson, J. D. Sutherland, *Nat. Chem.* **2012**, 4, 895. (b) J. D. Sutherland, *Angew. Chem. Int. Ed.* **2016**, 55, 104.



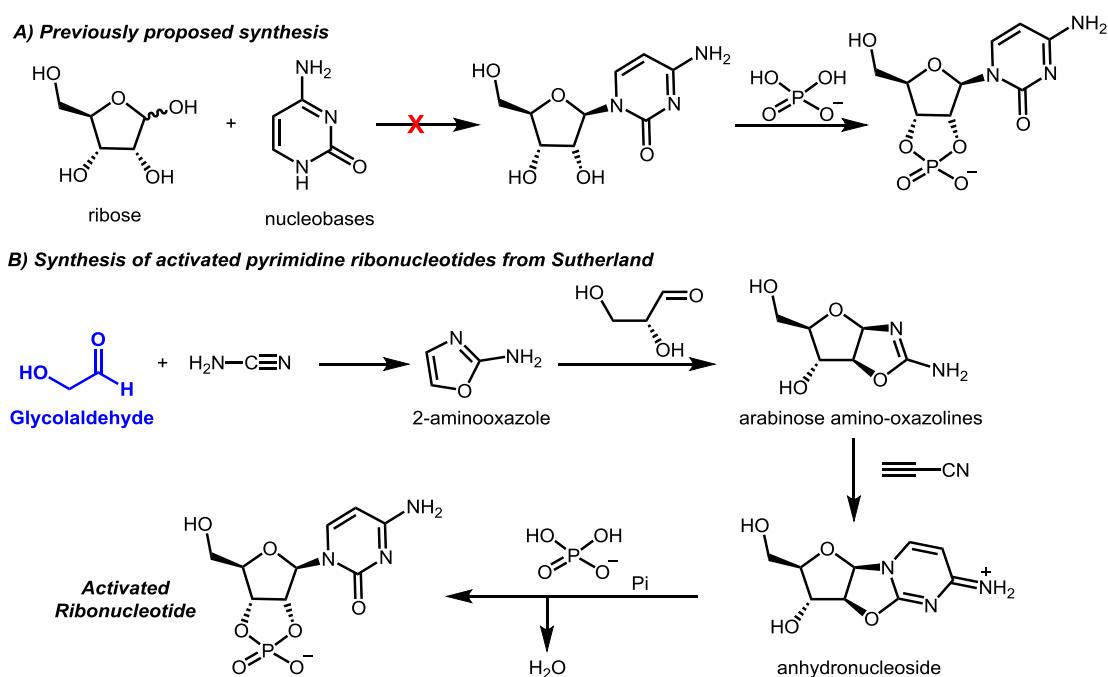
Scheme 4.3. Preparation of glycolaldehyde in prebiotic manner

Since the Miller-Urey experiment,¹⁶³ glycolaldehyde is believed to be an important starting material for biologically-relevant building blocks such as ribonucleotides, imidazoles and sugars. In the following section, the important applications of glycolaldehyde as the starting material towards complex biologically-relevant building blocks will be introduced.

4.2.1 Formation of ribonucleotides

As is known, the polymeric form of ribonucleotide is an important informational polymer—RNA, which must have arisen at some stage during the emergence of life in a chemical reaction manner. Even though, there were some successful examples to show that RNA could form from polymerization of ‘activated’ ribonucleotides, it was not clear that how these ribonucleotides arose from their components: ribose and

nucleobases.¹⁶⁹ On one hand, it took efforts to form ribose selectively;¹⁷⁰ on the other hand, adding nucleobases to ribose was problematic with purines¹⁷¹, and not even possible in some cases of canonical pyrimidines¹⁷² (**Scheme 4.4, a**). In 2009, Sutherland and co-workers reported an efficient approach for the formation of activated ribonucleotides from simple precursors¹⁷³ (**Scheme 4.4, b**). They started from plausible prebiotic feedstock molecules, including glycolaldehyde, and went through arabinose amino-oxazoline and anhydronucleoside intermediates; therefore bypassing the free ribose and nucleobases and eventually generated the activated ribonucleotides. This pathway to generate activated ribonucleotides was a clear example emphasizing the importance of glycolaldehyde which provided solutions to a long-standing problem/challenge.



Scheme 4.4. Prebiotic synthesis of activated ribonucleotides from Sutherland

¹⁶⁹ (a) J. P. Ferris, A. R. Hill Jr, R. Liu, L. E. Orgel, *Nature* **1996**, 381, 59. (b) M. S. Verlander, R. Lohrmann, L. E. Orgel, *J. Mol. Evol.* **1973**, 2, 303.

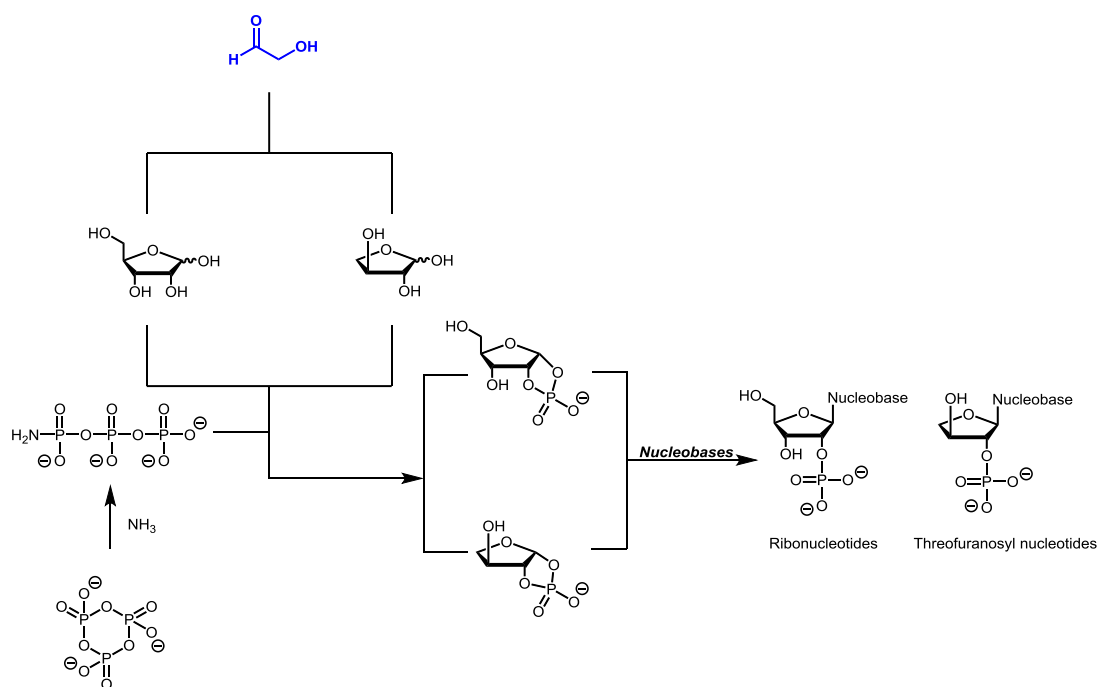
¹⁷⁰ (a) J. Kofoed, J.-L. Reymond, T. Darbre, *Org. Biomol. Chem.* **2005**, 3, 1850. (b) A. Ricardo, M. A. Carrigan, A. N. Olcott, S. A. Benner, *Science* **2004**, 303, 196.

¹⁷¹ W. D. Fuller, R. A. Sanchez, L. E. Orgel, *J. Mol. Biol.* **1972**, 67, 25.

¹⁷² L. E. Orgel, *Crit. Rev. Biochem. Mol. Biol.* **2004**, 39, 99.

¹⁷³ M. W. Powner, B. Gerland, J. D. Sutherland, *Nature* **2009**, 459, 239.

In 2017, Benner and co-workers reported a prebiotic stereoselective coupling approach to directly prepare purine and noncanonical pyrimidine nucleotides from phosphorylated carbohydrates and free nucleobases¹⁷⁴ (**Scheme 4.5**). With this development, the formation of ribonucleotides from the protected-ribose and nucleobases was achieved in short sequence.



Scheme 4.5. Prebiotic synthesis of ribonucleotides from Benner

With all these listed approaches, the important role of glycolaldehyde has been clearly demonstrated towards the formation of ribonucleotides, which also supported the hypothesis of the current “RNA world” for the origin of life.

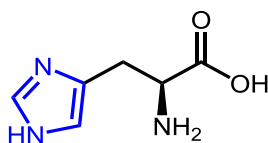
4.2.2 Formation of imidazoles and oxazoles

Imidazoles are biologically important and they are found in histidine residues in proteins (**Scheme 4.6**). They are also found to be catalytically¹⁷⁵ helpful for the

¹⁷⁴ (a) H.-J. Kim, S. A. Benner, *PNAS* **2017**, *114*, 43, 11315. (b) H.-J. Kim, J. Kim, *Astrobiology* **2019**, *19*:5, 669.

¹⁷⁵ J. Oró, B. Basile, S. Cortes, C. Shen, T. Yamrom, *Origins Life* **1984**, *14*, 237.

oligomerization of amino acids,¹⁷⁶ phosphates¹⁷⁷ and nucleotides.¹⁷⁸



Scheme 4.6. Structure of histidine

Glycolaldehyde has been extensively studied as the starting material for prebiotic formation of imidazoles and oxazoles. For example, glycolaldehyde could be utilized to prepare 2-aminooxazole,¹⁷³ 2-aminoimidazole,¹⁷⁹ and 2-thiooxazole¹⁸⁰ (**Scheme 4.7**). In the field of prebiotic chemistry, 2-aminooxazole has been demonstrated by Sutherland and co-workers as the key precursor to prebiotically synthesize pyrimidine nucleotides.¹⁷³ Moreover, the importance of imidazoles, in particular 2-aminoimidazole, was emphasized by their ability to serve as an efficient activation agent, which allowed enhanced rate of non-enzymatic template-directed RNA primer extension.¹⁸¹ Synthesis of 2-thiooxazole was also achieved using glycolaldehyde as the starting material and was further utilized as the key prebiotic precursor to prepare both 8-oxo-purine nucleotides and pyrimidine nucleotides.¹⁸⁰

¹⁷⁶ R. Lohrmann, L. E. Orgel, *Nature* **1973**, *244*, 418.

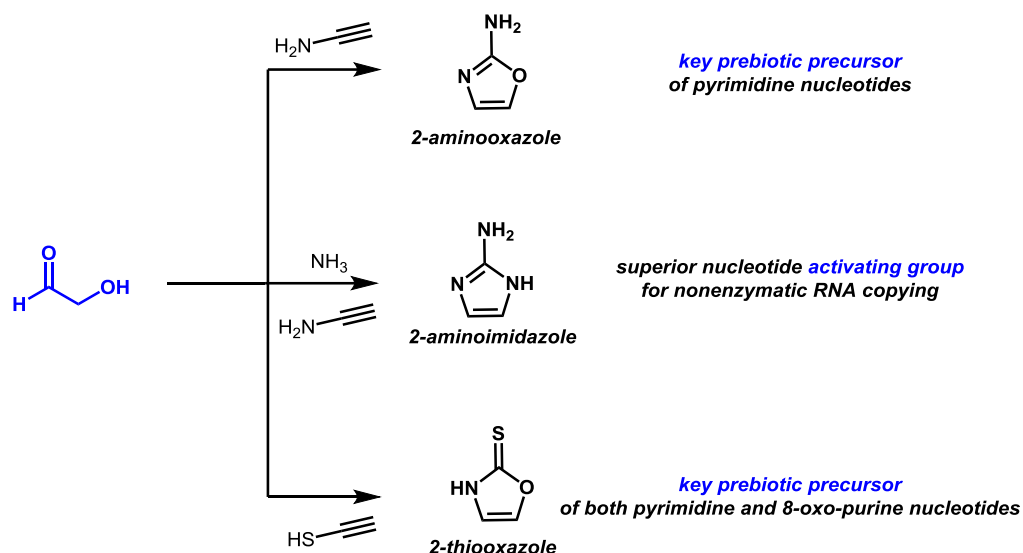
¹⁷⁷ (a) A. L. Weber, *J. Mol. Evol.* **1981**, *18*, 24. (b) A. D. Keefe, S. L. Miller, *Origins Life Evol. Biospheres* **1996**, *26*, 15.

¹⁷⁸ (a) O. Pongs, P. O. P. Ts'o, *J. Am. Chem. Soc.* **1971**, *93*, 5241. (b) J. Oró, E. Stephen-Sherwood, *Origins Life Evol Biophere* **1974**, *5*, 159.

¹⁷⁹ A. C. Fahrenbach, C. Giurgiu, C. P. Tam, L. Li, Y. Hongo, M. Aono, J. W. Szostak, *J. Am. Chem. Soc.* **2017**, *139*, 26, 8780.

¹⁸⁰ S. Stairs, A. Nikmal, D.-K. Bucar, S.-L. Zheng, J. W. Szostak, M. W. Powner, *Nat. Comm.* **2017**, *8*, 15270.

¹⁸¹ (a) T. Wu, L. E. Orgel, *J. Am. Chem. Soc.* **1992**, *114*, 5496. (b) J. C. Blain, J. W. Szostak, *Annu. Rev. Biochem.* **2014**, *83*, 615. (c) A. C. Fahrenbach, *Pure Appl. Chem.* **2015**, *87*, 205. (d) E. C. Izgu, A. C. Fahrenbach, N. Zhang, L. Li, W. Zhang, A. T. Larsen, J. C. Blain, J. W. Szostak, *J. Am. Chem. Soc.* **2015**, *137*, 6373. (e) L. Li, N. Prywes, C. P. Tam, D. K. O'Flaherty, V. S. Lelyveld, E. C. Izgu, A. Pal, J. W. Szostak, *J. Am. Chem. Soc.* **2017**, *139*, 1810.



Scheme 4.7. Glycolaldehyde as the precursor for imidazoles and oxazoles

These achievements further suggested the paramount importance of glycolaldehyde as a prebiotic precursor towards the formation of complex building blocks.

4.2.3 Formation of sugars: Formose synthesis

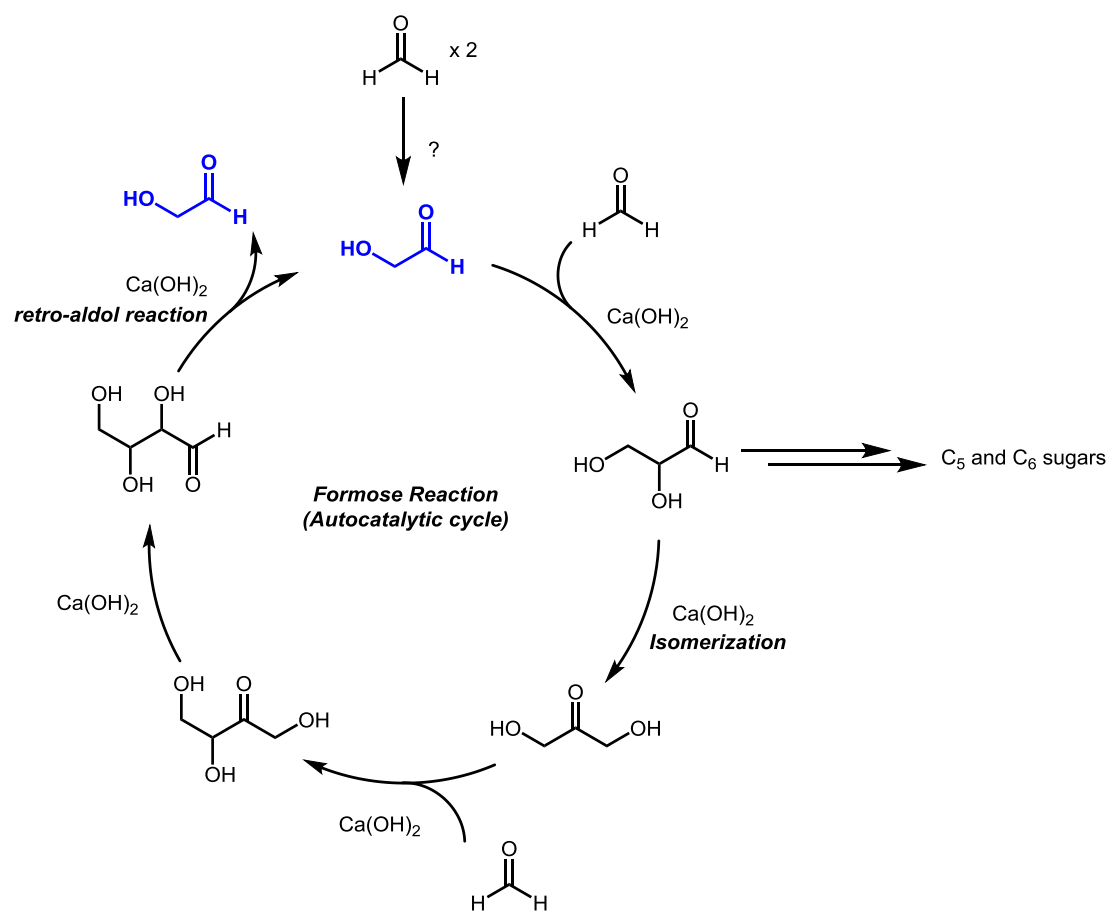
In 1861, Butlerow first discovered a complex autocatalytic reaction to generate sugar-type substances from formaldehyde¹⁸² (**Scheme 4.8**). This reaction is known as the formose reaction, which is a portmanteau of *formaldehyde* and *aldose*. This discovery was noteworthy in the field of prebiotic chemistry since this is a chemical pathway to generate carbohydrates and in the context of origin of an RNA world, ribose is potentially important.¹⁸³ No doubt that this discovery led to a massive investigation, with extensive discussion and debate regarding to the mechanism. In the most accepted mechanism,¹⁸⁴ the formose reaction is extremely slow at the beginning, until glycolaldehyde is formed from the dimerization of formaldehyde (via an unknown

¹⁸² A. C. R. Butlerow, *Acad. Sci.* **1861**, *53*, 145.

¹⁸³ H. J. Cleaves, in *Encyclopedia of Astrobiology*, eds. R. Amils, M. Gargaud, J. Cernicharo Quintanilla, H. J. Cleaves, W. M. Irvine, D. Pinti and M. Viso, Springer Berlin Heidelberg, Berlin, Heidelberg, 2014, pp. 1-8.

¹⁸⁴ R. Breslow, *Tetrahedron Lett.* **1959**, *1*, 22.

mechanism that may involve radiation). After, the autocatalytic cycle performs efficiently to generate different intermediates and sugar-like substances. This process involves aldol reactions, reverse aldol reactions and isomerization reactions. It is worth mentioning that, the induction period could be accelerated by the addition of glycolaldehyde or other analogous ketols. Notably, glycolaldehyde is believed to serve as a key precursor and initiator of this autocatalytic system. It was worth mentioning that under dry conditions, the formation of carbohydrates was also achieved, with preferable formation of unbranched monosaccharides.¹⁸⁵



Scheme 4.8. Most accepted mechanism for Formose reaction

With this range of experimental support, it is broadly accepted that glycolaldehyde is a

¹⁸⁵ S. Lamour, S. Pallmann, M. Haas, O. Trapp, *life*, **2019**, *9*, 52.

key precursor and reagent for the preparation of more complex molecules. Despite the evidence, very little, other than the formose reaction, has been achieved to exploit its ability to act as a catalyst. Given the paramount importance of glycolaldehyde in prebiotic chemistry and our interest in discovering the catalytic role of aldehydes, we decided to systematically study the catalytic importance of glycolaldehyde in hydrolysis reactions of Strecker products and the compounds containing the P(=O)-N bonds.

4.3 Glycolaldehyde catalyzed hydrolysis of Strecker adduct

In the Miller-Urey experiment,¹⁶³ amino acids were the first prebiotic molecules to be identified.¹⁸⁶ Amino acids are fundamental unit for proteins and exist in high quantities on some chondritic meteorites.¹⁸⁷ Among the different prebiotic synthesis of amino acids,¹⁸⁸ the Strecker reaction¹⁸⁹ followed by hydration and hydrolysis is considered as the most straightforward pathway to achieve amino acids.

4.3.1 Strecker reaction

The Strecker reaction allows to combine carbonyl compounds (e.g. glycolaldehyde could be used as a Strecker precursor to form serine^{186a}), ammonia and HCN together^{186a} (**Scheme 4.9**). This reaction has been studied for more than 160 years, involving formation of α -aminonitriles. Importantly, it can be followed by the hydration and hydrolysis of nitrile group to generate amino acids. Moreover, the precursors for the Strecker reaction are prebiotically important substrates, for example HCN can be

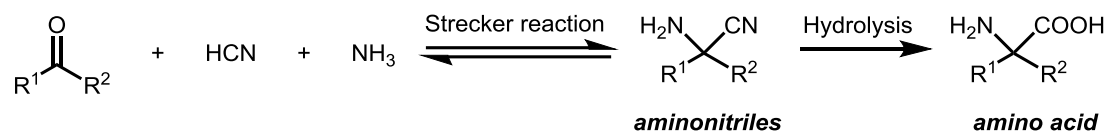
¹⁸⁶ (a) K. Ruiz-Mirazo, C. Briones, A. de la Escosura, *Chem. Rev.* **2014**, *114*, 1, 285. (b) A. P. Johnson, H. J. Cleaves, J. P. Dworkin, D. P. Glavin, A. Lazcano, J. L. Bada, *Science* **2008**, *322*, 404.

¹⁸⁷ (a) S. Pizzarello, *Acc. Chem. Res.* **2006**, *39*, 231. (b) S. Pizzarello, E. Shock, *Cold Spring Harbor Perspect. Biol.* **2010**, *2*, a002105. (c) A. S. Burton, J. C. Stern, J. E. Elsila, D. P. Glavin, J. P. Dworkin, *Chem. Soc. Rev.* **2012**, *41*, 5459.

¹⁸⁸ D. Fitz, H. Reiner, B. M. Rode, *Pure Appl. Chem.* **2007**, *79*, 2101.

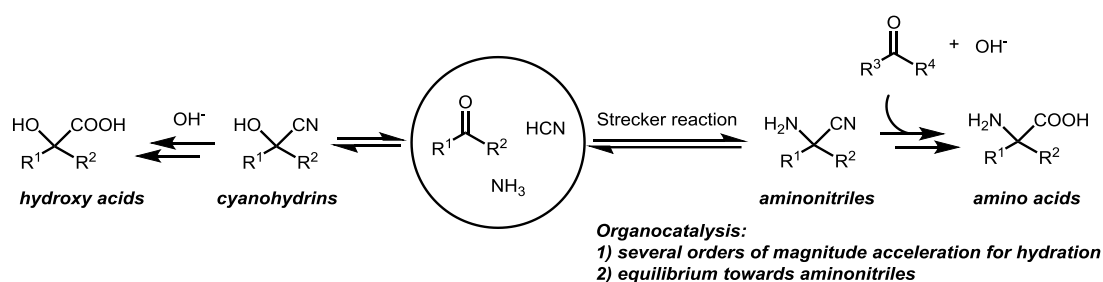
¹⁸⁹ A. Strecker, *Liebigs. Ann. Chem.* **1850**, *75*, 27.

used as the starting material for the prebiotic synthesis of purines. Aldehydes, as discussed above, are main reagents of the formose reaction to provide sugar-type substances. Therefore, the prebiotic relevance of the Strecker reaction is generally accepted.



Scheme 4.9. Strecker Reaction to produce α -aminonitriles

In the Strecker reaction (**Scheme 4.10**), the first step involves an equilibrium where both α -aminonitriles and cyanohydrins can form. After the reaction, hydration and hydrolysis of the nitrile group forms a mixture of α -amino acids and α -hydroxy acids, respectively. This irreversible and slow process goes through the hydration of α -aminonitriles to generate α -amino amides followed by their hydrolysis of α -amino amides to provide different amino acids. The hydrolysis step was found to be accelerated by the addition of carbonyl compounds^{190a} that pushes the equilibrium towards the formation of α -aminonitriles. Therefore the hydrolysis of α -aminonitriles also attracted extensive attention.

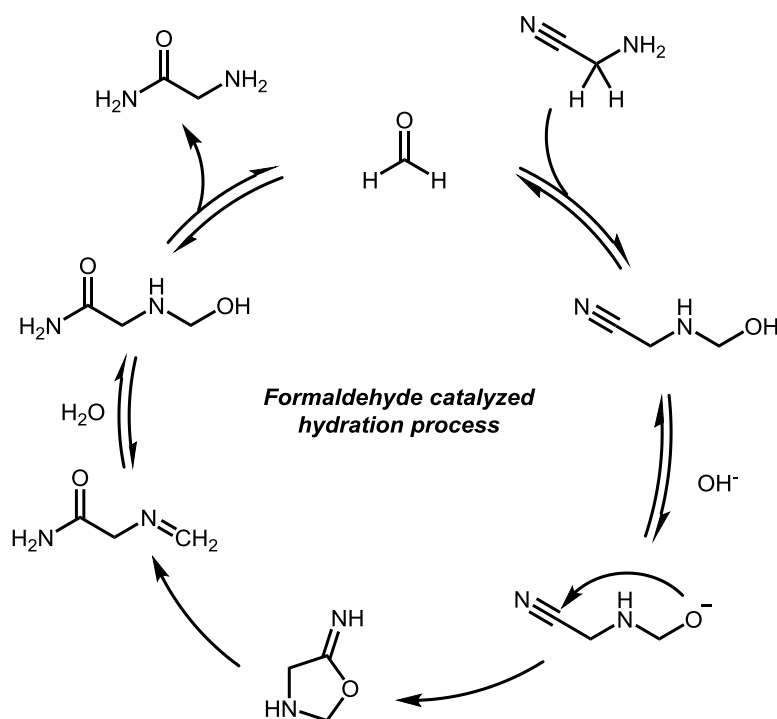


Scheme 4.10. Carbonyl compounds promoted the formation of amino acids from α -aminonitriles

4.3.2 Hydration of α -aminonitriles (Strecker adduct)

Decades ago, Commeyras and co-workers demonstrated that addition of aldehydes or

ketones into Strecker reactions could shift the initial equilibrium to favor the formation of α -aminonitriles and generated α -amino amides, precursors of amino acids, as the product¹⁹⁰ (**Scheme 4.11**). Simply adding aldehydes or ketones into the system could accelerate this process by several orders of magnitude. Strategically, this also applied the concept of temporary intramolecularity to form the intramolecular nucleophiles to facilitate this slow hydration process. These studies demonstrated the catalytic importance of carbonyl compounds for the formation of amino acids in the field prebiotic chemistry.



Scheme 4.11. Proposed catalytic cycle for formaldehyde-catalyzed hydration of α -aminonitriles

In summary, aspects of prebiotic chemistry have been introduced, focusing on glycolaldehyde. This molecule has been used as a key starting material to synthesize

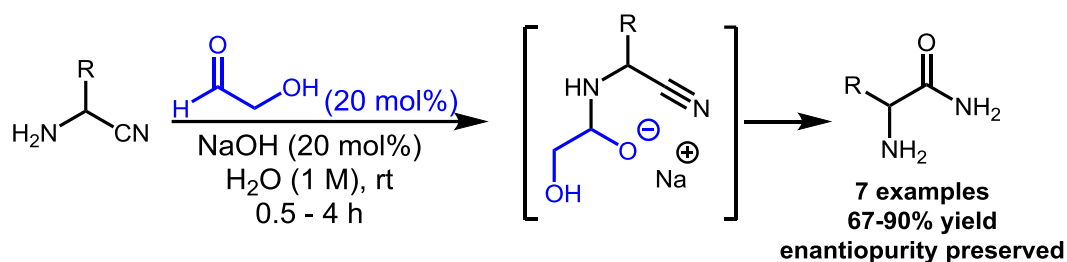
¹⁹⁰ (a) R. Pascal, J. Taillades and A. Commeyras, *Bull. Soc. Chim. Fr., II*, **1978**, 3-4, 177; (b) R. Pascal, J. Taillades and A. Commeyras, *Tetrahedron*, **1978**, 34, 2275; (c) R. Pascal, J. Taillades and A. Commeyras, *Tetrahedron*, **1980**, 36, 2999; (d) R. Pascal, M. L. Marnier, A. Rousset, A. Commeyras, J. Taillades and L. Mion, US4243814, **1981**. For efforts toward asymmetric variants; (e) P.-H. Lagriffoul, Z. Tadros, J. Taillades and A. Commeyras, *J. Chem. Soc., Perkin Trans. 2*, **1992**, 1279. See also: (f) R. Sola, J. Taillades, J. Brugidou and A. Commeyras, *New J. Chem.*, **1989**, 13, 881; (g) Taillades, J.; Beuzelin, I.; Garrel, L.; Tabacik, V.; Bied, C.; Commeyras, A. *Origins Life Evol. Biospheres*, **1998**, 28, 61.

different prebiotic building blocks. In addition, the Strecker reaction, a reaction relevant to the prebiotic generation of amino acids was also discussed, in particular, the difficult hydration/hydrolysis of Strecker adducts. Even though different methodologies have been developed to solve this problem, a prebiotic process involving glycolaldehyde as an efficient catalyst to produce amino acids has not been reported.

4.3.3 Glycolaldehyde catalyzed hydration reaction of α -aminonitriles

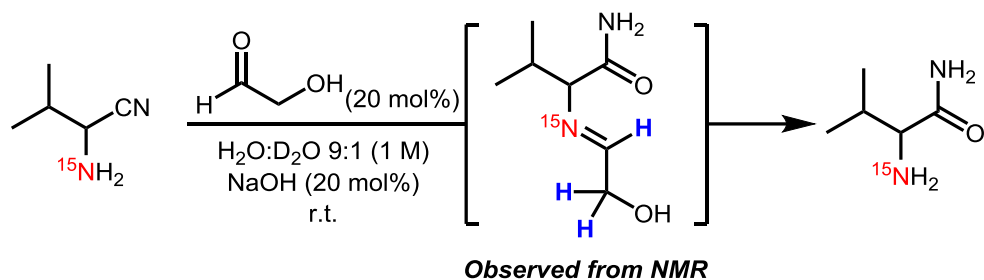
Noticing the gap in the literature for applying glycolaldehyde as a catalyst, and given previous results that the benzyl-protected glycolaldehyde could act as a tethering catalyst to carry out alkene hydroamination,⁴⁰ we were excited to exploit the catalytic efficiency of glycolaldehyde starting from the hydrations of the Strecker adducts, α -aminonitriles, under prebiotic conditions. This part of the work for glycolaldehyde-catalyzed hydrolysis reaction of α -aminonitriles was performed by Dr. Claudia El-Nachef with Aidan Pezacki, an undergraduate student.

Gratifyingly, our previously reported conditions for formaldehyde-catalyzed hydration reaction³² could be applied for this system, with catalytic amount of the glycolaldehyde and sodium hydroxide. Excellent catalytic efficiency of glycolaldehyde was obtained with different primary α -amino nitriles as substrates (**Scheme 4.12**). In this reaction system, different functional groups could be tolerated providing moderate to excellent yields. Depending on the nature of different substrates and of their solubility in water, the reaction time varied from 0.5 to 4 hours. It is worth mentioning that an enantiomerically pure α -amino nitrile was also compatible with the reaction conditions resulting to a minimal loss of enantiopurity (97% ee), which indicated that glycolaldehyde was not acting as a racemization catalyst in this system.



Scheme 4.12. Glycolaldehyde catalyzed hydration of α -aminonitriles

It should be noted that no evidence was obtained to directly prove the formation of intermediate as shown in **Scheme 4.12**. Instead the formation of an imine intermediate from the condensation of glycolaldehyde and ^{15}N labelled substrate was observed by NMR (**Scheme 4.13**).



Scheme 4.13. Observed intermediate of glycolaldehyde-catalyzed hydration reaction of α -aminonitriles

In order to gain more insight into this glycolaldehyde-catalyzed hydration of α -aminonitriles, the reaction order with respect to glycolaldehyde was examined. The kinetic experiment results elucidated this hydrolysis reaction was approximately first-order in glycolaldehyde. These results clearly demonstrated that glycolaldehyde could reveal the catalytic efficiency operating via temporary intramolecularity. Since the intermediate can be observed, the rate-limiting step was proposed to be the formation of α -amino amides from α -imino amides intermediates.

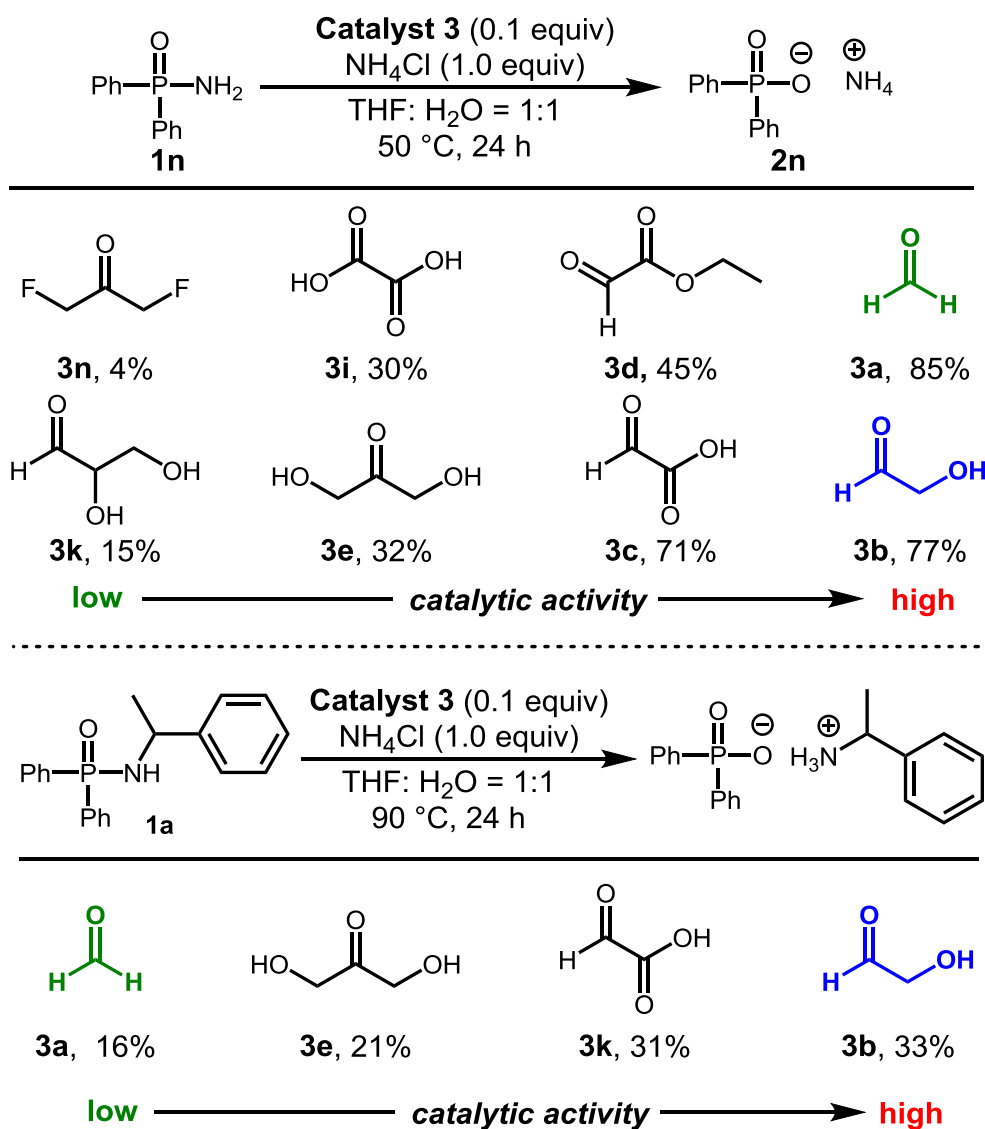
With the promising results regarding hydration reaction of α -aminonitriles in hand, my attention was directed to re-investigate Jencks' work⁹¹ on the hydrolysis of phosphoramidate.

4.4 Results and Discussion: Comparison of catalytic efficiency of glycolaldehyde vs formaldehyde

It was demonstrated by Jencks and co-workers that formaldehyde could facilitate the hydrolysis of phosphoramidate through electrophilic activation, which has been discussed in detail in Chapter 2. Inspired by Jencks' work, we have shown that *o*-phthalaldehyde, compared to formaldehyde, is a more applicable catalyst with a broad substrate scope and could achieve efficient chemoselectivity. In prebiotic chemistry, phosphoryl transfer reactions are of paramount importance, especially in the context of RNA replication. Given the importance of glycolaldehyde in prebiotic chemistry and the encouraging results achieved from hydrolysis reactions of α -aminonitriles with glycolaldehyde as the catalyst, we decided to investigate the catalytic efficiency of glycolaldehyde in the hydrolysis of P-N bond system as an outset.

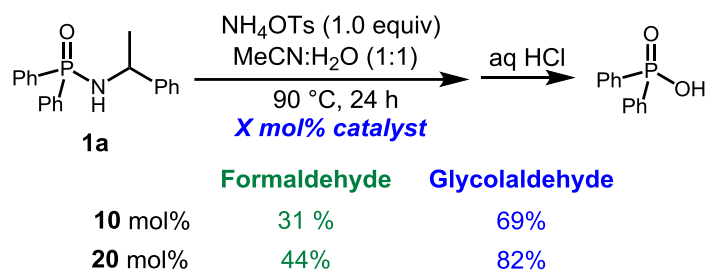
The investigation started with the screening of different prebiotic and non-prebiotic aldehydes and ketones as catalysts, which has been presented in Chapter 2 (**Table 4.1**, review of **Tables 2.1** and **2.3**). With primary phosphinic amide **1n** as the substrate, both formaldehyde and glycolaldehyde could provide the product with good yields with only 10 mol% loading of the catalyst. However, with a more hindered secondary phosphinic amide, glycolaldehyde was a more efficient catalyst than formaldehyde.

Table 4.1. Review on aldehyde screening for model primary and secondary substrates^a



^a Reaction conditions: **4a** (0.2 mmol), NH₄Cl (0.2 mmol), **3** (0.02 mmol) in 0.4 mL of THF/H₂O (1:1) at 50 °C for 24 h in a sealed tube. NMR yields were determined using 1,3,5-trimethoxybenzene as internal standard.

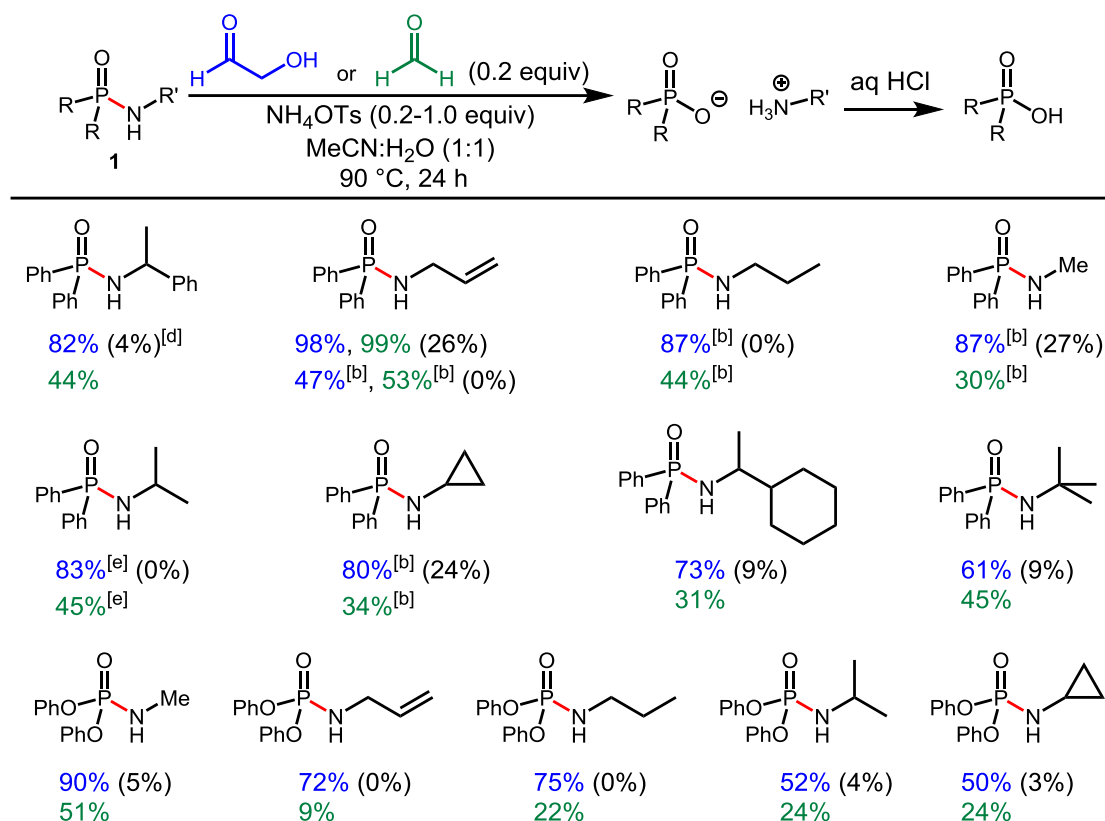
By combining this encouraging result with insights from our previous study of *o*-phthalaldehyde, this reaction was promoted to be even more efficient by applying 20 mol% of glycolaldehyde as a catalyst. (**Scheme 4.14**)



Scheme 4.14. Comparison of 10 and 20 mol% amount of formaldehyde and glycolaldehyde

This result encouraged us to further investigate this hydrolysis reaction with glycolaldehyde as a catalyst for different substrates (**Table 4.2**). As can be seen, in most cases, glycolaldehyde proved to be a competent catalyst for this hydrolysis reaction, offering even better results than formaldehyde. Many reactions had to be carried out at 90 °C, but depending on the nature of the substrates, some reactions worked at lower temperatures.

Table 4.2. Comparison of the catalytic efficiency between glycolaldehyde and formaldehyde^a



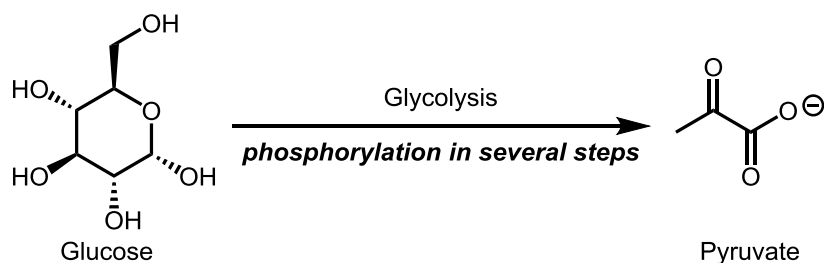
^a Reaction conditions: **1** (0.2 mmol), NH₄OTs (0.2 mmol), aldehyde (0.04mmol) in 0.4 mL of MeCN/H₂O (1:1) at 90 °C for 24 h in a sealed tube. Isolated yields after quenching with aqueous HCl are shown (corresponding acid). ^b In the presence of 0.04 mmol at 50 °C. ^c Yields in blue (with glycolaldehyde) and green (with formaldehyde) are isolated yields. ^d Yields in parentheses are NMR yields of the background reaction (hydrolysis in the absence of glycolaldehyde). ^e At 50 °C.

These results clearly demonstrated the catalytic potential with glycolaldehyde as a catalyst for the hydrolysis of P(=O)-N bonds. This proved to be a good starting point for us to investigate the phosphoryl activation with glycolaldehyde as a catalyst and we finally could move on to apply this method to the electrophilic activation of more prebiotic-relevant substances.

4.5 Phosphorylation process

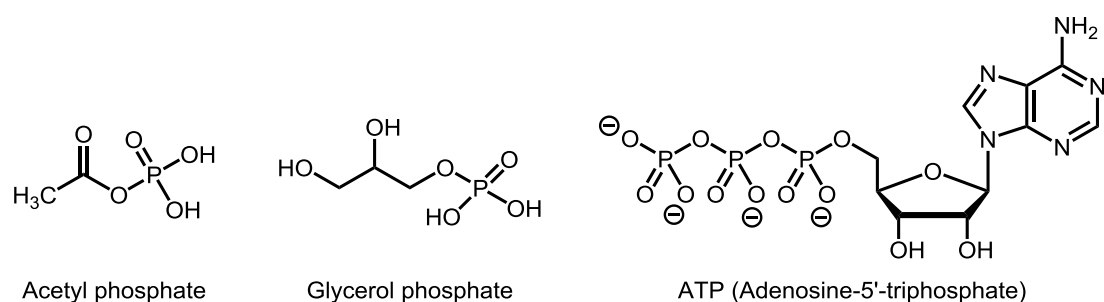
Phosphorylation is an important process in biology and biochemistry. One of the most discussed phosphorylation processes, in Nature, is glycolysis (**Scheme 4.15**).

Glycolysis is an enzyme-catalyzed metabolic pathway to convert glucose into pyruvate, meanwhile, free energy was released to form ATP and NADH molecules. In this process, several phosphorylation steps are performed with the assistance of different enzymes.



Scheme 4.15. An outline for the process of glycolysis

Moreover, many other phosphorylated organic molecules are essential in living organisms. For example acetyl phosphate (reactive organophosphates), glycerol phosphates (stable phosphorylated biomolecules) and ATP (poly-phosphates)¹⁹¹ (**Scheme 4.16**).



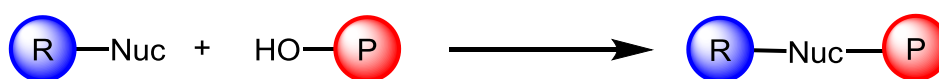
Scheme 4.16. Selected examples for phosphorylated biomolecules

4.5.1 Prebiotic phosphorylation

In the context of prebiotic chemistry, as has been discussed above, this field investigated on the formation of simple biomolecules such as amino acids (e.g. Strecker reaction), sugars (e.g. formose reaction) and etc. Moreover, the processes to form more complex molecules from simple precursors have also been extensively studied. Another aspect

¹⁹¹ M. Gull, *Challenges* **2014**, *5*, 193.

that has attracted increasing attention is ‘the problem of phosphorus and phosphorylation’. However, it was interesting to realize the challenge of prebiotic phosphorylation (**Scheme 4.17**) especially in the aqueous media given that 1) it is thermodynamically unfavorable to ‘kick out’ water into the environment and 2) water as a nucleophile can react with the phosphorylating reagents and undergo hydrolysis of the reagents.¹⁹¹ Due to these difficulties, different possible phosphorylating reagents, conditions and catalysts have been developed for different substrates.



Scheme 4.17. An outline for phosphorylation process

Orthophosphates as phosphorylating reagents

Orthophosphates could be applied as the phosphorylating reagents especially in the presence of condensation agents. Back in 1968, Lohrmann and Orgel systematically studied the phosphorylation of uridine with inorganic phosphate to form uridine-5'-phosphate, in the presence of different condensing agents in aqueous solution.¹⁹² However, even with a large excess of condensing agents, the yields (with NaH_2PO_4 , up to 12%) were still low. Other phosphorylation reactions with different substrates have also been developed.¹⁹¹ For example, with the assistance of cyanogen, glucose 1,6-diphosphate could be prepared from glucose-1-phosphate at room temperature (with Na_2HPO_4 , 1-3% yields).¹⁹³ Moreover, numerous studies also demonstrated that clays, minerals and salts could catalyze the phosphorylation by orthophosphates.¹⁹⁴

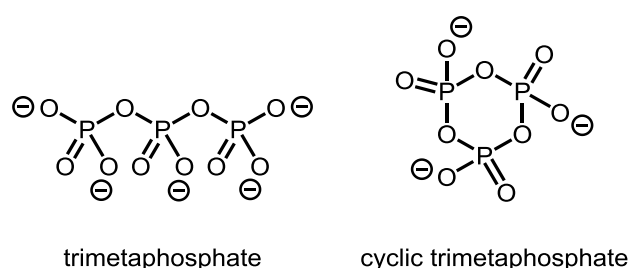
¹⁹² R. Lohrmann, L. E. Orgel, *Science* **1968**, *161*, 64.

¹⁹³ C. Degani, M. Halmann, *J. Chem. Soc. Chem. Commun.* **1971**, 1459.

¹⁹⁴ For clays, minerals and salts catalyzed phosphorylation reactions, please see: (a) W. R Hargreaves, S. J. Mulvihill, D. W. Deamer, *Nature* **1977**, *266*, 78. (b) M. Gull, T. Ge, W. Yingwu, H. Chao, S. Zhan, Y. Hongming, F. Shouhua, *Heteroat. Chem.* **2010**, *21*, 161. (c) M. Gull, W. Yu, W. Yingwu, S. Zhan, T. Ge, F. Shouhua, *Heteroat. Chem.* **2011**, *22*, 186. (d) G. J. Handschuh, R. Lohrmann, L. E. Orgel, *J. Mol. Evol.* **1973**, *2*, 251. (e) L. Lohrmann, L. E. Orgel, L.E. *Science* **1971**, *171*, 490–494. For other recent variants of orthophosphates as phosphorylating reagents, please

Poly-phosphates as phosphorylating reagents

Even if orthophosphates have been largely used as the phosphorylating reagents, it was clearly demonstrated that this type of reagents is not as efficient as expected. Therefore, poly-phosphates, long-chain compounds with stable P-O-P bonds, were investigated for this special process. In 1991, Yamagata and co-workers demonstrated that water-soluble poly-phosphates could be produced from volcanic activity through partial hydrolysis of P_4O_{10} .¹⁹⁵ For a long time, (cyclic)trimetaphosphate (**Scheme 4.18**) has been used to phosphorylate different prebiotic-relevant substances, such as amino acids,¹⁹⁶ and nucleoside,¹⁹⁷ with limited substrate scope.¹⁹⁸ However, these molecules were found to be ineffective for phosphorylation of glycolaldehyde in aqueous solution towards the formation of glycolaldehyde phosphate. This led to the development of other potential phosphorylating reagents.



Scheme 4.18. Structures of trimetaphosphate and cyclic triphosphate

DAP as a common phosphorylating source

Amidotriphosphate (AmTP)¹⁹⁹ and diamidophosphate (DAP)²⁰⁰ were investigated

see: (f) B. Burcar, M. Pasek, M. Gull, B. J. Cafferty, F. Velasco, N. V. Hud, C. Menor-Salván, *Angew. Chem. Int. Ed.* **2016**, *55*, 13249. (g) H.-J. Kim, Y. Furukawa, T. Kakegawa, A. Bitá, R. Scorei, S. A. Benner, *Angew. Chem. Int. Ed.* **2016**, *55*, 15816.

¹⁹⁵ Y. Yamagata, H. Watanabe, M. Saitoh, T. Namba, *Nature* **1991**, *352*, 516.

¹⁹⁶ F. Ni, S. Sun, C. Huang, Y. Zhao, *Green Chem.* **2009**, *11*, 569.

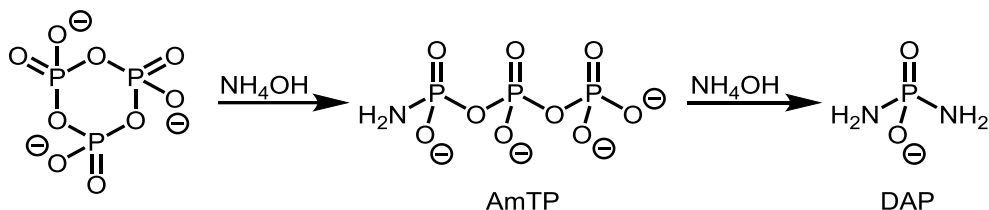
¹⁹⁷ R. Saffhill, *J. Org. Chem.* **1970**, *35*, 2881.

¹⁹⁸ (a) W. Feldmann, *Chem. Ber.* **1967**, *100*, 3850. (b) A. Schwartz, C. Ponnampereuma, *Nature* **1968**, *218*, 443. (c) A. Schwartz, *J. Chem. Soc. D* **1969**, 1393a.

¹⁹⁹ Formation of AmTP: O. T. Quimby, T. J. Flautt, *Z. Anorg. Allg. Chem.* **1958**, *296*, 220.

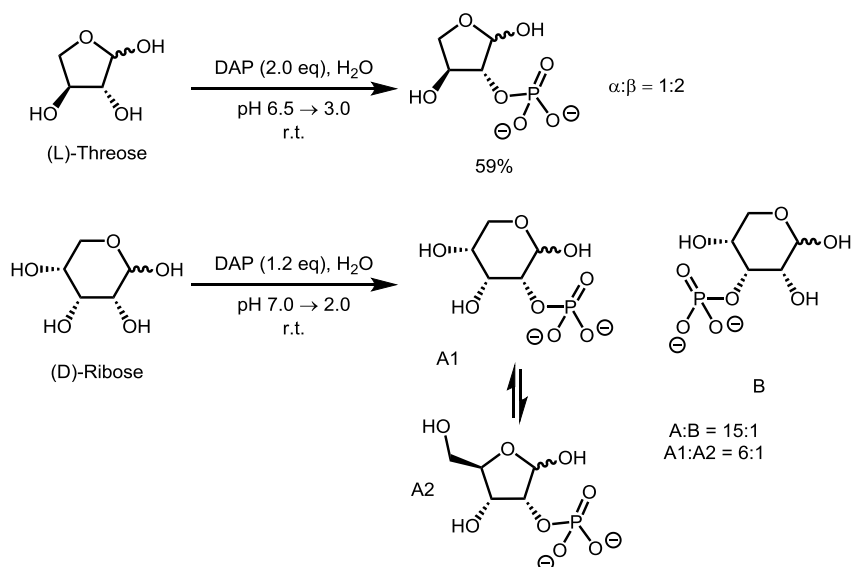
²⁰⁰ Formation of DAP: W. Feldmann, E. Thilo, *Z. Anorg. Allg. Chem.* **1964**, *328*, 113.

particularly for the phosphorylation of glycolaldehyde. AmTP and DAP are plausible prebiotic agents generated from cyclic-trimetaphosphate (**Scheme 4.19**), and have been shown to phosphorylate different prebiotic-relevant substances.



Scheme 4.19. Generation of DAP from cyclo-trimetaphosphate

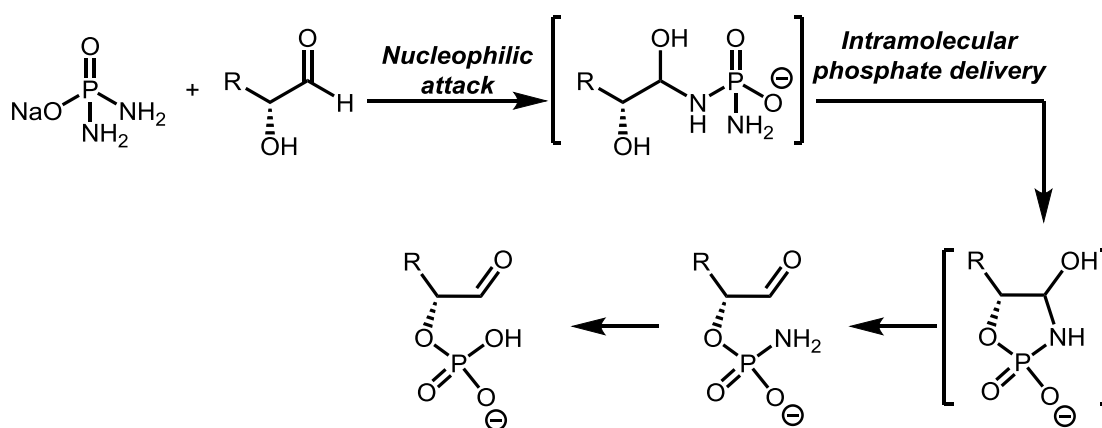
In 1999, Krishnamurthy, Arrhenius and Eschenmoser demonstrated at near neutral pH AmTP could phosphorylate glycolaldehyde in aqueous solution within days.²⁰¹ The reaction was performed in the presence of Mg^{2+} and the product was isolated in 76% yield. In 2000, DAP was applied as a potential phosphorylating reagent by the same group^{201b} and successfully achieved phosphorylated aldoses in aqueous environment (**Scheme 4.20**).



Scheme 4.20. Phosphorylation of aldoses with DAP

²⁰¹ (a) R. Krishnamurthy, G. Arrhenius, A. Eschenmoser, *Orig. Life Evol. Biosph.* **1999**, *29*, 333. For a follow-up work to phosphorylate different α -hydroxy aldehydes, please see: R. Krishnamurthy, S. Guntha, A. Eschenmoser, *Angew. Chem. Int. Ed.* **2000**, *39*, 2281

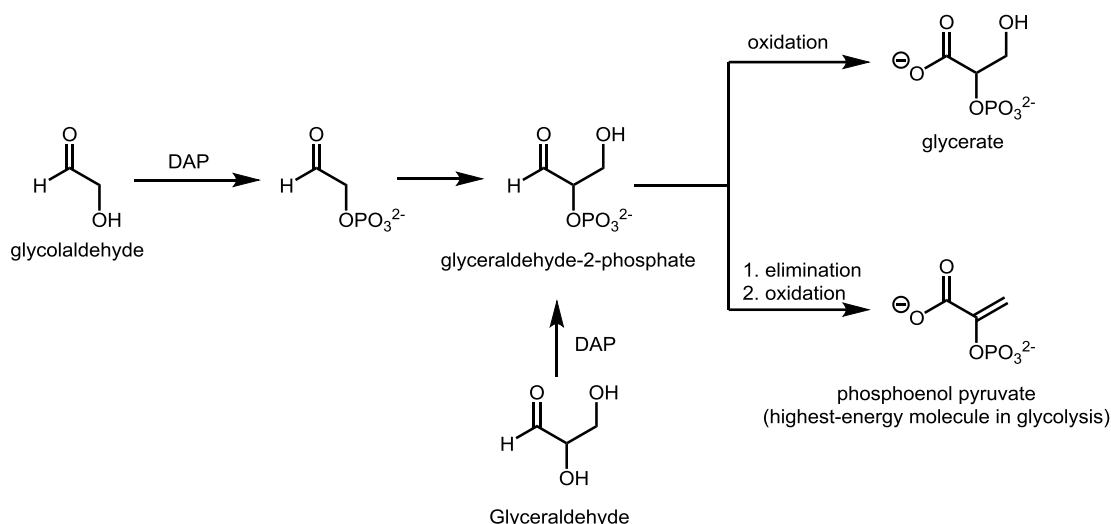
This phosphorylation process started with a nucleophilic attack of the NH₂-group of DAP onto the aldehyde, then adjacent OH-group would be phosphorylated via an intramolecular manner (**Scheme 4.21**). This intramolecular phosphate delivery process was faster than the hydrolysis of DAP, and no discernible side reactions were observed in this system even if the reaction times varied from days to weeks.



Scheme 4.21. Intramolecular phosphorylation of α -hydroxy aldehyde with DAP

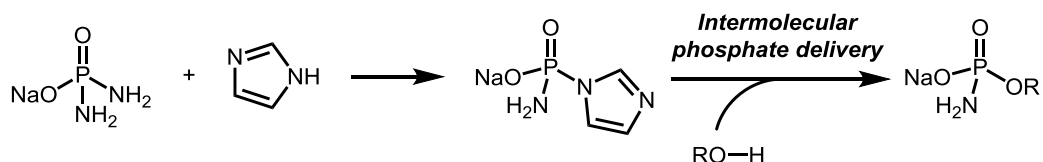
In 2016, Powner and co-workers utilized DAP to synthesize phosphoenol pyruvate from simple prebiotic precursors, glycolaldehyde and glyceraldehyde²⁰² (**Scheme 4.22**). They demonstrated that both glycolaldehyde and glyceraldehyde can regioselectively generate glyceraldehyde-2-phosphate, which could be further converted into glycerate or phosphoenol pyruvate.

²⁰² A. J. Coggins, M. W. Powner, *Nat. Chem.* **2017**, *9*, 310.



Scheme 4.22. DAP as phosphorylating reagent to prepare phosphoenol pyruvate

More recently, Krishnamurthy and co-workers reported that DAP could be utilized as an efficient phosphorylating reagent to phosphorylate various more complex (pre)biological building blocks without the use of a condensing agent.²⁰³ In this newly discovered methodology, the direct phosphorylation of different nucleophiles was realized via the direct nucleophilic attack on the phosphorus center, taking advantage of imidazole as an activating group for DAP (**Scheme 4.23**).

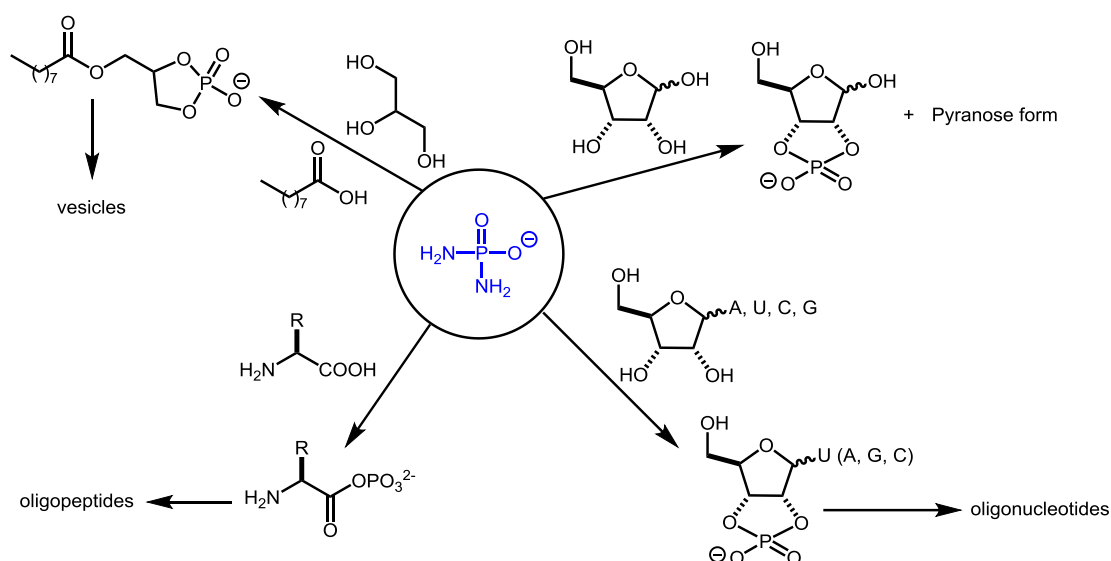


Scheme 4.23. Imidazole activated phosphorylation process of DAP

Their unique reaction conditions were described as *'paste reaction'* conditions, which consisted of mixing all the materials with *drops of water* at room temperature. In summary, they could achieve phosphorylation for nucleosides/tides, amino acids and lipid precursors in moderate yields. Moreover, under the same conditions,

²⁰³ C. Gibard, S. Bhowmik, M. Karki, E.-K. Kim, R. Krishnamurthy, *Nat. Chem.* **2018**, *10*, 212.

corresponding high-order structures, oligonucleotides, peptides and liposomes, could also be produced with trace to low yields in days to weeks (**Scheme 4.24**).



Scheme 4.24. DAP as the phosphorylating reagent for different building blocks

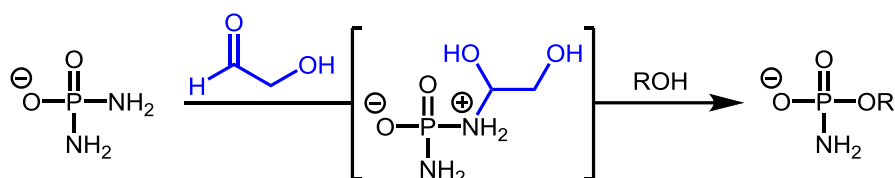
Even it was definitely reasonable to come up with this ‘*paste reaction*’ to minimize the hydrolysis of DAP, arguably, these unique conditions are likely not common especially with continuous addition of large excess of DAP into the ‘*paste*’ (Approximately 5 M – 15 M of DAP). Presumably, on the primitive Earth it was unlikely for this particular environment to exist, which was needed for these chemical reactions to occur. Applicability of such reactions therefore appears to be limited to scenarios where, for example evaporation of water could occur to a large extent, thus increasing the concentration and mimicking these conditions.²⁰⁴

Inspired by the electrophilic activation of the phosphorus center with imidazole, we wondered if it was possible to develop an efficient activation method for DAP with glycolaldehyde as the catalytic activating agent to allow the use of more dilute conditions exploiting a glycolaldehyde-catalyzed prebiotic phosphorylation process.

²⁰⁴ K. E. Nelson, M. P. Robertson, M. Levy, S. L. Miller, *Orig. Life Evol. Biosph.* **2001**, *31*, 221.

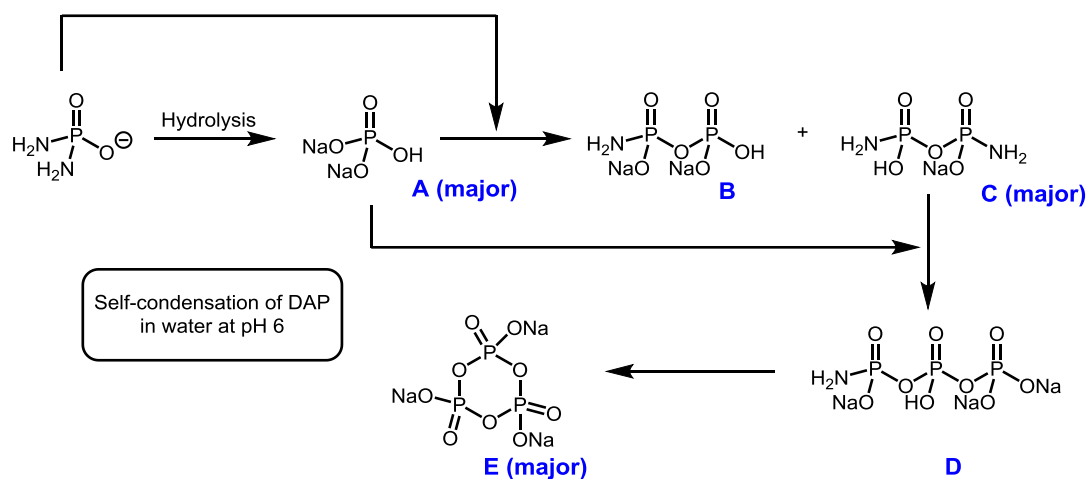
4.5.2 Results and Discussion: Glycolaldehyde-catalyzed phosphorylation with DAP

To start the investigation, we decided to study the hydrolysis reaction of DAP considering that water was always a factor that cannot be avoided in primitive Earth. Therefore, the reaction was tested under our previous conditions. (20 mol% glycolaldehyde, 100 mol% NH₄OTs in H₂O) This reaction was expected to go through the mechanism where the free NH₂-group would first attack the glycolaldehyde to form an activated intermediate, then other nucleophiles would directly attack the phosphorus center and finish the phosphorylation process (**Scheme 4.25**).



Scheme 4.25. Activation of DAP through glycolaldehyde catalysis

According to the study from the Krishnamurthy group,²⁰³ the self-condensation of DAP in water would mainly produce hydrolysis product **A** and products **C**, **E** and other phosphorus-containing species (**Scheme 4.26**). This study came up during my research process, and clearly demonstrated the possible difficulty to realize the phosphorylation with DAP in water because that hydrolysis of DAP would compete with other nucleophiles.



Scheme 4.26. Self-condensation of DAP in water at pH 6 from Krishnamurthy group

However, it is worth investigating: 1) how DAP would respond to a different activation mode, specifically the electrophilic catalysis with the application of glycolaldehyde as catalyst; 2) whether the reactivity of DAP could be improved and other nucleophiles could potentially compete with water to realize phosphorylation reactions under the electrophilic catalysis conditions, especially under diluted conditions; 3) how the products would distribute for hydrolysis reaction, oligomerization and phosphorylation reaction. Thanks to the study from Krishnamurthy,²⁰³ the complex NMR spectra could be analyzed reliably.

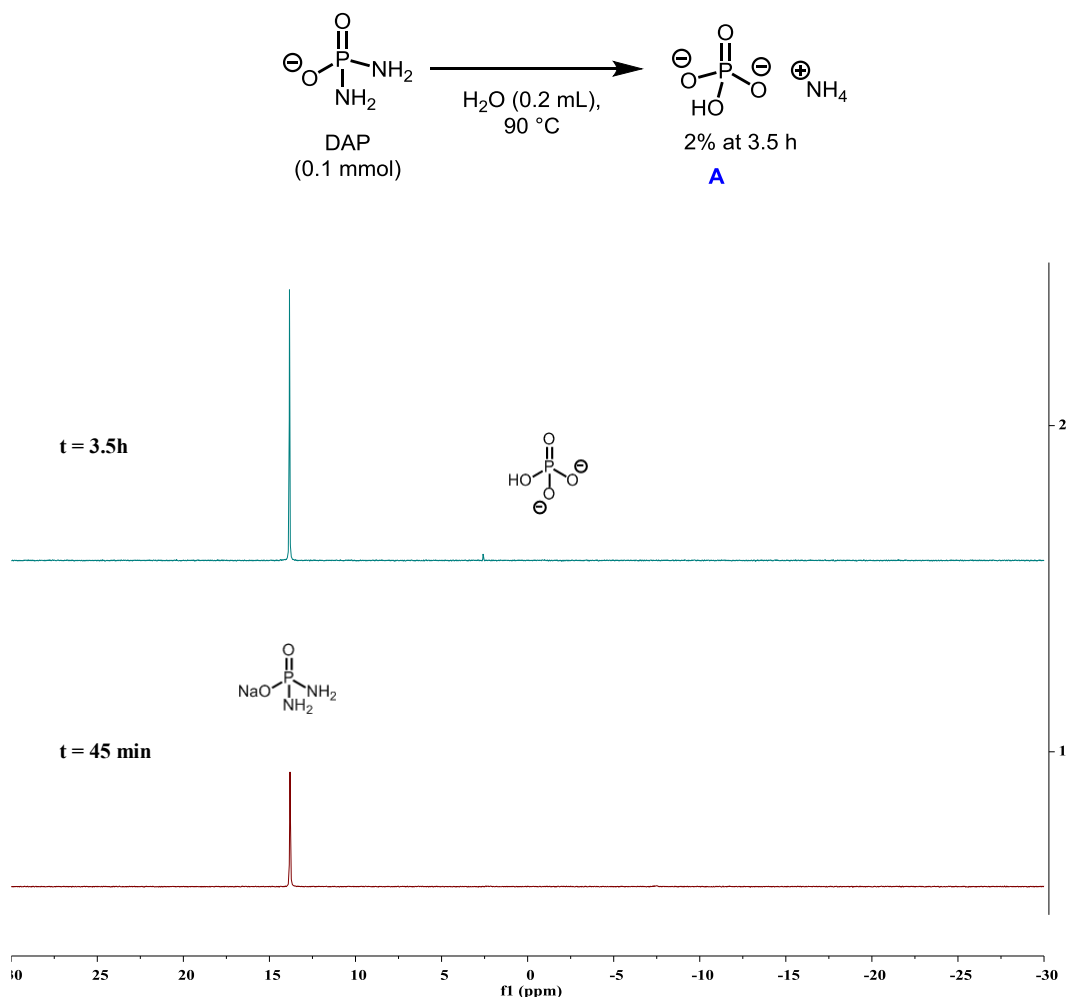
The reactions were shown below and were monitored by ³¹P NMR at various time points: 45 min, 3.5 h, 24 h, 48 h, 72 h, 96 h and up to 7 days. It is worth mentioning that in order to monitor the reaction, instead of taking aliquots from one reaction, several identical reactions were performed in parallel and monitored according to different time points. This would also allow us to detect small peaks and obtain more information on products distribution. The spectra collected with different reaction conditions and catalysts are shown in the following pages.

First, the blank reaction in the absence of glycolaldehyde and NH₄OTs was performed.

As was shown in **Figure 4.1**, this background reaction was monitored at 45 min and

3.5 h. Delightfully, the hydrolysis reaction of DAP was not as fast as expected. After 45 min, DAP was not hydrolyzed and after 3,5 h, only 2% of the hydrolysis product **A** was produced.

Figure 4.1. Background reaction (without glycolaldehyde and NH₄OTs)



With this in hand, we continued to perform the reaction in the presence of glycolaldehyde and NH₄OTs and this reaction was monitored for up to 7 days. The stacked spectra were shown in **Figure 4.2**. The products distribution calculation was based on spectrum obtained at 3.5 hours (For an enhanced spectrum at 3.5 h, please see **Figure 4.3**).

Figure 4.2. Glycolaldehyde catalyzed activation of DAP under full reaction

conditions

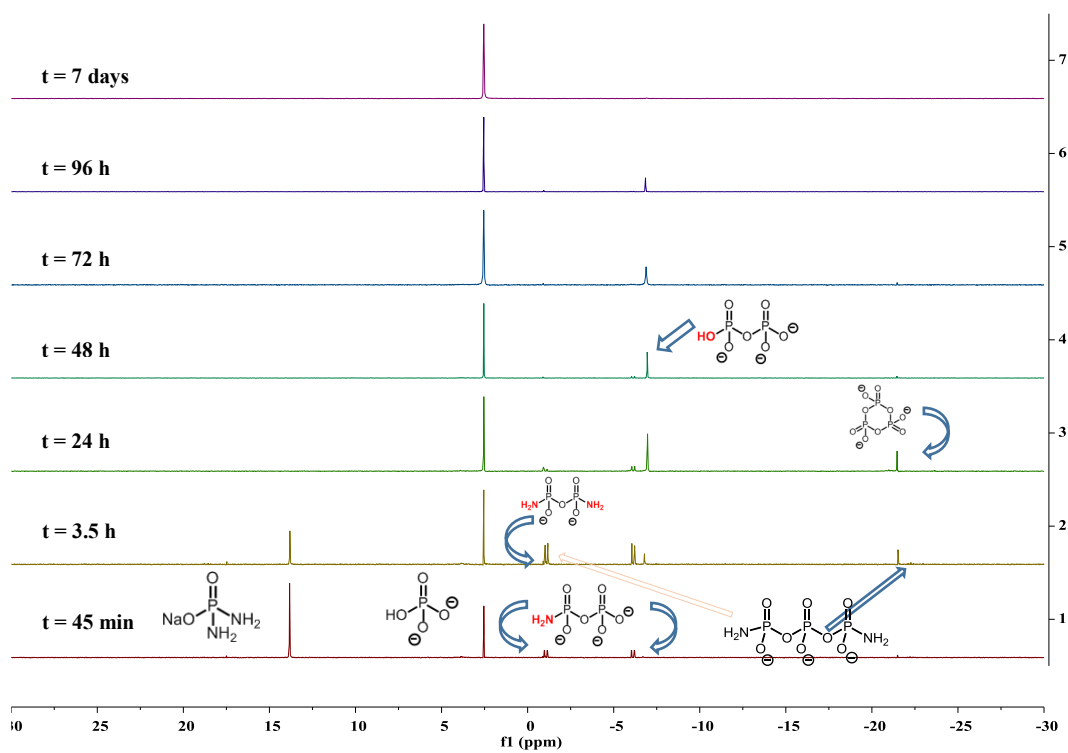
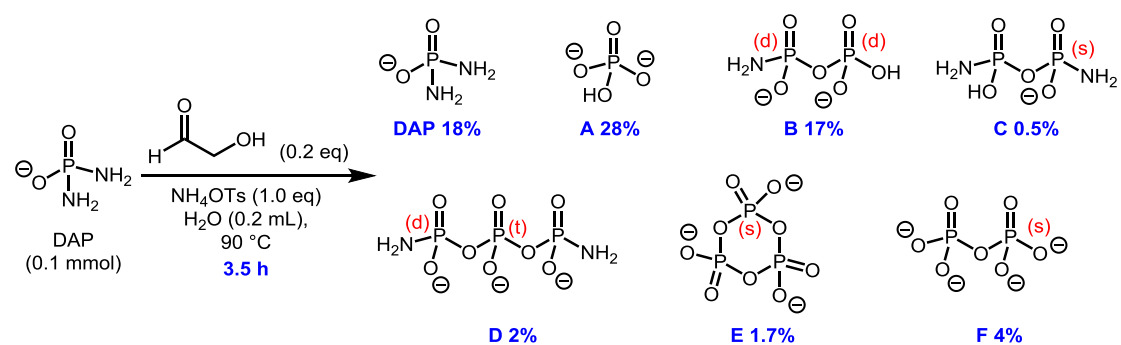
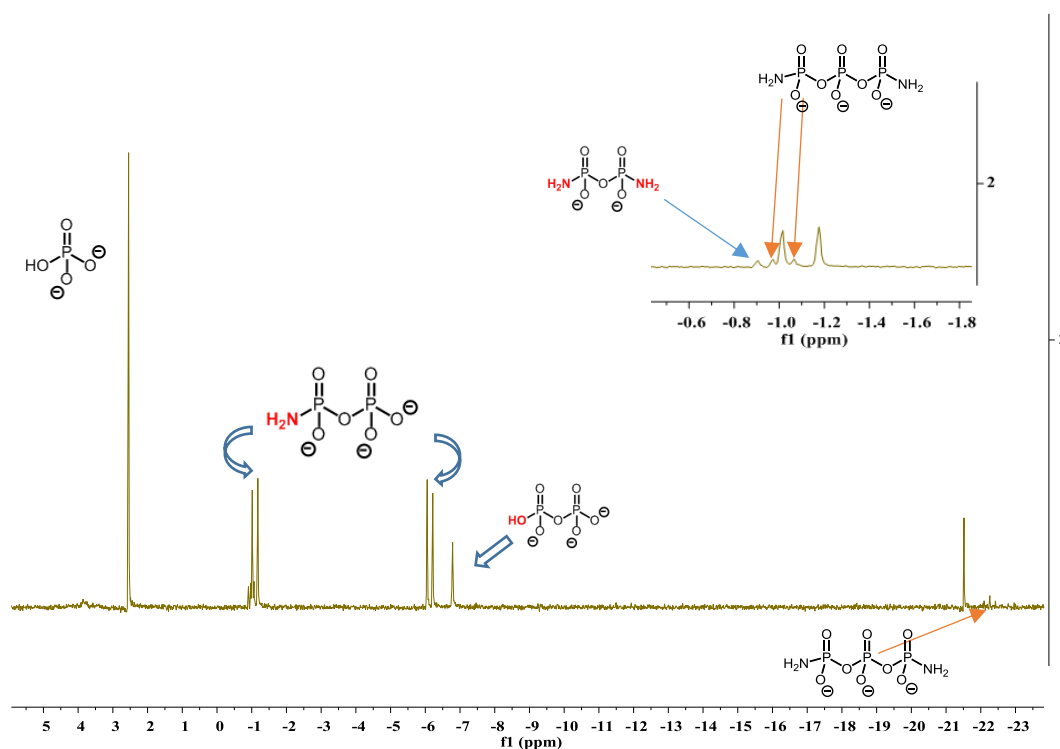


Figure 4.3. Enhanced spectrum for $t = 3.5$ h



Combining these sets of the results, it was exciting to find out that the reactivity of DAP was significantly increased. This indicated the activation of DAP by utilizing glycolaldehyde as the catalyst could be realized. For example, even only after 45 min, the reaction already showed good transformation towards the fully hydrolyzed product **A**, which showed our hypothesis to activate DAP with glycolaldehyde was possible and water could serve as a simple nucleophile to directly attack at the phosphorus center.

To our delight, other prebiotically relevant compounds besides the hydrolysis product were generated from intermolecular reactions in most of these reactions. This suggested that, under these reaction conditions, besides water, a variety of phosphates could also act as nucleophiles to react with activated DAP (and derivatives) to generate more species that can be applied in further reactions.

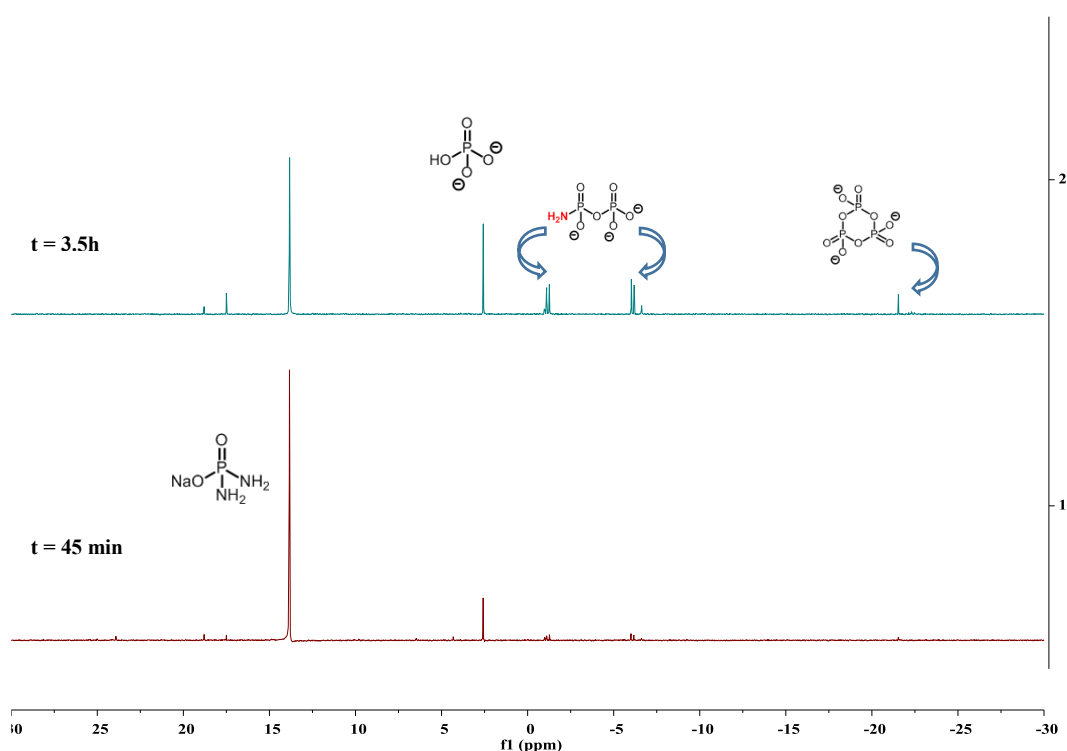
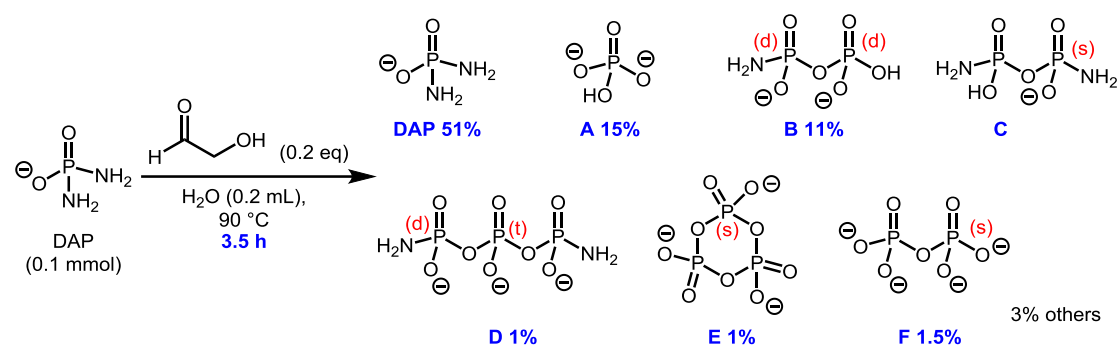
It was also noticed that the hydrolysis product **A** (fully hydrolyzed product) was likely formed first and then phosphorylation product **B** also started to be generated and

accumulated. After 3.5 h, only 18% of DAP (98% of DAP in the absence of glycolaldehyde and NH_4OTs) remained and various phosphorus-containing products were formed under the reaction conditions. It was interesting to find that the NH_2 -containing species, which were almost all consumed at 24 h, seems more reactive than other species. This fits our proposed hypothesis that free NH_2 -group could react with glycolaldehyde to form a better leaving group. For example, between 3.5 h and 24 h, products **B** was accumulated and then consumed, instead products **E** and **F** started to accumulate during this period. After 48 h, the product **E** started to disappear and product **F** still existed in this reaction system after 96h. After 7 days, the only detected product was the hydrolyzed product **A**.

It was worth mentioning that our results are very different from previous results from Krishnamurthy.²⁰³ After 6 days, the self-condensation of DAP was reported to generate product **A** (hydrolysis product) and **C**, **E** (cyclotriphosphate) as the major products. Their reaction environment was more acidic (pH 6 vs. 8.7 at 45 min in our case).

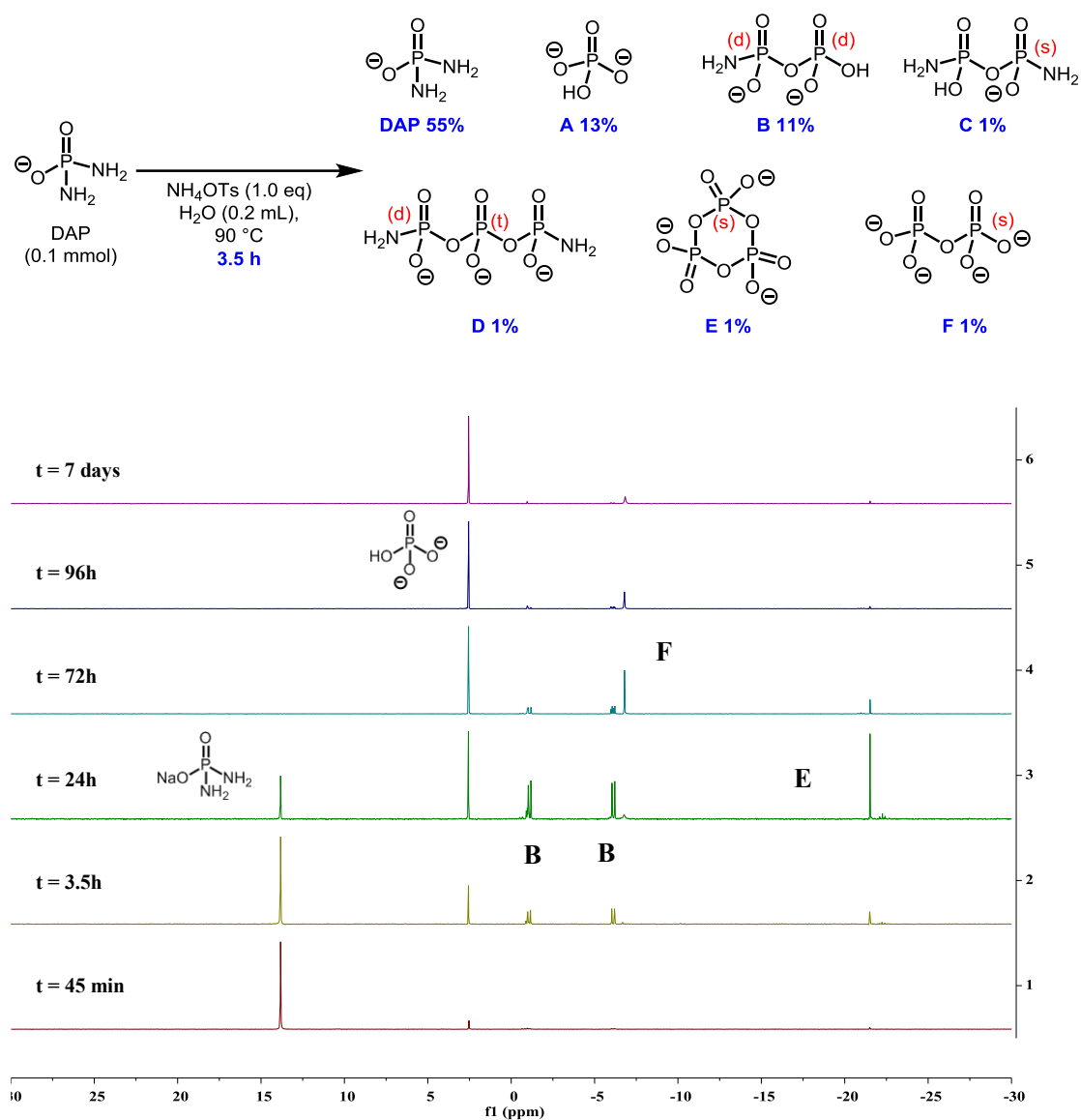
To gain more information of the system, other control experiments were performed in order to understand the role of glycolaldehyde and the effect of NH_4OTs . First the reaction was carried out only in the presence of glycolaldehyde (**Figure 4.4**). The products distribution calculation was based on spectrum obtained at 3.5 hours.

Figure 4.4. Control experiment in the presence of glycolaldehyde



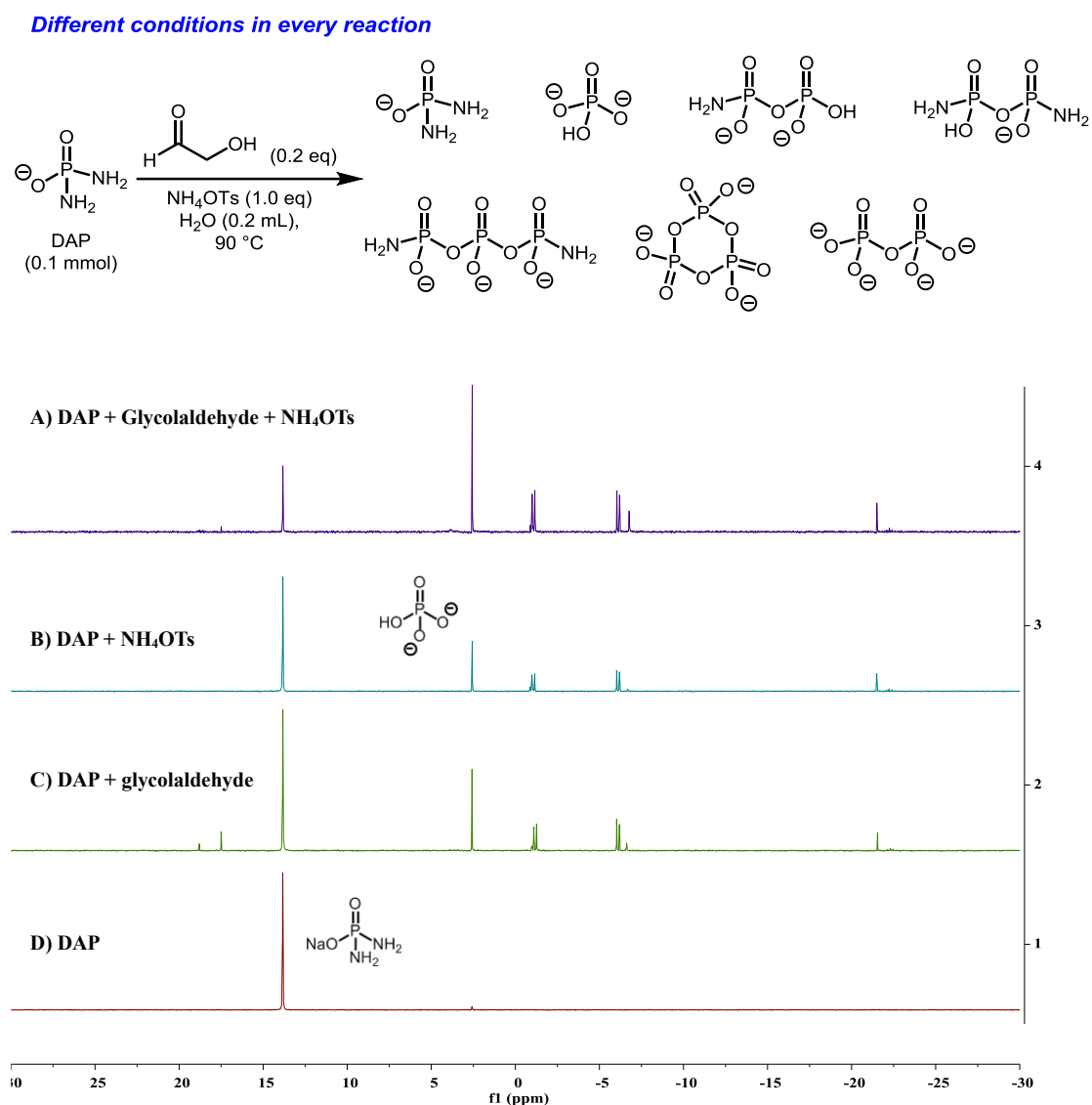
Comparing to the spectra in **Figure 4.1** (in the absence of glycolaldehyde and NH_4OTs), this set of results clearly demonstrated that acceleration of the reactivity of DAP was achieved by glycolaldehyde activation. After 45 min, hydrolysis product **A** and phosphorylation product **B** were generated. Almost half of the DAP were converted after 3.5 h. However, it was not as efficient as the reaction in **Figure 4.2**. From this comparison, NH_4OTs seems to play an important role in this reaction. Therefore, the control experiment was performed only in the presence of NH_4OTs (**Figure 4.5**).

Figure 4.5. Control reaction (in the presence of NH_4OTs , without glycolaldehyde)



With this set of results, the reactivity of DAP in the presence of NH_4OTs or glycolaldehyde was not much differentiated. However, the combination of glycolaldehyde and NH_4OTs could have synergy effect on the reaction. Stacked spectra (at 3.5 h) could clearly demonstrate the difference among these conditions (**Figure 4.6**).

Figure 4.6. Stacked spectra for different reaction conditions at 3.5 h



This stacked spectrum showed the necessity to have both glycolaldehyde and NH₄OTs in the reaction that the reactivity of DAP was significantly improved. Both hydrolysis of DAP and the formation of other phosphorylating products were accelerated. Meanwhile, we also noticed NH₄OTs as an additive favored the reaction towards the formation of fully hydrolyzed product of DAP, however, the role of NH₄OTs was still not clear. Likely, the NH₄OTs could: 1) Serve as proton source and potentially facilitate the activation of DAP and other P(O)-N intermediate by forming the protonated adduct; 2) Be as source of nucleophiles (NH₃ or TsO⁻). Therefore, the potential effects of the

NH₄OTs additive were tested by changing NH₄OTs to NH₄Cl and NaCl (**Figure 4.7** and **Figure 4.8**). The products distribution was based on spectrum obtained at 3.5 h. The stacked spectra for different additives at 3.5 hours will also be demonstrated (**Figure 4.9**).

Figure 4.7. Potential effect of anion by changing NH₄OTs to NH₄Cl

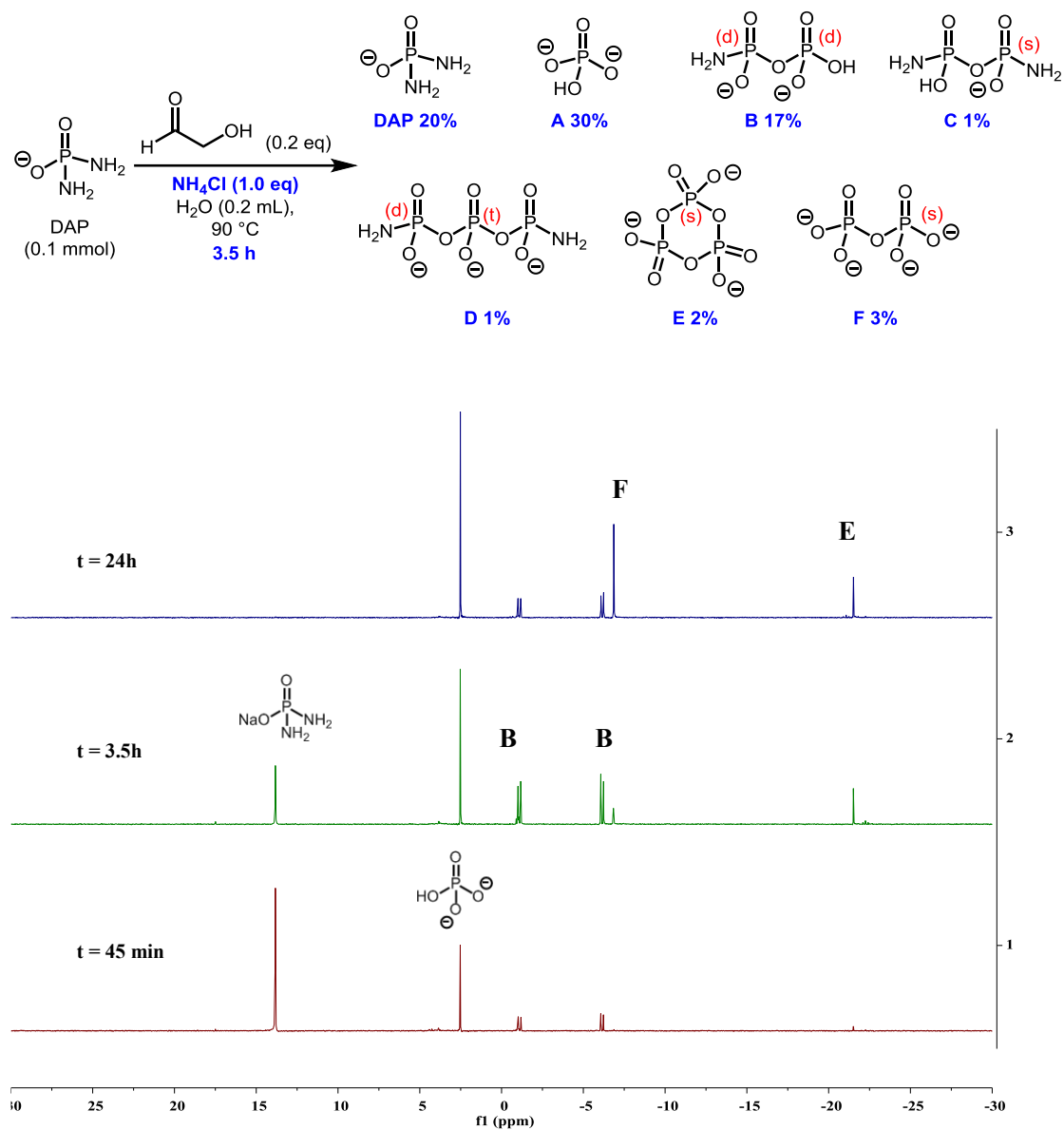


Figure 4.8. Potential effect of additives by changing NH₄OTs to NaCl

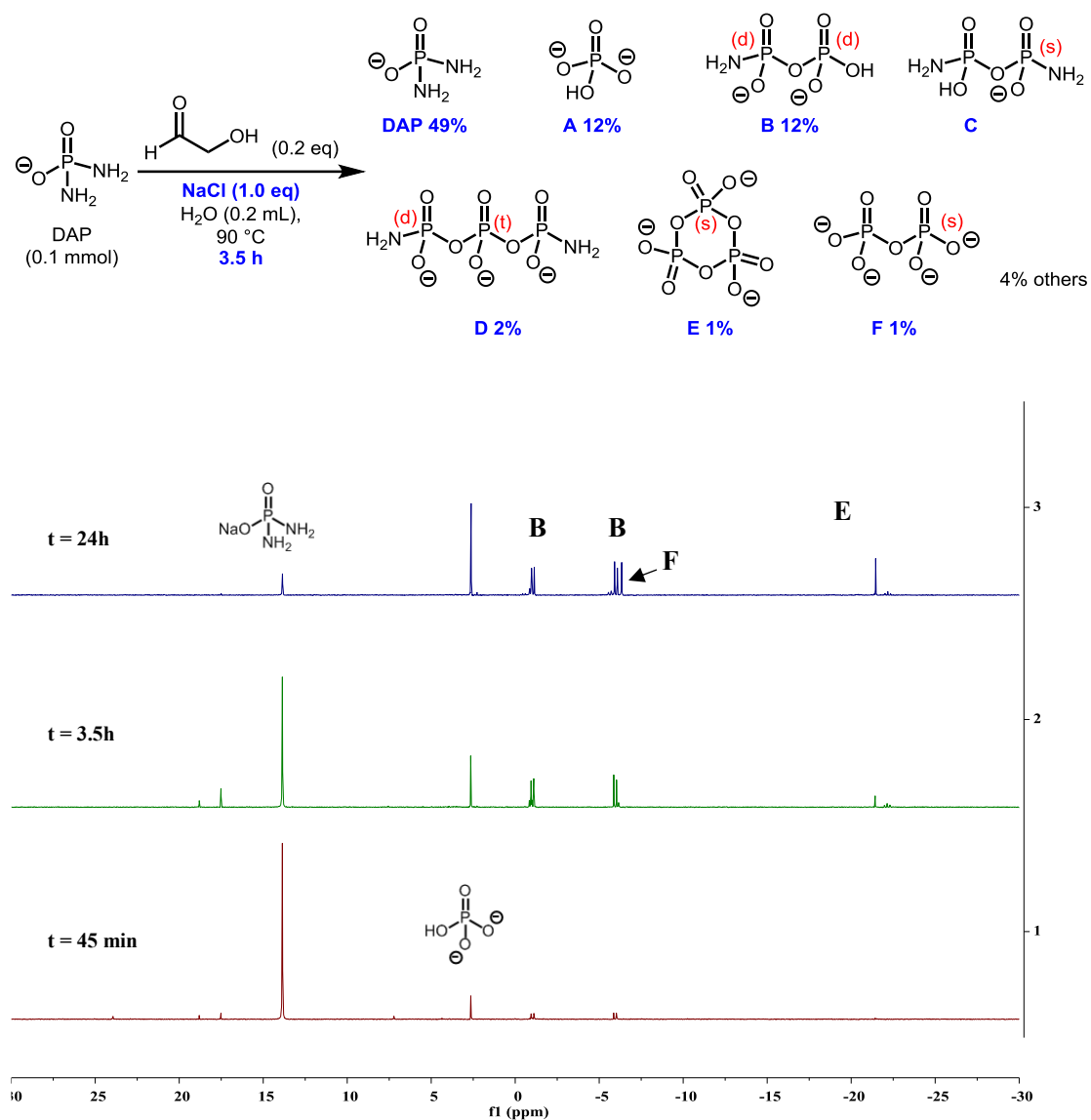
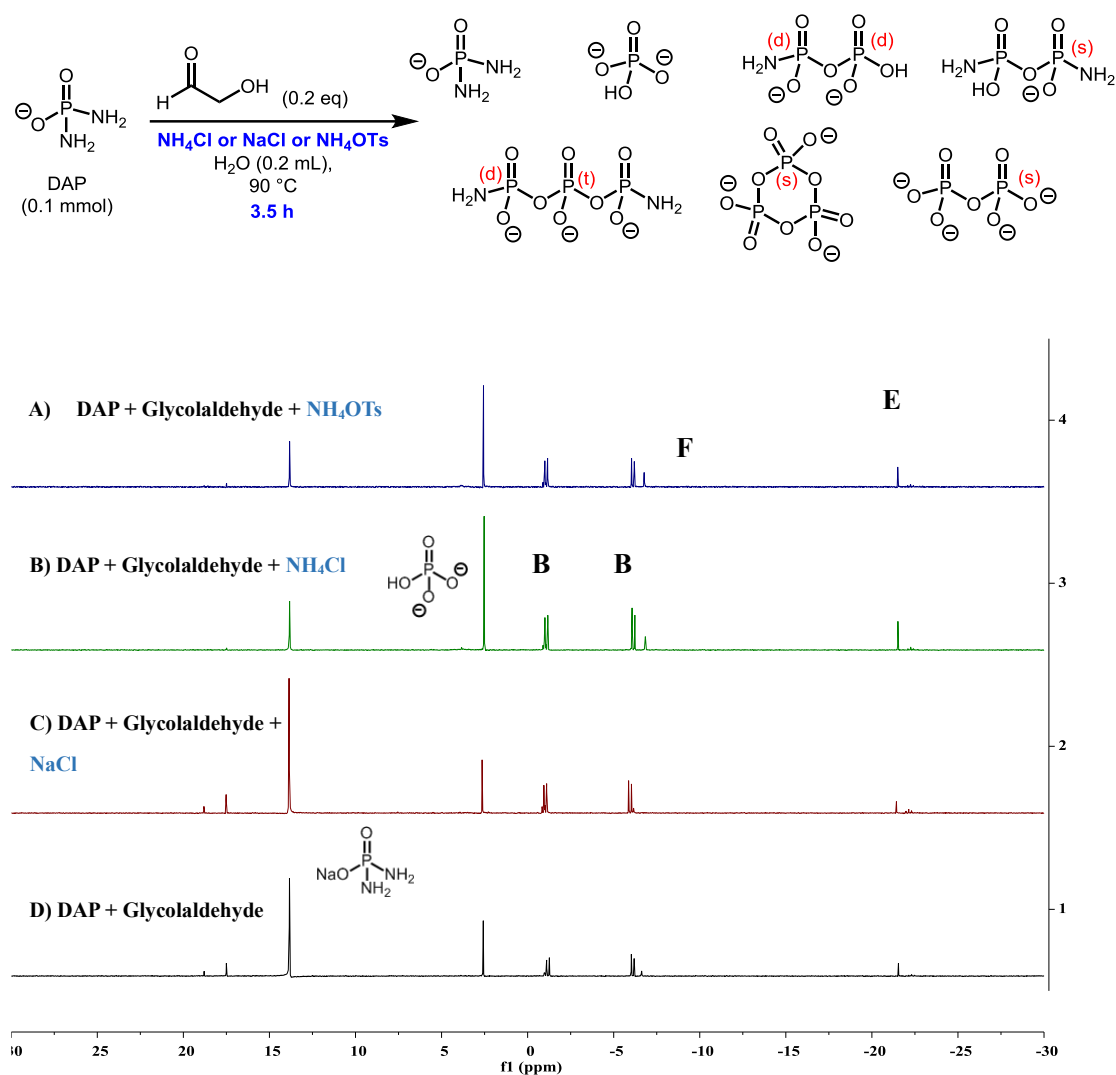


Figure 4.9. Stacked spectra for different additives at 3.5 h



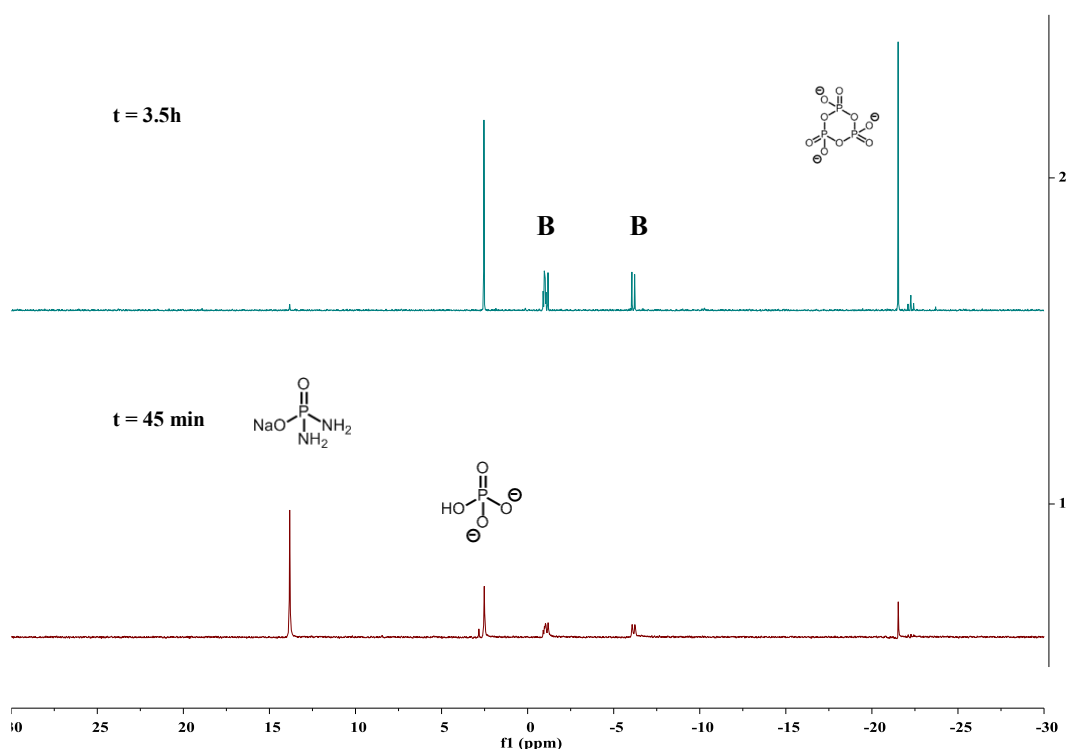
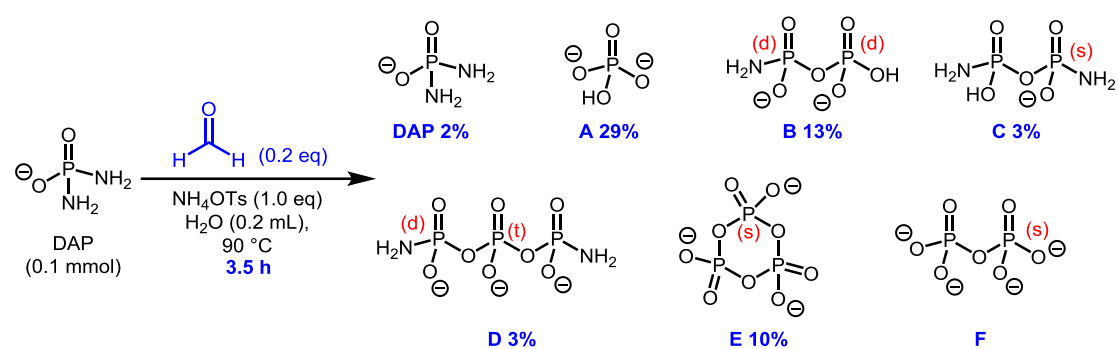
From these spectra obtained at 3.5 h for different reactions, changing the anion of the additive from OTs^- to Cl^- did not affect the reaction significantly (**Figure 4.9 A and B**). Instead, in the absence of NH_4^+ (**Figure 4.9 B and C**) the reaction efficiency was decreased which elucidated that the NH_4^+ might be more effective for this reaction. Presumably, NH_4OTs could assist the reaction by serving as a proton source or a potential nucleophile. Unfortunately, the exact role of NH_4OTs was not fully elucidated. With these studies and comparison, it was clear that with the addition of catalytic amount of glycolaldehyde, the reactivity of DAP could be improved via electrophilic activation and this process could be further facilitated by the addition of NH_4OTs . These

results emphasized the importance of glycolaldehyde as a catalyst to activate DAP for further transformation.

Furthermore, we also carried out the reaction with formaldehyde as the catalyst to compare the reactivity and catalytic efficiency in this prebiotic system (**Figure 4.10**).

The products distribution calculation was based on spectrum obtained at 3.5 hours.

Figure 4.10. Formaldehyde catalyzed activation of DAP under full reaction conditions



From this set of results, formaldehyde could react even more efficiently than glycolaldehyde providing a different major product **E** (cyclotriphosphate). The control

experiment (only in the presence of formaldehyde) was further carried out (**Figure 4.11**).

The products distribution calculation was based on spectrum obtained at 3.5 hours. A

stacked spectra to compare the reactivity of DAP in the presence of formaldehyde and

glycolaldehyde is also provided (**Figure 4.12**).

Figure 4.11. Formaldehyde activated DAP (only in the presence of formaldehyde)

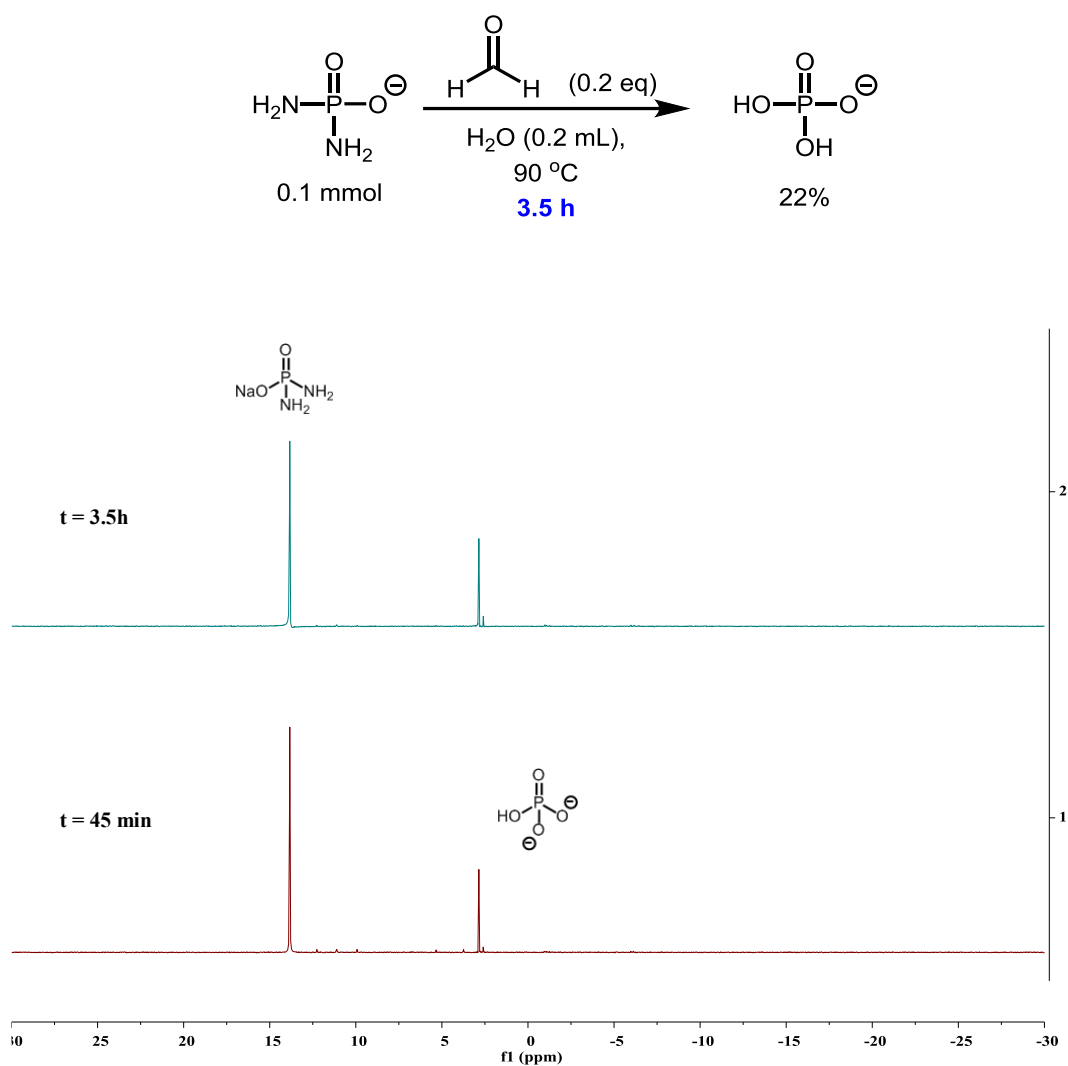
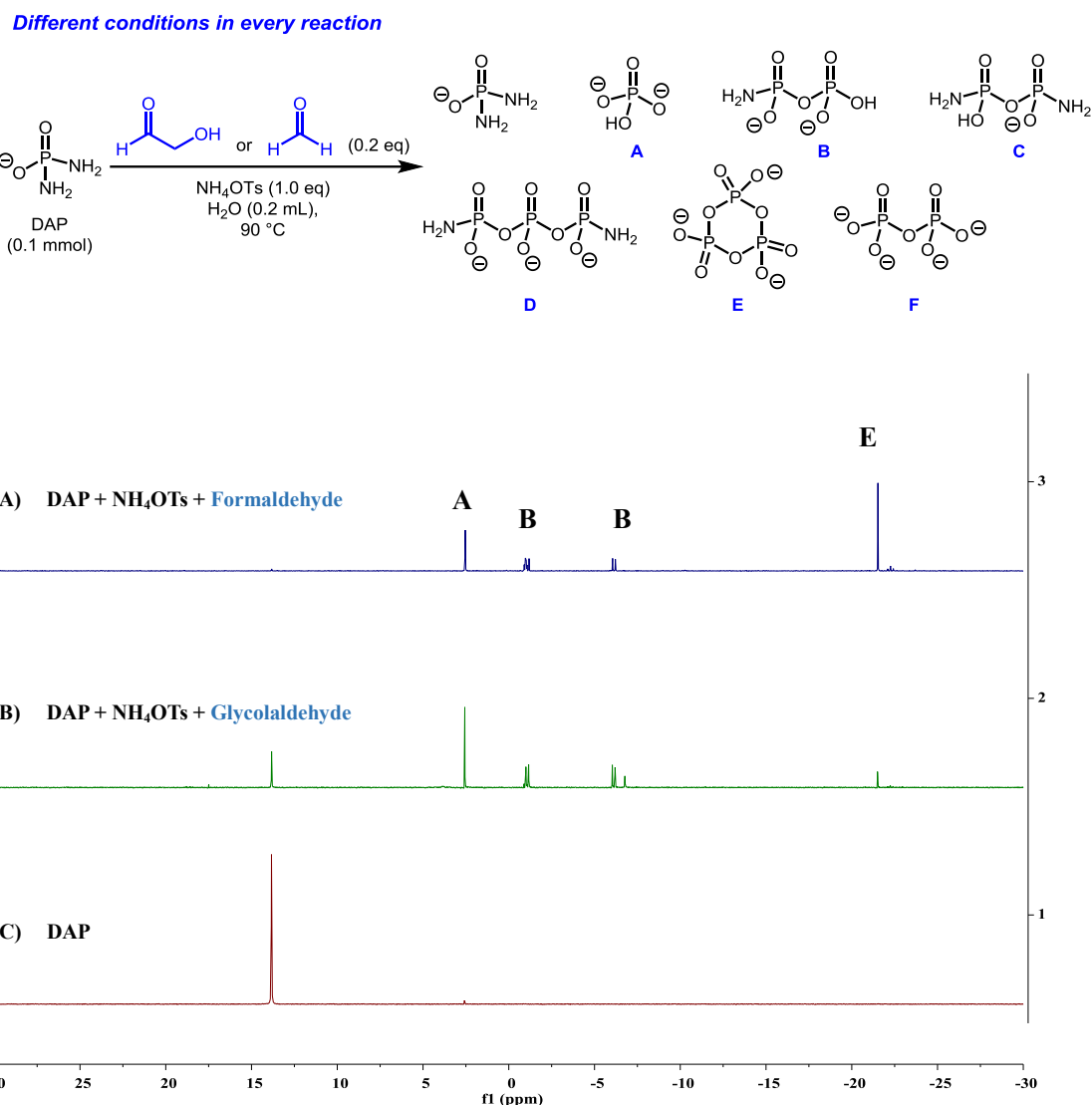


Figure 4.12. Comparison of catalytic efficiency between glycolaldehyde and formaldehyde



By this comparison of the catalytic efficiency of glycolaldehyde and formaldehyde, it was encouraging to develop and control this reactivity by two different prebiotically relevant simple aldehydes with different major products at 3.5 h (Glycolaldehyde: product **A** and **B**; Formaldehyde: product **A** and **E**).

As mentioned above, other prebiotically relevant compounds besides the hydrolysis product were generated from intermolecular reaction in most of these reactions. This suggested that, besides water, a variety of phosphates could also act as nucleophiles to react with activated DAP to generate more species that can be applied in further reaction. Inspired by these initial results, we were wondering if other nucleophiles, for example,

other phosphates formed in the reaction, could potentially influence the reaction rate.

We continued to investigate the impact of orthophosphates, as potential nucleophiles

for the reaction in the presence of water (**Figure 4.13 - 4.16**). The products distribution

calculation (from DAP) was based on spectrum obtained at **45 min**.

Figure 4.13. Glycolaldehyde-catalyzed activation of DAP in the presence of NH_4Cl and Na_3PO_4

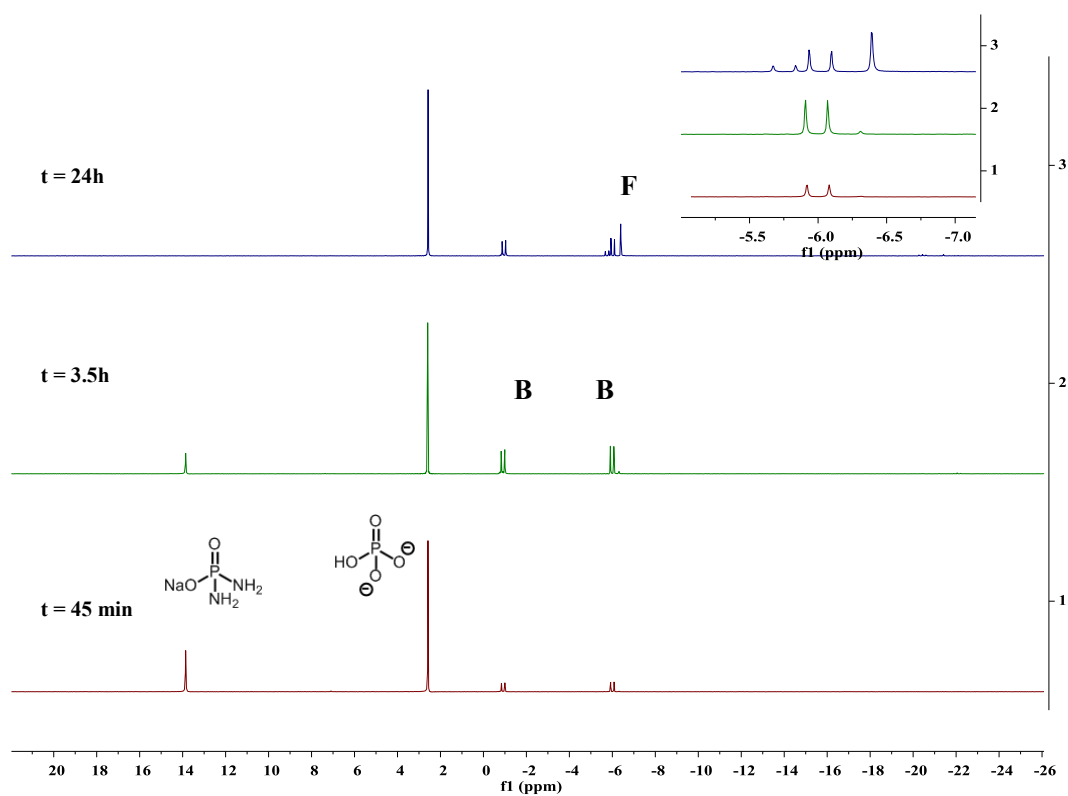
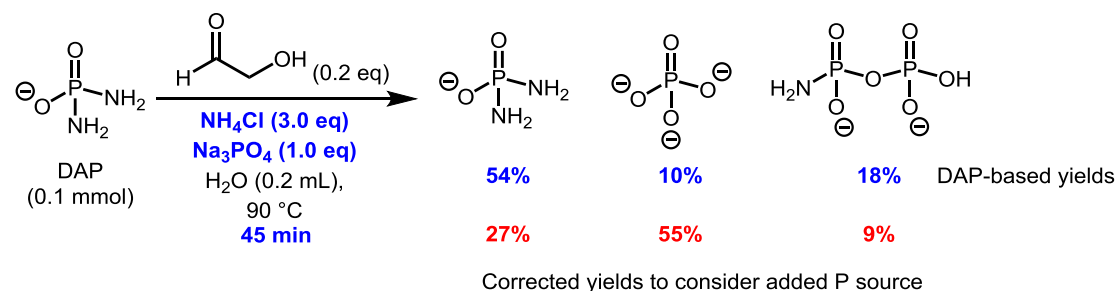


Figure 4.14. Glycolaldehyde catalyzed activation of DAP in the presence of $(\text{NH}_4)_2\text{HPO}_4$

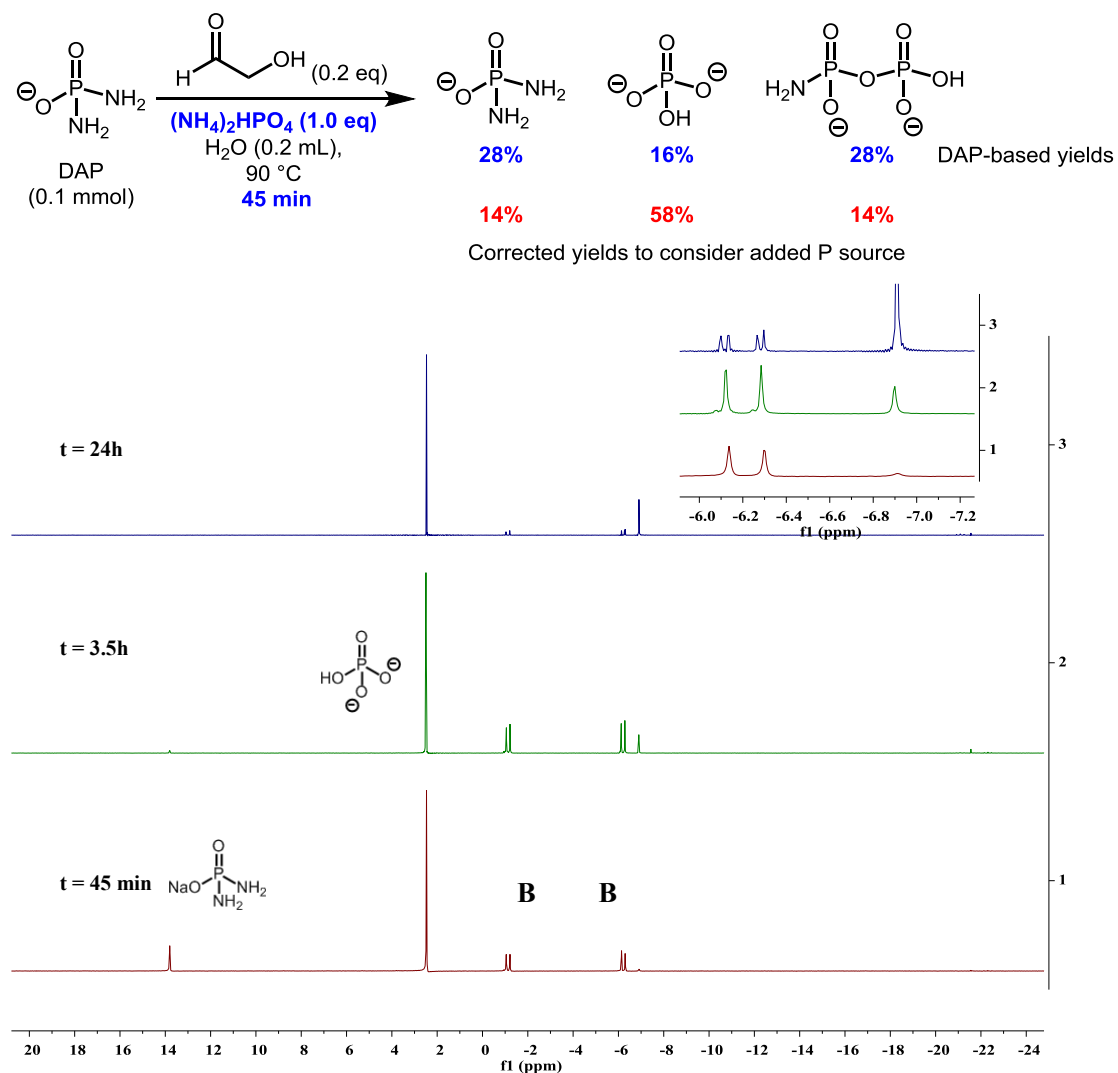


Figure 4.15. Glycolaldehyde catalyzed activation of DAP in the presence of $\text{NH}_4\text{H}_2\text{PO}_4$

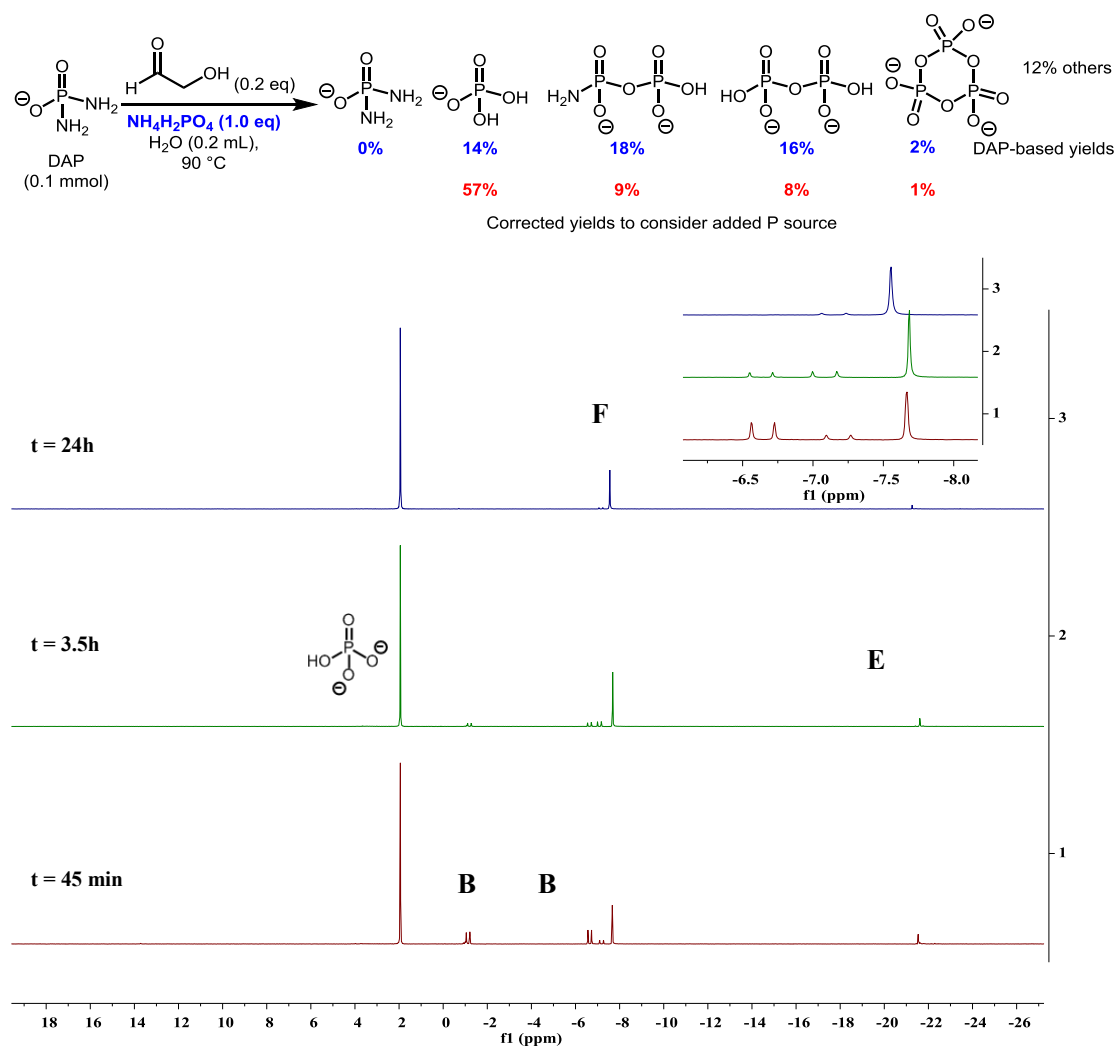
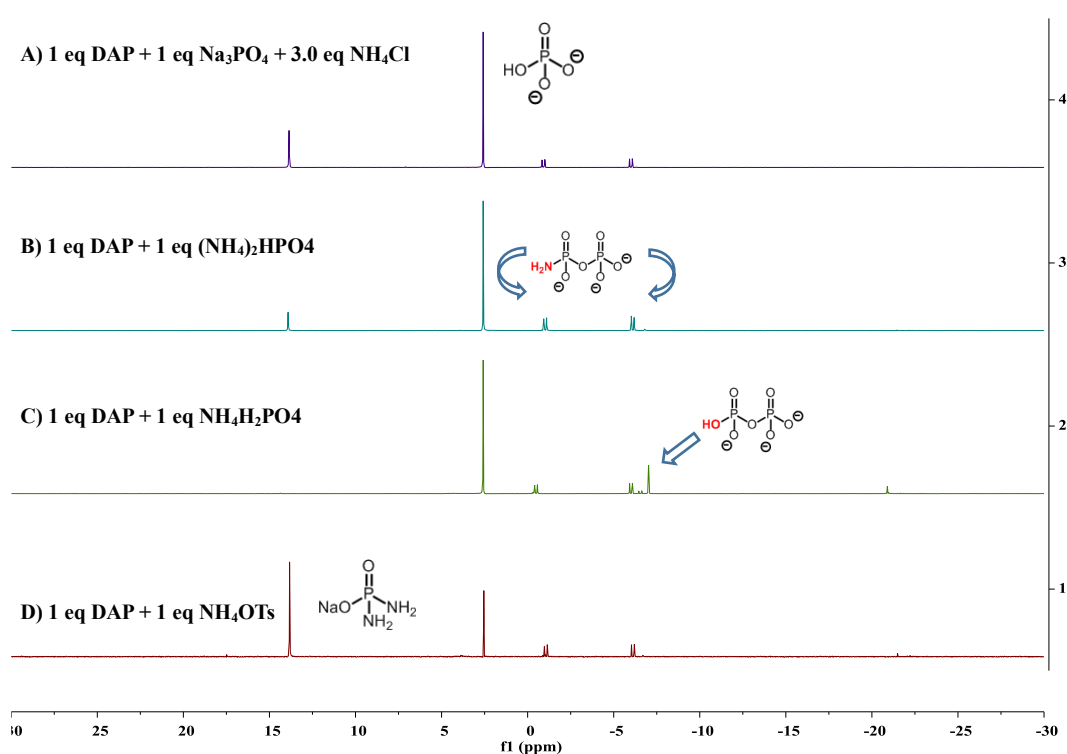
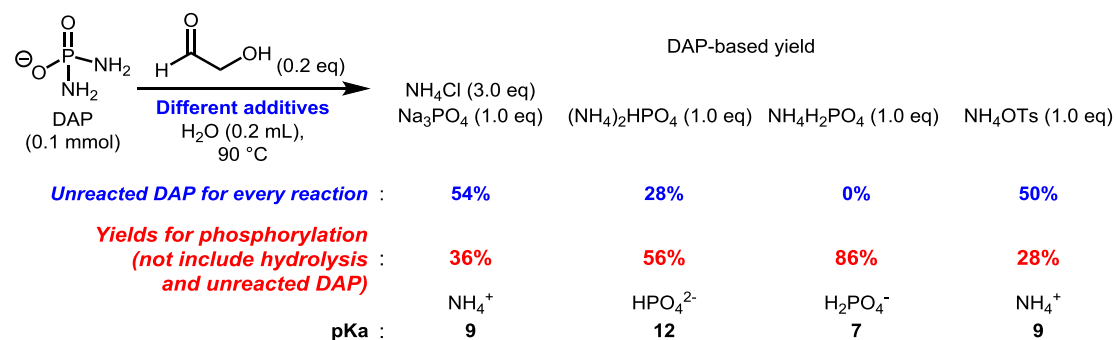


Figure 4.16. Comparison for activation of DAP under different conditions after 45 min (in presence of glycolaldehyde)



In order to gain better understanding of this reaction, the reaction was tested and monitored in the presence of different phosphate sources as additives. Surprisingly, changing the additive to other orthophosphates has a major impact on the reaction efficiency. After 45 min, all reactions proceeded efficiently and formed different products, and the spectra were demonstrated in **Figure 4.16**. As shown in Spectrum A, B and C, with 1 eq of PO_4^{3-} , HPO_4^{2-} and H_2PO_4^- as other phosphorus containing nucleophiles, the reaction showed better conversion than the original reaction (**Figure 4.16, D**). Especially, with the addition of other nucleophiles, products of

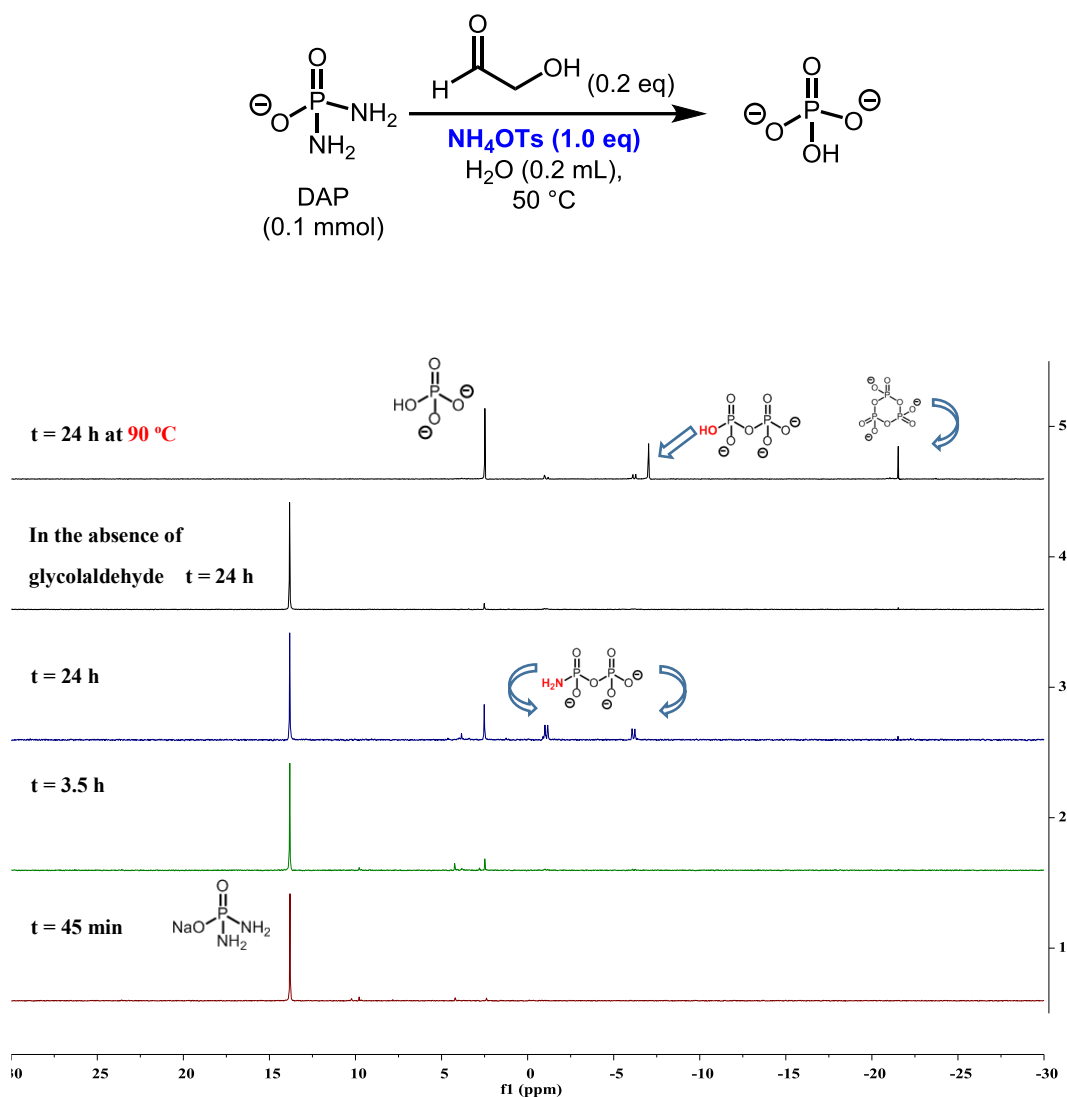
phosphorylation could be formed in higher yields (**Figure 4.16, in red**). This difference may be due to the different pKa of the additives (**Figure 4.16, pKa**).²⁰⁵ In the situation that when the additive is more acidic (lower pKa), the reactivity is more efficient. Besides being a nucleophile under the reaction conditions, the additives might improve the reaction in two different pathways: 1) the additive could facilitate the formation of the adduct between DAP and glycolaldehyde, or 2) the additive could protonate the NH₂-group on DAP to be a better leaving group.

Overall, this comparison indicated that glycolaldehyde could serve as a catalyst to facilitate further phosphorylation with DAP in the presence of other nucleophiles with significantly improved reactivity.

Arguably, the reaction temperature is not that ideal for the prebiotic transformation. Therefore, we attempted to perform the reaction at lower temperature, 50 °C, demonstrated as below (**Figure 4.17**).

²⁰⁵ J. Rumble, *Handbook of Chemistry and Physics 100th Edition* CRC Press, **2019**.

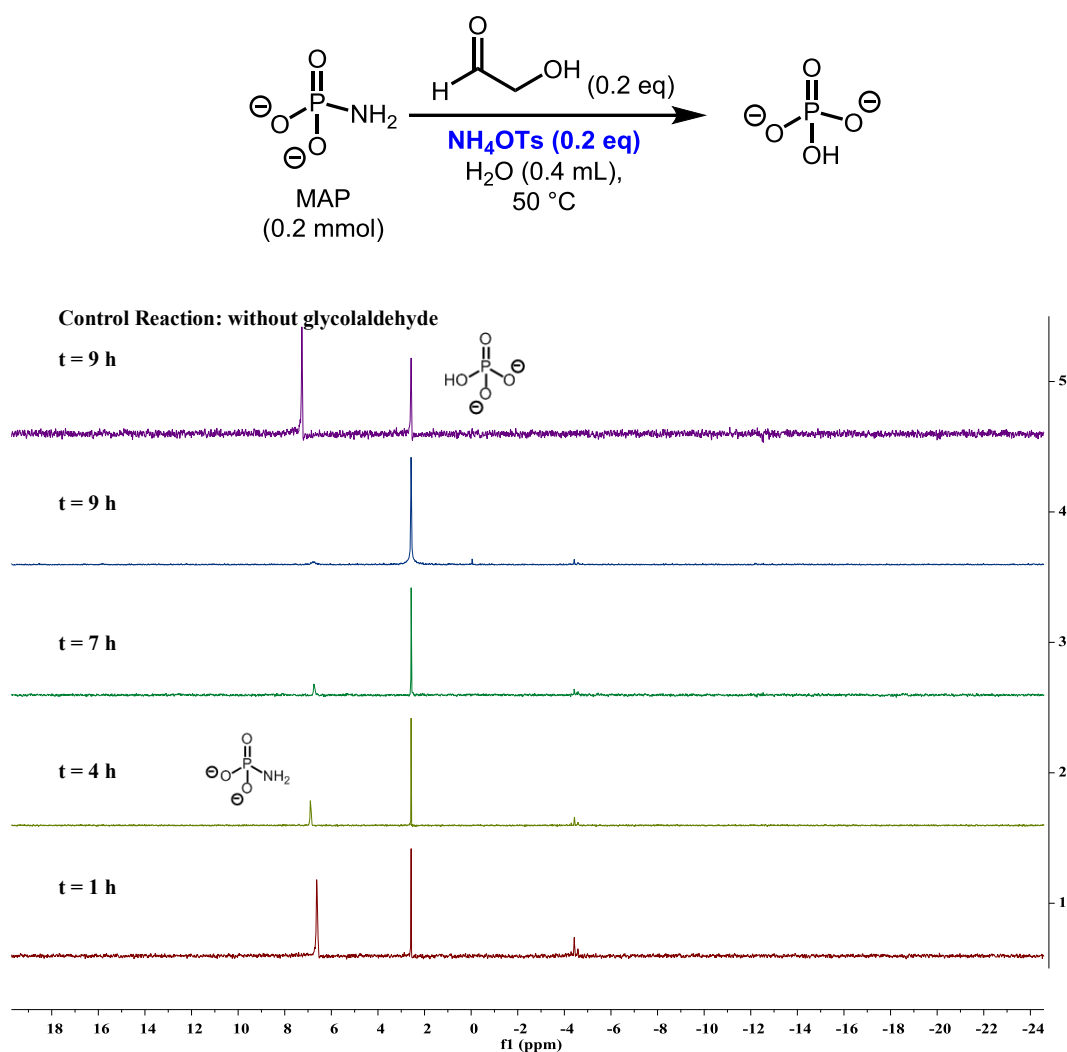
Figure 4.17. Glycolaldehyde catalyzed activation of DAP at 50 °C



This results indeed demonstrated better reactivity with the addition of catalytic amount of glycolaldehyde at 50 °C. The product distribution was not exactly the same as the one at 90 °C (Products **E** and **F** were not produced at 50 °C after 24 hours). With longer reaction time, the hydrolysis reaction of DAP at 50 °C could be possibly realized.

With the investigation of DAP, we continued to study another potential phosphorylating reagents, monoamidophosphate. Therefore, the hydrolysis of MAP in the presence of catalytic amount of glycolaldehyde was also performed (**Figure 4.18**).

Figure 4.18. Glycolaldehyde catalyzed activation of MAP



This set of results signified the importance of glycolaldehyde to serve as a catalyst, facilitating the hydrolysis reaction of MAP, and water could be a nucleophile to react at the phosphorus center after the activation with glycolaldehyde. However, other phosphorylation products that were observed with DAP were not formed in this reaction conditions. Efforts were made to identify the peaks around -4 ppm, unfortunately, the analysis of these peaks were not achieved.

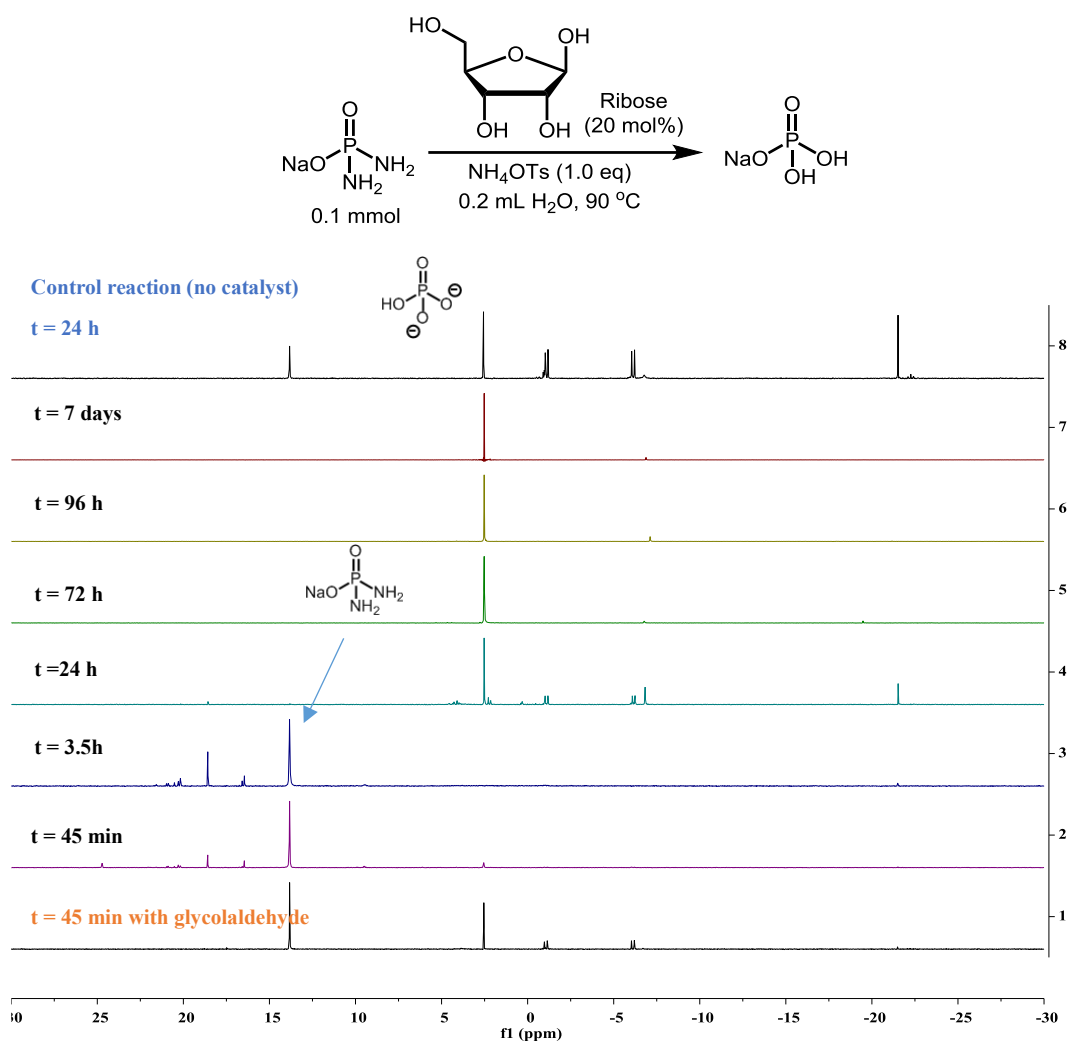
Combining these studies, it was reasonable to propose that in this glycolaldehyde catalyzed electrophilic activation process, water and other nucleophiles could be potentially phosphorylated.

Finally, to fit this piece in the bigger picture, this reaction was tested with ribose as a catalyst. The prebiotic synthesis of carbohydrates has been discussed in previous sections. In most of cases, the importance of carbohydrates was highlighted as a component for the formation of complex biologically important building blocks. However, very little has been done to investigate the catalytic efficiency of sugars, especially for the introduction of enantioselectivity. Recently, Blackmond and co-workers reported that chiral sugars could induce the enantioenrichment in a prebiotic synthesis of amino acids²⁰⁶ and it was observed that ribose and lyxose would lead to the opposite chiral preference.

In our prebiotic hydrolysis system, the addition of a simple sugar as a catalyst was expected to give only slightly better or equal reactivity, considering the nature of the sugar that preferred for the ring form than the open-chain form. The reaction was tested with the addition of catalytic amount of ribose (**Figure 4.19**).

²⁰⁶ A. J. Wagner, D. Y. Zubarev, A. Aspuru-Guzik, D. G. Blackmond. *ACS Cent. Sci.* **2017**, 3, 4, 322.

Figure 4.19. Investigation of ribose as a potential catalyst



This set of results was again achieved by monitoring the reaction for 7 days by ^{31}P NMR. At the beginning, the reaction did not show good conversion comparing to that with glycolaldehyde. Interestingly, however, more phosphorus species (ppm 15-30) were detected, with peaks that were not observed before in other reactions. Although, the reaction with the addition of ribose did not go well at the beginning, most of the DAP surprisingly disappeared after 24 hours. The comparison between this result and the control reaction with no glycolaldehyde added indeed has obvious difference. It was definitely encouraging that the reaction showed better conversion with the addition of catalytic amount of ribose, and only a trace of the DAP was left after 24 hours, while around 15% of DAP was left in the control experiment. This small difference clearly

indicated the possibility to develop this catalytic reaction with ribose or other sugars with more systematic investigation.

4.6 Conclusion and future work

In summary, this chapter demonstrated the paramount importance of glycolaldehyde acting as an efficient prebiotic catalyst for the hydrolysis of organophosphinic amides derivatives under plausible prebiotic conditions. This transformation was achieved via electrophilic activation. This work added strong evidence that glycolaldehyde could have played an important role in chemical evolution as catalyst for difficult hydration and hydrolysis reactions, especially considering that glycolaldehyde could be regenerated in the formose reaction (see introduction). The catalytic reactivity of glycolaldehyde was also systematically investigated for two prebiotically important substances, diamidophosphate (DAP) and monoamidophosphate (MAP). The results supported that glycolaldehyde could also activate DAP and allow other nucleophiles to directly attack at the phosphorus center, which provides more opportunities for further phosphorylating transformations. With these results in hand, this research definitely calls for the future study on more organic nucleophiles. It is important to investigate the possibility to phosphorylate more complex and biologically important building blocks for this system. Moreover, the outcome for using ribose as a catalyst is promising and calls for more in-depth studies. With more research and understanding it is also possible to study potential for enantioenrichment associated with optically active carbohydrates.

Chapter 5

Conclusion

To sum up, this thesis first introduced the development of organocatalysis and in particular carbonyl catalysis. Electrophilic activation via nucleophilic catalysis (e.g. DMAP-type compounds as catalysts) was also discussed in detail (Chapter 1). The *electrophilic activation via carbonyl catalysis* was further proposed and successfully applied to the hydrolysis of organophosphorus compounds that contain P(=O)-N motif. The reactivity and catalytic efficiency between *o*-phthalaldehyde and formaldehyde were compared, and *o*-phthalaldehyde was identified as a superior catalyst to formaldehyde. Moreover, chemoselective hydrolysis of the P(=O)-N bonds could be accomplished in the presence of P(=O)-O bonds (Chapter 2). Using a different activation mode, carbonyl compounds can be used as a catalyst to install transient intramolecular nucleophile: this strategy was applied to α -amino phosphonates. As a result, the challenging mono hydrolysis of α -amino phosphonates could be realized under mild conditions. A reliable isolation procedure was also discovered, and successfully implemented for a variety of substrates. Kinetic resolution with chiral aldehydes as catalysts demonstrated promising preliminary results (Chapter 3). Furthermore, the methodology developed in Chapter 2 was applied to the field of prebiotic chemistry. Glycolaldehyde, a prebiotic important substance was successfully developed as a catalyst for the hydrolysis reaction of organophosphorus compounds that bear P(=O)-N motif. More importantly, DAP as a potential phosphorylating reagent was systematically studied under the glycolaldehyde-catalyzed systems. In total, DAP

could be activated by glycolaldehyde towards the hydrolysis reaction and as a potential phosphorylating reagent for nucleophiles under diluted conditions.

Claims to Original Research

- 1) Development and optimization of *o*-phthalaldehyde-catalyzed hydrolysis reactions for P(=O)-N bond in organophosphorus compounds, including a significant expansion of substrate scope for both phosphinic amides and phosphoramidates, early test for kinetic resolution to achieve chiral organophosphorus compounds with different chiral aldehydes.
- 2) Development and optimization of formaldehyde-catalyzed hydrolysis reaction for α -amino phosphonates to achieve mono ester of α -amino phosphonic acids, including expansion of substrate scope for both *N*-primary and secondary substances, preliminary establishment for kinetic resolution to obtain chiral α -amino phosphonates with chiral aldehydes.
- 3) Development of glycolaldehyde-catalyzed hydrolysis for P(=O)-N bond in phosphinic amides and phosphoramidates, systematic ^{31}P NMR investigation for reactions related to DAP as a potential phosphorylation reagent in the presence of glycolaldehyde as a catalyst.

Publication from This Work

- 1) *o*-Phthalaldehyde Catalysed Hydrolysis of Organophosphinic Amides and Other P(=O)-NH Containing Compounds, Bin-Jie Li, Ryan D. Simard, André M. Beauchemin, *Chem. Commun.* **2017**, 53, 8667.
- 2) *Organocatalysis Using Aldehydes: The Development and Improvement of Catalytic Hydroaminations, Hydrations and Hydrolyses*, Bin-Jie Li, Claudia El-Nachef, André M. Beauchemin, *Chem. Commun.* **2017**, 53, 13192.

3) *Glycolaldehyde-Catalyzed Hydration and Hydrolysis Reactions*, Claudia El-Nachef,[§] Bin-Jie Li,[§] Aidan T. Pezacki, André M. Beauchemin, Manuscript in preparation.

Presentations from This Work

Oral presentation

1) Bin-Jie Li, Ryan D. Simard, Claudia El-Nachef, Philippe Lemire, André M. Beauchemin, *New Reactivity Using Aldehyde Catalysis*, CCRI Technical Seminar, Department of Chemistry and Biomolecular Sciences, University of Ottawa, Mar 8th, 2018.

Poster presentation

1) Bin-Jie Li, Ryan D. Simard, André M. Beauchemin, *Electrophilic Catalysis: Hydrolysis of Phosphinic Amides and Related Derivatives*, 26st Quebec & Ontario Mini-Symposium on Biological and Organic Chemistry, November 6-8th, 2015.

2) Bin-Jie Li, Ryan D. Simard, Claudia El-Nachef, Philippe Lemire, André M. Beauchemin, *Aldehyde Catalysis: Hydrolysis of Organophosphorus Compounds*, 28st Quebec & Ontario Mini-Symposium on Biological and Organic Chemistry, November 17-19th, 2017.

3) Bin-Jie Li, Ryan D. Simard, André M. Beauchemin, *Electrophilic Activation: Simple Aldehydes Catalyzed Hydrolysis of Organophosphinic Amides and Related Derivatives*, 100th Canadian Chemistry Conference and Exhibition, May 28th – Jun 1st, 2017.

Chapter 6

Experiment Section

6.1. General Information

Unless otherwise mentioned, all commercially available materials were purchased from Alfa Aesar, Aldrich or Combi Blocks and used without further purification. Solvents were obtained from LC Technology solvent system or distilled before using. All reactions involving moisture sensitive reactants were executed under an argon atmosphere using oven dried and/or flame dried glassware. Flash column chromatography was performed using 40 – 63 μm Silicycle silica gel. Reactions were monitored by analytical thin layer chromatography (TLC), using aluminium based plates, and cut to size. TLC visualization was achieved by UV, I_2 stain and KMnO_4 stain. Bruker AVANCE 300 MHz, 400 MHz, 500 MHz and 600 MHz spectrometers were used to obtain ^1H NMR, ^{13}C NMR, ^{31}P NMR and ^{19}F NMR spectra at ambient temperature. Spectral data is reported in ppm using solvents as the reference (CDCl_3 at 7.26 ppm, CD_3OD at 3.31 ppm and DMSO at 2.50 ppm for ^1H NMR/ CDCl_3 at 77.16 ppm, CD_3OD at 49.00 ppm and DMSO at 39.52 ppm for ^{13}C NMR). ^1H NMR data was reporting as: multiplicity (s = singlet, d = doublet, t = triplet, q = quartet, m = multiplet), coupling constant(s) in Hz, and integration. Infrared (IR) spectra were obtained as neat solids on an Agilent Cary 630 Fourier transform infrared spectrometer. Electron impact and electrospray ionisation high-resolution mass spectroscopy (EI-HRMS/ESI-HRMS) were recorded on a Kratos Concept 11-A mass spectrometer at the Ottawa-Carleton

Mass Spectrometry Centre. ^1H NMR yields were determined using 1,3,5-trimethoxybenzene as an internal standard. The NMR integrations were exposed to uncertainty.

6.2. Experimental section for Chapter 2

General procedure for the synthesis of diphenylphosphinic amides and diphenylphosphoramidates.

Diphenylphosphinic amides and *O,O*-diphenyl phosphoramidates were synthesized according to a reported general procedure.²⁰⁷ To a stirred solution of amines (10 mmol) in THF (25 mL) was added trimethylamine (21 mmol) at room temperature. Diphenylphosphinic chloride (12 mmol) or *O,O*-diphenyl chlorophosphate (12 mmol) in 25 mL of THF was added to the solution at 0 °C. After being stirred for 15 min at 0 °C, the reaction solution was allowed back to ambient temperature and stirred for overnight. The resulting mixture was cooled in ice bath, and diluted with CHCl_3 and water. The product was extracted with CHCl_3 and combined organic layer was washed by brine, 1 N HCl, saturated NaHCO_3 and brine. The combined organic phases were dried over Na_2SO_4 and filtered and concentrated *in vacuo*. The crude product was purified by column chromatography using CH_2Cl_2 -MeOH (95:5) as eluent to give the corresponding phosphinic amides or phosphoramidates.

General procedure to generate products

Procedure for hydrolysis of diphenylphosphinic amides and

²⁰⁷ M. Hatano, T. Miyamoto, K. Ishihara, *Org. Lett.* **2007**, *9*, 4535.

diphenylphosphoramidates

Diphenylphosphinic amide **1** (0.2 mmol), *o*-phthalaldehyde **3f** (0.04mmol) and NH₄OTs (0.2 mmol) were added into a sealed tube. 0.2 mL MeCN and 0.2 mL H₂O were followed. Then the reaction mixture was stirred under 90 °C for 24 hours.

Isolation of diphenylphosphinic acid

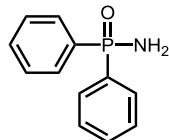
After the completion, the solvent was removed by high vacuum and following adding H₂O (10 mL) and toluene (10 mL). The mixture was stirred for 10 minutes and the aqueous layer was collected. After acidification of the aqueous layer by 1 M HCl to pH = 1~2, then the aqueous layer was extracted using 5% methanol in dichloromethane (20 mL x 3). The organic layers was combined, dried over Na₂SO₄ and filtered and concentrated *in vacuo*.

Isolation of amine component

After the completion, the solvent was removed by high vacuum and following adding H₂O (10 mL) and toluene (10 mL). The mixture was stirred for 10 minutes and the aqueous layer was collected. After basification of the aqueous layer by 1 M NaOH to pH = 8~9, then the aqueous layer was extracted using ethyl acetate (20 mL x 3). The organic layers was combined, dried over Na₂SO₄ and filtered and concentrated *in vacuo*.

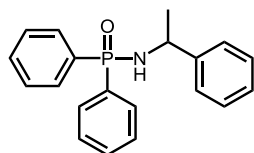
Phosphinic Amides

P,P-Diphenylphosphinic amide (*1n*)



Synthesized according to general procedure. The title compound was isolated as white solid (1.70 g, 78% yield). ^1H NMR (300 MHz, CDCl_3) 8.10 – 7.72 (4 H, m), 7.57 – 7.33 (6 H, m), 3.12 (2 H, s). ^{13}C NMR (75 MHz, CDCl_3) 133.6 (d, $J=129.9$ Hz), 131.9 (d, $J = 9.7$ Hz), 131.8 (d, $J = 2.8$ Hz), 128.5 (d, $J = 12.7$ Hz). ^{31}P NMR (121 MHz, CDCl_3) 19.12. IR 3286, 3244, 3129, 3056, 1618, 1573, 1541, 1435, 1306, 1168, 1121, 1105, 994, 978, 909, 755, 720, 690 cm^{-1} . HRMS (EI): Exact mass calculated for $\text{C}_{12}\text{H}_{12}\text{NOP}$ $[\text{M}]^+$ 217.06565, found 217.06572. Spectral data was found to be in good agreement with literature.²⁰⁸

P,P-Diphenyl-*N*-(1-phenylethyl)phosphinic amide (*1a*)

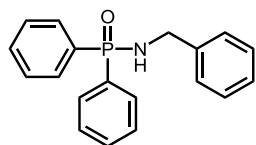


Synthesized according to general procedure. The title compound was isolated as white solid (2.44 g, 76% yield). ^1H NMR (300 MHz, CDCl_3) 8.15 – 7.60 (4 H, m), 7.55 – 7.27 (10 H, m), 7.25 – 7.15 (1 H, m), 4.68 – 4.05 (1 H, m), 3.43 – 3.00 (1 H, m), 1.57 (3 H, d, $J = 6.7$ Hz). ^{13}C NMR (75 MHz, CDCl_3) 145.2 (d, $J = 7.0$ Hz), 133.4 (d, $J = 79.6$ Hz), 132.6 (d, $J = 9.7$ Hz), 132.1 (d, $J = 9.9$ Hz), 131.9 (d, $J = 3.3$ Hz), 131.7 (d, J

²⁰⁸ B. Wahl, A. Cabré, S. Woodward, W. Lewis, *Tetrahedron Lett.* **2014**, *55*, 5829.

= 81.7 Hz), 131.4 (d, $J = 10.4$ Hz), 128.7, 128.6 (d, $J = 6.9$ Hz), 128.4 (d, $J = 3.1$ Hz), 127.2, 126.1, 51.3, 26.1 (d, $J = 3.4$ Hz). ^{31}P NMR (121 MHz, CDCl_3) 19.64. IR 3152, 3057, 3029, 2972, 2867, 1459, 1434, 1176, 1122, 1106, 1082, 1034, 969, 870, 781, 750, 725, 691 cm^{-1} . HRMS (ESI): Exact mass calculated for $\text{C}_{20}\text{H}_{20}\text{NOPNa}$ $[\text{M}+\text{Na}]^+$: 344.1175, found: 374.1180. Spectral data was found to be in good agreement with literature.²⁰⁹

N-Benzyl-P,P-diphenylphosphinic amide (1b)

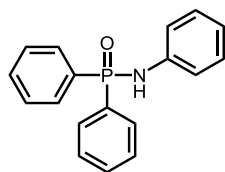


Synthesized according to general procedure. The title compound was isolated as white solid (1.69 g, 55% yield). ^1H NMR (500 MHz, CD_3OD) 8.00 – 7.67 (4 H, m), 7.58 – 7.51 (2 H, m), 7.50 – 7.42 (4 H, m), 7.36 – 7.31 (2 H, m), 7.30 – 7.24 (2 H, m), 7.24 – 7.14 (1 H, m), 4.06 (2 H, d, $J = 10.1$ Hz). ^{13}C NMR (75 MHz, CD_3OD) 139.7 (d, $J = 8.7$ Hz), 132.3 (d, $J = 129.2$ Hz), 132.3 (d, $J = 9.6$ Hz), 132.1 (d, $J = 2.8$ Hz), 128.8, 128.7 (d, $J = 9.3$ Hz), 127.8, 127.5, 44.8. IR 3280, 3212, 3166, 3063, 2873, 1588, 1484, 1452, 1243, 1219, 1185, 1162, 1099, 1073, 1024, 1003, 929, 899, 772, 748, 687 cm^{-1} . HRMS (EI): Exact mass calculated for $\text{C}_{19}\text{H}_{18}\text{NOP}$ $[\text{M}]^+$ 307.11260, found 307.11029. Spectral data was found to be in good agreement with literature.²¹⁰

²⁰⁹ B. Burns, N. Paul King, H. Tye, J. R. Studley, M. Gamble, M. Wills, *J. Chem. Soc., Perkin Trans.1*, **1998**, 1027.

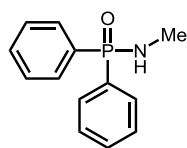
²¹⁰ A. Martínez-Asencio, D. J. Ramón, M. Yus, *Tetrahedron*, **2011**, 67, 3140.

***N,P,P*-Triphenylphosphinic amide (1c)**



Synthesized according to general procedure. The title compound was isolated as white solid (1.58 g, 54% yield). ^1H NMR (300 MHz, CDCl_3) 7.96 – 7.83 (4 H, m), 7.62 – 7.37 (6 H, m), 7.20 – 7.08 (2 H, m), 7.01 – 6.84 (3 H, m). ^{13}C NMR (76 MHz, CDCl_3) 140.5, 132.2 (d, $J = 2.8$ Hz), 132.0 (d, $J = 10.1$ Hz), 131.9 (d, $J = 129.1$ Hz), 129.2, 128.8 (d, $J = 13.0$ Hz), 121.7, 118.5 (d, $J = 6.6$ Hz). ^{31}P NMR (122 MHz, CDCl_3) 18.56. IR 3106, 3072, 3043, 3018, 2964, 2883, 2819, 2726, 1591, 1558, 1487, 1434, 1415, 1303, 1280, 1233, 1185, 1170, 1123, 1104, 1067, 1028, 996, 932, 895, 845, 796, 759, 742, 724, 688 cm^{-1} . HRMS (EI): Exact mass calculated for $\text{C}_{18}\text{H}_{16}\text{NOP}$ $[\text{M}]^+$ 293.09695, found 293.09484. Spectral data was found to be in good agreement with literature.²¹¹

***N*-Methyl-*P,P*-diphenylphosphinic amide (1d)**

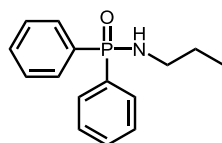


Synthesized according to general procedure. The title compound was isolated as white solid (0.81 g, 35% yield). ^1H NMR (300 MHz, CDCl_3) 8.15 – 7.78 (4 H, m), 7.64 – 7.33 (6 H, m), 2.80 (1 H, m), 2.73 – 2.57 (3 H, m). ^{13}C NMR (75 MHz, CDCl_3) 132.1 (d, $J = 129.5$ Hz), 132.1 (d, $J = 9.4$ Hz), 131.8 (d, $J = 2.7$ Hz), 128.5 (d, $J = 12.5$ Hz), 26.7 (d, $J = 2.0$). ^{31}P NMR (121 MHz, CDCl_3) 22.46. IR (ATR Diamond): 3186, 2916,

²¹¹ C. Shen, G. Yang, W. Zhang, *Org. Lett.* **2013**, *15*, 5722.

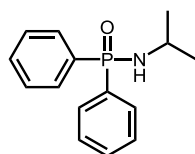
2819, 1478, 1432, 1175, 1108, 1069, 838, 755, 724, 695, 556 cm^{-1} . HRMS (EI): Exact mass calculated for $\text{C}_{13}\text{H}_{14}\text{NOP}$ $[\text{M}]^+$ 231.08130, found 231.08103. Spectral data was found to be in good agreement with literature.²¹²

N-Propyl-*P,P*-diphenylphosphinic amide (**1e**)



Synthesized according to general procedure. The title compound was isolated as white solid (1.40 g, 54% yield). ^1H NMR (300 MHz, CDCl_3) δ 7.98 – 7.76 (m, 4H), 7.60 – 7.35 (m, 6H), 3.09 (s, 1H), 2.98 – 2.82 (m, 2H), 1.68 – 1.46 (m, 2H), 0.90 (t, $J = 7.4$ Hz, 3H). ^{13}C NMR (101 MHz, CDCl_3) δ 132.5 (d, $J = 129.3$ Hz), 132.1 (d, $J = 9.3$ Hz), 131.8 (d, $J = 2.8$ Hz), 128.5 (d, $J = 12.5$ Hz), 42.6 (d, $J = 2.0$ Hz), 25.3 (d, $J = 7.3$ Hz), 11.3. ^{31}P NMR (121 MHz, CDCl_3) δ 20.6. IR (ATR Diamond): 3171, 2963, 2842, 1590, 1435, 1179, 1124, 1102, 1074, 1010, 995, 885, 842, 749, 773, 701, 692 cm^{-1} . HRMS (EI) for: Exact mass calculated for $\text{C}_{15}\text{H}_{18}\text{NOP}$ $[\text{M}]^+$: 259.11260, found 259.11133.

N-Isopropyl-*P,P*-diphenylphosphinic amide (**1f**)

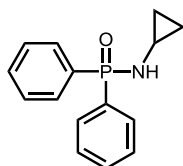


Synthesized according to general procedure. The title compound was isolated as white solid (1.74 g, 67% yield). ^1H NMR (300 MHz, CDCl_3) 8.18 – 7.78 (4 H, m), 7.67 –

²¹² N. A. Bondarenko, A. V. Kharlamov, A. G. Vendilo, *Russ. Chem. Bull.* **2009**, 58, 1872.

7.37 (6 H, m), 3.37 (1 H, ddt, $J = 10.5, 8.4, 6.4$ Hz), 2.67 (1 H, s), 1.24 (6 H, d, $J = 6.4$ Hz). ^{13}C NMR (75 MHz, CDCl_3) 132.9 (d, $J = 129.8$ Hz), 132.1 (d, $J = 9.4$ Hz), 131.7 (d, $J = 2.8$ Hz), 128.5 (d, $J = 12.4$ Hz), 43.8 (d, $J = 1.8$ Hz), 26.2 (d, $J = 5.5$ Hz). ^{31}P NMR (121 MHz, CDCl_3) 19.28. IR 3117, 3060, 2961, 2851, 1469, 1438, 1382, 1362, 1309, 1199, 1183, 1167, 1133, 1106, 1070, 1010, 891, 838, 741, 720, 690 cm^{-1} . HRMS (EI): Exact mass calculated for $\text{C}_{15}\text{H}_{18}\text{NOP} [\text{M}]^+$ 259.11260, found 259.11512. Spectral data was found to be in good agreement with literature.²¹³

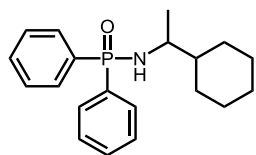
N-Cyclopropyl-P,P-diphenylphosphinic amide (1g)



Synthesized according to general procedure. The title compound was isolated as white solid (1.49 g, 58% yield). ^1H NMR (400 MHz, CDCl_3) δ 7.91 – 7.79 (4H, m), 7.52 – 7.42 (2H, m), 7.42 – 7.36 (4H, m), 3.54 (1H, s), 2.44 (1H, tq, $J = 7.1, 3.6$ Hz), 0.53–0.57 (2H, m), 0.40–0.46 (2H, m). ^{13}C NMR (101 MHz, CDCl_3) δ 132.7 (d, $J = 128.2$ Hz), 131.9 (d, $J = 9.6$ Hz), 131.6 (d, $J = 2.7$ Hz), 128.3 (d, $J = 12.6$ Hz), 23.0, 7.3 (d, $J = 5.1$ Hz). ^{31}P NMR (121 MHz, CDCl_3) δ 20.7. IR (ATR Diamond): 3173, 3053, 1438, 1421, 1405, 1356, 1190, 1157, 1113, 1070, 1039, 1019, 1007, 995, 878, 819, 749, 721, 693 cm^{-1} . HRMS (EI): Exact mass calculated for $\text{C}_{15}\text{H}_{16}\text{NOP} [\text{M}]^+$: 257.09695, found 257.09772.

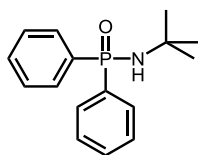
²¹³ A. Brück, W. Kuchen, W. Peters, *Phosphorus, Sulfur Silicon Relat. Elem.* **1995**, 107, 129.

***N*-(1-Cyclohexylethyl)-*P,P*-diphenylphosphinic amide (1h)**



Synthesized according to general procedure. The title compound was isolated as white solid (2.71 g, 83% yield). ^1H NMR (300 MHz, CDCl_3) 7.91 (4 H, m), 7.59 – 7.33 (6 H, m), 3.01 (1 H, m), 2.78 (1 H, s), 1.89 – 1.52 (5 H, m), 1.49 – 0.64 (9 H, m). ^{13}C NMR (76 MHz, CDCl_3) 133.9 (d, $J=38.5$ Hz), 132.6 – 131.9 (m), 131.7 (t, $J=2.5$ Hz), 128.4 (dd, $J=12.6, 3.2$ Hz), 52.0 (d, $J=2.2$ Hz), 44.9 (d, $J=6.1$ Hz), 28.8 (d, $J=79.6$ Hz), 26.5, 26.3 (d, $J=4.9$ Hz), 20.6 (d, $J=3.8$ Hz). ^{31}P NMR (122 MHz, CDCl_3) 21.82. IR 3117, 3060, 2961, 2851, 1589, 1469, 1438, 1382, 1362, 1309, 1199, 1183, 1167, 1133, 1106, 1070, 1010, 925, 891, 838, 774, 741, 720, 690 cm^{-1} . HRMS (ESI): Exact mass calculated for $\text{C}_{20}\text{H}_{27}\text{NOP}$ $[\text{M}+\text{H}]^+$: 328.1825, found: 328.1278. Spectral data was found to be in good agreement with literature.²¹⁴

***N*-(*t*-Butyl)-*P,P*-diphenylphosphinic amide (1i)**

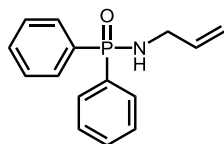


Synthesized according to general procedure. The title compound was isolated as white solid (1.37 g, 50% yield). ^1H NMR (300 MHz, CDCl_3) 7.89 (4 H, m), 7.45 (6 H, m), 1.30 (9 H, d, $J=0.5$ Hz). ^{13}C NMR (76 MHz, CDCl_3) 135.1 (d, $J=128.6$ Hz), 131.8

²¹⁴ C. R. Graves, K. A. Scheidt, S. T. Nguyen, *Org. Lett.* **2006**, *8*, 1229.

(d, $J = 9.4$ Hz), 131.4 (d, $J = 2.7$ Hz), 128.3 (d, $J = 12.5$ Hz), 53.1 (d, $J = 3.1$ Hz), 32.3 (d, $J = 4.6$ Hz). ^{31}P NMR (122 MHz, CDCl_3) 19.47. IR 3184, 3058, 2968, 2913, 1475, 1475, 1433, 1388, 1359, 1230, 1174, 1108, 1043, 1019, 995, 923, 852, 798, 745, 718, 692, 664 cm^{-1} . HRMS (EI): Exact mass calculated for $\text{C}_{16}\text{H}_{20}\text{NOP}$ $[\text{M}]^+$ 273.12825, found 273.12711. Spectral data was found to be in good agreement with literature.²¹⁵

N-Allyl-*P,P*-diphenylphosphinic amide (**1j**)

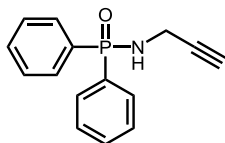


Synthesized according to general procedure. The title compound was isolated as white solid (2.19 g, 85% yield). ^1H NMR (300 MHz, CDCl_3) 8.06 – 7.77 (4 H, m), 7.63 – 7.36 (6 H, m), 6.14 – 5.69 (1 H, m), 5.27 (1H, dq, $J = 17.1$ Hz, 1.6 Hz), 5.13 (1H, dqd, $J = 10.2, 1.5, 0.4$ Hz), 3.59 (2 H, dddt, $J = 8.7, 7.2, 5.6, 1.6$ Hz), 2.89 (1 H, d, $J = 6.8$ Hz). ^{13}C NMR (75 MHz, CDCl_3) 136.3 (d, $J = 8.1$ Hz), 132.2 (d, $J = 129.6$ Hz), 132.1 (d, $J = 9.4$ Hz), 131.9 (d, $J = 2.8$ Hz), 128.6 (d, $J = 12.6$ Hz), 115.8, 43.2. ^{31}P NMR (121 MHz, CDCl_3) 21.15. IR 3164, 3081, 3058, 2981, 2835, 1644, 1435, 1401, 1240, 1176, 1122, 1065, 1021, 1005, 903, 868, 753, 724, 692 cm^{-1} . HRMS (ESI) for: Exact mass calculated for $\text{C}_{15}\text{H}_{16}\text{NOPNa}$ $[\text{M}+\text{Na}]^+$ 280.0867, found 280.0839. Spectral data was found to be in good agreement with literature.²¹⁶

²¹⁵ V. Moodley, L. Mthethwa, M. N. Pillay, B. Omondi, W. E. van Zyl, *Polyhedron* **2015**, 99, 87.

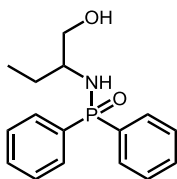
²¹⁶ A. M. Z. Slawin, J. Wheatley, J. D. Woollins, *Eur. J. Inorg. Chem.* **2005**, 2005, 713.

***P,P*-Diphenyl-*N*-(prop-2-yn-1-yl)phosphinic amide (1k)**



Synthesized according to general procedure. The title compound was isolated as white solid (1.58 g, 62% yield). ^1H NMR (300 MHz, CDCl_3) 8.04 – 7.72 (4 H, m), 7.65 – 7.37 (6 H, m), 3.72 (2 H, dd, $J = 8.6, 2.5$ Hz), 3.37 (1 H, s), 2.24 (1 H, t, $J = 2.5$ Hz). ^{13}C NMR (75 MHz, CDCl_3) 132.2, 132.1, 131.6 (d, $J = 129.4$ Hz), 128.6 (d, $J = 12.7$ Hz), 81.3 (d, $J = 10.4$ Hz), 71.8, 30.2. ^{31}P NMR (121 MHz, CDCl_3) 21.68. IR 3300, 3281, 3178, 3061, 2860, 1589, 1486, 1436, 1341, 1310, 1246, 1219, 1183, 1122, 1103, 1073, 1025, 1001, 931, 875, 832, 751, 722, 693, 668 cm^{-1} . HRMS (ESI) for: Exact mass calculated for $\text{C}_{15}\text{H}_{14}\text{NOPNa}$ $[\text{M}+\text{Na}]^+$ 278.0711, found 278.0697. Spectral data was found to be in good agreement with literature.²¹⁷

***N*-(1-Hydroxybutan-2-yl)-*P,P*-diphenylphosphinic amide (1l)**

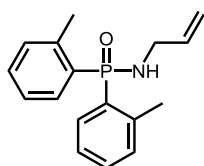


Synthesized according to general procedure. The title compound was isolated as white solid (1.62 g, 56% yield). ^1H NMR (400 MHz, CDCl_3) δ 7.97 – 7.80 (4H, m), 7.55 – 7.35 (6H, m), 4.85 (1H, s), 3.62 (1H, dd, $J = 11.7, 2.6$ Hz), 3.43 (1H, dd, $J = 11.6, 7.3$ Hz), 3.13 (1H, s), 2.99 – 2.80 (1H, m), 1.65 – 1.35 (2H, m), 0.96 (3H, t, $J = 7.5$ Hz).

²¹⁷ D. A. Erzunov, G. V. Latyshev, A. D. Averin, I. P. Beletskaya, N. V. Lukashev, *Eur. J. Org. Chem.* **2015**, 2015, 6289.

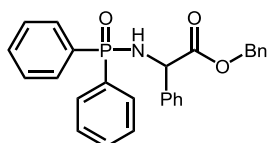
^{13}C NMR (101 MHz, CDCl_3) δ 132.6 (d, $J=9.5$ Hz), 132.3 (d, $J=148.2$ Hz), 132.0 (d, $J=2.5$ Hz), 131.9 (d, $J=2.6$ Hz), 131.7 (d, $J=9.4$ Hz), 130.2, 128.6 (d, $J=1.5$ Hz), 128.5 (d, $J=1.8$ Hz), 67.0, 56.8 (d, $J=2.2$ Hz), 26.5 (d, $J=9.6$ Hz), 10.8. ^{31}P NMR (121 MHz, CDCl_3) δ 23.7. IR (ATR Diamond): 3249, 3187, 1142, 1436, 1169, 1112, 1093, 1063, 1021, 995, 946, 873, 851, 754, 748, 724, 694 cm^{-1} . HRMS (ESI) for: Exact mass calculated for $\text{C}_{16}\text{H}_{21}\text{NO}_2\text{P}$ $[\text{M}+\text{H}]^+$ 290.1310, found 290.1300.

N-Allyl-P,P-di-o-tolylphosphinic amide (1m)



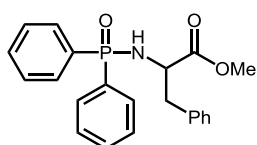
Synthesized according to general procedure. The title compound was isolated as white solid (1.99 g, 70% yield). ^1H NMR (400 MHz, CDCl_3) δ 7.73-7.67 (2H, m), 7.40-7.35 (2H, m), 7.24 – 7.16 (4H, m), 6.03-5.93 (1H, m), 5.24 (1H, dq, $J=17.1, 1.6$ Hz), 5.11 (1H, dq, $J=10.2, 1.5$ Hz), 3.70-3.64 (2H, m), 2.73 (1H, d, $J=7.4$ Hz), 2.46 (6H, s). ^{13}C NMR (101 MHz, CDCl_3) δ 142.3 (d, $J=9.9$ Hz), 136.5 (d, $J=7.3$ Hz), 132.9 (d, $J=10.7$ Hz), 131.8, 131.7 (d, $J=15.2$ Hz), 131.0 (d, $J=123.5$ Hz), 125.4 (d, $J=12.6$ Hz), 115.8, 43.5, 21.5 (d, $J=4.0$ Hz). ^{31}P NMR (121 MHz, CDCl_3) δ 25.5. IR (ATR Diamond): 3117, 3062, 1645, 1591, 1452, 1433, 1275, 1201, 1166, 1136, 1076, 1030, 998, 910, 866, 806, 762, 716, 691, 671 cm^{-1} . HRMS (ESI): Exact mass calculated for $\text{C}_{17}\text{H}_{20}\text{NOPNa}$ $[\text{M}+\text{Na}]^+$ 308.1180, found 308.1181.

Benzyl 2-((diphenylphosphoryl)amino)-2-phenylacetate (1o)



Synthesized according to general procedure. The title compound was isolated as white solid (2.96 g, 67% yield). ^1H NMR (400 MHz, CDCl_3) δ 7.90 – 7.81 (2H, m), 7.78 – 7.70 (2H, m), 7.54 – 7.48 (1H, m), 7.47 – 7.40 (3H, m), 7.34 – 7.26 (10H, m), 7.17 – 7.11 (2H, m), 5.16 – 5.09 (2H, m), 4.99 (1H, dd, $J = 10.7, 9.7$ Hz), 4.30 (1H, dd, $J = 9.7, 6.6$ Hz). ^{13}C NMR (101 MHz, CDCl_3) δ 172.0 (d, $J = 5.7$ Hz), 138.1 (d, $J = 4.4$ Hz), 135.1, 132.5 (d, $J = 48.5$ Hz), 132.3 (d, $J = 9.8$ Hz), 132.1 (d, $J = 2.8$ Hz), 131.9, 131.9 (d, $J = 9.6$ Hz), 131.2 (d, $J = 51.7$ Hz), 129.2, 128.6 (d, $J = 12.7$ Hz), 128.6 (d, $J = 23.9$ Hz), 128.3 (d, $J = 24.4$ Hz), 128.3, 128.1, 127.9, 127.0, 67.5, 57.0. IR (ATR Diamond): 3059, 1743, 1591, 1538, 1436, 1248, 1222, 1160, 1065, 1040, 1019, 955, 741, 754, 717, 692 cm^{-1} . HRMS (ESI): Exact mass calculated for $\text{C}_{27}\text{H}_{25}\text{NO}_3\text{P}$ $[\text{M}+\text{H}]^+$ 442.1572, found 442.1594.

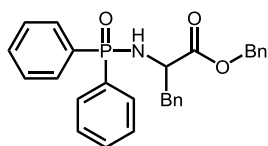
Methyl (diphenylphosphoryl)phenylalaninate (1p)



Synthesized according to general procedure. The title compound was isolated as white solid (2.27g, 60% yield). ^1H NMR (400 MHz, CDCl_3) δ 7.83-7.78 (2H, m), 7.69-7.63 (2H, m), 7.51 – 7.38 (4H, m), 7.36-7.32 (2H, m), 7.30 – 7.22 (3H, m), 7.13 (2H, dd, J

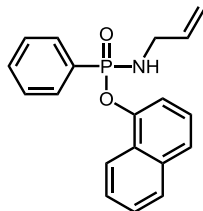
7.7, 1.8 Hz), 4.09-4.01 (1H, m), 3.64 (3H, s), 3.49 (1H, dd, $J = 11.2, 6.9$ Hz), 3.08 (2H, dd, $J = 6.0, 1.8$ Hz). ^{13}C NMR (101 MHz, CDCl_3) δ 173.2 (d, $J = 5.6$ Hz), 135.9, 132.6 (d, $J = 11.7$ Hz), 132.1 (d, $J = 9.7$ Hz), 132.0 (d, $J = 2.8$ Hz), 131.9 (d, $J = 9.8$ Hz), 131.9 (d, $J = 2.8$ Hz), 131.3 (d, $J = 10.1$ Hz), 129.7, 128.5 (d, $J = 2.7$ Hz), 128.5 (d, $J = 22.8$ Hz), 128.5, 127.0, 54.7, 52.2, 41.2 (d, $J = 5.0$ Hz). ^{31}P NMR (121 MHz, CDCl_3) δ 20.3 IR (ATR Diamond): 3145, 1732, 1659, 1591, 1433, 1282, 1243, 1182, 1125, 1108, 1096, 1043, 1016, 940, 918, 748, 726, 691 cm^{-1} . HRMS (ESI) for: Exact mass calculated for $\text{C}_{22}\text{H}_{22}\text{NO}_3\text{PNa}$ $[\text{M}+\text{Na}]^+$ 402.1235, found 402.1241.

Benzyl (diphenylphosphoryl)phenylalaninate (1q)



Synthesized according to general procedure. The title compound was isolated as white solid (3.19 g, 70% yield). ^1H NMR (300 MHz, CD_3OD) δ 7.82 – 7.66 (2H, m), 7.61 – 7.40 (6H, m), 7.40 – 7.23 (10H, m), 7.21 – 7.11 (2H, m), 5.17 – 4.98 (2H, m), 3.85 (1H, td, $J = 8.4, 6.5$ Hz), 3.17 – 2.94 (2H, m). ^{13}C NMR (75 MHz, CD_3OD) δ 172.8 (d, $J = 3.2$ Hz), 136.9, 135.7, 132.5, 132.0 (d, $J = 2.7$ Hz), 131.9, 131.8, 131.7 (d, $J = 1.4$ Hz), 131.6, 130.7, 130.1, 129.4, 128.3, 128.1, 128.1 (d, $J = 1.8$ Hz), 127.9, 126.6, 66.5, 55.7, 40.1 (d, $J = 7.2$ Hz). ^{31}P NMR (121 MHz, CDCl_3) δ 22.93. IR (ATR Diamond): 3172, 3059, 1738, 1434, 1383, 1159, 1177, 1125, 1106, 1091, 919, 902, 742, 727, 693 cm^{-1} . HRMS (ESI): Exact mass calculated for $\text{C}_{28}\text{H}_{26}\text{NO}_3\text{PNa}$ $[\text{M}+\text{Na}]^+$ 478.1548, found 478.1541.

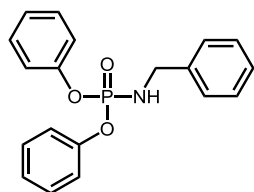
Naphthalen-1-yl-N-allyl-P-phenylphosphonamidate (1r)



Synthesized according to general procedure. The title compound was isolated as white solid (2.58 g, 80% yield). ^1H NMR (400 MHz, CDCl_3) δ 8.18 – 8.10 (1H, m), 8.03 – 7.92 (2H, m), 7.87 – 7.78 (1H, m), 7.61 (2H, dd, $J = 7.9, 1.2$ Hz), 7.59 – 7.52 (1H, m), 7.48 (4H, ddt, $J = 8.3, 6.9, 2.8$ Hz), 7.35 (1H, t, $J = 8.0$ Hz), 5.67 (1H, ddt, $J = 17.2, 10.6, 5.5$ Hz), 5.06 (1H, dd, $J = 17.1, 1.6$ Hz), 4.96 (1H, dd, $J = 10.3, 1.5$ Hz), 3.57 (2H, ddt, $J = 9.2, 5.5, 1.6$ Hz), 3.03 (1H, s). ^{13}C NMR (101 MHz, CDCl_3) δ 146.7 (d, $J = 8.4$ Hz), 135.5 (d, $J = 6.3$ Hz), 134.8, 132.3 (d, $J = 3.2$ Hz), 131.4 (d, $J = 10.0$ Hz), 131.2, 129.4, 128.6 (d, $J = 14.7$ Hz), 127.9, 126.6 (d, $J = 5.9$ Hz), 126.3 (d, $J = 28.5$ Hz), 125.7 (d, $J = 0.9$ Hz), 124.3, 121.5, 115.9, 115.3 (d, $J = 4.0$ Hz), 43.6. ^{31}P NMR (121 MHz, CDCl_3) δ 17.8. IR (ATR Diamond): 3207, 1574, 1462, 1437, 1392, 1262, 1214, 1125, 1077, 1046, 913, 853, 795, 771, 750, 718, 694 cm^{-1} . HRMS (ESI): Exact mass calculated for $\text{C}_{19}\text{H}_{18}\text{NO}_2\text{PNa}$ $[\text{M}+\text{Na}]^+$ 346.0973, found 346.0971.

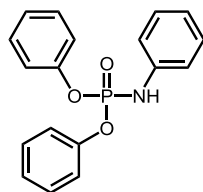
Phosphoramidates

Diphenyl benzylphosphoramidate (1s)



Synthesized according to general procedure. The title compound was isolated as white solid (3.09 g, 91% yield). ^1H NMR (300 MHz, CDCl_3) 7.38 – 7.26 (8 H, m), 7.26 – 7.21 (5 H, m), 7.21 – 7.14 (2 H, m), 4.26 (2 H, dd, $J = 10.5, 4.0$ Hz), 3.88 (1 H, s). ^{13}C NMR (75 MHz, CDCl_3) 150.8 (d, $J = 6.7$ Hz), 138.8 (d, $J = 6.6$ Hz), 129.7, 128.6, 127.5, 127.4, 124.9 (d, $J = 1.2$ Hz), 120.3 (d, $J = 4.9$ Hz), 45.7. ^{31}P NMR (121 MHz, CDCl_3) -3.94. IR 3163, 3065, 3029, 2936, 2894, 2876, 1588, 1484, 1454, 1243, 1313, 1243, 1213, 1185, 1157, 1106, 1074, 1022, 1004, 927, 901, 770, 744, 687 cm^{-1} . HRMS (ESI): Exact mass calculated for $\text{C}_{19}\text{H}_{18}\text{NO}_3\text{PNa}$ $[\text{M}+\text{Na}]^+$: 362.0917, found: 362.1526. Spectral data was found to be in good agreement with literature.²¹⁸

Diphenyl phenylphosphoramidate (1t)

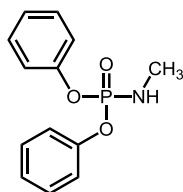


Synthesized according to general procedure. The title compound was isolated as white solid (1.69 g, 52% yield). ^1H NMR (300 MHz, CDCl_3) 7.39 – 7.26 (5 H, m), 7.26 –

²¹⁸ C. S. Jones, S. D. Bull, J. M. J. Williams, *Org. Biomol. Chem.* **2016**, *14*, 8452.

7.17 (6 H, m), 7.18 – 7.11 (3 H, m), 7.08 – 6.99 (1 H, m). ^{13}C NMR (75 MHz, CDCl_3) 150.3 (d, $J = 6.5$ Hz), 139.1, 129.7, 129.3, 125.3, 122.2, 120.4 (d, $J = 4.8$ Hz), 118.2 (d, $J = 7.7$ Hz). ^{31}P NMR (121 MHz, CDCl_3) -9.36. IR 3172, 3094, 3062, 3031, 2988, 2916, 1586, 1486, 1423, 1330, 1305, 1289, 1260, 1229, 1177, 1165, 1071, 1028, 1008, 980, 945, 922, 903, 819, 754, 688 cm^{-1} . HRMS (ESI) for: Exact mass calculated for $\text{C}_{18}\text{H}_{16}\text{NO}_3\text{PNa}$ $[\text{M}+\text{Na}]^+$ 348.0766, found 348.0789. Spectral data was found to be in good agreement with literature.²¹⁹

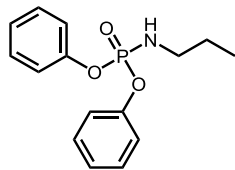
Diphenyl methylphosphoramidate (1u)



Synthesized according to general procedure. The title compound was isolated as yellow solid (1.58 g, 60% yield). ^1H NMR (400 MHz, CDCl_3) δ 7.37 – 7.31 (m, 4H), 7.26 (dq, $J = 7.9, 1.2$ Hz, 5H), 7.21 – 7.14 (m, 2H), 3.03 (s, 1H), 2.76 (d, $J = 12.5$ Hz, 3H). ^{13}C NMR (75 MHz, CDCl_3) δ 150.7 (d, $J = 6.7$ Hz), 129.7, 124.9, 120.2 (d, $J = 4.7$ Hz), 27.9. ^{31}P NMR (121 MHz, CDCl_3) δ 0.42. IR (ATR Diamond): 3244, 3069, 2928, 2824, 1587, 1488, 1456, 1424, 1256, 1227, 1104, 1163, 1110, 1081, 1024, 1008, 949, 926, 905, 857, 750, 687, 613, 591, 568 cm^{-1} HRMS (EI) for: Exact mass calculated for $\text{C}_{13}\text{H}_{14}\text{NO}_3\text{P}$ $[\text{M}]^+$: 263.07113, found 263.07396.

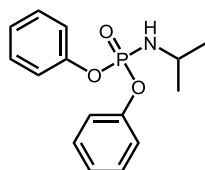
²¹⁹ M. E. Masri, K. D. Berlin, *Org. Prep. Proced. Int.* **1995**, 27, 161.

Diphenyl propylphosphoramidate (1v)



Synthesized according to general procedure. The title compound was isolated as white solid (2.47 g, 85% yield). ^1H NMR (400 MHz, CDCl_3) δ 7.31 (t, $J = 7.9$ Hz, 4H), 7.25 (d, $J = 3.5$ Hz, 3H), 7.23 (s, 1H), 7.14 (t, $J = 7.4$ Hz, 2H), 3.12 – 3.00 (m, 2H), 2.98 (d, $J = 14.0$ Hz, 1H), 1.48 (d, $J = 7.3$ Hz, 2H), 0.86 (t, $J = 7.4$ Hz, 3H). ^{13}C NMR (101 MHz, CDCl_3) δ 150.9 (d, $J = 6.7$ Hz), 129.6, 124.9, 120.2 (d, $J = 5.0$ Hz), 43.6, 24.7 (d, $J = 6.3$ Hz), 11.0. ^{31}P NMR (121 MHz, CDCl_3) δ -3.3. IR (ATR Diamond): 3174, 3055, 2963, 2932, 2875, 1589, 1486, 1456, 1250, 1233, 1213, 1187, 1167, 1104, 1069, 1036, 1021, 1006, 949, 927, 915, 773, 749, 688, 586, 545 cm^{-1} . HRMS (ESI): Exact mass calculated for $\text{C}_{15}\text{H}_{18}\text{NO}_3\text{PNa}$ $[\text{M}+\text{Na}]^+$ 314.0922, found 314.0920.

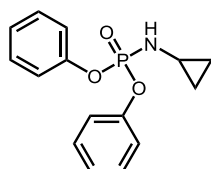
Diphenyl isopropylphosphoramidate (1w)



Synthesized according to general procedure. The title compound was isolated as white solid (2.03 g, 70% yield). ^1H NMR (400 MHz, CDCl_3) δ 7.34 – 7.27 (m, 4H), 7.24 – 7.26 (m, 4H), 7.16 – 7.10 (m, 2H), 3.65 – 3.51 (m, 1H), 2.99 (t, $J = 11.0$ Hz, 1H), 1.14 (d, $J = 1.0$ Hz, 3H), 1.13 (d, $J = 1.0$ Hz, 3H). ^{13}C NMR (101 MHz, CDCl_3) δ 150.9 (d,

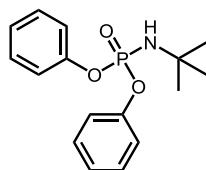
$J = 6.9$ Hz), 129.6, 124.7 (d, $J = 1.1$ Hz), 120.2 (d, $J = 5.1$ Hz), 44.5, 25.1 (d, $J = 5.8$ Hz). ^{31}P NMR (121 MHz, CDCl_3) δ -4.6. IR (ATR Diamond): 3261, 2967, 1590, 1484, 1464, 1422, 1385, 1369, 1245, 1220, 1191, 1163, 1144, 1126, 1042, 1026, 924, 906, 767, 751, 691 cm^{-1} . HRMS (ESI) for: Exact mass calculated for $\text{C}_{15}\text{H}_{18}\text{NO}_3\text{PNa}$ $[\text{M}+\text{Na}]^+$ 314.0922, found 314.0933

Diphenyl cyclopropylphosphoramidate (1x)



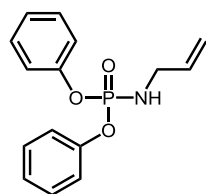
Synthesized according to general procedure. The title compound was isolated as white solid (2.60 g, 90% yield). ^1H NMR (300 MHz, CDCl_3) δ 7.31 (dd, $J = 8.7, 6.9$ Hz, 4H), 7.26 – 7.20 (m, 4H), 7.19 – 7.09 (m, 2H), 3.65 (d, $J = 14.9$ Hz, 1H), 2.43 – 2.51 (m, 1H), 0.74 – 0.41 (m, 4H). ^{13}C NMR (101 MHz, CDCl_3) δ 150.8 (d, $J = 6.6$ Hz), 129.6, 124.8 (d, $J = 1.1$ Hz), 120.1 (d, $J = 5.1$ Hz), 23.2, 7.1 (d, $J = 5.3$ Hz). ^{31}P NMR (121 MHz, CDCl_3) δ -3.6. IR (ATR Diamond): 3218, 1591, 1483, 1453, 1433, 1417, 1249, 1209, 1190, 1176, 1162, 1101, 1025, 1005, 929, 903, 777, 766, 752, 691 cm^{-1} . HRMS (ESI) for: Exact mass calculated for $\text{C}_{15}\text{H}_{16}\text{NO}_3\text{PNa}$ $[\text{M}+\text{Na}]^+$ 312.0766, found 312.0774.

Diphenyl tert-butylphosphoramidate (1y)



Synthesized according to general procedure. The title compound was isolated as white solid (2.28 g, 75% yield). ^1H NMR (400 MHz, CDCl_3) δ 7.34 – 7.27 (m, 4H), 7.24 (dq, $J = 7.4, 1.2$ Hz, 4H), 7.10 – 7.13 (m, 2H), 3.24 (s, 1H), 1.32 (s, 9H). ^{13}C NMR (101 MHz, CDCl_3) δ 151.1 (d, $J = 7.0$ Hz), 129.5, 124.6 (d, $J = 1.3$ Hz), 120.1 (d, $J = 5.2$ Hz), 51.7 (d, $J = 1.5$ Hz), 31.2 (d, $J = 4.9$ Hz). ^{31}P NMR (121 MHz, CDCl_3) δ -6.2. IR (ATR Diamond): 3264, 2974, 1588, 1484, 1409, 1388, 1365, 1260, 1219, 1192, 1156, 1047, 1021, 923, 867, 784, 757, 721, 690 cm^{-1} . HRMS (ESI): Exact mass calculated for $\text{C}_{16}\text{H}_{21}\text{NO}_3\text{P}$ $[\text{M}+\text{H}]^+$ 306.1255, found 306.1259

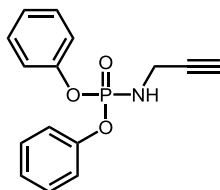
Diphenyl allylphosphoramidate (1z)



Synthesized according to general procedure. The title compound was isolated as white solid (2.34 g, 81% yield). ^1H NMR (300 MHz, CDCl_3) 7.39 – 7.26 (5 H, m), 7.25 – 7.20 (3 H, m), 7.20 – 7.11 (2 H, m), 5.95 – 5.67 (1 H, m), 5.18 (1H, dq, $J = 17.1, 1.6$ Hz), 5.08 (1H, dq, $J = 10.2, 1.4$ Hz) 3.70 (2 H, dddd, $J = 12.2, 5.5, 3.2, 1.6$ Hz), 3.14 (1 H, dt, $J = 13.2, 6.7$ Hz). ^{13}C NMR (75 MHz, CDCl_3) 150.8 (d, $J = 7.0$ Hz), 135.2 (d, J

= 6.1 Hz), 129.7, 124.9, 120.3 (d, $J = 4.9$ Hz), 116.1, 44.1. ^{31}P NMR (121 MHz, CDCl_3) -3.97. IR 3249, 3093, 3066, 3018, 2982, 2925, 2860, 1588, 1485, 1439, 1251, 1233, 1216, 1183, 1164, 1090, 1072, 1026, 1004, 977, 920, 868, 753, 685 cm^{-1} . HRMS (ESI) for: Exact mass calculated for $\text{C}_{15}\text{H}_{16}\text{NO}_3\text{PNa}$ $[\text{M}+\text{Na}]^+$ 312.0766, found 312.0772. Spectral data was found to be in good agreement with literature.²¹⁸

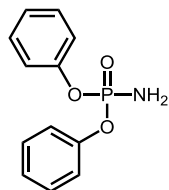
Diphenyl prop-2-yn-1-ylphosphoramidate (1aa)



Synthesized according to general procedure. The title compound was isolated as white solid (1.29 g, 45% yield). ^1H NMR (300 MHz, CDCl_3) 7.31 (5 H, m), 7.23 (3 H, m), 7.15 (2 H, m), 4.08 – 3.63 (3 H, m), 2.21 (1 H, t, $J = 2.4$ Hz). ^{13}C NMR (75 MHz, CDCl_3) 150.6 (d, $J = 6.7$ Hz), 129.7, 125.1, 120.3 (d, $J = 4.9$ Hz), 80.3, 72.0, 31.3. ^{31}P NMR (121 MHz, CDCl_3) -4.73. IR 3280, 3166, 3063, 2935, 2873, 1588, 1485, 1452, 1219, 1185, 1162, 1099, 1073, 1024, 1003, 929, 899, 772, 748, 687 cm^{-1} . HRMS (ESI) for: Exact mass calculated for $\text{C}_{15}\text{H}_{14}\text{NO}_3\text{PNa}$ $[\text{M}+\text{Na}]^+$ 310.0609, found 310.0631. Spectral data was found to be in good agreement with literature.²²⁰

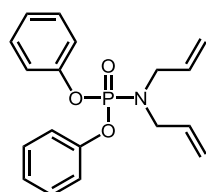
²²⁰ B. M. Trost, M. C. Ryan, M. Rao, T. Z. Markovic, *J. Am. Chem. Soc.* **2014**, *136*, 17422.

Diphenyl phosphoramidate (1ab)



Synthesized according to general procedure. The title compound was isolated as white solid (1.92 g, 77% yield). ^1H NMR (300 MHz, CD_3OD) 7.48 – 7.30 (4 H, m), 7.30 – 7.12 (6 H, m). ^{13}C NMR (76 MHz, CD_3OD) 151.0 (d, $J = 7.0$ Hz), 129.3, 124.7 (d, $J = 1.5$ Hz), 120.2 (d, $J = 4.9$ Hz). ^{31}P NMR (122 MHz, CD_3OD) 3.04. IR 3280, 3211, 3166, 3063, 2873, 1588, 1505, 1484, 1452, 1219, 1185, 1162, 1099, 1073, 1024, 1008, 950, 907, 780, 754, 695 cm^{-1} . HRMS (ESI) for: Exact mass calculated for $\text{C}_{12}\text{H}_{12}\text{NO}_3\text{PNa}$ $[\text{M}+\text{Na}]^+$ 272.0453, found 272.0463. Spectral data was found to be in good agreement with literature.²²¹

Diphenyl diallylphosphoramidate (1ac)

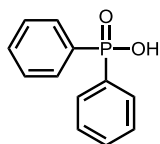


Synthesized according to general procedure. The title compound was isolated as white solid (2.87 g, 87% yield). ^1H NMR (300 MHz, CDCl_3) δ 7.38 – 7.09 (m, 10H), 5.56 (ddt, $J = 17.5, 9.7, 6.3$ Hz, 2H), 5.19 – 5.07 (m, 4H), 3.75 (ddt, $J = 11.3, 6.3, 1.3$ Hz, 4H). ^{13}C NMR (101 MHz, CDCl_3) δ 151.2 (d, $J = 6.7$ Hz), 133.9 (d, $J = 2.6$ Hz), 129.92,

²²¹ S. Kan, Y. Jin, X. He, J. Chen, H. Wu, P. Ouyang, K. Guo, Z. Li, *Polym. Chem.* **2013**, *4*, 5432.

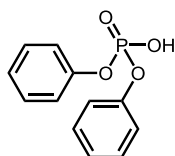
125.1 (d, $J = 1.1$ Hz), 120.5 (d, $J = 5.0$ Hz), 118.8, 48.1 (d, $J = 4.4$ Hz). ^{31}P NMR (121 MHz, CDCl_3) δ -2.77. IR (ATR Diamond): 3452, 1588, 1485, 1254, 1227, 1186, 1162, 1111, 1085, 1023, 993, 923, 910, 775, 762, 613 cm^{-1} . HRMS (EI): Exact mass calculated for $\text{C}_{18}\text{H}_{20}\text{NO}_3\text{P}$ $[\text{M}]^+$: 329.11808, found 329.11611

Diphenylphosphinic acid



White solid, ^1H NMR (400 MHz, CD_3OD) δ 7.85 – 7.71 (m, 4H), 7.59 – 7.50 (m, 2H), 7.50 – 7.41 (m, 4H). ^{13}C NMR (101 MHz, CD_3OD) δ 133.1 (d, $J = 138.4$ Hz), 131.8 (d, $J = 2.9$ Hz), 130.9 (d, $J = 10.3$ Hz), 128.2 (d, $J = 13.2$ Hz). Spectral data is in good agreement with literature data.²²²

Diphenyl hydrogen phosphate

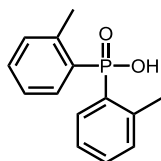


White solid, ^1H NMR (300 MHz, CD_3OD) δ 7.34 (dddd, $J = 9.0, 6.5, 1.2, 0.6$ Hz, 4H), 7.23 – 7.13 (m, 6H). ^{13}C NMR (101 MHz, CDCl_3) δ 150.3 (d, $J = 7.1$ Hz), 129.7, 125.4, 120.2 (d, $J = 4.9$ Hz). Spectral data is in good agreement with literature data.²²³

²²² Y. Hao, D. Wu, R. Tian, Z. Duan, F. Mathey, *Dalton Trans.* **2016**, 45, 891.

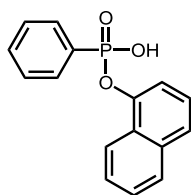
²²³ I. E. Nifant'ev, A. N. Tavtorkin, S. Y. A. Korchagina, I. F. Gavrilenko, N. N. Glebova, N. N. Kostitsyna, V. A.

Di-*o*-tolylphosphinic acid



Colorless oil. ^1H NMR (400 MHz, CD_3OD) δ 7.94-7.88 (m, 2H), 7.44 (tt, $J = 7.6$, 1.5 Hz, 2H), 7.33-7.28 (m, 2H), 7.26 – 7.18 (m, 2H), 2.27 (s, 6H). ^{13}C NMR (101 MHz, CD_3OD) δ 141.1 (d, $J = 11.4$ Hz), 132.5 (d, $J = 9.8$ Hz), 132.1, 132.0, 131.1 (d, $J = 12.5$ Hz), 125.2 (d, $J = 12.6$ Hz), 20.0 (d, $J = 4.6$ Hz). ^{31}P NMR (121 MHz, CD_3OD) δ 25.56. IR (ATR Diamond): 3183, 2919, 2848, 1645, 1594, 1276, 939, 715, 699 cm^{-1} . HRMS (ESI): Exact mass calculated for $\text{C}_{14}\text{H}_{15}\text{O}_2\text{PNa}$ $[\text{M}+\text{Na}]^+$ 269.0707, found 269.0726.

Naphthalen-1-yl hydrogen phenyl phosphonate



Colorless oil, ^1H NMR (400 MHz, CDCl_3) δ 11.50 (s, 1H), 8.06 (dd, $J = 8.3$, 1.2 Hz, 1H), 7.89-7.83 (m, 2H), 7.78 – 7.71 (m, 1H), 7.56 – 7.46 (m, 2H), 7.45 – 7.28 (m, 5H), 7.16 (t, $J = 7.9$ Hz, 1H). ^{13}C NMR (101 MHz, CDCl_3) δ 146.4 (d, $J = 8.4$ Hz), 134.7, 132.7 (d, $J = 3.1$ Hz), 131.5 (d, $J = 10.4$ Hz), 129.0, 128.4 (d, $J = 15.8$ Hz), 127.5, 127.0, 126.8 (d, $J = 5.4$ Hz), 126.3 (d, $J = 32.6$ Hz), 125.4 (d, $J = 1.6$ Hz), 124.7 (d, $J = 1.5$ Hz), 122.1, 115.6 (d, $J = 3.6$ Hz). ^{31}P NMR (121 MHz, CDCl_3) δ 17.3. IR (ATR Diamond): 3056, 1595, 1574, 1507, 1462, 1439, 1390, 1258, 1226, 1154, 1132, 1082,

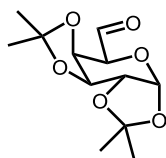
1043, 977, 914, 815, 795, 769, 749, 719, 691, 638, 596, 565, 544 cm^{-1} . HRMS (ESI):

Exact mass calculated for $\text{C}_{16}\text{H}_{13}\text{O}_3\text{PNa}$ $[\text{M}+\text{Na}]^+$ 307.0500, found 307.0506.

Chiral aldehydes

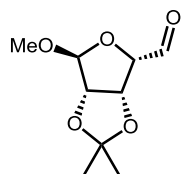
(3aR,5S,5aR,8aS,8bR)-2,2,7,7-tetramethyltetrahydro-5H

bis([1,3]dioxolo)[4,5-b:4',5'-d]pyran-5-carbaldehyde (3q)



Prepared according to a known procedure from D-Mannose.²²⁴ ^1H NMR(300 MHz, CDCl_3) 9.62 (1 H, d, $J = 0.5$ Hz), 5.67 (1 H, d, $J = 4.9$ Hz), 4.63 (2 H, qd, $J = 7.8, 2.2$ Hz), 4.39 (1 H, dd, $J = 4.9, 2.4$ Hz), 4.19 (1 H, dt, $J = 2.1, 0.6$ Hz), 1.51 (3 H, s), 1.44 (3 H, s), 1.35 (3 H, s), 1.32 (3 H, s). Spectral data was found to be in good agreement with literature.

(4S,6S)-6-methoxy-2,2-dimethyltetrahydrofuro[3,4-d][1,3]dioxole-4-carbaldehyde

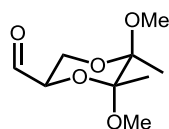


Prepared according to a known procedure from D-Mannose.²²⁴ ^1H NMR (300 MHz, $\text{DMSO}-d_6$) 9.55 (1 H, d, J 0.8), 5.23 – 5.12 (1 H, m), 5.04 (1 H, d, $J = 0.6$ Hz), 4.59 (1 H, d, $J = 5.9$ Hz), 4.47 (1 H, dt, $J = 4.3, 0.7$ Hz), 3.27 (3 H, s), 1.31 (3 H, s), 1.23 (3 H,

²²⁴ D. H. R. Barton, S. D. Gero, B. Quiclet-Sire, M. Samadi, M. *Tetrahedron: Asymmetry* **1994**, 5, 2123.

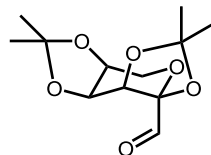
s). Spectral data was found to be in good agreement with literature.

(2*R*,5*R*,6*R*)-5,6-dimethoxy-5,6-dimethyl-1,4-dioxane-2-carbaldehyde



Prepared according to a known procedure from D-Mannitol.²²⁵ ¹H NMR (300 MHz, CDCl₃) 9.66 (1 H, s), 4.35 (1 H, ddd, *J* = 9.7, 5.5, 0.6 Hz), 3.75 – 3.66 (2 H, m), 3.32 (3 H, s), 3.27 (3 H, s), 1.38 (3 H, s), 1.30 (3 H, s). Spectral data was found to be in good agreement with literature.

(3*aR*,5*aS*,8*aS*,8*bS*)-2,2,7,7-tetramethyltetrahydro-3*aH*-bis([1,3]dioxolo)[4,5-*b*:4',5'-*d*]pyran-3*a*-carbaldehyde



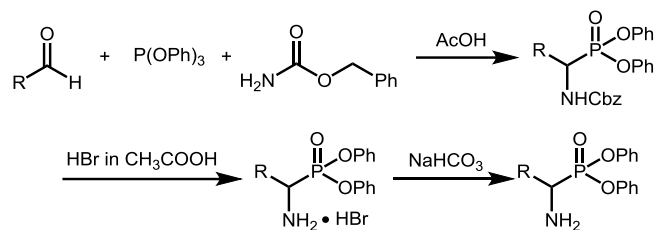
Prepared according to a known procedure.²²⁶ ¹H NMR (300 MHz, CDCl₃) 9.52 (1 H, s), 4.61 (1 H, dd, *J* = 7.9, 2.6 Hz), 4.49 (1 H, d, *J* = 2.5 Hz), 4.30 – 4.23 (1 H, m), 3.92 (2 H, qd, *J* = 12.9, 1.4 Hz), 1.56 (3 H, s), 1.43 (3 H, s), 1.40 (3 H, s), 1.34 (3 H, s). Spectral data was found to be in good agreement with literature.

²²⁵ P. Michel, S. V. Ley, *Synthesis* **2003**, 10, 1598.

²²⁶ Cubero, I. I.; Lopez-Espinosa, M T. Plaza. *Carbohydrate Res.* **1990**, 250, 293.

6.3. Experimental section for Chapter 3

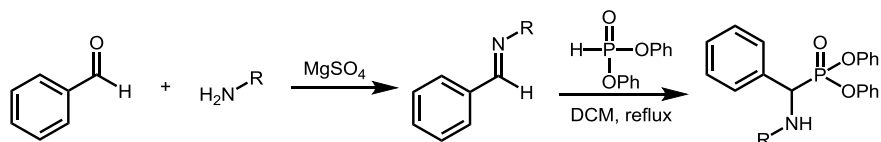
General procedure for the synthesis of α -amino phosphonates



To a round bottom flask, triphenyl phosphite (10 mmol), benzyl carbamate (10 mmol) and aldehyde (15 mmol) were added at room temperature then acetic acid (3mL) was added. Then the reaction mixture was heated at 50 °C for 4 hours and was monitored under UV. The product precipitated from the reaction mixture. After the completion, the reaction mixture was slowly cooled to room temperature and filtered to obtain the solid. 50 mL of cold ether was used to wash the solid in three portions. (Cbz-product)

Then the solid was placed into a round bottom flask and hydrogen bromide in acetic acid (5 mL) was added. After 1 hour, the reaction mixture was concentrated, and then cold ether (50 mL) was added and solid precipitated. Then the mixture was filtered and the powder was washed with ether. (HBr-product) The powder was placed into a round bottom flask and 50 mL of saturated $NaHCO_3$ solution was added, and the solution was stirred for 20 minutes. Then the solution was extracted with DCM (50 mLx3). The DCM was collected and dried with Na_2SO_4 . Then the solution was filtered and concentrated. The resulting oil was further purified by column chromatography using ethyl estate-hexanes (80:20 or 60:40) as eluent to give the corresponding free- NH_2 product.

General procedure for the synthesis of secondary α -amino phosphonates



To a round bottom flask, 50 mL of dichloromethane was added. Then benzaldehyde (10 mmol), amine (10.5 mmol) and MgSO_4 (2.5g) were added at room temperature. The reaction was stirred overnight. Then the reaction mixture was filtered and the solution was collected and concentrated. (Imine product) To the round bottom flask containing the imine intermediate, 50 mL of dichloromethane was added. Then diphenyl phosphite (10 mmol) was added. The reaction was heated to reflux for 2 hours. The reaction was monitored by TLC, and after the completion, the reaction was cooled down to room temperature. The reaction mixture was concentrated and the resulting mixture was further purified by column chromatography using ethyl ester-hexanes (80:20 or 60:40) as eluent to give the corresponding product.

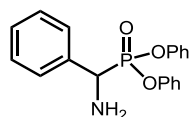
General procedure for the synthesis of mono ester of α -amino phosphonates

Freshly made α -amino phosphonates (0.1 mmol) was added into a tube, then 0.5 mL of 1,4-dioxane and 0.5 mL of distilled H_2O were added. Formaldehyde (0.02 mmol) was then added into the reaction mixture, followed by the addition of diisopropylethylamine

(0.02 mmol). The reaction was monitored by TLC. After the completion, ethanol (5 mLx2) was added then the reaction mixture and the mixture was transferred into a round bottom flask and then was concentrated. After, distilled H₂O (10 mL) and ethanol (10 mL) were added, followed by the addition of resin (2 mL). Then swirl the flask for 5 minutes. The mixture was filtered to obtain the solution. Then the solution was concentrated. Then methanol and ether was added into the flask. The flask was placed at -20 °C that solid slowly precipitated. Then it was filtered to obtain the solid as the desired product.

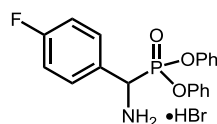
α -Amino phosphonates

Diphenyl (amino(phenyl)methyl)phosphonate (4a)



Prepared according to a known procedure.²²⁷ The titled compound was isolated as white solid. (1.87 g, 55%) ¹H NMR (300 MHz, DMSO-*d*₆) 7.65 – 7.52 (2 H, m), 7.46 – 7.25 (7 H, m), 7.23 – 7.05 (4 H, m), 7.00 – 6.88 (2 H, m), 4.68 (1 H, d, *J* = 17.8 Hz), 2.62 (2 H, br). ³¹C NMR (101 MHz, DMSO-*d*₆) 150.9 (d, *J* = 10.3 Hz), 150.7 (d, *J* = 10.1 Hz), 138.4 (d, *J* = 1.1 Hz), 130.2, 128.8, 128.7, 128.6 (d, *J* = 2.6 Hz), 128.1 (d, *J* = 3.4 Hz), 125.4, 125.4, 121.1 (d, *J* = 4.0 Hz), 120.9 (d, *J* = 4.1 Hz), 54.2 (d, *J* = 149.4 Hz). ³¹P NMR (121 MHz, DMSO-*d*₆) 16.60. IR (ATR Diamond): 3356, 3059, 2924, 1587, 1487, 1452, 1263, 1254, 1215, 1187, 1163, 1068, 1025, 1008, 978, 947, 928, 807, 777, 759, 714, 697, 686, 629, 615, 592, 557 cm⁻¹. HRMS (ESI) for: Exact mass calculated for C₁₉H₁₈NO₃PNa [M+Na]⁺: 362.0922, found 362.0902.

Diphenyl (amino(4-fluorophenyl)methyl)phosphonate hydrobromide (4b)

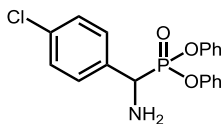


Prepared according to the general procedure. The titled compound was isolated as white powder. (2.5 g, 57%) ¹H NMR (300 MHz, CD₃OD) 7.74 (2 H, ddd, *J* = 9.0, 5.0, 2.2

²²⁷ Y.-M. Cao, F.-F. Shen, F.-T. Zhang, J.-L. Zhang, R. Wang, *Angew. Chem. Int. Ed.* **2014**, *53*, 1862.

Hz), 7.46 – 7.33 (2 H, m), 7.33 – 7.23 (5 H, m), 7.22 – 7.07 (3 H, m), 6.89 (2 H, dt, $J = 8.4, 1.3$ Hz), 5.56 (1 H, d, $J = 18.4$ Hz). ^{13}C NMR (75 MHz, CD_3OD) 163.8 (d, $J = 249.2$ Hz), 149.6 (d, $J = 9.9$ Hz), 149.5 (d, $J = 10.5$ Hz), 131.2 (dd, $J = 8.8, 6.2$ Hz), 129.7, 129.6, 125.9, 125.7, 125.3 (dd, $J = 5.1, 3.4$ Hz), 120.2 (d, $J = 4.2$ Hz), 119.9 (d, $J = 4.4$ Hz), 116.1 (dd, $J = 22.5, 2.2$ Hz), 50.4 (d, $J = 159.8$ Hz). ^{31}P NMR (121 MHz, CD_3OD) 7.01 (d, $J = 4.9$ Hz). ^{19}F NMR (282 MHz, CD_3OD) -112.18 (d, $J = 4.7$ Hz). IR (ATR Diamond) for free amine: 3059, 1588, 1509, 1487, 1455, 1420, 1264, 1234, 1209, 1186, 1158, 1092, 1067, 1024, 1006, 927, 906, 835, 833, 762, 726, 688, 616, 589, 573, 560 cm^{-1} . HRMS (ESI) for: Exact mass calculated for $\text{C}_{19}\text{H}_{17}\text{NO}_3\text{PFNa}$ [$\text{M}-\text{HBr}+\text{Na}$] $^+$: 380/0828, found 380.0817.²²⁸

Diphenyl (amino(4-chlorophenyl)methyl)phosphonate (4d)

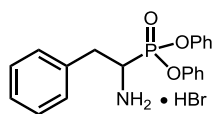


Prepared according to the general procedure. The titled compound was isolated as white solid. (1.9 g, 51%) ^1H NMR (300 MHz, $\text{DMSO}-d_6$) 7.60 (2 H, dd, $J = 8.6, 2.4$ Hz), 7.49 – 7.40 (2 H, m), 7.40 – 7.28 (4 H, m), 7.23 – 7.13 (2 H, m), 7.10 (2 H, dq, $J = 7.8, 1.2$ Hz), 7.00 (2 H, dq, $J = 7.8, 1.2$ Hz), 4.73 (1 H, d, $J = 18.2$ Hz), 2.66 (2 H, br). ^{13}C NMR (101 MHz, CDCl_3) 150.5 (d, $J = 4.3$ Hz), 150.4 (d, $J = 4.0$ Hz), 135.1 (d, $J = 3.6$ Hz), 134.4 (d, $J = 4.0$ Hz), 129.8 (d, $J = 7.2$ Hz), 129.6, 129.5, 129.0 (d, $J = 2.8$ Hz), 125.4, 125.3, 120.6 (d, $J = 4.3$ Hz), 120.5 (d, $J = 4.3$ Hz), 53.8 (d, $J = 151.4$ Hz). ^{31}P NMR

²²⁸ The HBr form of the starting material could not survive in ESI. Instead, HBr was placed by Na^+ .

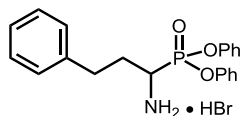
(121 MHz, DMSO-*d*₆) 15.98. IR 3384, 3314, 3058, 2925, 1587, 1483, 1411, 1265, 1212, 1190, 1159, 1099, 1085, 1069, 1007, 985, 931, 907, 886, 830, 764, 722, 688, 669 cm⁻¹. HRMS (ESI) for: Exact mass calculated for C₁₉H₁₇NO₃PNaCl [M+Na]⁺: 396.0532, found 396.0521.

Diphenyl (1-amino-2-phenylethyl)phosphonate hydrobromide (4g)



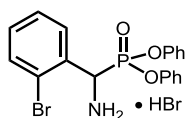
Prepared according to the general procedure. The titled compound was isolated as white solid. (1.96 g, 45%) ¹H NMR (300 MHz, CD₃OD) 7.50 – 7.32 (9 H, m), 7.30 – 7.19 (2 H, m), 7.15 – 7.04 (4 H, m), 4.45 (1 H, ddd, *J* = 14.3, 8.6, 6.7 Hz), 3.56 (1 H, ddd, *J* = 14.4, 10.2, 6.7 Hz), 3.39 – 3.20 (1 H, m). ¹³C NMR (76 MHz, CD₃OD) 149.5 (d, *J* = 6.5 Hz), 149.3 (d, *J* = 6.5 Hz), 134.0 (d, *J* = 9.9 Hz), 129.8, 129.7, 129.3, 128.8, 127.7, 125.9 (d, *J* = 1.0 Hz), 125.9 (d, *J* = 1.0 Hz), 120.2 (d, *J* = 1.7 Hz), 120.2 (d, *J* = 1.6 Hz), 49.4, 34.1 (d, *J* = 2.4 Hz). ³¹P NMR (122 MHz, CD₃OD) 12.96. IR (ATR Diamond) for free amine: 3359, 3287, 3054, 1588, 1487, 1455, 1246, 1213, 1186, 1162, 1071, 1025, 1006, 927, 902, 858, 786, 769, 750, 738, 687, 616, 597, 561 cm⁻¹. HRMS (ESI) for the free amine: Exact mass calculated for C₂₀H₂₀NO₃PNa [M+Na]⁺: 376.1079, found 376.1060.

Diphenyl (1-amino-3-phenylpropyl)phosphonate hydrobromide (4h)



Prepared according to the general procedure. The titled compound was isolated as white solid. (1.84 g, 41%) ^1H NMR (300 MHz, CD_3OD) 7.46 – 7.32 (5 H, m), 7.32 – 7.10 (10 H, m), 4.14 (1 H, ddd, $J = 14.1, 7.4, 6.6$ Hz), 3.13 – 2.81 (2 H, m), 2.65 – 2.16 (2 H, m). ^{13}C NMR (75 MHz, CD_3OD) 149.5 (d, $J = 3.1$ Hz), 149.4 (d, $J = 3.2$ Hz), 139.5, 129.8 (d, $J = 1.6$ Hz), 129.8, 128.4, 128.1, 126.3, 125.9 (d, $J = 1.6$ Hz), 125.9, 120.2 (d, $J = 2.0$ Hz), 120.2 (d, $J = 1.9$ Hz), 45.5, 31.3 (d, $J = 8.2$ Hz), 30.4 (d, $J = 2.6$ Hz). ^{31}P NMR (121 MHz, CD_3OD) 10.38. IR (ATR Diamond) for free amine: 3393, 3324, 3062, 3025, 2918, 2862, 1588, 1484, 1455, 1254, 1207, 1185, 1157, 1069, 1022, 1005, 991, 922, 903, 852, 815, 787, 767, 751, 689, 616, 595, 584, 568 cm^{-1} . HRMS (ESI) for: Exact mass calculated for $\text{C}_{21}\text{H}_{22}\text{NO}_3\text{PNa}$ $[\text{M}-\text{HBr}+\text{Na}]^+$: 390.1235, found 390.1213.²²⁸

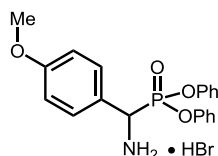
Diphenyl (amino(2-bromophenyl)methyl)phosphonate hydrobromide (4c)



Prepared according to the general procedure. The titled compound was isolated as white solid. (2.94 g, 59%) ^1H NMR (400 MHz, $\text{DMSO}-d_6$) 9.44 (3 H, br), 7.91 (1 H, m), 7.80 (1 H, m), 7.58 (1 H, m), 7.49 – 7.37 (3 H, m), 7.35 – 7.24 (3 H, m), 7.24 – 7.14 (3 H, m), 6.86 (2 H, m), 5.63 (1 H, d, $J = 18.5$ Hz). ^{13}C NMR (101 MHz, $\text{DMSO}-d_6$) 149.8

(d, $J = 8.3$ Hz), 149.7 (d, $J = 8.8$ Hz), 134.0, 132.2 (d, $J = 2.9$ Hz), 130.7, 130.5, 130.3, 130.3, 129.0 (d, $J = 2.8$ Hz), 126.5, 126.3, 125.0 (d, $J = 8.7$ Hz), 120.9 (d, $J = 4.4$ Hz), 120.3 (d, $J = 4.2$ Hz), 50.7 (d, $J = 158.0$ Hz). ^{31}P NMR (162 MHz, $\text{DMSO-}d_6$) 10.03. IR (ATR Diamond) for free amine: 3374, 3301, 3064, 1589, 1488, 1471, 1455, 1434, 1256, 1213, 1184, 1160, 1069, 1023, 1006, 931, 902, 820, 761, 729, 746, 706, 687, 666, 619, 584 cm^{-1} . HRMS (ESI) for: Exact mass calculated for $\text{C}_{19}\text{H}_{17}\text{NO}_3\text{PNaBr}$ $[\text{M-HBr}+\text{Na}]^+$: 440.0027, found 440.0024.²²⁸

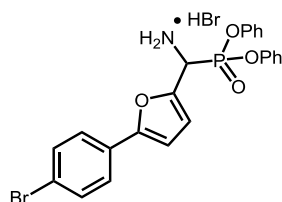
Diphenyl (amino(2-bromo-4-methoxyphenyl)methyl)phosphonate hydrobromide (4e)



Prepared according to the general procedure. The titled compound was isolated as white solid. (1.94g, 43%) ^1H NMR (400 MHz, $\text{DMSO-}d_6$) 9.39 (3 H, s), 7.63 (2 H, m), 7.40 (2 H, m), 7.33 (2 H, m), 7.27 – 7.22 (1 H, m), 7.22 – 7.16 (1 H, m), 7.14 (2 H, m), 7.09 – 7.03 (2 H, m), 6.92 (2 H, m), 5.60 (1 H, d, $J = 18.0$ Hz). ^{13}C NMR (101 MHz, $\text{DMSO-}d_6$) 160.6 (d, $J = 2.7$ Hz), 149.9 (d, $J = 8.8$ Hz), 149.8 (d, $J = 9.3$ Hz), 131.0 (d, $J = 6.1$ Hz), 130.5, 130.4, 126.2 (d, $J = 12.6$ Hz), 122.2 (d, $J = 5.5$ Hz), 120.9 (d, $J = 4.2$ Hz), 120.7 (d, $J = 4.1$ Hz), 114.83, 114.81, 55.8, 50.3 (d, $J = 158.0$ Hz). ^{31}P NMR (162 MHz, $\text{DMSO-}d_6$) 11.74. IR (ATR Diamond) for free amine: 3369, 3293, 3058, 2837, 1607, 1589, 1511, 1485, 1456, 1304, 1246, 1213, 1186, 1159, 1109, 1069, 1024, 1007, 950, 919, 893, 838, 826, 793, 763, 666, 637, 616, 599, 564 cm^{-1} . HRMS (ESI) for: Exact

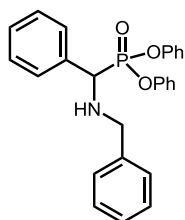
mass calculated for C₂₀H₂₀NO₄PNa [M-HBr+Na]⁺: 392.1028, found 392.1026.²²⁸

Diphenyl (amino(5-(4-bromophenyl)furan-2-yl)methyl)phosphonate hydrobromide (4f)



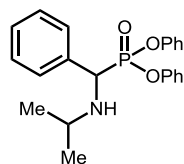
Prepared according to the general procedure. The titled compound was isolated as yellow solid. (1.67 g, 30%) ¹H NMR (300 MHz, CD₃OD) 7.56 (4 H, m), 7.28 (8 H, m), 7.04 (2 H, m), 6.90 (2 H, m), 5.80 (1 H, d, *J* = 19.1 Hz). ¹³C NMR (75 MHz, CD₃OD) 155.2 (d, *J* = 3.3 Hz), 149.6 (dd, *J* = 10.0, 5.4 Hz), 141.7 (d, *J* = 7.7 Hz), 131.6, 129.7 (d, *J* = 10.0 Hz), 128.6, 125.9 (d, *J* = 8.9 Hz), 125.4, 121.8, 119.9 (dd, *J* = 15.2, 4.3 Hz), 115.3 (d, *J* = 7.6 Hz), 106.9 (d, *J* = 2.3 Hz), 44.2. ³¹P NMR (121 MHz, CD₃OD) 4.45. IR 3037, 3012, 2995, 2924, 2886, 2806, 2742, 2647, 1586, 1559, 1486, 1456, 1405, 1336, 1309, 1265, 1207, 1192, 1157, 1087, 1069, 1022, 1006, 985, 931, 904, 825, 801, 762, 718, 686, 669 cm⁻¹. HRMS (ESI) for: Exact mass calculated for C₂₃H₁₉NO₄PNaBr [M-HBr+Na]⁺: 506.0133, found 506.0135.²²⁸

Diphenyl ((benzylamino)(phenyl)methyl)phosphonate (4m)



Prepared according to the general procedure. The titled compound was isolated as white solid. (3.48 g, 81%) ^1H NMR (300 MHz, CDCl_3) 7.59 – 7.47 (2 H, m), 7.45 – 7.26 (9 H, m), 7.26 – 7.03 (7 H, m), 6.88 (2 H, dt, $J = 8.4, 1.3$ Hz), 4.38 (1 H, d, $J = 20.0$ Hz), 3.94 (1 H, d, $J = 13.3$ Hz), 3.65 (1 H, d, $J = 13.3$ Hz), 2.33 (1 H, br). ^{13}C NMR (75 MHz, $\text{DMSO}-d_6$) 150.8 (d, $J = 9.8$ Hz), 150.5 (d, $J = 9.5$ Hz), 139.9, 135.6, 130.2, 130.1, 129.4, 129.3, 128.9 (d, $J = 2.5$ Hz), 128.6 (d, $J = 2.1$ Hz), 128.5 (d, $J = 3.3$ Hz), 127.3, 125.5, 125.4, 120.9 (d, $J = 4.2$ Hz), 120.7 (d, $J = 4.0$ Hz), 59.3 (d, $J = 157.5$ Hz), 50.9 (d, $J = 18.7$ Hz). ^{31}P NMR (121 MHz, CDCl_3) 13.49. IR 3278, 3066, 3026, 3004, 2834, 1590, 1487, 1453, 1365, 1261, 1213, 1190, 1156, 1113, 1091, 1068, 1021, 1006, 986, 930, 902, 875, 854, 804, 765, 732, 687 cm^{-1} . HRMS (ESI) for: Exact mass calculated for $\text{C}_{26}\text{H}_{24}\text{NO}_3\text{PNa}$ $[\text{M}+\text{Na}]^+$: 452.1392, found 452.1377.

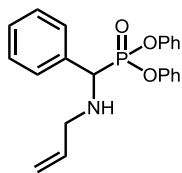
Diphenyl ((isopropylamino)(phenyl)methyl)phosphonate (4p)



Prepared according to the general procedure. The titled compound was isolated as white solid. (2.14 g, 56%) ^1H NMR (300 MHz, CDCl_3) 7.53 – 7.43 (2 H, m), 7.39 – 7.24 (5 H, m), 7.24 – 7.02 (6 H, m), 6.92 – 6.82 (2 H, m), 4.46 (1 H, d, $J = 21.9$ Hz), 2.78 (1 H,

pd, $J = 6.3, 1.1$ Hz), 1.92 (1 H, br), 1.02 (6 H, dd, $J = 10.9, 6.2$ Hz). ^{13}C NMR (75 MHz, CD_3OD) 150.5 (d, $J = 10.0$ Hz), 150.2 (d, $J = 10.1$ Hz), 135.3 (d, $J = 1.6$ Hz), 129.4, 129.3, 128.6 (d, $J = 7.1$ Hz), 128.4 (d, $J = 2.4$ Hz), 128.1 (d, $J = 3.3$ Hz), 125.1 (d, $J = 1.4$ Hz), 124.9 (d, $J = 1.2$ Hz), 120.5 (d, $J = 4.0$ Hz), 120.2 (d, $J = 4.0$ Hz), 57.7 (d, $J = 158.6$ Hz), 46.1 (d, $J = 17.0$ Hz), 22.5, 20.3. ^{31}P NMR (121 MHz, CDCl_3) 14.04. IR 3321, 3056, 2957, 2904, 2839, 1588, 1486, 1453, 1379, 1333, 1263, 1202, 1179, 1162, 1101, 1068, 1024, 1005, 984, 921, 908, 840, 802, 763, 687 cm^{-1} . HRMS (ESI) for: Exact mass calculated for $\text{C}_{22}\text{H}_{24}\text{NO}_3\text{PNa}$ $[\text{M}+\text{Na}]^+$: 404.1392, found 404.1418.

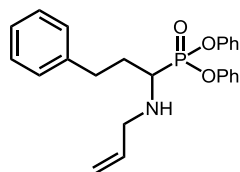
Diphenyl ((allylamino)(phenyl)methyl)phosphonate (4n)



Prepared according to the general procedure. The titled compound was isolated as white solid. (2.2 g, 58%) ^1H NMR (300 MHz, C_6D_6) 7.55 – 7.42 (2 H, m), 7.31 (2 H, dq, $J = 7.8, 1.3$), 7.14 – 7.04 (5 H, m), 7.02 – 6.69 (6 H, m), 5.66 (1 H, dddd, $J = 17.0, 10.2, 6.6, 5.1$ Hz), 5.02 (1H, dq, $J = 17.2, 1.7$ Hz), 4.95 (1H, dq, $J = 10.2, 1.5$ Hz), 4.42 (1 H, d, $J = 20.2$ Hz), 3.20 – 3.01 (1 H, m), 2.90 (1 H, dd, $J = 14.1, 6.6$ Hz), 2.15 (1 H, br). ^{13}C NMR (101 MHz, CD_3OD) 150.4 (d, $J = 10.3$ Hz), 150.3 (d, $J = 10.0$ Hz), 135.6, 134.6 (d, $J = 2.1$ Hz), 129.5 (d, $J = 1.1$ Hz), 129.4, 128.9, 128.9, 128.5 (d, $J = 2.5$ Hz), 128.3 (d, $J = 3.3$ Hz), 125.2 (d, $J = 1.4$ Hz), 125.1 (d, $J = 1.3$ Hz), 120.5 (d, $J = 4.1$ Hz), 120.2 (d, $J = 4.1$ Hz), 116.5, 58.9 (d, $J = 159.0$ Hz), 49.5 (d, $J = 18.0$ Hz). ^{31}P NMR (121 MHz, C_6D_6) 16.63. IR 3306, 3057, 3009, 2909, 2884, 2831, 2805, 1638, 1587,

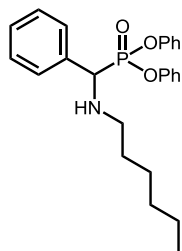
1486, 1452, 1275, 1250, 1210, 1178, 1158, 1111, 1070, 1046, 1022, 1005, 993, 940, 918, 859, 834, 763, 742, 683, 656 cm^{-1} . HRMS (ESI) for: Exact mass calculated for $\text{C}_{22}\text{H}_{22}\text{NO}_3\text{PNa}$ $[\text{M}+\text{Na}]^+$: 402.1235, found 402.1259.

Diphenyl (1-(allylamino)-3-phenylpropyl)phosphonate (4o)

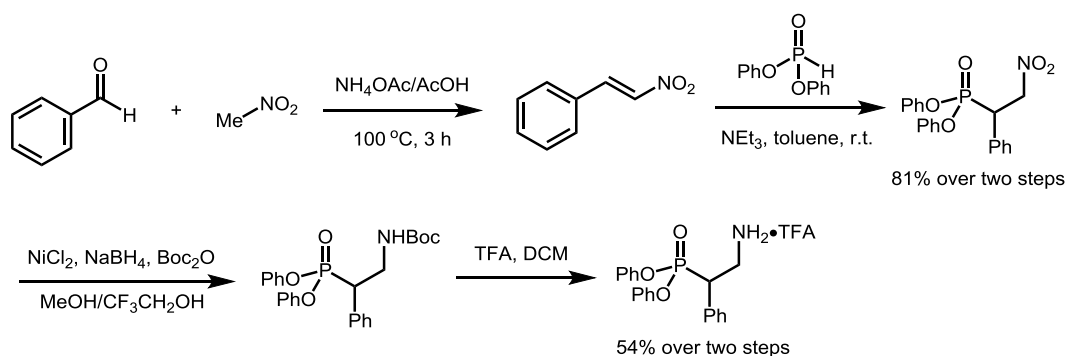


Prepared according to the general procedure. The titled compound was isolated as white solid. (1.55 g, 38%) ^1H NMR (300 MHz, CDCl_3) 7.34 – 7.26 (6 H, m), 7.25 – 7.20 (3 H, m), 7.20 – 7.09 (6 H, m), 6.13 – 5.72 (1 H, m), 5.19 (1H, dq, $J = 17.2, 1.6$ Hz), 5.11 (1H, dq, $J = 10.2, 1.3$ Hz), 3.64 – 3.50 (1 H, m), 3.46 (1 H, ddt, $J = 6.2, 2.2, 1.4$ Hz), 3.26 (1 H, ddd, $J = 11.6, 9.2, 4.3$ Hz), 2.99 (1 H, td, $J = 8.9, 4.6$ Hz), 2.85 (1 H, ddd, $J = 13.8, 9.0, 7.2$ Hz), 2.44 – 2.23 (1 H, m), 2.21 – 1.95 (1 H, m), 1.52 (2 H, br). ^{13}C NMR (75 MHz, CD_3OD) 150.3 (d, $J = 10.2$ Hz), 141.0, 136.2, 129.5 (d, $J = 4.0$ Hz), 128.2, 128.2, 125.8, 125.4 – 124.0 (m), 120.3 (d, $J = 4.0$ Hz), 115.8, 53.0 (d, $J = 150.4$ Hz), 50.3 (d, $J = 5.8$ Hz), 35.4 – 23.8 (m). ^{31}P NMR (121 MHz, CDCl_3) 18.63. IR 3279, 3062, 3024, 2932, 2835, 2712, 1591, 1542, 1487, 1453, 1419, 1394, 1369, 1305, 1209, 1190, 1161, 1069, 1023, 1004, 927, 813, 751, 688 cm^{-1} . HRMS (ESI) for: Exact mass calculated for $\text{C}_{24}\text{H}_{26}\text{NO}_3\text{PNa}$ $[\text{M}+\text{Na}]^+$: 430.1548, found 430.1548.

Diphenyl ((hexylamino)(phenyl)methyl)phosphonate (4q)

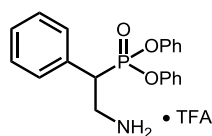


Prepared according to the general procedure. The titled compound was isolated as white solid. (1.69 g, 40%) ^1H NMR (300 MHz, CDCl_3) 7.57 – 7.49 (2 H, m), 7.40 – 7.27 (4 H, m), 7.25 – 7.08 (7 H, m), 6.91 (2 H, dt, $J = 8.5, 1.3$ Hz), 4.38 (1 H, d, $J = 19.6$ Hz), 2.74 – 2.40 (2 H, m), 1.95 (1 H, br), 1.59 – 1.42 (2 H, m), 1.38 – 1.17 (6 H, m), 0.87 (3 H, t, $J = 6.8$ Hz). ^{13}C NMR (101 MHz, CDCl_3) 150.6 (d, $J = 9.9$ Hz), 150.5 (d, $J = 9.8$ Hz), 135.2 (d, $J = 3.0$ Hz), 129.6, 129.5, 128.8 (d, $J = 6.8$ Hz), 128.6 (d, $J = 2.5$ Hz), 128.3 (d, $J = 3.2$ Hz), 125.1 (d, $J = 0.6$ Hz), 124.9 (d, $J = 0.6$ Hz), 120.8 (d, $J = 4.4$ Hz), 120.5 (d, $J = 4.2$ Hz), 61.0 (d, $J = 156.1$ Hz), 48.2 (d, $J = 17.1$ Hz), 31.7, 29.8, 26.8, 22.6, 14.1. ^{31}P NMR (121 MHz, CDCl_3) 13.65. IR (ATR Diamond): 3303, 3062, 2926, 2855, 1590, 1487, 1375, 1267, 1186, 1071, 1024, 929, 758, 688, 587 cm^{-1} . HRMS (ESI) for: Exact mass calculated for $\text{C}_{25}\text{H}_{30}\text{NO}_3\text{PNa}$ $[\text{M}+\text{Na}]^+$: 446.1861, found 446.1873.



Diphenyl (2-amino-1-phenylethyl)phosphonate with trifluoroacetic acid

(4l)

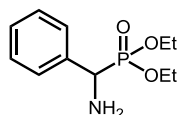


Synthesized according to a step-wise procedure as shown above.²²⁹ The title compound was isolated as white solid. (4.3 g, 44%) ¹H NMR (400 MHz, CD₃OD) 7.55 (2 H, d, *J* = 6.9), 7.44 (3 H, q, *J* = 7.7, 6.9 Hz), 7.34 (2 H, t, *J* = 7.8 Hz), 7.28 – 7.16 (3 H, m), 7.18 – 7.04 (3 H, m), 6.76 (2 H, d, *J* = 7.9 Hz), 4.13 (1 H, ddd, *J* = 24.8, 11.2, 4.4 Hz), 4.01 – 3.54 (2 H, m). ¹³C NMR (101 MHz, CD₃OD) 161.8 (q, *J* = 34.1, 33.1 Hz), 149.9 (d, *J* = 9.9 Hz), 149.8 (d, *J* = 10.3 Hz), 130.1 (d, *J* = 8.3 Hz), 129.8, 129.7 (d, *J* = 6.8 Hz), 129.5, 129.2 (d, *J* = 2.8 Hz), 129.0 (d, *J* = 3.3 Hz), 125.7 (d, *J* = 1.3 Hz), 125.4 (d, *J* = 1.2 Hz), 120.3 (d, *J* = 4.2 Hz), 120.0 (d, *J* = 4.2 Hz). 115.5 (q, *J* = 294.3 Hz), 43.0 (d, *J* = 142.0 Hz), 39.1 (d, *J* = 3.7 Hz). ³¹P NMR (162 MHz, CD₃OD) 16.92. ¹⁹F NMR (282 MHz, CD₃OD) -76.91. IR 3070, 3040, 3017, 2994, 2948, 2901, 1678, 1635, 1587, 1541, 1488, 1249, 1232, 1202, 1180, 1161, 1131, 1071, 1024, 1007, 949, 929, 908, 833, 797, 768, 743, 720, 689 cm⁻¹. Exact mass calculated for C₂₀H₂₀NO₃PNa (without TFA)

²²⁹ For the synthesis of alkene: (a) Q. V. Vo, C. Trenerry, S. Rochfort, J. Wadeson, C. Leyton, A. B. Hughes, *Bioorg. Med. Chem.* **2013**, *21*, 5945. For the synthesis of NO₂ product: (b) Y. Zhu, J. P. Malerich, V. H. Rawal, *Angew. Chem. Int. Ed.* **2009**, *49*, 153. For the synthesis of Boc protection: (c) M. Terada, T. Ikehara, H. Ube, *J. Am. Chem. Soc.* **2007**, *129*, 14112.

$[M+Na]^+$: 376.1079, found 376.1073.

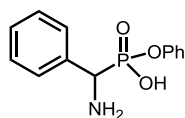
Diethyl (amino(phenyl)methyl)phosphonate



Prepared according to a known procedure.²³⁰ The titled compound was isolated as clear oil. (1.63 g, 67%) ¹H NMR (300 MHz, CDCl₃) 7.49 – 7.42 (2 H, m), 7.40 – 7.27 (3 H, m), 4.25 (1 H, d, $J = 17.2$ Hz), 4.16 – 3.73 (4 H, m), 1.27 (3 H, td, $J = 7.0, 0.4$ Hz), 1.17 (3 H, td, $J = 7.1, 0.5$ Hz). Spectral data was found to be in good agreement with literature.

Mono ester of α -Amino phosphonates

Phenyl hydrogen (amino(phenyl)methyl)phosphonate (5a)

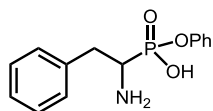


¹H NMR (300 MHz, CD₃OD) 7.57 (2 H, dt, $J = 7.6, 1.8$ Hz), 7.47 – 7.33 (3 H, m), 7.30 – 7.19 (2 H, m), 7.15 – 7.00 (3 H, m), 4.44 (1 H, d, $J = 16.4$ Hz). ¹³C NMR (101 MHz, CD₃OD) 153.4 (d, $J = 8.1$ Hz), 134.8, 130.2, 129.8 (d, $J = 1.7$ Hz), 129.7 (d, $J = 2.5$ Hz), 129.6 (d, $J = 5.2$ Hz), 124.6, 121.7 (d, $J = 4.3$ Hz), 54.8 (d, $J = 145.3$ Hz). ³¹P NMR (121 MHz, CD₃OD) 4.34. IR (ATR Diamond): 2853, 1591, 1538, 1489, 1455,

²³⁰ B. Kaboudin, M. Sorbiun, *Heteroatom Chem.* **2010**, *21*, 284.

1212, 1165, 1069, 1026, 912, 826, 824, 767, 734, 689, 586 cm^{-1} . HRMS (ESI) for:
Exact mass calculated for $\text{C}_{13}\text{H}_{14}\text{NO}_3\text{PNa}$ $[\text{M}+\text{Na}]^+$: 286.0609, found 286.0605.

Phenyl hydrogen (1-amino-2-phenylethyl)phosphonate (5g)



^1H NMR (300 MHz, CD_3OD) 7.40 – 7.24 (7 H, m), 7.24 – 7.15 (2 H, m), 7.13 – 7.03 (1 H, m), 3.46 (2 H, dtd, $J = 14.4, 10.7, 3.8$ Hz), 2.94 (1 H, ddd, $J = 14.7, 11.3, 8.0$ Hz).

^{13}C NMR (75 MHz, CD_3OD) 153.2 (d, $J = 8.1$ Hz), 137.65 (d, $J = 12.5$ Hz), 130.4, 130.3, 130.1, 128.4, 124.8, 121.8 (d, $J = 4.3$ Hz), 51.7 (d, $J = 147.5$ Hz), 36.08. ^{31}P NMR: (121 MHz, CD_3OD) δ 6.74. IR (ATR Diamond): 2851, 1592, 1529, 1490, 1455, 1242, 1211, 1166, 1131, 1077, 1064, 1024, 915, 894, 770, 757, 732, 691, 617, 604, 548 cm^{-1} . HRMS (ESI) for: Exact mass calculated for $\text{C}_{14}\text{H}_{17}\text{NO}_3\text{P}$ $[\text{M}+\text{H}]^+$: 278.0946, found 278.0955.

Phenyl hydrogen (amino(4-methoxyphenyl)methyl)phosphonate (5e)



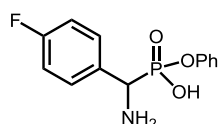
^1H NMR (300 MHz, CD_3OD): 7.50 (2 H, dt, $J = 7.2, 1.8$ Hz), 7.31 – 7.20 (2 H, m), 7.16 – 7.01 (3 H, m), 6.95 (2 H, d, $J = 8.7$ Hz), 4.38 (1 H, d, $J = 16.1$ Hz), 3.80 (3 H, s). ^{13}C

NMR (76 MHz, CD_3OD) 161.6, 153.4 (d, $J = 8.5$ Hz), 131.1 (d, $J = 5.5$ Hz), 130.3,

126.5 (d, $J = 4.3$ Hz), 124.6, 121.7 (d, $J = 4.5$ Hz), 115.2, 55.8, 54.1 (d, $J = 147.9$ Hz).

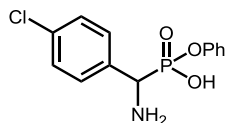
^{31}P NMR: (121 MHz, CD_3OD) δ 4.76. IR (ATR Diamond): 2836, 1612, 1588, 1518, 1490, 1463, 1308, 1256, 1213, 1064, 1027, 921, 831, 776, 752, 722, 686, 635, 615, 599 cm^{-1} . HRMS (ESI) for: Exact mass calculated for $\text{C}_{14}\text{H}_{17}\text{NO}_4\text{P}$ $[\text{M}+\text{H}]^+$: 294.0895, found 294.0899.

Phenyl hydrogen (amino(4-fluorophenyl)methyl)phosphonate (5b)



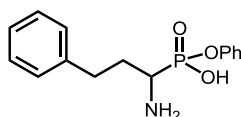
^1H NMR (300 MHz, CD_3OD) 7.77 – 7.49 (2 H, m), 7.25 (2 H, t, $J = 7.7$ Hz), 7.17 – 6.97 (5 H, m), 4.45 (1 H, d, $J = 16.2$ Hz). ^{13}C NMR (76 MHz, CD_3OD) 164.3 (dd, $J = 246.2, 2.2$ Hz), 153.4 (d, $J = 8.1$ Hz), 131.9 (dd, $J = 8.4, 5.2$ Hz), 130.9 (t, $J = 3.8$ Hz), 130.3, 124.6, 121.7 (d, $J = 4.3$ Hz), 116.5 (dd, $J = 22.0, 1.6$ Hz), 53.9 (d, $J = 145.8$ Hz). ^{31}P NMR: (121 MHz, CD_3OD) δ 4.05. ^{19}F NMR (282 MHz, CD_3OD) -115.53 (d, $J = 3.8$ Hz). IR (ATR Diamond): 2866, 1592, 1512, 1489, 1209, 1163, 1067, 1026, 912, 837, 759, 689, 634, 617, 586, 568, 549 cm^{-1} . HRMS (ESI) for: Exact mass calculated for $\text{C}_{13}\text{H}_{13}\text{FNO}_3\text{PNa}$ $[\text{M}+\text{Na}]^+$: 304.0515, found 304.0517.

Phenyl hydrogen (amino(4-chlorophenyl)methyl)phosphonate (5d)



^1H NMR (400 MHz, CD_3OD) 7.55 (2 H, m), 7.39 (2 H, m), 7.26 (2 H, m), 7.18 – 7.02 (3 H, m), 4.49 (1 H, d, $J = 16.6$ Hz). ^{13}C NMR (101 MHz, CD_3OD) 153.2 (d, $J = 8.4$ Hz), 135.7 (d, $J = 2.8$ Hz), 133.5 (d, $J = 4.7$ Hz), 131.3 (d, $J = 5.2$ Hz), 130.4, 129.9 (d, $J = 1.8$ Hz), 124.8, 121.6 (d, $J = 4.4$ Hz), 53.9 (d, $J = 145.6$ Hz). ^{31}P NMR (162 MHz, CD_3OD) δ 6.83. IR: 3355, 3230, 2964, 2852, 2625, 2378, 2343, 2317, 2116, 2101, 1991, 1733, 1664, 1616, 1590, 1541, 1488, 1404, 1338, 1209, 1165, 1069, 1024, 1006, 916, 821, 791, 753 cm^{-1} . HRMS (ESI) for: Exact mass calculated for $\text{C}_{13}\text{H}_{13}\text{ClNO}_3\text{PNa}$ $[\text{M}+\text{Na}]^+$: 320.0219, found 320.0210.

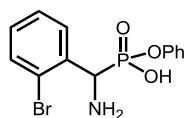
Phenyl hydrogen (1-amino-3-phenylpropyl)phosphonate (5h)



^1H NMR (500 MHz, CD_3OD) 7.32 – 7.25 (4 H, m), 7.26 – 7.22 (2 H, m), 7.20 (3 H, dd, $J = 7.6, 5.8$ Hz), 7.08 (1 H, t, $J = 7.3$ Hz), 3.27 (1 H, ddd, $J = 13.6, 7.7, 6.3$ Hz), 2.86 (2 H, m), 2.34 (1 H, m), 2.06 (1 H, m). ^{13}C NMR (101 MHz, CD_3OD) 153.3 (d, $J = 8.0$ Hz), 142.1, 130.4, 129.6, 129.5, 127.3, 124.7, 121.8 (d, $J = 4.3$ Hz), 50.3, 33.3 (d, $J = 7.8$ Hz), 32.5 (d, $J = 2.0$ Hz). ^{31}P NMR (162 MHz, CD_3OD) δ 10.07. IR: 3024, 2854, 2652, 2371, 2343, 2316, 2117, 1941, 1788, 1617, 1591, 1538, 1488, 1453, 1404, 1213,

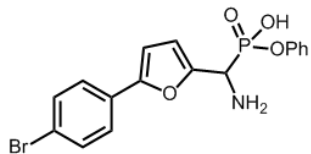
1167, 1067, 1023, 910, 895, 822, 767, 752 cm^{-1} . HRMS (ESI) for: Exact mass calculated for $\text{C}_{15}\text{H}_{18}\text{NO}_3\text{PNa}$ $[\text{M}+\text{Na}]^+$: 314.0922, found 314.0935.

Phenyl hydrogen (amino(2-bromophenyl)methyl)phosphonate (5c)



^1H (300 MHz, CD_3OD) 7.89 (1 H, d, $J = 8.0$ Hz), 7.68 (1 H, d, $J = 8.0$ Hz), 7.43 (1 H, t, $J = 7.5$ Hz), 7.25 (3 H, m), 7.13 (2 H, d, $J = 7.9$ Hz), 7.05 (1 H, t, $J = 7.3$ Hz), 5.06 (1 H, d, $J = 16.6$ Hz). ^{13}C NMR (75 MHz, CD_3OD) 151.9 (d, $J = 8.0$ Hz), 133.3 (d, $J = 3.2$ Hz), 132.9 (d, $J = 1.4$ Hz), 130.0 (d, $J = 2.1$ Hz), 129.3 (d, $J = 3.3$ Hz), 128.8, 127.8 (d, $J = 2.1$ Hz), 124.7 (d, $J = 7.9$ Hz), 123.1, 120.1 (d, $J = 4.7$ Hz), 51.5 (d, $J = 144.8$ Hz). ^{31}P NMR: (121 MHz, CD_3OD) δ 3.32. IR: 3242, 3012, 2854, 2833, 2623, 2371, 2343, 2114, 1991, 1884, 1635, 1616, 1590, 1542, 1487, 1404, 1338, 1210, 1165, 1066, 1024, 911, 895, 822, 734, 711 cm^{-1} . HRMS (ESI) for: Exact mass calculated for $\text{C}_{13}\text{H}_{13}\text{NO}_3\text{PBrNa}$ $[\text{M}+\text{Na}]^+$: 363.9714, found 363.9708.

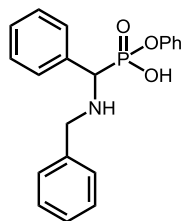
Phenyl hydrogen (amino(5-(4-bromophenyl)furan-2-yl)methyl)phosphonate (5f)



^1H NMR (400 MHz, CD_3OD) 7.66 – 7.60 (2 H, m), 7.58 – 7.50 (2 H, m), 7.24 (2 H, m), 7.17 (2 H, m), 7.05 (1 H, t, $J = 7.3$ Hz), 6.83 (1 H, d, $J = 3.5$ Hz), 6.74 (1 H, dd, $J = 3.5$ Hz, 2.2), 4.66 (1 H, d, $J = 17.0$ Hz). ^{13}C NMR (101 MHz, CD_3OD) 155.0 (d, $J = 2.1$ Hz), 153.4 (d, $J = 8.2$ Hz), 147.7 (d, $J = 3.6$ Hz), 132.9, 130.7, 130.3, 126.7, 124.73, 122.4, 121.6 (d, $J = 4.3$ Hz), 114.1 (d, $J = 4.7$ Hz), 108.1 (d, $J = 1.9$ Hz), 47.5. ^{31}P NMR (162 MHz, CD_3OD) 4.34. IR: 3031, 2926, 2852, 2743, 2618, 2374, 2343, 2114, 1590, 1541, 1489, 1456, 1404, 1213, 1164, 1069, 1025, 1006, 968, 917, 820, 788, 751 cm^{-1} . HRMS (ESI) for: Exact mass calculated for $\text{C}_{17}\text{H}_{15}\text{NO}_4\text{PBrNa}$ $[\text{M}+\text{Na}]^+$: 429.9820, found 429.9790.

Secondary products

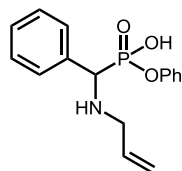
Phenyl hydrogen ((benzylamino)(phenyl)methyl)phosphonate (5m)



^1H NMR (400 MHz, CD_3OD) 7.52 (2 H, m), 7.43 (8 H, m), 7.20 (2 H, m), 7.03 (1 H, t, $J = 7.4$ Hz), 6.97 (2 H, d, $J = 8.0$ Hz), 4.36 – 4.27 (2 H, m), 4.19 (1 H, d, $J = 13.2$ Hz).

^{13}C NMR (151 MHz, CD_3OD) 151.9 (d, $J = 8.2$ Hz), 131.6, 130.6, 130.0, 129.4 (d, $J = 5.3$ Hz), 129.4, 128.89, 128.88, 128.8 (d, $J = 1.9$ Hz), 128.7 (d, $J = 1.4$ Hz), 123.3, 120.2 (d, $J = 4.3$ Hz), 59.2 (d, $J = 141.6$ Hz), 50.0 (d, $J = 5.6$ Hz). ^{31}P NMR (162 MHz, CD_3OD) 5.54. IR: 3066, 2927, 2852, 2716, 2612, 2548, 2448, 2395, 2343, 2247, 1990, 1938, 1590, 1489, 1471, 1455, 1212, 1163, 1074, 1028, 1002, 970, 920, 902, 885, 768, 47, 522 cm^{-1} . HRMS (ESI) for: Exact mass calculated for $\text{C}_{20}\text{H}_{20}\text{NO}_3\text{PNa}$ $[\text{M}+\text{Na}]^+$: 376.1079, found 376.1082.

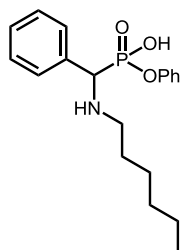
Phenyl hydrogen ((allylamino)(phenyl)methyl)phosphonate (5n)



^1H NMR (400 MHz, CD_3OD) 7.61 – 7.54 (2 H, m), 7.43 (3 H, m), 7.23 (2 H, t, $J = 7.8$ Hz), 7.09 – 7.01 (3 H, m), 5.92 (1 H, ddt, $J = 17.1, 10.3, 6.9$ Hz), 5.53 – 5.36 (2 H, m), 4.42 (1 H, d, $J = 16.0$ Hz), 3.68 (1 H, dd, $J = 13.6, 6.3$ Hz), 3.59 (1 H, dd, $J = 13.6, 7.6$ Hz). ^{13}C NMR (101 MHz, CD_3OD) 153.3 (d, $J = 8.5$), 133.0 (d, $J = 4.2$ Hz), 130.78(d,

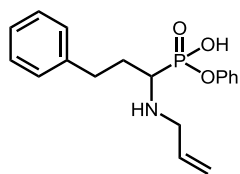
$J = 5.3$ Hz), 130.3, 130.2 (d, $J = 1.9$ Hz), 130.1 (d, $J = 1.3$ Hz), 129.0, 124.8, 124.6, 121.6 (d, $J = 4.4$ Hz), 60.7 (d, $J = 142.5$ Hz), 50.1 (d, $J = 5.9$ Hz). ^{31}P NMR (162 MHz, CD_3OD) 5.78. IR: 3036, 2982, 2923, 2797, 2726, 2688, 2641, 2552, 2484, 2434, 2392, 2344, 2247, 2118, 2071, 1629, 1589, 1487, 1453, 1420, 1257, 1193, 1176, 1154, 1092, 1079, 1034, 1009, 908, 885, 845, 767, 736 cm^{-1} . HRMS (ESI) for: Exact mass calculated for $\text{C}_{16}\text{H}_{18}\text{NO}_3\text{PNa}$ $[\text{M}+\text{Na}]^+$: 326.0922, found 326.0918.

Phenyl hydrogen ((hexylamino)(phenyl)methyl)phosphonate (5q)



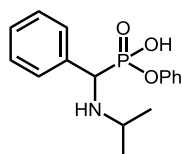
^1H NMR (300 MHz, CD_3OD) 7.60 (2 H, m), 7.49 – 7.34 (3 H, m), 7.31 – 7.14 (2 H, m), 7.10 – 6.94 (3 H, m), 4.44 (1 H, d, $J = 16.0$ Hz), 3.06 (1 H, ddd, $J = 12.3, 10.7, 5.8$ Hz), 2.92 (1 H, ddd, $J = 12.3, 10.7, 5.8$ Hz), 1.69 (2 H, ddt, $J = 17.0, 11.3, 6.5$ Hz), 1.43 – 1.15 (6 H, m), 1.00 – 0.77 (3 H, m). ^{13}C NMR (76 MHz, $\text{DMSO}-d_6$) 153.2, 133.92, 130.0, 129.2, 128.5, 128.3, 122.9, 120.7 (d, $J = 4.3$ Hz), 60.6 (d, $J = 138.0$ Hz), 46.9 (d, $J = 6.7$ Hz), 31.2, 26.3, 25.1, 22.3, 14.2. ^{31}P NMR (121 MHz, CD_3OD) 2.83. IR: 2923, 2853, 2705, 2615, 2542, 2497, 2447, 2394, 2344, 2243, 2119, 1940, 1590, 1488, 1210, 1161, 1081, 1025, 972, 883, 843, 767 cm^{-1} . HRMS (ESI) for: Exact mass calculated for $\text{C}_{19}\text{H}_{26}\text{NO}_3\text{PNa}$ $[\text{M}+\text{Na}]^+$: 370.1548, found 370.1575.

Phenyl hydrogen (1-(allylamino)-3-phenylpropyl)phosphonate (5o)



^1H NMR (600 MHz, CD_3OD) 7.39 – 7.22 (9 H, m), 7.15 (1 H, tq, $J = 7.4, 1.0$ Hz), 5.92 (1 H, ddt, $J = 17.2, 10.5, 6.9$ Hz), 5.46 (1H, q, $J = 1.2$ Hz), 5.44 (1H, dq, $J = 9.1, 1.1$ Hz), 3.94 – 3.77 (2 H, m), 3.36 – 3.30 (1 H, m), 3.06 – 2.86 (2 H, m), 2.50 – 2.34 (1 H, m), 2.21 – 2.07 (1 H, m). ^{13}C NMR (101 MHz, CD_3OD) 153.3 (d, $J = 8.0$ Hz), 142.1, 130.5, 129.7, 129.6, 129.3, 127.3, 124.7, 124.6, 121.6 (d, $J = 4.5$ Hz), 54.8 (d, $J = 144.7$ Hz), 49.8 (d, $J = 3.7$ Hz), 33.3 (d, $J = 4.1$ Hz), 31.3 (d, $J = 2.0$ Hz). ^{31}P NMR (162 MHz, CD_3OD) 8.61. IR: 3448, 2995, 2983, 2958, 2782, 2678, 2617, 2535, 2459, 1623, 1582, 1482, 1454, 1426, 1407, 1246, 1213, 1162, 1153, 1130, 1100, 1064, 1054, 989, 948, 915, 898, 757 cm^{-1} . HRMS (ESI) for: Exact mass calculated for $\text{C}_{18}\text{H}_{22}\text{NO}_3\text{PNa}$ $[\text{M}+\text{Na}]^+$: 354.1235, found 354.1240.

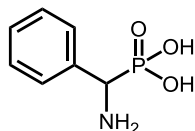
Phenyl hydrogen ((isopropylamino)(phenyl)methyl)phosphonate (5p)



^1H NMR (300 MHz, CD_3OD) 7.72 – 7.54 (2 H, m), 7.42 (3 H, m), 7.22 (2 H, m), 7.11 – 6.77 (3 H, m), 4.51 (1 H, d, $J = 16.6$ Hz), 3.49 (1 H, dt, $J = 13.4, 7.0$ Hz), 1.34 (6 H, dd, $J = 11.7, 6.5$ Hz). ^{13}C NMR (151 MHz, CD_3OD) 152.0 (d, $J = 8.2$ Hz), 132.3, 129.28, 129.24, 128.9, 128.6, 123.2, 120.2 (d, $J = 4.4$ Hz), 58.2 (d, $J = 142.5$ Hz), 49.8, 17.6. ^{31}P NMR (122 MHz, CD_3OD) 6.07. IR: 3059, 3010, 2976, 2936, 2814, 2784, 2686, 2633, 2554, 2521, 2464, 2403, 2360, 2255, 2130, 2093, 1985, 1719, 1628, 1590,

1489, 1454, 1390, 1333, 1283, 1214, 1144, 1095, 1025, 1001, 908, 860, 804, 783, 754 cm^{-1} . HRMS (ESI) for: Exact mass calculated for $\text{C}_{16}\text{H}_{20}\text{NO}_3\text{PNa}$ $[\text{M}+\text{Na}]^+$: 328.1079, found 328.1080.

(amino(phenyl)methyl)phosphonic acid



Prepared according to a known procedure.²³¹ ^1H NMR (300 MHz, D_2O) 7.35 (4 H, s), 4.32 (1 H, d, $J = 16.0$ Hz). ^{31}P NMR (121 MHz, D_2O) 7.46. Spectral data was found to be in good agreement with literature.²³²

²³¹ K. C. Kumara Swamy, S. Kumaraswamy, K. Senthil Kumar, C. Muthiah, *Tetrahedron Lett.* **2005**, 46, 3347.

²³² K. Kozyra, M. Brzezinska-Rodak, M. Klimek-Ochab, E. Zymanczyk-Duda, *J. Mol. Catal. B: Enzy.* **2013**, 91, 32.

6.4. Experiment section for Chapter 4

General procedure to generate products with glycolaldehyde or formaldehyde

Procedure for hydrolysis of diphenylphosphinic amides and diphenylphosphoramidates in the presence of glycolaldehyde

Diphenylphosphinic amide (0.2 mmol), glycolaldehyde (0.04mmol) and NH_4OTs (0.2 mmol) were added into a sealed tube. 0.2 mL MeCN and 0.2 mL H_2O were followed.

Then the reaction mixture was stirred under 90 °C for 24 hours.

Procedure for hydrolysis of diphenylphosphinic amides and diphenylphosphoramidates in the presence of formaldehyde

Diphenylphosphinic amide (0.2 mmol), formaldehyde (0.04mmol) and NH_4OTs (0.2 mmol) were added into a sealed tube. 0.2 mL MeCN and 0.2 mL H_2O were followed.

Then the reaction mixture was stirred under 90 °C for 24 hours.

Isolation of diphenylphosphinic acid

After the completion, the solvent was removed by high vacuum and following adding H_2O (10 mL) and toluene (10 mL). The mixture was stirred for 10 minutes and the aqueous layer was collected. After acidification of the aqueous layer by 1 M HCl to pH = 1~2, then the aqueous layer was extracted using 5% methanol in dichloromethane (20 mL x 3). The organic layers were combined, dried over Na_2SO_4 and filtered and concentrated *in vacuo*.

Isolation of amine component

After the completion, the solvent was removed by high vacuum and following adding H₂O (10 mL) and toluene (10 mL). The mixture was stirred for 10 minutes and the aqueous layer was collected. After basification of the aqueous layer by 1 M NaOH to pH = 8~9, then the aqueous layer was extracted using ethyl acetate (20 mL x 3). The organic layers were combined, dried over Na₂SO₄ and filtered and concentrated *in vacuo*.

General procedure when DAP or MAP were used

In a sealed tube, diamidophosphate (DAP) (0.10 mmol) (and other substances) was dissolved in H₂O (0.2 mL). The reaction mixture was heated at 90 °C. Several reactions were performed in parallel. At certain time point, 0.4 mL of D₂O was added and the reaction mixture was monitored by ³¹P NMR. The assignment of ³¹P NMR peaks was based on an informative study.²⁰³

Procedure for background reaction with DAP. In a sealed tube, diamidophosphate (DAP) (0.10 mmol) was dissolved in H₂O (0.2 mL). The reaction mixture was heated at 90 °C and monitored by ³¹P NMR. Two reactions were performed in parallel that one reaction was monitored after 45 min and the other one was monitored after 3.5 h. The spectra were presented in Chapter 4. The assignment of ³¹P NMR peaks was based on an informative study.²⁰³

Procedure for reaction with DAP. In a sealed tube, diamidophosphate (DAP) (0.10 mmol), glycolaldehyde (0.02 mmol) and NH₄OTs (0.10 mmol) were dissolved in H₂O

(0.2 mL). The reaction mixture was heated at 90 °C and monitored by ^{31}P NMR. Seven reactions were performed in parallel and they were monitored for different time points, 45 min, 3.5 h, 24 h, 48 h, 72 h, 96 h and 7 days. The spectra were presented in Chapter 4. The assignment of ^{31}P NMR peaks was based on an informative study.²⁰³

Procedure for control experiment with DAP in the presence of glycolaldehyde. In a sealed tube, diamidophosphate (DAP) (0.10 mmol) and glycolaldehyde (0.02 mmol) were dissolved in H_2O (0.2 mL). The reaction mixture was heated at 90 °C and monitored by ^{31}P NMR. Two reactions were performed in parallel that one reaction was monitored after 45 min and the other one was monitored after 3.5 h. The spectra were presented in Chapter 4. The assignment of ^{31}P NMR peaks was based on an informative study.²⁰³

Procedure for control experiment with DAP in the presence of NH_4OTs . In a sealed tube, diamidophosphate (DAP) (0.10 mmol) and NH_4OTs (0.10 mmol) were dissolved in H_2O (0.2 mL). The reaction mixture was heated at 90 °C and monitored by ^{31}P NMR. Seven reactions were performed in parallel and they were monitored for different time points, 45 min, 3.5 h, 24 h, 48 h, 72 h, 96 h and 7 days. The spectra were presented in Chapter 4. The assignment of ^{31}P NMR peaks was based on an informative study.²⁰³

Procedure for reaction with DAP in the presence of glycolaldehyde and different additives. In a sealed tube, diamidophosphate (DAP) (0.10 mmol), glycolaldehyde (0.02 mmol) and NH_4Cl (0.10 mmol) or NaCl (0.10 mmol) or were dissolved in H_2O (0.2 mL). The reaction mixture was heated at 90 °C and monitored by ^{31}P NMR. Three reactions were performed in parallel and they were monitored for different time points,

45 min, 3.5 h, and 24 h. The spectra were presented in Chapter 4. The assignment of ^{31}P NMR peaks was based on an informative study.²⁰³

Procedure for reaction with DAP in the presence of formaldehyde with or without NH_4OTs . In a sealed tube, diamidophosphate (DAP) (0.10 mmol) and formaldehyde (0.02 mmol) with or without NH_4OTs (0.10 mmol) were dissolved in H_2O (0.2 mL). The reaction mixture was heated at 90 °C and monitored by ^{31}P NMR. Three reactions were performed in parallel and they were monitored for different time points, 45 min, 3.5 h, and 24 h. The spectra were presented in Chapter 4. The assignment of ^{31}P NMR peaks was based on an informative study.²⁰³

Procedure for reaction with DAP in the presence of different phosphates. In a sealed tube, diamidophosphate (DAP) (0.10 mmol), glycolaldehyde (0.02 mmol) and $(\text{NH}_4)_2\text{PO}_4$ (0.10 mmol) were dissolved in H_2O (0.2 mL). The reaction mixture was heated at 90 °C and monitored by ^{31}P NMR. Three reactions were performed in parallel and they were monitored for different time points, 45 min, 3.5 h, and 24 h. The spectra were presented in Chapter 4. The assignment of ^{31}P NMR peaks was based on an informative study.²⁰³

Procedure for reaction with DAP in the presence of different phosphates. In a sealed tube, diamidophosphate (DAP) (0.10 mmol), glycolaldehyde (0.02 mmol) and $\text{NH}_4\text{H}_2\text{PO}_4$ (0.10 mmol) were dissolved in H_2O (0.2 mL). The reaction mixture was heated at 90 °C and monitored by ^{31}P NMR. Three reactions were performed in parallel and they were monitored for different time points, 45 min, 3.5 h, and 24 h. The spectra were presented in Chapter 4. The assignment of ^{31}P NMR peaks was based on an

informative study.²⁰³

Procedure for reaction with DAP in the presence of different phosphates. In a sealed tube, diamidophosphate (DAP) (0.10 mmol), glycolaldehyde (0.02 mmol) Na_3PO_4 (0.1 mmol), NH_4Cl (0.3 mmol) were dissolved in H_2O (0.2 mL). The reaction mixture was heated at 90 °C and monitored by ^{31}P NMR. Three reactions were performed in parallel and they were monitored for different time points, 45 min, 3.5 h, and 24 h. The spectra were presented in Chapter 4. The assignment of ^{31}P NMR peaks was based on an informative study.²⁰³

Procedure for reaction with MAP. In a sealed tube, monoamidophosphate (MAP) (0.20 mmol), glycolaldehyde (0.04 mmol) and NH_4OTs (0.20 mmol) were dissolved in H_2O (0.4 mL). The reaction mixture was heated at 50 °C and monitored by ^{31}P NMR. Four reactions were performed in parallel and they were monitored for different time points, 45 min, 3.5 h, 7 h, and 9 h. The spectra were presented in Chapter 4.

Procedure for reaction with MAP without glycolaldehyde. In a sealed tube, monoamidophosphate (MAP) (0.20 mmol) and NH_4OTs (0.20 mmol) were dissolved in H_2O (0.4 mL). The reaction mixture was heated at 50 °C and monitored by ^{31}P NMR after 9 h. The spectra were presented in Chapter 4.

Procedure for reaction with DAP in the presence of ribose. In a sealed tube, diamidophosphate (DAP) (0.10 mmol), ribose (0.02 mmol) and NH_4OTs (0.10 mmol) were dissolved in H_2O (0.2 mL). The reaction mixture was heated at 90 °C and monitored by ^{31}P NMR. Six reactions were performed in parallel and they were

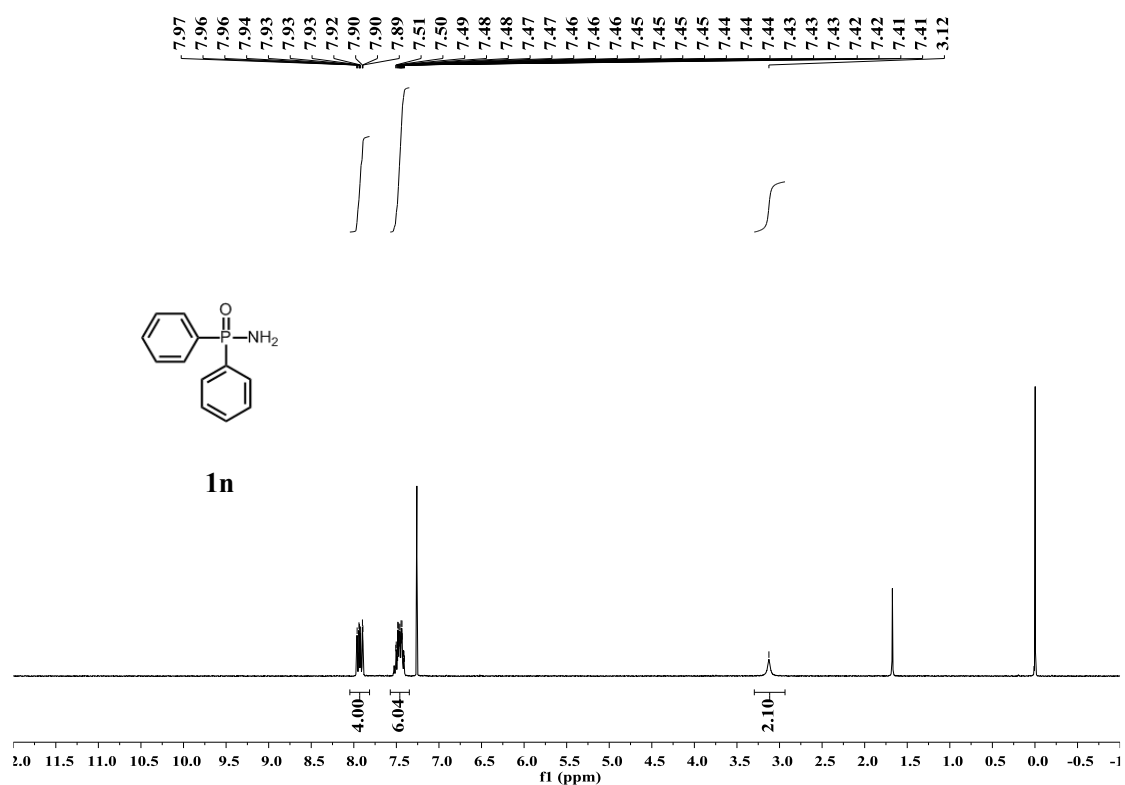
monitored for different time points, 45 min, 3.5 h, 24 h, 72 h, 96 h and 7 days. The spectra were presented in Chapter 4. The assignment of ^{31}P NMR peaks was based on an informative study.²⁰³

Substrates used in Chapter 4 were characterized in Chapter 2.

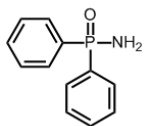
Appendix I

NMR and HPLC spectra data

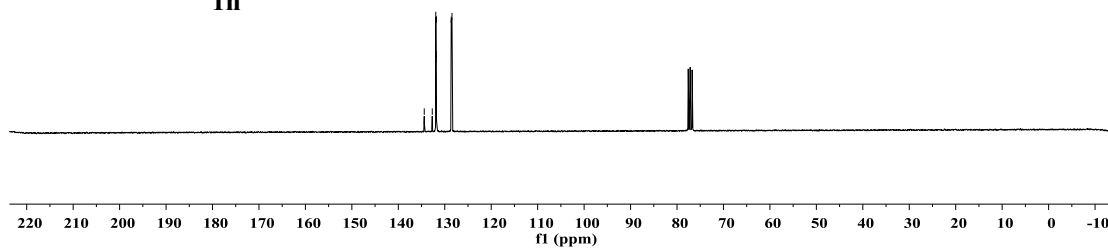
Spectra for starting materials in Chapter 2



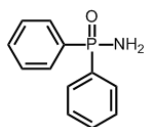
134.41
132.69
131.93
131.86
131.83
131.80
128.61
128.45



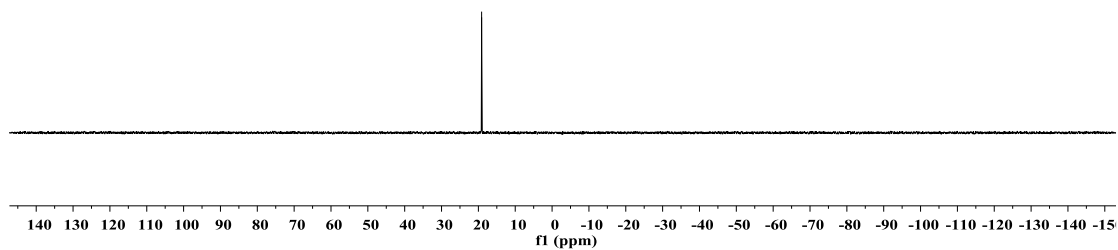
1n

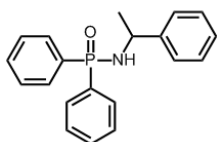
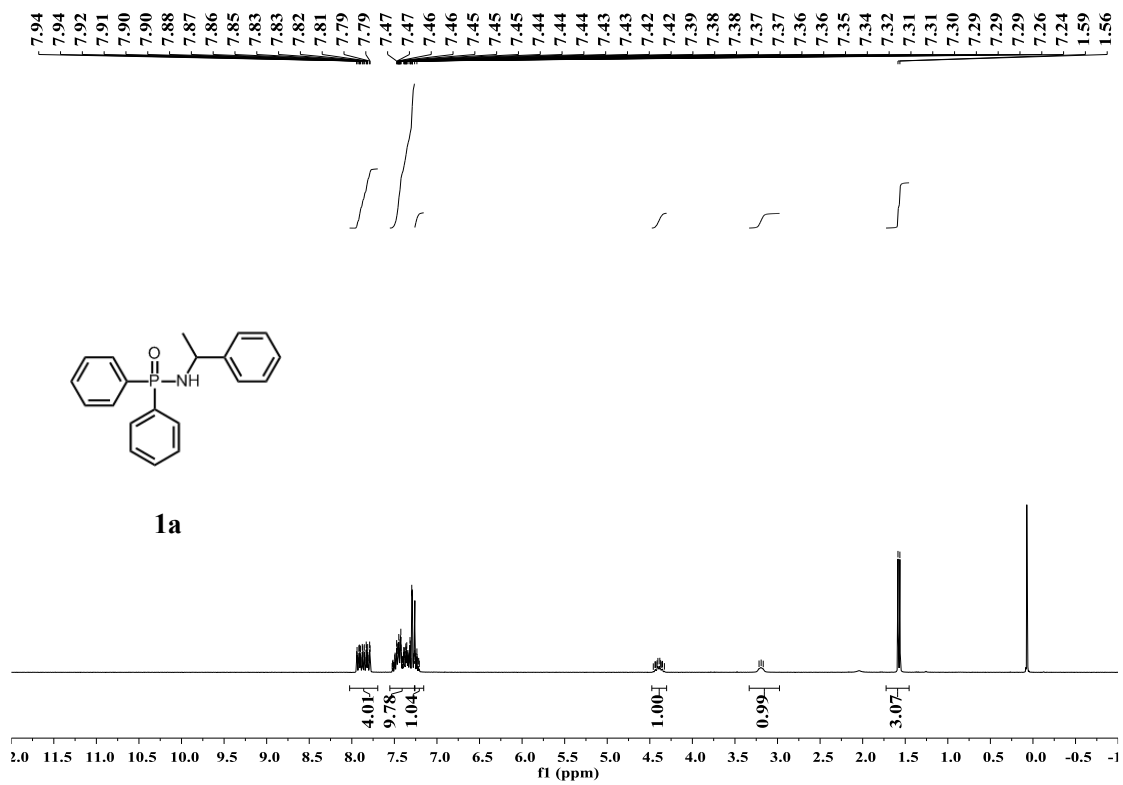


19.12

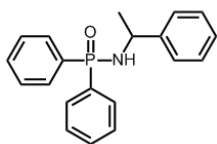
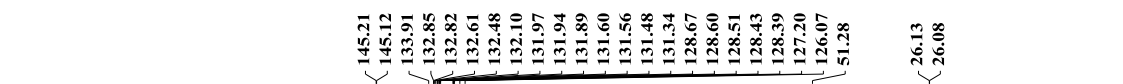


1n

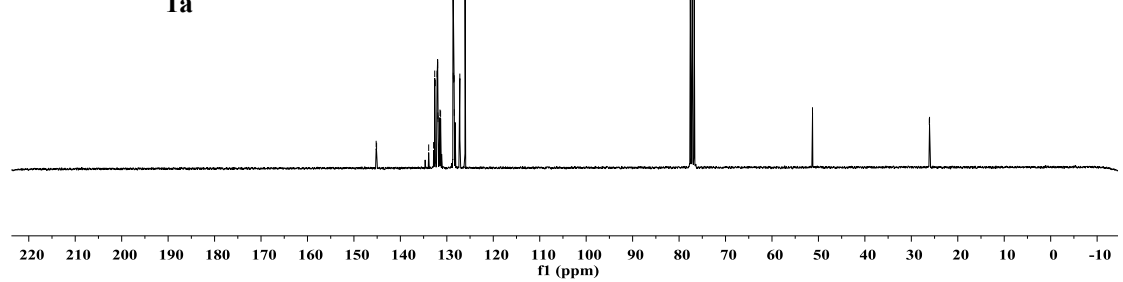




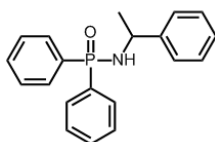
1a



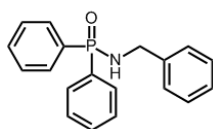
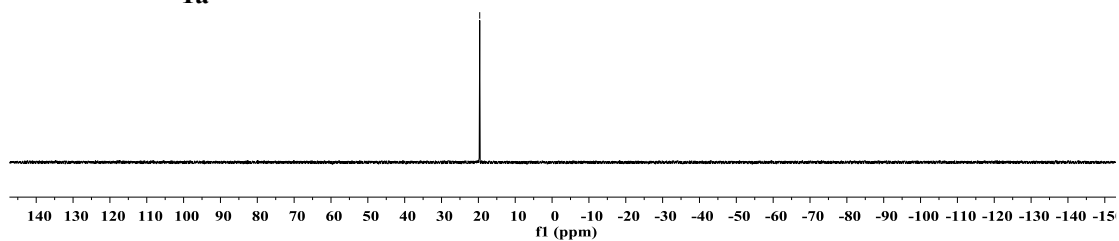
1a



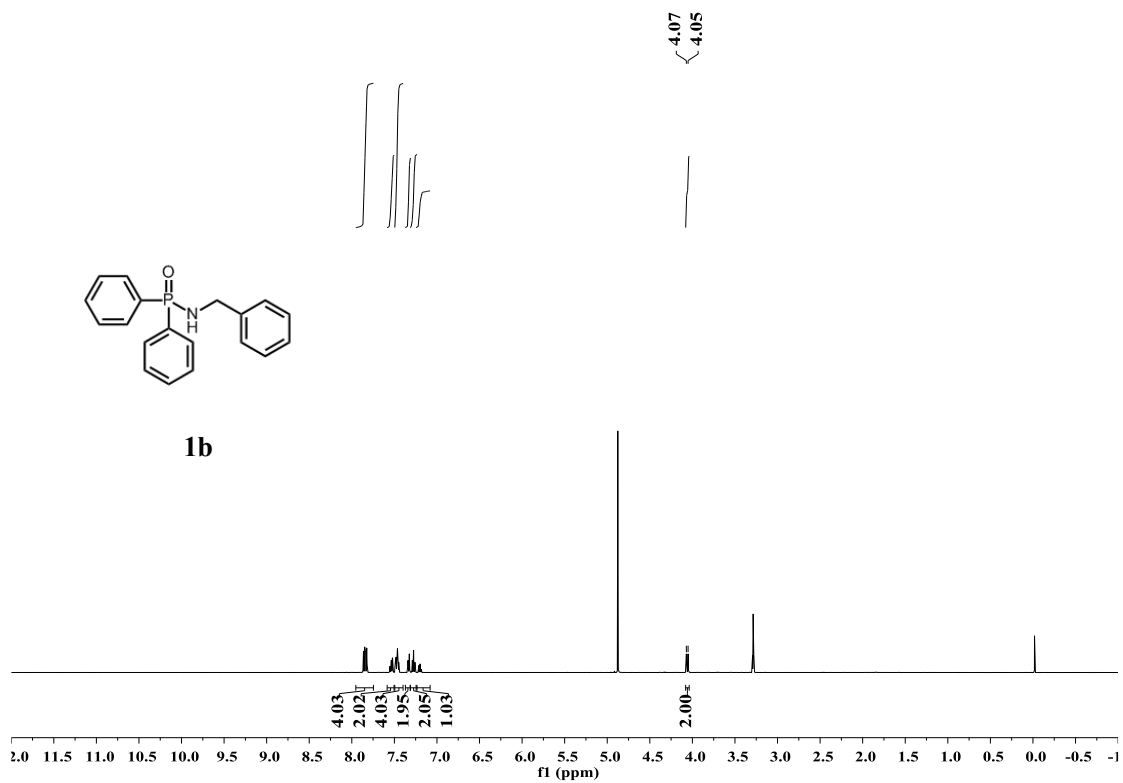
- 19.64

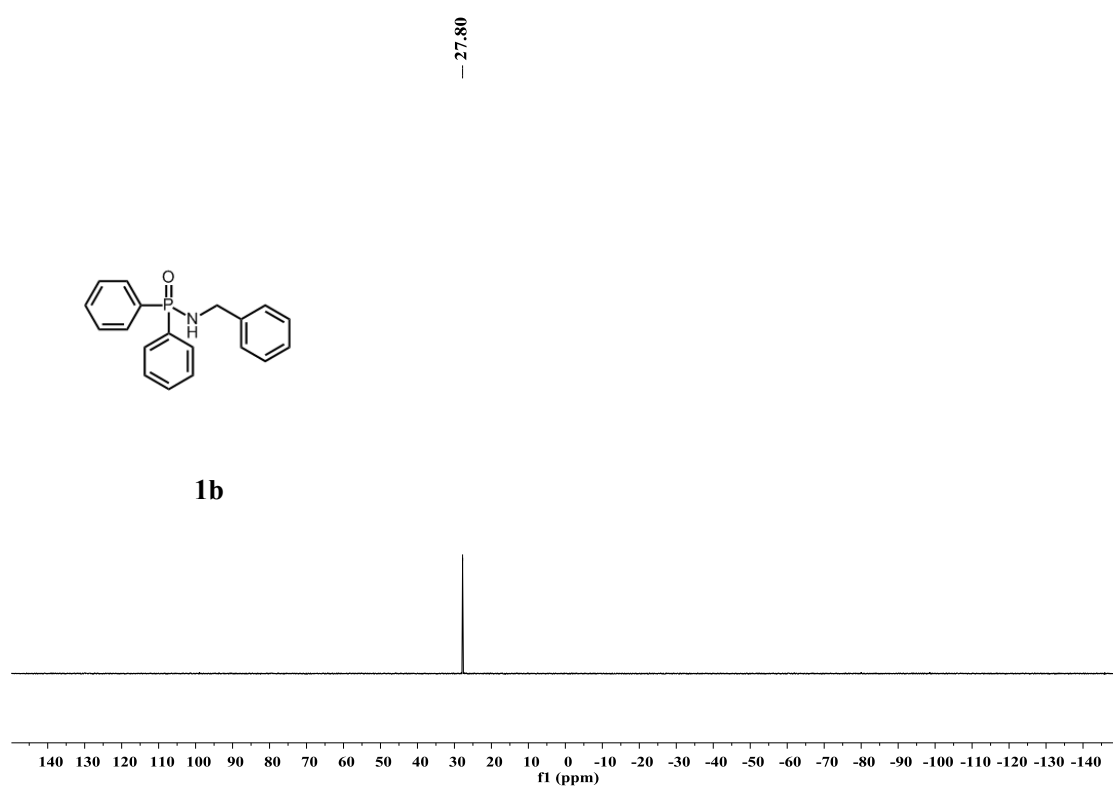
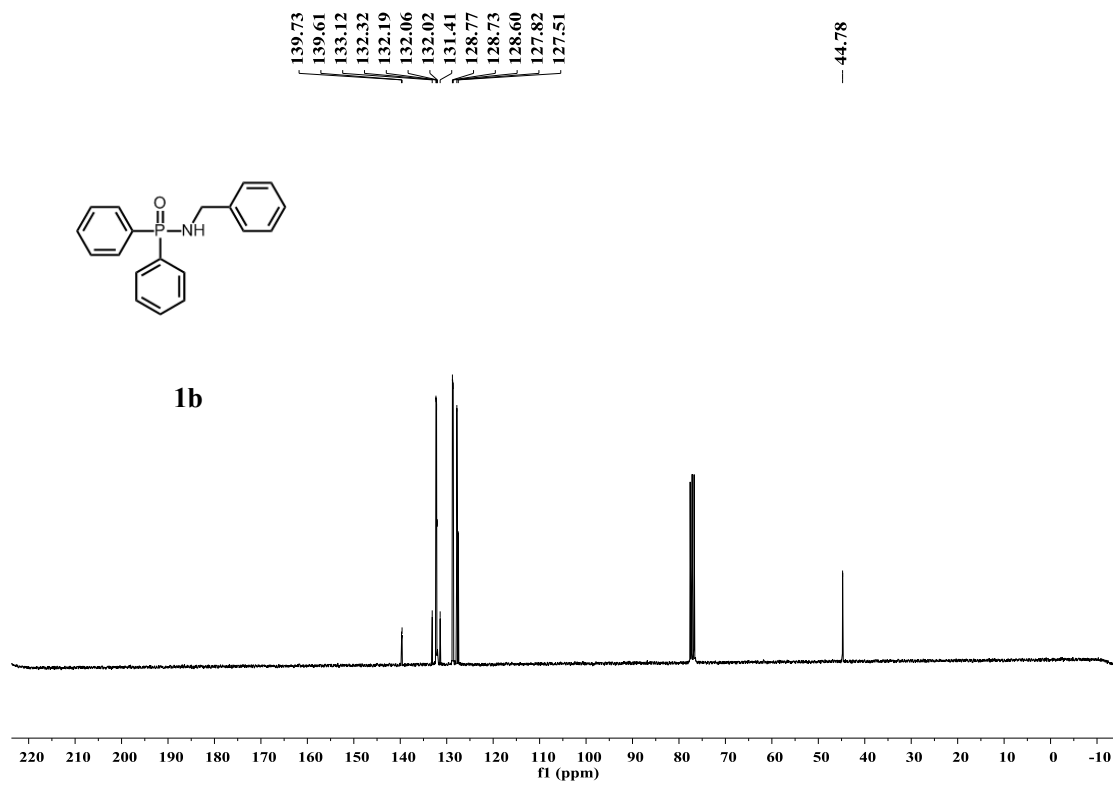


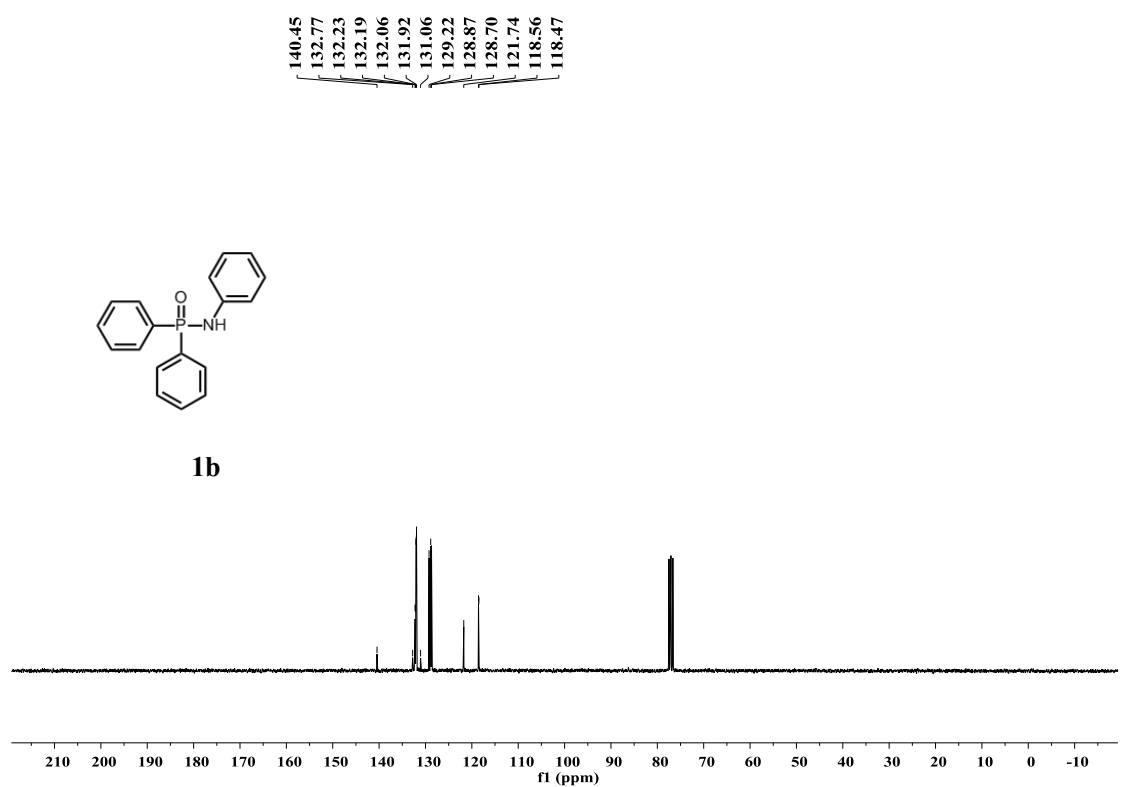
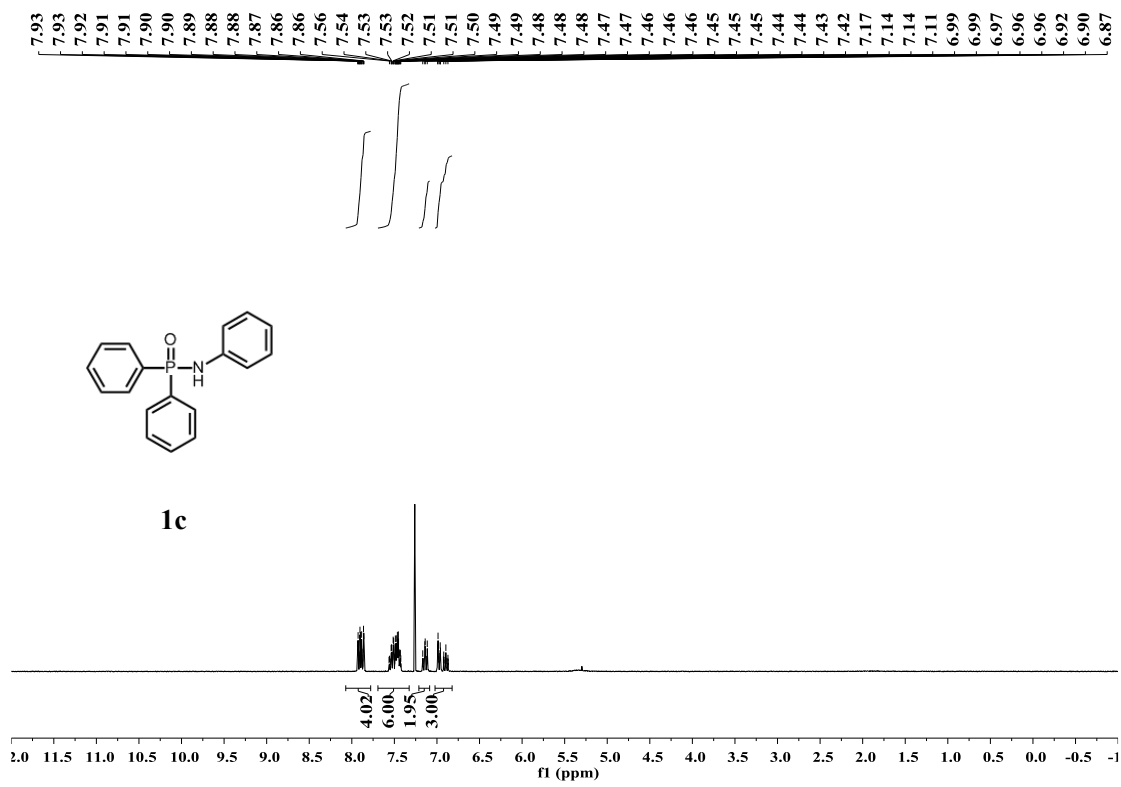
1a



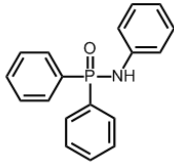
1b



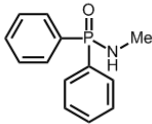
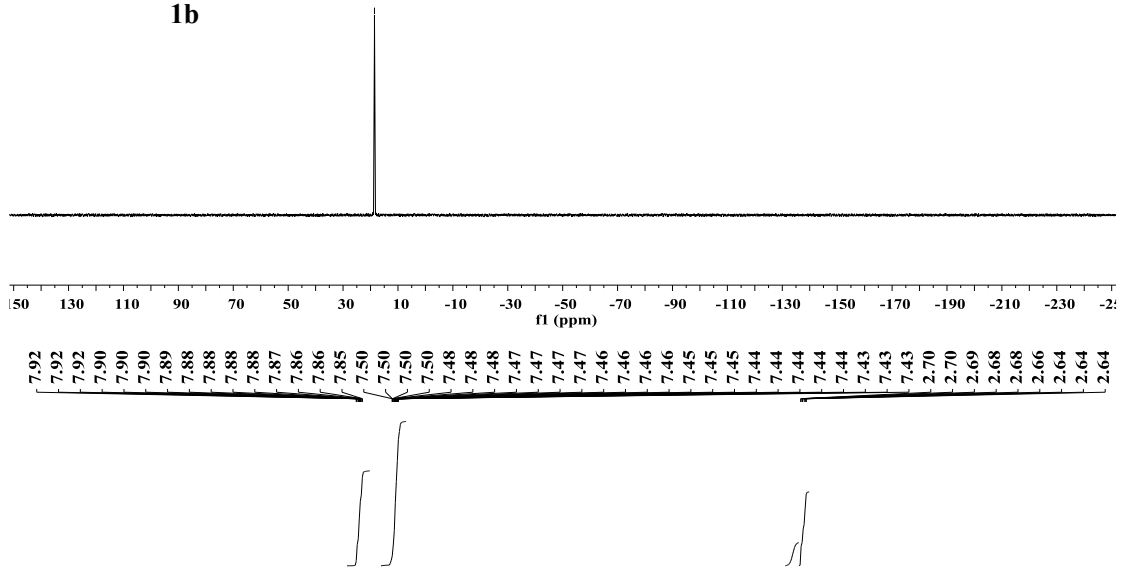




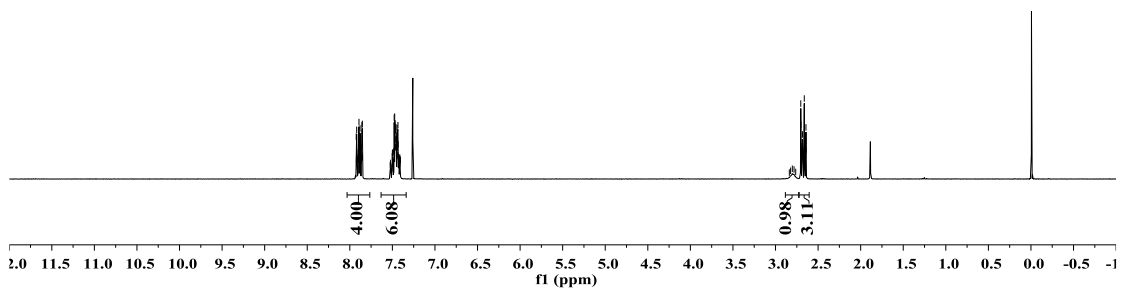
- 18.56

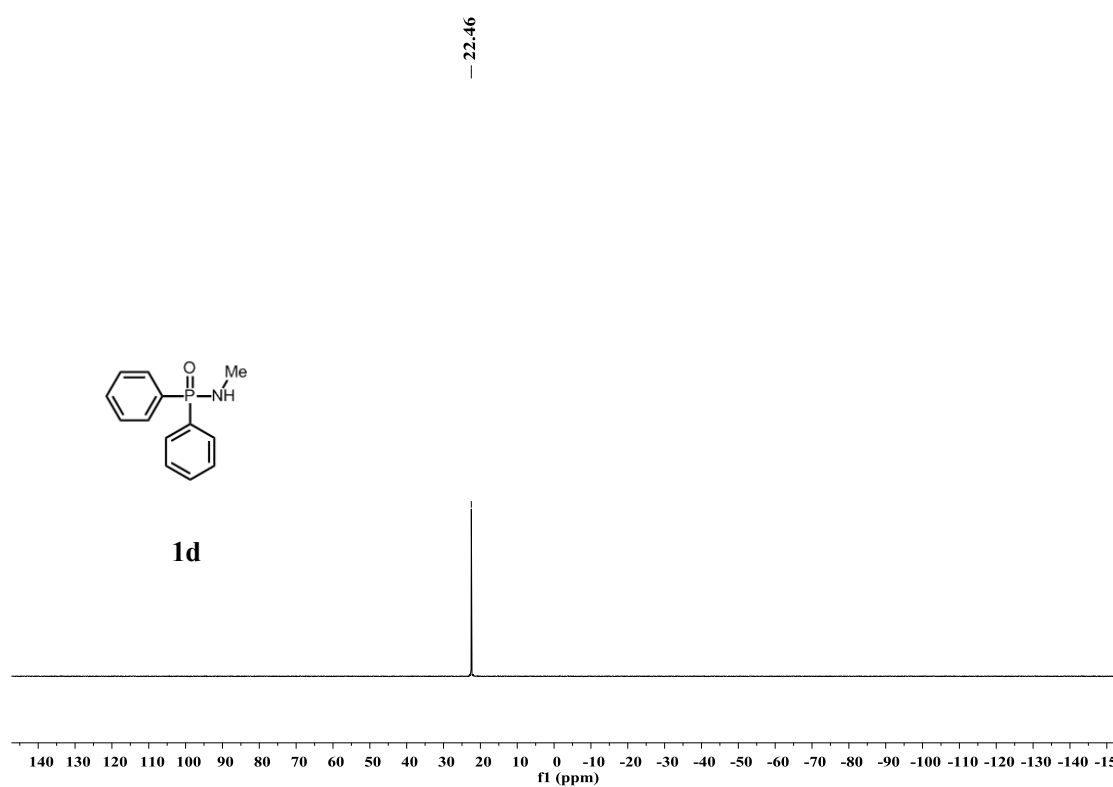
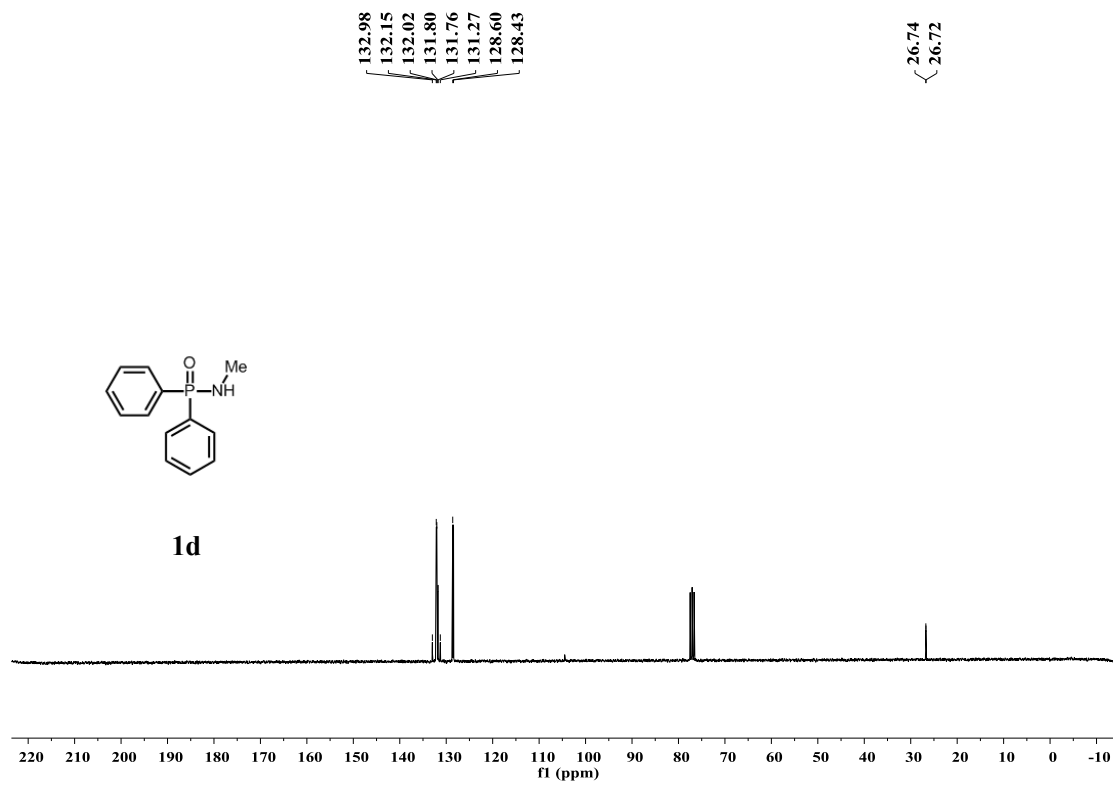


1b

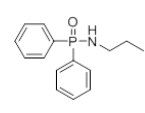


1d

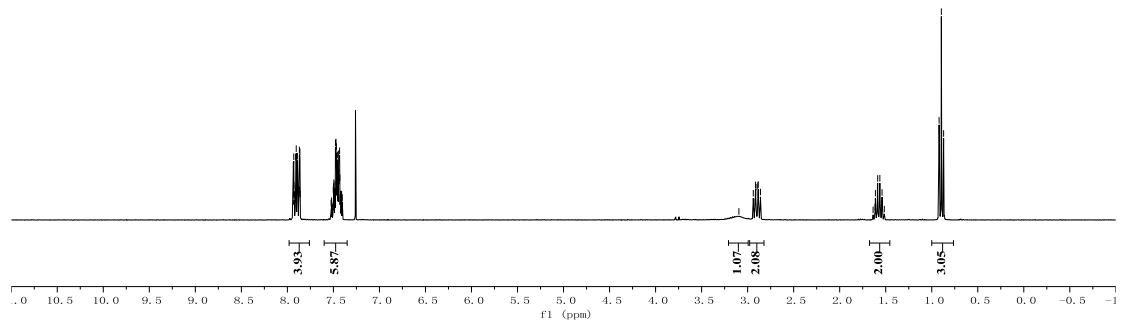




7.94
7.93
7.93
7.93
7.92
7.91
7.91
7.90
7.90
7.89
7.89
7.88
7.87
7.87
7.86
7.86
7.82
7.82
7.80
7.80
7.49
7.49
7.48
7.48
7.47
7.47
7.47
7.47
7.46
7.46
7.46
7.45
7.45
7.44
7.44
7.44
7.44
7.43
7.43
7.43
7.42
7.42
7.42
7.41
7.41
7.40
2.94
2.92
2.92
2.91
2.91
2.89
2.88
2.86
1.61
1.59
1.59
1.57
1.56
1.54
0.92
0.90
0.87

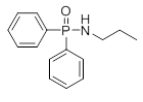


1e

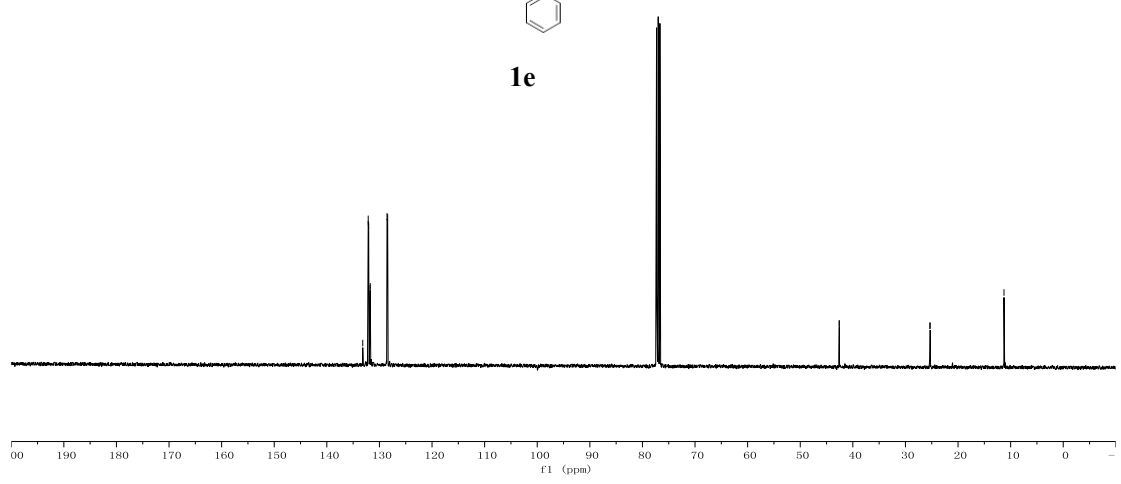


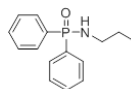
133.17
132.13
132.04
131.89
131.78
131.75
128.56
128.44

42.60
42.58
25.37
25.29
11.27

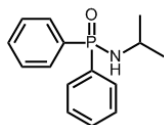
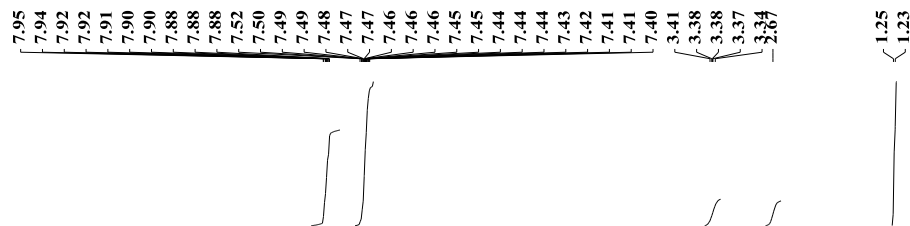
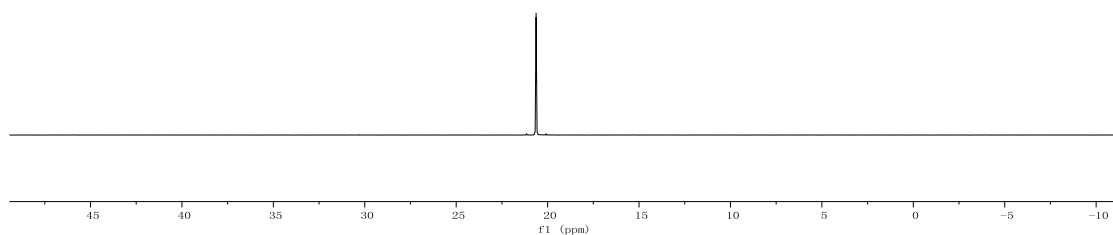


1e

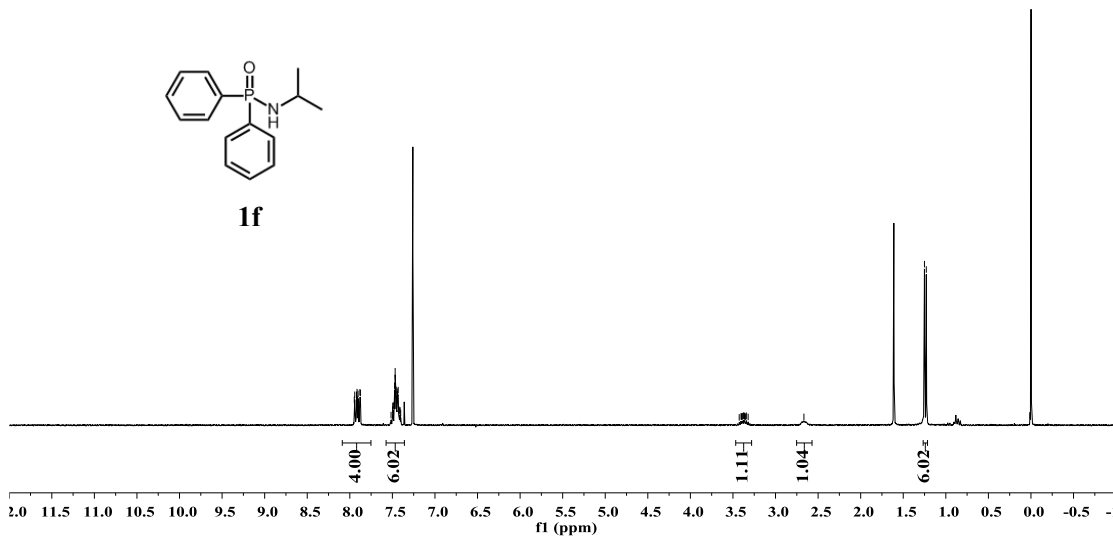


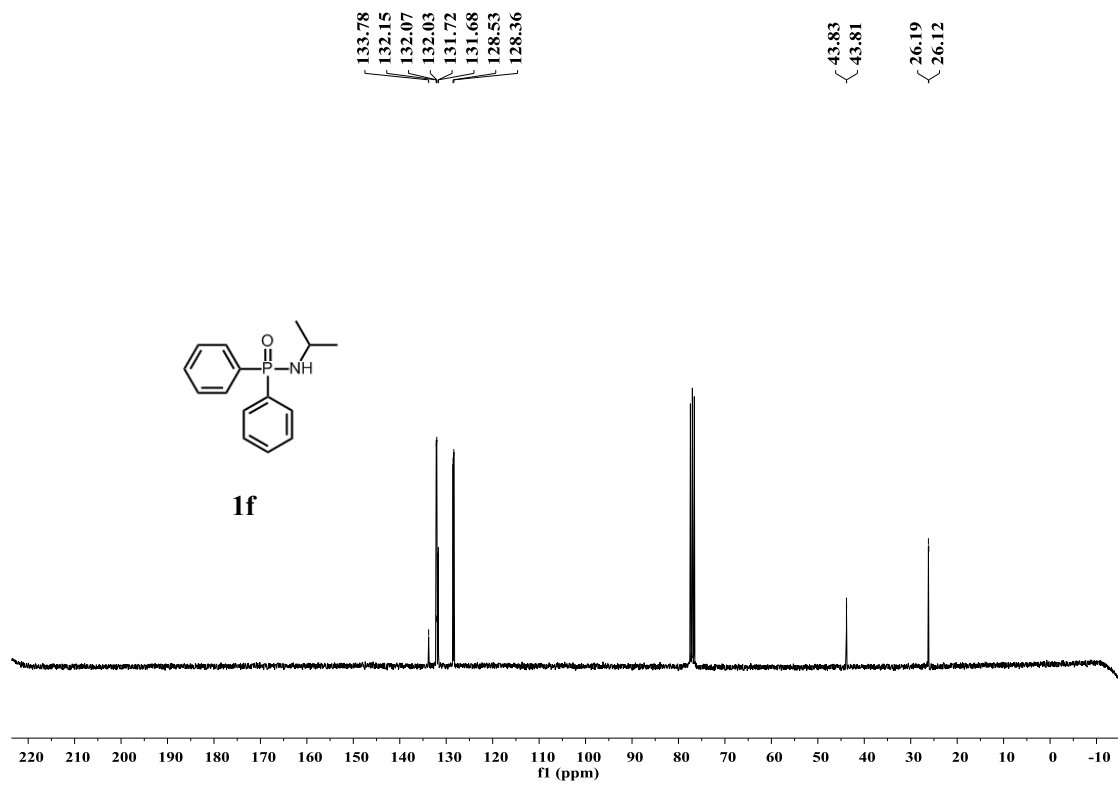


1e

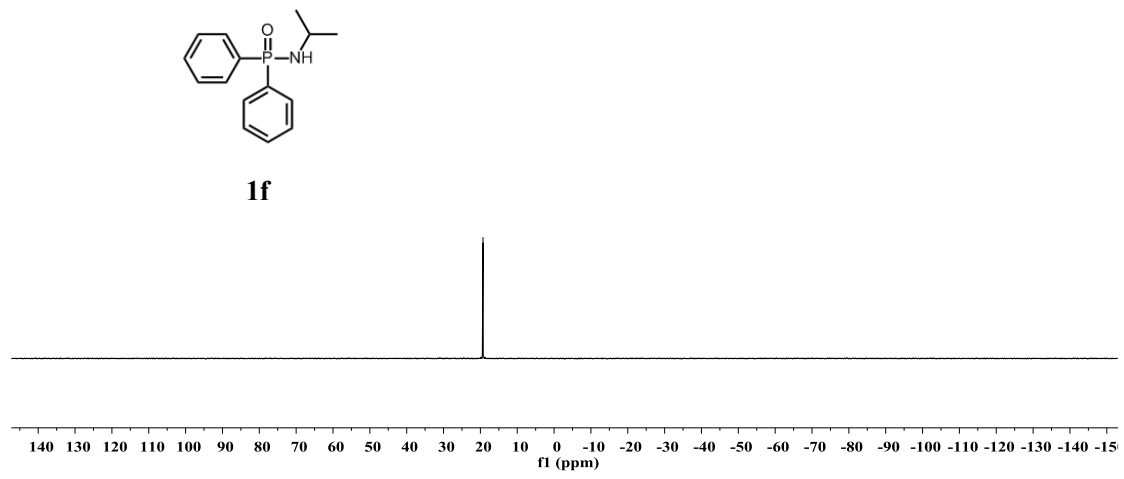


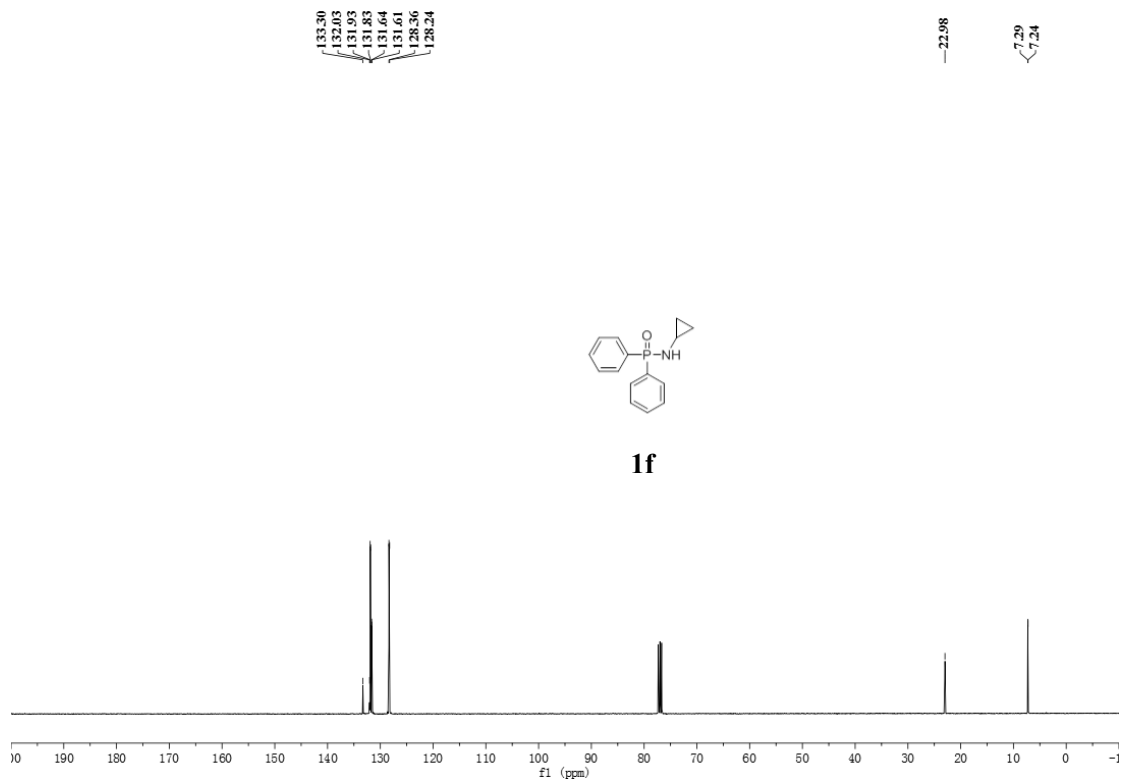
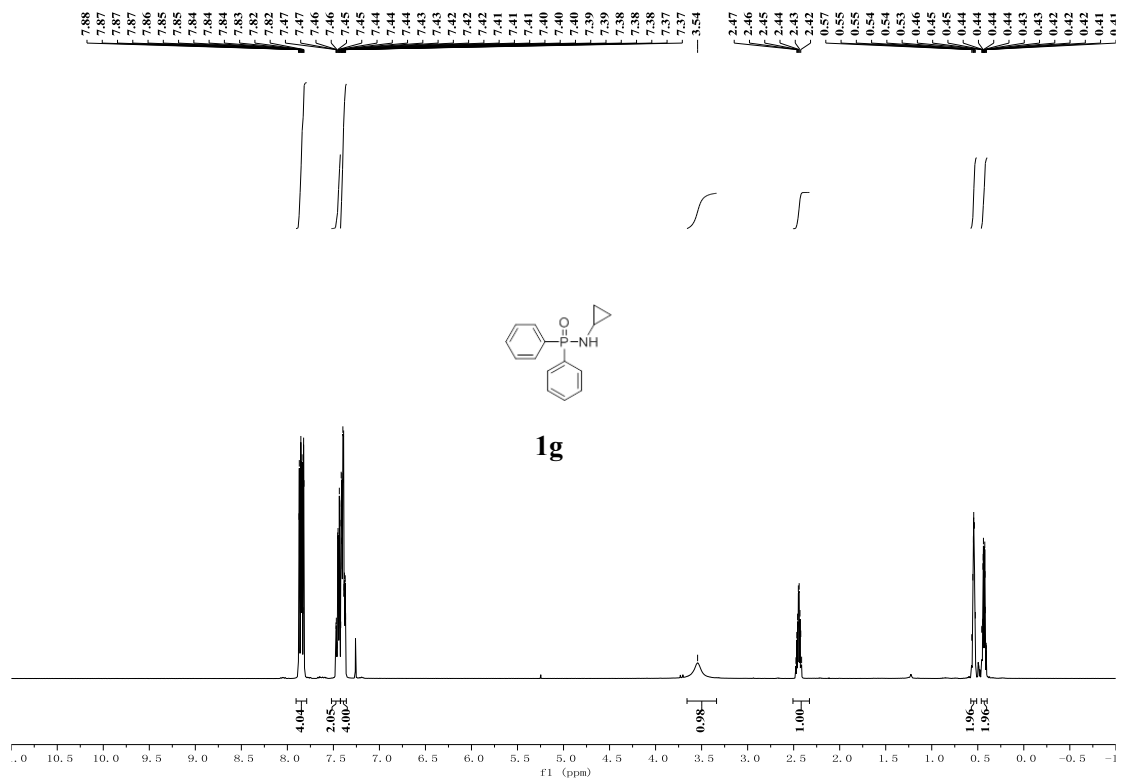
1f

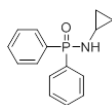




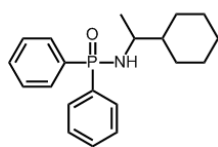
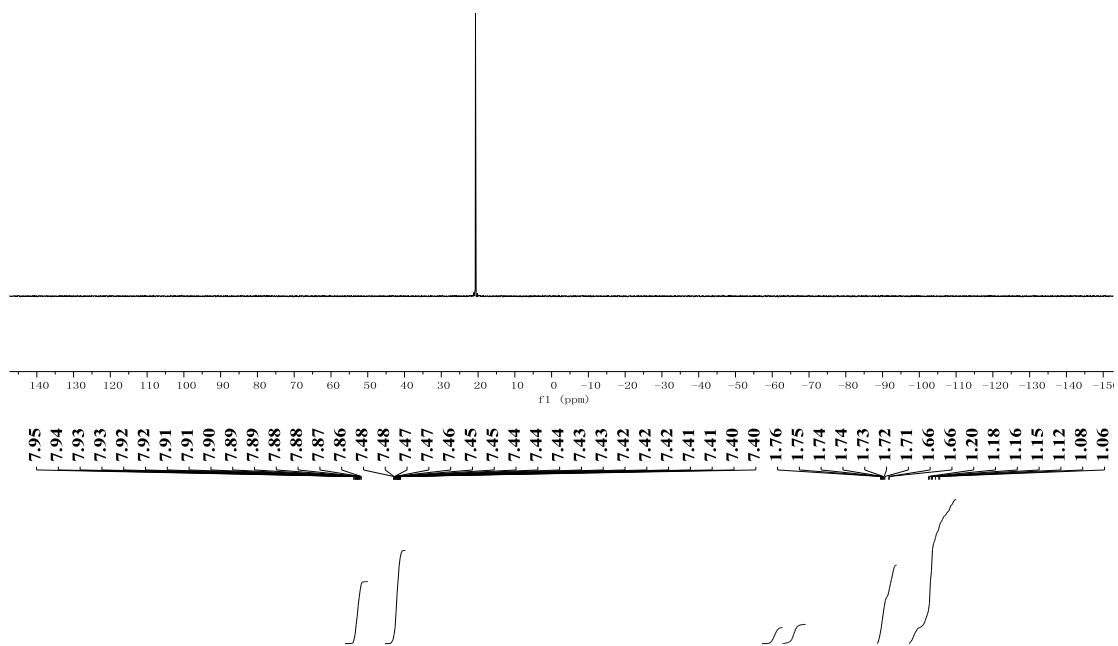
19.28



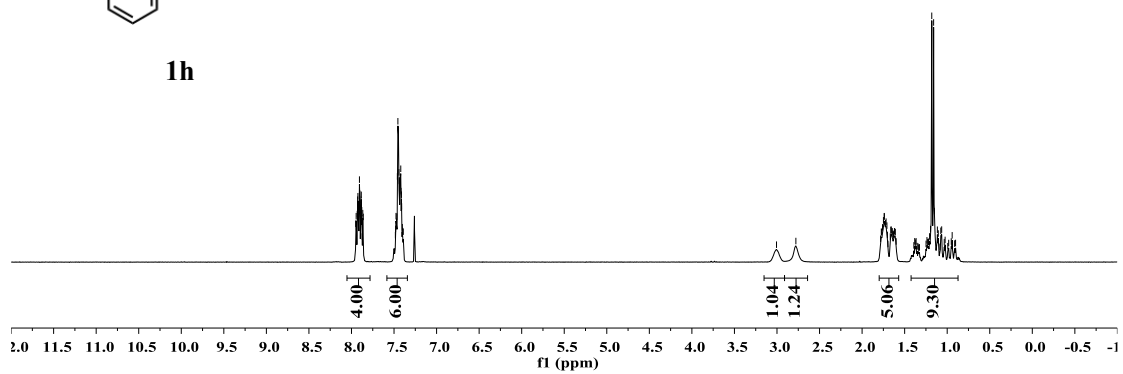


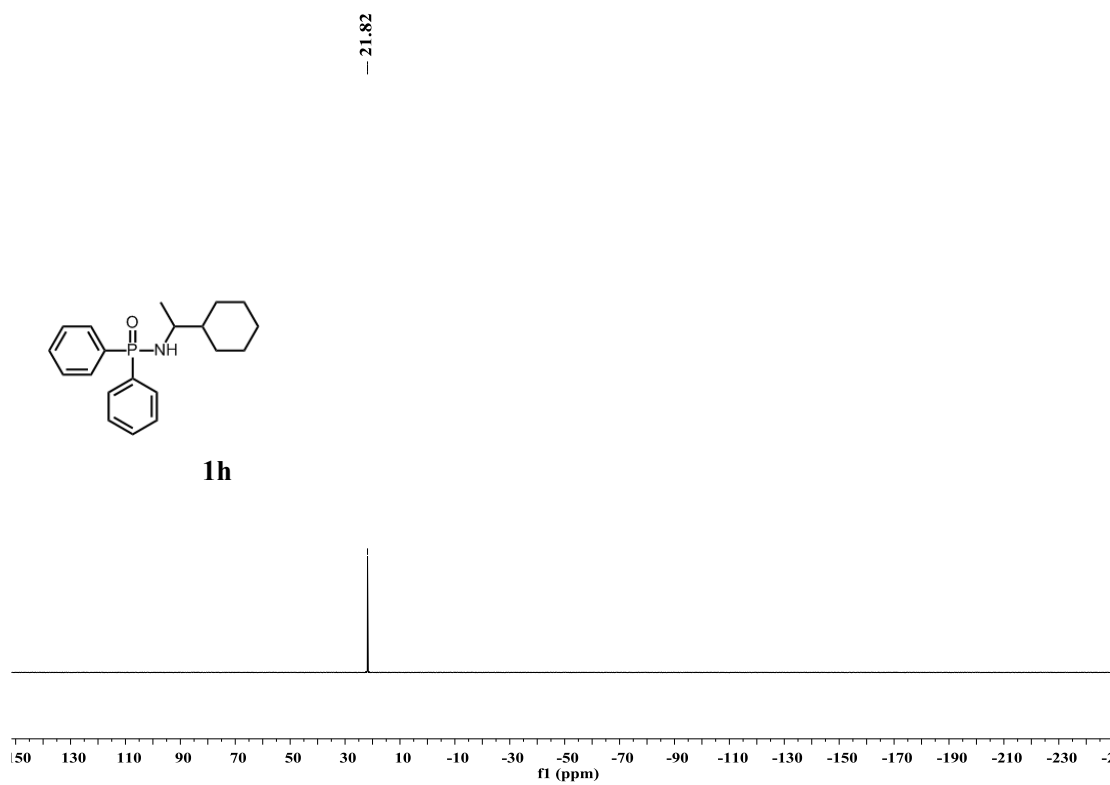
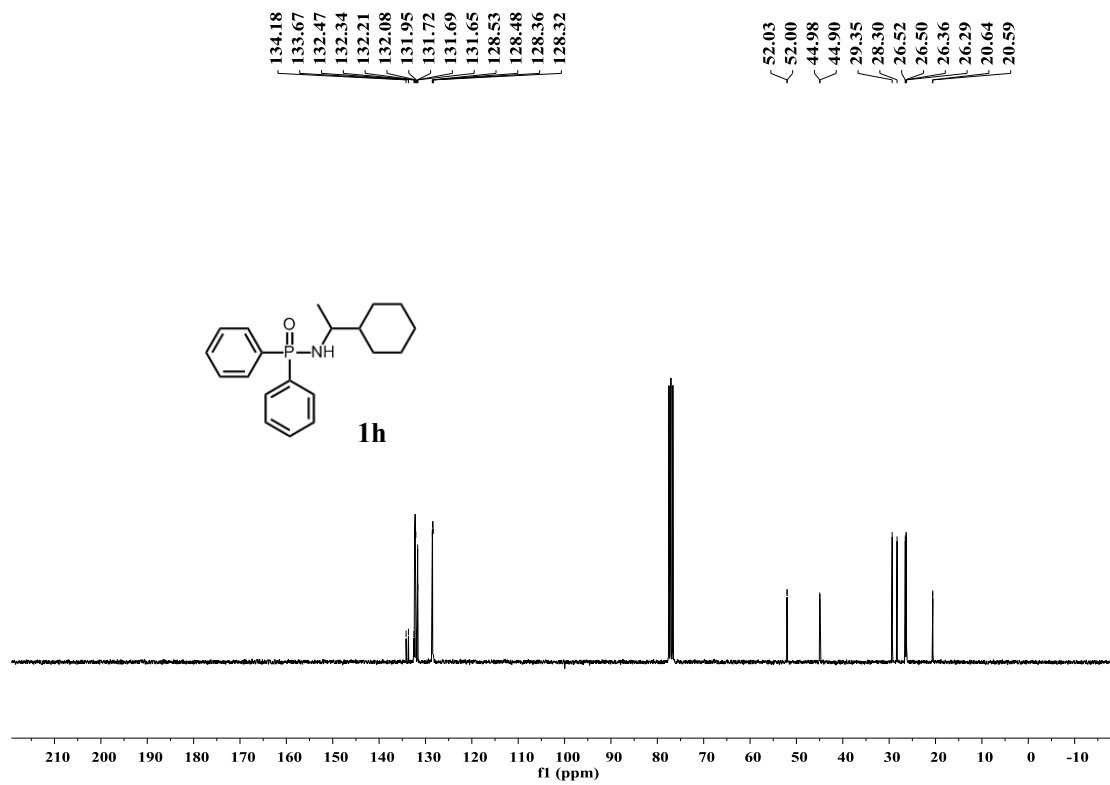


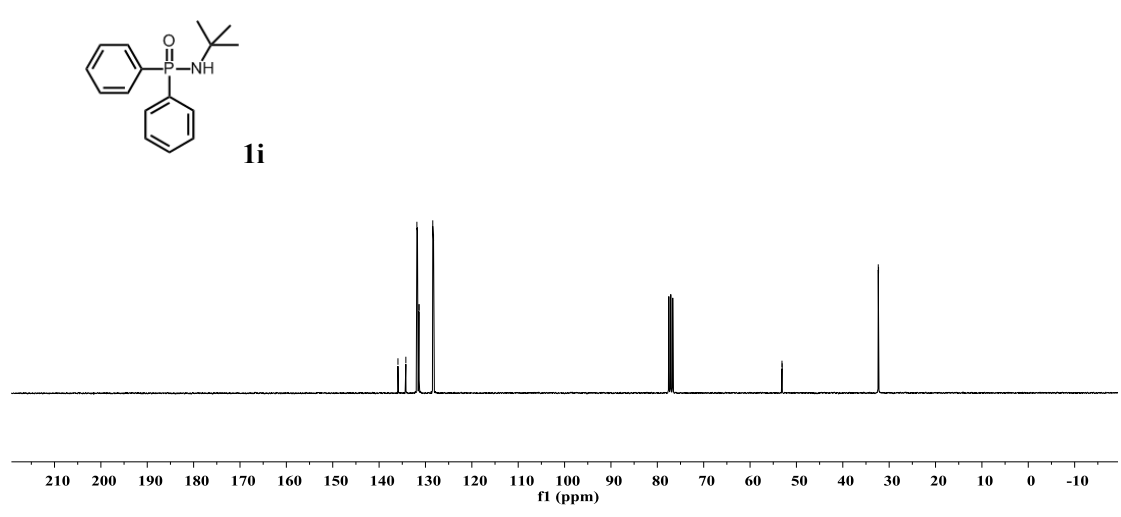
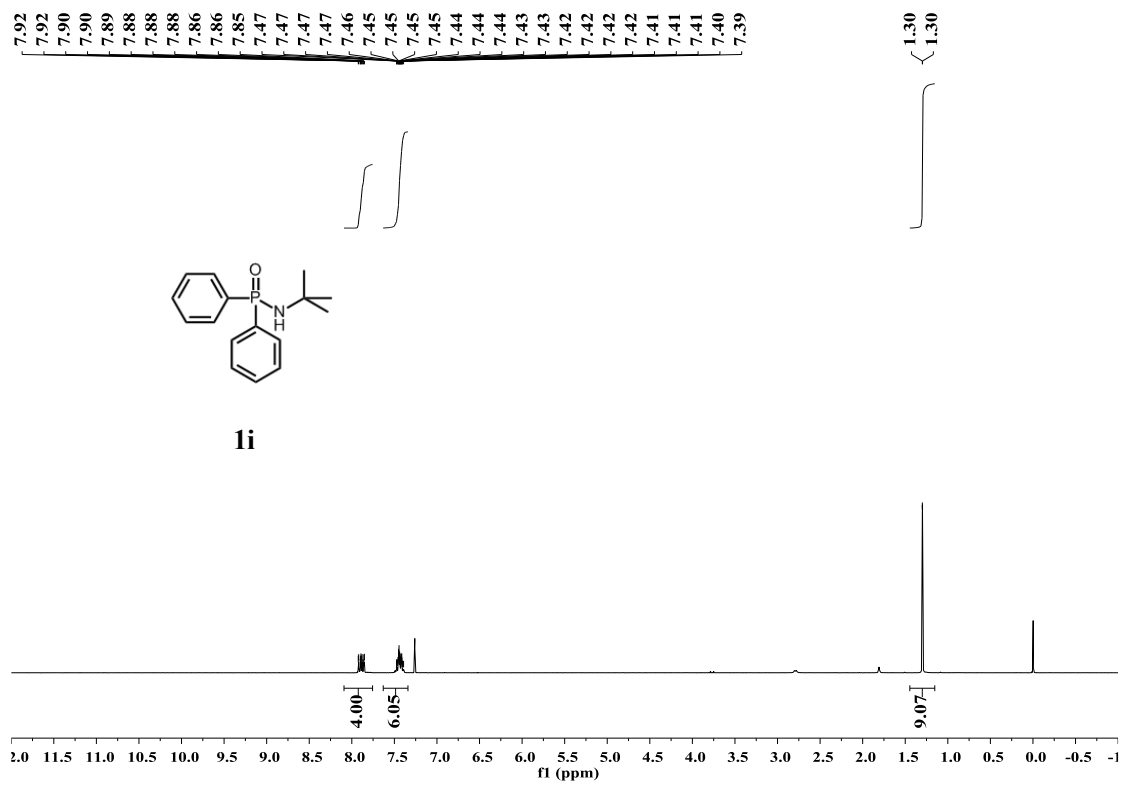
1f



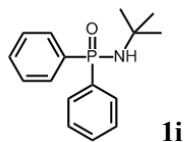
1h







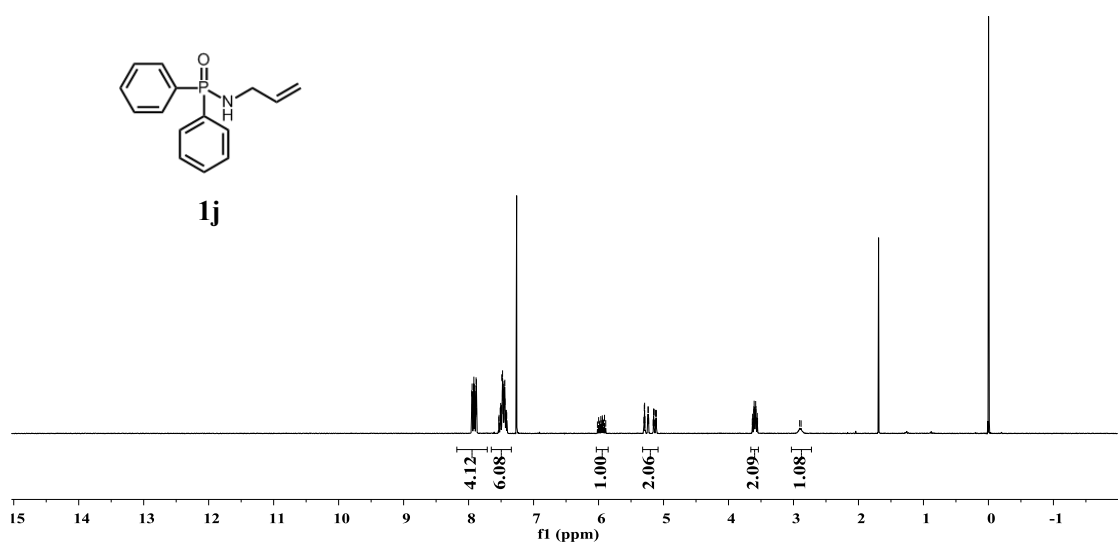
- 19.47



150 130 110 90 70 50 30 10 -10 -30 -50 -70 -90 -110 -130 -150 -170 -190 -210 -230 -2

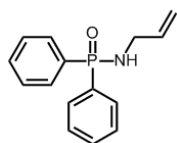
fl (ppm)

7.95 7.95 7.94 7.92 7.92 7.91 7.91 7.90 7.90 7.88 7.88 7.88 7.88 7.51 7.51 7.51 7.51 7.49 7.49 7.48 7.48 7.48 7.48 7.47 7.47 7.47 7.47 7.47 7.46 7.46 7.46 7.45 7.45 7.45 7.45 7.45 7.44 7.44 7.44 5.30 5.29 5.24 5.24 5.15 5.15 5.15 5.15 3.61 3.61 3.60 3.59 3.58 3.58

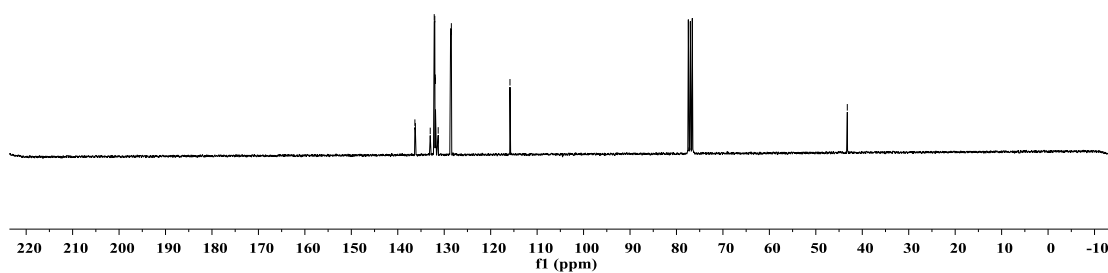


136.31
136.21
133.01
132.15
132.03
131.92
131.88
131.30
128.63
128.47
115.84

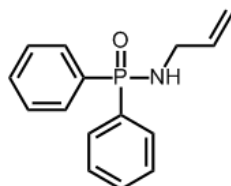
43.22



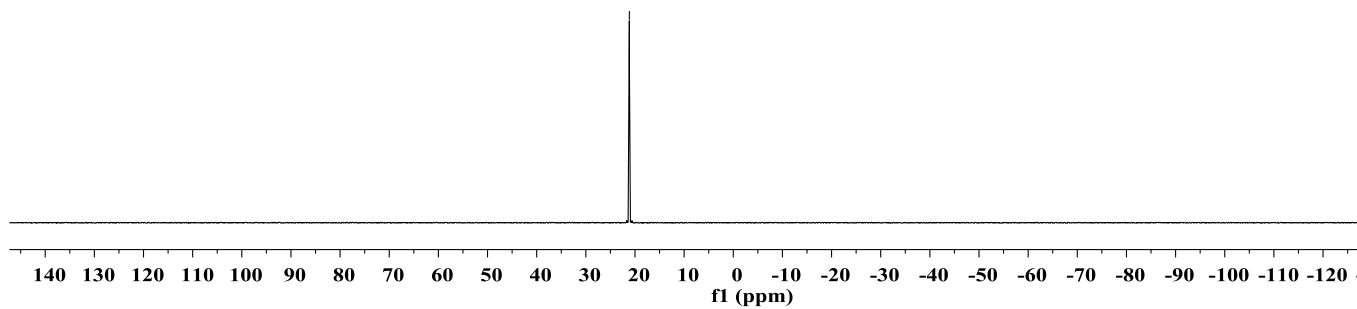
1j

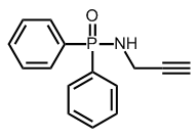
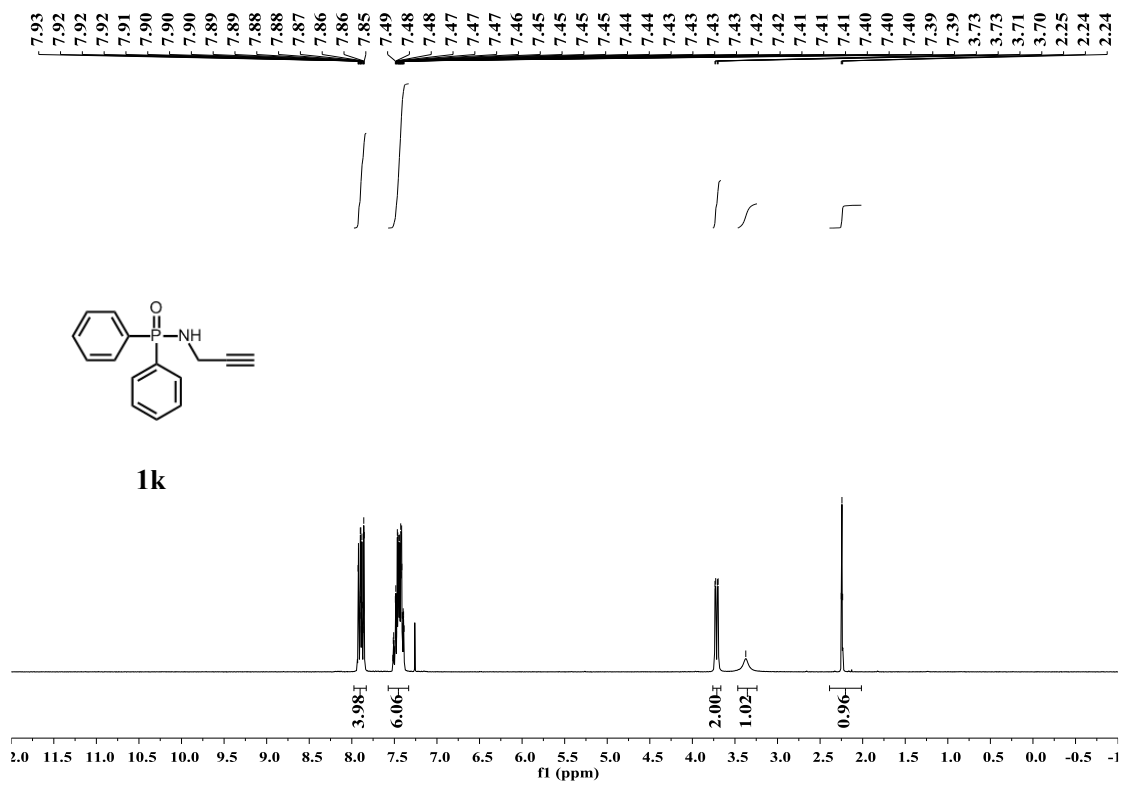


21.15

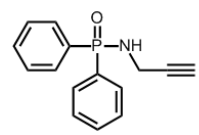


1j

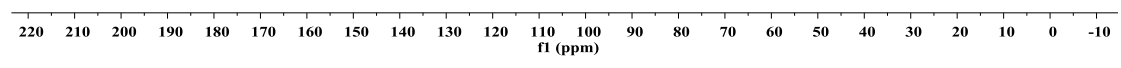


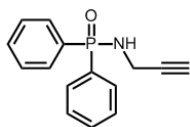


1k

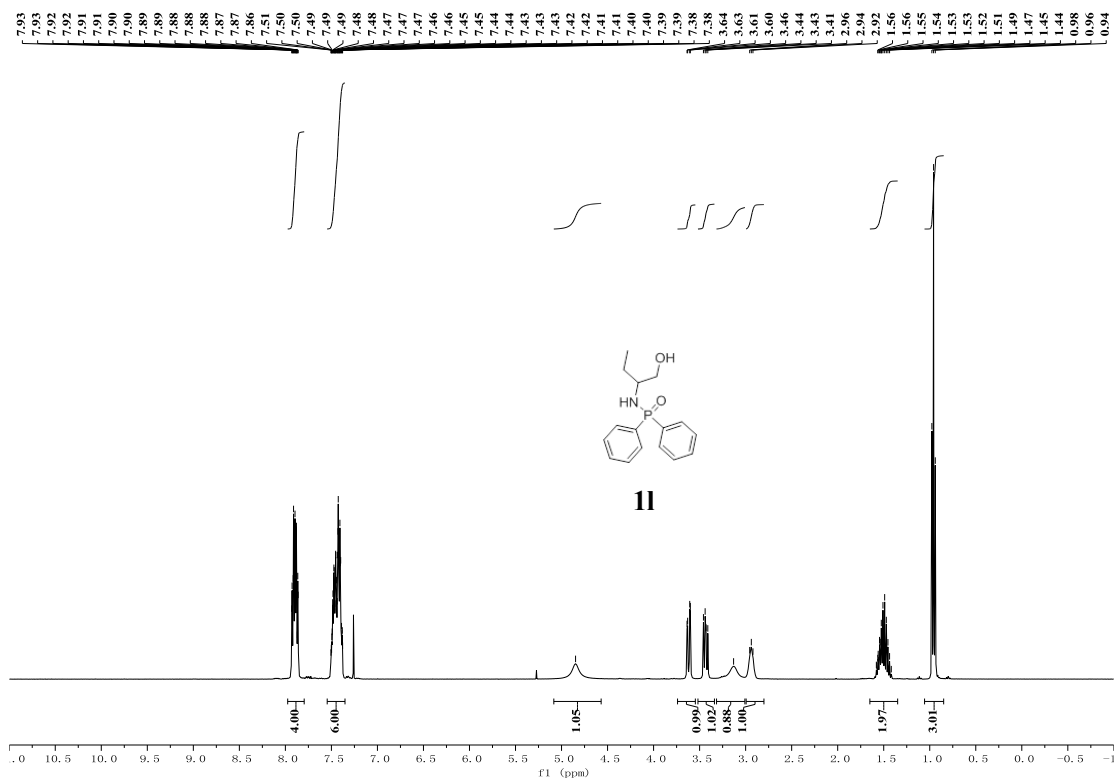
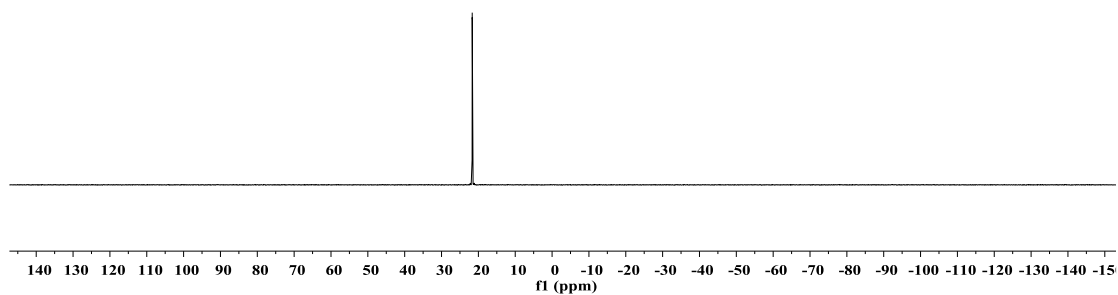


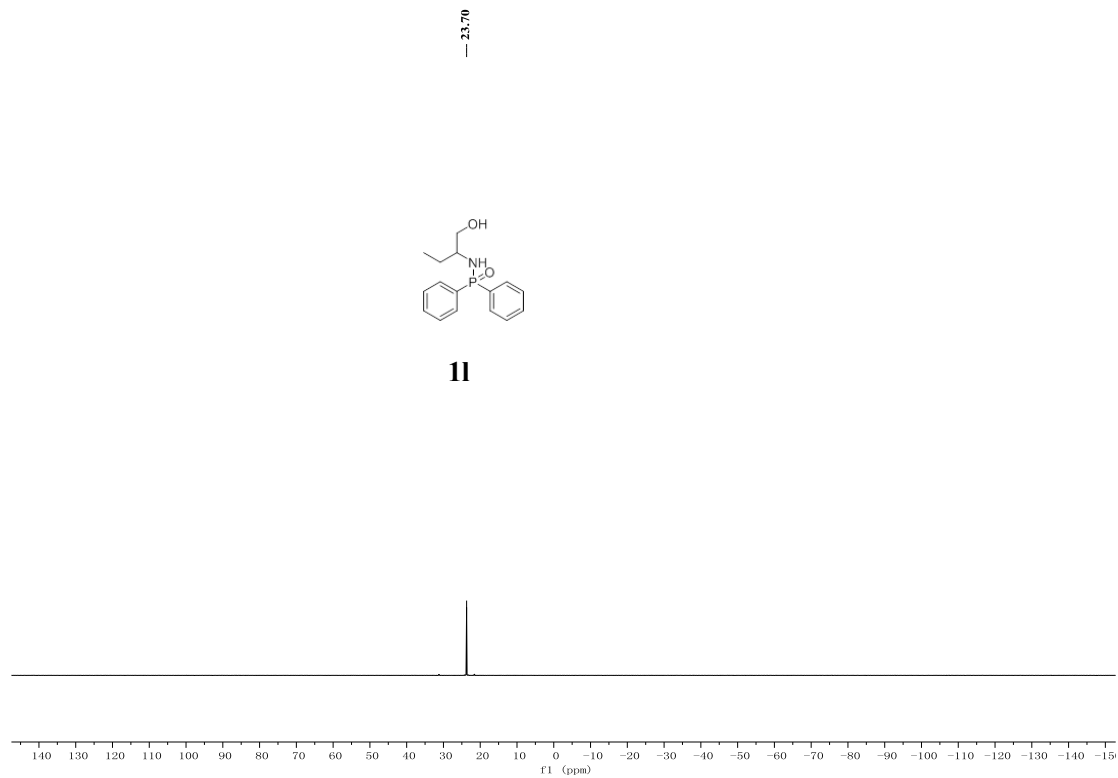
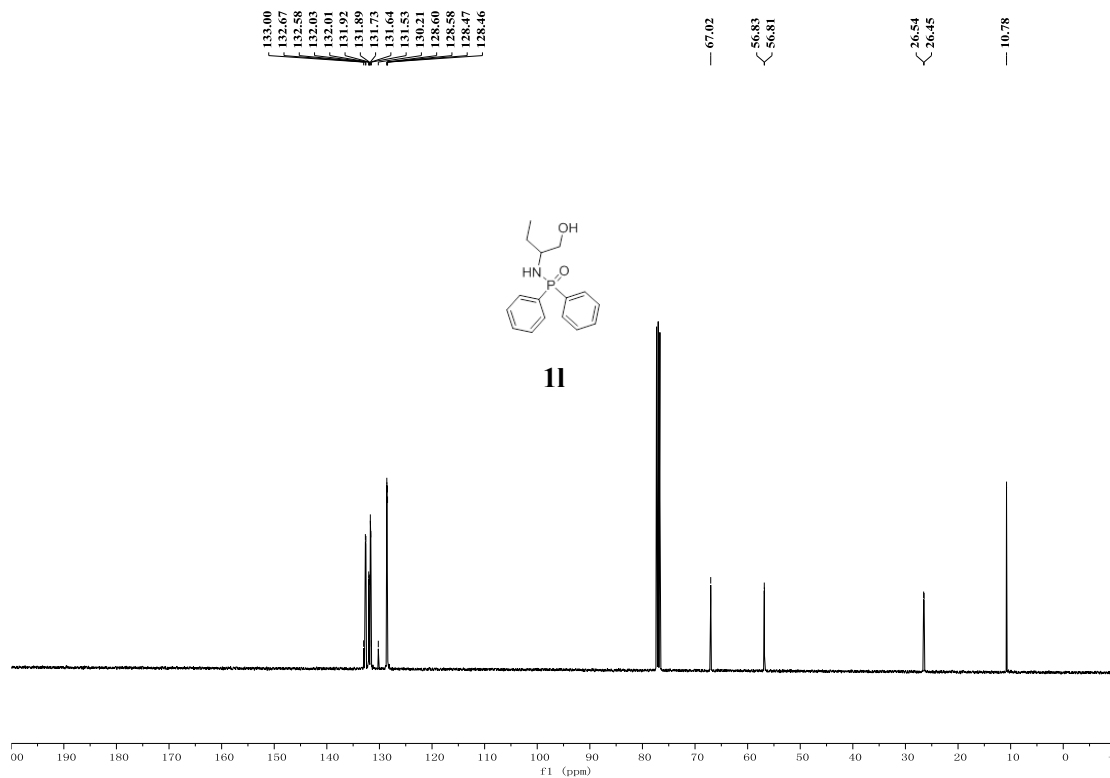
1k

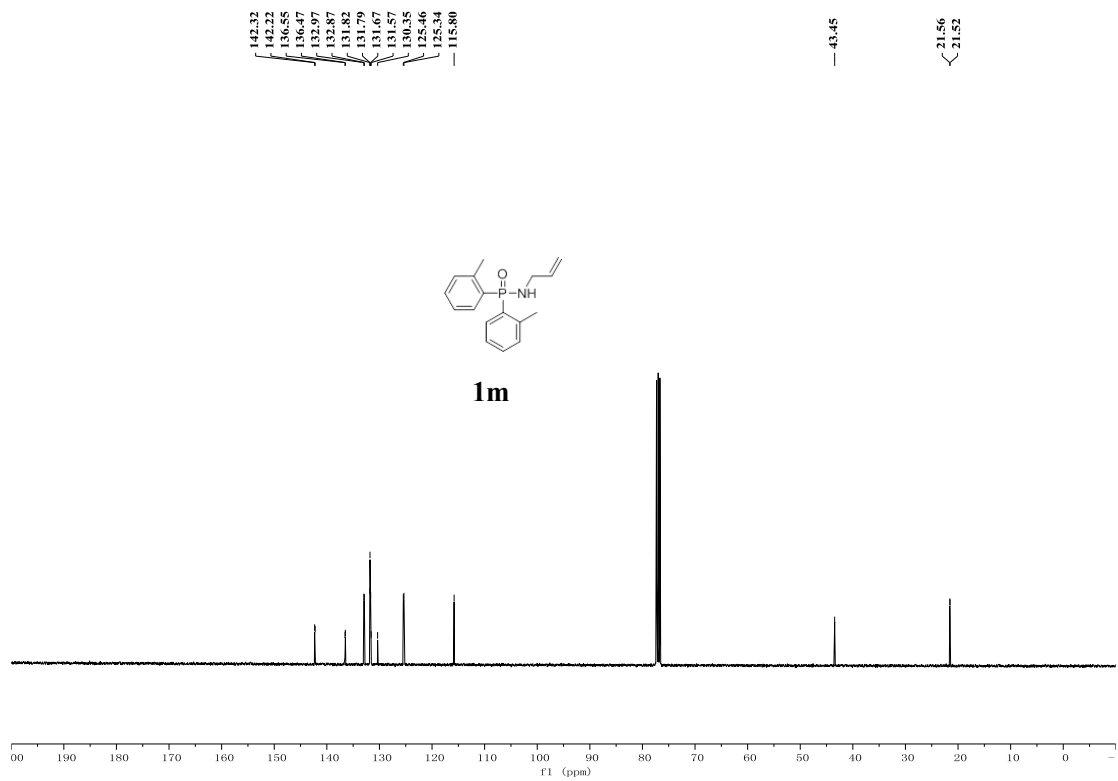
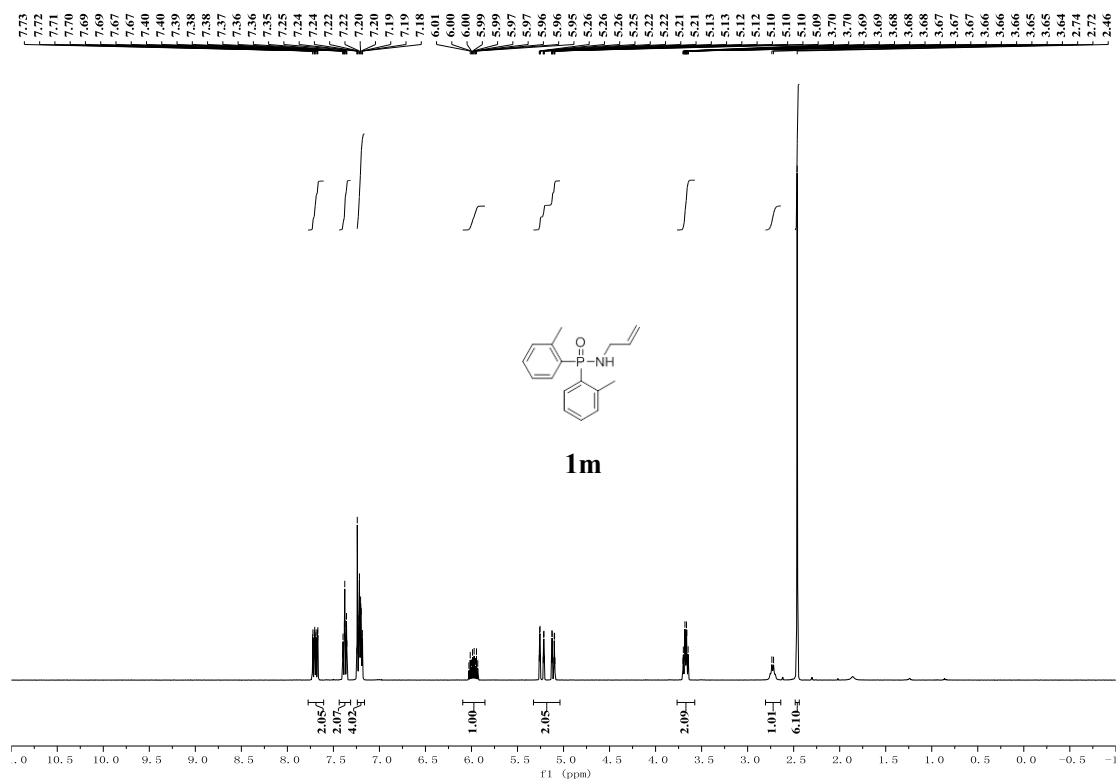




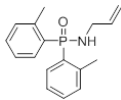
1k



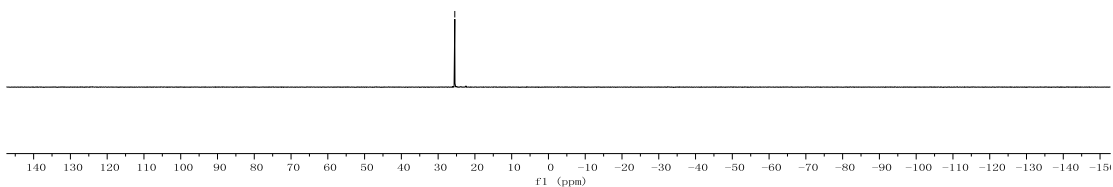




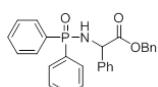
- 25.47



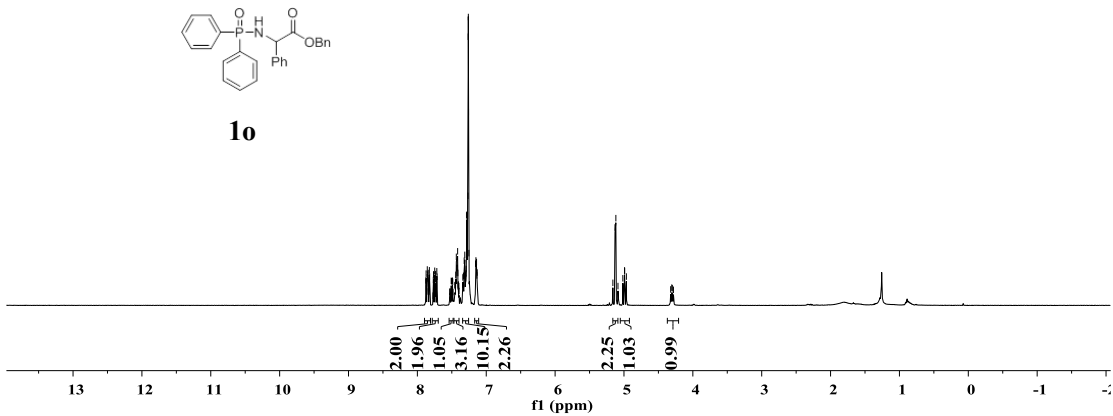
1m

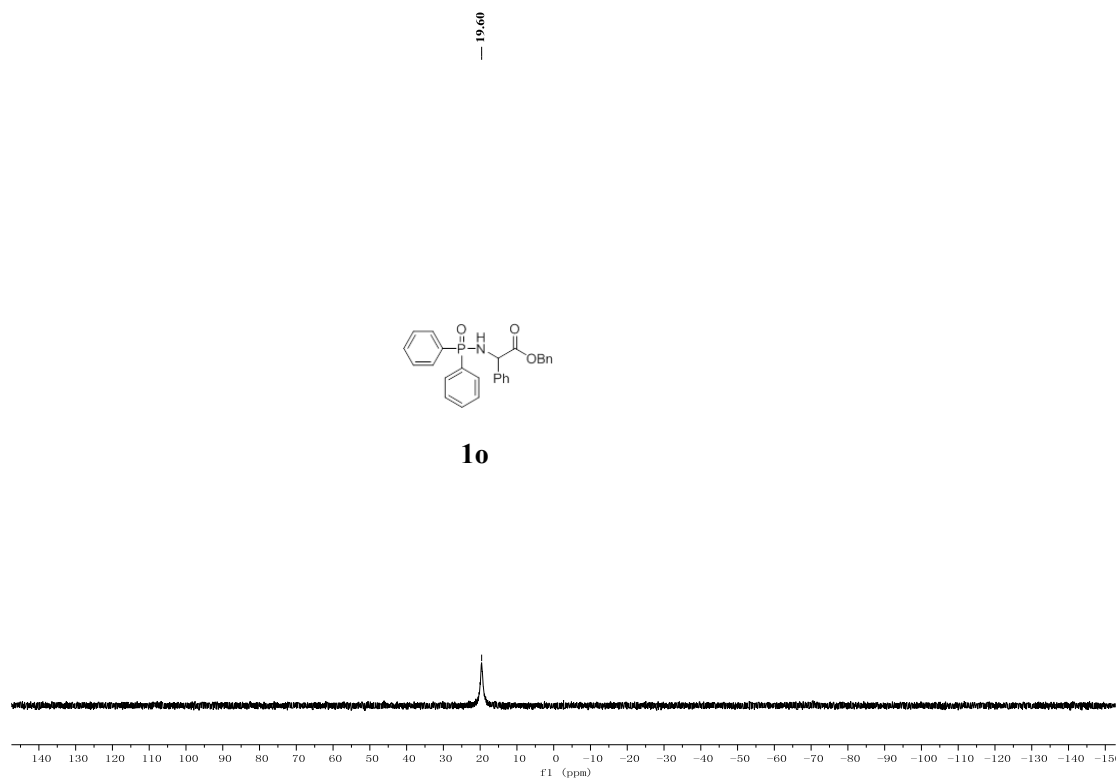
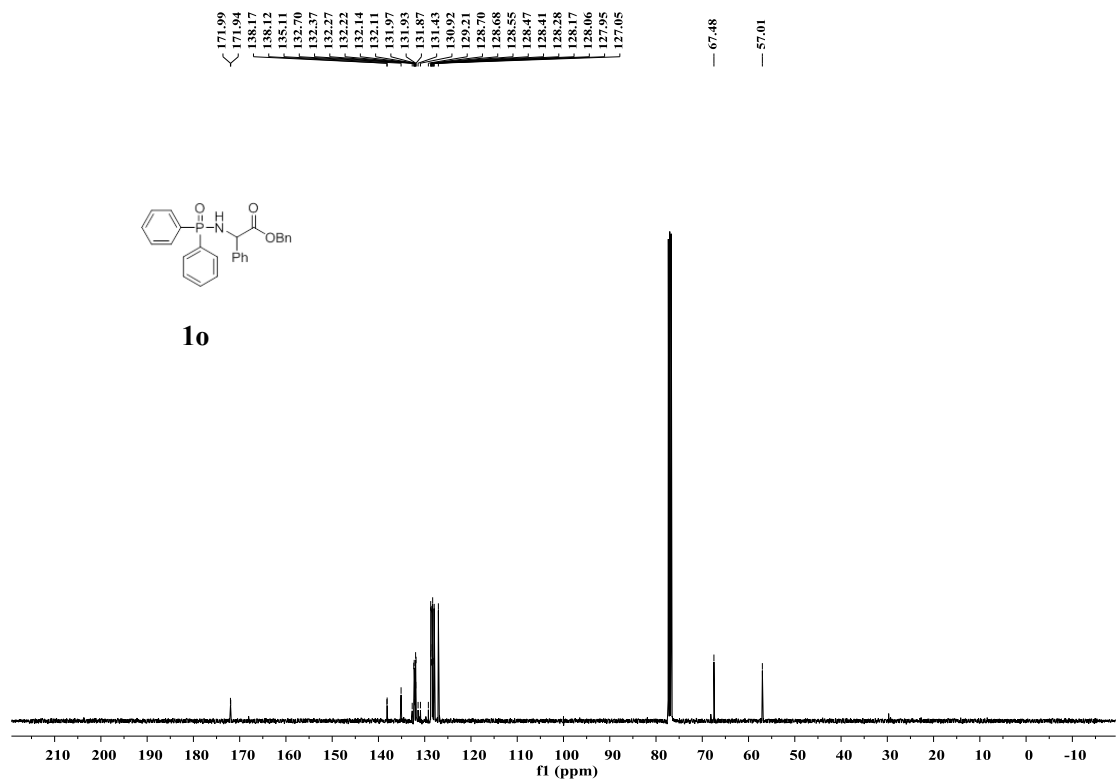


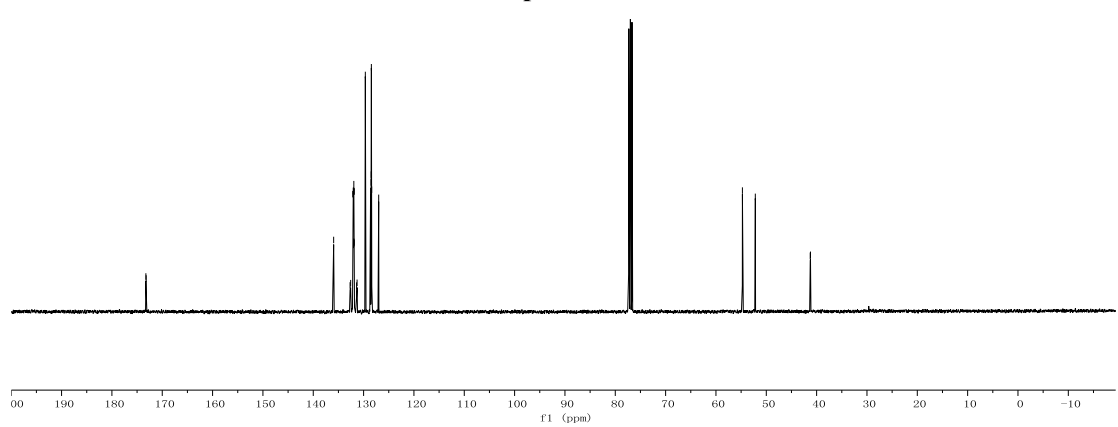
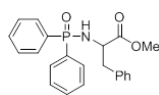
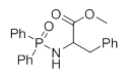
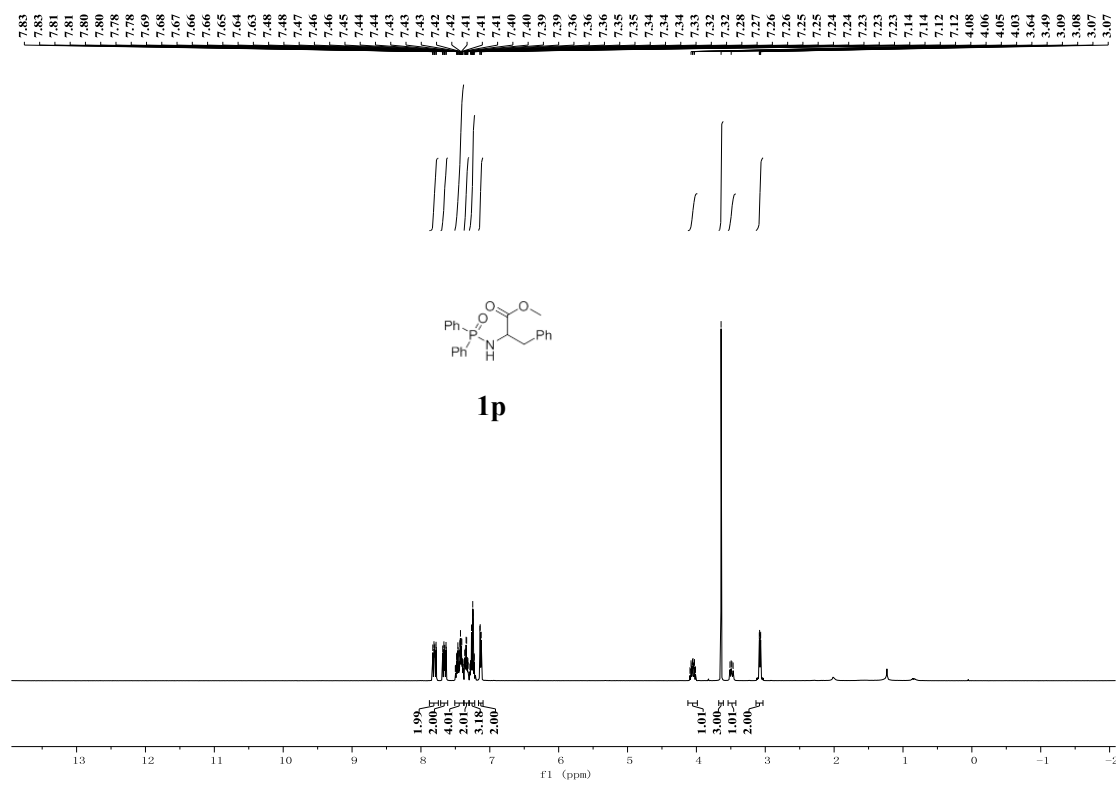
7.87
7.86
7.85
7.84
7.83
7.82
7.77
7.75
7.74
7.73
7.72
7.71
7.44
7.43
7.43
7.43
7.42
7.42
7.41
7.33
7.32
7.32
7.32
7.31
7.31
7.30
7.29
7.29
7.28
7.28
7.27
7.26
7.26
7.26
7.25
7.16
7.15
7.14
7.14
7.14
7.13
5.12
4.99
4.97



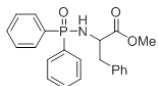
1o



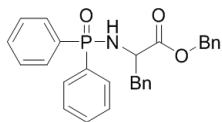
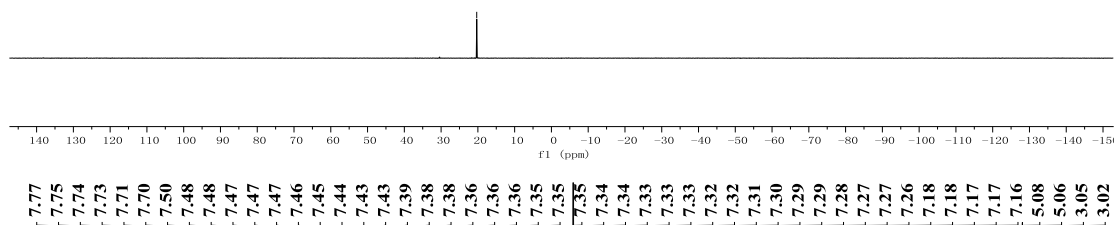




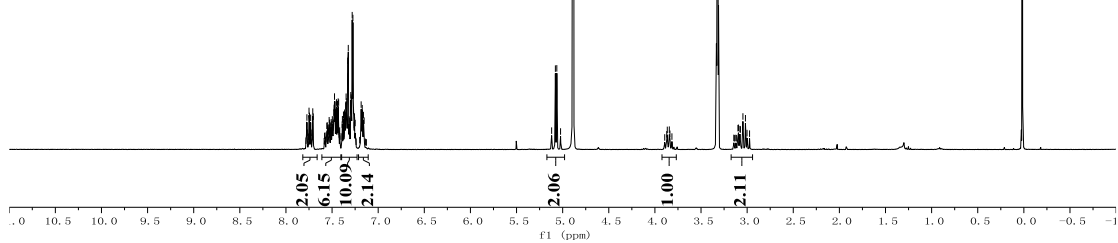
— 20.31

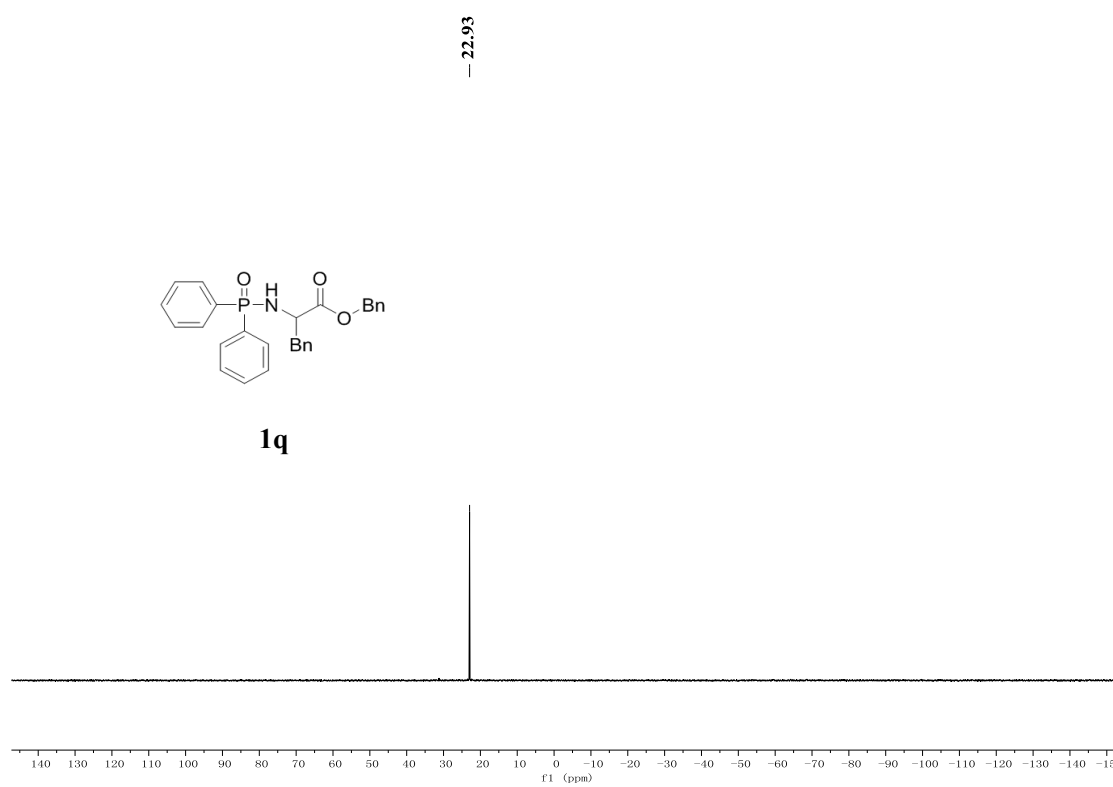
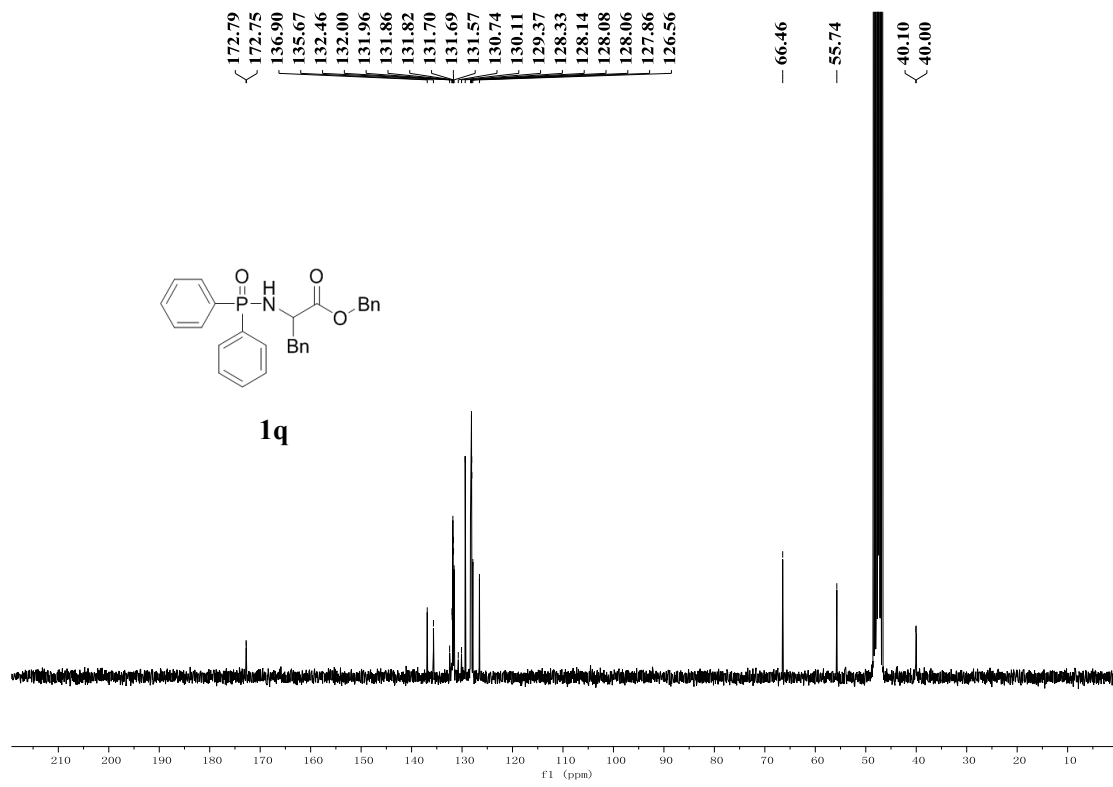


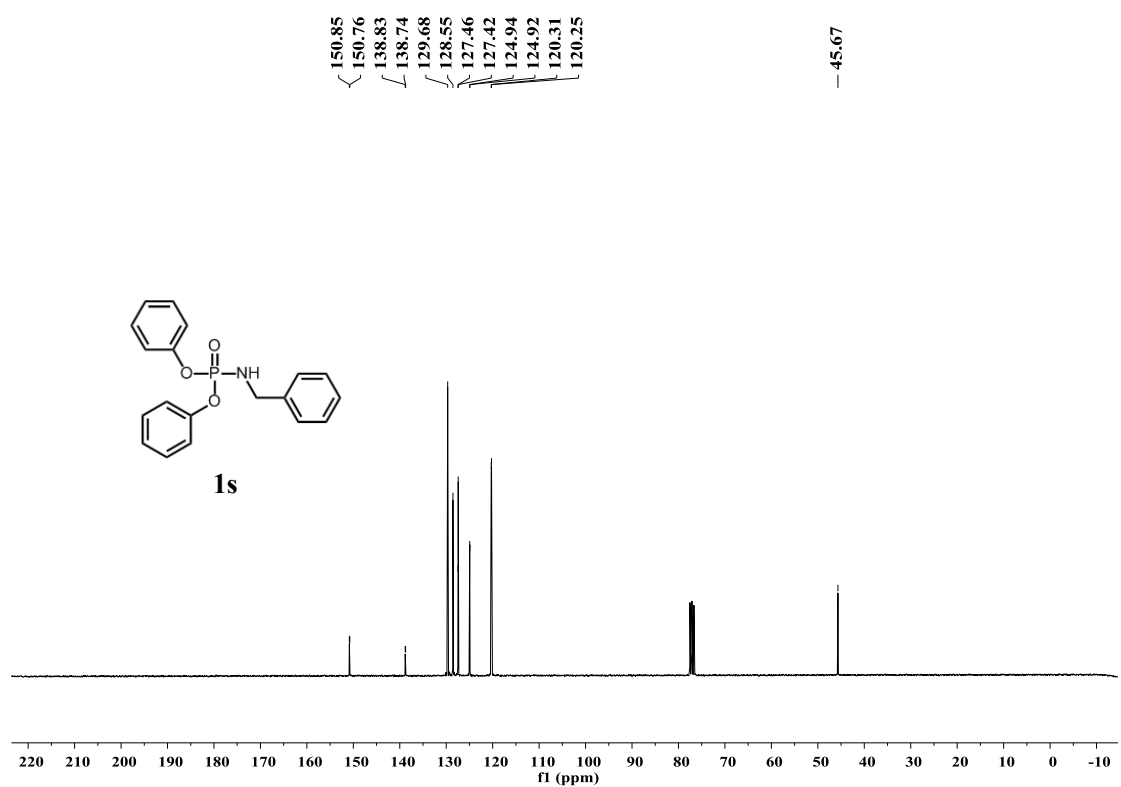
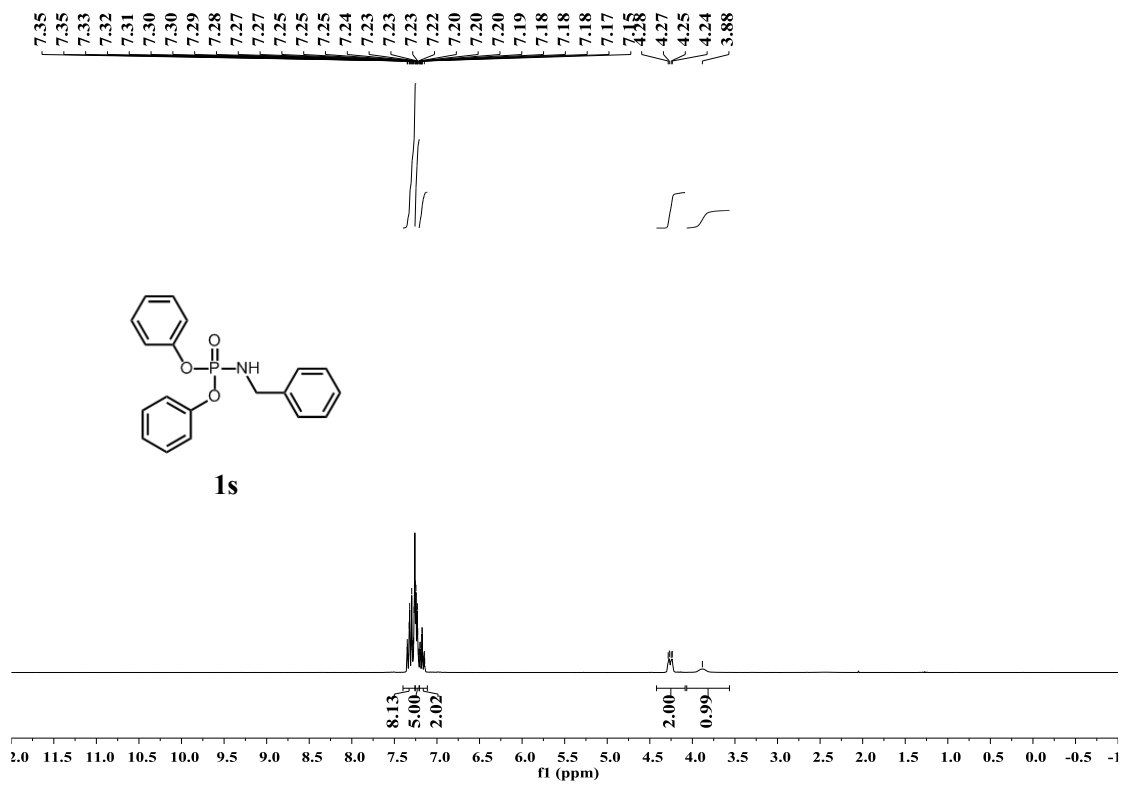
1p

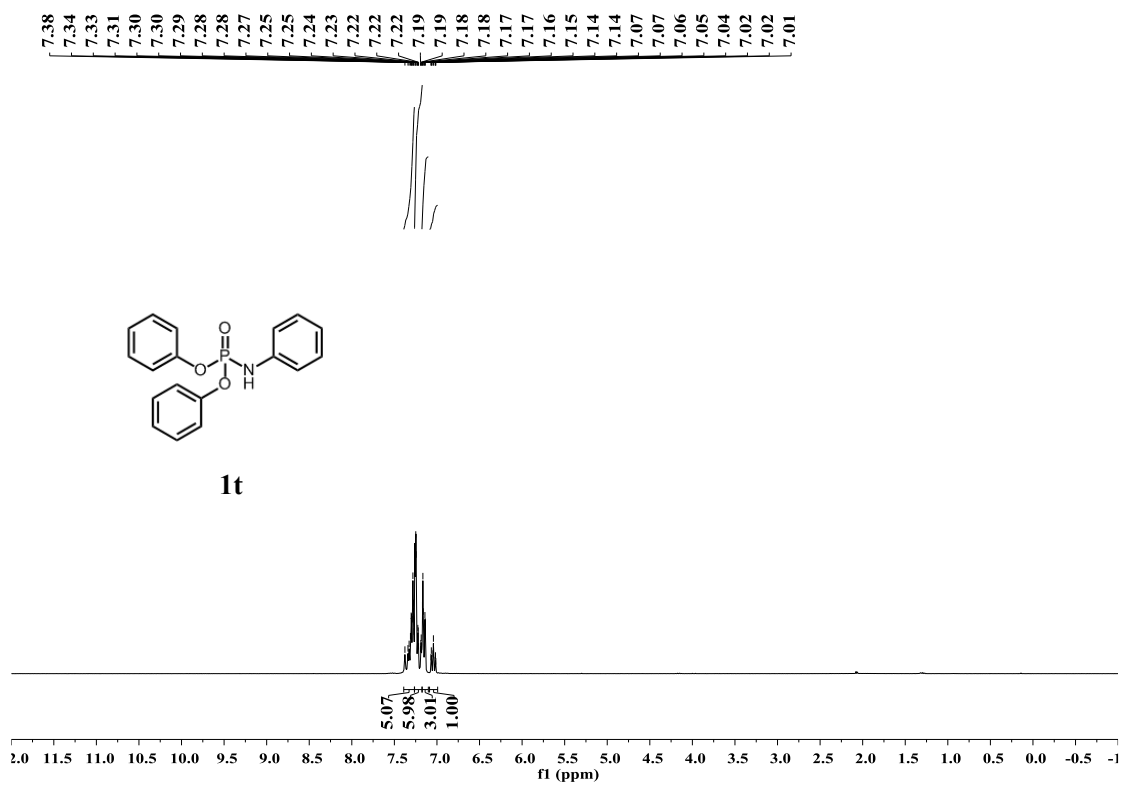
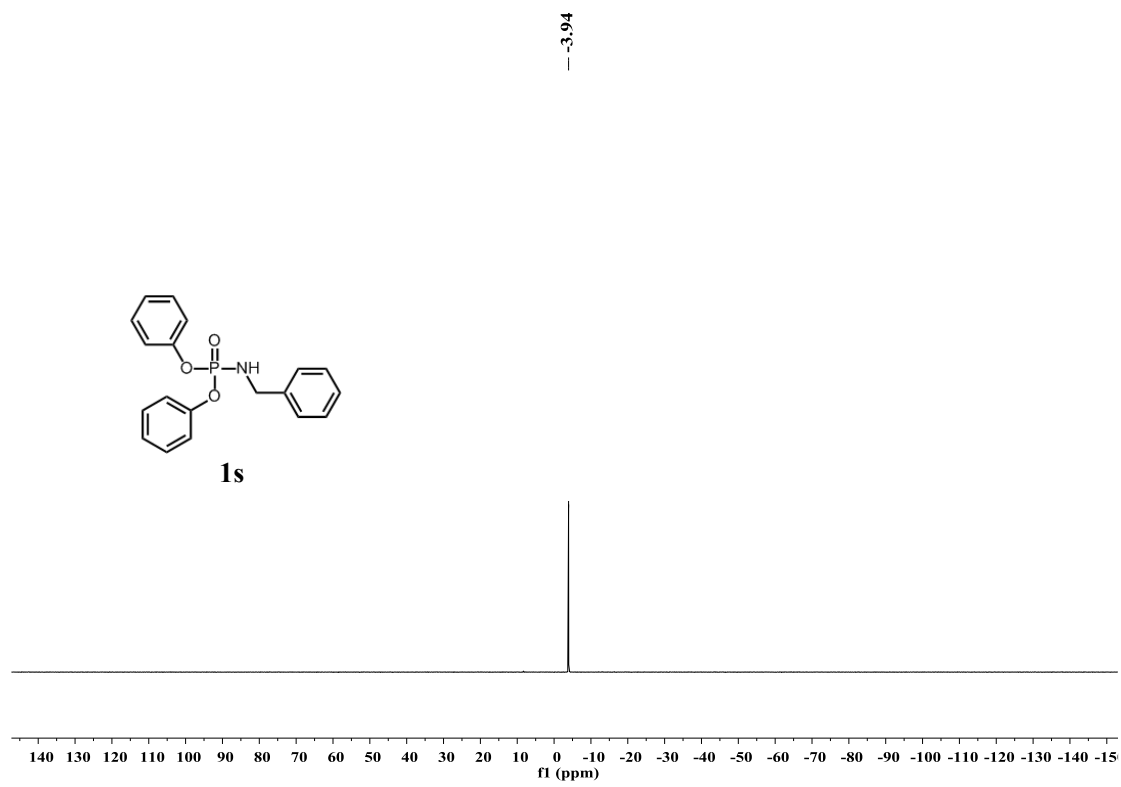


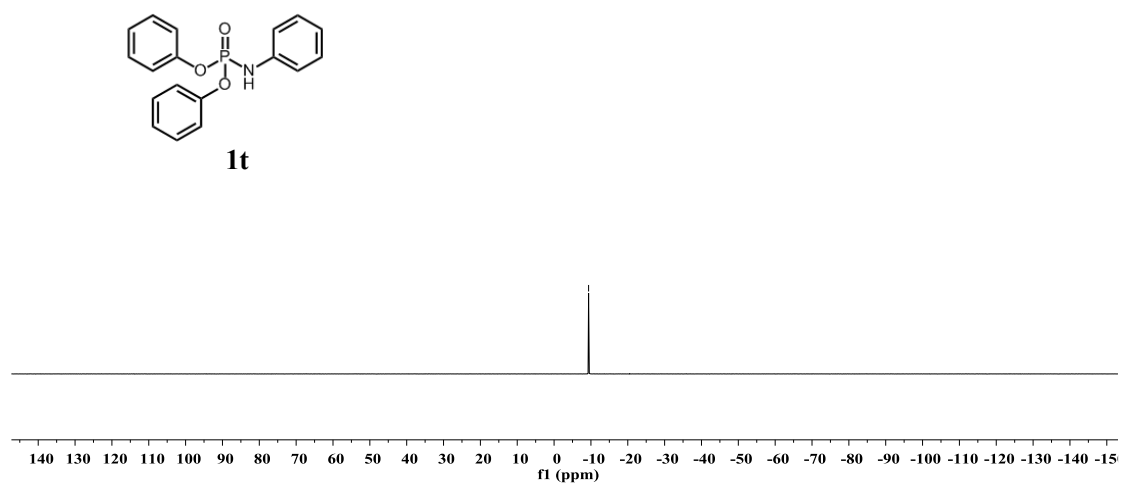
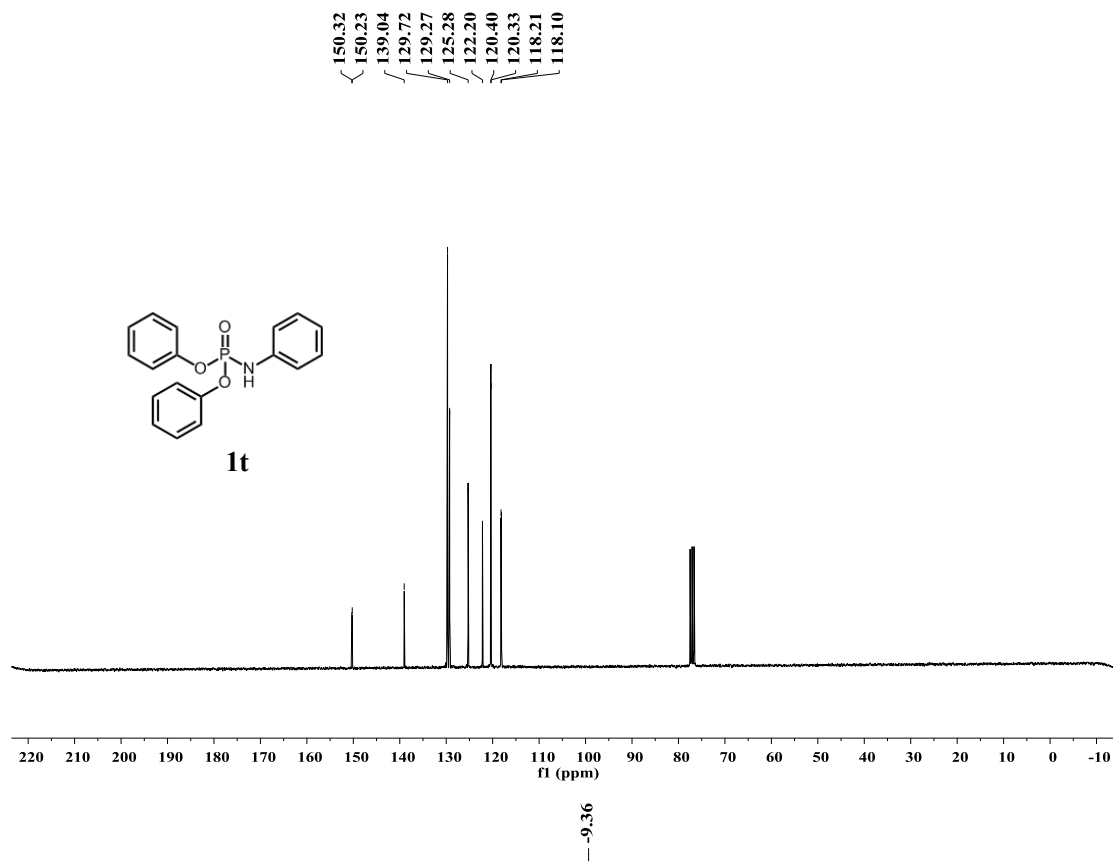
1q

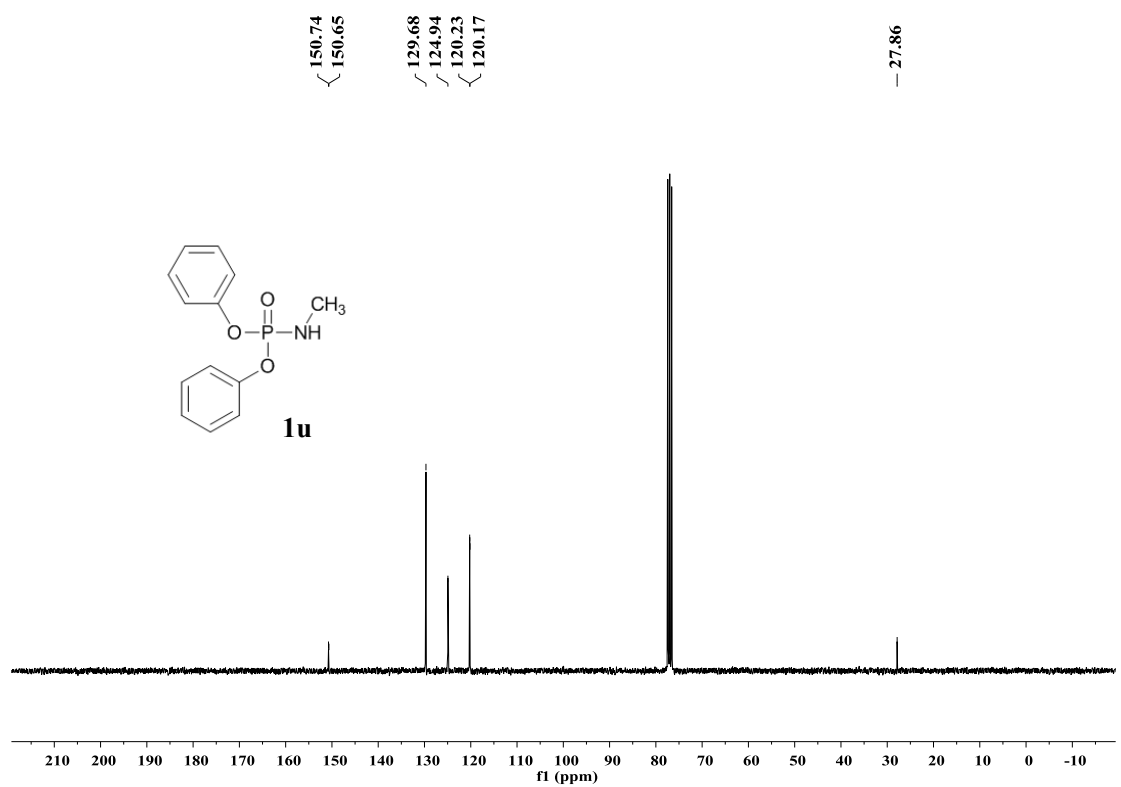
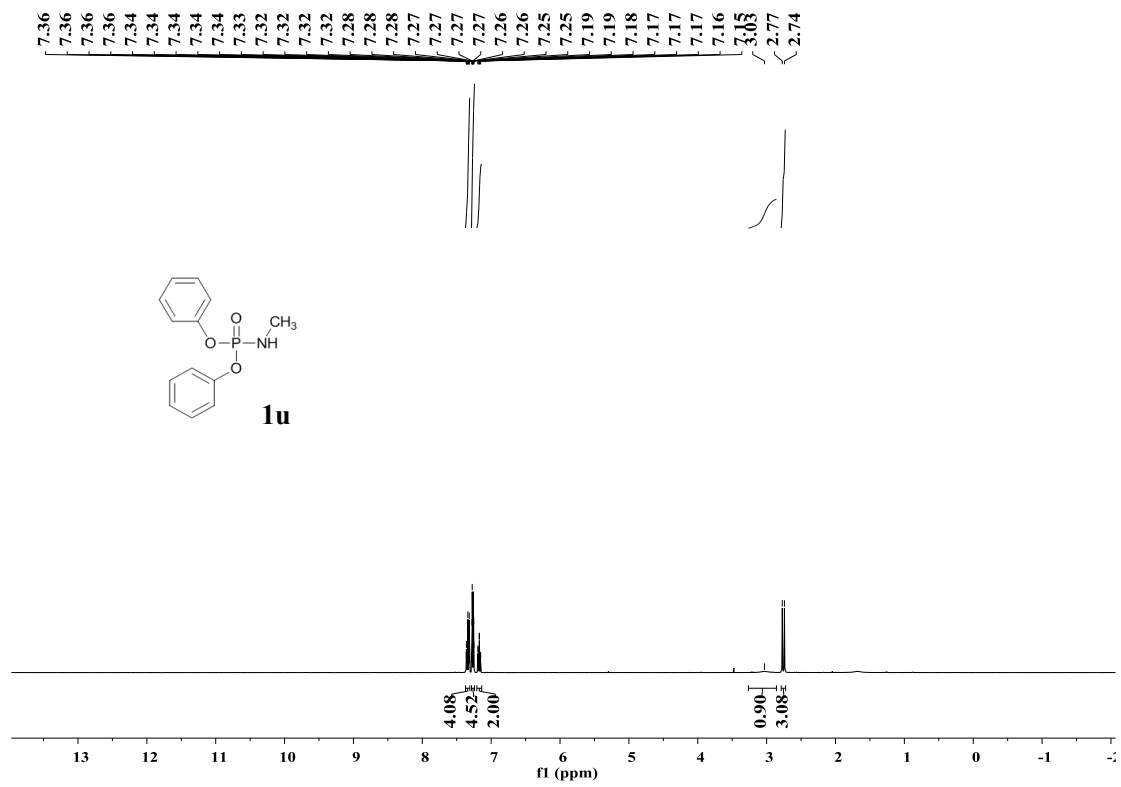




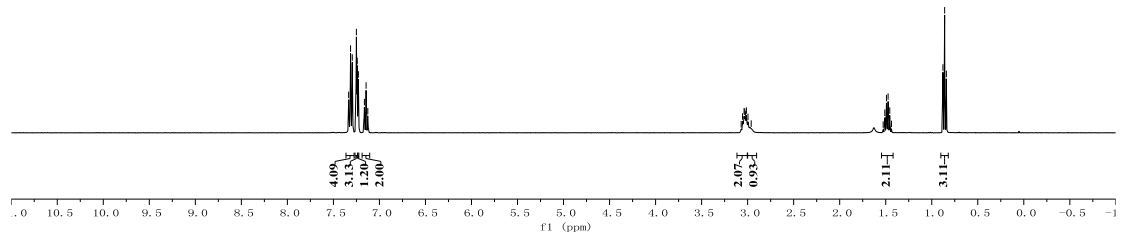
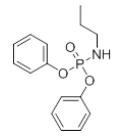
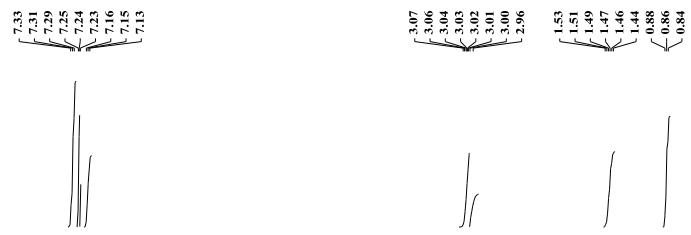
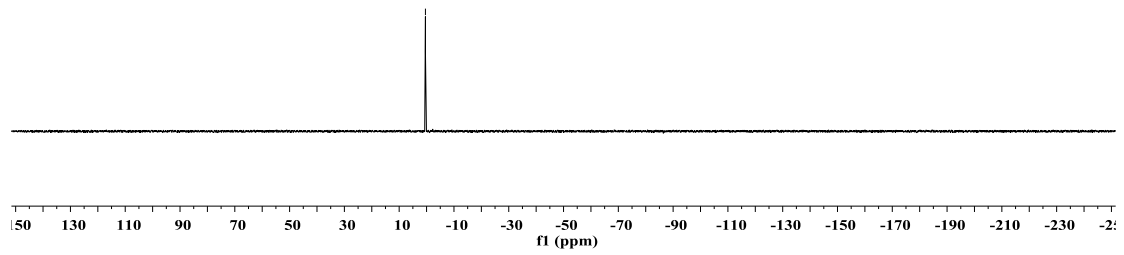
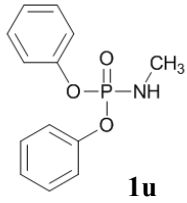


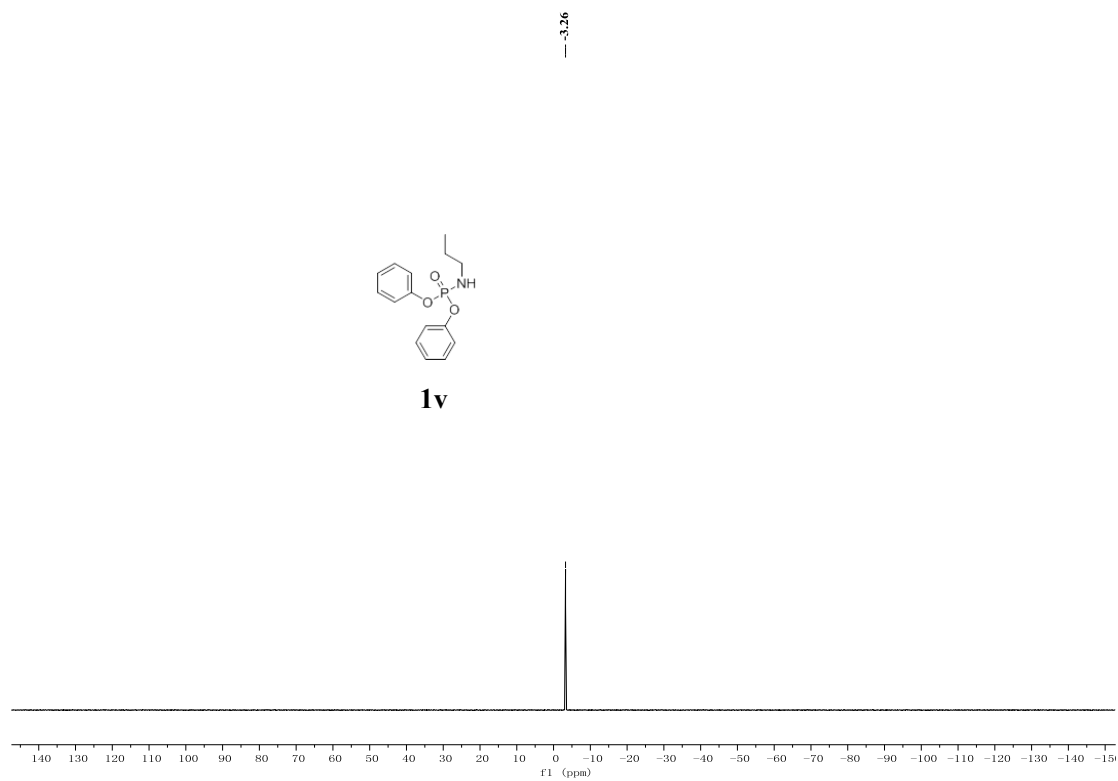
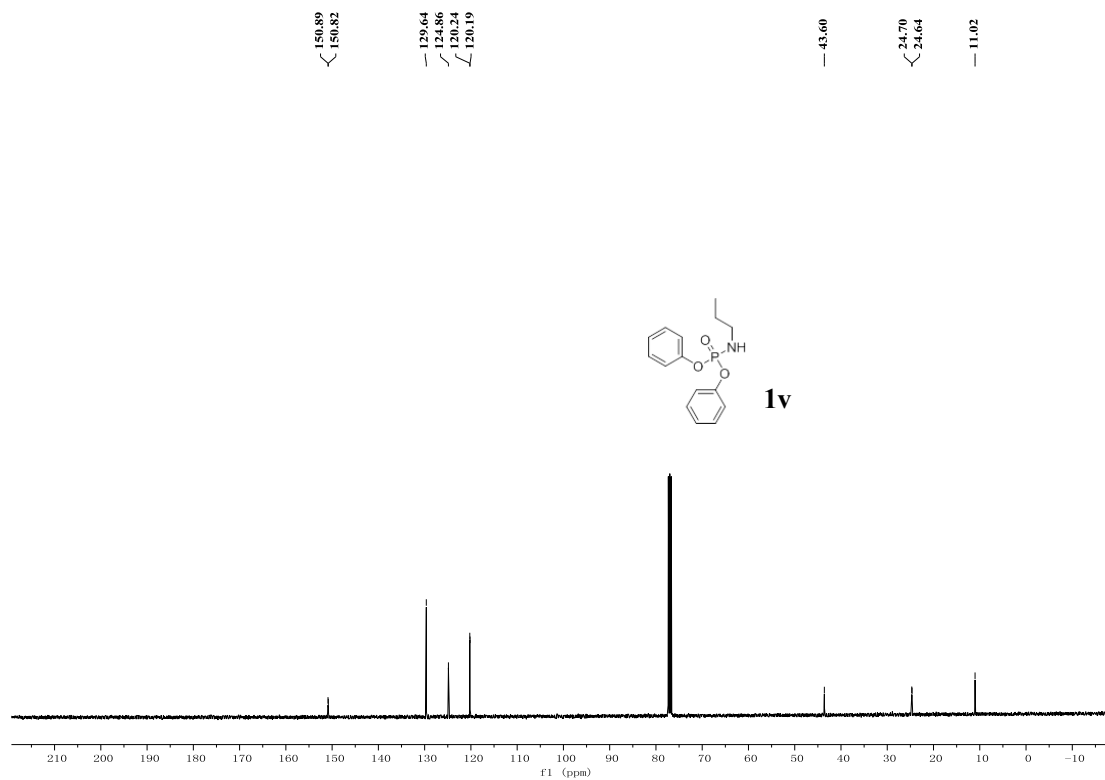


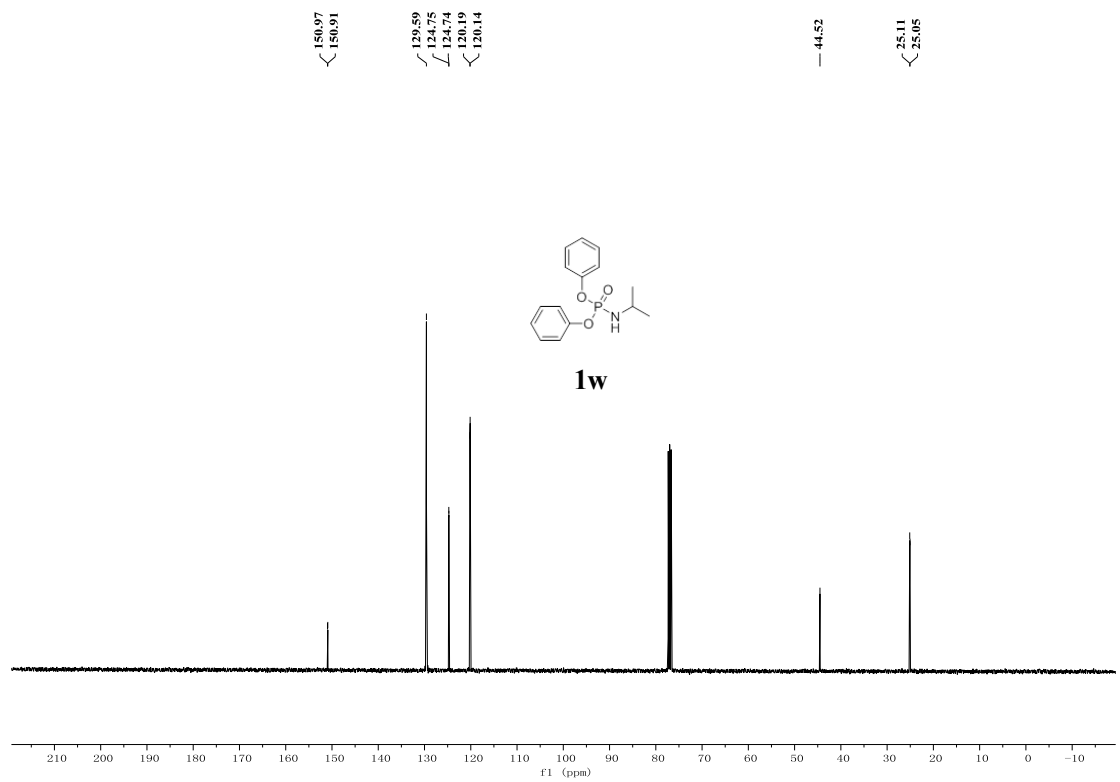
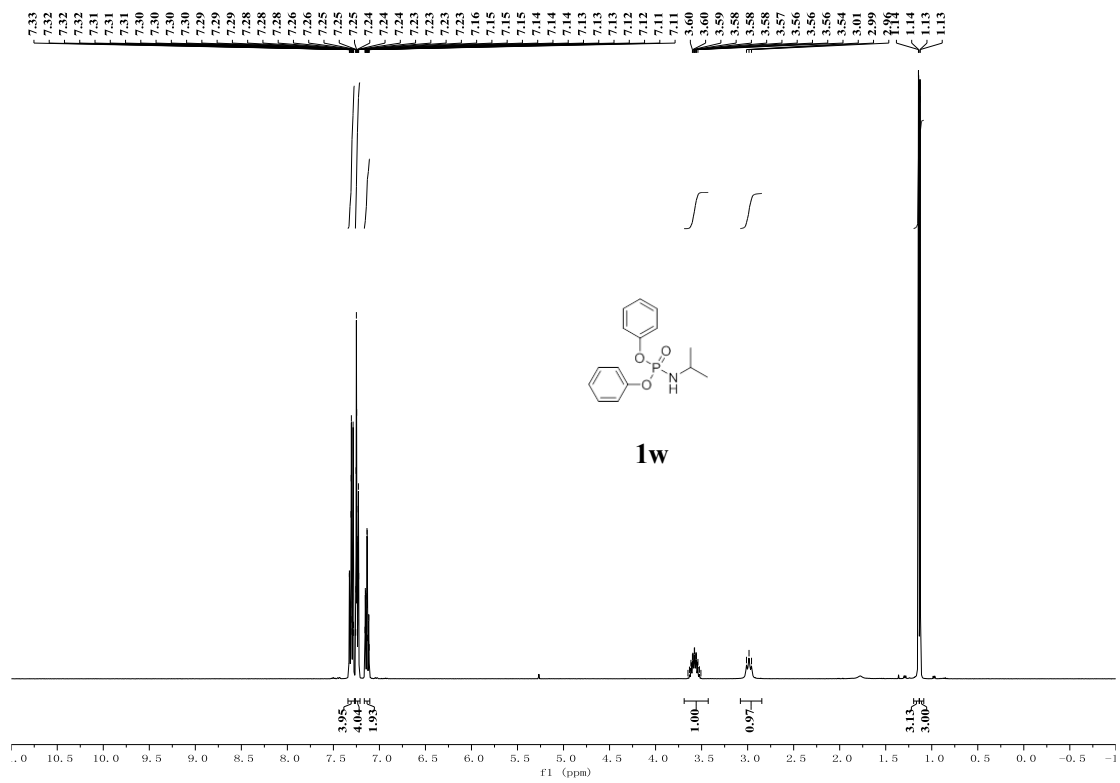




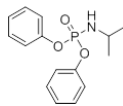
-0.42



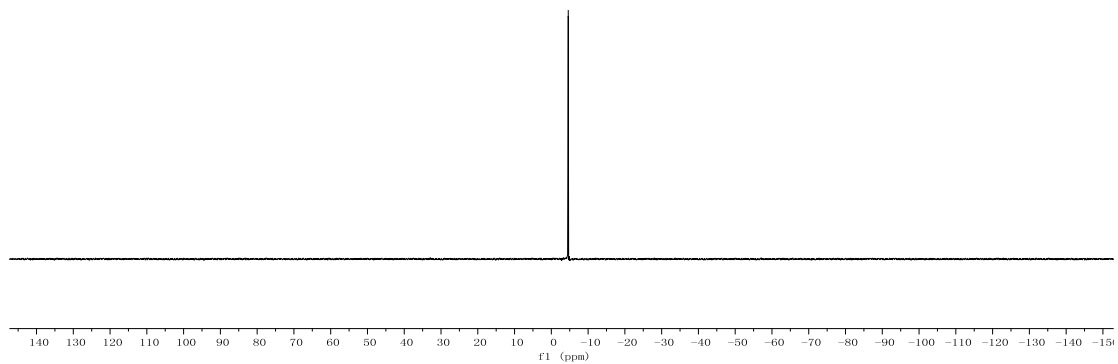




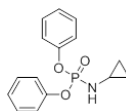
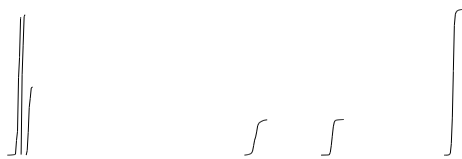
-4.60



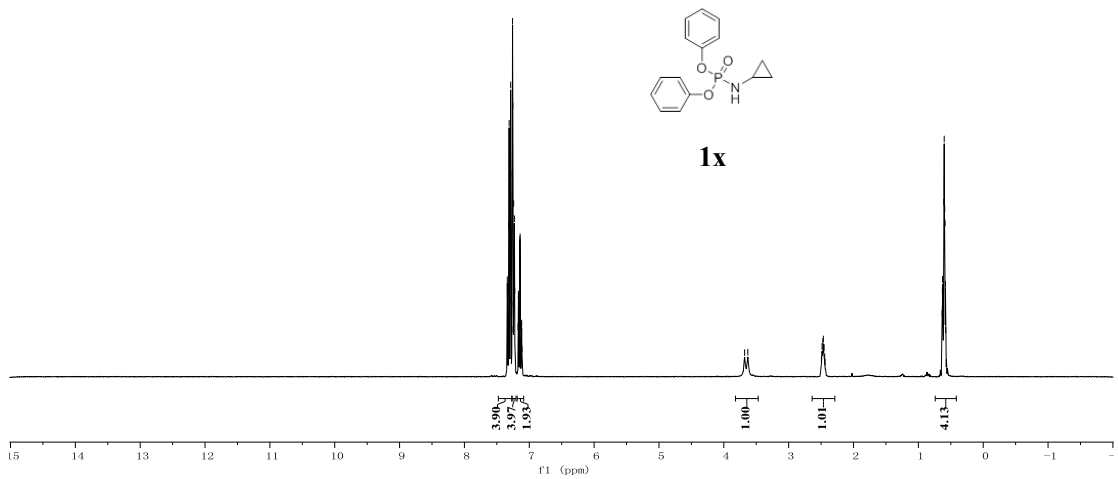
1w



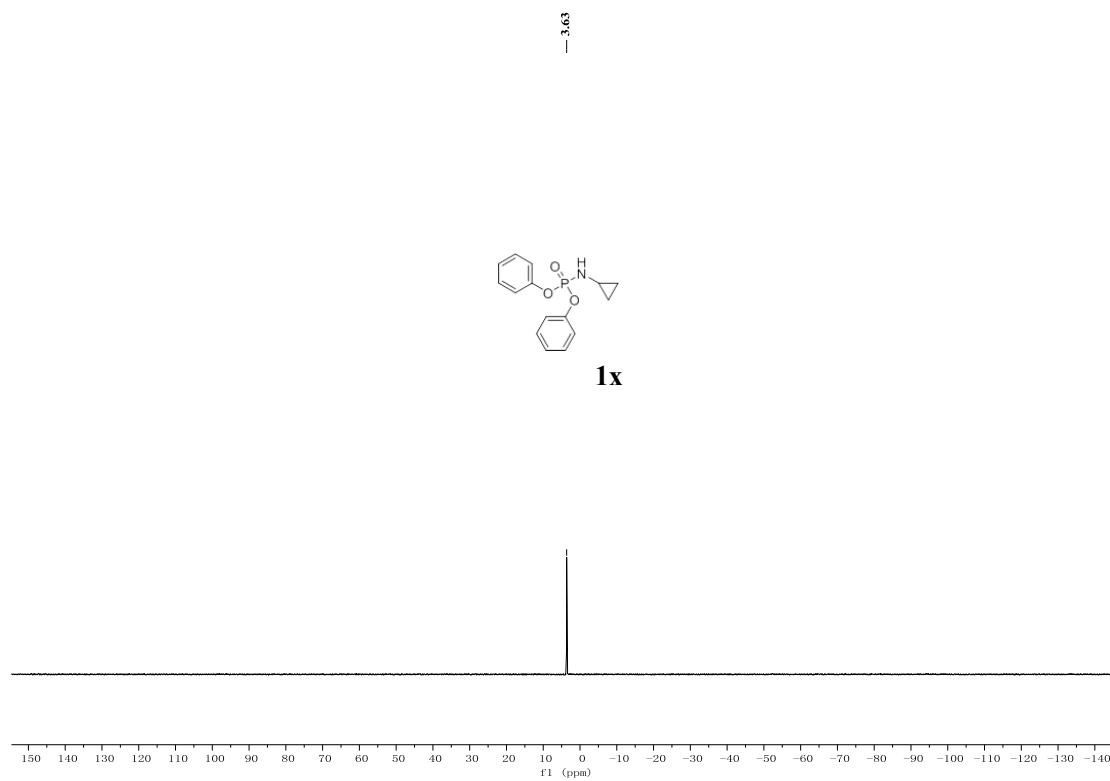
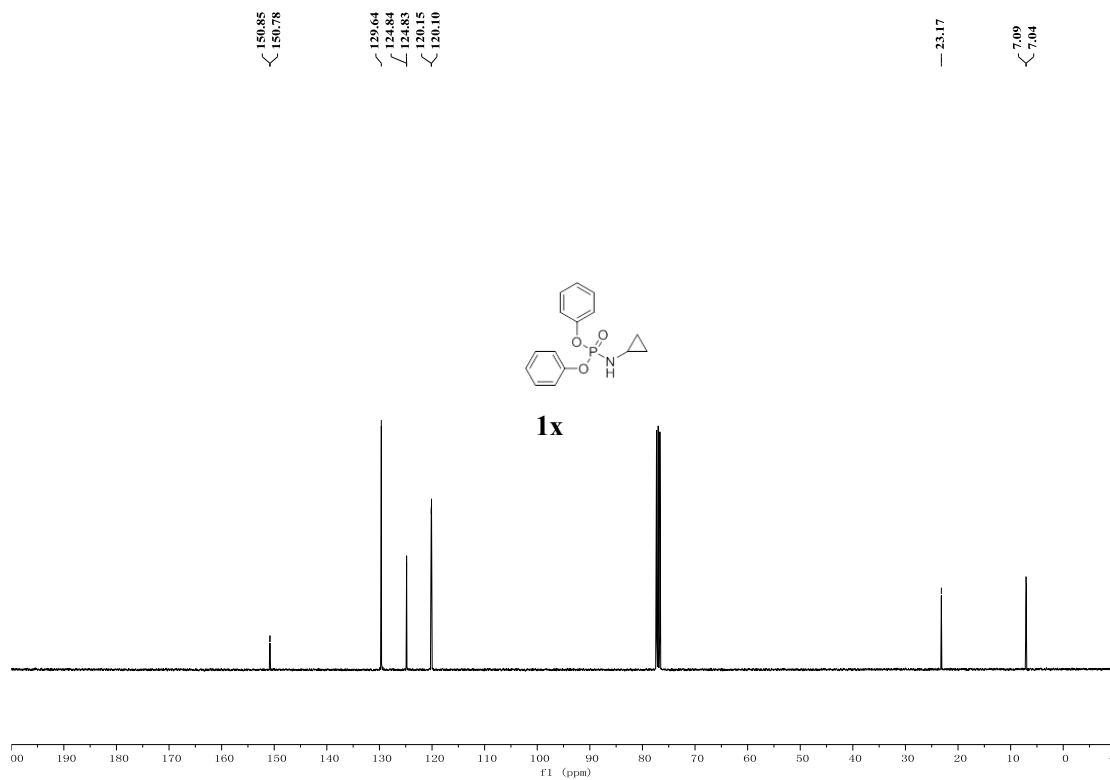
7.34
7.33
7.32
7.31
7.30
7.29
7.28
7.27
7.26
7.25
7.25
7.25
7.24
7.24
7.23
7.23
7.22
7.17
7.17
7.16
7.16
7.15
7.15
7.14
7.14
7.14
7.13
7.13
7.12
7.12
7.12
7.11
7.11
3.68
3.63
2.50
2.49
2.47
2.47
2.45
2.45
2.44
2.44
0.63
0.63
0.62
0.62
0.61
0.61
0.60
0.60
0.59
0.59
0.58
0.58

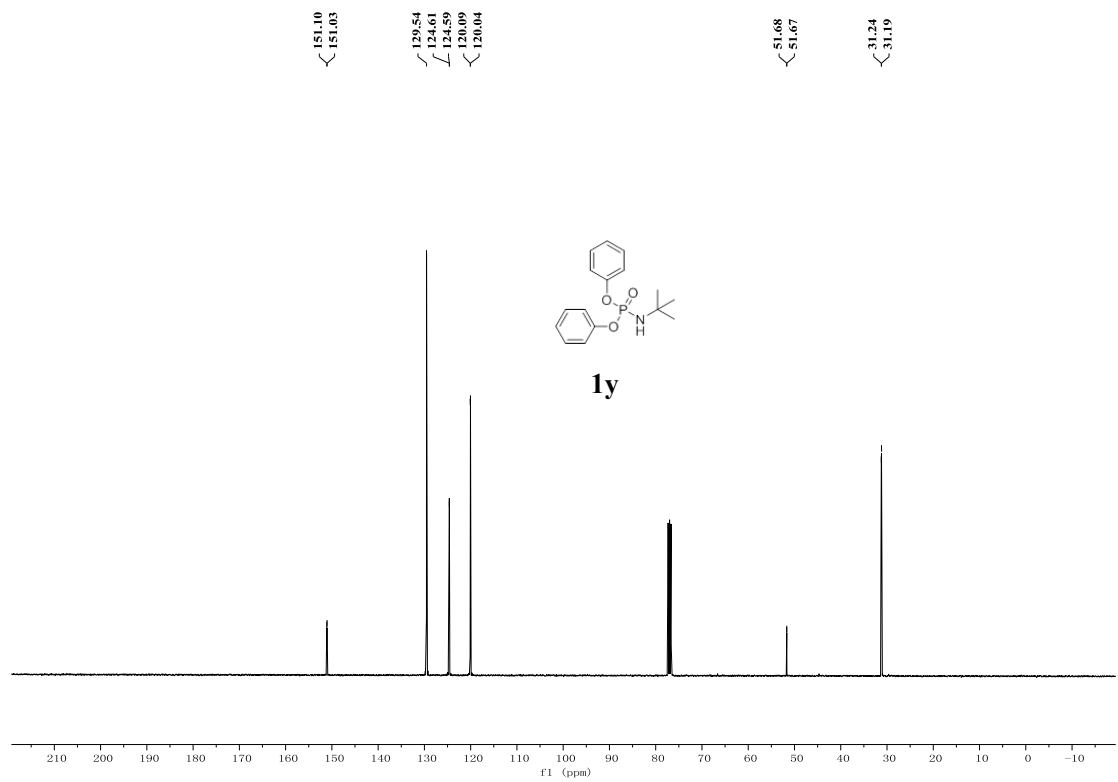
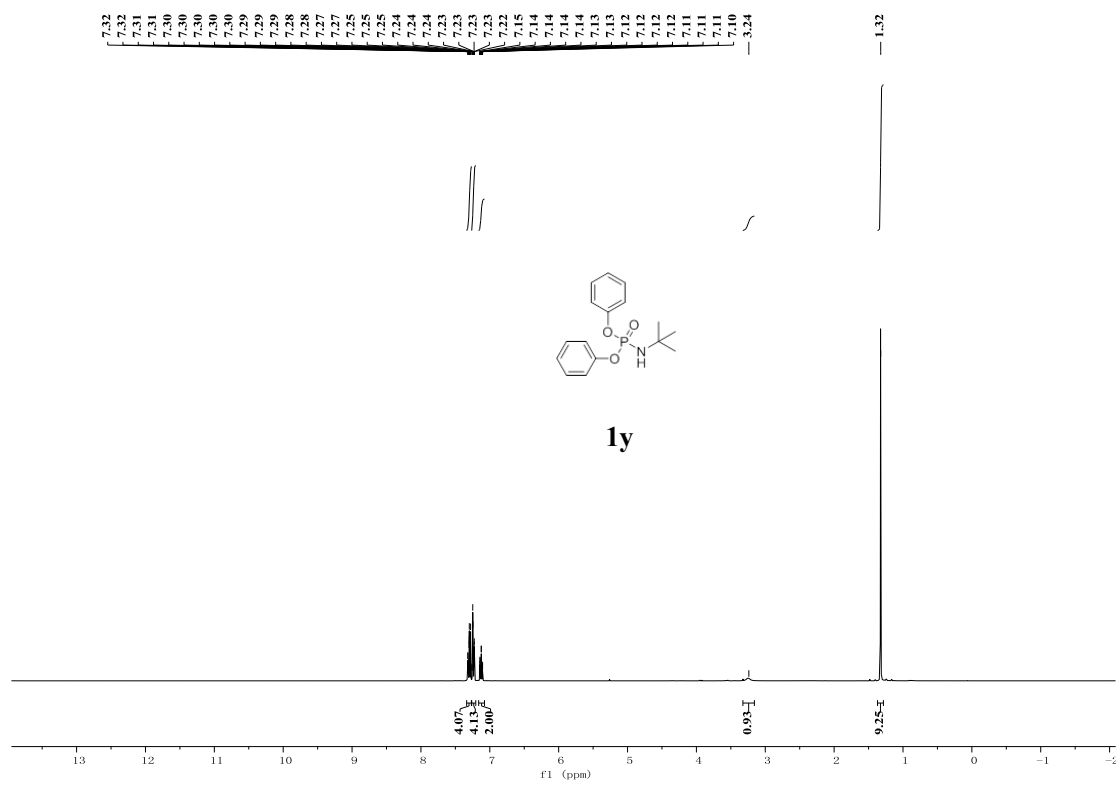


1x

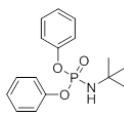


3.90
3.97
1.93
1.00
1.01
4.13

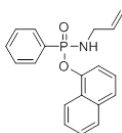
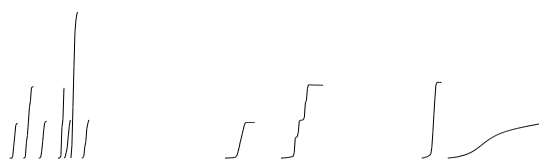
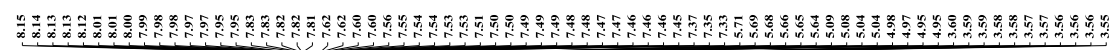
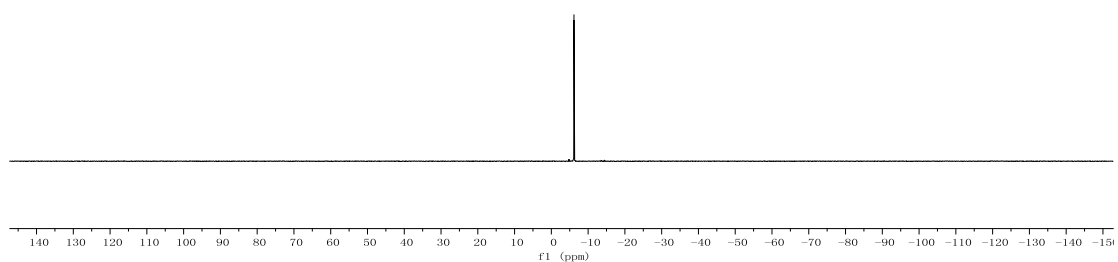




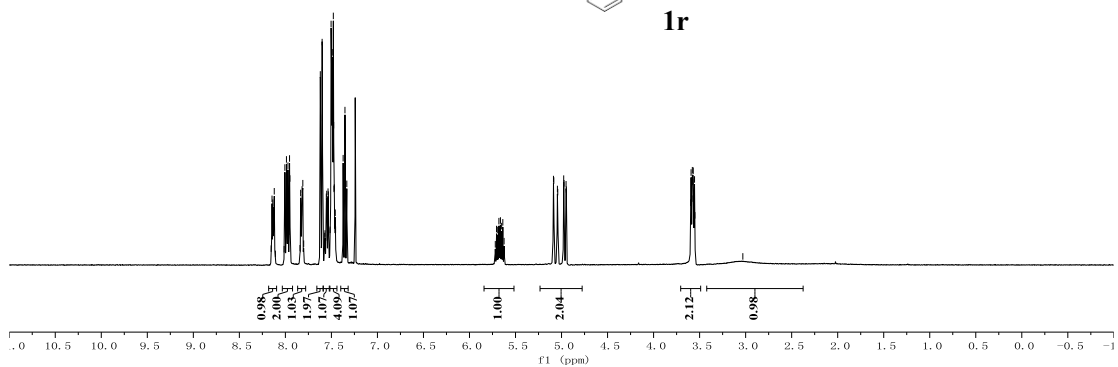
-6.15



1y

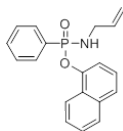


1r

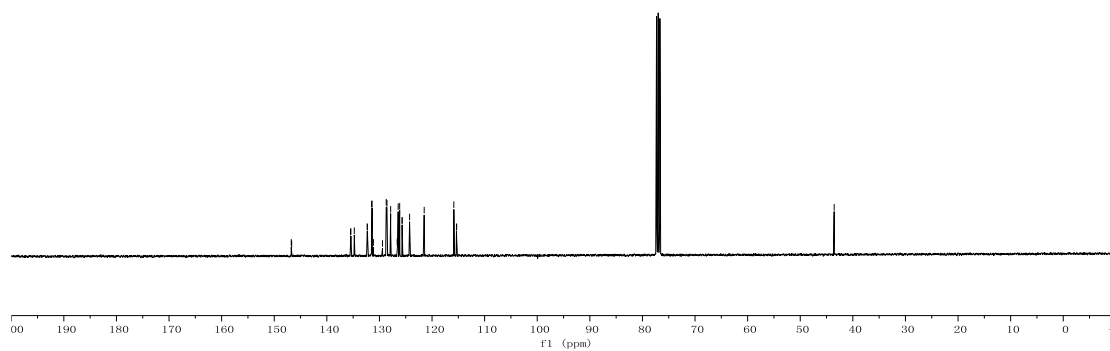


146.77
146.68
135.49
135.43
134.77
132.72
132.26
131.50
131.40
131.18
131.18
129.42
128.71
128.57
127.87
126.63
126.57
126.44
126.15
125.69
125.68
124.27
121.49
115.86
115.32

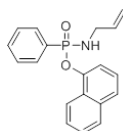
— 43.55



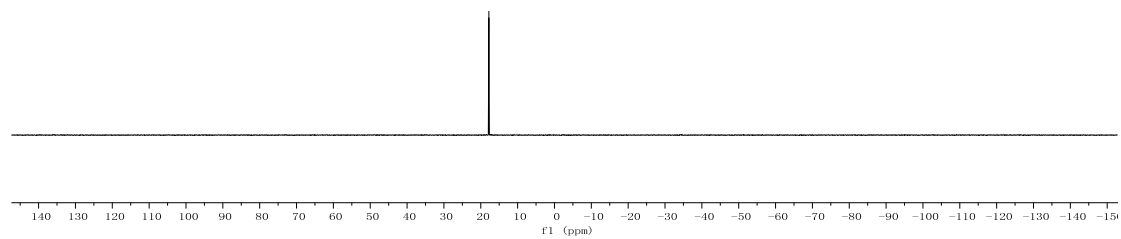
1y

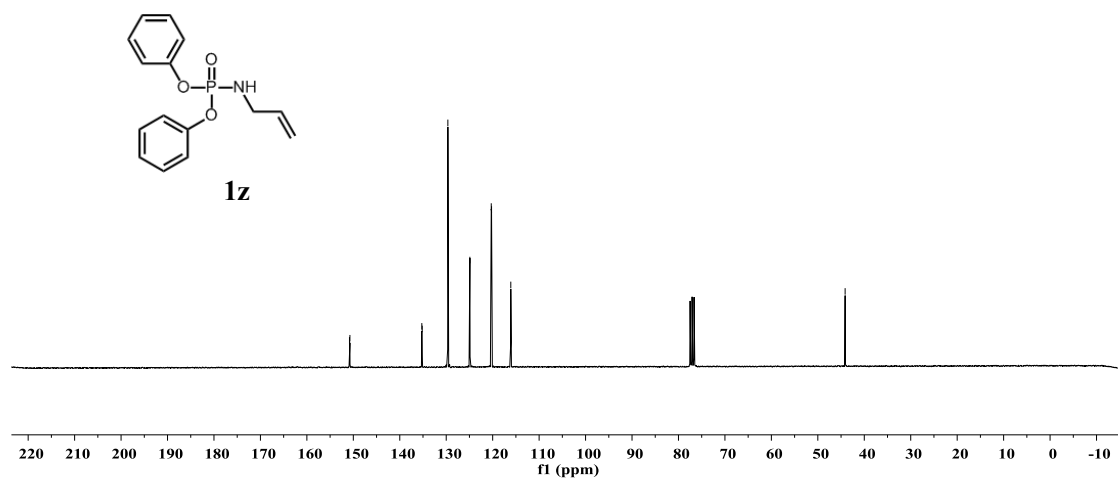
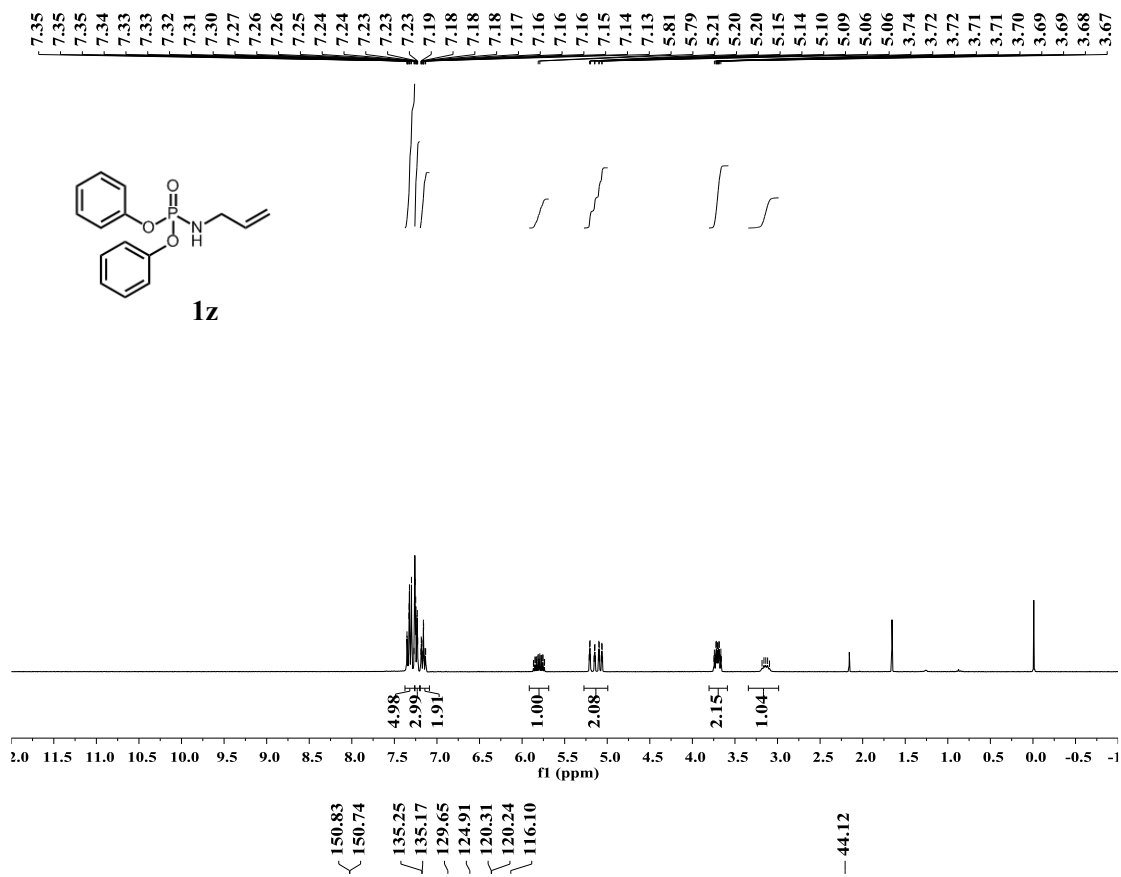


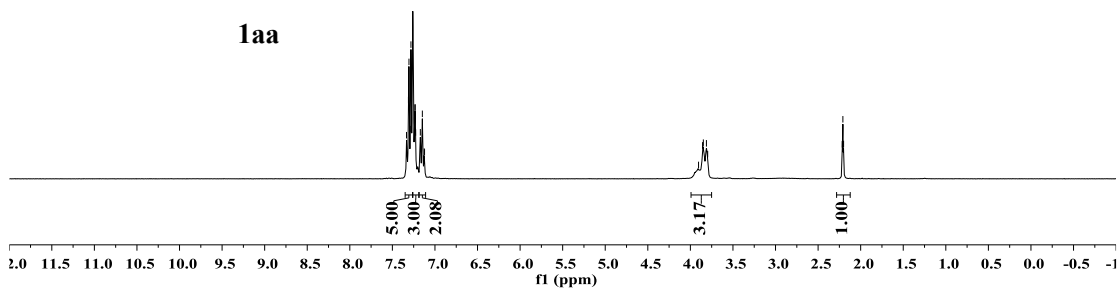
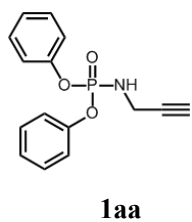
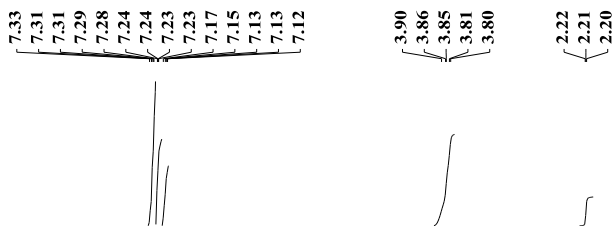
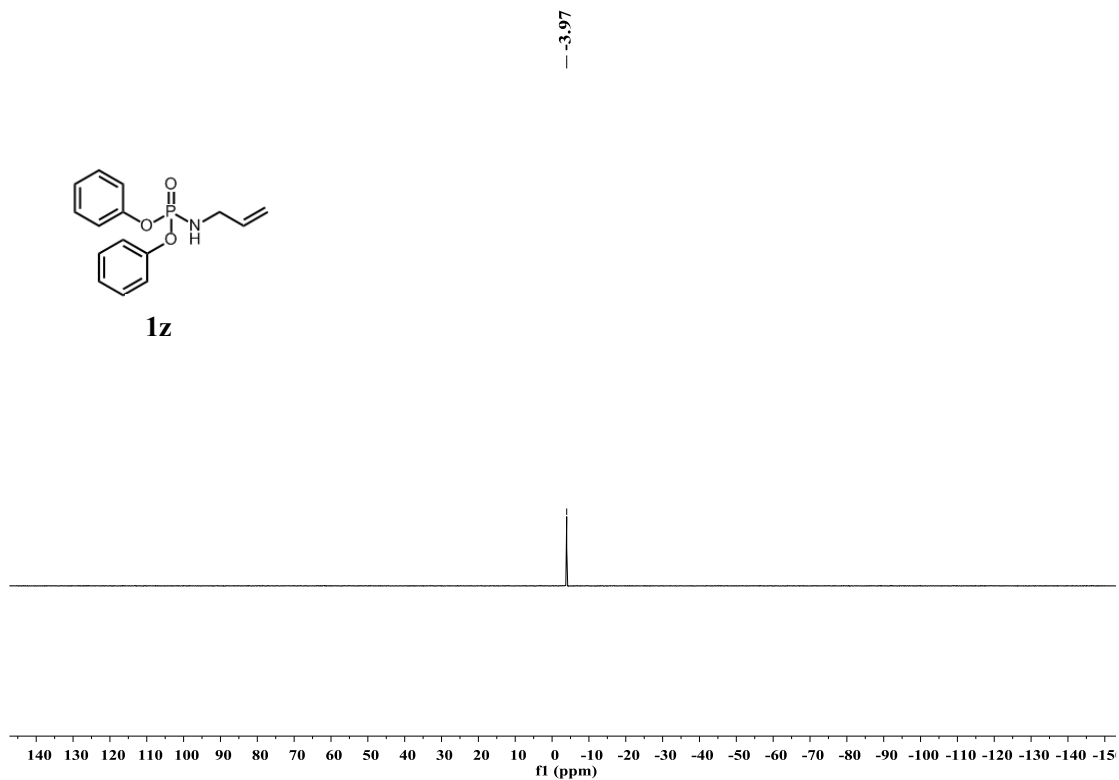
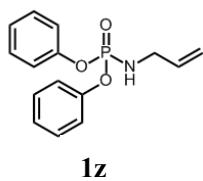
— 17.80

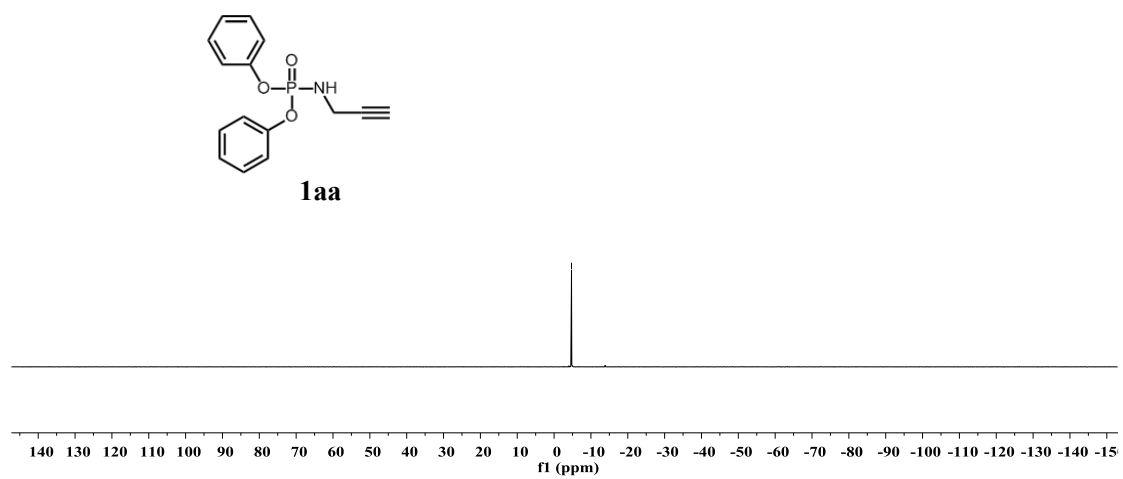
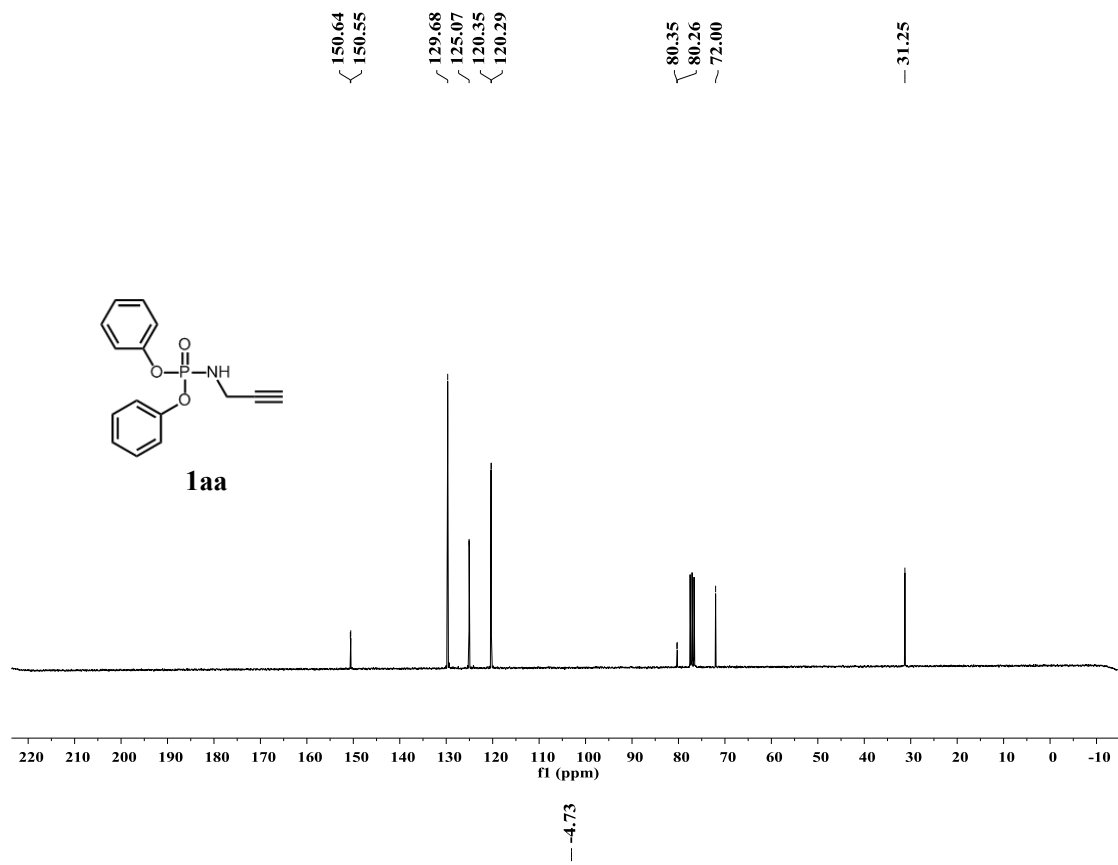


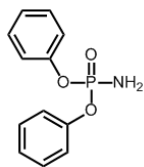
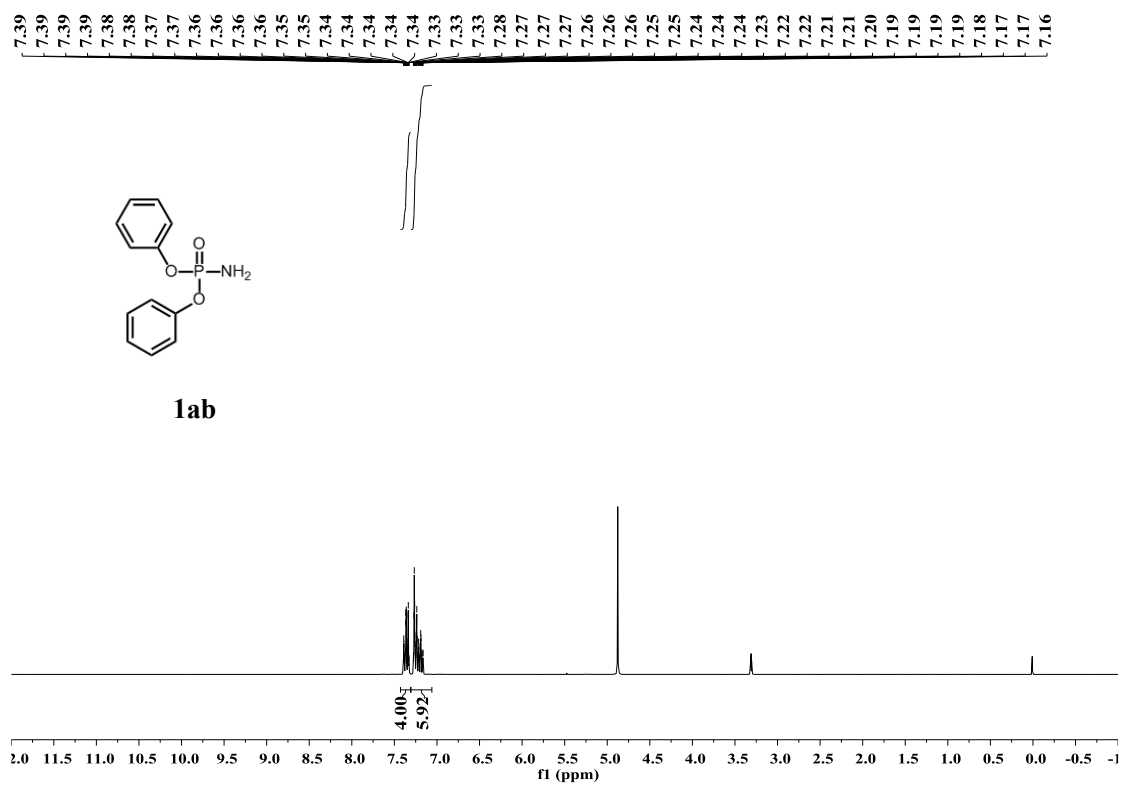
1y





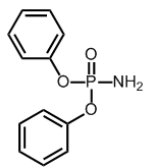
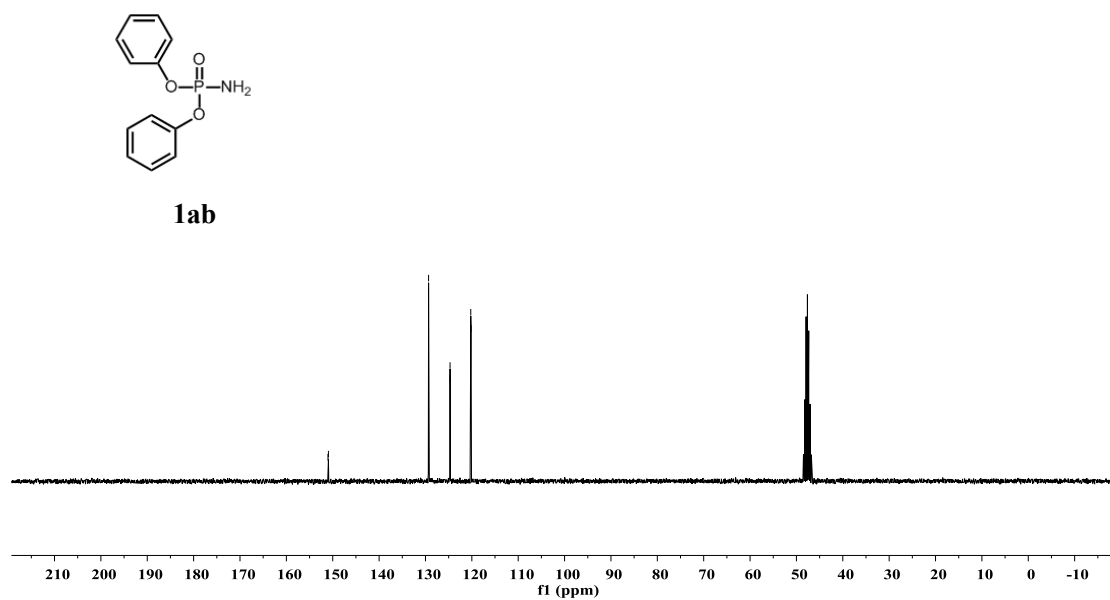






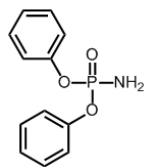
1ab

151.02
150.93
129.33
124.72
124.70
120.23
120.17

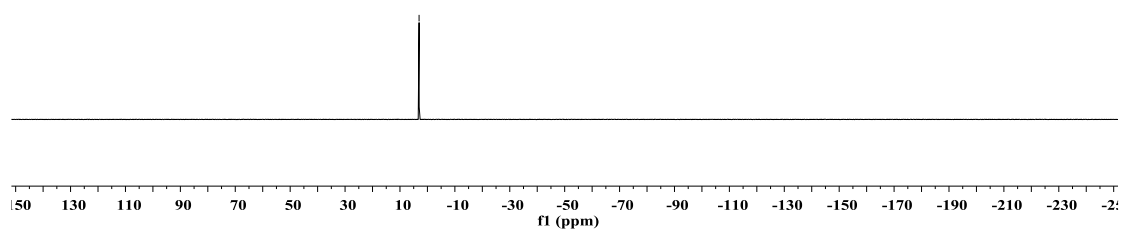


1ab

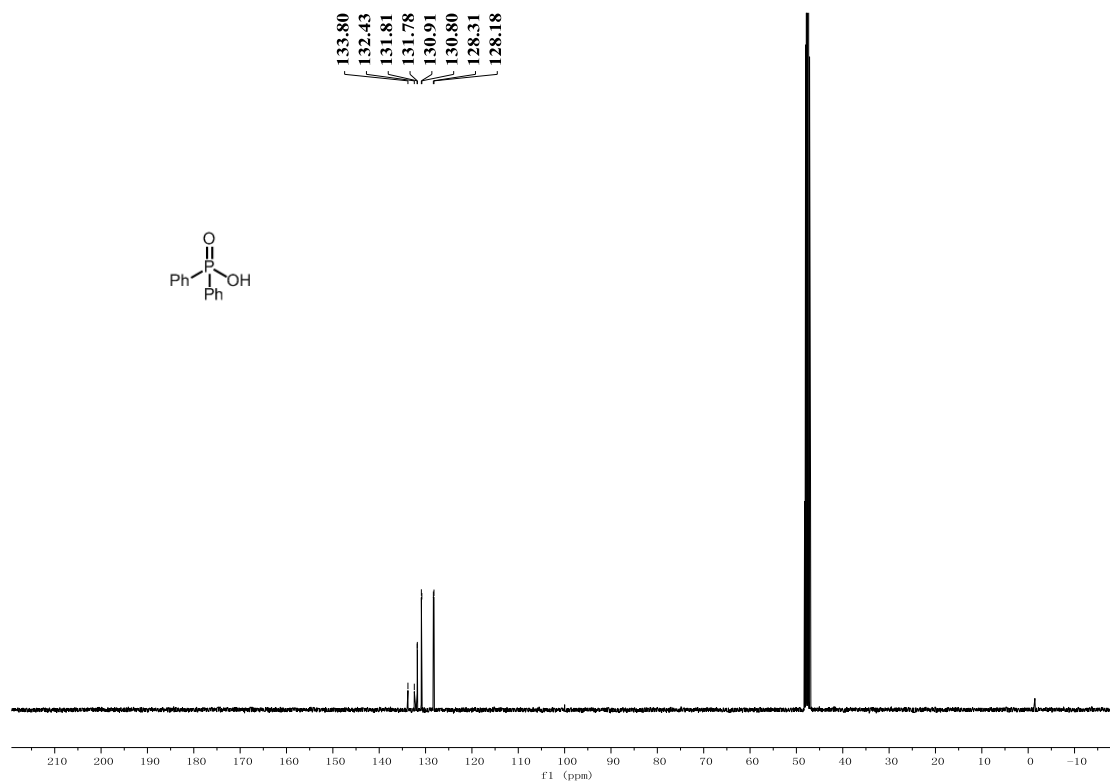
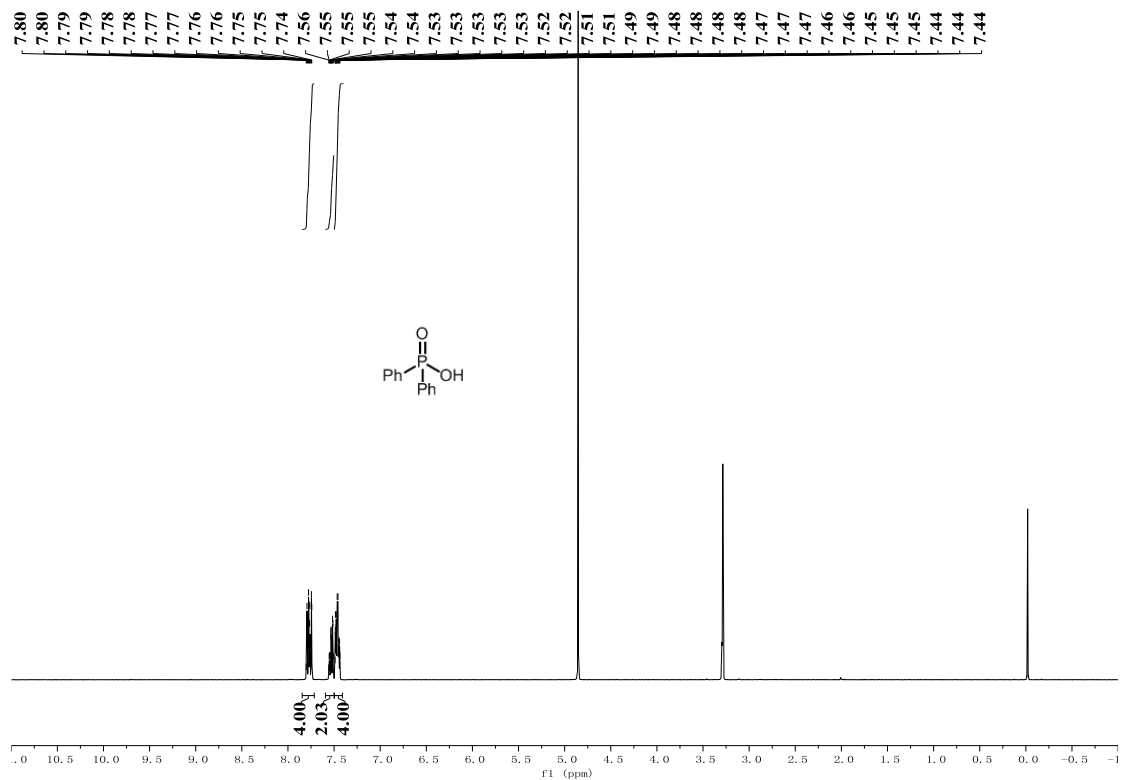
- 3.04

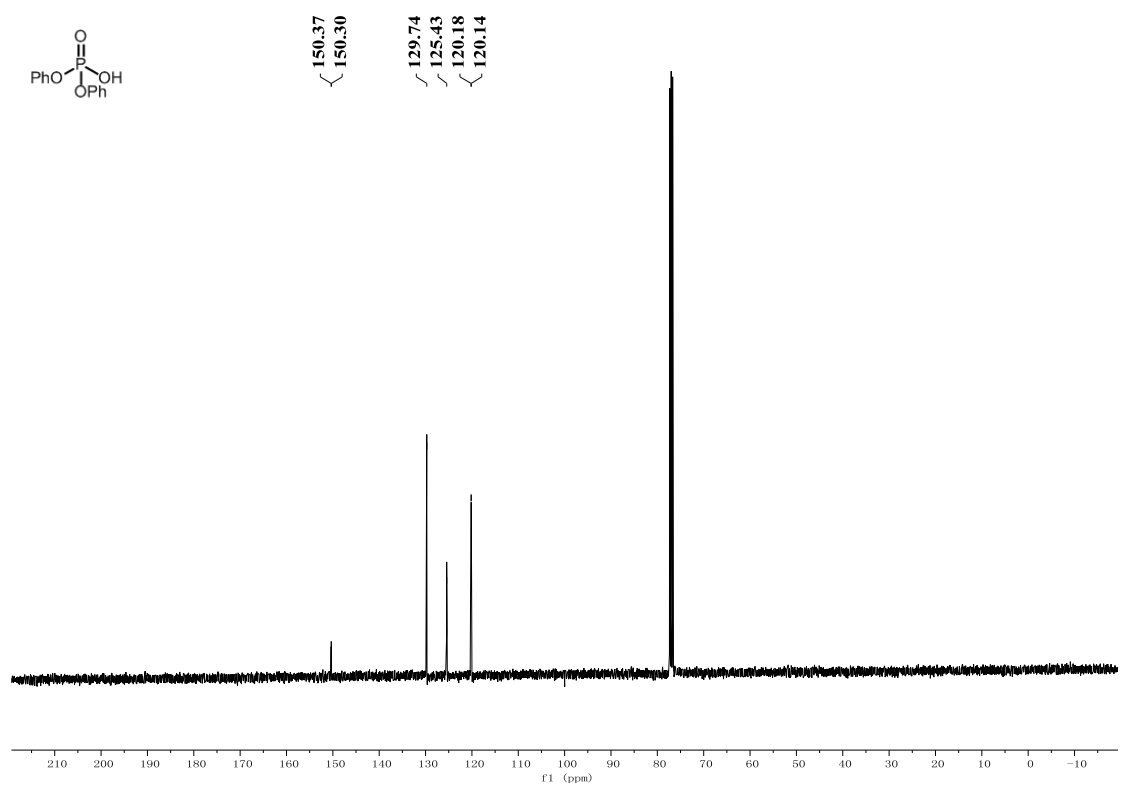
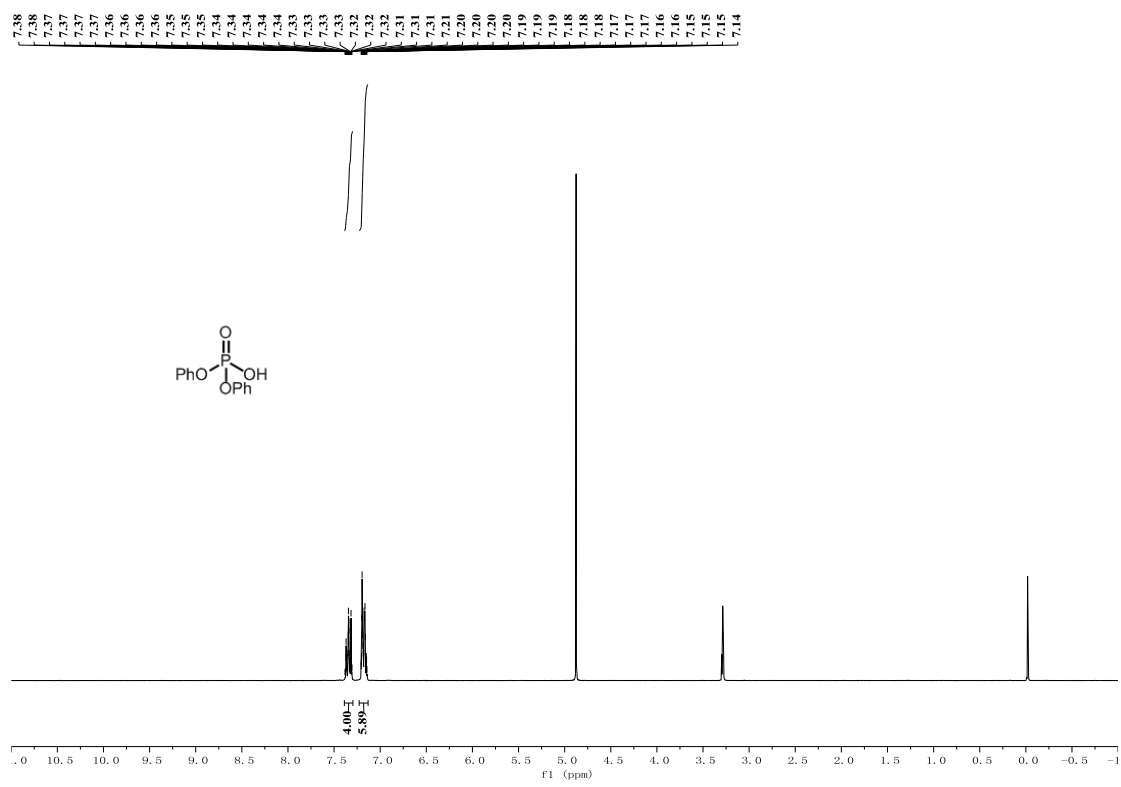


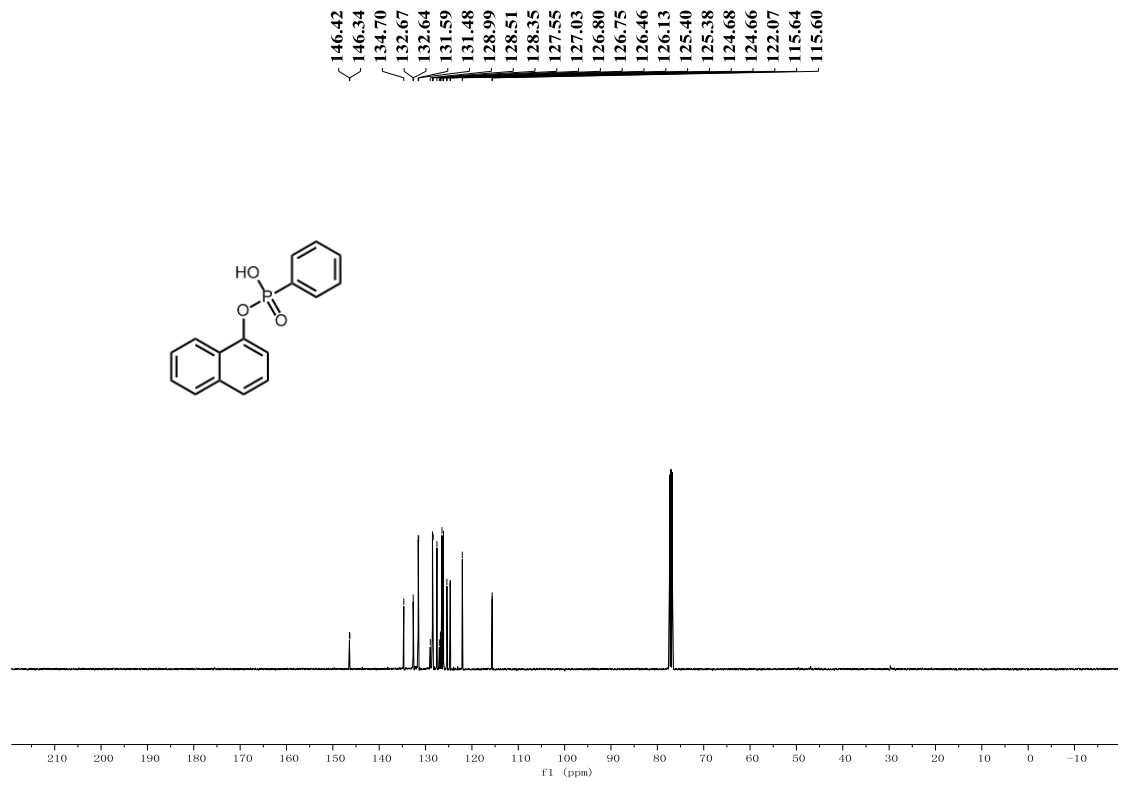
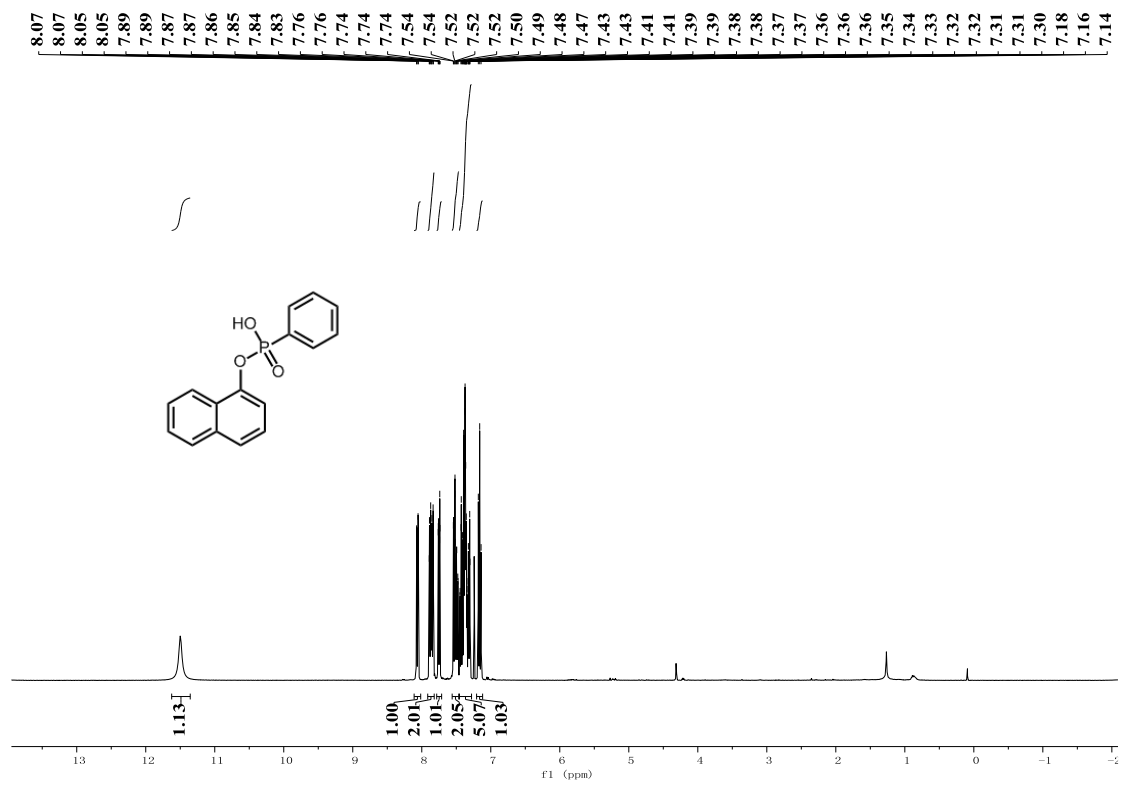
1ab

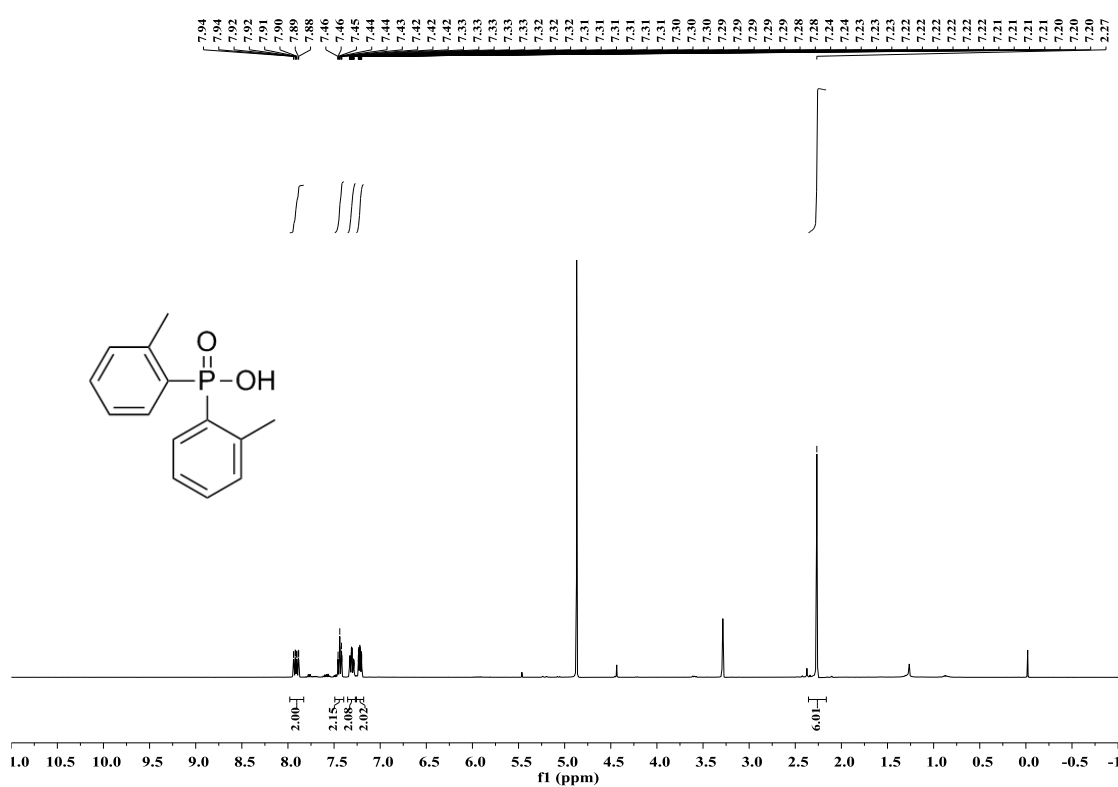
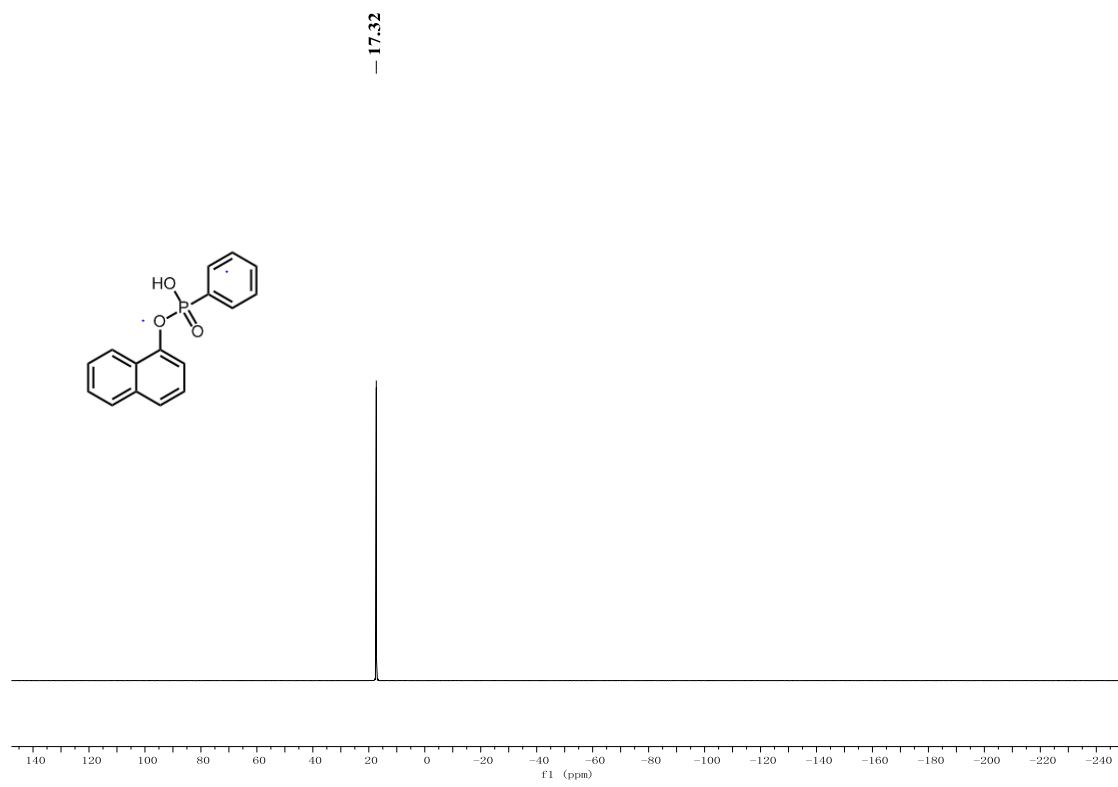


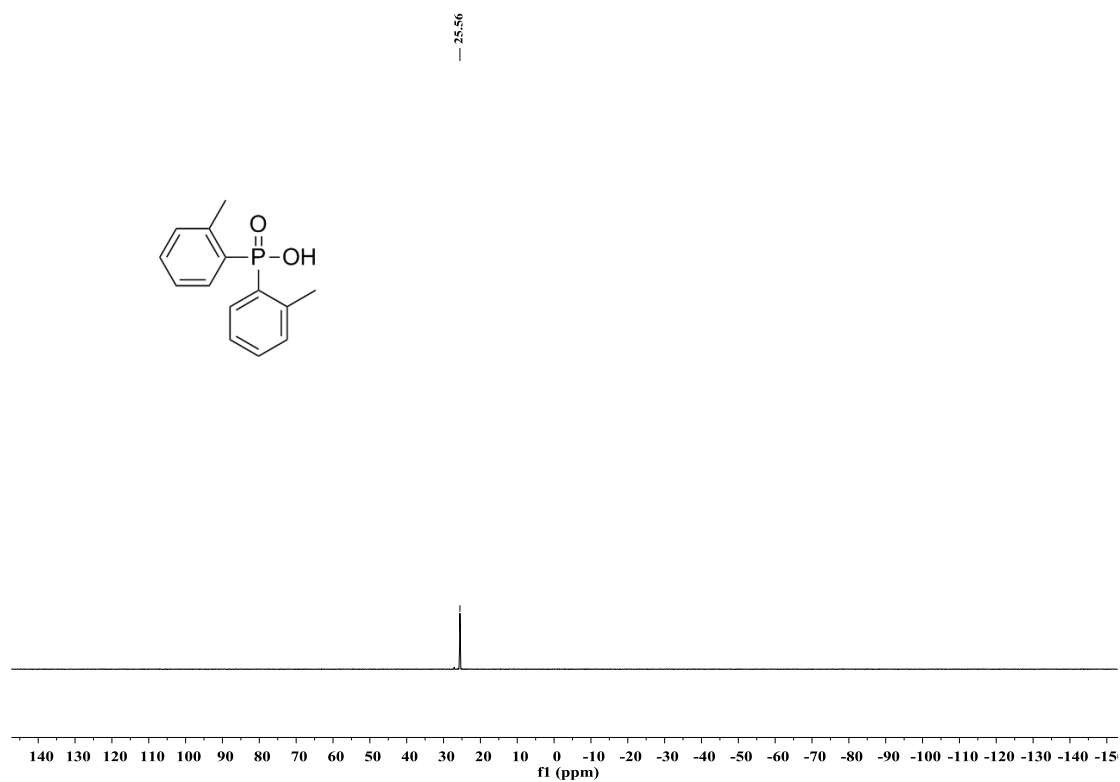
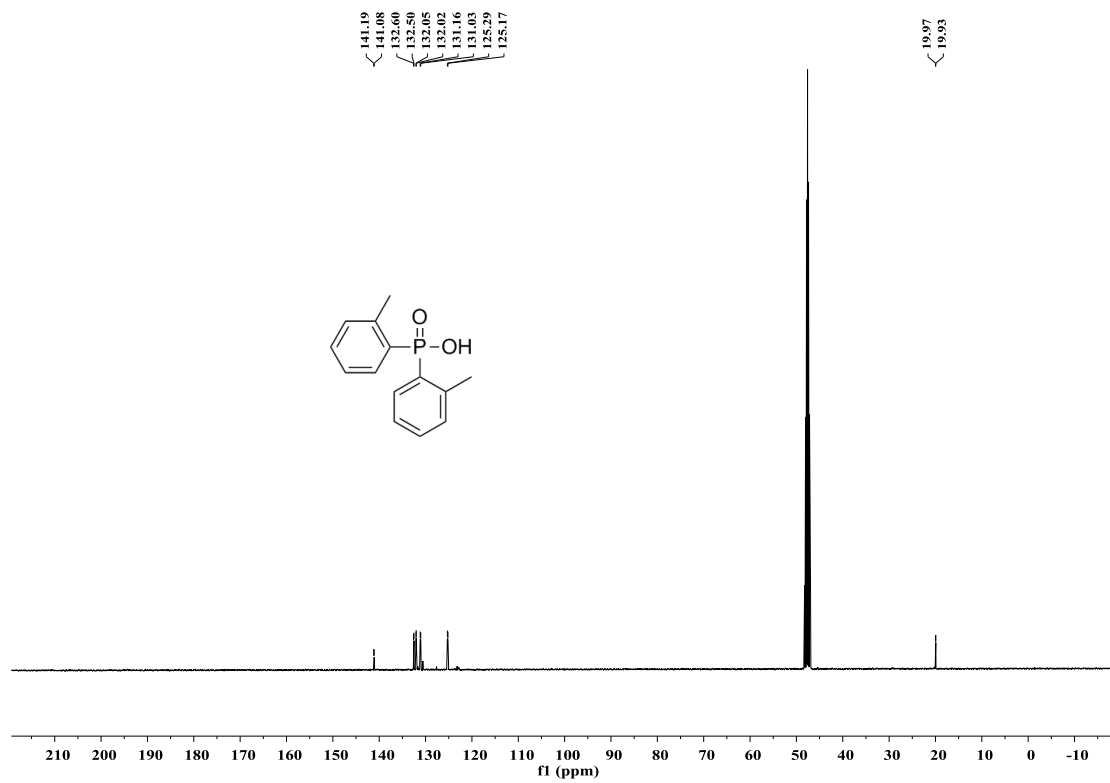
Spectra for products in Chapter 2



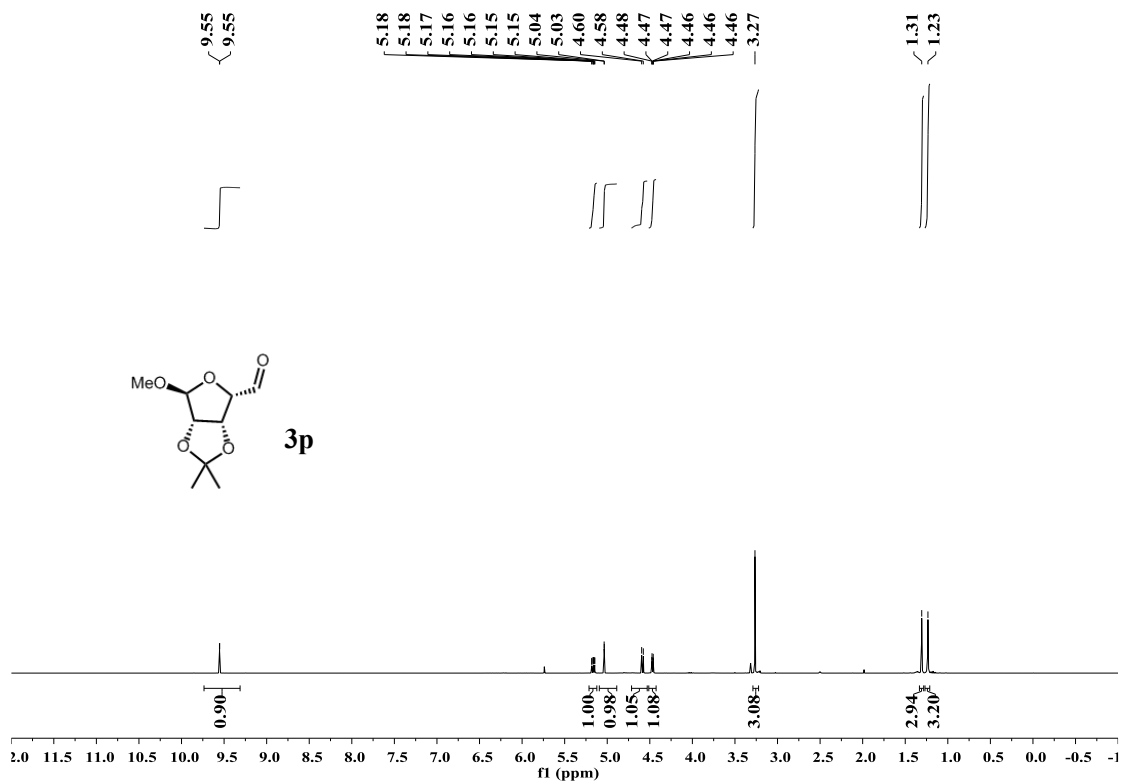
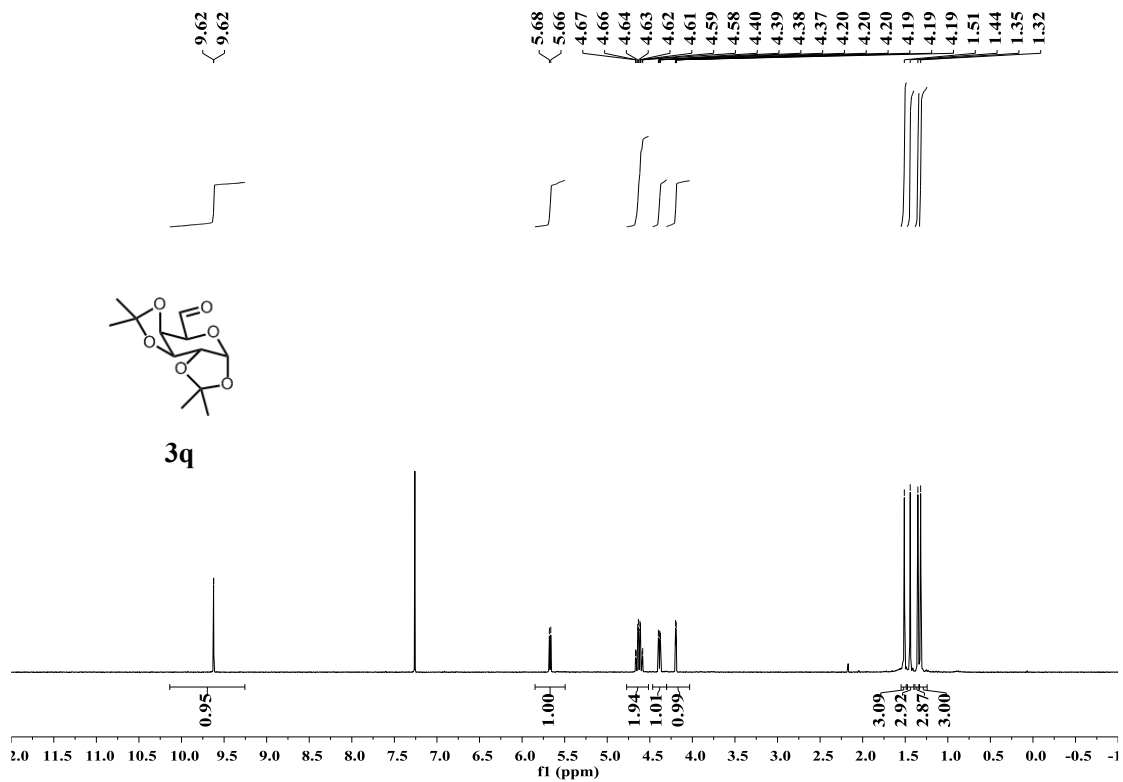


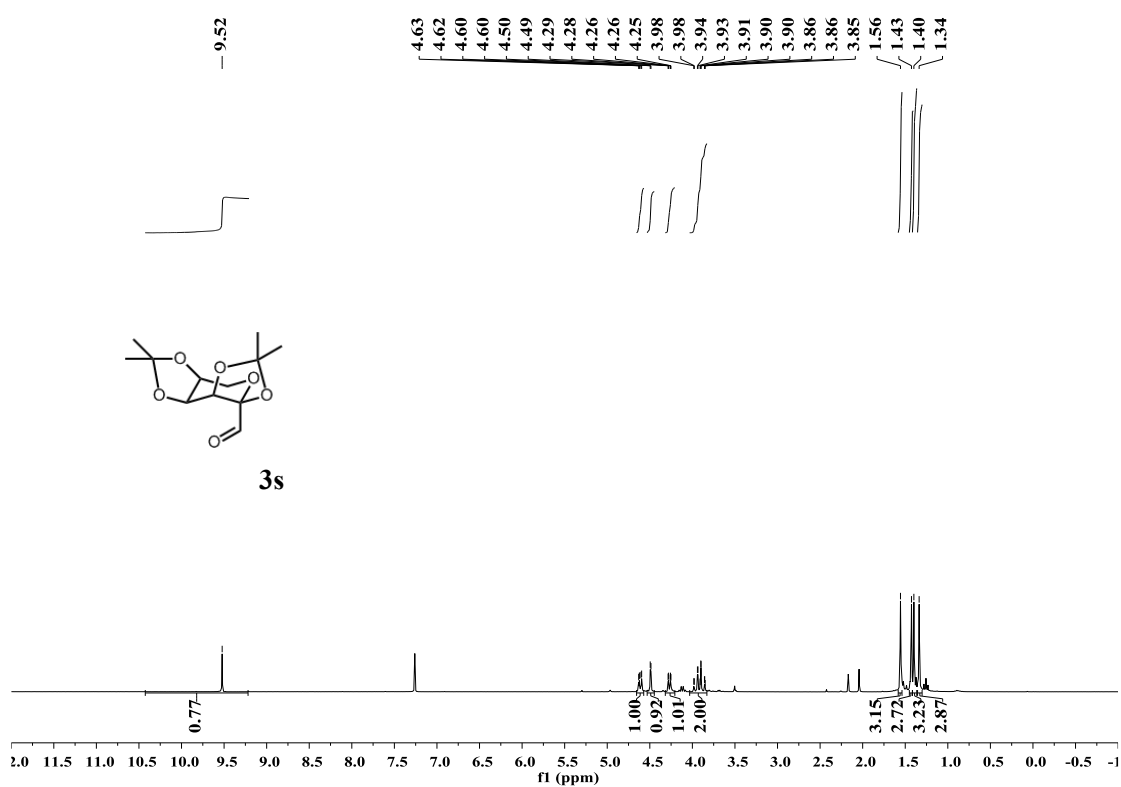
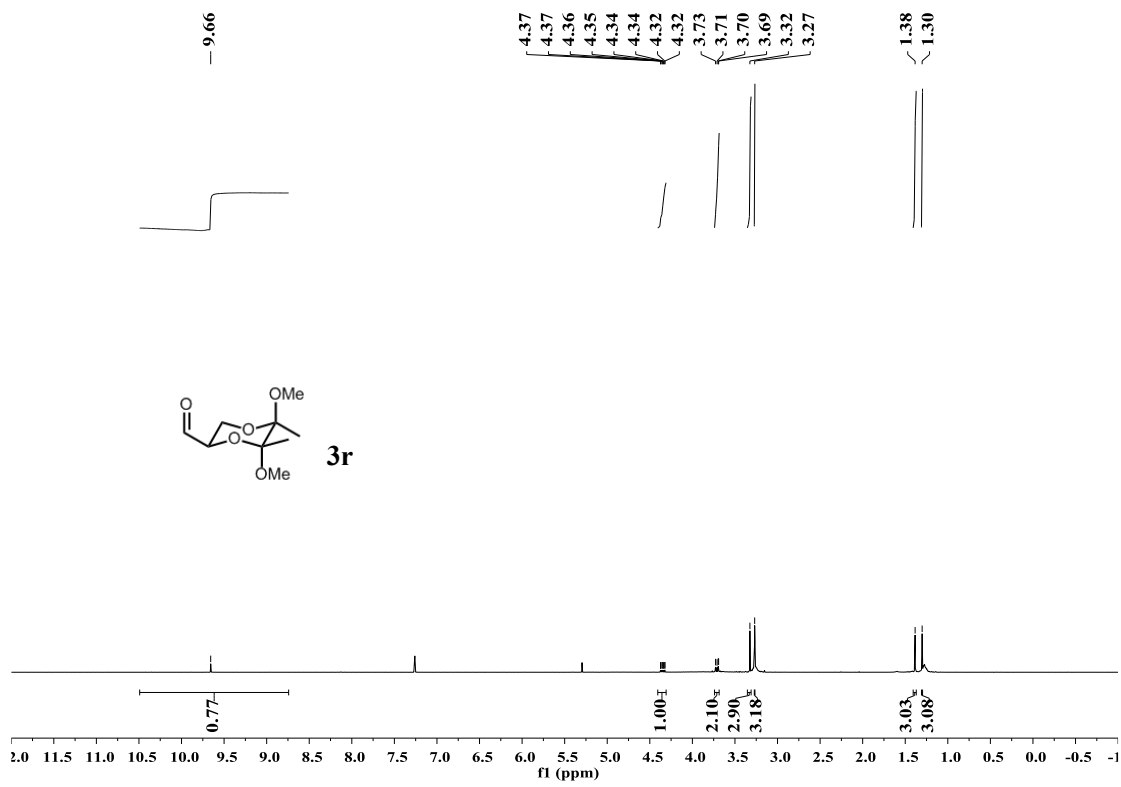




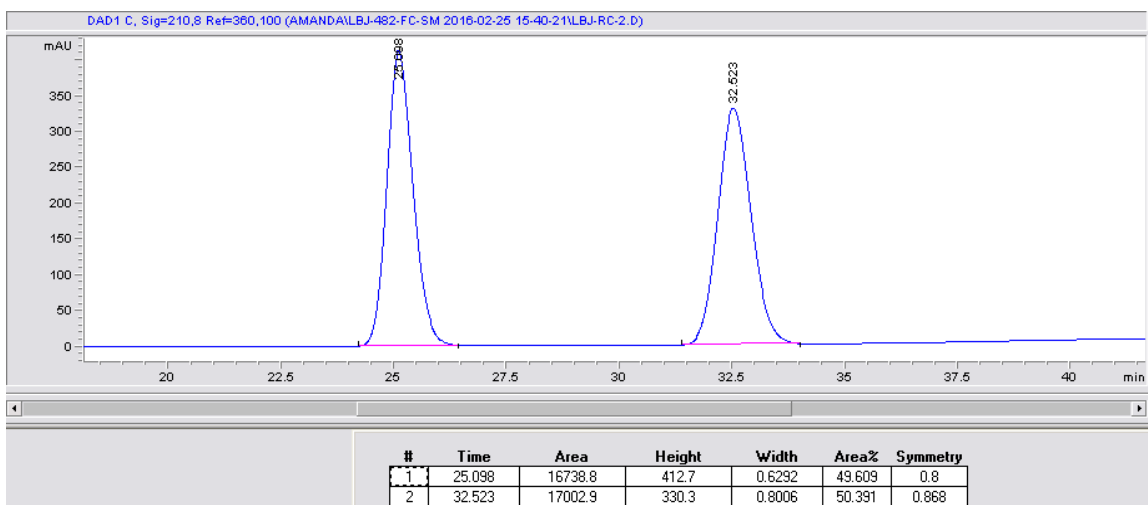
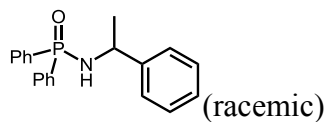
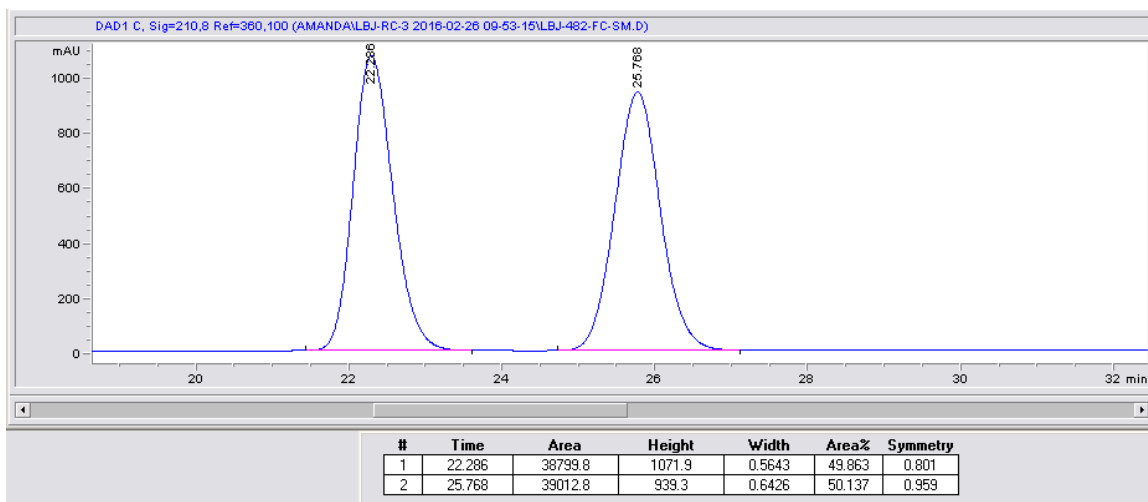
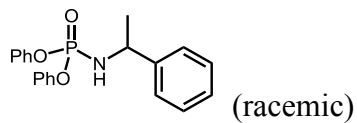


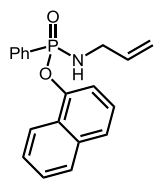
Spectra for chiral aldehydes in Chapter 2



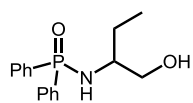
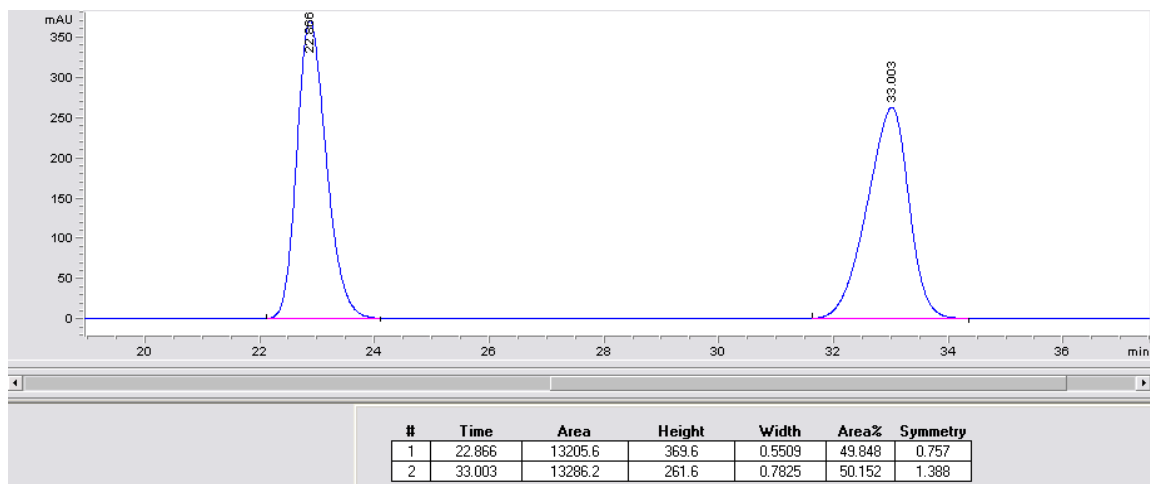


HPLC data for racemic in Chapter 2

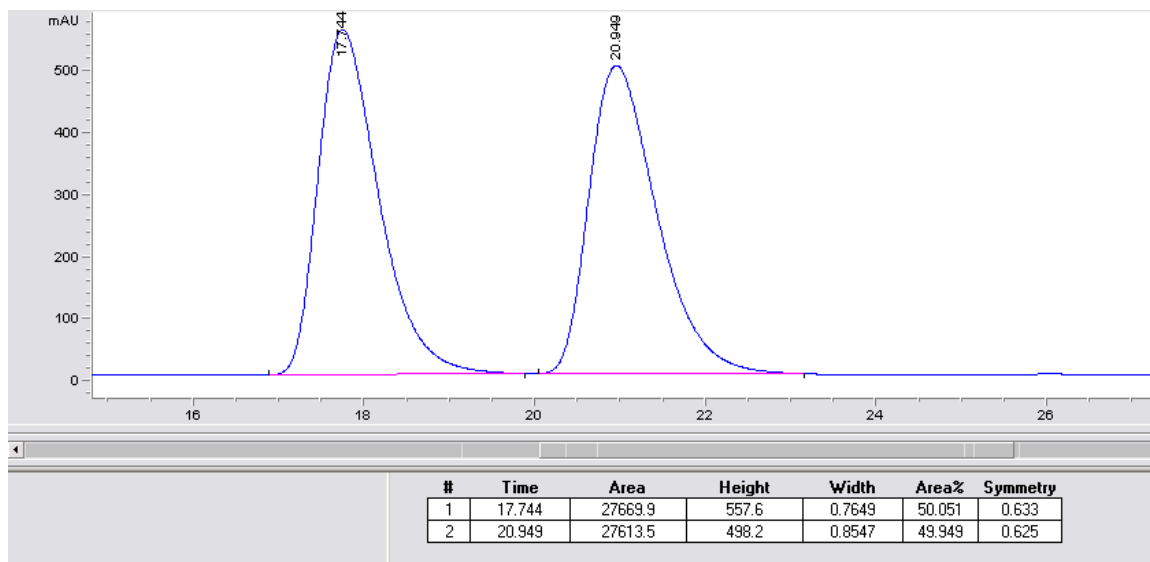




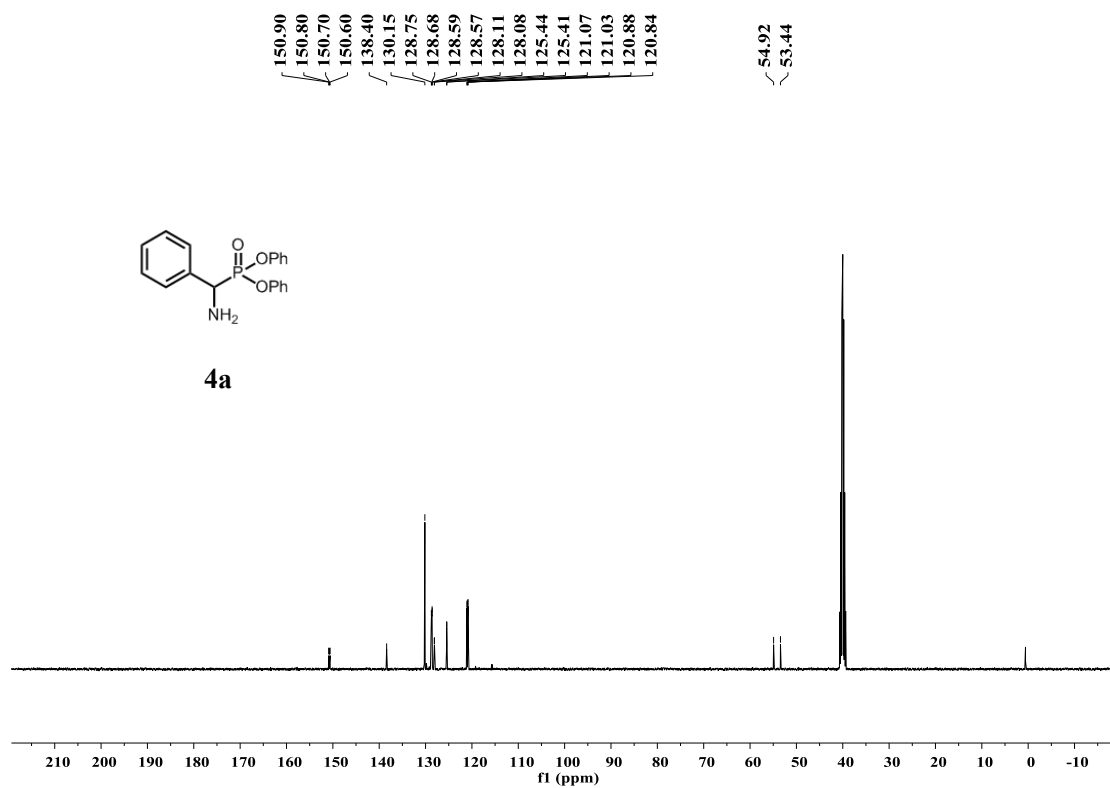
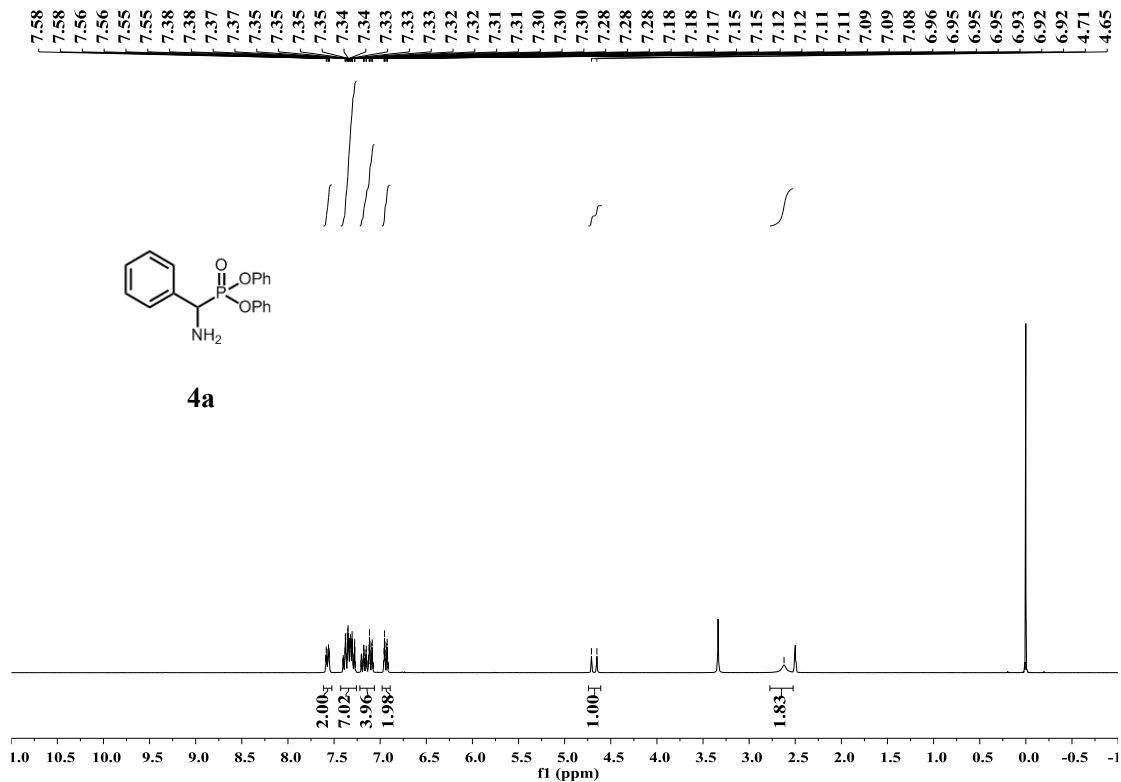
(racemic)

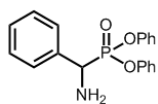


(racemic)

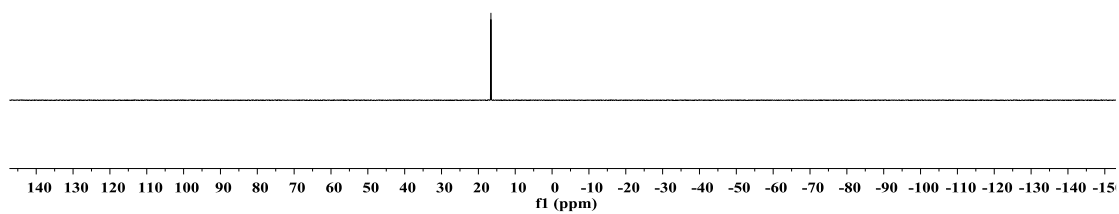


Spectra for starting materials in Chapter 3

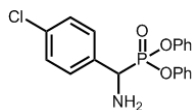




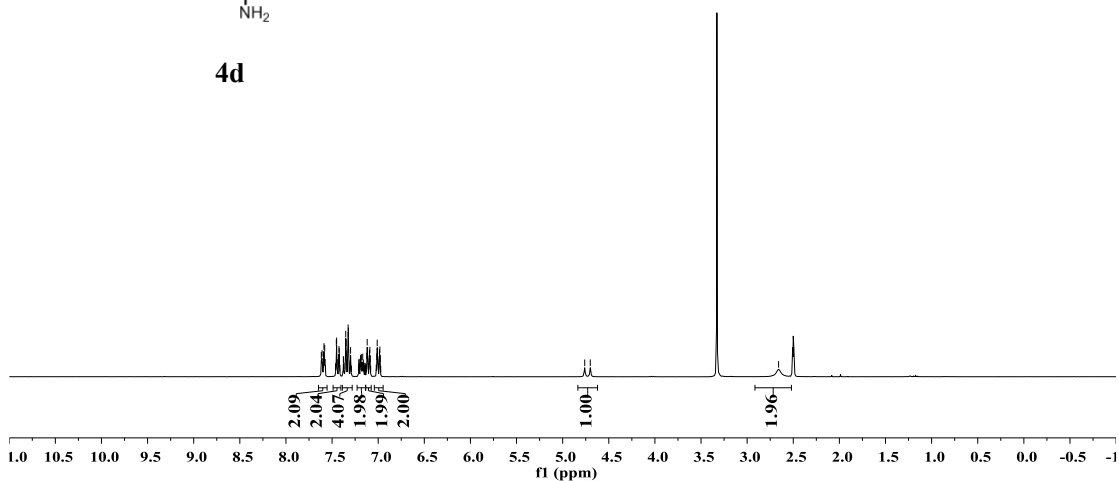
4a



7.62
7.61
7.60
7.60
7.59
7.58
7.45
7.45
7.44
7.43
7.43
7.42
7.38
7.38
7.37
7.35
7.35
7.35
7.33
7.32
7.31
7.30
7.21
7.21
7.19
7.19
7.19
7.18
7.17
7.16
7.16
7.12
7.12
7.12
7.11
7.11
7.10
7.09
7.09
7.09
7.02
7.01
7.01
7.00
6.99
6.99
6.98
6.98
4.76
4.70
2.66

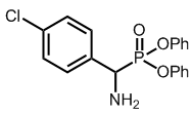


4d

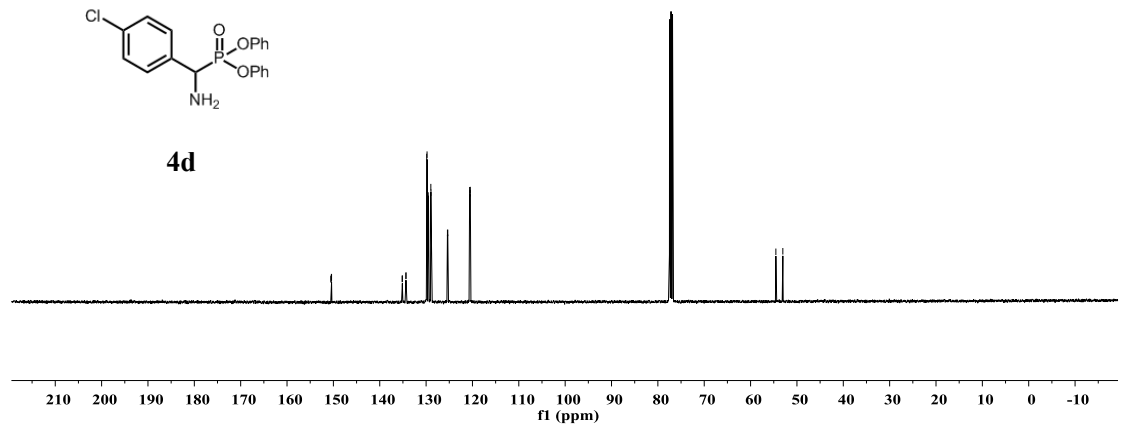


150.54
 150.49
 150.43
 150.39
 135.16
 135.12
 134.37
 134.33
 129.87
 129.79
 129.55
 128.98
 128.95
 125.40
 125.32
 120.61
 120.57
 120.50
 120.46

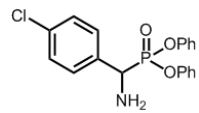
54.55
 53.04



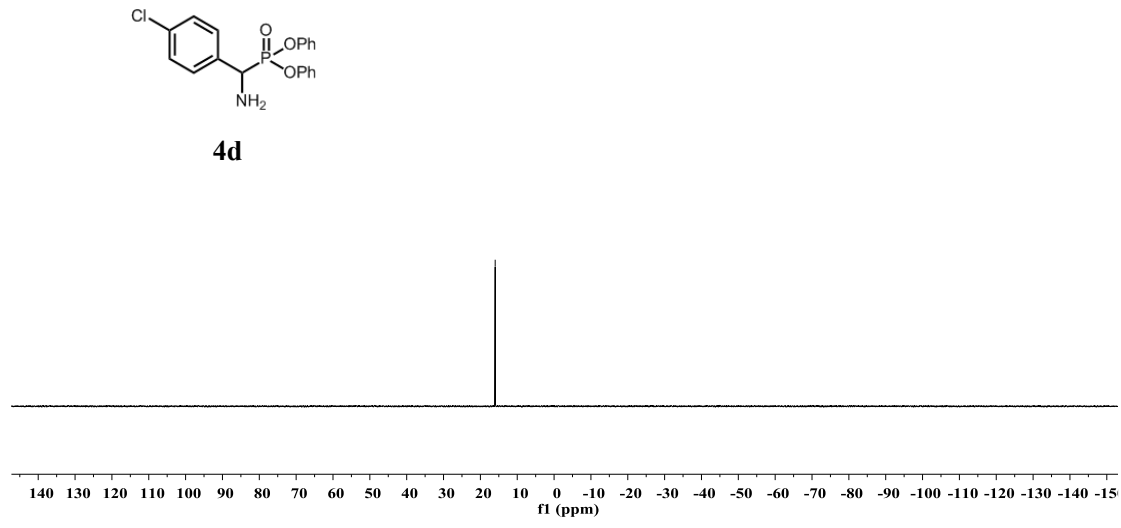
4d

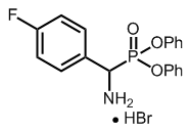
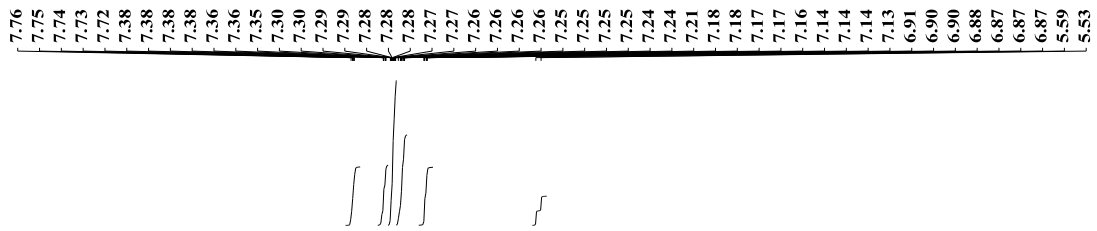


15.98

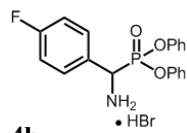
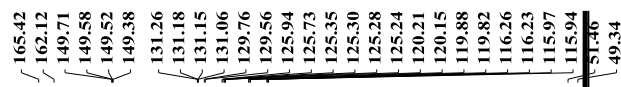
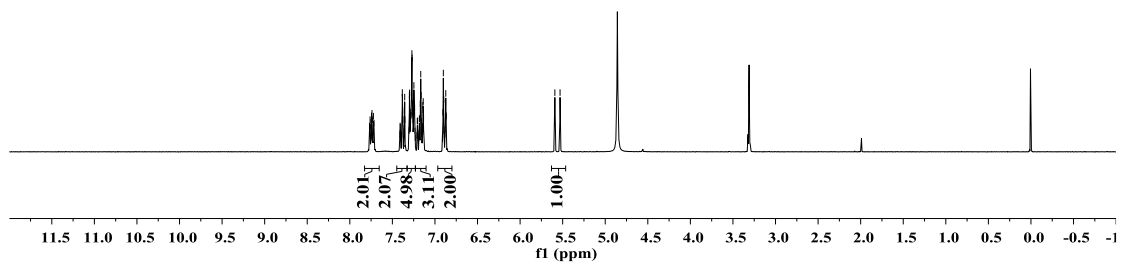


4d

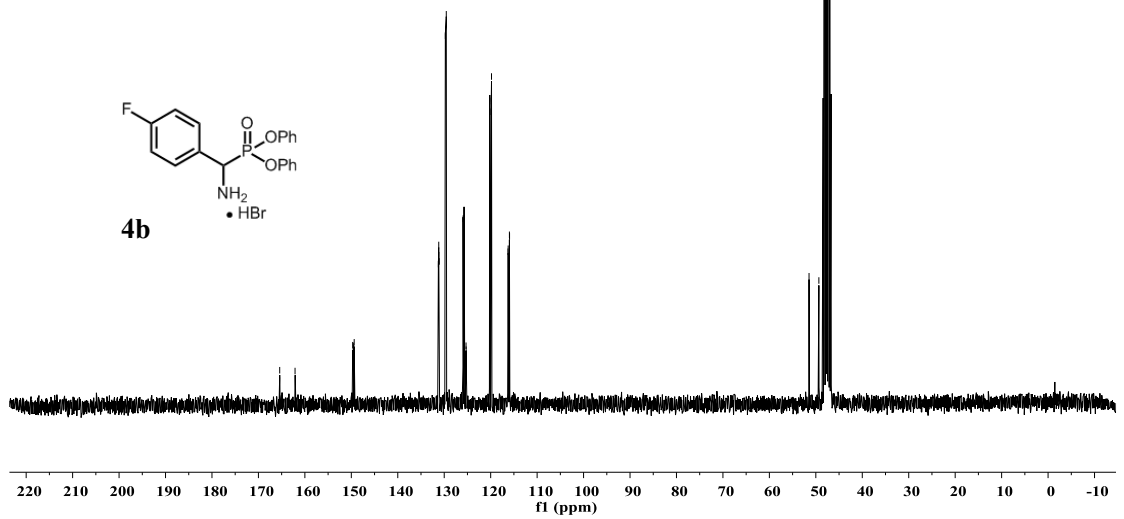




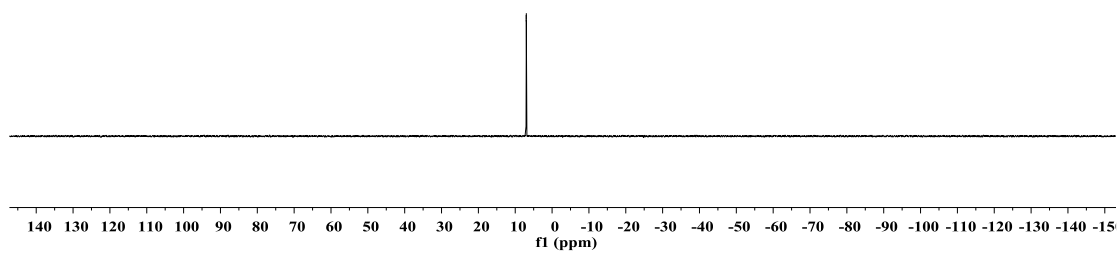
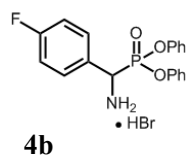
4b



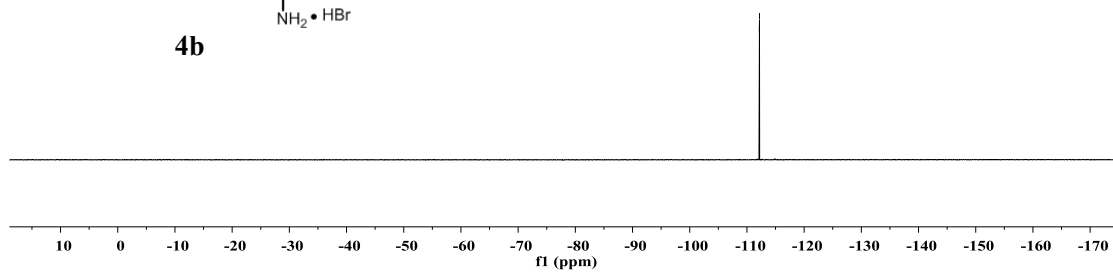
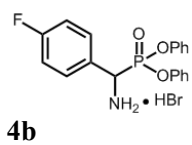
4b

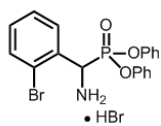
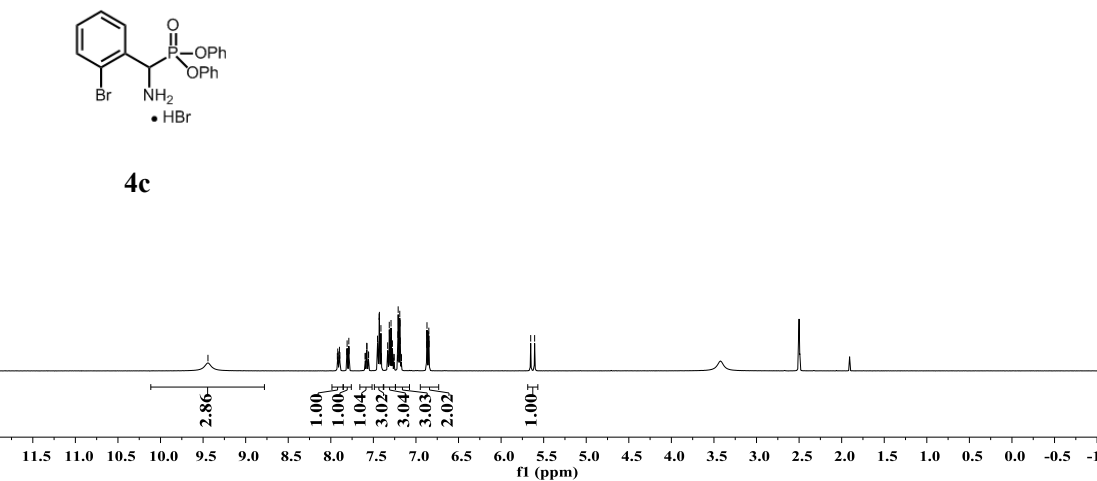
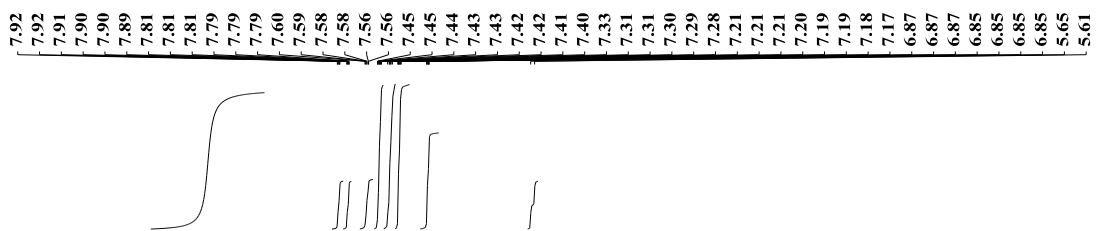


7.03
6.99

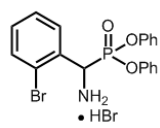


-112.17
-112.19

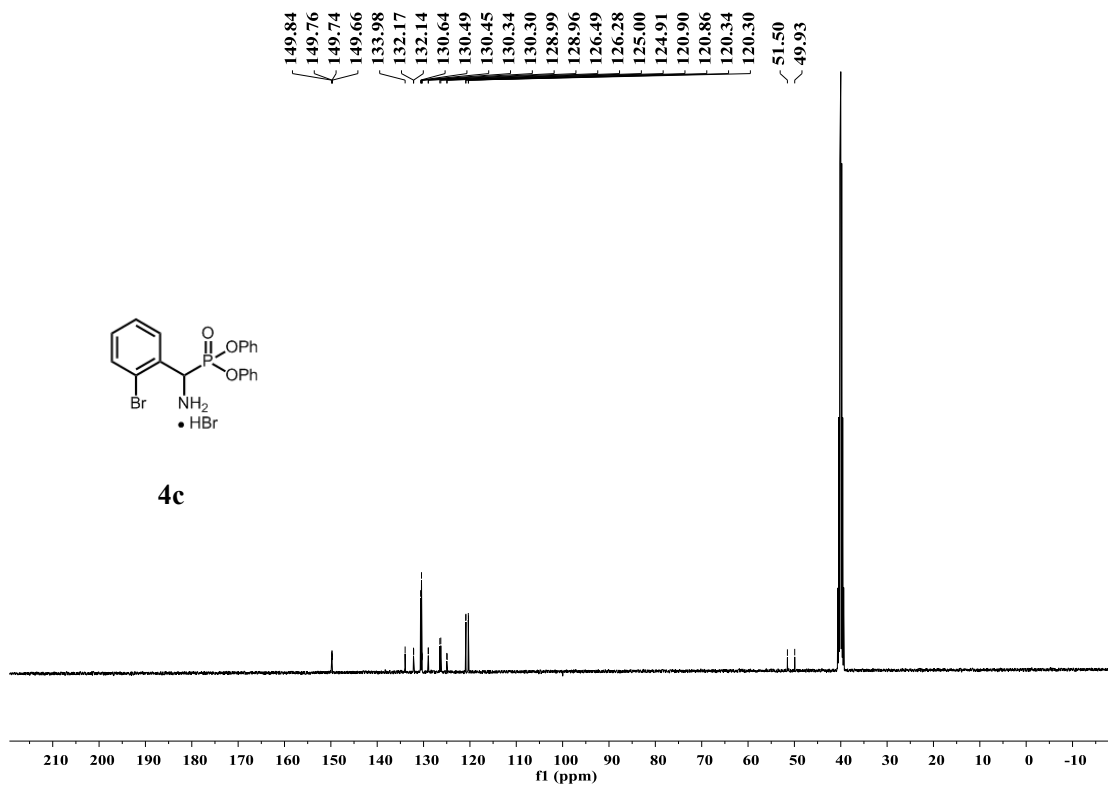


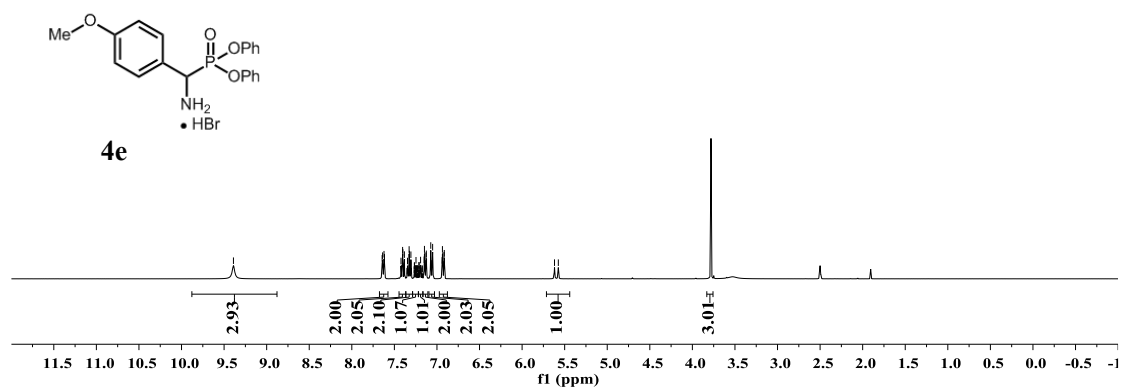
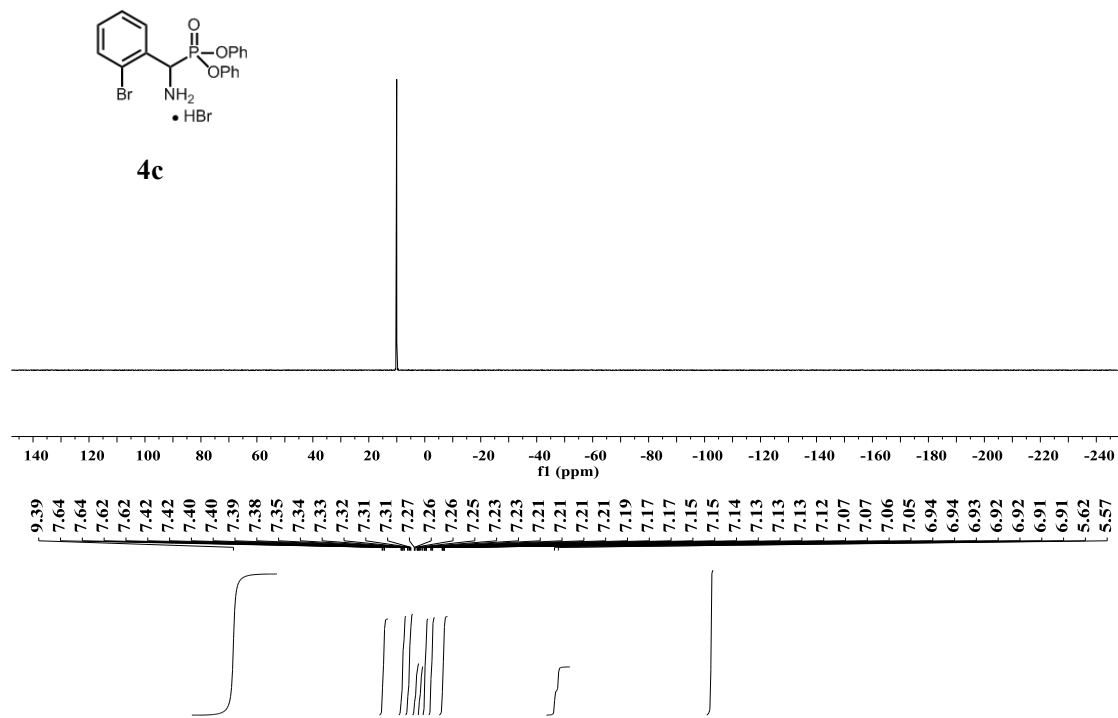


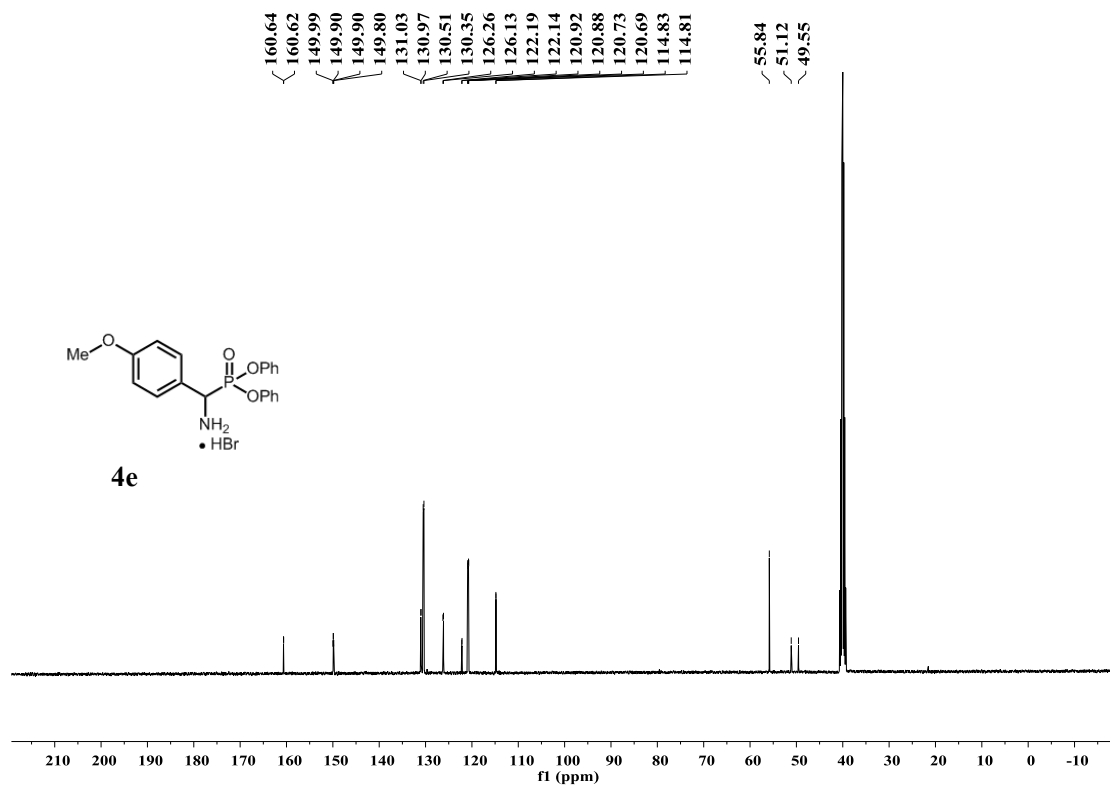
4c



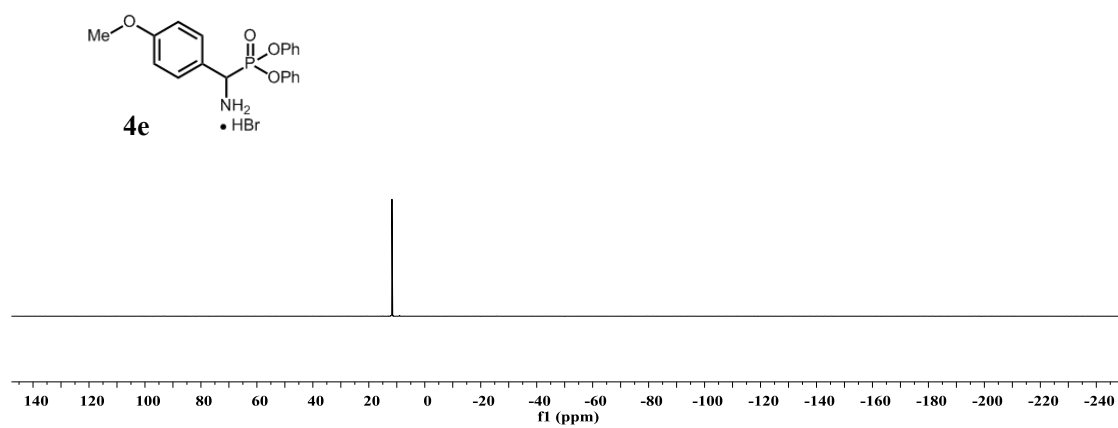
4c

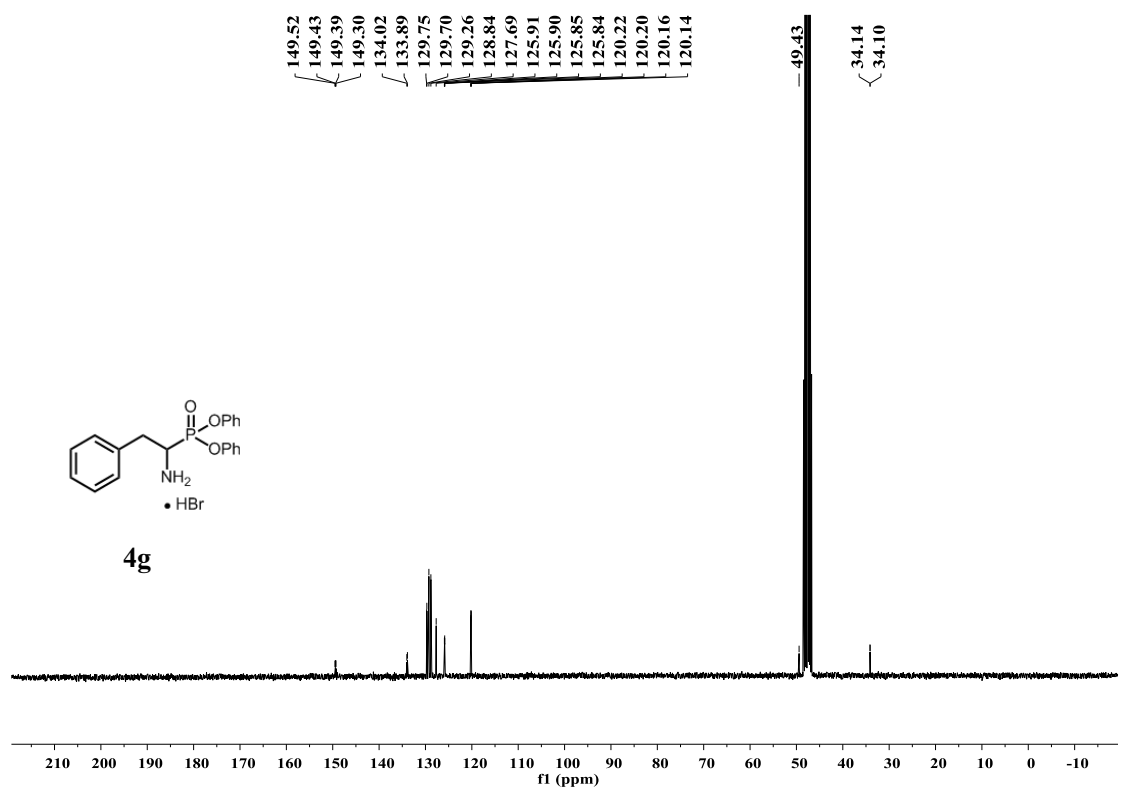
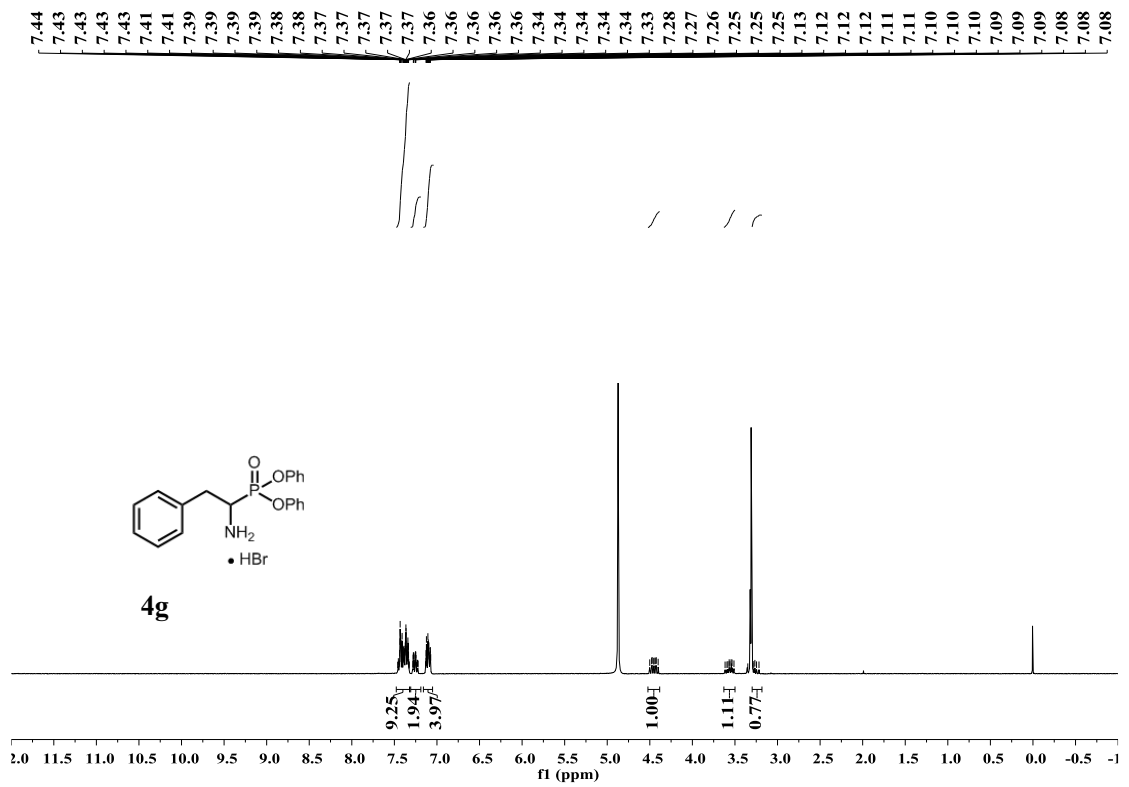




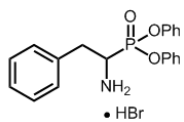


— 11.74

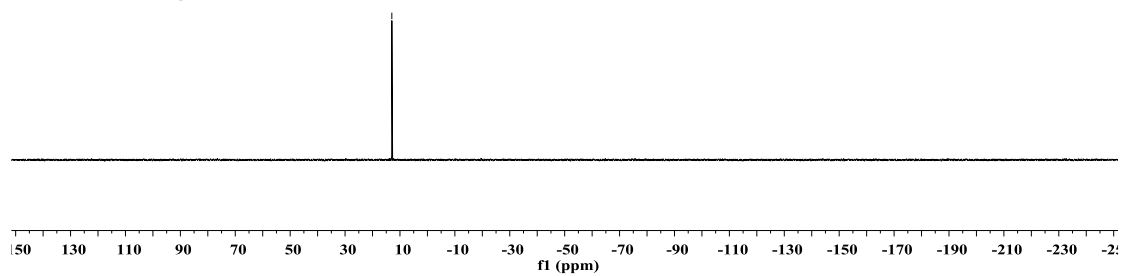




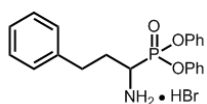
-12.96



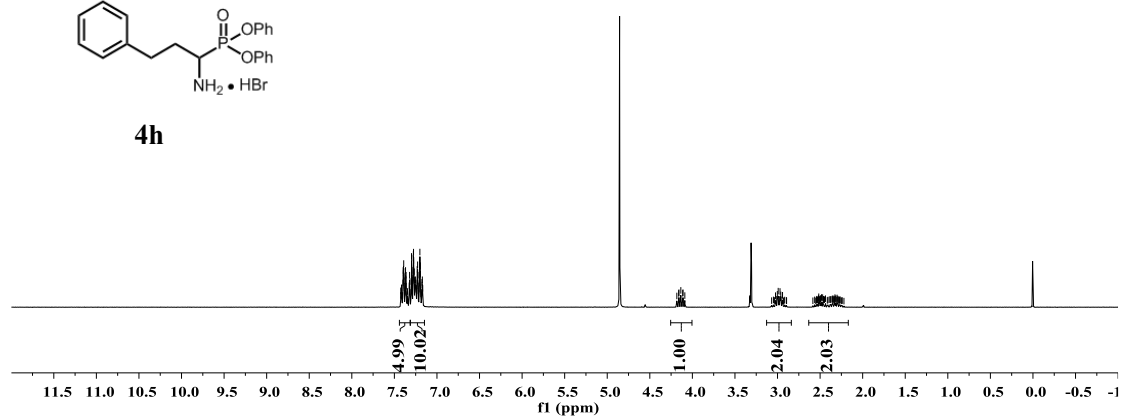
4g

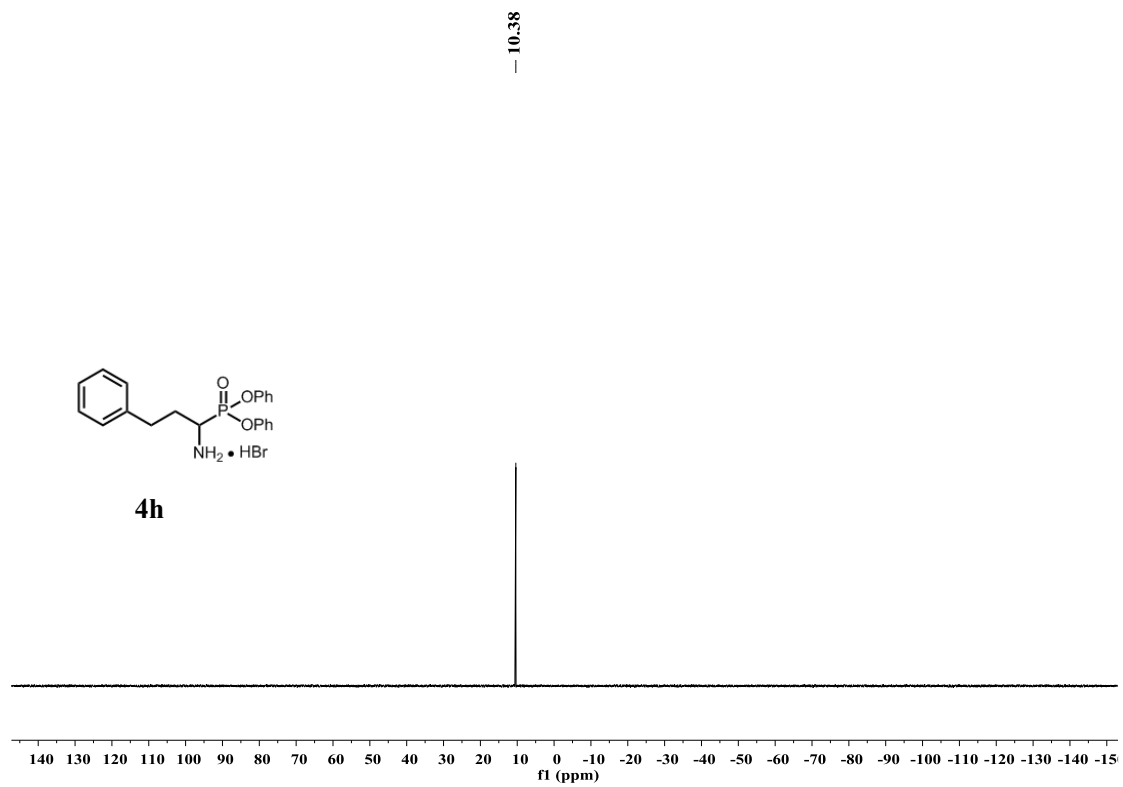
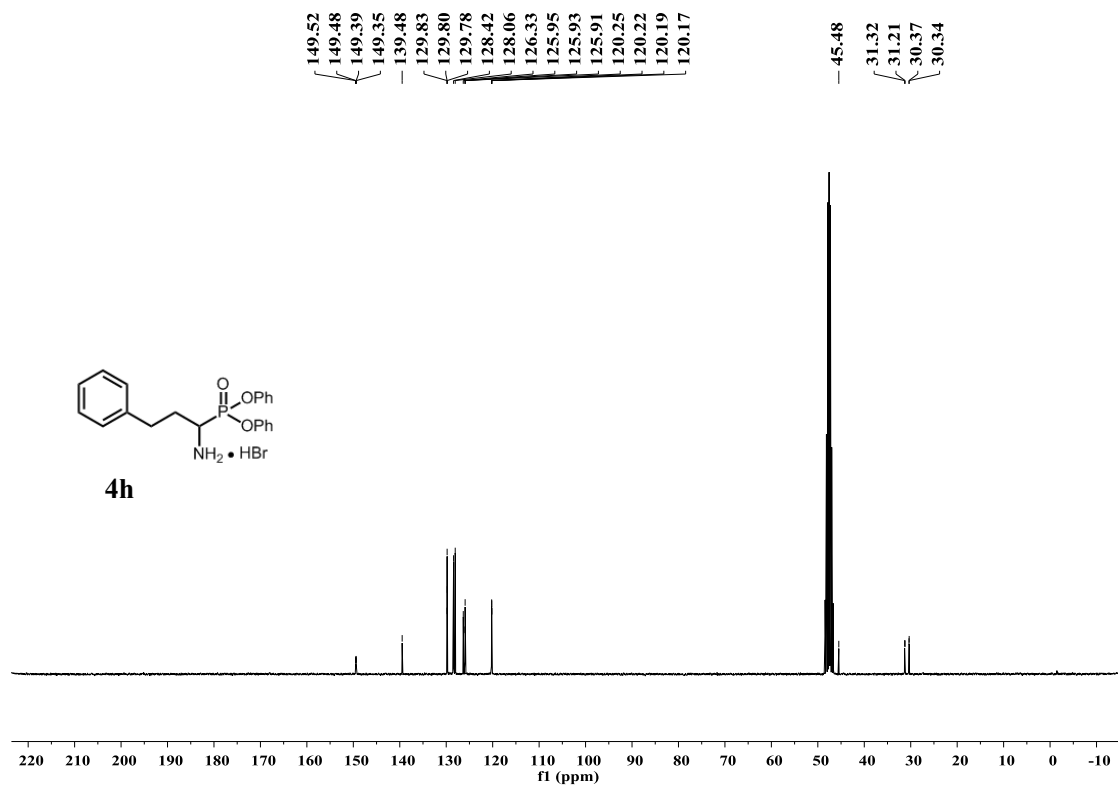


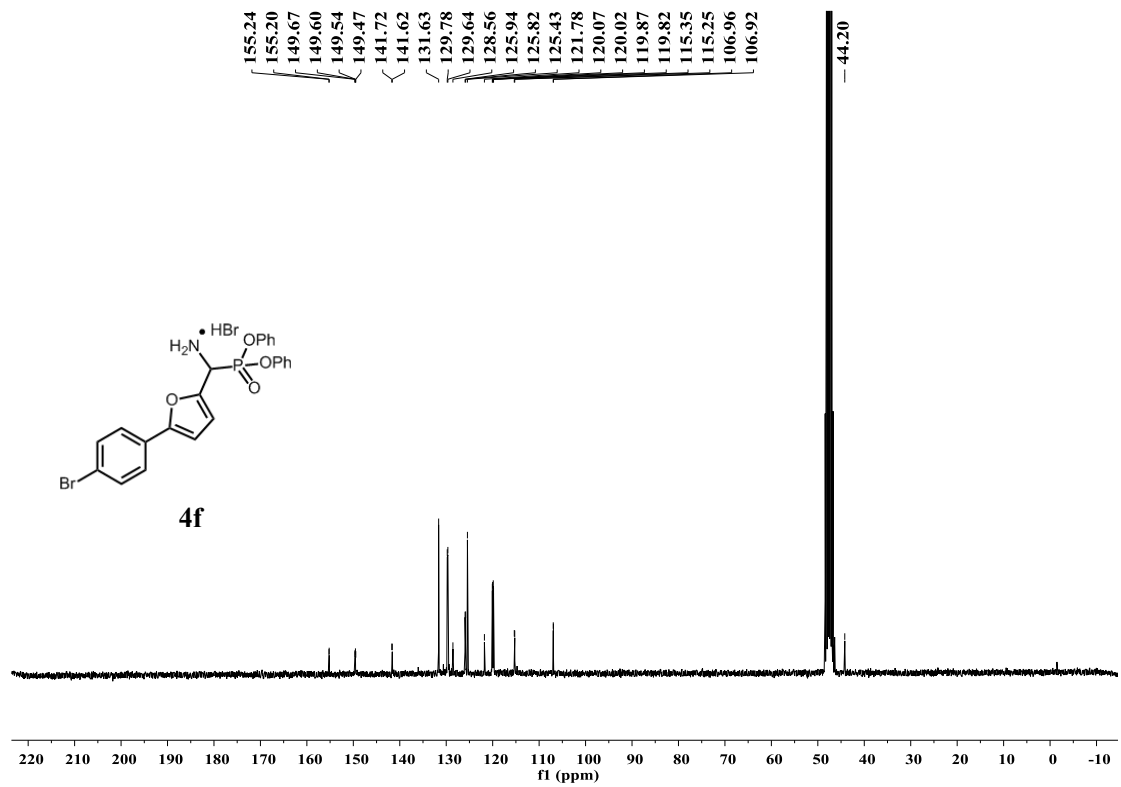
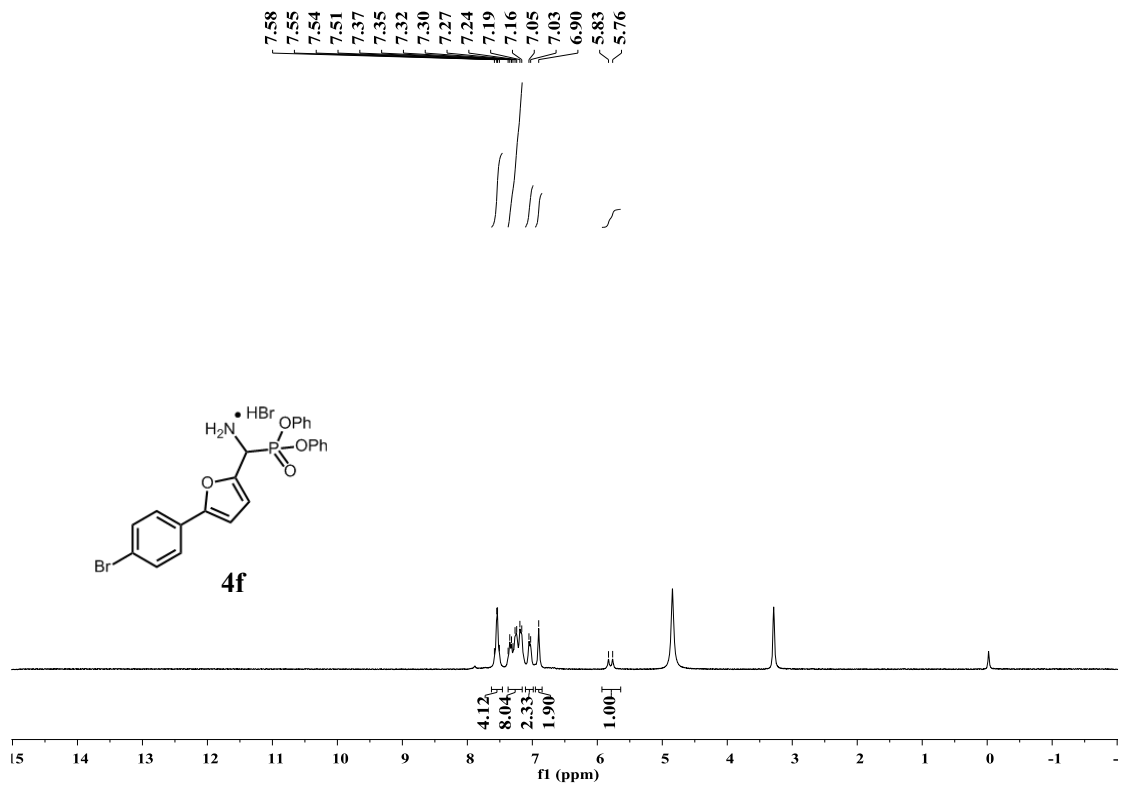
7.42
7.40
7.40
7.39
7.39
7.39
7.39
7.38
7.37
7.37
7.37
7.36
7.36
7.36
7.33
7.32
7.32
7.30
7.30
7.29
7.29
7.29
7.28
7.28
7.28
7.27
7.27
7.27
7.27
7.26
7.26
7.25
7.25
7.23
7.23
7.22
7.22
7.21
7.21
7.20
7.20
7.20
7.20
7.20
7.20
7.18
7.17
7.17



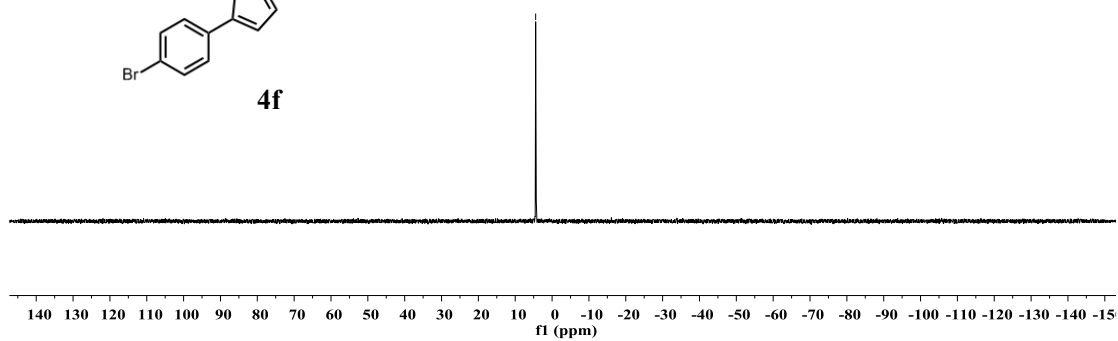
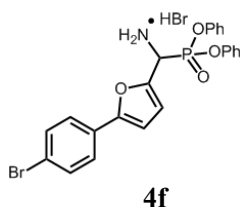
4h



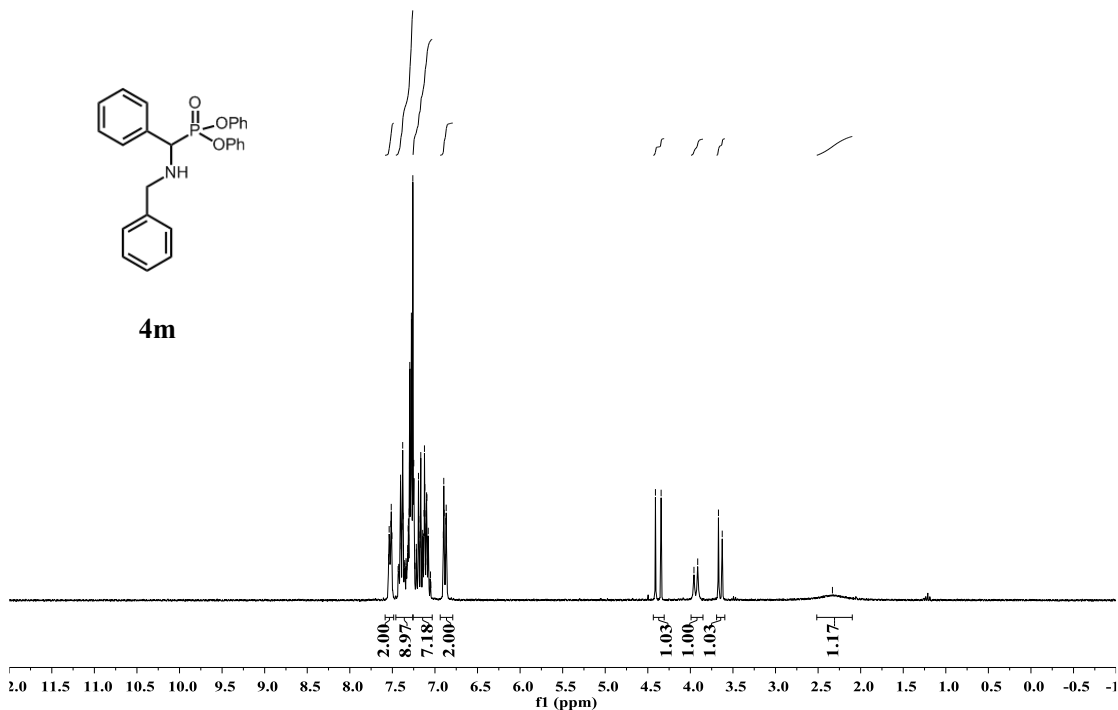
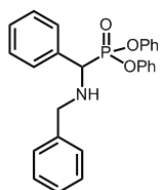




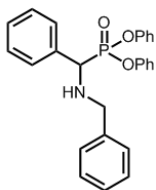
- 4.45



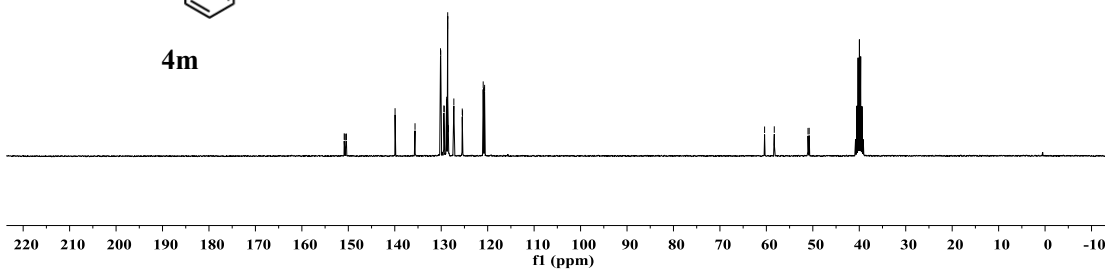
7.54
7.53
7.52
7.51
7.51
7.40
7.39
7.38
7.37
7.31
7.31
7.30
7.30
7.30
7.29
7.29
7.28
7.27
7.26
7.26
7.26
7.25
7.19
7.19
7.19
7.17
7.17
7.14
7.13
7.12
7.12
7.12
7.10
7.10
7.10
7.09
7.09
7.08
6.90
6.90
6.89
6.89
6.87
6.87
6.86
4.41
4.34
3.67
3.63



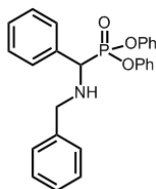
150.89
 150.76
 150.53
 150.41
 139.94
 135.64
 130.15
 130.10
 129.43
 128.86
 128.83
 128.63
 128.60
 128.49
 128.44
 127.28
 125.47
 125.41
 120.96
 120.91
 120.72
 120.66
 60.38
 58.30
 51.03
 50.79



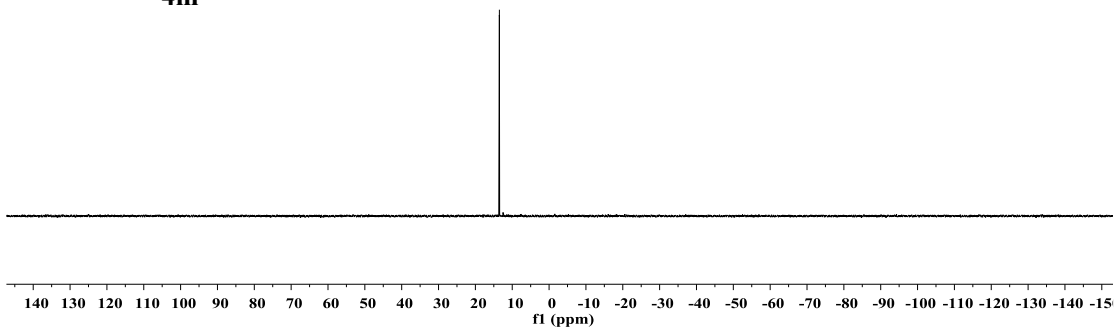
4m

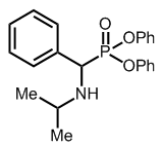
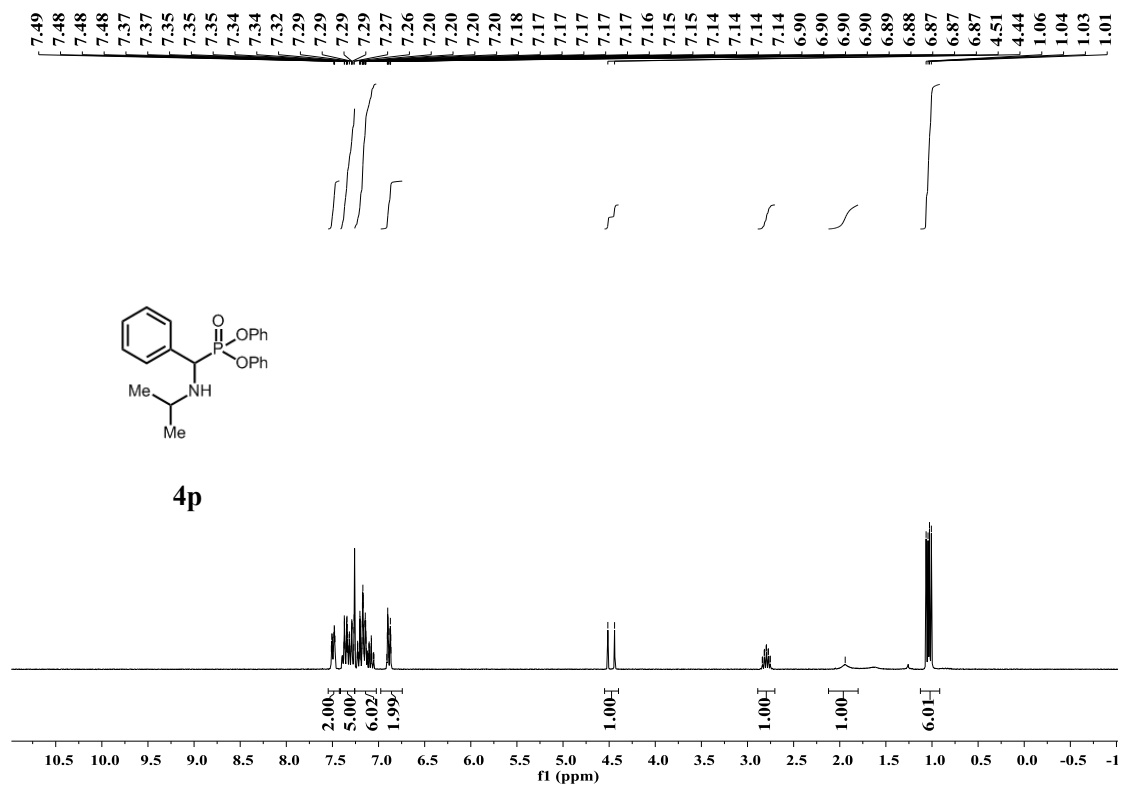


- 13.49

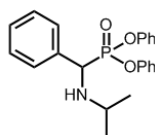
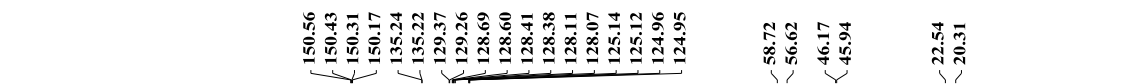


4m

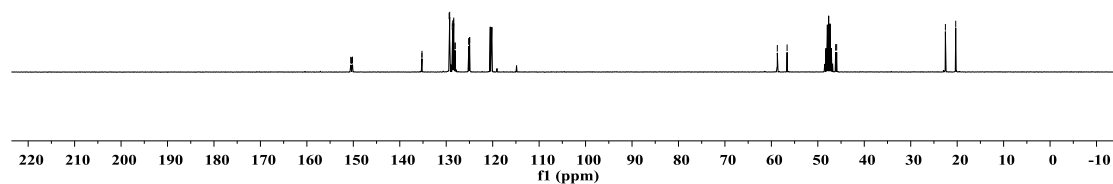


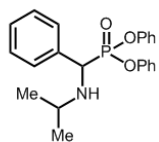


4p

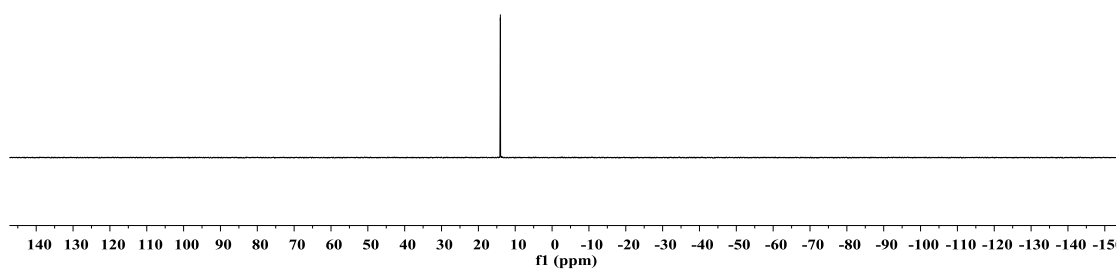


4p

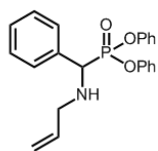




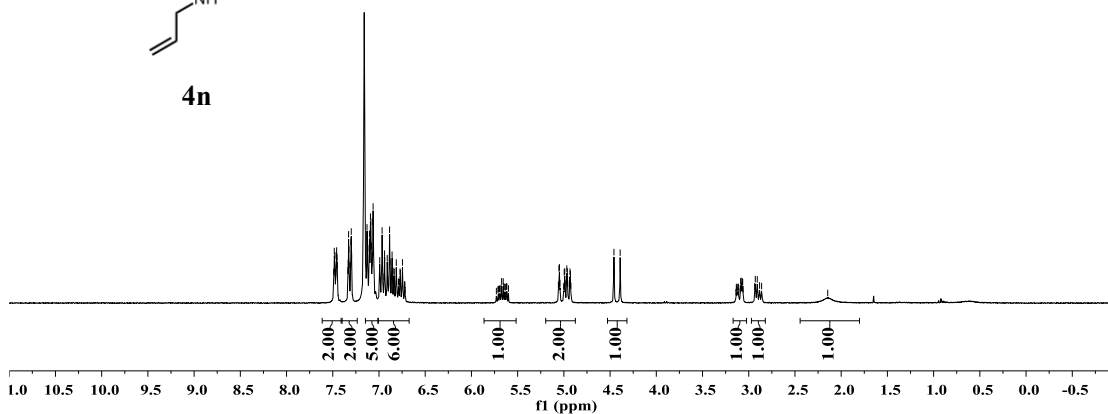
4p



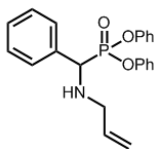
7.49
7.48
7.48
7.46
7.46
7.45
7.45
7.33
7.32
7.32
7.31
7.30
7.30
7.30
7.13
7.13
7.12
7.11
7.11
7.10
7.10
7.09
7.09
7.08
7.07
7.07
7.07
7.06
7.06
6.99
6.97
6.96
6.94
6.91
6.89
6.88
6.86
6.84
6.84
6.81
6.77
6.75
5.05
4.99
4.97
4.96
4.93
4.46
4.39



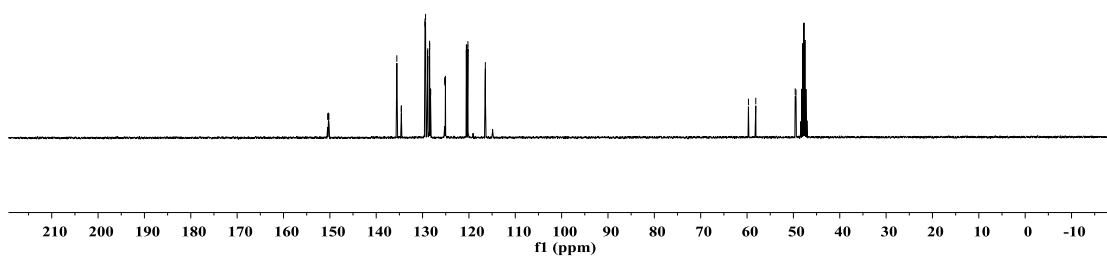
4n



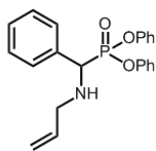
150.47
 150.36
 150.30
 150.20
 135.55
 134.60
 134.58
 129.47
 129.46
 129.35
 128.94
 128.87
 128.49
 128.46
 128.28
 128.25
 125.22
 125.20
 125.07
 125.05
 120.56
 120.52
 120.26
 120.22
 116.46
 59.70
 58.12
 49.62
 49.44



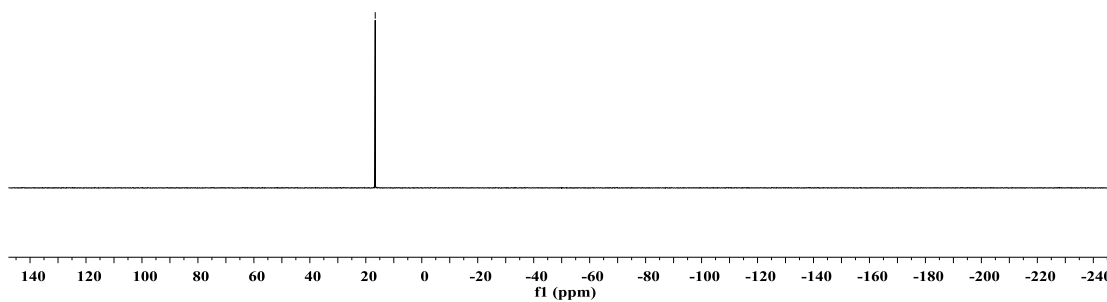
4n

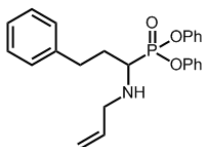
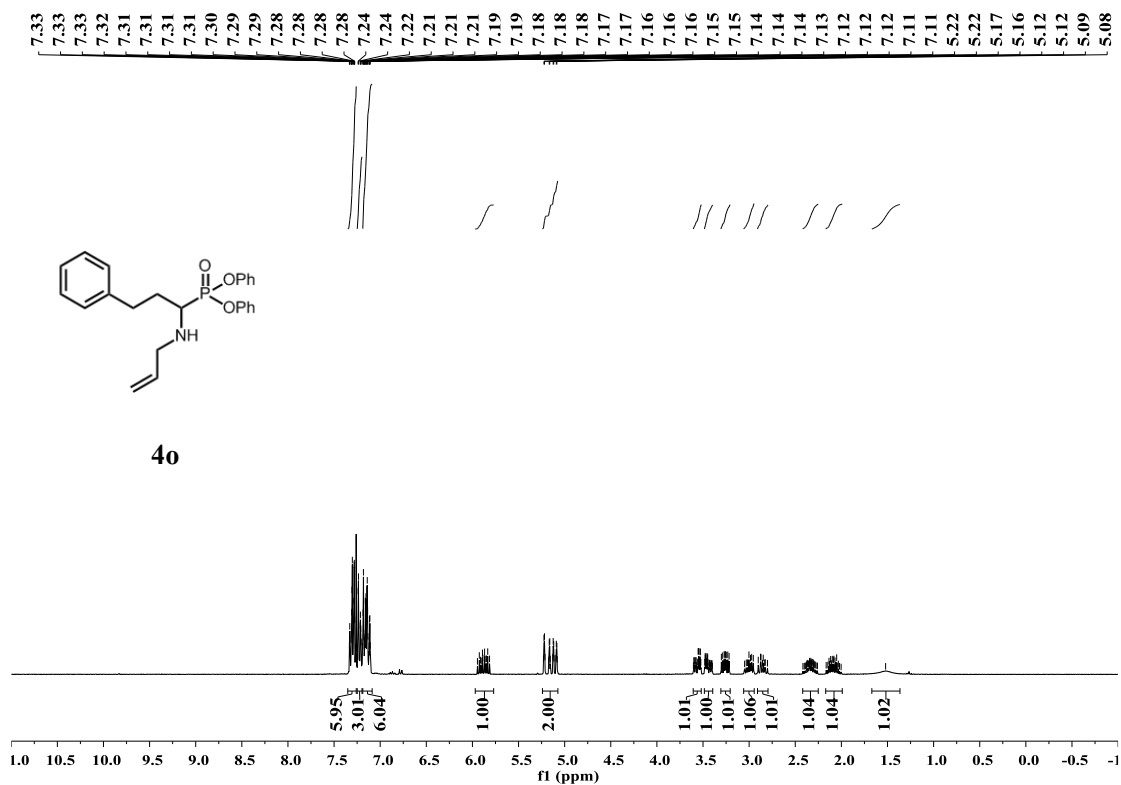


- 16.63

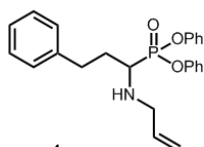
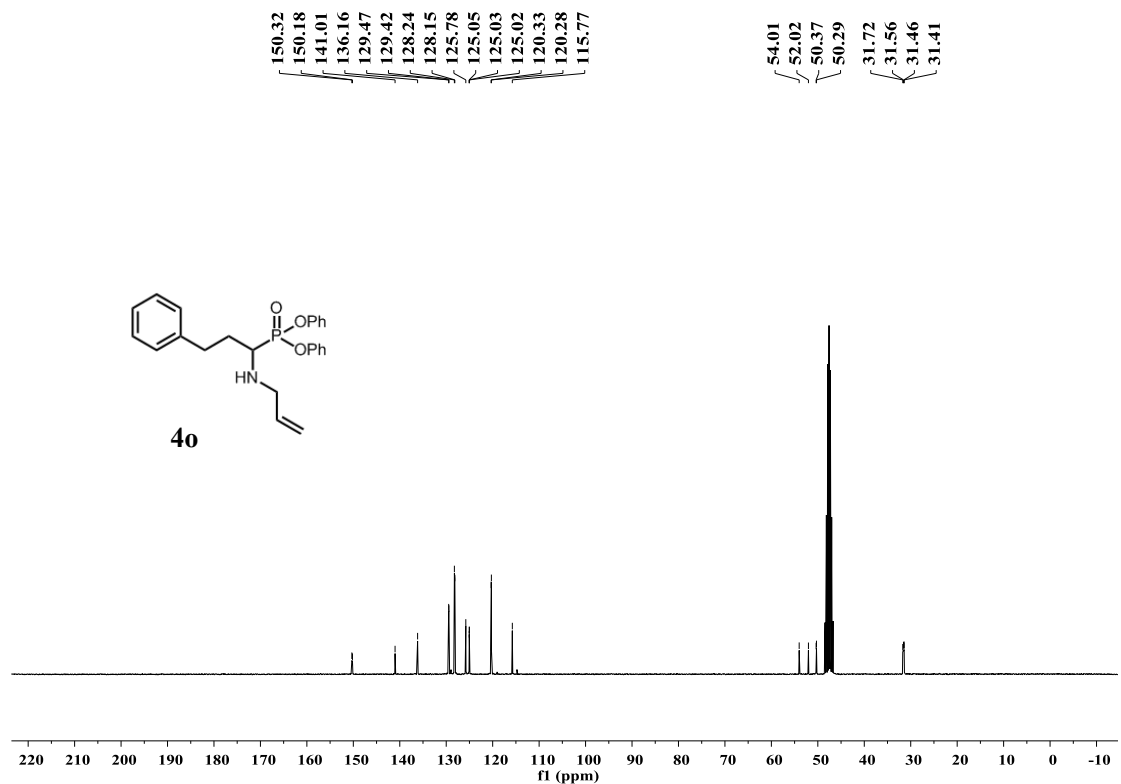


4n

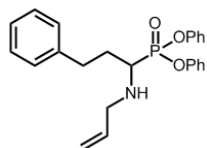




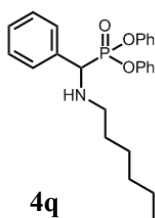
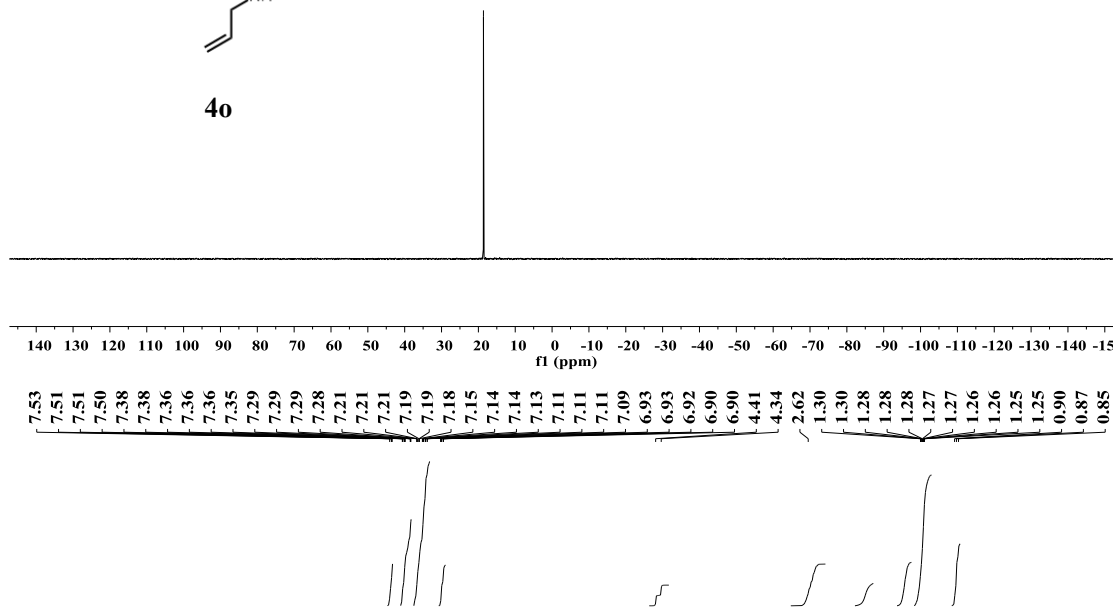
40



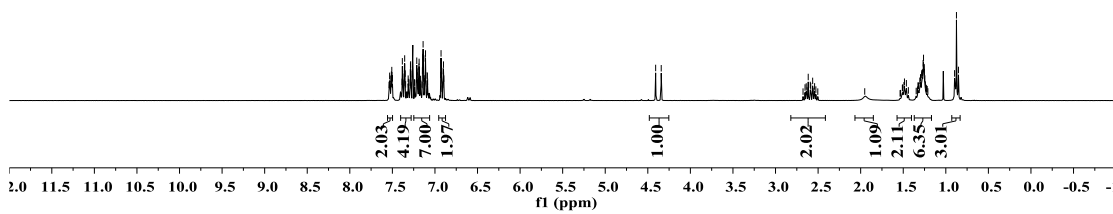
40

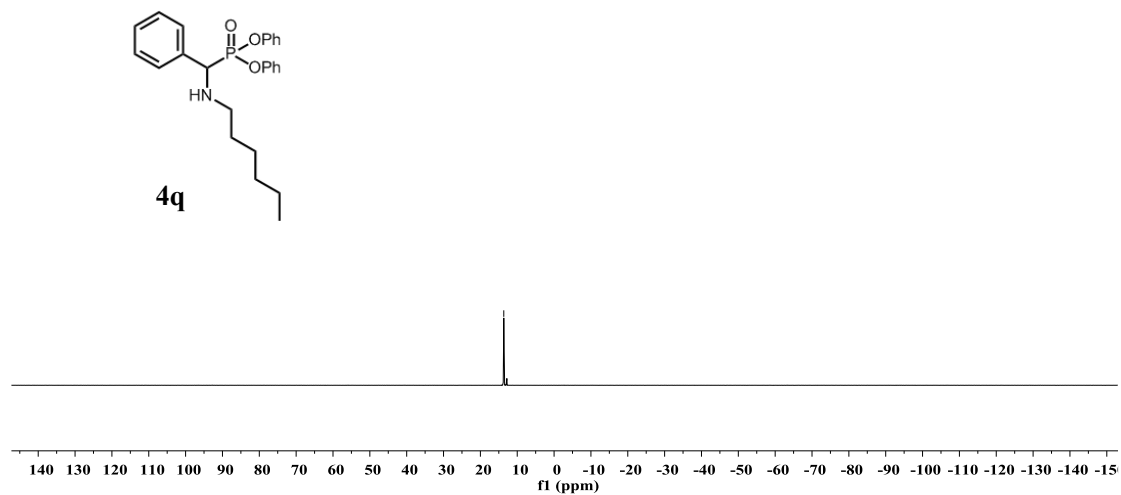
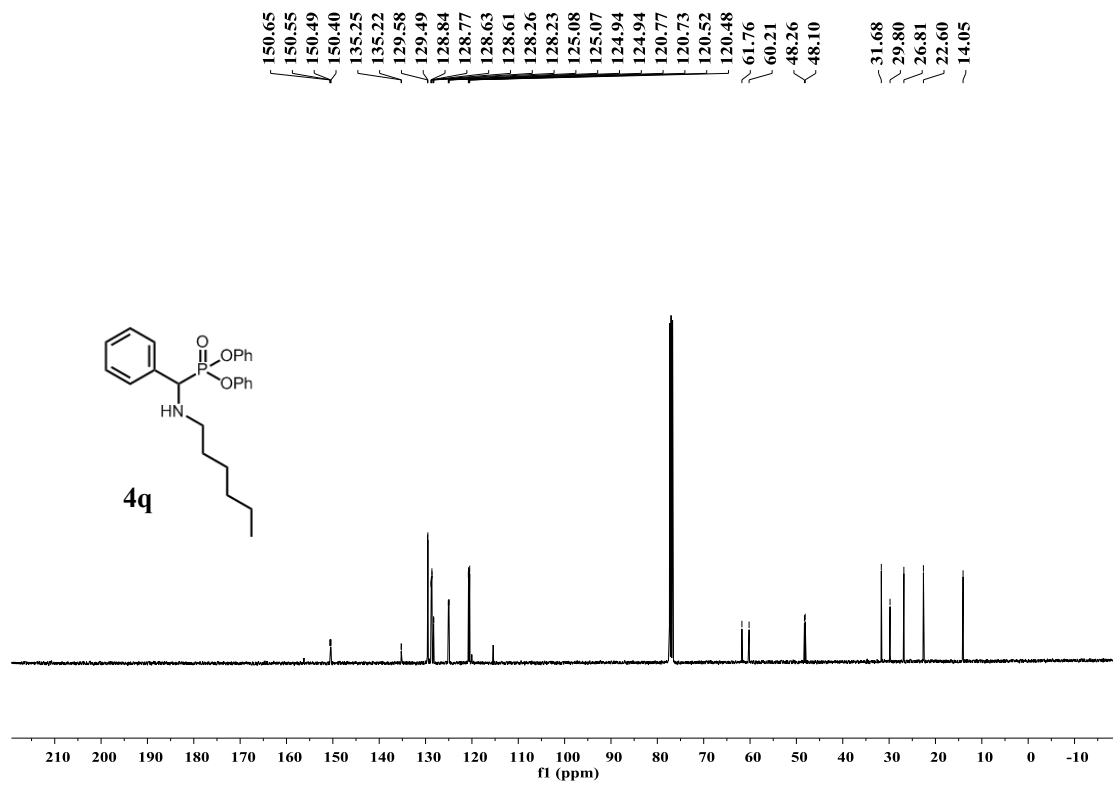


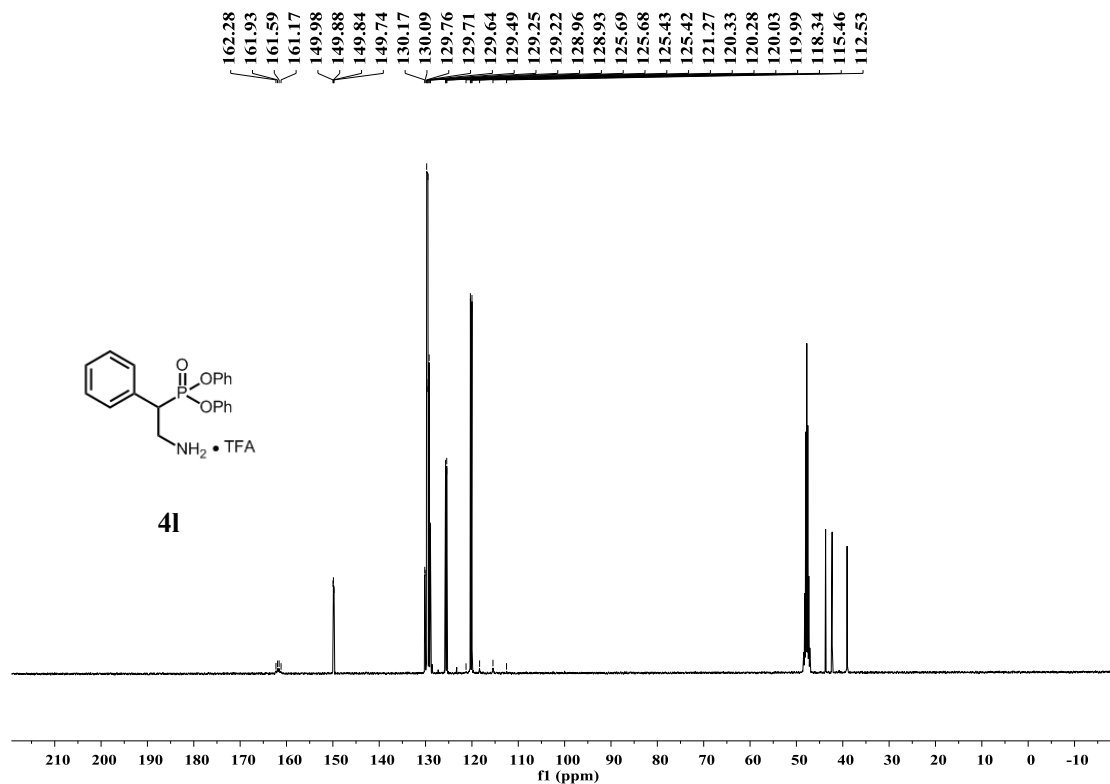
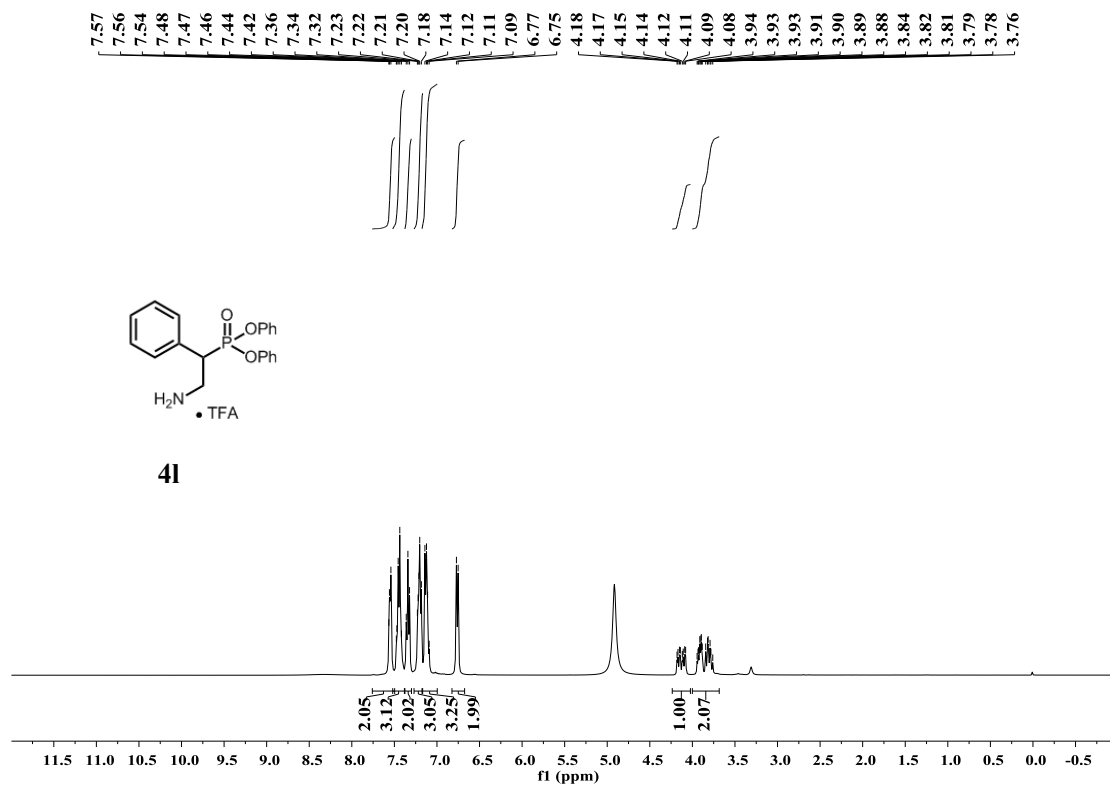
40



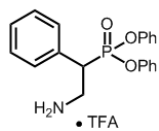
4q



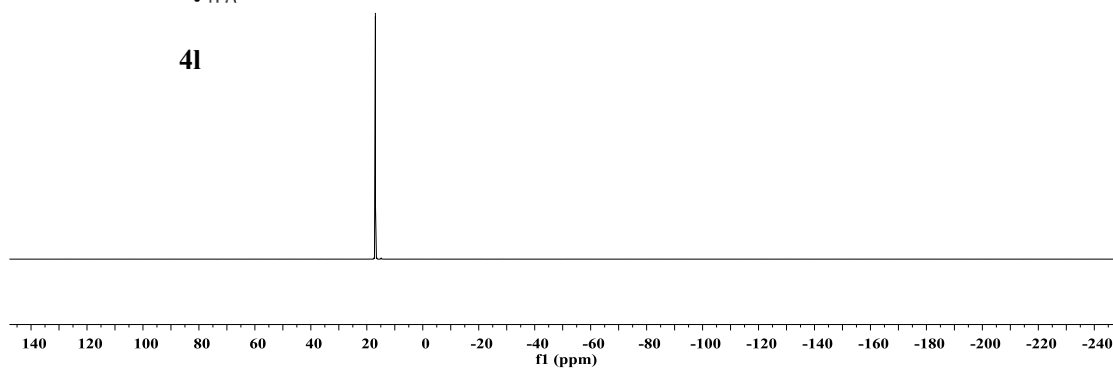




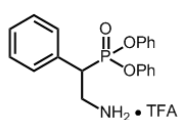
— 16.92



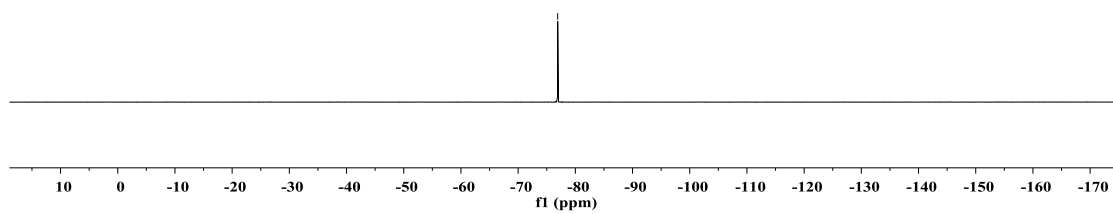
4l

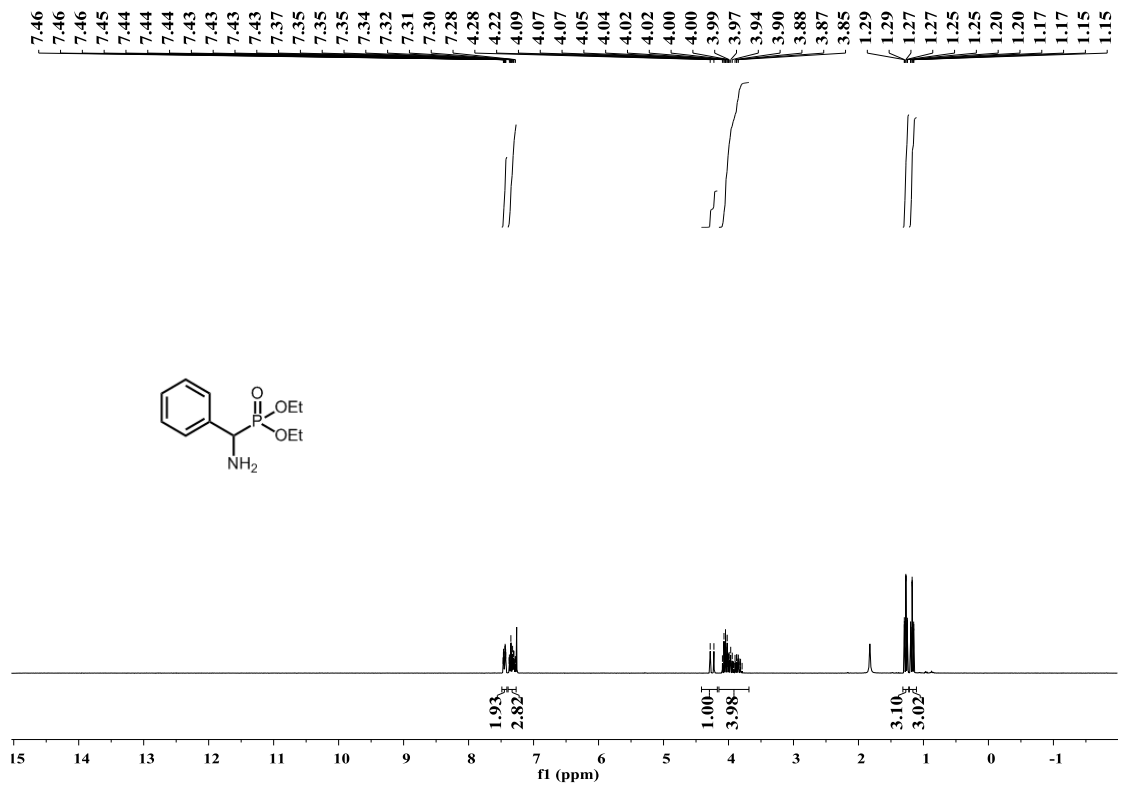


— -76.91

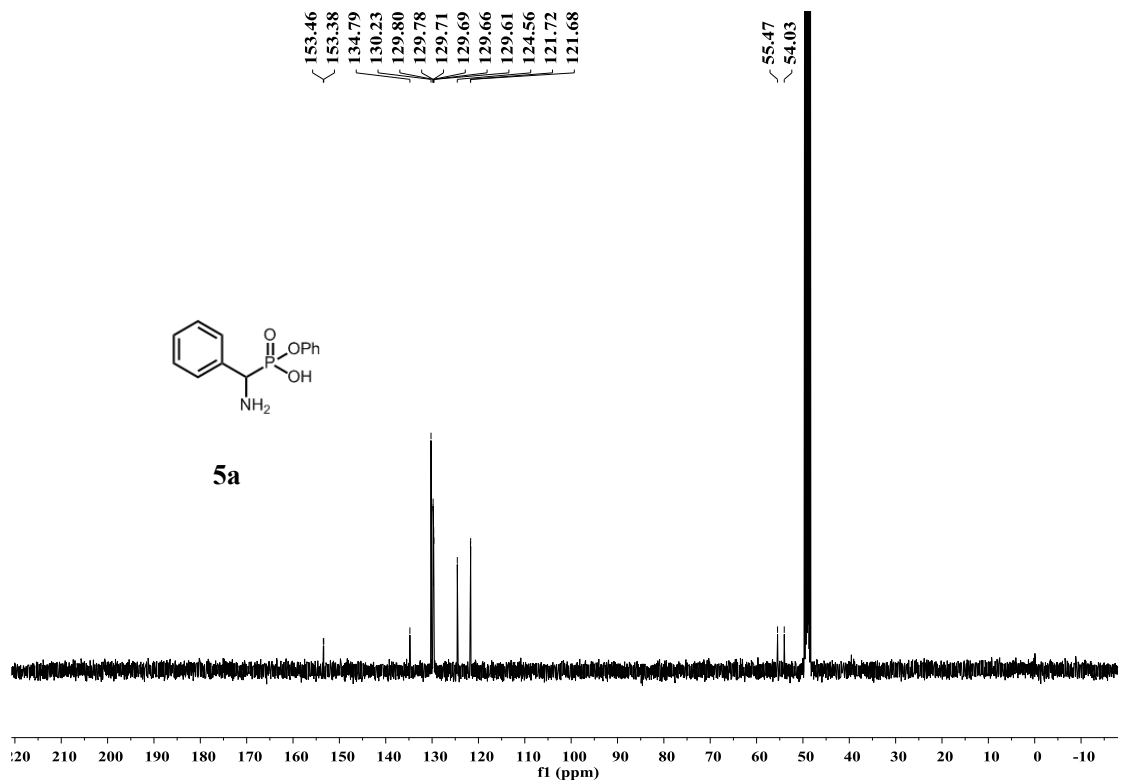
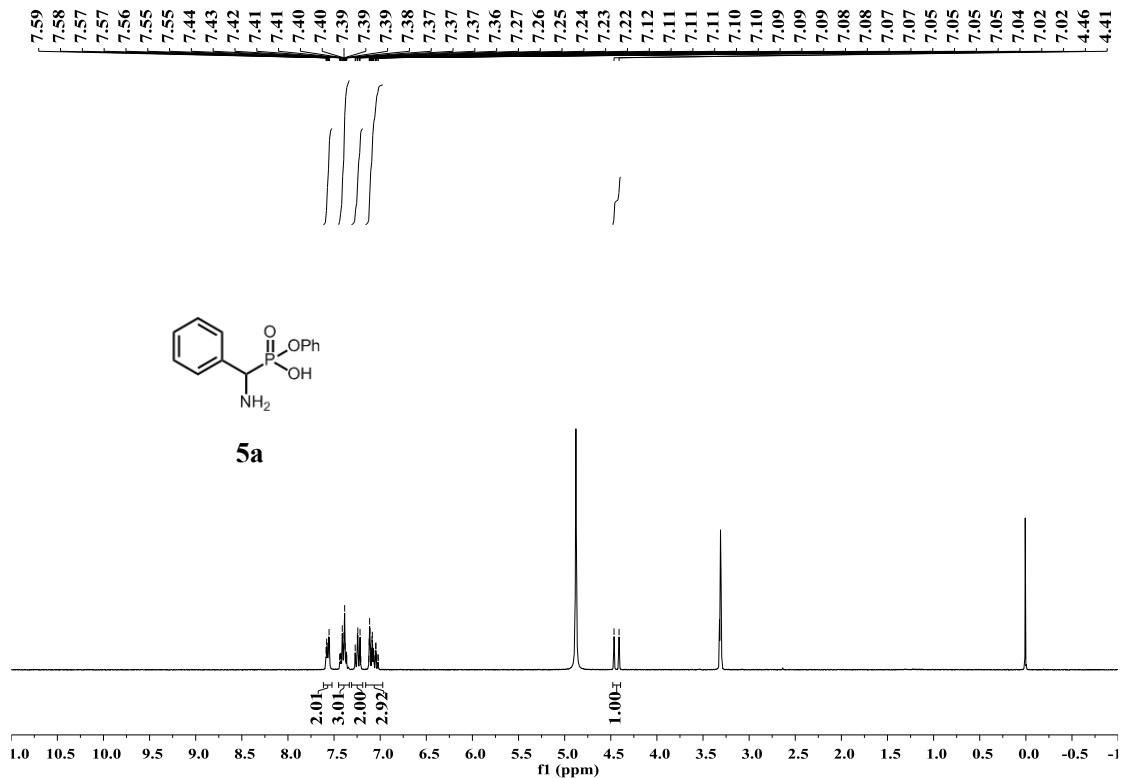


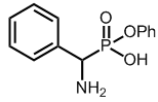
4l



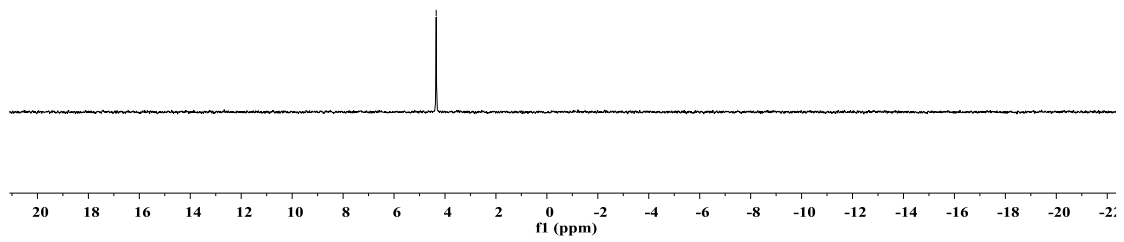


Spectra for products in Chapter 3

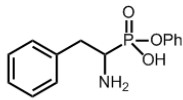




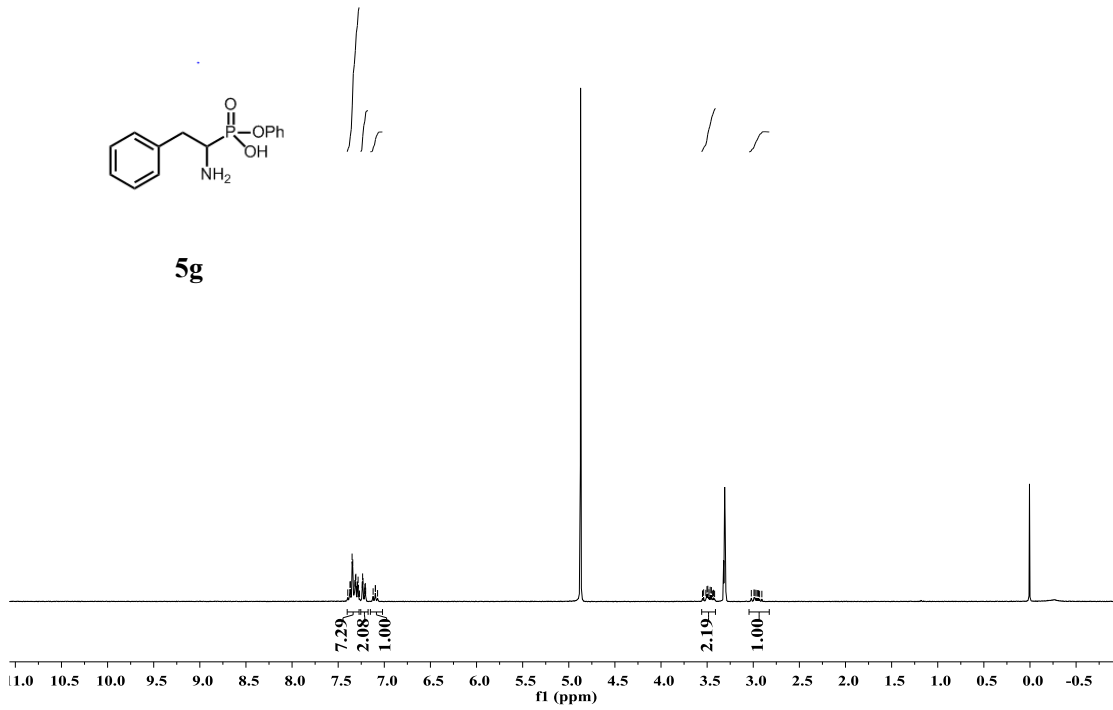
5a



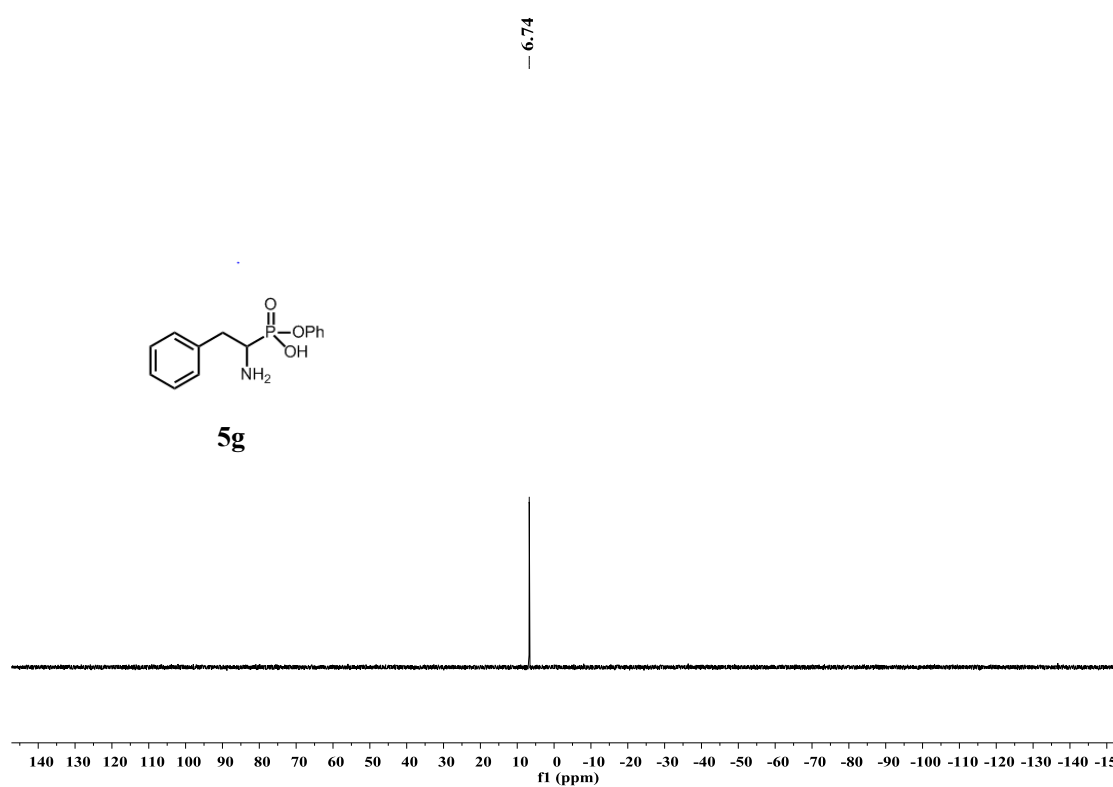
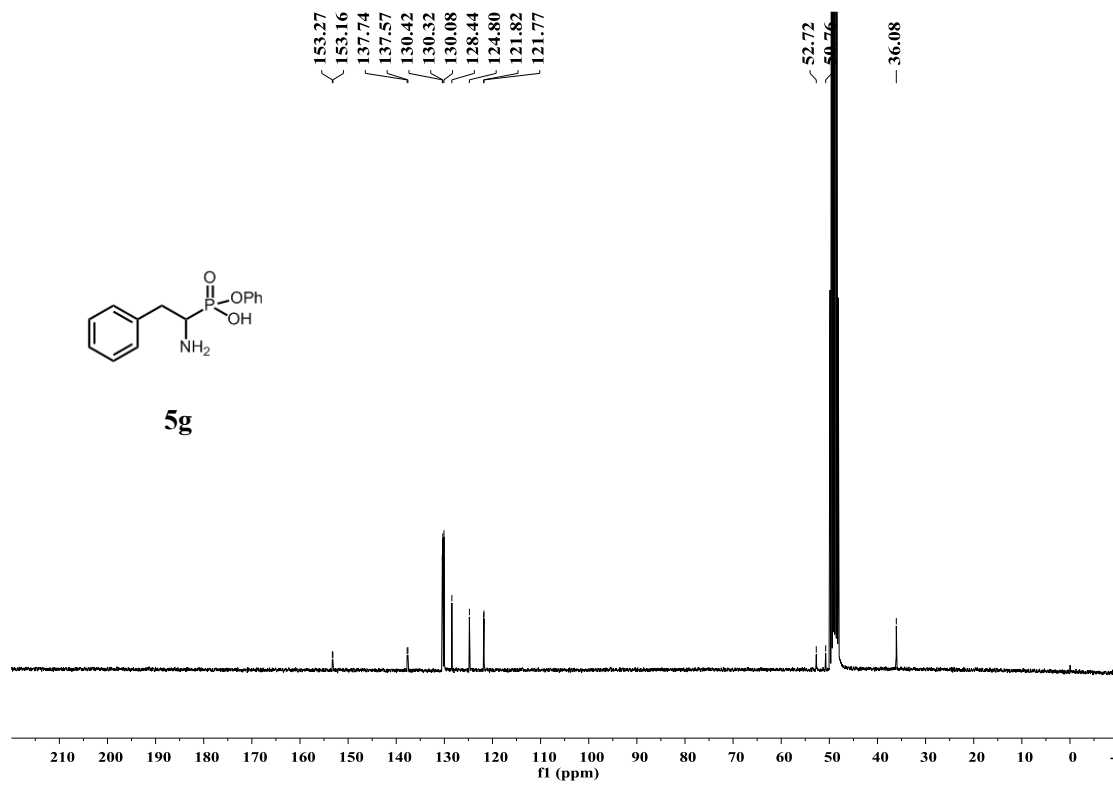
7.40
7.37
7.36
7.35
7.34
7.32
7.31
7.31
7.30
7.30
7.29
7.28
7.24
7.24
7.23
7.21
7.21
7.21
7.20
7.12
7.10
7.10
7.10
7.07
3.85
3.85
3.54
3.51
3.50
3.49
3.48
3.47
3.45
3.44
3.44
3.42
3.02
2.99
2.98
2.97
2.96
2.94
2.93
2.91

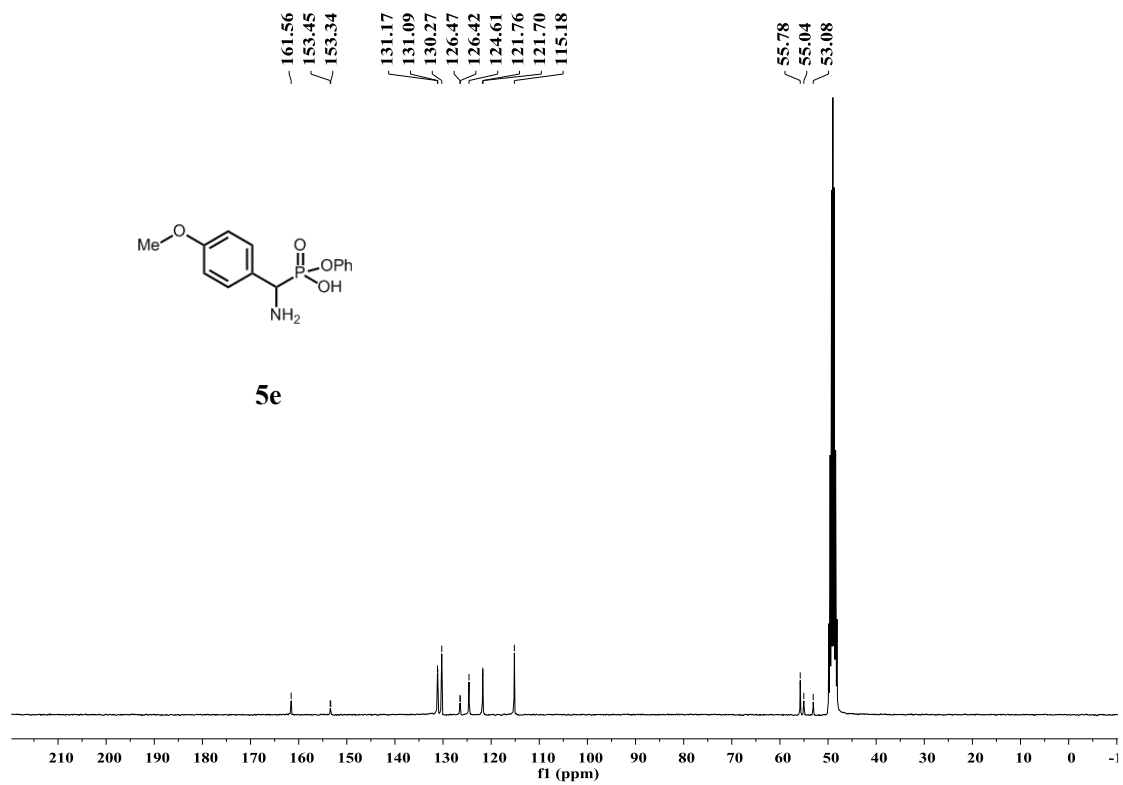
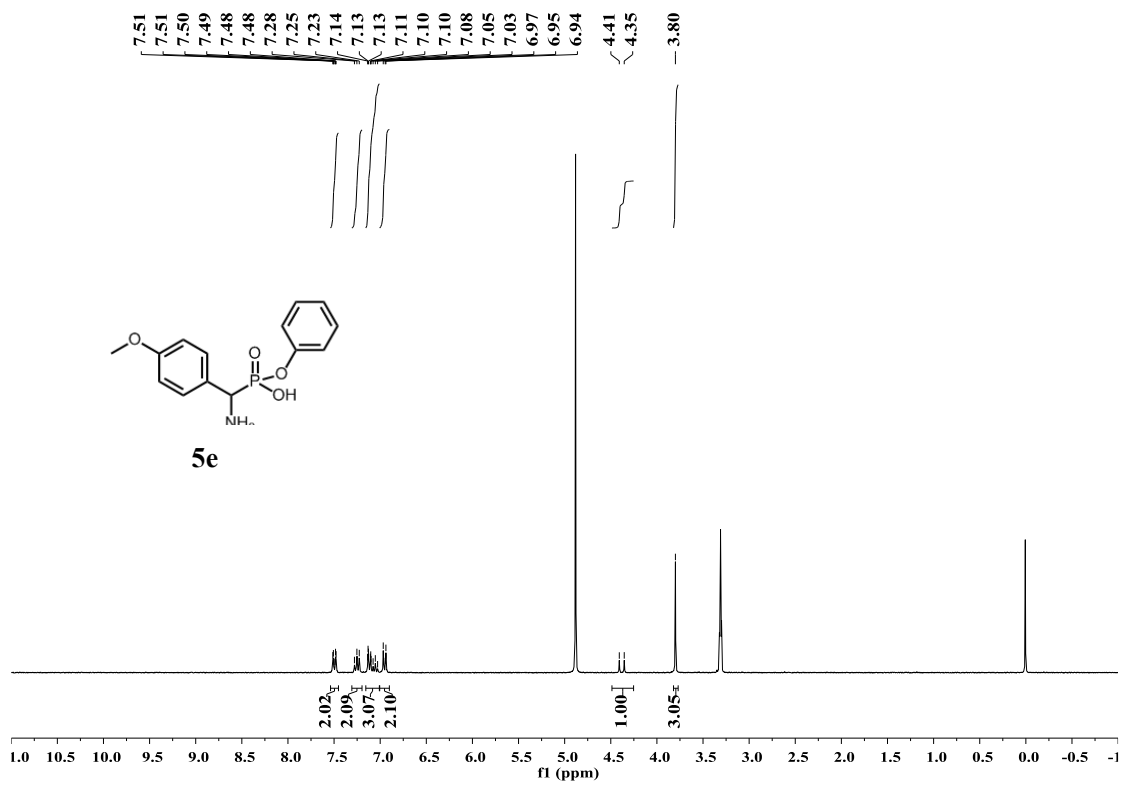


5g

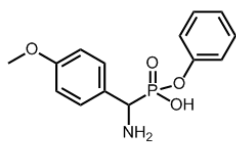


7.29
2.08
1.00
2.19
1.00

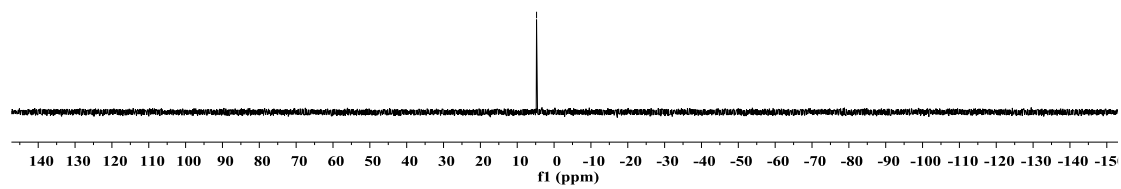


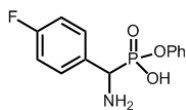
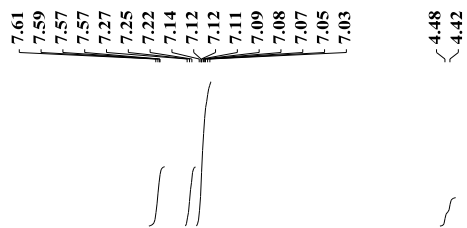


— 4.76

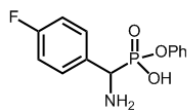
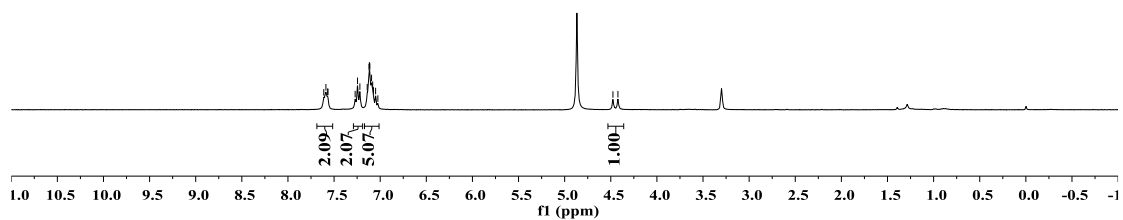


5e

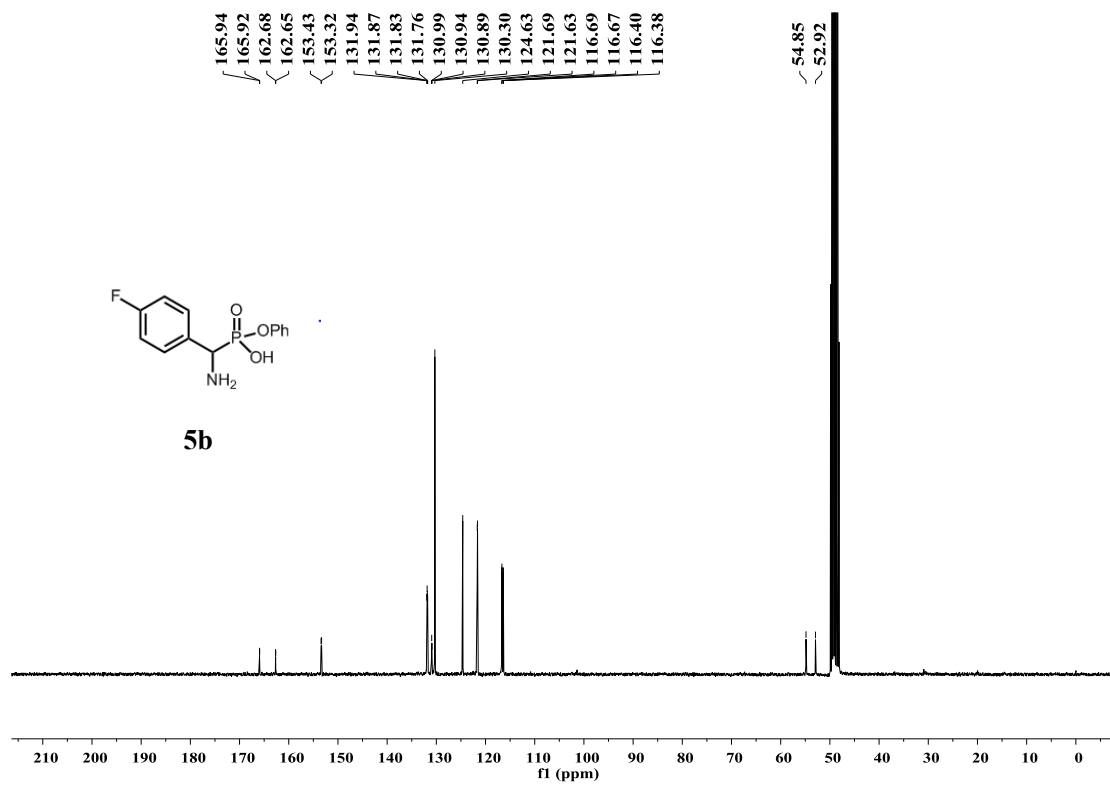




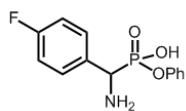
5b



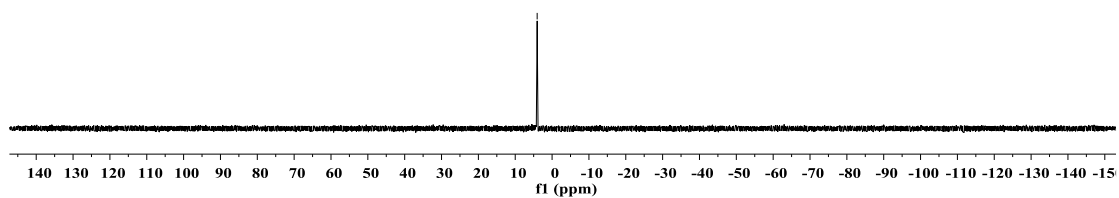
5b



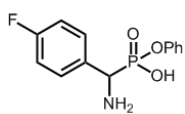
- 4.05



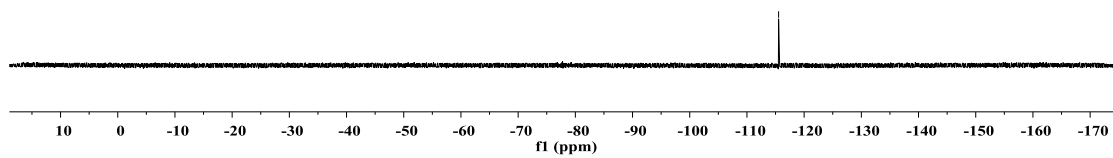
5b

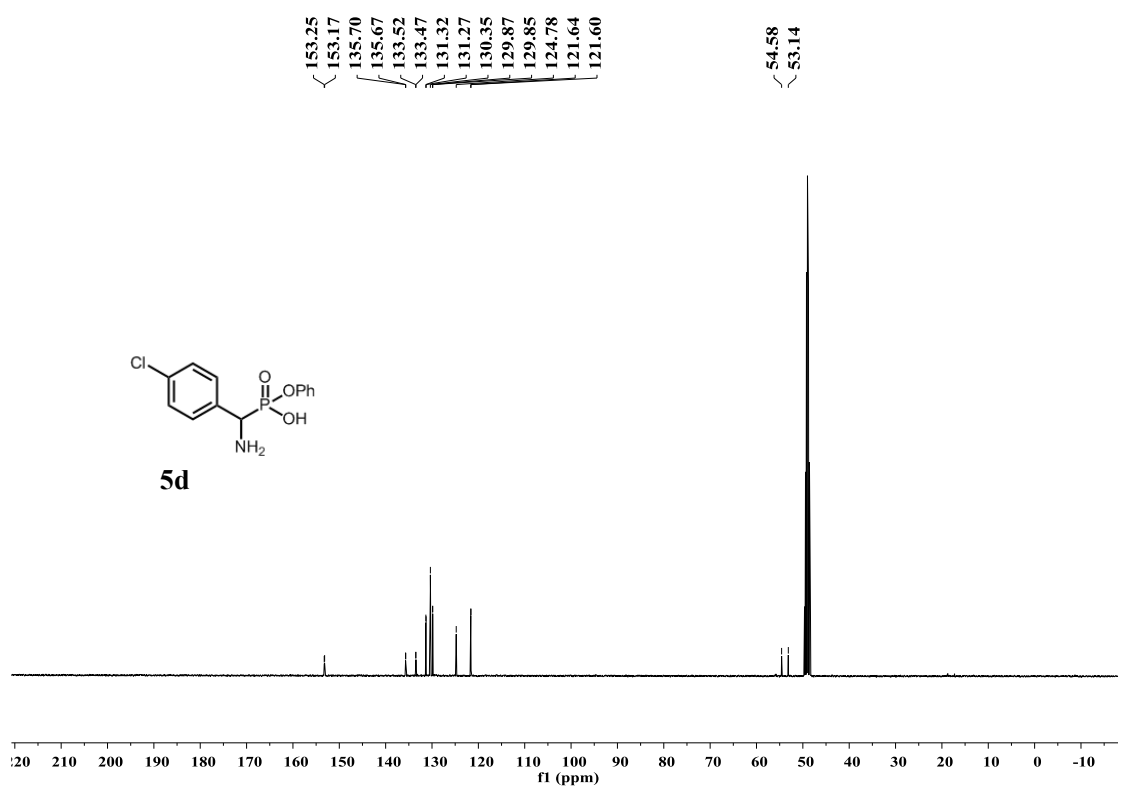
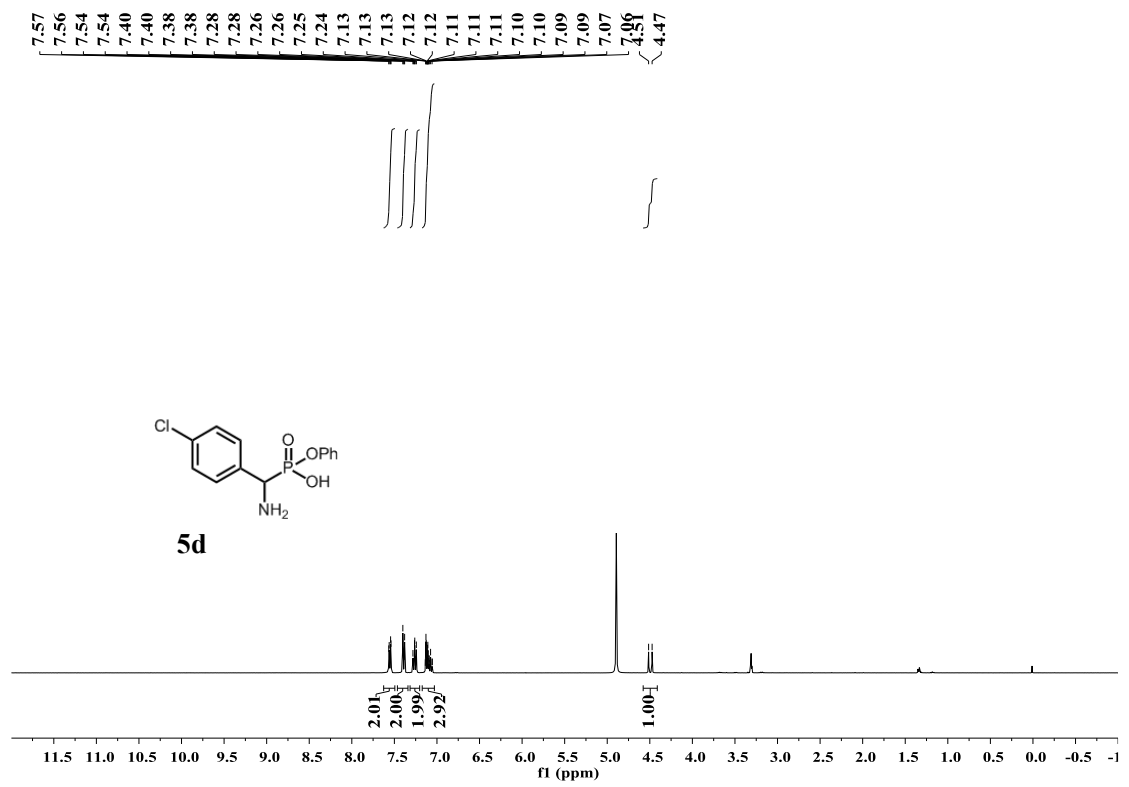


{ -115.52
-115.53

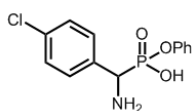


5b

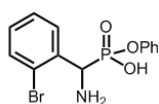
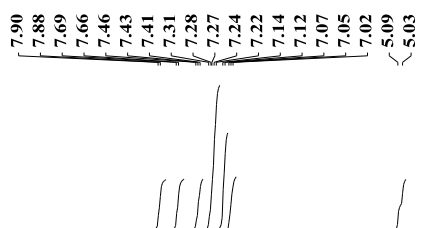
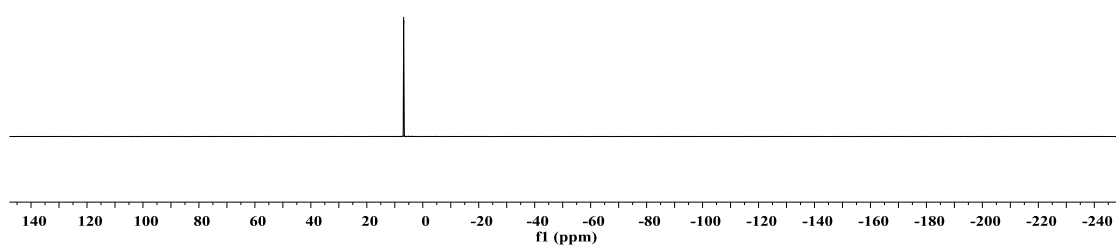




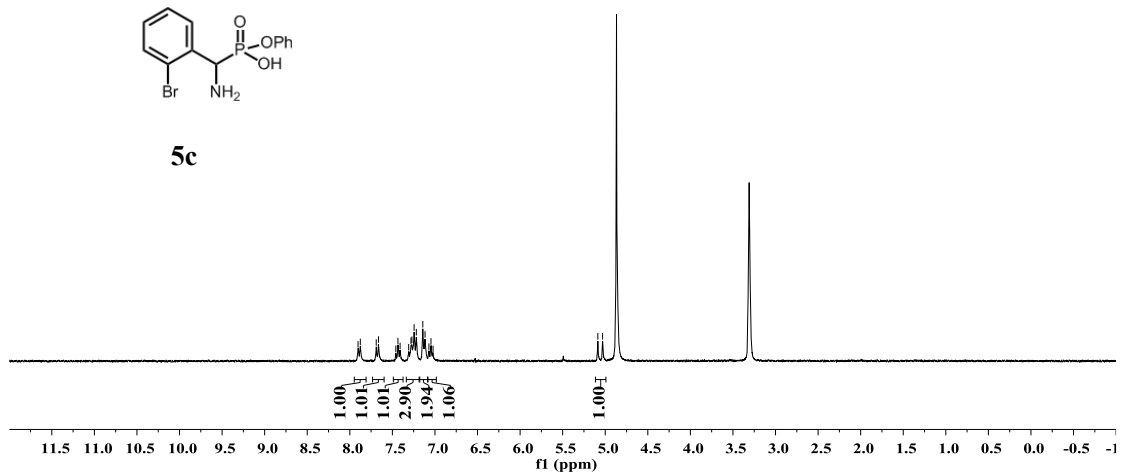
6.83

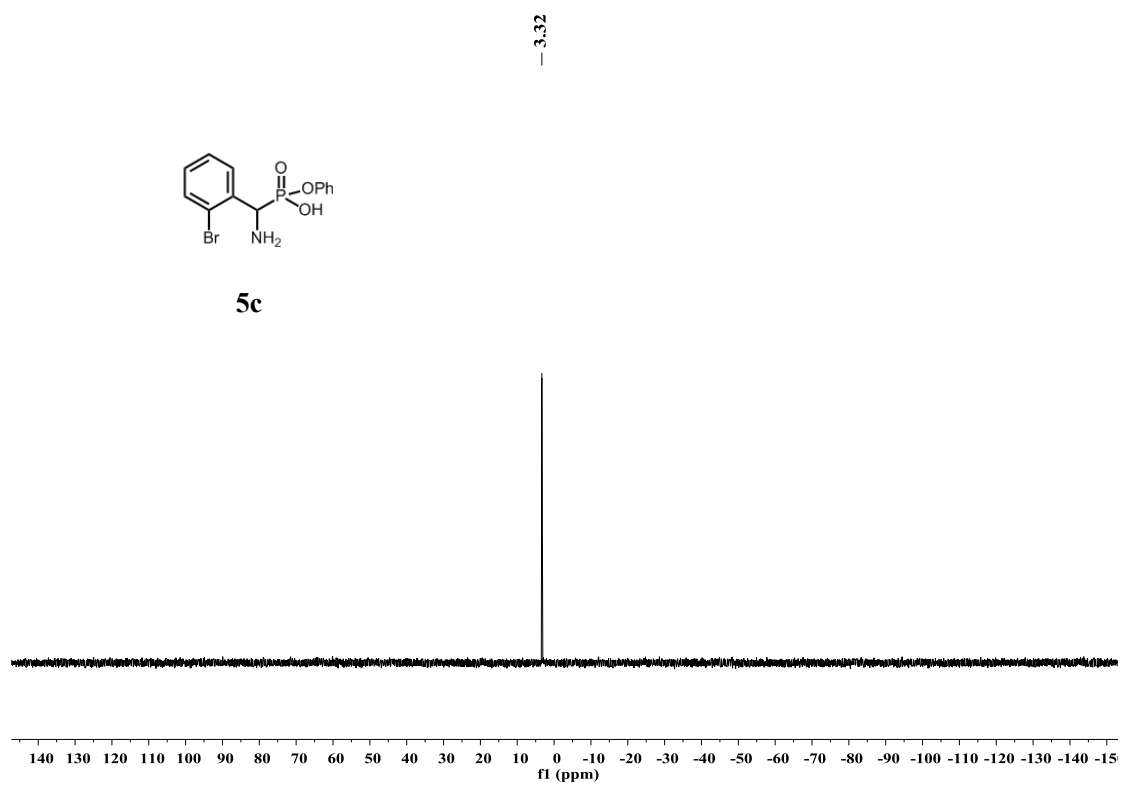
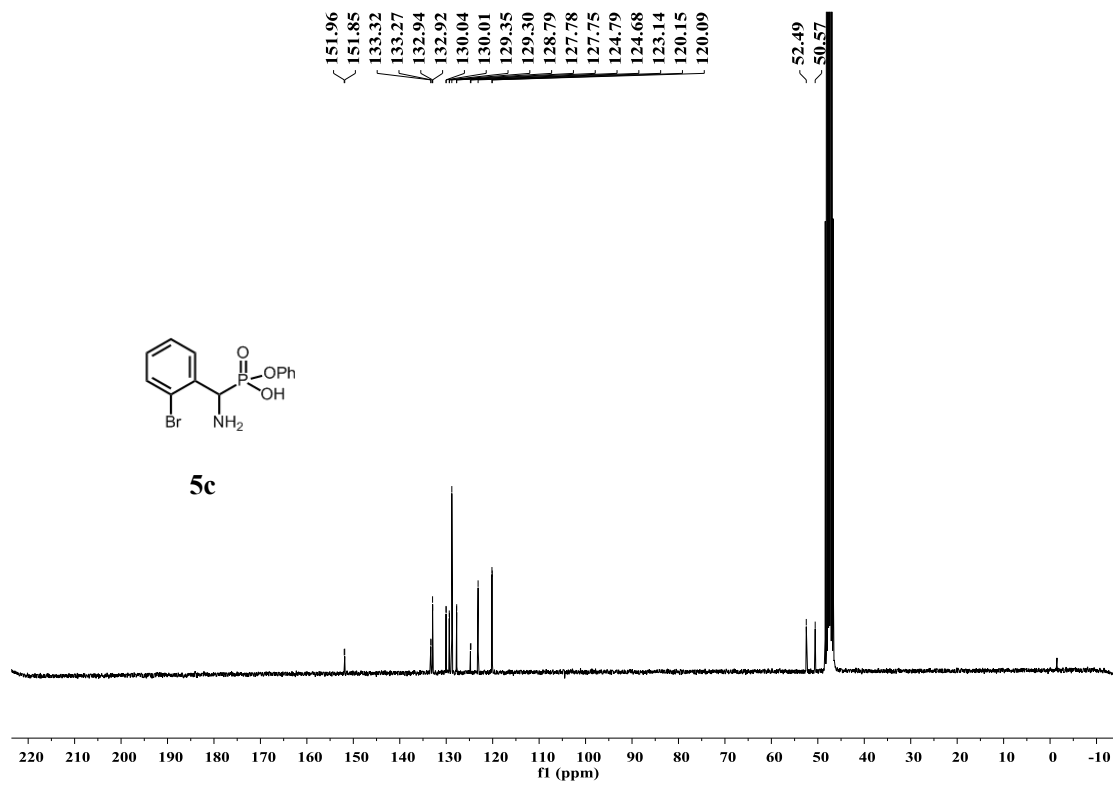


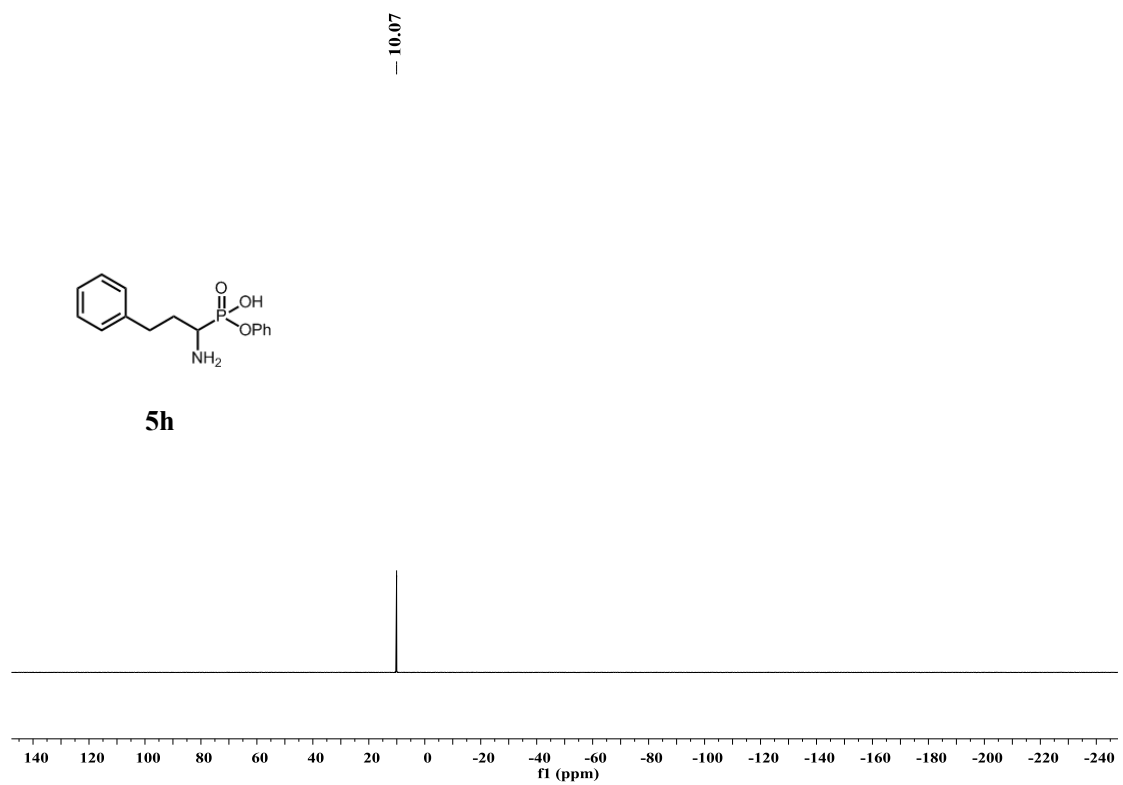
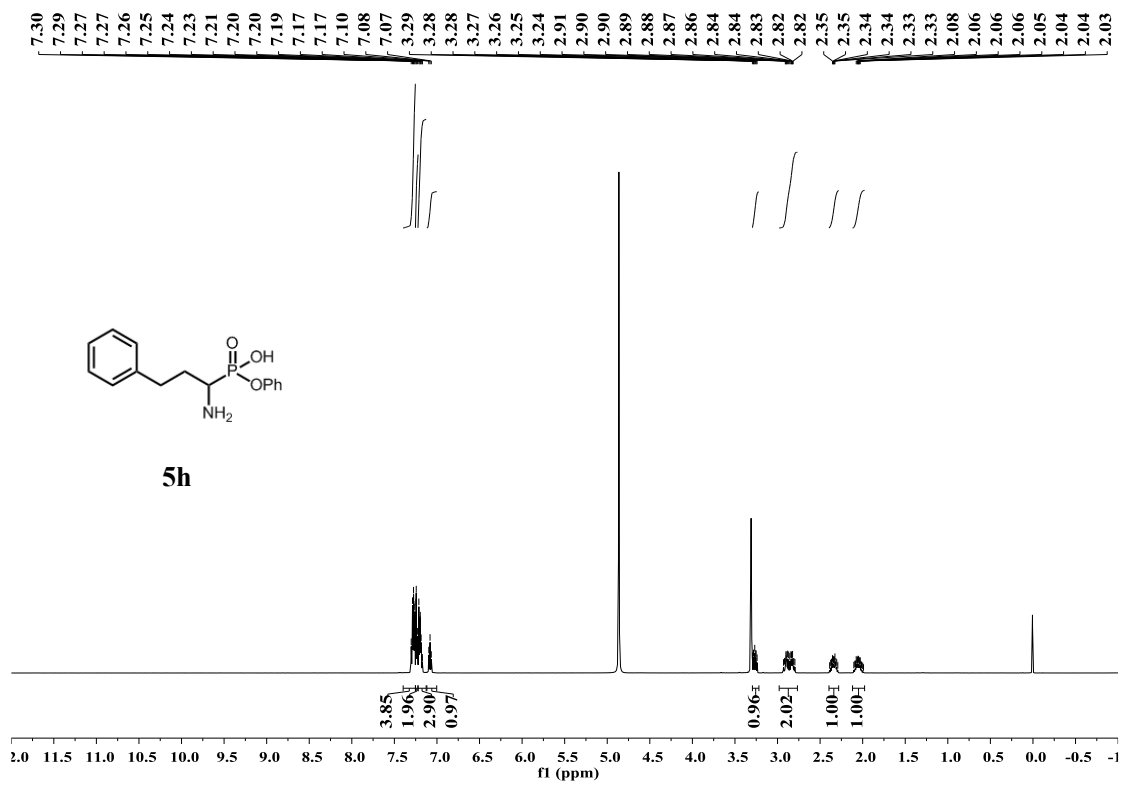
5d

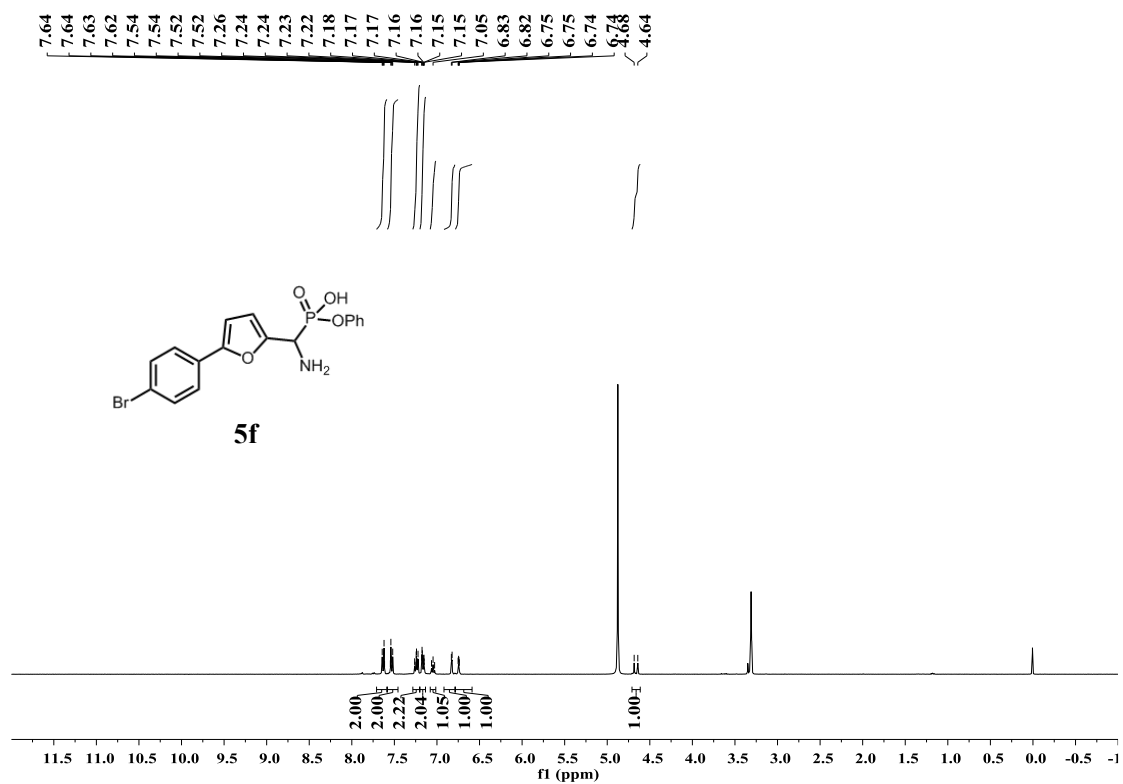
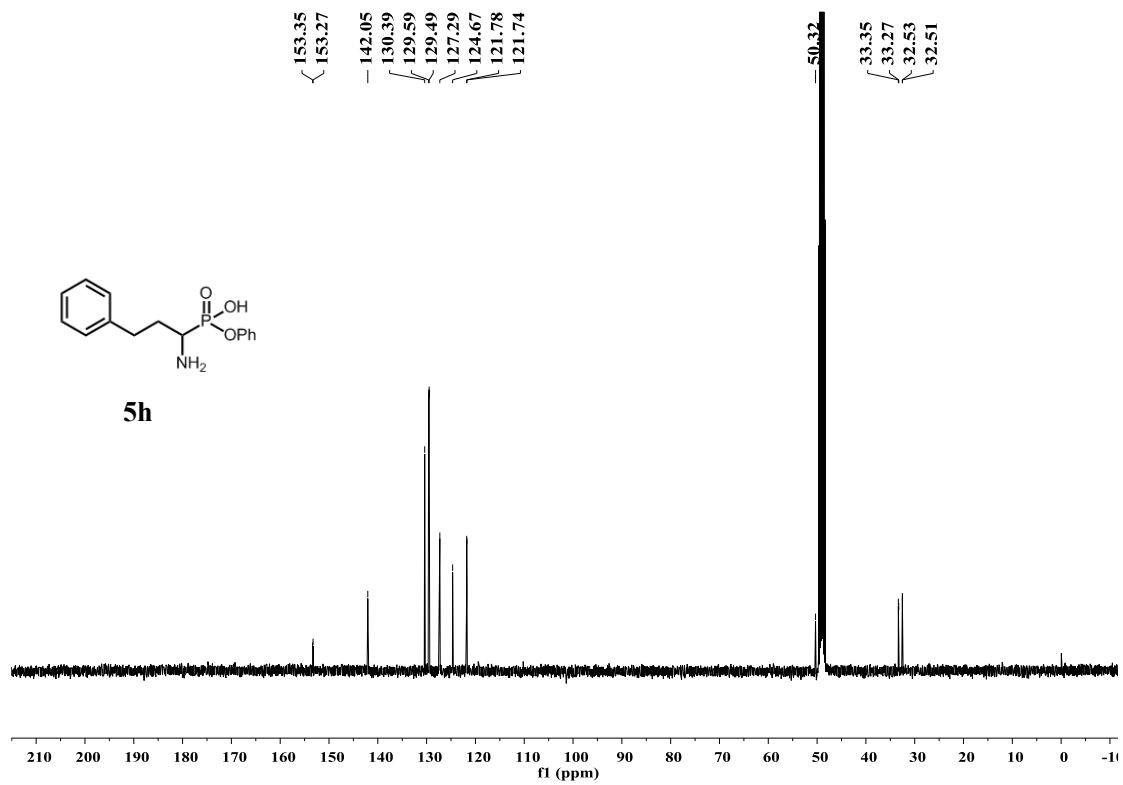


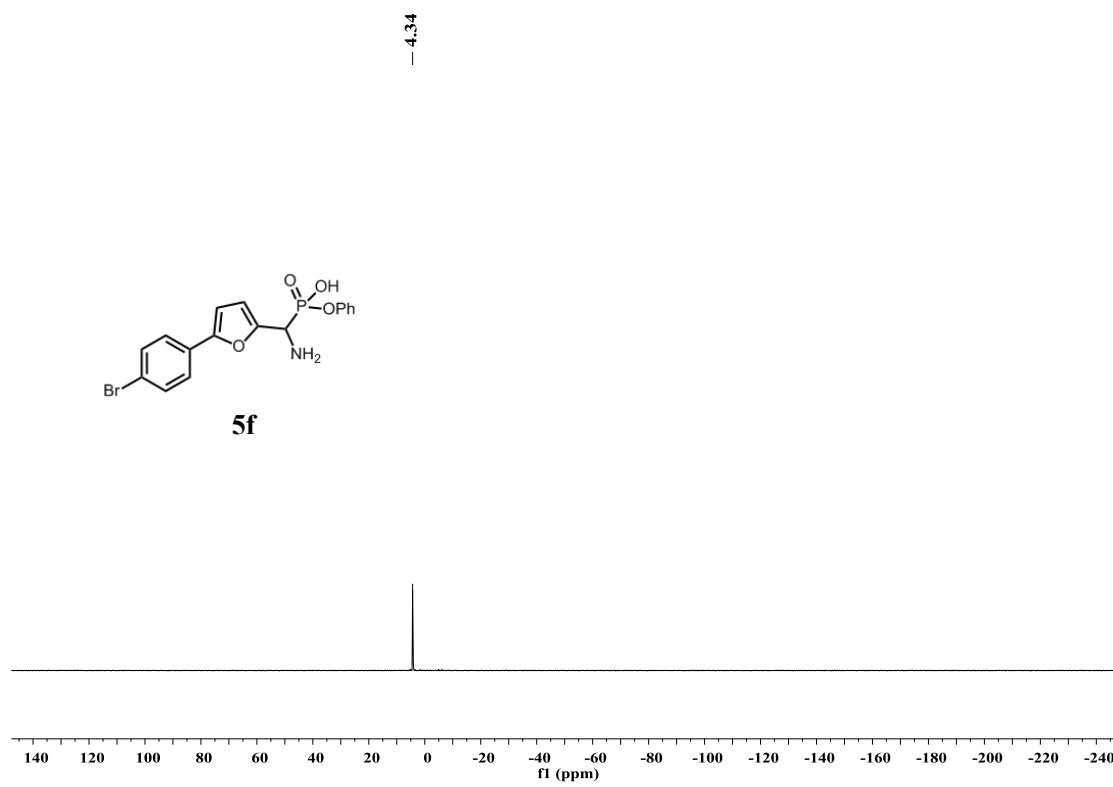
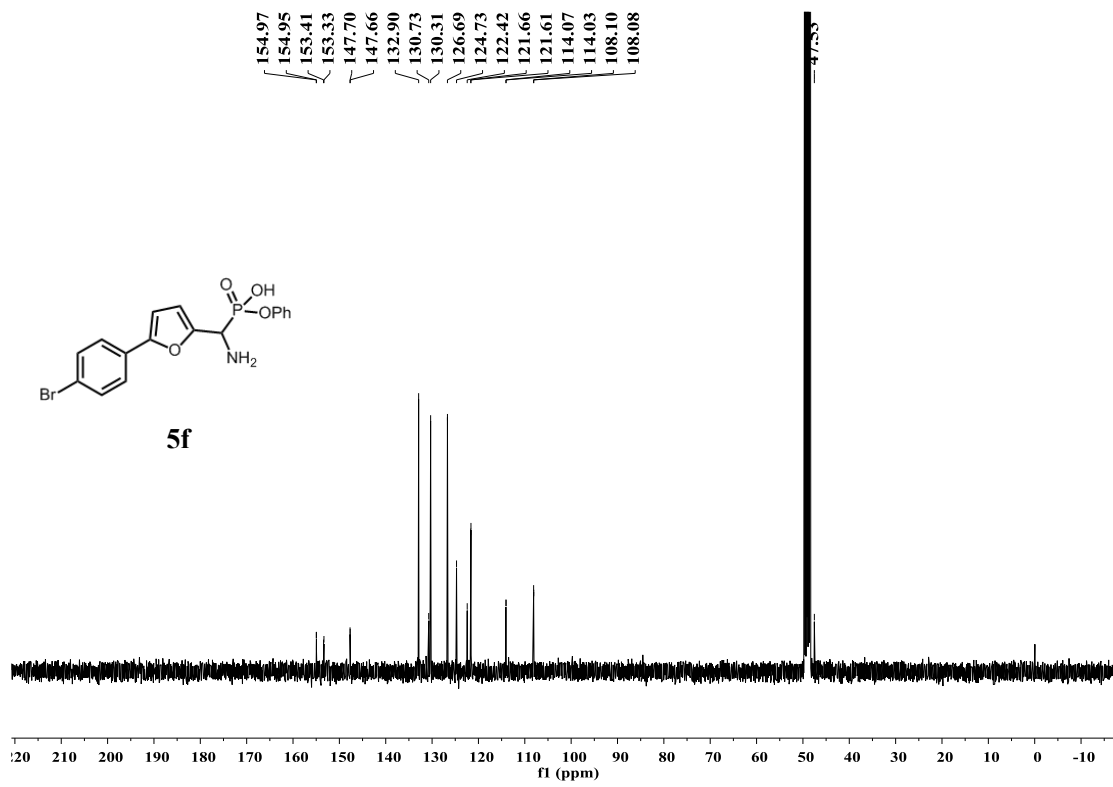
5c

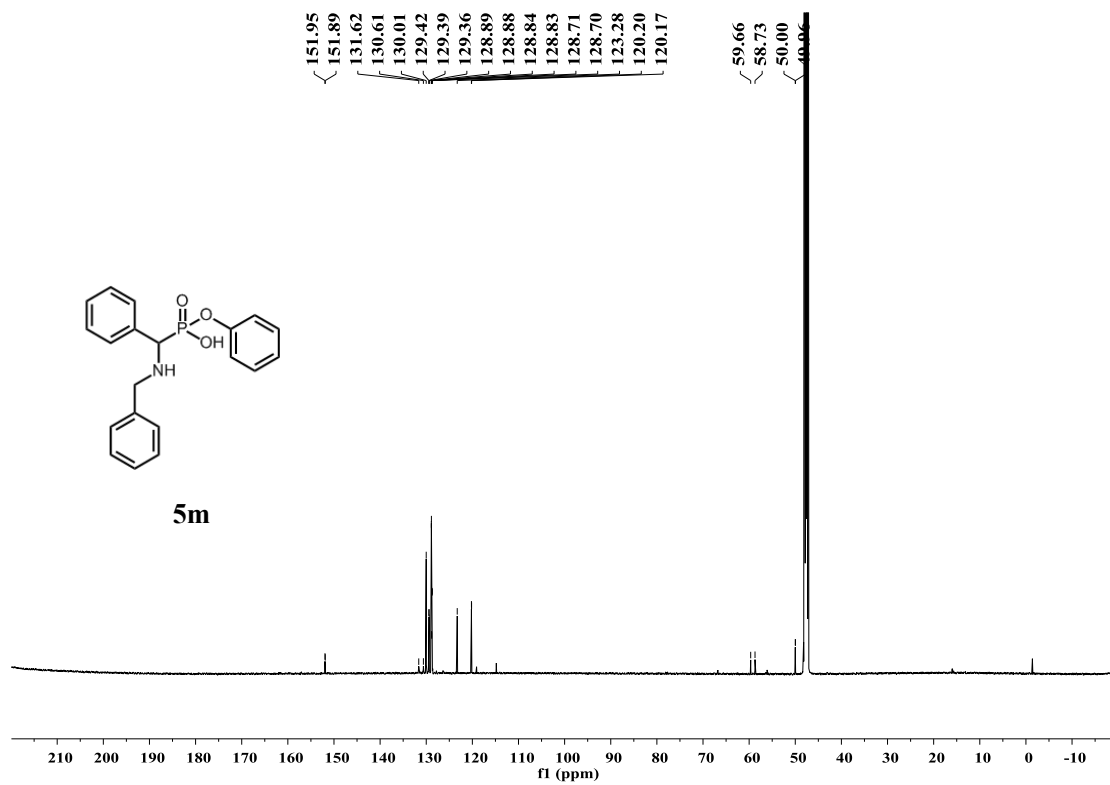
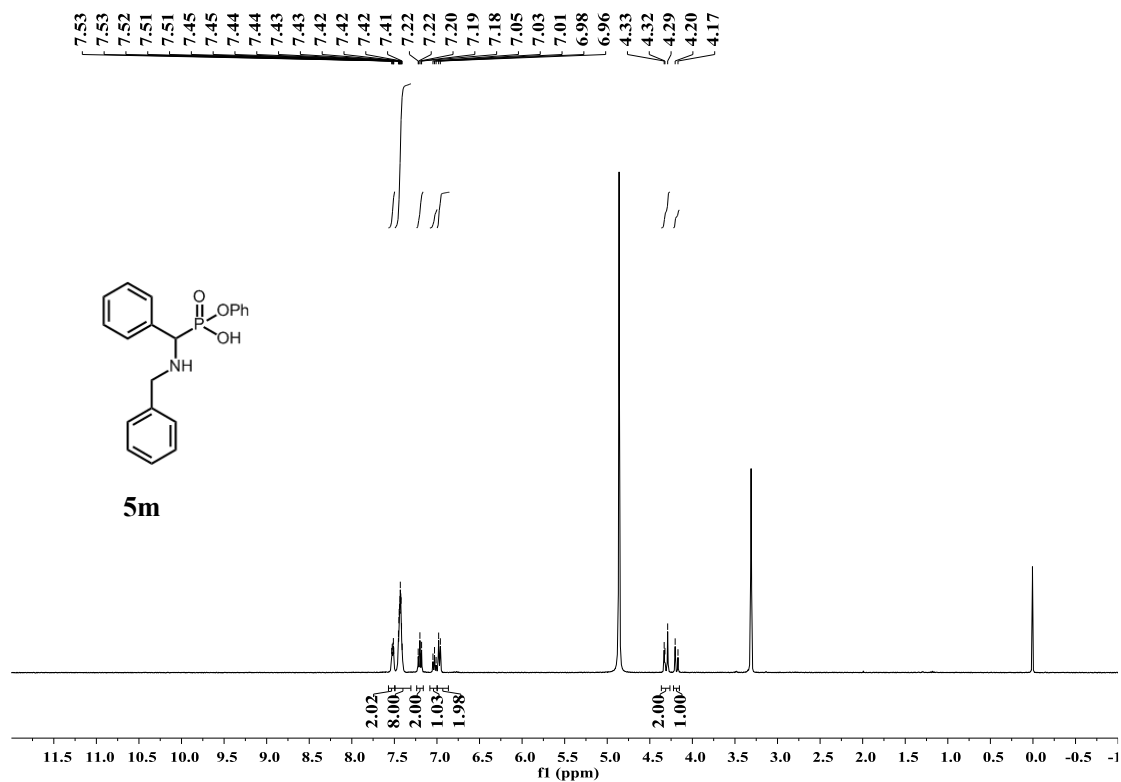


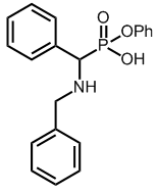




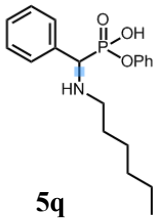
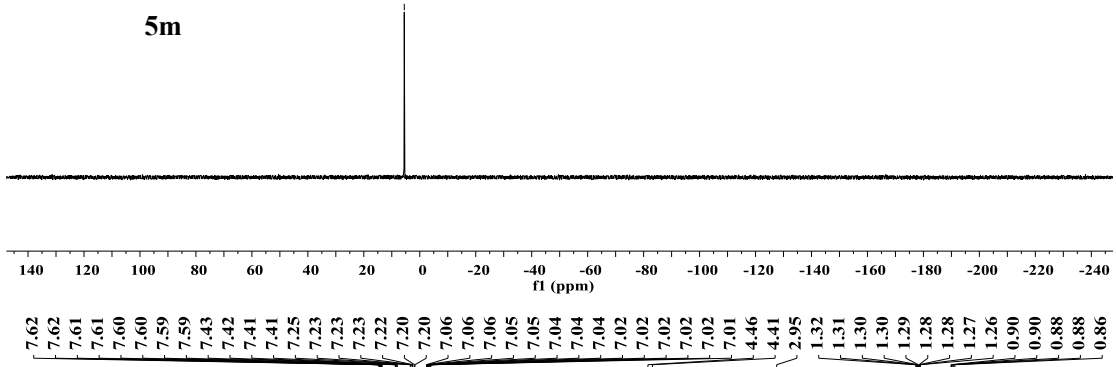




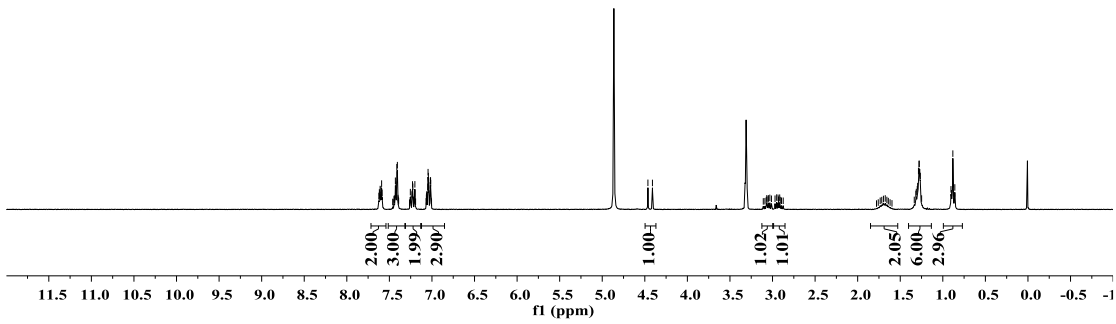


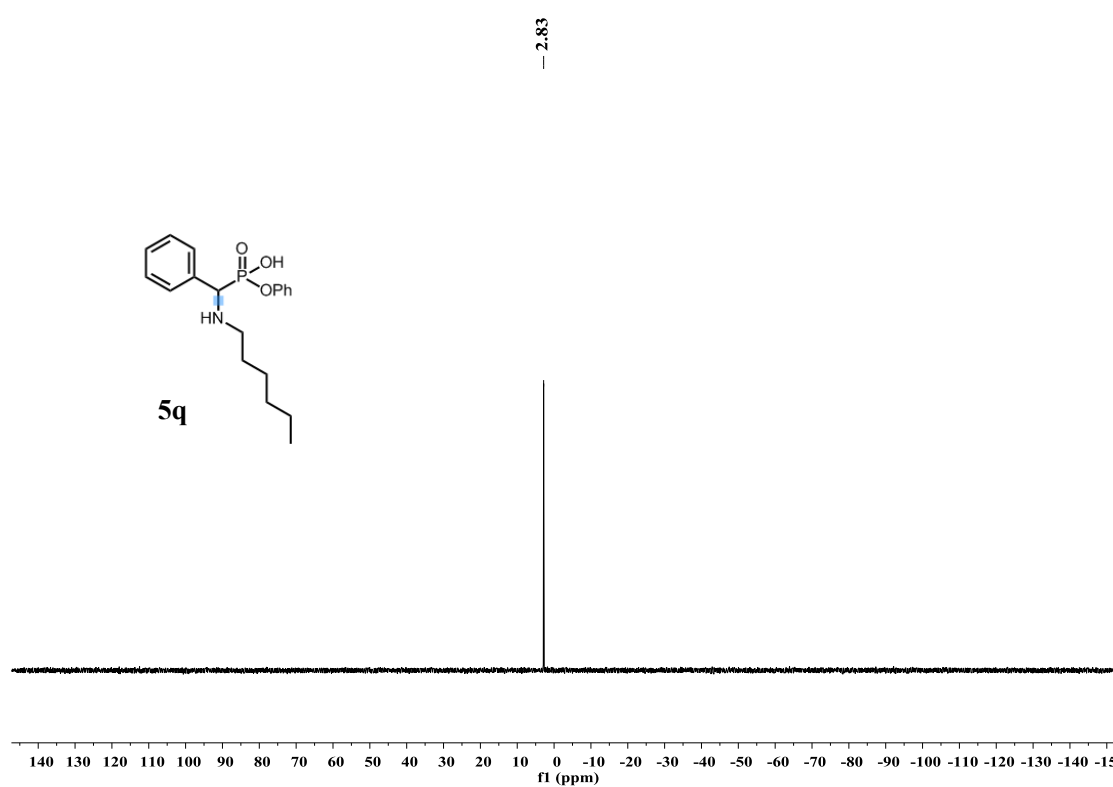
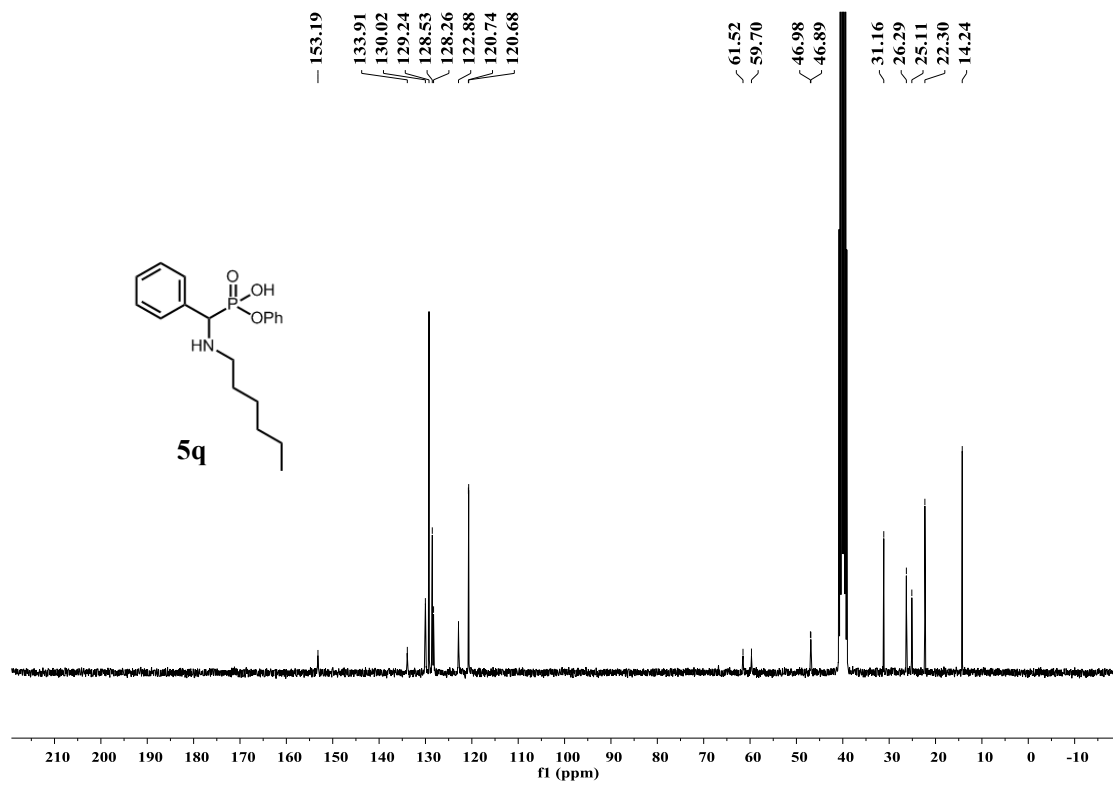


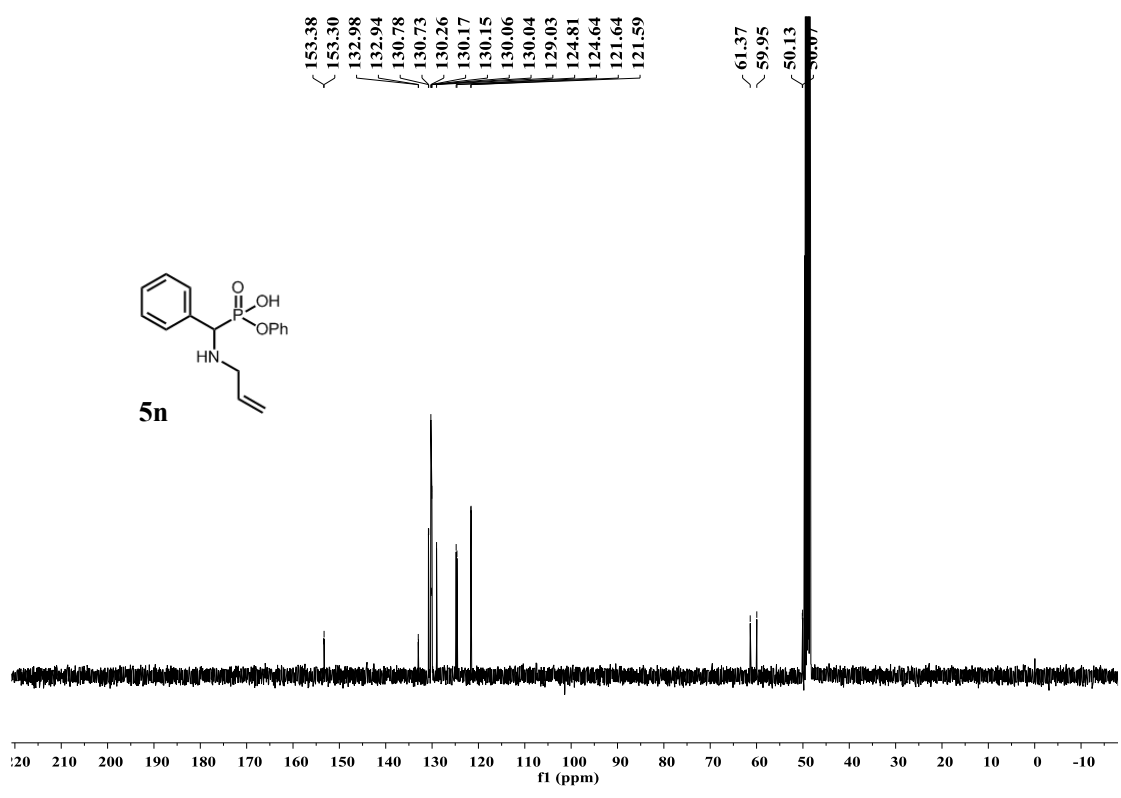
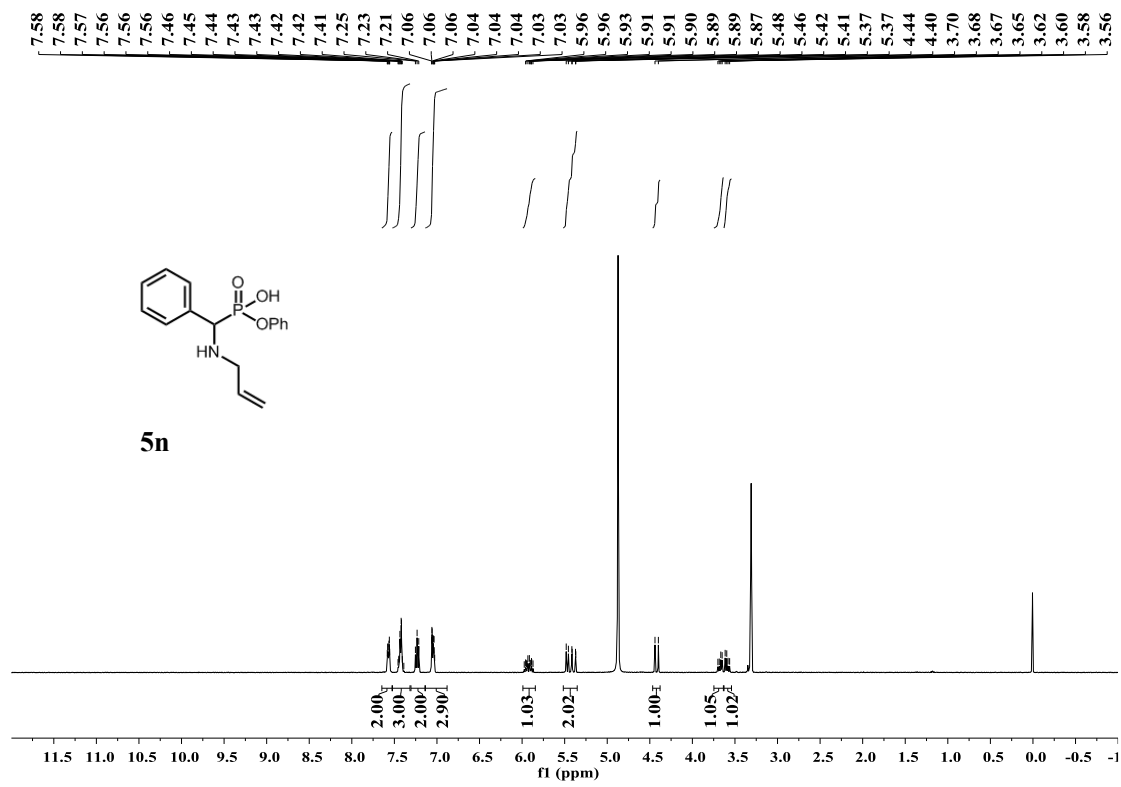
5m



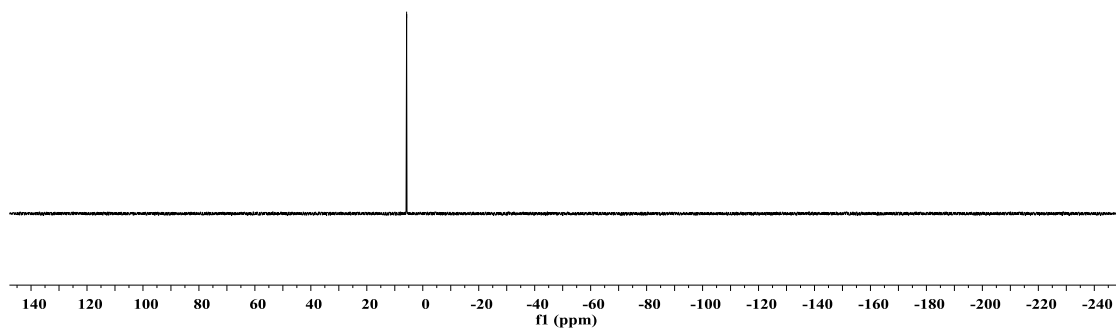
5q

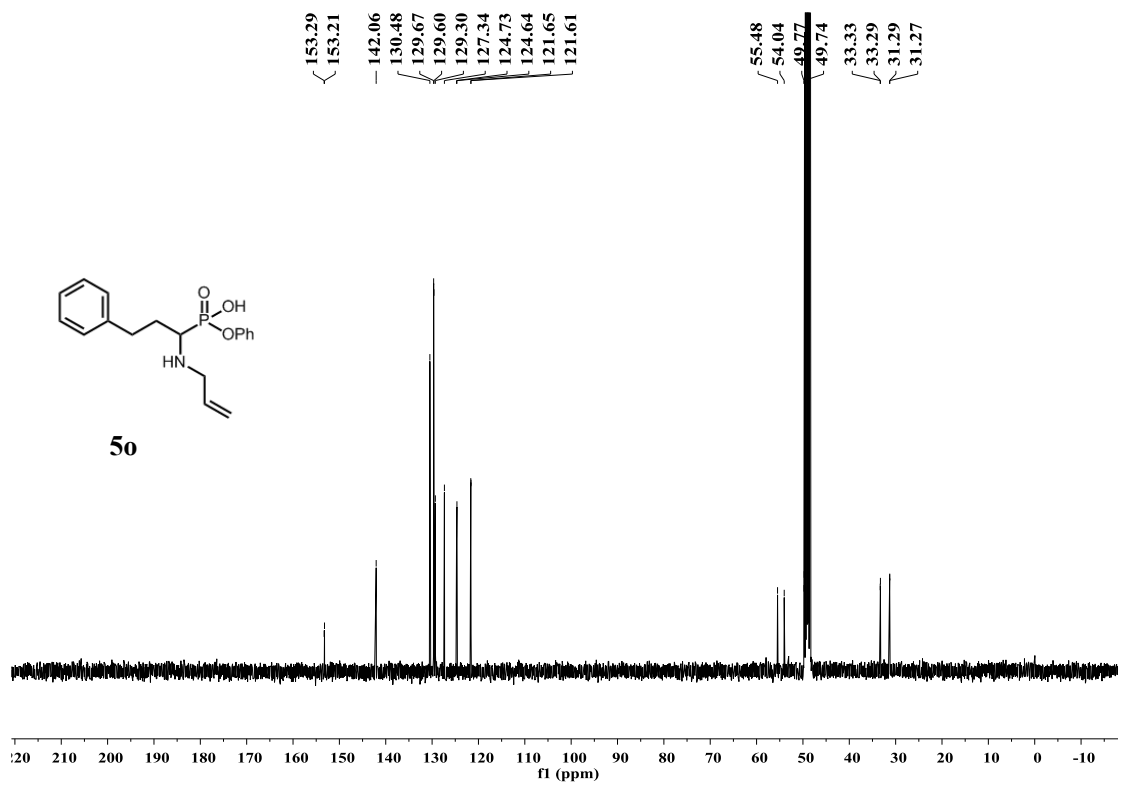
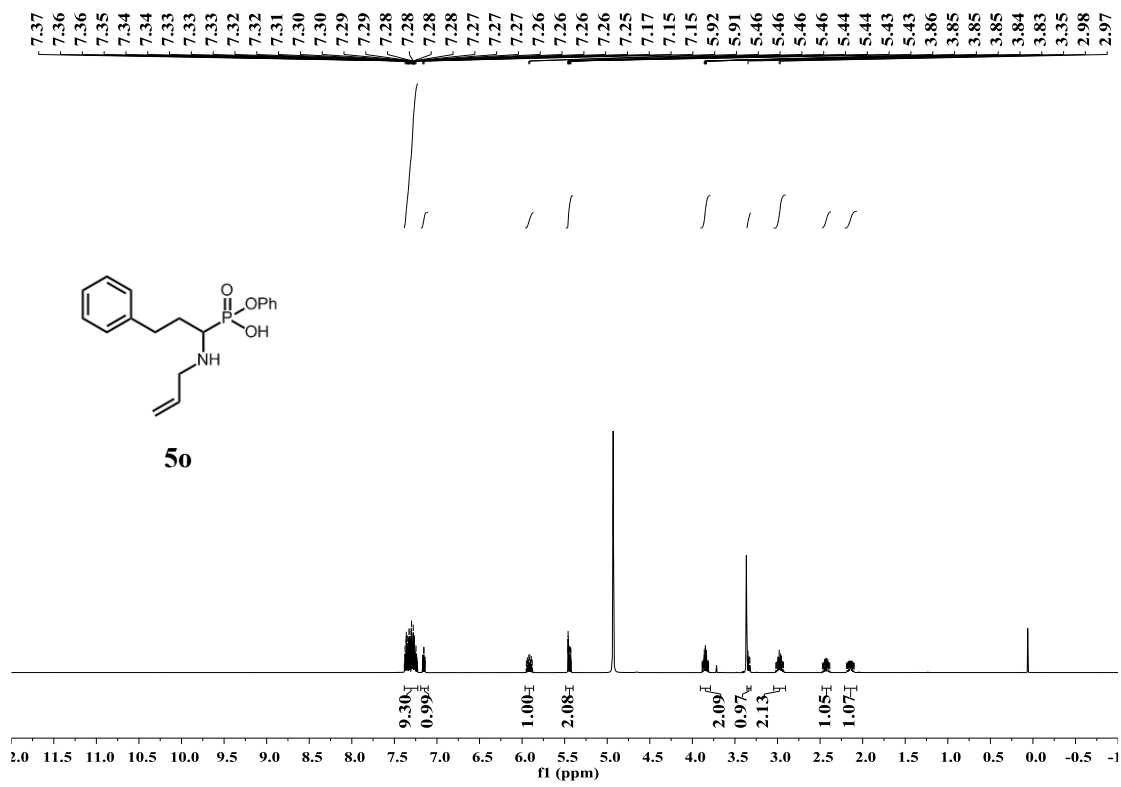




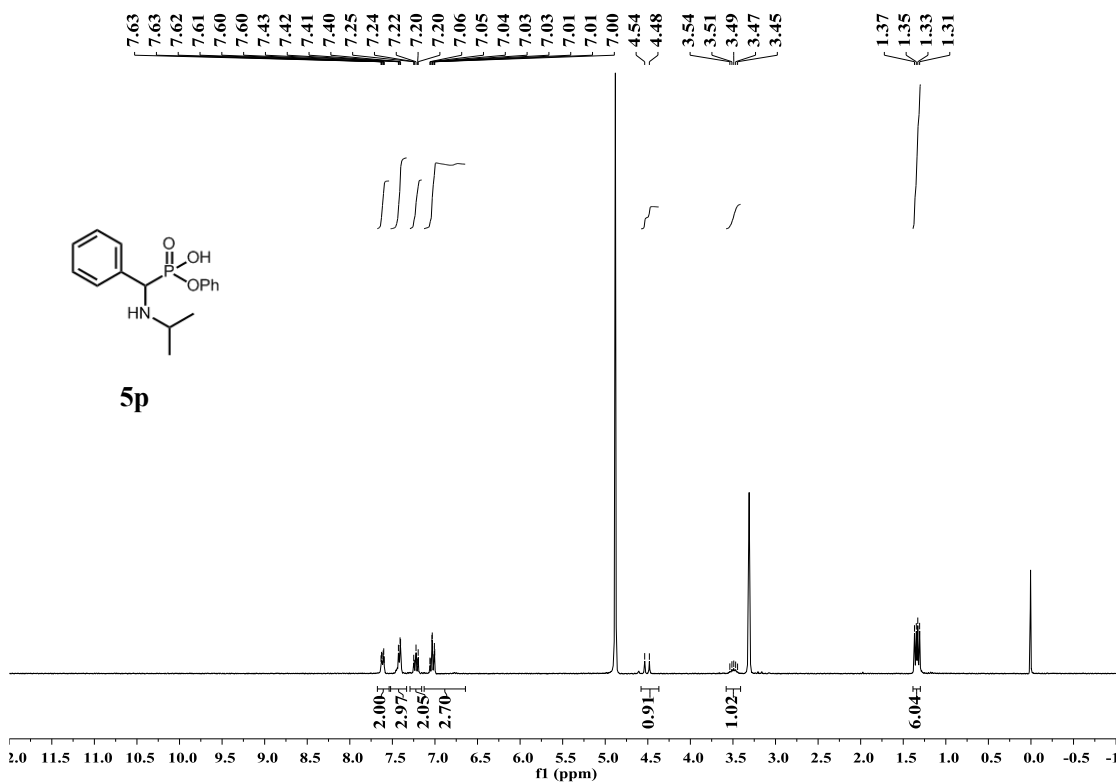
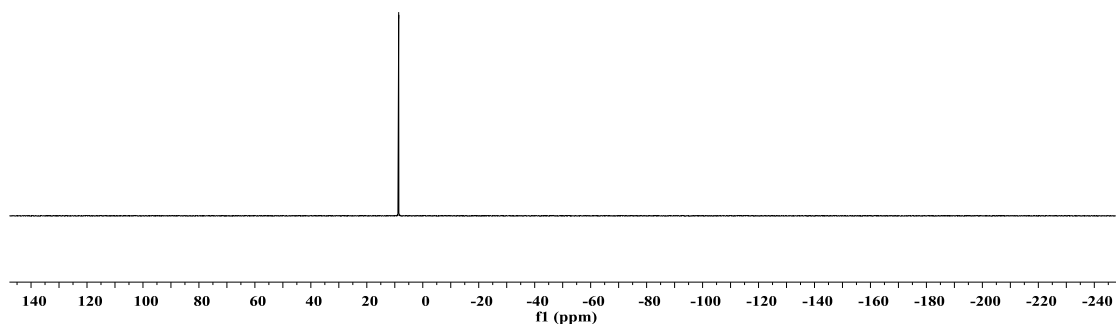
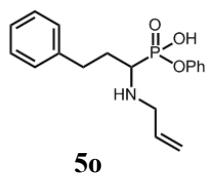


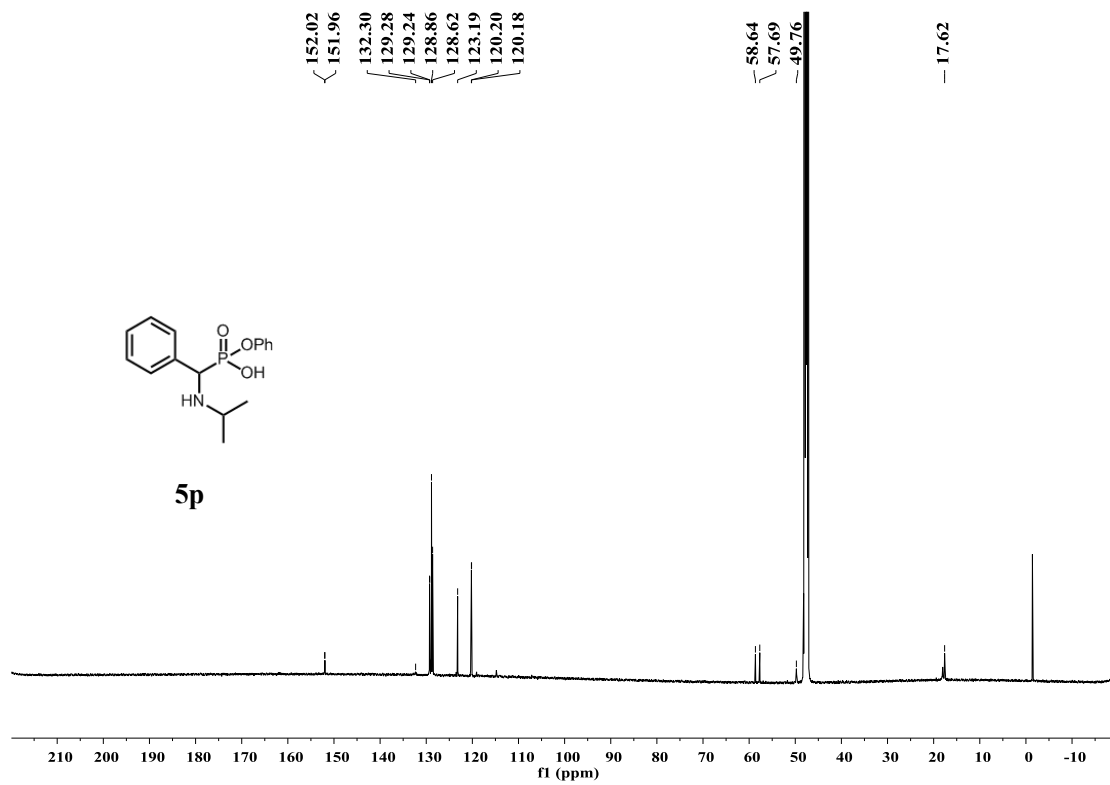
- 5.78



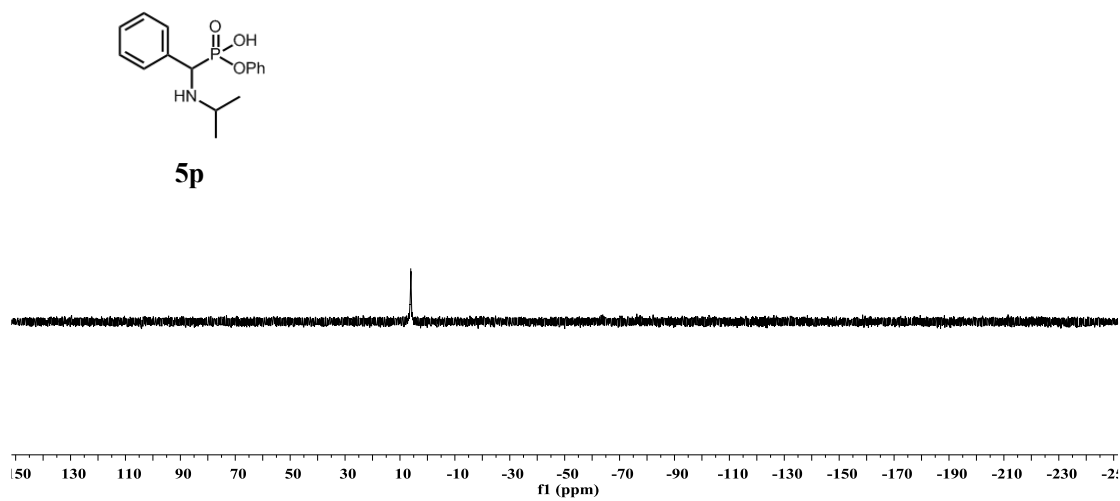


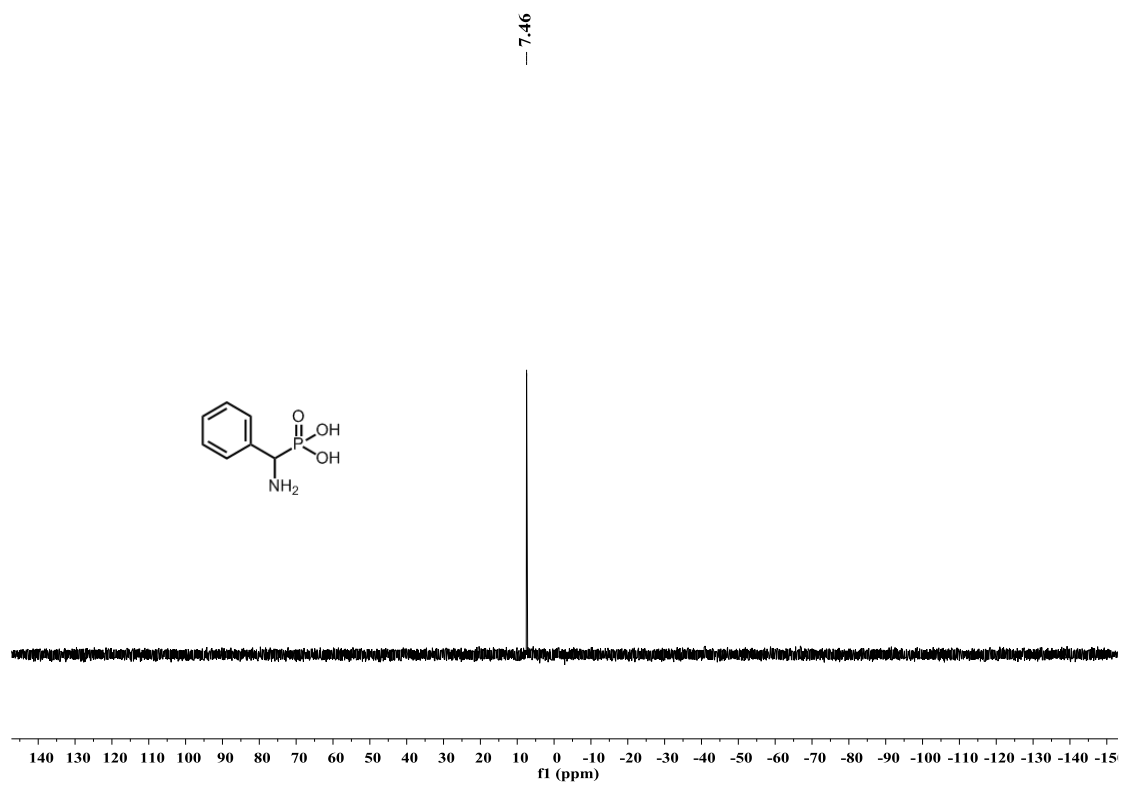
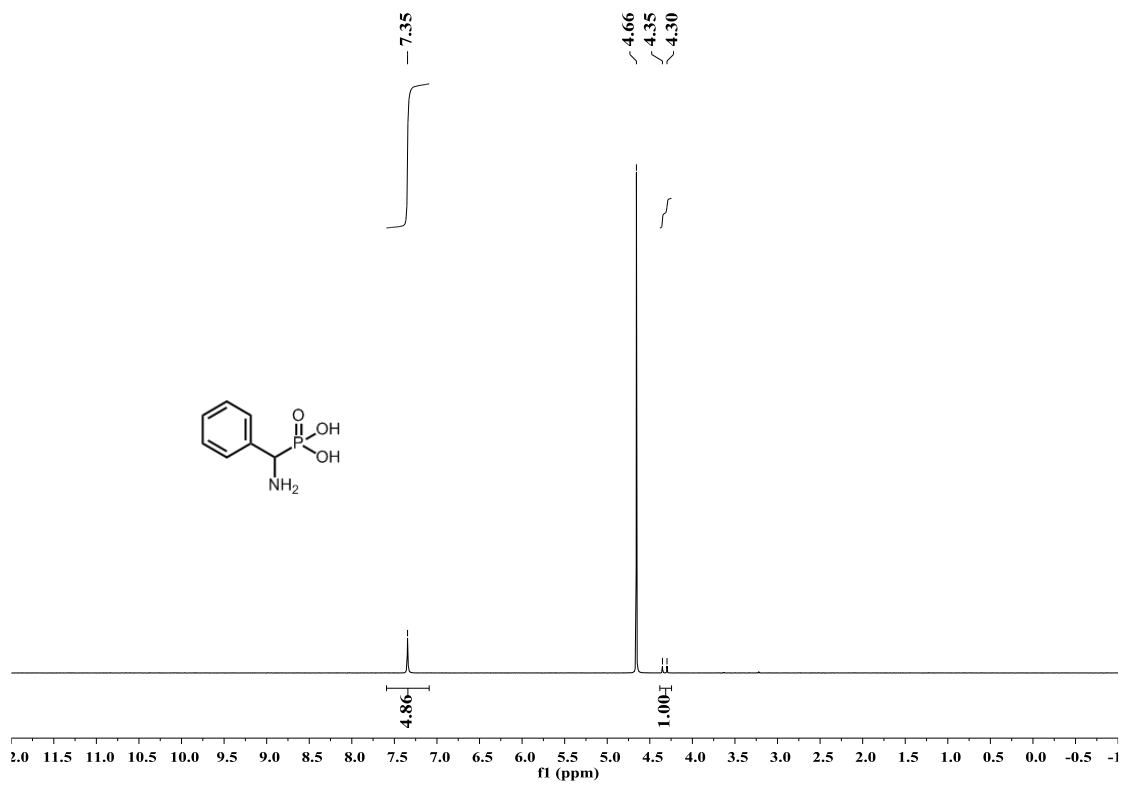
8.61





6.07





HPLC data for racemic in Chapter 3

